RETINAL DISEASES: MULTIFOCAL PUPILLOGRAPHIC OBJECTIVE PERIMETRY, AND EPIDEMIOLOGY

by

Bhim Bahadur Rai

A thesis submitted for the Doctor of Philosophy degree

Eccles Institute of Neuroscience

John Curtin School of Medical Research

The Australian National University

Primary Supervisor and Chair: Professor Ted Maddess

Advisor: Associate Professor Krisztina Valter-Kocsi

Associate Supervisors:

Professor Christopher James Nolan

Associate Professor Rohan William Essex

Dr Corinne Frances Carle

Dr Faran Sabeti

Preface

This thesis had two aims: 1) to develop a reliable objective functional assessment tool for early diagnosis and monitoring of disease activity and visual outcomes, and 2) to more broadly understand the pattern and magnitude of vitreoretinal diseases in the developing countries. So this thesis is comprised of two sets of data: first the functional assessment of retinal diseases using multifocal pupillographic objective perimetry **(**mfPOP), and second the epidemiological studies of vitreoretinal diseases in Bhutan and Nepal. The Chapter 1 is the Introduction, which describes the overview of the socio-economic burden of visual impairment and blindness, visual pathways, pupillary system and responses, and visual field testing and perimetric methods including mfPOP. It also summarises the common vitreoretinal diseases and treatment approaches in the context of the epidemiology.

The Chapter 2 is entitled: *Recovery dynamics of multifocal pupillographic objective perimetry from tropicamice dilation*. It provides clinical guidelines for the use of mfPOP in the clinical settings following pupillary dilation. It was important to report on it because mydriasis obviously affects the responses such as constriction amplitude and time-to-peak. It is published in the *Graefe's Archive for Clinical and Experimental Ophthalmology*. [DOI:10.1007/s00417-019-04523-8]

The Chapter 3 is entitled: *Multifocal pupillographic objective perimetry as a biomarker for anti-VEGF injection requirements in neovascular age-related macular degeneration.* It is part of a clinical trial on anti-VEGF treatment, and explores if mfPOP can possibly predict the need for retreatment among the patients of neovascular AMD.

The Chapter 4 is titled*: Correlation between Retinal Structure and Function measured with Multifocal Pupillographic Objective Perimetry in early-stage Type 2 Diabetic Macular Oedema.* This study maps macular OCT, and macular mfPOP data onto the Matrix 10-2 format to allow direct comparison between those three ways of assessing structure and function in diabetic macular oedema. The strongest structure/function correlations appear to be for outer macular locations, and especially between mfPOP sensitivity and delay and outer macular OCT thickness.

The Chapter 5 is entitled: *Pattern and presentation of vitreoretinal diseases: an analysis of retrospective data at a tertiary eye care centre in Nepal.* This covers 1905 cases over one year at a major hospital. It makes interesting observations on asymmetry of AMD and DR

and also the effect of dominant eye on reporting symptoms. It makes specific recommendations for screening programs. It is published in the *Asia-Pacific Journal of Ophthalmology*. [DOI:10.1097/01.APO.0000604400.50700.2d]

The Chapter 6 is entitled: *Pattern of vitreoretinal diseases at the national referral hospital in Bhutan: a retrospective, hospital-based study*. This study covers all 2913 new vitreoretinal cases in Bhutan over s 3-year period, all were patients of the author BBR. The profile of VR diseases in Bhutan is quantified and compared with other countries. Specific recommendations are made. It is published in the BMC Ophthalmology. [DOI:10.1186/s12886-020-01335-x]

The Chapter 7 is entitled: *Rural-urban difference in Myopia prevalence among myopes presenting to Bhutanese retinal clinical services: a 3-year national study*. Univariate and multivariate analyses of myopes referred for retinal assessment confirm that, as elsewhere in Asia, a lack of sunlight associated with education is causing an explosion of myopia. Fortunately, things are not as advanced in Bhutan. All the myopes were seen by BBR. It is published in the *Graefe's Archive for Clinical and Experimental Ophthalmology*. [DOI:10.1007/s00417-020-04891-6]

The Chapter 8 is entitled: *Surgical Management of Vitreoretinal Diseases in Bhutan: a 3-year national study*. The patient demography, number, types and indications of vitreoretinal surgery, including intravitreal injections of anti-vascular endothelial growth factor administered in the operating theatres as mandated in Bhutan are quantified. All patients were treated by BBR. It is published in New Frontiers in Ophthalmology. DOI:10.15761/NFO.1000251

The Chapter 9 is entitled: *Retinal laser services in Bhutan: a 3-year national survey*. It reports on the demographic characteristics of patients receiving laser services, and types and indications of laser therapies performed for vitreoretinal diseases in Bhutan over the study period. All patients were treated by BBR. It is published in the BMC Ophthalmology. [DOI:10.1186/s12886-020-01675-8]

The Chapter 10 is on the *Summary and Recommendations*. It highlights the critical findings from the mfPOP and the epidemiological studies.

Besides the above mentioned studies I had other achievements during the course of my PhD candidature. I made two presentations at the annual meetings of the Association for Research in Vision and Ophthalmology in the USA. Both the abstracts, *Pupillary response dynamics of*

*mydriasis measured with multifocal pupillography***,** and *Comparing retinal thickness and Matrix 10-2 functional testing in diabetic macular oedema*, which are published in the Investigative Ophthalmology and Visual Science in 2018 and 2020. I also presented my research at the New Investigator Forum, Australian Society of Medical Research, and other local health conferences. For my combined tertiary teaching experience at: the Postgraduate Medical Education Centre; and in the Faculty of Nursing and Public Health of the University Medical Sciences of Bhutan; and my work as a sessional Academic at the ANU Medical School; and a short thesis on tertiary teaching, I was awarded a *Fellowship of the Higher Education Academy*, UK by the ANU branch in August 2019.

Acknowledgement

As a clinician my life counted on like that of a cricketer counting number of runs scored, centuries or half-centuries made, wickets taken, and the catches. For me, the laurels were just giving back vision to the patients, performing cataract surgeries, fixing detached retinas, sealing macular holes, retinal lasers, intravitreal injections, and retrieving dislocated lenses from the vitreous cavity. My happiest moments would be celebrating my patients' emotions, who had been blind and bed-ridden for years, when they were able to see the faces of their loved ones again. I then took up a new venture, a PhD course by research. I have several people to thank because they have walked me through this wonderful journey called *research* holding my hands as I stepped along different steppingstones.

First, I thank Professor Ted Maddess for embracing me as his PhD candidate. His very friendly and approachable nature, and readiness to help at any time are true assets for any student to bank on. Supervisors count their success on number of publications, students, or grants won. Atop of all these, Prof. Maddess ensures that his students are well-placed in the job market. I have learnt not only about research from him but also other aspects such as humour, humanity, and importance of effective and timely communications. He has introduced me to the research world, including peer-reviewing of journal articles, which I now do regularly.

I thank Associate Professor Rohan Essex for being my clinical supervisor and allowing me to work with him closely in various research studies and as an Observer in the Ophthalmology Department of The Canberra Hospital. In the process I learnt not only about research but also many clinical pearls through examining our research participatory patients, hospital clinics, operating theatres and some academic sessions, which I was naïve about.

I thank Dr. Faran Sabeti for taking me as his PhD student and working with me very closely in all the research studies carried out at the ANU. I am also thankful to him for allowing me to deliver public lectures on diabetes and diabetic eye diseases at the Health Hub, University of Canberra, which helped us recruit our research participants. Through daily discussions with him I have learnt a lot about Australian eye care services and teaching strategies.

I thank Dr. Corinne Carle for always being there for me: be it a procedure in the research activities, or a missing or misplaced data, she always helped me to find a way out.

I thank Professor Christopher Nolan, endocrinologist and diabetologist for his suggestions and advice on the clinical ground. The instant feedback that I got from him on diabetes helped me streamline my research studies on diabetes. He has been like a guardian figure in Australia for my family and I.

I thank Associate Professor Krisztina Valter-Kocsi for being my PhD course advisor. With her vast experience in the research field I got constant and close guidance which helped me sail smoothly at different stages of my PhD course, including planning of thesis chapters.

Besides my supervisory panel members, I must thank Ms. Emilie Rohan who helped me recruit my patients, perform eye tests, and maintain data. I also thank Joshua van Kleef for helping to analyse some of my data.

It would be incomplete if I do not thank the research participants, from both the patient and control groups, without whom this venture would be impossible. I also thank the John Curtin School of Medical Research, Australian National University and the Australian Government for providing me the PhD research and HDR fee remission merit scholarships, which were definitely above my reach.

Lastly, but not the least, I thank my family, wife Deepa and sons Yogit and Yodeep for being understanding and allowing me to perform my studies. I know every success comes with compromise at least, if not sacrifice.

Dedication

I dedicate this research project to the elders of my family, who worked hard and supported my upbringing and education:

Elder brother: Late Nar Bahadur Rai (1.1.1967-13.10.2020)

Mother: Late Nar Lachi Rai

Father: Bindu Man Rai

Grandmother: Late Run Maya Rai

Grandfather: Late Maha Pal Rai

Declaration

I hereby declare that the research materials submitted in this thesis have not been submitted or accepted for the award of any other degree at any university. The research studies presented in this thesis are my own original work. To the best of my knowledge, the thesis contains no material published previously or written by another person. The three research studies on the application of multifocal pupillographic objective perimetry are conducted as prospective studies during my PhD course at the John Curtin School of Medical Research, Australian National University. For the other studies on the pattern and treatment of vitreoretinal diseases in Bhutan and Nepal the data was collected when I was working as the vitreoretinal surgeon, and the analysis and writing are done exclusively during my PhD course, but were entirely analysed, written up, and published while I was at JCSMR.

Thesis abstract

My thesis entitled *Retinal Diseases: Multifocal pupillographic objective perimtery, and epidemiology* comprises two parts. First, retinal function measured with multifocal pupillographic objective perimetry (mfPOP) in neovascular AMD (nAMD) and diabetic macular oedema (DMO), and second, epidemiology of vitreoretinal diseases (VRD) in Bhutan and Nepal. The epidemiological chapters cover 1905 new VRD patients in Nepal, and 2913 in Bhutan. Those studies identified the common, preventable, VRDs including: diabetic retinopathy and macular oedema, nAMD, high myopia, hypertensive retinopathy, retinal vein occlusion, retinal breaks, retinal vasculitis, retinopathy of prematurity, etc. In Nepal, females presented later than males by 9 years ($p<0.0001$), age or disease duration for diabetic retinopathy did not correlate with severity, presenting visual acuity (VA) was asymmetric between eyes ($p<0.0001$), and patients often only reported once their right (dominant) eyes had VA of 6/18 or worse. In Bhutan, females presented earlier: ($p=0.003$). Myopia constituted 92.1% of refractive error with myopia prevalence (MP) of 12.3%, more common among females ($p=0.01$) and urbanites ($p=0.02$). MP was highest among urban females (20.9%), followed by urban males (11.9%), rural females (6.8%), and rural males (5.2%). Logistic regression revealed that the odds of having myopia were increased by being a student (4.96 ×) or professional (1.96 ×), and decreased by rural living (1.75 ×), all $p \leq 0.038$.

Those diseases are treatable with complete recovery if managed early. To improve management, we address the knowledge gap in developing countries by advancing a reliable objective diagnostic method: an FDA-cleared prototype of mfPOP, the ObjectiveFIELD Analyser (OFA) (Konan Medical USA, Irvine, CA).

In nAMD, the per-region central OFA sensitivities decreased and delays increased with disease severity in patients tested monthly for up to 2 years. Central sensitivity of eyes needing anti-VEGF treatment was less sensitive than in the untreated eyes by -2.23 ± 0.051 dB ($p<0.0002$). Based on the peripheral responses we have noticed 2 types of patients: *positive* with peripheral hypersensitivity and longer delays than normal, and *negative* with peripheral hyposensitivity and shorter delays. Among the positive eyes the peripheral sensitivity increased on average by 9.88 ± 4.41 dB/month ($p=0.042$), and the delay increased at 3.49 ± 1.75 ms/month ($p=0.049$) before the clinical decision to treat. For the negative eyes, the peripheral sensitivity dropped, and the delay was shorter a month before the treatment by 9.38 ± 3.59 ($p=0.013$), and a month following treatment it improved (shorter by 8.50 ± 2.71

ms, p=0.004). Treatment drove subsequent responses towards normality either from the positive or negative patient condition. Importantly, changes occurred 1-3 months before treatment was indicated clinically or by other diagnostic methods.

We followed Type 2 diabetes patients for up to 2 years. Reduced mean sensitivities and longer delays were seen compared to normal. Peripheral hypersensitivity and shorter delays were associated with shorter diabetes duration. Principal curve analysis showed correlation between OFA and Matrix values. Outer macular thickness correlated significantly with inner and outer OFA sensitivity and delay, all $p<0.0012$ with DMO, and median $p=0.001$ without DMO, while the inner thickness was not correlated. A mixed-effects logistic regression determined that outer thickness and OFA sensitivity contributed independently to a clinical diagnosis of DMO. Outer thickness, number of visits and male gender increased the odds of having DMO.

From a practical standpoint dilation with tropicamide 1% affected per-region sensitivities for more hours than either delays or signal-to-noise ratios (SNRs). So sensitivity measurements should be considered only after 48 hours, but delays or SNRs can be measured after 8–12 hours following mydriasis with tropicamide.

Contents

1. Introduction ……1
1.1 Overview ……2
1.2 Visual pathway ……3
1.2.1 Human Retinal Circuitry ……3
1.2.2 Retinal Ganglion Cell Projection: Optic Nerve, Optic Chiasma, Optic Tract ……16
1.2.3 Lateral Geniculate Nucleus ……19
1.2.4 Optic Radiation ……22
1.2.5 Visual Cortex ……23
1.3 Pupillary System and Responses – Neural pathways and mechanisms ……26
1.3.1 Pupil: Anatomy and function ……26
1.3.2 Sub-cortical pathways ……27
1.3.3 Cortical input ……29
1.3.4 Direct and consensual responses ……30
1.4 Visual Field Testing and Perimetry ……31
1.4.1 History and Evolution of Perimetry ……31
1.4.2 Subjective Perimetric Methods ……33
1.4.3 Objective Perimetric Methods ……40
1.5 Vitreoretinal diseases and their treatment ……50
1.5.1 AMD, mainly neovascular ……51
1.5.2 Anti-VEGF treatments ……53
1.5.3 Diabetic eye diseases ……56
1.5.4 Hypertensive retinopathy ……58
1.5.5 Retinal vein occlusions ……59
1.5.6 Retinal detachments ……60
1.5.7 Complications of myopia ……61
1.5.8 Retinopathy of prematurity ……62
1.5.9 Ocular trauma……62
1.6 References ……64

2. Recovery Dynamics of Multifocal Pupillographic Objective Perimetry from Tropicamide Dilation. ……88
2.1 Abstract ……88
2.2 Introduction ……88
2.2 Methods ……89
2.2.1 Subjects ……89
2.2.2 Multifocal Pupillographic Objective Perimetry ……89
2.2.3 Test Procedures ……90
2.2.4 Analysis ……90
2.3 Results ……91
2.4 Discussion ……94
2.5 Conclusions ……96
2.6 References ……96

3. Multifocal Pupillographic Objective Perimetry as a biomarker for anti-VEGF injection requirements in neovascular Age-related Macular Degeneration. …….....98
3.1 Abstract …….…99
3.2 Introduction ……..…..102
3.3 Methods …….….103
3.3.1 Subjects …….…. 103
3.3.2 Study design …….…104
3.3.3 Test Procedures ……104
3.3.4 Multifocal Pupillographic Objective Perimetry …….……..105
3.3.5 Analysis …….……...106
3.4 Results …….…110
3.5 Discussion …….…..131
3.6 Conclusions……..136
3.7 References ……...138

4. Correlation between Retinal Structure and Function measured with Multifocal Pupillographic Objective Perimetry in early-stage Type 2 Diabetic Macular Oedema..142
4.1 Abstract ……...143
4.2 Introduction …….……145
4.3 Methods ……...146
4.3.1 Subjects ……146
4.3.2 Study design ……..147
4.3.3 Test Procedures ……147
4.3.4 Multifocal Pupillographic Objective Perimetry …….....148
4.3.5 Analysis ……149
4.4 Results ……149
4.5 Discussion ……..….…170
4.6 Conclusions ……..…...175
4.7 References ……..……..…177

5. Pattern and presentation of vitreo-retinal diseases: an analysis of retrospective data at a tertiary eye care centre in Nepal. ……180
5.1 Abstract ……....180
5.2 Introduction ……180
5.3 Methods …….....180
5.3.1 Study design ……..181
5.3.2 Setting ……181
5.3.3 Participants ……181
5.3.4 Clinical examination and data collection ……..181
5.3.5 Analysis ……181
5.4 Results ……181
5.5 Discussion ……185
5.6 Conclusions ……186
5.7 References ……...187
5.8 Supplementary data ……188

6. Pattern of vitreoretinal diseases at the national referral hospital in Bhutan: a retrospective, hospital-based study. ……..194
6.1 Abstract …….……..194
6.2 Introduction ……194
6.3 Methods …….……195
6.3.1 Study design ……195
6.3.2 Setting …….,……..195
6.3.3 Participants …….,…..195
6.3.4 Clinical examination and data collection …….,……195
6.3.5 Analysis ……196
6.4 Results …….…....196
6.5 Discussion …….……..201
6.6 Conclusions …….……203
6.7 References …….…..204
6.8 Supplementary data ……....205

7. Rural-urban difference in Myopia prevalence among myopes presenting to Bhutanese retinal clinical services: a 3-year national study. ……..……..209
7.1 Abstract ……..…….209
7.2 Introduction …….....210
7.3 Methods …….…….210
7.3.1 Study design ……..…210
7.3.2 Setting ……..….210
7.3.3 Participants …….….….210
7.3.4 Clinical examination and data collection ……..…211
7.3.5 Analysis ……..…...211
7.4 Results …….....211
7.5 Discussion ……..…….213
7.6 Conclusions ……..……..215
7.7 References ……..…216

8. Surgical Management of Vitreoretinal Diseases in Bhutan: a 3-year national study. 218
8.1 Abstract ……...218
8.2 Introduction …….....218
8.3 Methods …….…..219
8.3.1 Study design ……..……219
8.3.2 Setting ……..….219
8.3.3 Participants ……..……219
8.3.4 Clinical examination and data collection …….……219
8.3.5 Analysis …….……219
8.4 Results ……..…...219
8.5 Discussion ……..….220
8.6 Conclusions ……..……...221
8.7 References ……..……..…222
8.8 Supplementary data ……..….…..223

9. Retinal laser services in Bhutan: a 3-year national survey. ……..……...225
9.1 Abstract ……...225
9.2 Introduction ……...……..225
9.3 Methods …….…..…226
9.3.1 Study design ……..……226
9.3.2 Setting ……..…….….226
9.3.3 Participants ……..…….….226
9.3.4 Clinical examination and data collection …….….…226
9.3.5 Analysis ……...……..227
9.4 Results ……..….…..227
9.5 Discussion ……..….…227
9.6 Conclusions ……..……...229
9.7 References ……...229

10. Summary and Recommendations ……231
10.1 Summary ..……232
10.2 Recommendations ……234
10.3 Future directions ……...236

11. Appendix ……238

11.1 Set of plots of data mapped to the 10-2 format ..……239

Chapter 1

Introduction

1

1.1 Overview

World Health Organization estimated 285 million people of all ages were living with visual impairment, of whom 39 million were blind, and of them 82% of population aged 50 years and above were blind (Pascolini & Mariotti, 2012). Vision loss often leads to a lifetime of inequality leaving the individuals with poorer health and barriers to education and employment. The consequence of vision loss and impairment burdens not only the blind or visually impaired individuals but also the other members of the family. The consequent caring responsibilities can reduce the opportunities of other family members to thrive, and increases a family's risk of poverty. The impact is also experienced at the national level, where vision loss can lead to economic deficits and increased direct and indirect costs to the health sector. With a rapidly accelerating ageing population, the impact of vision loss is expected to rise. The *World report on vision* stated that investing in vision offers a good return on investment and that people with visual impairment can lead full and productive lives with the right support (Ulldemolins *et al.*, 2012). The prevalence of visual impairment or blindness goes hand in hand with the lack of socio-economic development. For this reason, blindness prevention programmes must address not only the elimination of avoidable blindness but also focus on the economic development simultaneously. The socio-economic burden of vision loss can obviously be estimated from the costs of rehabilitation and care provided to the visually impaired, and less apparent but just as significant, however, are the indirect costs resulting from the loss of productivity. *Quality-Adjusted Life Years* is being used by the economists to calculate the economic burden of visual impairment, including prevention and care (Thavorncharoensap *et al.*, 2013).

The International Agency for the Prevention of Blindness (IAPB) is an alliance of civil society organisations, corporates and professional bodies promoting eye health through advocacy, knowledge and partnerships. Its mission is to eliminate the main causes of avoidable blindness and visual impairment by bringing together governments and non-governmental agencies to facilitate the planning, development and implementation of sustainable national eye care programmes. IAPB promotes *VISION 2020: The Right to Sight*, its joint initiative with the WHO. *World Sight Day* is an annual event observed on the second Thursday of October, though which IAPB creates awareness about blindness and visual impairment (IAPB, 2017a). The WHO Global Action Plan 2014-2019 supports the provision

2

of effective and accessible eye care services for effectively controlling visual impairment including blindness to achieve the goal of VISIN 2020 (IAPB, 2017b).

The WHO suggested that estimating the magnitude of blindness and visual impairment, and working out the graphical distribution, along with the causes, was an important initial step to reducing the load of blindness and visual impairment (Pascolini & Mariotti, 2012). The developed countries have done the national surveys on the causes, incidence, prevalence and current structure of treatment of blindness and visual impairment and can formulate the action plans based on available data. But among the developing countries one very important barrier to the implementation of the programs is the insufficient national data. Very few developing countries have conducted nationwide surveys, and there have been no follow-up surveys to provide the current data. There have been only six national studies being completed and published since 2012 (Ramke *et al.*, 2012; Lepcha *et al.*, 2013; Isipradit *et al.*, 2014; Park *et al.*, 2015; Zatic *et al.*, 2015).

The aims of this thesis are based on two levels. First, to report on the use of the new objective method of visual field testing multifocal objective pupillographic perimetry (mfPOP) in diagnosing common retinal diseases, responses to the treatment, and reporting on its characteristic findings as biomarkers for categorising the disease activities and further need of treatments. Second, to highlight epidemiological data on the prevalence, pattern and presentation of vitreoretinal (VR) diseases and the treatment modalities in the developing countries like Bhutan and Nepal in the perspective of patients presenting to the tertiary eye care centre for VR services. The information will inform policy making at the national level in framing action plans to control blindness and visual impairment due to VR diseases.

1.2 VISUAL PATHWAYS

1.2.1 Human Retinal Circuitry

Basic Anatomy

Vision, one of the five senses of human beings, is the function of eye, a complex optical organ system. The development of the eye is an extremely complex process with different inductive events, each step requiring exquisite coordination among the various tissues that contribute to it, which is beyond the scope of this chapter. In brief, from the first recognition of the eye as optic vesicle, an evagination from the diencephalon of the neural tube at around

3

the 25th postovulatory day in the human embryo. *Sonic hedgehog* (Shh) is an extracellular glycoprotein released initially by the prechordal mesoderm, acts on the ventral diencephalon so that the initial cyclopean eye primordium is split into two. The optic vesicle folds in on itself to become a two layered optic cup (Reh & Moshiri, 2006). The outer layer forms the retinal pigment epithelium (RPE), while the inner layer forms the sensory retina (Reese, 2011). The retina is the inner most of the three layers of the eyeball, with a surface area of human retina is about 1094 square mm (Bernstein). The thickness of retina is 0.10 mm at ora serrata, 0.18 mm at the equator and 0.56 mm near the optic disc. Out of ten layers of retina, the RPE layer is the outer most bordered externally by Bruch's membrane. The rest of the inner nine layers are referred together as the neuro-sensory retina and consists of the layer of photoreceptors, external limiting membrane, outer nuclear layer, outer plexiform layer, inner nuclear layer, inner plexiform layer, ganglion cell layer, nerve fibre layer and internal limiting membrane (Bron, 1997a). With the advent of OCT each of these layers can be visualised and studied in normal, ageing or pathological conditions as in **Figure 1.1**. Identifying each retinal layer is useful in diagnosis and management of different retinal diseases.

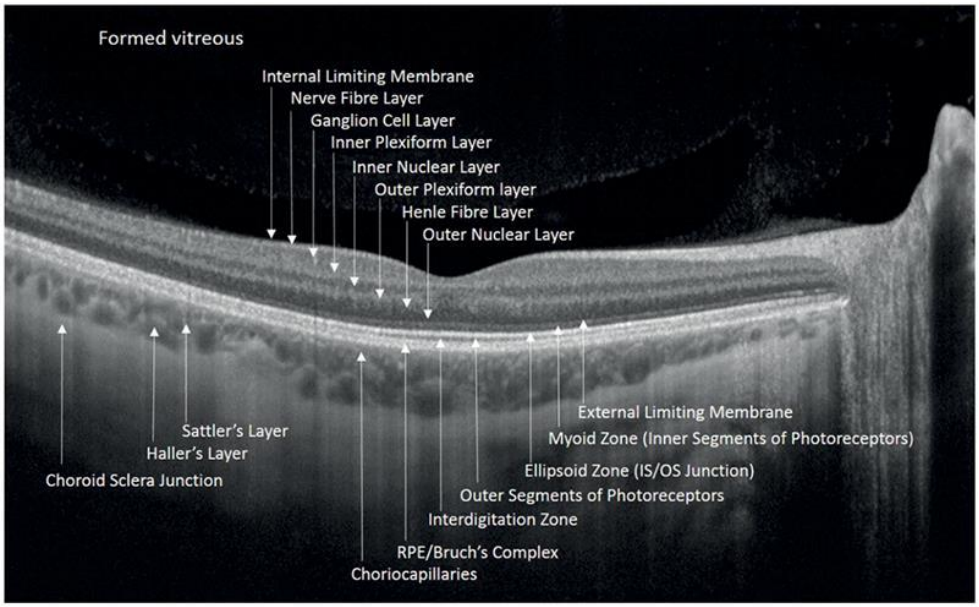

Figure 1.1. Optical Coherence Tomography of a normal retina showing different layers. (Adapted from https://www.opticianonline.net/cet-archive/153)

At the beginning of embryogenesis the fovea is the thickest portion of the retina. Soon different retinal cells, particularly the photoreceptors migrate towards the centre of the fovea, creating centripetal displacement. This process continues throughout the intrauterine life until some months or years postnatally. This migration of cells into the central fovea results

4

metabolic starvation of the inner retina. To overcome this starvation there is adaptive centrifugal migration of cells from the inner retina towards the encroaching perifoveal capillary network, thereby forming the foveal depression (Provis *et al.*, 1998; Tick *et al.*, 2011). The fovea as the thinnest portion of the retina consists only six layers, namely RPE layer, photoreceptors, external limiting membrane, outer plexiform layer, Henle's layer and internal limiting layer. This results uneven distributions of different types of cells as well as ratios between photoreceptors and the ganglion cells (Perlman *et al.*, 1995; Bron, 1997a; Reese, 2011; Bowling, 2016a). The same information is reflected in **Figure 1.2**.

5

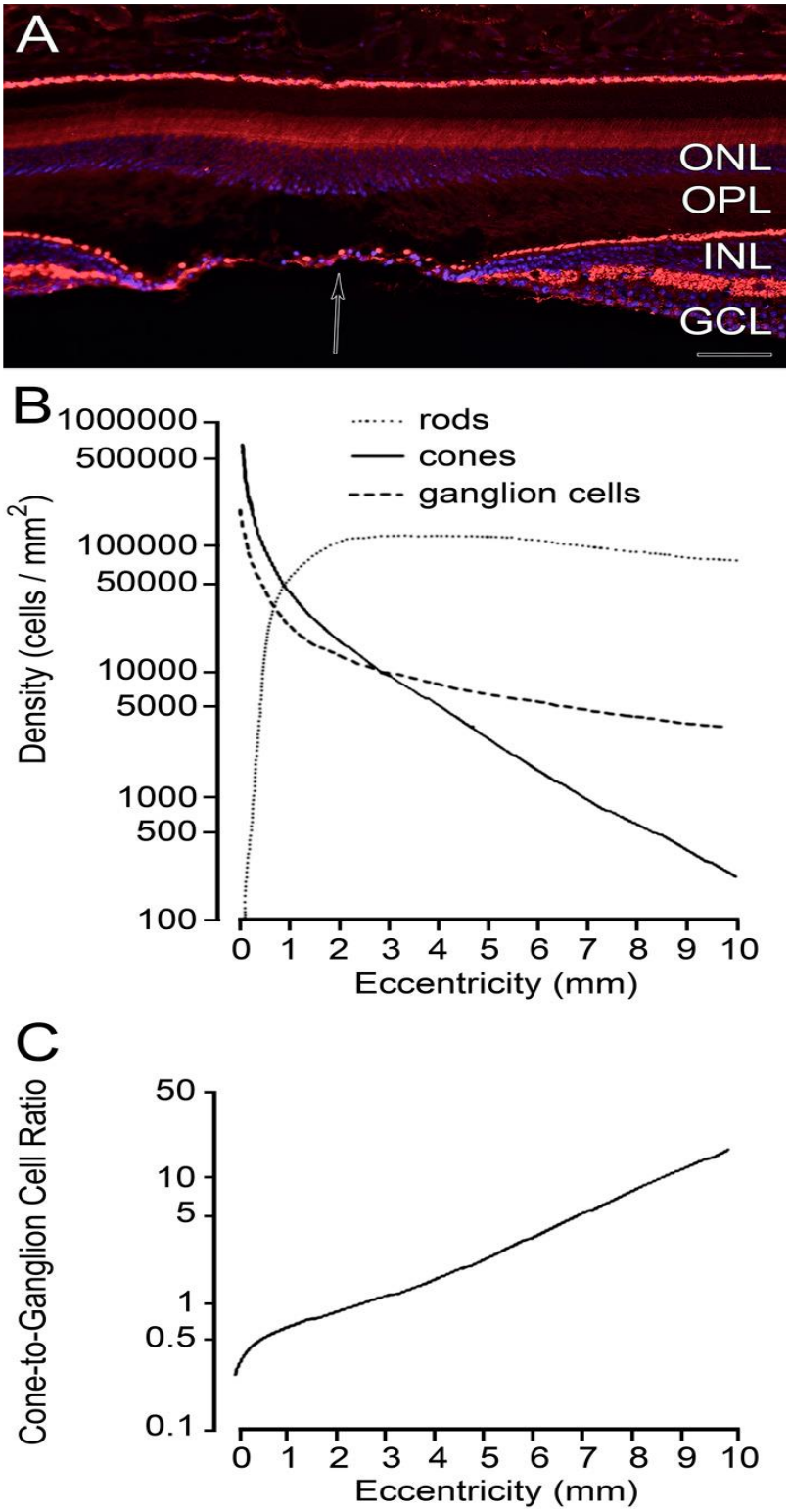

Figure 1.2. Regional distribution of neurons in the retina. (**A**)Vertical section through the human fovea. (**B**) Density of rods, cones and ganglion cells throughout the primate retina. Densities in the rhesus monkey retina were measured along the temporal horizontal meridian; zero eccentricity represents the fovea. (**C**) Cone-to-ganglion cell ratio throughout the monkey retina. Divergence is maximal in the fovea, where there are almost 3 ganglion cells per cone. As eccentricity increases, divergence decreases and convergence increases. At the retinal periphery, there are more than 10 cones per GC. Reproduced from (Joselevitch, 2008).

6

Different landmarks and functional zones in the retina

The inner two-thirds of the retina is supplied by the central retinal artery (CRA) through its retinal arterioles and capillaries, whereas the outer third is supplied by the choriocapillaries, with sympathetic autoregulation. The CRA first divides into superior and inferior branches, each of which further branches into temporal and nasal arterioles, namely supero-temporal, infero-temporal, supero-nasal and infero-nasal arterioles. These arterioles run from the optic disc to respective directions. The supero-temporal and infero-temporal arterioles mark the peripheral extends of the macula as shown in **Figure 1.3**. The venules and vein follow the corresponding course and drain the retina (Harris *et al.*, 1998; Bowling, 2016e). The macula is sub-divided into foveal, parafoveal and perifoveal zones. The fovea has different zones: outer most foveal avascular zone (FAZ), foveola in the middle and umbo the innermost.

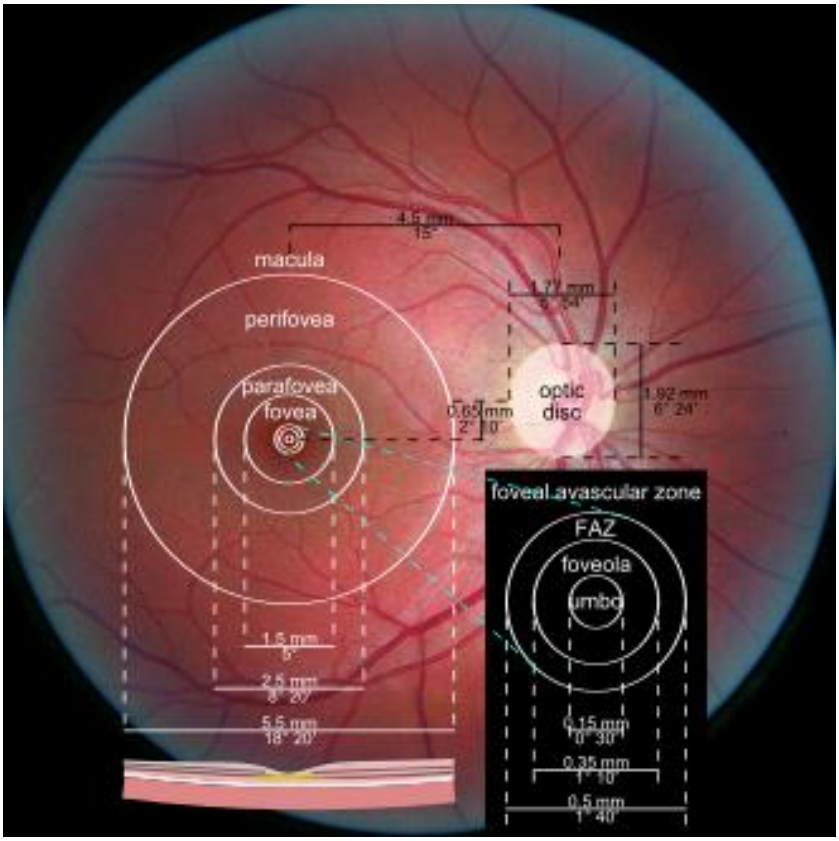

Figure 1.3. Different landmarks and functional zones of macula. It also shows different demarcated zones within the macula with dimensions. Inset depicts the structure within the fovea. (Adapted from https://en.wikipedia.org/wiki/Foveola)

7

For the precise location and mapping of the macular diseases the macula is divided into nine subfields by the ETDRS grid (Group, 1991). The central subfield has 1 mm diameter area overlaying the fovea. The pericentral ring is the area of 3 mm diameter outside central subfield. The peripheral ring is the area of 6 mm diameter outside the pericentral ring. The pericentral and peripheral rings are further subdivided into four subfields each by the diagonal lines as shown in **Figure 1.4** (Demirkaya *et al.*, 2013). These subfields are used conveniently in localising the pathology and mapping out the visual function or dysfunction.

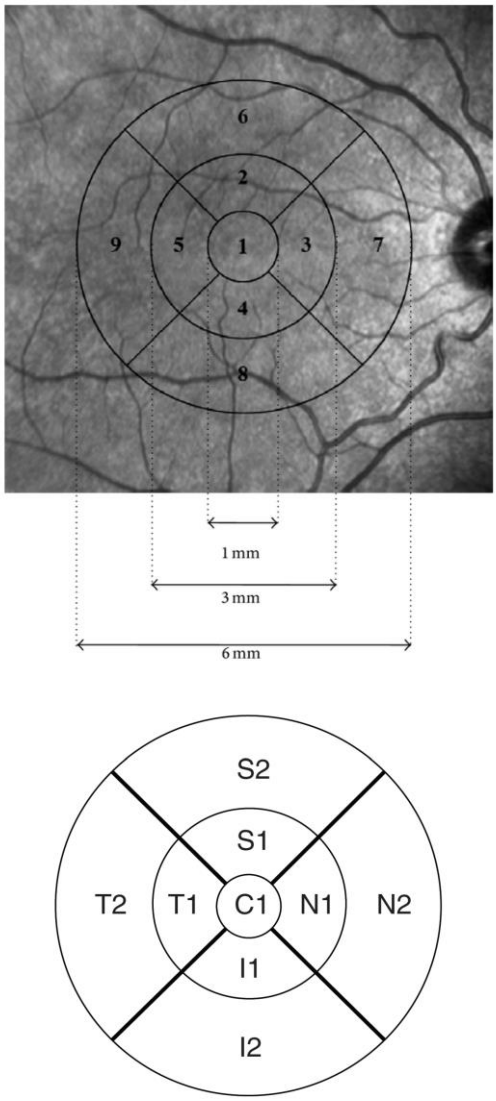

Figure 1.4. ETDRS grid. Nine ETDRS subfields of macula in each eye, right and left representing the mirror-image demarcation (Demirkaya *et al.*, 2013). The figure illustrates the two numbering schemes used in the literature: T,S,N,I and C referring to temporal, superior, nasal, inferior and central. Diagram Courtesy Ted Maddess.

8

RPE Cells

The functions of RPE layer are to form the outer retinal barrier (zonula occludentes) which prevents leakage of extracellular fluids from the choriocapillaris into the subretinal space and actively pumping ions and water out of the space; maintenance of continued adhesion with Bruch's membrane; phagocytosis and lysosomal degradation of shed outer segments of photoreceptors; storage, metabolism and transport of vitamin A; absorbing excess light and clearance of metabolic wastes (Binder, 2006; Gullapalli *et al.*, 2008; Strauss, 2011; Xu & Le, 2011; Che *et al.*, 2014).

The retina consists of five distinct classes of neuronal cells, namely photoreceptors, amacrine, bipolar, horizontal and retinal ganglion cells; and other non-neuronal cells like Muller cells, astrocytes and microglial cells (Curcio *et al.*, 1990). There are three nuclear layers in the retina, namely outer nuclear, inner nuclear and ganglion cell layers; and two plexiform layers, namely outer and inner plexiform layers. The outer nuclear layer contains cell bodies of the photoreceptors whose photosensitive outer segments are wrapped in the RPE layer. The inner nuclear layer contains soma of three main classes of retinal second order neuronal cells: bipolar, horizontal and amacrine cells. The functional unit of photoreceptors, bipolar cells and horizontal cells are called *triads* in the outer plexiform layer, whereas that of bipolar cells, amacrine cells and ganglion cells are called *dyads* in the inner plexiform layer (Joselevitch, 2008) as shown in **Figure 1.5**.

9

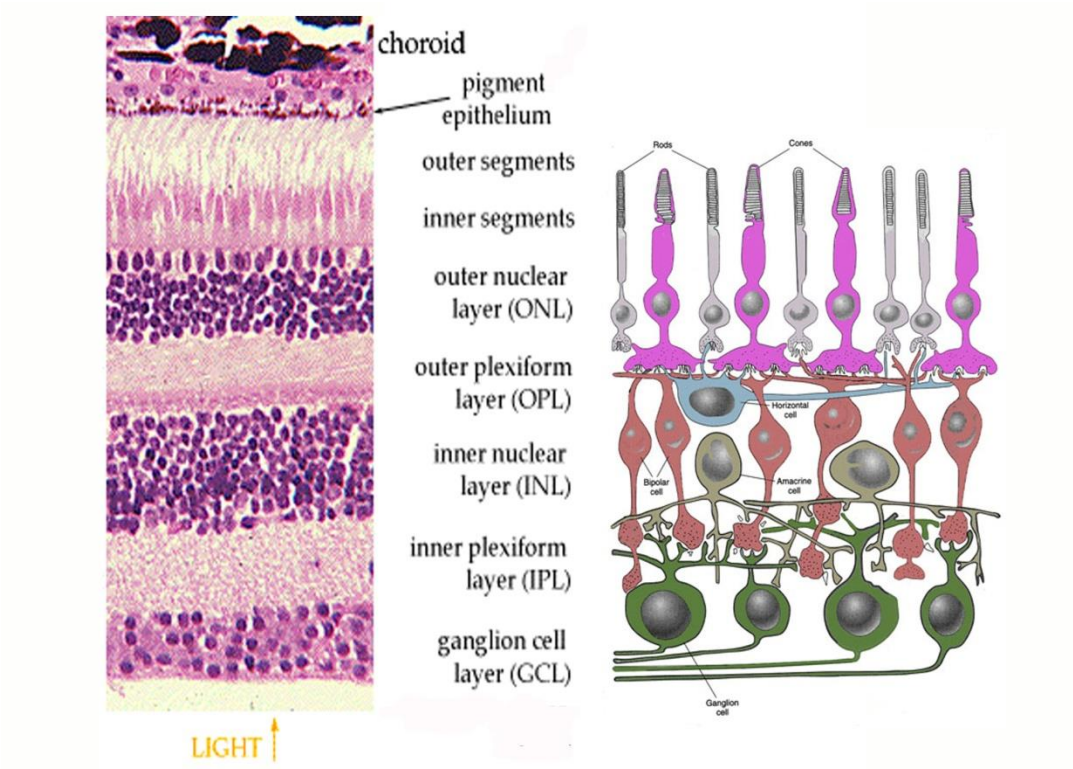

Figure 1.5. Depicting the inverted arrangement of different layers of retina. The light passes through all the retinal layers before it reaches the outer segment of the photoreceptors. (**Left**) Histological section with hematoxylin and eosin stain identifying the layers of retina. (**Right**) A schematic illustration of the interactions of neuronal cells in the retina (Sabeti, 2011). (Reproduced from Thesis by Faran Sabeti, Neuroscience, JCSMR, ANU)

Photoreceptors

The photoreceptors, rods and cones are named based on the morphology of their outer segments. Rods have rod-like outer segments while cones have conical ones, at least outside the fovea. The membranous disks containing the visual pigments in rods are like flattened sealed vesicles stacked within the outer segment, and the plasma membrane surrounds the disks and the cytoplasm. In contrast, the disks in cones have a single membrane which forms multiple invaginations that resemble disks but are not sealed and are continuous with the plasma membrane (Curcio *et al.*, 1990; Joselevitch, 2008; Gross, 2011) as shown in **Figure 1.6**.

10

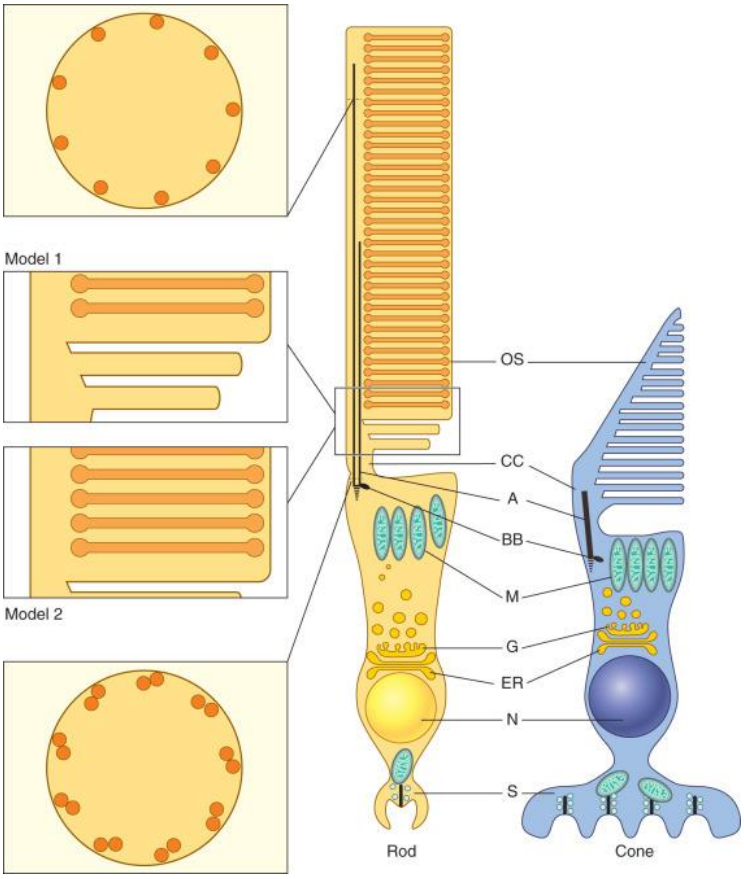

Figure. 1.6. The fundamental organization of vertebrate rod and cone photoreceptors. Parts of the cell include: OS, outer segment; A, axoneme; CC, connecting cilium; BB, basal body; M, mitochondria; G, Golgi apparatus; ER, endoplasmic reticulum; N, nucleus; S, synaptic terminal. Both rod and cone outer segments are connected to the inner segments via a connecting cilium. Membrane topologies of rods and cones are similar near the base, with both rods and cones showing disc-like membranes as invaginations of the plasma membrane. Along the outer segment axis moving from the inner segment towards the distal tips, the rod discs become sealed compartments, completely surrounded by, but distinct from the plasma membrane; whereas the cone disk and plasma membranes are continuous with the plasma membranes and their interior is continuous with the extracellular space. Insets depict the structure of the axoneme at the level of the OS where microtubule structure is 9x1+0(top), and where the IS and OS join the microtubule structure is 9x2+0 (bottom). Middle panels depict two models for OS disc formation. In model 1, OS disc originates from evaginations of the plasma membrane but become closed off and separate from the plasma membrane. In model 2, newly generated discs are already closed and separate from the plasma membrane. (Reproduced from Ryan's Retina: Chen J, Sampath AP. Structure and Function of Rod and cone Photoreceptors)

The kinds of photopigments and the regulation of intracellular reactions are different in rods and cones resulting differences in visual function. Rods are more sensitive to light than cones and enable our scotopic vision (Ebrey & Koutalos, 2001). Rods have limited ability to adapt to ambient light intensity while cones have the ability to shift the range to avoid saturation (Burkhardt, 1994). The rods and cones also differ in their sensitivity to lights of distinct

11

wavelengths. Human rods have maximal sensitivity at around 495 nm, whereas the cones are divided into three distinct types according to the wavelength of peak adsorption called *λmax.* First, the short wavelength-sensitive cones (S-cones) which have *λmax* of around 420 nm; second, the medium wavelength-sensitive cones (M-cones) which have *λmax* of around 530 nm and third, the long wavelength-sensitive cones (L-cones) which have *λmax* of around 560 nm (Dartnall *et al.*, 1983). This basic physiology of different cones with different peak absorptions helps us to perceive different colours.

Horizontal cells

Horizontal cells are interneurons that modulate the information flow from the photoreceptors to the bipolar cells in the outer plexiform layers (Müller & Peichl, 1993). These generate both positive and negative feedbacks at the photoreceptor-horizontal cell synapses. The cone neurotransmitter glutamate triggers a retrograde signal from the horizontal cells, which elevates the intracellular Ca^{2+} in the cones and enhances the release of neurotransmitters. The positive feedback synapse between horizontal cells and photoreceptors locally offsets the effect of negative feedback and boosts photoreceptor transmission, preserving signal strength in the visual system without sacrificing the contrast enhancement mediated by the horizontal cells (Jackman *et al.*, 2011).

Amacrine Cells

Amacrine cells mediate the lateral inhibitory interactions between the vertical excitatory channels composed of bipolar and retinal ganglion cells. They are synaptically active in the inner plexiform layer and the neurotransmitters associated in amacrine functions include GABA and glycine (Watanabe *et al.*, 2000). They integrate, modulate and interpose a temporal domain to the visual message presented to the ganglion cells (Kolb, 2007). More than 40 different morphological subtypes of Amacrine cells have been described based on the measurement of their dendritic field diameters and stratification of cells (Kolb, 2007).

Muller Cells & Vertical transmission of light

Muller cells are the predominant and modified glial cells of the vertebrate retina. They span the region from the internal limiting membrane to the external limiting membrane, giving support to the neural elements of the retina (Arevalo, 2006; Wang *et al.*, 2017). One Muller cell together with a specific number of rod photoreceptor cells, bipolar cells and a sub-set of amacrine cells form a *columnar unit* within the retinal tissue. Thus, the Muller cells, also

12

known as the radial glial cells, act as fibreoptic materials, whose processes wrap around the neuronal cell bodies, axonal and dendritic processes reducing light scatter (Joselevitch, 2008; Agte *et al.*, 2011). Muller cells also express functional insulin receptors and enzymes for glycogen metabolism. These are thought to be essential for rapid and effective retinal K^+ homeostasis due to presence of inwardly rectifying K^+ channels. This property imparts spatial buffering current, which greatly limits lateral spread of excitation beyond the borders of light-stimulated retinal columns, thus helps in maintaining visual acuity (Newman & Reichenbach, 1996; Wang *et al.*, 2005). They also produce retinal vascular endothelial growth factor, in high levels, especially in pathological conditions like diabetic retinopathy, to maintain the retinal homeostasis (Wang *et al.*, 2015). Muller cells and microglial cells feature prominently in responses to diseases and injury to the retina. Their mutual interactions appear to be a mode of bi-directional communications that help shape the overall injury response in the retina (Wang & Wong, 2014).

Retinal Circuitry

The retina is responsible for sensing the environmental light (and motion) and transforming it into electrical impulses that are sent to the brain where they are processed centrally and interpreted. It is an exceptionally approachable part of the brain, hence deciphering the retinal neural circuitry was one of the earliest triumphs of neuroscience (Cohen, 1988). The retinal sensory neuroepithelium phenotype, photoreceptors and bipolar cells are polarised with apical ciliary-dendritic and basal axonal-exocytotic poles. These cell types form the first stage of synaptic gain in the glutamatergic photoreceptors. The impulse signal passes forward from the photoreceptors to the bipolar cells and from the bipolar cells to the ganglion cells and ultimately to the CNS vertical chain (Dowling & Werblin, 1971; Marc, 2011). In vertebrate eyes, the images are projected onto an inverted retina where light passes through all the retinal layers before it reaches the outer segment of the photoreceptors that have the photopigments as shown in **Figure 1.5**. This makes the system very prone to light scattering and a potentially poor visual system, especially in the disease conditions. However, as explained above the Muller cells can act as fibreoptic materials reducing light scatter in thick retinas. This leads to an optimized signal-to-noise ratio, which increases visual acuity and contrast sensitivity (Joselevitch, 2008; Agte *et al.*, 2011). As the visual information gets conveyed from the retina to the visual cortex it is also transformed at each and every synapse in both plexiform layers. Some animals like the human there is a foveal pit where much of the neural machinery is swept to the side, obviating the need for fibre-optic Mueller cells. The

13

vertically permeated and laminated organization of the retina generates two streams of visual information (Fig. 1.5). First, the *vertical pathway*, from the photoreceptors to bipolar cells to ganglion cells; and second, the *lateral pathway*, comprising local feedback circuits from horizontal cells back to photoreceptors (Byzov, 1977; Joselevitch, 2008), and from amacrine cells back to bipolar cells (Kaneko, 1973; Kaneko & Tachibana, 1987; Joselevitch, 2008).

Membrane Potential

Every living cell has membrane potential as a result of differential accumulation of cations and anions on either side of the cell membrane. In the dark-adapted state the photoreceptors (rods and cones) have a resting membrane potential of about -40 mV, which means that there are more cations on the outside of the plasma membrane. The source of this membrane potential is generated by the Na^+/K^+-ATPase active pumps present in the plasma membrane of the outer segments of rods and cones. These pumps use the energy released by the hydrolysis of ATP to pump sodium ions out of the cells and potassium ions into the cell. However, there are other K^+ channels in the plasma membrane which allow the potassium ions to flow out of the cells passively along the concentration gradient. This results in net accumulation of positive charges outside and negative charge inside the cell membranes, thus generating the negative resting membrane potential (Gross, 2011; MacLeish & Makino, 2011). Most of the neurons in the central nervous system have resting membrane potential of about -70 mV but rods and cones have only about -40 mV, so these are said to be in a partially depolarised state. That is due to the presence of cGMP-gated cation channels in the plasma membrane of inner segments of the photoreceptors. This light sensitive channel allows all types of cations like Na^+, K^+ and $Ca^{2+,}$ but not anions, to pass through the plasma membrane resulting partially depolarised state of the photoreceptors. These cation channels are held open in the absence of light stimuli. A light stimulus causes the closure of these channels resulting hyperpolarisation of the cells. cGMP is produced continuously from GTP by enzyme *guanylate cyclase*, but on the other hand it is continuously broken down by another enzyme *phosphodiesterase*. The basal activities of these two enzymes maintain high concentration of cGMP, thereby cGMP-gated cation channels open in the darkness (MacLeish & Makino, 2011).

Graded Action Potentials

Action potentials are characteristics of spiking neurons and cells. The graded action potentials (GAP) are primarily generated by sensory input, causing a change in the

14

conductance of the membrane of the sensory receptor cells, such as photoreceptors. The spiking potentials are observed as an all-or-none phenomenon, while the characteristics of GAP depends on the size of the stimulus resulting the release of neurotransmitters at the synapses (Webb, 2017). The amplitude of GAP is proportional to the strength of the stimulus. Depending on the stimulus, graded potentials can be excitatory (depolarizing) as seen in the photoreceptor and bipolar vertical circuit (Miller & Schwartz, 1983), or inhibitory (hyperpolarizing) as seen in the Amacrine in the inner plexiform layer or horizontal cells in the outer plexiform layer (Watanabe *et al.*, 2000).

Phototransduction

Phototransduction is a cascade of biochemical reactions triggered by a light stimulus, which ultimately leads to the closure of cGMP-gated cation channels in the membrane of the photoreceptors and consequently causes voltage-dependent modulation of release of the neurotransmitter (glutamate). This results in change in the concentration of the glutamate in the outer plexiform layer, which is sensed by the glutamate receptors on the dendrites of bipolar and horizontal cells (Miller & Schwartz, 1983). G-protein-coupled receptors called *rhodopsin* in rods and *opsin* in cones are found inserted into the membranous discs of the outer segments of the photoreceptors. They contain the photosensitive chromophore called *11-cis-retinal*, which is inactive in the dark. When a photon is absorbed the photopigment changes its conformation activating rhodopsin in rods and opsin in cones, which in turn activate *transducin.* Each activated transducin activates a catalytic subunit of phosphodiesterase enhancing the breakdown of cGMP. Decreased concentration of cGMP cause closure of the cGMP-gated cation channels resulting membrane hyperpolarization (Leskov *et al.*, 2000). When the light stimulus ceases, or in darkness the concentration of cGMP regains its baseline level, the cGMP-gated cation channels reopen and the photoreceptors depolarize back to the resting membrane potential (Baylor, 1987).

Light-evoked hyperpolarization signals in rods and cones are transmitted to the second order retinal cells, the bipolar and the horizontal cells in the outer plexiform layer, which is the first synaptic layer of the retina. Here the signals are processed and modulated through a highly organized network of electrical and chemical synapses (Cohen, 1988). Horizontal cells send feedback signals to the photoreceptors and feed forward synaptic signals to the bipolar cells (Baylor *et al.*, 1971). The signals are then passed on to the second synaptic layer in the inner plexiform layer. Here the amacrine cells shape the bipolar cells signalling to retinal ganglion

15

cells, which are the third order retinal neuron cells. A variety of bipolar cell types form parallel signalling pathways that relay the processed photoreceptor signals to the inner plexiform layer. The synaptic interactions between bipolar cells, amacrine cells and ganglion cells in the inner plexiform layer produce complex processing of the visual signals. These interactions also process spatial, motion and directional information. The bipolar cells have been found to use kinate and AMPA (Alpha-amino-3-hydroxy-5-Methyl-4-isoxazole Propionic Acid) receptors to filter visual information into separate channels (DeVries, 2000). Finally, the processed signal outputs from the inner plexiform layer are transmitted to the retinal ganglion cells, which convey visual signals to the brain via the ganglion cell axon in the optic nerve.

1.2.2 Retinal Ganglion Cell Projections

The axons of the retinal ganglion cells form a compact layer called the *retinal nerve fibre layer* and establish a retinotopic orientation as these approach and converge the optic disc before passing through the lamina cribrosa, exiting the eye ball to form the optic nerve. The foveal fibres form the papillomacular bundle (PMB) as these approach the optic nerve head (ONH) and occupy a large proportion of the temporal aspect of the ONH. The fibres from retinal areas temporal to the fovea displaced themselves superiorly and inferiorly forming temporal retinal nerve fibre layer raphe as they approach the disc, forming superior arcuate fibres (SAF) and inferior arcuate fibres (IAF) bundles. Other fibres from the superior retina form superior retinal fibres (SRF) and those from inferior retina form inferior retinal fibres (IRF) and encroach onto the ONH. The fibres from the peripheral retina remain less organized (Vrabec, 1966; Ogden, 1983; Fitzgibbon & Taylor, 1996; Takayama *et al.*, 2012; Bedggood *et al.*, 2016; Bowling, 2016b) as shown in **Figure 1.7**.

16

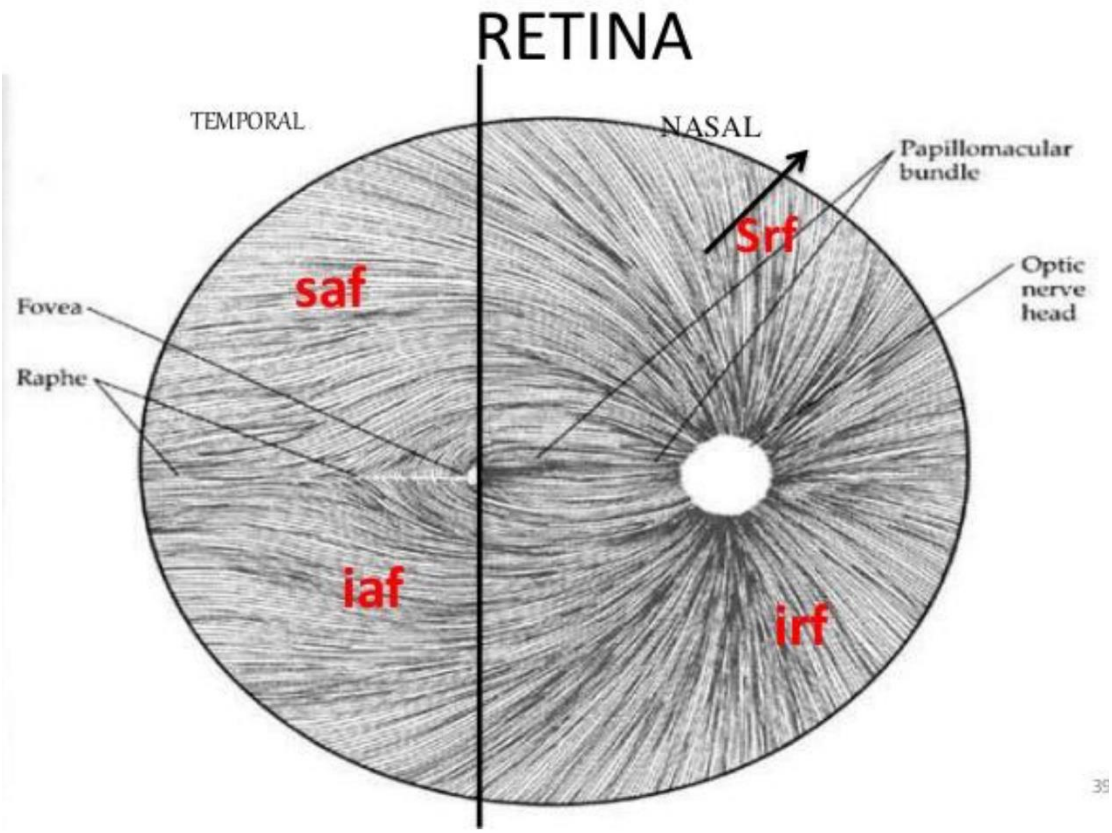

Figure 1.7. Schematic representation of the optic nerve fibres in the nerve fibre layer of the retina: The central retinal nerve fibres between the fovea and the optic nerve head forms the papillo-macular bundle. Fibres from the superior temporal quadrant temporal to fovea form SAF, from the inferior temporal quadrant form IAF, from the superior nasal quadrant form SRF and from the inferior nasal quadrant form IRF. Fibres from the peripheral retina are less organised. (Adapted from https://www.slideshare.net/nikhilprerna/visual-pathway-52468042)

There is systematic arrangement of nerve fibres as these converge to the optic disc. The fibres from the most peripheral retina maintain deeper position along the scleral side forming the outer most layer of the retinal nerve fibre layer, whereas the fibres originating from more central retina take more superficial or more vitreal in position. Thus, the longer and more peripheral nerve fibres lie deeper in the nerve fibre layer in comparison with the shorter fibres, which arise nearer the optic disc. This organization is maintained in the optic nerve head (Hayreh, 2011a, b) as shown in **Figure 1.8**.

At the peripapillary region the retinal nerve thickness shows a double hump pattern with thicker superiorly and inferiorly; and thinner temporally and nasally (Kaliner *et al.*, 2007). This characteristic may have diagnostic implications. The nerve fibres represent 90 percent of

17

the tissue of the optic nerve head, where these make right-angle turn and continue into the optic nerve (Walsh & Hoyt, 2008).

Optic Nerve

The optic nerve is the bundle of 0.8 -1.4 million axons of the retinal ganglion cells covered by sheath of astrocytes. The mean diameter of the axon is about 0.8 micron, which increases with age (Sanchez *et al.*, 1986; Mikelberg *et al.*, 1991; Bowling, 2016d). The length of optic nerve varies widely even between two eyes of the same person, measuring between 35 mm to 55 mm. It is divided into four parts: intraocular 1 mm, intraorbital 25 mm, intracanalicular 4-10 mm and intracranial part 10 mm. The common site of traumatic optic neuropathy is the junction between the mobile orbital and anchored intracanalicular parts (Duke-Elder, 1961; Hayreh, 2011b; Jeffrey, 2011). The retinotopic arrangement of the retinal nerve fibres are maintained in the optic nerve as well at least in the distal part of the optic nerve. However, these start scattering as they approach the optic chiasma. The prechiasmal visual pathway receives its blood supply from the ophthalmic artery and the internal carotid artery via the pial vessels (Pula & Yuen, 2017).

Optic Chiasma

In the optic chiasma the retinal nerve fibres decussate. The retinal nerve fibres from the ipsilateral temporal hemiretina pass onto the lateral horn of the optic chiasma forming the uncrossed axons and continue in the ipsilateral optic tract with crossed axons from the nasal hemiretina of the contralateral eye, whereas the fibres from the nasal hemiretina cross over to the contralateral optic tract where these bundle up with the uncrossed axons from the temporal hemiretina of the contralateral eye (Hoyt & Luis, 1962). The ratio of crossed to the uncrossed fibres is 53:47 in the optic chiasma (O'Connell, 1973). The optic chiasma receives its blood supply from the Circle of Willis (Pula & Yuen, 2017).

Optic Tract

The optic tract begins at the postero-lateral angle of the optic chiasma. After sweeping round the side of the cerebral peduncle, it divides into lateral and medial roots. The lateral root is larger and majority of its fibres terminate into lateral geniculate body, while some fibres reach pretectal region and superior colliculus (LeVere, 1978; Ahmed, 2011). The axons of the third generation retinal neurons end in the lateral geniculate body. It receives its blood supply

18

from anterior choroidal artery, which is a branch of internal carotid artery (Pula & Yuen, 2017).

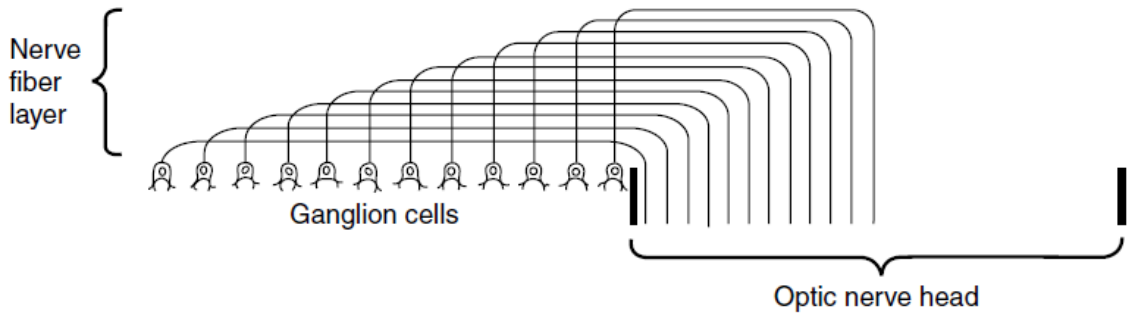

Figure 1.8. Schematic representation of arrangement of nerve fibres within the nerve fibre layer of the retina and the optic nerve head (Hayreh, 2011a).

1.2.3 Lateral Geniculate Nucleus

Lateral Geniculate Nucleus, located at the postero-lateral margin of the dorsal thalamus, is the gateway to the conscious visual perception. Conscious perception requires the visual information that passes through the dorsal lateral geniculate nucleus in primates. Although the retinal ganglion cell axons terminate in many sub-cortical nuclei, only the pathway from the retina to the LGN to cortex is critical to the visual awareness (Derrington, 2001; Casagrande, 2011; Ling *et al.*, 2015). The LGN first appears as a distinct structure along the dorsolateral wall of the diencephalon at around the 10th week of gestation. Rapid growth of th pulvinars displaces it laterally, caudally and ventrally to take the adult position (Hitchcock & Hickey, 1980). In the beginning the LGN appears as a homogeneous aggregation of cells. Anatomically, the axons from the two retina initially invade the LGN in an extensively over-lapped manner giving rise to functional binocularly innervated LGN neurons (Shatz & Kirkwood, 1984; Sretavan & Shatz, 1986). With further development eye-specific segregation and development of different layers of LGN achieved as seen in the adult anatomy. It is proven that action potentials and generation of spontaneous retinal activities are required for the eye-specific segregation and development of different laminae of the LGN (Penn *et al.*, 1998; Ballesteros *et al.*, 2005; Koch, 2011). Retinal activities, described as *retinal waves* are important for refinement of retinogeniculate projections. Stage I wave

19

consists of infrequent bursts of patterned activity which occur embryonically and are largely mediated by communication through gap junctions. Stage II waves are mediated by acetyl-choline release from starburst amacrine cells. The final stage of patterned spontaneous activity, stage III, is mediated by glutamatergic transmission from bipolar cells (Wong, 1999; Syed *et al.*, 2004; Firth *et al.*, 2005). With completion of the development the LGN takes as a six-layered asymmetrical cone with rounded apex. The LGN contains two principal *cell classes*. First, the *relay cells* that send axons to the visual cortex and *interneurons* whose axons remain within the LGN. Furthermore, based on the cell size the relay cells are categorized into three sub-types: large cells called magno or M cells, medium sized cells called parvo or P cells and very small cells called konio or K cells. The histological section of the LGN shows ventral two layers made up of M cells, so are called Magnocellular layers, whereas the dorsal four layers are made up of P cells so are called Parvocellular layers. K cells form lighter layers which lie below each parvocellular and magnocellular layer (Derrington, 2001; de Sousa *et al.*, 2013) **Figure 1.9**.

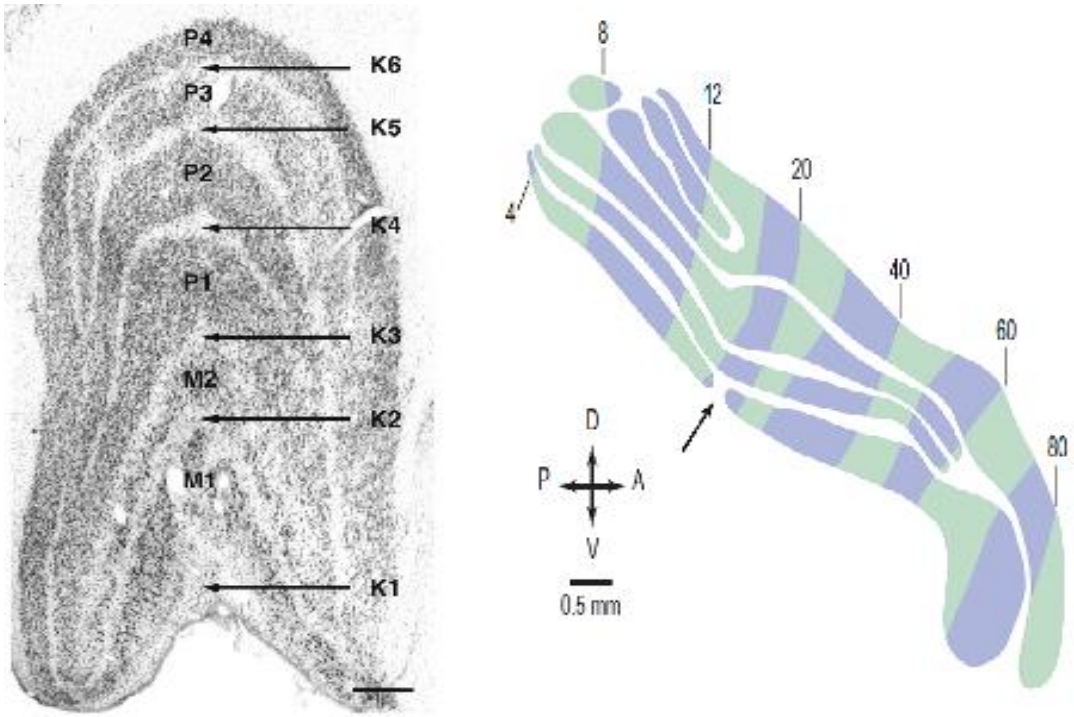

Figure 1.9. Lateral Geniculate Nucleus (LGN). (**Right)** A coronal Nissl (cell) stained section through LGN of a macaque monkey showing the parvocellular (P), magnocellular (M), and koniocellular (K) layers. At this cross-sectional level of the nucleus there are four P layers, two M layers, and six K layers. Scale bar = 500 um. **(Left)** A reconstructed parasagittal section through the LGN of a macaque monkey. Light and dark bands represent eccentricity hemizones that have been mapped onto the LGN layers. Numbers refer to the eccentricity at the border between two adjacent eccentric hemizones. The

20

gap in magnocellular layer 1 (M1) represents the optic disc (arrow). The cluster of arrows indicates anatomical orientation (D, dorsal; V, ventral; P, posterior; A, anterior). (Reproduced from Adler's Physiology of the Eye, 2011).

The rostral region represents the peripheral vision by only four layers due to fusion of the dorsal layers. The caudal region represents the central vision in its six layers. Crossed axonal fibres from the contralateral nasal retina converge into layers 1, 4 and 6, whereas the uncrossed fibres from the ipsilateral temporal retina converge into layers 2, 3 and 5 resulting in homonymous regions of the visual fields input into the adjacent laminae (Malpeli & Baker, 1975; Connolly & Van Essen, 1984).

The parvocellular layers are sensitive to colour vision and have high spatial resolution, whereas the magnocellular layers are more sensitive to the luminance contrast and have higher temporal resolution (Livingstone & Hubel, 1987).

The maps in each layer are retinotopically aligned such that each point in visual space is represented along a line perpendicular to the layers. The alignment of the maps is so precise that a cell-free gap representing the optic disc exists in all contralaterally innervated layers in order to maintain retinotopic alignment with the ipsilaterally innervated layers as the disc located in the nasal half of the retina does not contain photoreceptors (Derrington, 2001). (**Figure 1.9, left**)

The LGN receives *inputs or the afferents* from the retina with glutamate as neurotransmitter. Additionally, it receives inputs from a variety of visual and non-visual extraretinal sources, which also regulate the information flow in the LGN. Extraretinal visual input has been documented in the form of glutamate from the primary visual cortex as feedback mechanism, some extrastriate areas and superior colliculus; gamma-aminobutyric acid (GABA) from pretectum and the visual sector of the thalamic reticular nucleus; and acetylcholine from parabigeminal nucleus (Ichida & Casagrande, 2002; Casagrande *et al.*, 2005). Non-visual sources of extra-retinal inputs to LGN include cholinergic afferents from the pons and also contain nitric oxide; serotonergic input from the dorsal raphe nucleus; and histaminergic input from the hypothalamus (Morrison & Foote, 1986; Kayama *et al.*, 1989; Bickford *et al.*, 1993; Gastinger *et al.*, 1999).

The main *output or the efferents* from the LGN terminate within the primary visual cortex and the visual sector of the thalamic reticular nucleus. A smaller efferent projection, involving only about 1 percent of the LGN cells has been reported to terminate in several

21

extrastriate visual areas, the most well documented being the middle temporal area. These fibres have been implicated for the residual vision referred to as *blindsight* in patients who have lost their primary visual cortex (Morris *et al.*, 1999; Nassi & Callaway, 2006).

Similar to the retina, the LGN cells also have their receptive fields defined as ON or OFF centre with opposing surrounds. The majority of the optic tract axons innervating four parvocellular layers are red/green opponent colour units. The corresponding geniculate cells in these parvocellular layers are also mostly red/green units. The majority of the axons innervating, as well as the geniculate cells, in the layers 6 and 5 are on-center units; while those in layers 4 and 3 are off-center units. In brief, it is accepted that these mainly display center-only blue ON, yellow-OFF receptive fields (Michael, 1988). The LGN receives a dual blood supply from the anterior choroidal and lateral posterior choroidal artery, a branch of posterior cerebral artery (Pula & Yuen, 2017).

1.2.4 Optic Radiations

The efferent fibres those leave the LGN are bundled up as optic radiations, which is a sheet of white matter, innervating ipsilateral occipital lobe. The inferior fibres in the optic radiation representing the superior hemifield travel along the temporal horn of the lateral ventricle, forming *Meyers' loop*, projects to the temporal lobe. The inferior hemifield represented by the superior fibres, and central fibres travel more straight to the visual cortex through the white matter of the parietal lobe (Bron, 1997b). The corresponding retinal quadrants, visual fields and the visual pathway including Meyers' loop are explained with schematic diagram in **Figure 1.10**. However, newer studies have argued that this loop may also contain other fibre projections (Goga & Türe, 2015). The optic radiation receives blood supply from posterior and middle cerebral arteries and also from the anterior choroidal artery (Pula & Yuen, 2017).

22

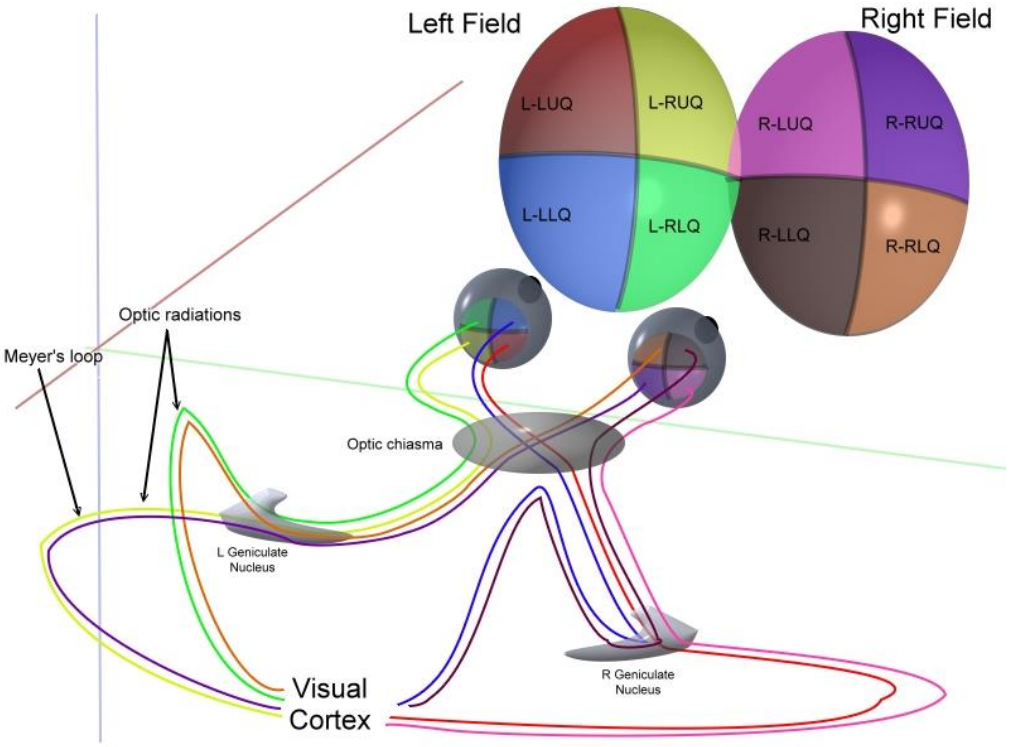

Figure 1.10. Schematic representation of optic radiations and Meyers' loop. The corresponding retinal quadrants, visual fields and the nerve fibres are shown in colour codes. Reproduced from Wikiwand (Wikiwand, 2018).

1.2.5 Visual Cortex

The visual cortex is anatomically located in the occipital lobe of cerebral cortex of the brain. It includes the primary visual cortex, also called as *striate cortex* and *extrastriate visual cortex*, which includes all visually responsive cortex other than the primary visual cortex (Allison *et al.*, 1994).

The cytoarchitecture of the brain mapping in terms of both the functional and pathological criteria was done by Korbinian Brodmann based on the regional differences in the distribution, density, shape, and size of the cell bodies (Amunts & Zilles, 2015). The primary visual cortex, designated as V1 area or Brodmann area 17 is on both upper and lower banks of the calcarine sulcus. This striate cortex, also known by the eponyms of the *stria or line of Gennari*, to honour the Italian medical student, Francesco Gennari who found striking white stripe on dissecting the visual cortex more than 200 years ago (Walters *et al.*, 2003). Immediately surrounding it is the Brodmann area 18, which is designated as V2 area and is the secondary visual cortex. Concentrically next to it lies the Brodmann area 19, designated as V3 area is the associative visual cortex. The left visual field is represented in the right

23

hemisphere of the visual cortex. The macula is represented in the posterior or caudal part of V1 area, and 60% of the V1 area is devoted to the central 10º of the visual field explaining that the lesions of the occipital pole result in a contralateral homonymous defect of the macular vision. (Daniel & Whitteridge, 1961). The periphery of the retina is represented in the anterior of V1 area. The upper hemifield is represented in cortical area below the calcarine sulcus, whereas the lower hemifield in areas above it (Dougherty *et al.*, 2003) as explained by the schematic diagram (**Figure 1.11**). The representation is asymmetric with more cortical areas devoted to the lower than to the upper visual fields. Much of the striate cortex shows anisotropic representation, in that the magnification factor depends upon the direction along which it is measured. Outside the fovea the magnification factor is proportional to the inverse of eccentricity in the visual field (Van Essen *et al.*, 1984).

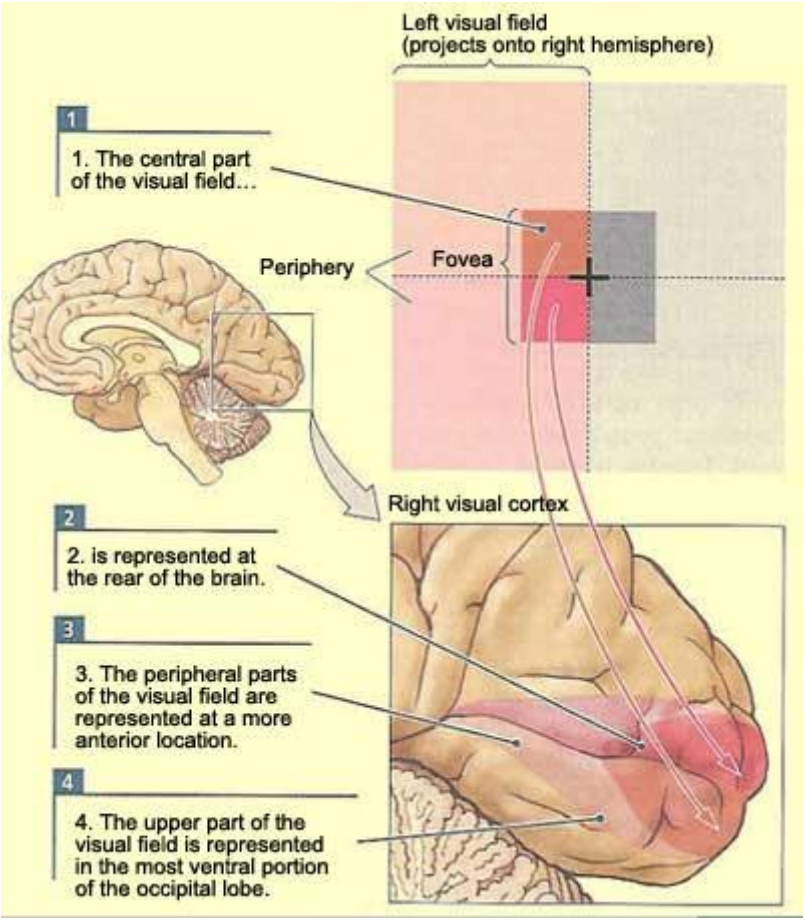

Figure 1.11. Schematic diagram with colour codes explaining the visual fields projection to the visual cortex. The left visual field is represented in the right visual cortex, central vision projects more caudal and the peripheral vision is represented anteriorly in the visual cortex. (Adapted from https://thebrain.mcgill.ca/flash/d/d_02/d_02_cr/d_02_cr_vis/d_02_cr_vis.html).

24

The cortex, including V1 and extrastriate cortex has six layers composed of mainly two types of cells, pyramidal and stellate in 80/20 proportion. Layer 1, the most superficial layer is non-neuronal, predominantly composed of connections between dendrites and axons. 80% of the neurons present in the layer are GABAergic. Approximately 20% of the neurons present in layers 2-6 are also GABAergic maintaining local feedback function within V1 circuits but do not project axons outside this area. Layers 2 and 3 are termed as *supragranular* layers that contain many excitatory neurons projecting their axons to the extrastriate cortical regions like V2, V3, V4, middle temporal, etc. Layer 4 termed as the *granular* layer has four sub-divisions, 4A, 4B, 4C alpha and 4C beta. The projections from magnocellular layers and parvocellular layers input to 4C alpha and 4C beta layers respectively. Layers 5 and 6 termed as *infragranular* layers contain many excitatory projection neurons that innervate LGN to provide feedback (Fitzpatrick *et al.*, 1987; Nie & Wong-Riley, 1999; Tehovnik & Slocum, 2003; Kolb, 2007).

Besides the inputs from the LGN, V1 also receives a variety of other modulatory inputs both from cortical and sub-cortical areas, like serotonergic and noradrenergic from brainstem and cholinergic inputs from basal forebrain nuclei. Other inputs are into layers 1 and 2 of V1 from the intralaminar nuclei of the thalamus and the pulvinar. V1 area also receives inputs from all other visual areas like V2, V3, V4, V5, middle temporal and parietal lobes. In short and practically, any area the V1 projects sends back the feedback projections to V1 (Walters *et al.*, 2003; Morgenstern *et al.*, 2016).

All layers of V1, except 4C, send output projections to other brain areas. The layer 6 cells provide direct feedback to the LGN and indirect inhibitory feedback to the LGN via axon collaterals to the thalamic reticular nucleus. The layer 5 provides major excitatory input to pulvinars nucleus of the thalamus, which in turn, provides inputs to a number of extrastriate areas that also provide feedback signals to V1. Layer 5 also projects to superior colliculus and other midbrain areas like pretectal and pons nuclei that are concerned with eye movements. The superficial layers of V1 projects to the extrastriate cortical areas, the largest connection being sent to V2 (Casagrande & Kaas, 1994; Walters *et al.*, 2003).

Organization of extrastriate visual areas:

The extrastriate areas receiving inputs directly from the primary visual cortex are classified as *lower tier* in the image processing hierarchy, such as V2, V3, middle temporal and parieto-occipital. The *higher tier ventral stream* areas are sensitive to object recognition include area

25

V4, posterior inferotemporal, central inferotemporal, anterior inferotemporal and temporal areas. The *higher tier dorsal stream* areas sensitive to motion and location of objects include medial and superior temporal areas, lateral intraparietal area, Brodmann area 7a, ventral intraparietal and anterior intraparietal areas (Allison *et al.*, 1994). Each unit area of the striate cortex receives equal number of LGN afferents and fovea has higher density of retinal ganglion cell in comparison to the peripheral retina (Wassle *et al.*, 1989, 1990).

The visual cortex receives its blood supply from the posterior cerebral artery as the terminal branches of the basilar artery (Pula & Yuen, 2017).

1.3 Pupillary System and Responses – Neural pathways and mechanisms

1.3.1 Pupil: Anatomy and function

In daylight the pupil is a 2-4 mm round opening situated in the centre of the iris diaphragm but slightly inferior and nasal to the centre of the cornea. The main functions of the pupil are to regulate the right amount of light entering the eye so that there is controlled retinal illumination, increasing depth of focus with miosis during near vision, and reducing both the chromatic and spherical aberrations. The size of the pupil is regulated by two intrinsic muscles, namely sphincter pupillae and dilator pupillae with the neuronal pathway. The sphincter pupillae is composed of a small group of 5-8 smooth muscle cells. It is situated in the posterior layer of the iris and just inside the pupillary margin. It measures about 0.75 mm wide and 0.15 mm thick. It is supplied by the parasympathetic fibres through short ciliary nerves. The dilator pupillae consists of radial smooth muscle situated in the mid periphery of the iris and just anterior to the pigmented epithelium. The muscle fibres, in 3-5 layers are oriented in a radial direction from the iris root towards the pupillary margin. It is supplied by the sympathetic fibres through the long ciliary nerves (Watson & Vijayan, 1995; Kardon, 2011).

The pupillary reactions are indirect but objective measure of the visual function. This is mainly regulated by a subcortical neural pathway, with some cortical inputs.

26

1.3.2 Sub-cortical pathways:

Anatomy

The afferent pathway of the pupillary system begins with the intrinsically photosensitive retinal ganglion cells (ipRGCs), which convey information via their axons through optic nerve, optic chiasma and until the later part of the optic tract, where the fibres deviate from the main visual pathway and continue along the brachium of the superior colliculus. These axonal fibres terminate in the pretectal olivary nucleus (PON) within the pretectal complex located in the dien-mesencephalic junction of the midbrain (Gamlin *et al.*, 2007; Distler & Hoffmann, 2009). The rostral extreme of it extends lateral to the third ventricle, just caudal to the posterior thalamus. Caudally, it extends in oblique plane and ends lateral to the rostral portions of the intermediate layers of the superior colliculus. It consists of nucleus of the optic tract (NOT), PON, medial, anterior and posterior pretectal nuclei. The pattern of retinal innervations to the pretectum determined by injecting ^{3}H-Proline into one eye found more on the contralateral than the ipsilateral nuclei in the ratio of 4:1 (Hutchins & Weber, 1985; Gamlin & Reiner, 1991; Clarke *et al.*, 2003). However, the previous studies have reported this ratio as 3:2 (Giolli & Tigges, 1970; Noback, 1975). From the PON the *internuncial* nerve fibres dissuade in the posterior commissure and directly project to both the contralateral and ipsilateral Edinger-Westphal Nucleus (EWN). This direct projections provide the anatomical pathway for the pupillary response (Benevento *et al.*, 1977; Berman, 1977; Kozicz *et al.*, 2011). In addition, there is a subset of afferent fibres from PON innervating lateral visceral cell column of Edinger-Westphal Complex, which are mainly contralateral (Buttner-Ennever *et al.*, 1996).

Melanopsin-containing ipRGCs have been described recently as the predominant origin of all the retinal input to the pupillary response. In primates the PON receives comparable input from ipRGCs and cortical structures (Gamlin *et al.*, 2007). In turn, the PON is the main source of input into the EWN and subsequently to the ciliary ganglion completing the parasympathetic reflex loop. Anatomically, the pupillary system receives significant input from the extra-striate cortex through the PON (Gamlin, 2006). More on cortical input is given at section 1.3.3 below. The strength of afferent signal transferred by the ipRGCs depends on the location of the luminance stimulus in the visual field corresponding to the retinal region. The density of ipRGCs range from 20-25 cells per mm square in the parafoveal retina to only 3-5 cells per mm square in the peripheral retina (Dacey *et al.*, 2005, Gamlin, 2007 #75).

27

The efferent fibres from the NOT innervate ipsilateral medial accessory nucleus of Bechterew, which is concerned with vestibular function. The NOT is associated with the generation of the optokinetic nystagmus (Berman, 1977).

EWN is classically defined as the oculomotor complex that is the source of the cholinergic, parasympathetic preganglionic motoneuron input to the ciliary ganglion through which it controls the pupillary constriction and accommodation (Warwick, 1954). However, some literature portrays the Edinger-Westphal as a complex perioculomotor nuclei, containing several functional cell groups, including papasympathetic preganglionic neurons to the ciliary ganglion, motoneurons of multiply innervated muscle fibres of extraocular muscles and urocortin-positive neurons that appear to play a role in eating and drinking behaviour and stress-related functions (Warwick, 1954; Horn *et al.*, 2008; May *et al.*, 2008a; Horn *et al.*, 2009).

The efferent pathway of the pupillary light reflex consists of fibres from the EWN. The fibres also travel in the medial most aspect to the *medial longitudinal fasciculus* and terminates in the dorsal accessory olive. The medial longitudinal fasciculus is a set of crossed fibres on each side of the brainstem, which links three main nerves which control eye movements: oculomotor, trochlear and abducent nerves, as well as the vestibulocochlear nerve (Loewy & Saper, 1978). The parasympathetic preganglionic nerves from the EWN emerge from the midbrain in the oculomotor nerve and run along and within it (May *et al.*, 2008b). These fibres pass through the oculomotor nerve, enter its inferior division and reach the ciliary ganglion via the nerve to the inferior oblique muscle. The ciliary ganglion is a small structure measuring 2 mm horizontally and 1 mm vertically, located within the muscle cone, just behind the globe. Although the ciliary ganglion serves as a conduit for other nerve fibres, only the parasympathetic fibres synapse here. Post-ganglionic parasympathetic nerve course along the short ciliary nerves to innervate the sphincter pupillae and the ciliary mucsles (Warwick, 1954; May, 2004). However, the ciliary ganglion is not always the gateway to the efferent arm of the pupillary reflex. Foerster showed (Foerster *et al.*, 1936) that ganglionectomy of ciliary ganglion produced a pupil not to react to light but did not prevent pupillary constriction in near reflex (Kuwayama *et al.*, 1987; Kuchiiwa *et al.*, 1989; Kuchiiwa, 1990; Kuchiiwa *et al.*, 1994). It has been found that an ectopic neurons in the communicating branch from the long ciliary nerve to the accessory ciliary ganglion bypassing the ciliary ganglion by way of the trigeminal nerve (Kuchiiwa *et al.*, 1993).

28

Sympathetic supply

Pupillary size is regulated by the interplay between the parasympathetic pupilloconstrictor reflex pathways described above, and sympathetic pupillodilator reflex pathways. The sympathetic efferent pathway is ipsilateral and has three neurons. The first order neurons, supranuclear arise from the posterior and lateral hypothalamus (diencephalon) and descends through the lateral tegmentum of the midbrain, pons and medulla to synapse on the intermediolateral cell column of the upper thoracic and cervical spinal cord, C8-T2 level, the region termed as the *ciliospinal centre of Budge*. Second order neurons are preganglionic axons arising from this region project to the sympathetic chain of ganglia and travel in the sympathetic trunk to reach the superior cervical ganglion and synapse there. Third order neurons are the postganglionic neurons arising from this ganglion, travel along the carotid plexus and enter the orbit and then into the eye via the short and long ciliary nerves, as well as through the optic canal. On entering the eye these nerves supply intrinsic smooth muscles like dilator pupillae, and Muller's muscles in the upper and lower tarsal plates in the eye lids (Greaves & Perkins, 1952; Reeves & Posner, 1969; Passatore & Pettorossi, 1976; Simons & Smith, 1994; Szabadi, 2013; McDougal & Gamlin, 2015).

On applying a noxious stimulus to the cervical region there is dilatation of the ipsilateral pupil. This finding is termed as the *Ciliospinal Reflex.* An interruption of this sympathetic nerve supply to the eye results in a clinical condition called *Horner's syndrome*, consisting of miosis, upside down ptosis, anhydrosis, enophthalmos and loss of ciliospinal reflex (Watson & Vijayan, 1995; Reede *et al.*, 2008; Kanagalingam & Miller, 2015). The co-existance of Horner's syndrome with heterochromia iridis is termed as Von Passow syndrome (Bhattacharyya, 2011). The EWN receives afferent projections from the reticular formation and other suprachiasmatic nuclei (Steiger & Büttner-Ennever, 1979).

1.3.3 Cortical input

As mentioned above the main input to the irides is from the PON, which receives afferent input from the retina as retinopretectal projections, and from the visual cortex (Gamlin, 2006; Sabeti *et al.*, 2017). Numerous studies have identified well-defined ipsilateral projections from both striate and extra-striate visual areas (Benevento *et al.*, 1977; Dineen & Hendrickson, 1983; Asanuma *et al.*, 1985; Distler & Hoffmann, 1989; Leichnetz, 1990;

29

Steele & Weller, 1993; Lui *et al.*, 1995). The PON also receives bilateral input from the LGN and intergeniculate leaflet, which contains luminance -sensitive neurons (see Melanopsin-containing ipRGCs below) which subserve visual and circadian systems (Harrington, 1997). The details of the non-retinal afferent connections of the PON is shown in **Figure 1.12**.

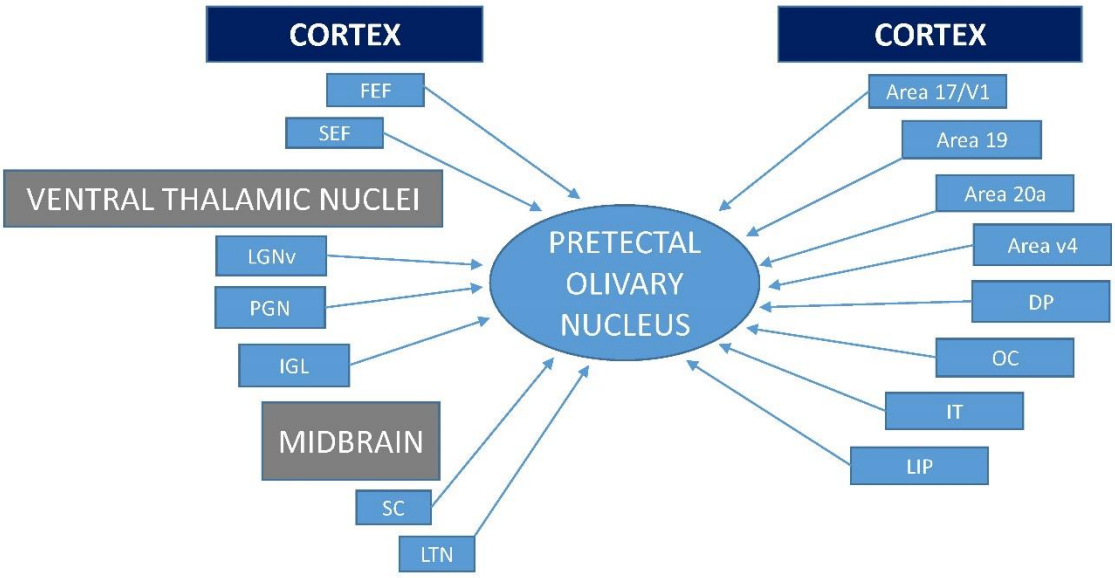

Figure 1.12 Non-retinal afferent connections of the pretectal olivary nucleus. (Reproduced and modified from Gamlin 2006 (Gamlin, 2006)).
DP: dorsal prelunate; FEF: frontal eye fields; IGL: intergeniculate leaflet; IT: inferior temporal cortex; LGNv: ventral lateral geniculate nucleus; LIP: lateral intraparietal region; LTN: lateral terminal nucleus; PGN: pregeniculate nucleus; POC: preoccipital cortex; SC: superior colliculus; SEF: supplementary eye fields.

1.3.4 Direct and consensual responses

As discussed previously, the decussation of nerve fibres of the pupillary light response occur at two levels: first at the level of optic chiasma, where the retinal ganglion cell axons from the nasal half of the retina cross over to the contralateral optic tract while the axons from the temporal half continue in the ipsilateral optic tract (Hoyt & Luis, 1962; O'Connell, 1973); secondly, each PON communicates through the internuncial fibres to both the ipsilateral and contralateral EWN (Benevento *et al.*, 1977; Berman, 1977; Kozicz *et al.*, 2011). The double decussation of afferent pupillary light reflex is the fundamental basis for direct and

30

consensual light reflexes. So both the pupils react even if only one eye is stimulated by light source.

The pupillary response controls the diameter of the pupil, in response to the intensity or luminance of light that falls on the retinal ganglion cells. To understand the pupillary responses to light stimulus first we must understand the terminologies. *Pupillary response* is conceptually linked to the side (right or left) of the reacting pupil, and not to the side from which light stimulation originates. For example, left pupillary response refers to the response of the left pupil to light regardless of which eye is exposed to a light source. In contrast, the term *direct* and *consensual* responses refer to the side where the light source comes from, relative to the side of the reacting pupil. For example, a direct pupillary response is pupillary response to light that enters the ipsilateral eye. A consensual pupillary response is response of a pupil to light that enters the contralateral eye. Thus there are four types of pupillary light responses: *Right direct pupillary response* is the right pupil reacting to light entering the right eye. *Right consensual pupillary response* is the response of left pupil to light entering the right eye. *Left direct pupillary response* is the response of left pupil to light entering the left eye. *Left consensual pupillary response* is the response of the right pupil to light entering the left eye (Smith *et al.*, 1979; Ellis, 1981; Naber *et al.*, 2011). Therefore, when one is subjected to a stimulus there are two recordable pupillary responses, and when both the eyes are subjected to a stimulus, four responses can be recorded simultaneously. The same principle is applied in multifocal pupillographic objective perimetry (mfPOP) which is the main equipment for the studies for this thesis.

1.4 Visual Field Testing and Perimetry

Accurately tested visual fields give clue to several eye, brain and neurological diseases. This is the most commonly used clinical diagnostic test procedure for evaluating the status of visual function in the diagnosis, management and prognostication of ocular and neurological diseases (Johnson, 2013). Examining the visual fields was, is and will remain an integral part of a comprehensive ophthalmic evaluation.

1.4.1 History and Evolution of Perimetry

Historically, the first recorded accounts of the peripheral visual field evaluation was from Hippocrates around late fifth century B.C., when he observed and described a hemianopia

31

(Lascaratos & Marketos, 1988; Johnson *et al.*, 2011). In 150 B.C., Ptolemy attempted to quantify the visual field and described that shape was roughly circular. Extramacular visual field testing was performed by Galen in 175 A.D. The first known illustration of the visual fields was published by Ulmas in 1602, and in 1668 Mariotte reported the physiological blind spot and related it to the optic disc (Lascaratos & Marketos, 1988; Johnson *et al.*, 2011). In the early nineteenth century Thomas Young reported the extent of the visual field in normal humans to be 50° radius superiorly, 70° radius inferiorly, 60° radius nasally and 90° radius temporally. Albrecht von Graefe is credited for being a pioneer in bringing perimetry and visual field testing to clinical ophthalmology (Johnson *et al.*, 2011).

Basically, visual field testing methods can be qualitative or quantitative. Qualitative methods were used early on, when the technique of visual field testing was picking up pace. The commonest qualitative method used was the **confrontation method**. The examiner and the patient sit face to face at about a meter apart, looking at the eyes of each other. Both of them cover one eye with the palm of hand. Assuming that the examiner has normal field of vision he moves his fingers or other objects from the far periphery to the central field slowly midway between the patient and the examiner and asking the patients when he detects the target. The procedure is repeated in different meridia and the other eye closed. The findings of the patient are compared with those of the examiner (Johnson *et al.*, 2011; Broadway, 2012).

The other qualitative method is the **Amsler Grid**. It is performed by placing the grid at a reading distance from the eye (30-33 cm) and the patient is asked to report on any missing or blurry part of the grid with each eye closed (Wall & May, 1987; Johnson *et al.*, 2011). The efficacy of the technique is good for diagnosing the central visual field defects (Greenberg *et al.*, 2012).

The **Tangent screen** technique, a quantitative method, was popularised initially by Jannik Bjerrum for detailed mapping of central 30° of visual fields, and later Harry Traquair further developed it and published a book describing its uses in diagnosing and evaluating a variety of ocular and neurological disorders (Traquair, 1927; Johnson *et al.*, 2011). The disadvantage of the tangent screen technique was that it measured only the central 30° of the visual field. In 1869 to overcome this limitation and provide a means of testing the full peripheral vision psychiatrist Hermann Rudloph Aubert and ophthalmologist Carl Friedrich Richard Foerster invented **Arc Perimete**r, which is commonly known as Foerster Perimeter (Johnson *et al.*,

32

2011; Strasburger *et al.*, 2011). This arc perimeter was effective in evaluating the full extent of the peripheral visual field but was not able to provide a consistent background illumination and adaptation. In 1945 and thereafter, Hans Goldmann made enormous contributions to the modern perimetry. He developed hemispheric bowl perimeter with uniform background illumination, performing both static and kinetic perimetry using targets of varying size, luminance and colour characteristics. Felicitating his noble work this perimeter was named as **Goldmann Perimeter** (Gloor, 2010; Johnson *et al.*, 2011).

The limitations of manual perimetry like inaccurate results resulting from errors from both the patient and the examiner lead to the curious search for automated perimetry (Fankhauser *et al.*, 1977). Many investigators worked towards developing automated perimeter, and Franz Fankhauser and his co-workers were undoubtedly the fore runners, who developed the *Octopus*, the first automated perimeter (Bebie *et al.*, 1976). Franz Fankhauser is honoured as the *Father of the Automated Perimeter* (Gloor, 2009). Anders Heijl and his colleagues have been instrumental in the development of the **Humphrey Field Analyzer**, including different types of visual field test and analytical methods (Heijl, 2012).

Subjective Perimetric methods

Standard Automated Perimetry (SAP): Automated perimetry has become the mainstream for the assessment of the functional visual loss and the progressive damage (Alencar & Medeiros, 2011). The principles of Goldmann Perimeter, devised in 1945 are still applied in the current SAP. The method uses white-on-white perimetry to measure the threshold at which a small bright white stimulus against a dim white background can be detected. The tests can be static or kinetic. In the *static perimetry* each stimulus is presented at predetermined locations with varying intensities of luminance and sizes until it is recognized by the patient. In *kinetic perimetry* a fixed stimulus is moved inward from the peripheral visual field until it is visible to the patient with their vision fixed in the field-centre. For the past several years, different test strategies and perimeters have been experimented and brought into clinical practices. The recent improvements with the Swedish Interactive Threshold Algorithm (SITA) strategy and the Guided Progression Analysis (GPA) have further made SAP as the preferred method of investigation of visual function (Alencar & Medeiros, 2011). SAP is usually performed with one of four similar threshold measuring tests, namely 30-2 or 24-2 SITA Standard™, or 30-2 or 24-2 SITA Fast™. SITA Standard offers very high accuracy and has relatively short test time of about four to eight minutes per

33

eye, depending on the test point pattern used. SITA Fast is a very fast threshold test taking only two to six minutes per eye with diagnostic sensitivity similar to that of full threshold test (Heijl, 2002).

Although the SAP remains the most commonly performed method of visual field assessment, clinical and histological studies have shown that in most cases the visual fields defects in SAP are detectable only when substantial amount of retinal ganglion cells (RGC) have been damaged (Quigley *et al.*, 1982; Quigley *et al.*, 1989; Quigley, 1999; White *et al.*, 2002; Anderson, 2006).

The perception of light is the function of almost all types of RGC. So even if a specific subset of RGC is affected in a particular retinal region it is not detected as other subsets of retinal cells are still functioning. However, specific functions like the detection of contrast sensitivity, motion-perception and colour vision are specific to different subsets of RGC. So isolating a single pathway or specific function, a deficit may be manifested even if a smaller proportion of cells are affected and can be mapped as visual field defects. Short Wavelength Automated Perimetry and Frequency Doubling Technology Perimetry have proven useful in cases where the visual field dysfunction is suspected and SAP is within normal limits. The techniques of new generation perimetry are based on this principle.

Short Wavelength Automated Perimetry (SWAP): It isolates the short-wavelength sensitive pathway and differs from the conventional perimetry for its narrow band of blue light stimulus on the yellow background illumination. The software has been installed in the Humphrey Field Analyzer and the latest version of it is based on the SITA strategy which reduces the test duration (Moss *et al.*, 1995). The total and pattern deviation plots, GHT and global indices should be interpreted in the same way as for the SAP. However, the grayscale map on SWAP printouts may be misleading because of the reduced visual perception of blue cones, resulting in a darker map even for normal subjects. It is proven with evidence that the SWAP is more sensitive than full-threshold SAP in detecting early functional deficits due to glaucoma (Adams *et al.*, 1982; Flammer & Drance, 1984; Hamill *et al.*, 1984). Longitudinal studies have shown that the SWAP can detect visual field defects 3-5 years earlier than the full-threshold SAP (Johnson *et al.*, 1993a, b; Sample *et al.*, 1993). Some of the limitations of SWAP are that the yellow colour of early cataracts acts as blue filter resulting in significant diffuse depression of sensitivity, and long duration of test time causing patient fatigue and discomfort (Sample *et al.*, 1994).

34

Frequency Doubling Technology (FDT) Perimetry: In 1991 Maddess presented data suggesting that the frequency doubling illusion might have special value for the diagnosis of glaucoma (Maddess, 1991a). Frequency-doubling illusion is an apparent doubling of spatial frequency when a sinusoidal grating pattern is presented at high temporal and low spatial frequency. It has been agreed that this illusion of frequency doubling phenomenon was mediated by a subset of magnocellular RGC (Maddess, 1991b). It is also suggested the origin of the response to be most likely cortical instead of magnocellular RGC (White *et al.*, 2002). The FDT Matrix by Carl Zeiss Meditec is the latest version of the technology. It performs with grating targets smaller than that used in the original FDT machine, to enable 24-2 and 30-2 test patterns, which look identical to those in SAP. It provides reliability indices similar like that in SAP, namely fixation loss, flase-positive and false-negative. The statistical analysis package provides the total and pattern deviation plots, GHT, and the global indices MD and PSD. FDT perimetry has high sensitivity and specificity in diagnosing the early visual field defects and its results are predictive of future onset and localization of functional loss when assessed by SAP (Medeiros *et al.*, 2004). Some prospective studies have proven that a patient with abnormal FDT test at baseline was three times more likely to develop SAP visual field defects than a patient with normal FDT findings (Landers *et al.*, 2003; Landers *et al.*, 2006). Other advantages of FDT perimetry are it is portable, easier to perform to both the operator and the patient, shorter test time, more resistant to blurring effects and is especially very helpful in patients who cannot perform SAP (Patel *et al.*, 2007).

High-pass Resolution Perimetry (HRP): HRP, or also known as *Ring Perimetry* aims to provide a patient- and user-friendly, full-threshold perimetric method. The test is best adapted to IBM personal computers with 17 inch black-and-white monitors. It utilizes fixed luminance and contrast with varying stimulus sizes to measure the threshold levels in very fine manner. The stimuli are arranged in ring fashion with boarders at 5 cd/m^2 darker, and the core at a 5 cd/m^2 brighter, than the background. This special arrangement effectively removes the low spatial frequency information creating *vanishing optotypes* so that the stimulus is not detectable at sizes below the acuity threshold levels (Wall *et al.*, 2004). It is thought that HRP findings are not direct indicators of RGC density or damage though it targets the sensitivity of high spatial frequency of the parvocellular pathway (Chauhan, 2000; Ennis & Johnson, 2002; McKendrick, 2005). HRP tests 50 locations per eye over an area extending up to 30° from the fixation, using staircase algorithm (Ennis & Johnson, 2002)**.** Advantages of HRP are the shorter test duration is only five to six minutes per eye, lower variability in the peripheral

35

visual fields, and is a suitable method for detection of early visual field loss (Kalaboukhova & Lindblom, 2003; Wall *et al.*, 2004). The limitations of HRP being its dependence on visual acuity results it being susceptible to interference from low visual acuity and media opacities; and large size stimuli it uses has given rise to suspicion over its ability to detect small scotomas (Delgado *et al.*, 2002).

Motion Automated Perimetry (MAP): While the central few degrees of visual field are important for perception of fine detail and colour, peripheral visual field is optimized for motion perception (McKee & Nakayama, 1984; Traschütz *et al.*, 2012). A motion detection perimetry measures a subject's ability to detect a coherent shift of position of dots (stimuli) in a circular area against a background of non-moving dots (Wall & Montgomery, 1995; Wall, 1997). The motion size threshold is the smallest detectable circular area in which the subject can detect motion. Subjects responds by touching a computer screen with a light pen where they detect motion stimuli. Their localization errors indicated as the number of pixels from the target centre and the reaction times are calculated (Wall, 1997). It has been found very sensitive and specific to localize early visual field defects in glaucoma (Wall & Ketoff, 1995), idiopathic intracranial hypertension (Wall, 1995a), and optic disc edema and cotton wool spots (Wall, 1995b). Motion Automated Perimetry has a reported sensitivity of 96% and specificity of 87% for identified glaucoma subjects (Bosworth *et al.*, 1997). Although it has high accuracy in detecting early visual field defects, its long test duration of fifteen minutes may impose limitations to the clinical usefulness of this perimetric method.

Moorfields Motion-Displacement Test (MDT): It has been developed as a perimetric method for the early diagnosis of glaucoma. The original MDT was presented as a single vertical-line stimulus and has been shown by several studies to have higher sensitivity than the SAP in detecting early visual field defects secondary to glaucoma (Ruben & Fitzke, 1994; Baez *et al.*, 1995). MDT determines the smallest perceptible positional displacement giving rise to the sensation of motion. Each stimulus presentation passes through three displacement cycles at 5 Hz (Verdon-Roe *et al.*, 2006). It has been shown to be more resistant to the effect of cataract than both SAP and FDT perimetry (Membrey, 2000). It is portable, being performed on a laptop computer, easy to perform, more robust against media opacities and has high accuracy. Atop, it is advantaged with short duration of test time ranging from 1.3 to 3.2 minutes per eye. With these advantages the MDT may accomplish as a convenient perimetric method fir the screening of large population (Ong *et al.*).

36

Rarebit Perimetry (RBP): It is also known as microdot perimetry is a new perimetric method developed by Frisen in 2002, is designed to detect subtle visual field damage (Frisen, 2002). Instead of measuring threshold for light sensitivity, it uses spatially and temporally minute test stimuli called *microdots* or *rare bits* to avoid simultaneous stimulation of numerous retinal receptive fields, which tend to cause underestimation of the visual field defects. It uses a regular computer LCD monitor to present stimuli against a dark background. The stimuli presented as small dots and the patient has to indicate whether one or two dots were observed for each presentation. Rarebit perimetry has shown promising preliminary results in the early detection of visual field defects in cases of neurologic disorders (Frisen, 2002, 2003) and glaucoma (Brusini *et al.*, 2005). Some of the advantages of Rarebit perimetry are simple, rapid and inexpensive besides its ability to detect subtle visual field deficit (Salvetat *et al.*, 2007).

Microperimetry: Microperimetry, also known as fundus-controlled perimetry, is an increasingly utilized form of static automated perimetry that tracks the fundal landmarks to correct rapidly for shifts in gaze and enables manual centration of testing grid at the anatomic fovea (Wong *et al.*, 2017). It is implemented for simultaneous observation of the fundus and correction for eye movements during perimetric examination (Springer *et al.*, 2005). It is considered superior to SAP for residual visual functional assessment. It accurately determines the location of a Preferred Retinal Location (PRL), and fixation stability estimates in low vision cases are reliable predictors of visual acuity estimates (Markowitz & Reyes, 2013). The earliest microperimeter invented was the scanning laser ophthalmoscope (SLO) microperimeter (SLO101) (Rodenstock, Munich, Germany) (Mainster *et al.*, 1982). The Nidek MP-1 microperimter (Nidek Technologies, Padova, Italy) followed. It uses a Liquid Crystal Display (LCD) to present the stimuli, and simultaneous SLO scans for fundus examination, and a fundus camera to capture fundus images and automated real-time fundus tracking (Chen *et al.*, 2009; Wong *et al.*, 2017). OPKO/OTI (OPKO Instrumentaion, Miami, FL) subsequently introduced the spectral optical coherence tomography SLO, which offers the advantage of correlating functional deficits with SLO infrared images and also bi-dimensional cross-sectional OCT retinal images (Wong *et al.*, 2017). Nidek MP-3 is newer version with wider range of stimulus intensity (0 to 34 dB) and provides better test-retest reproducibility (Palkovits *et al.*, 2018). CenterVue Macular Integrity Assessment (MAIA) (CenterVue, Padova, Italy) is a recent development (Wong *et al.*, 2017) and is quite similar to the Nidek.

37

Limitations of subjective perimetry

The limitations of the subjective tests are well known. Elderly people not only find difficulty in understanding and performing subjective perimetric methods, but also find equally stressful. A study conducted on the performance of gold standard perimeter, HFA SITA full-threshold, the specificity in normal subjects was only 38% at the first test and 73.7% after two tests (Schimiti *et al.*, 2002). So there is a learning curve associated with the subjective perimetry that complicates the interpretation in new patients, such that two to three field tests need to be done before a reliable result is achieved. Therefore, any objective functional information is useful, particularly among those who are poor performers in the subjective perimetry (Shaarawy, 2009). SAP also has huge test-retest variability partly due to undersampling caused by relative influence of fixation and variation in sensitivity across a visual field faster than the Nyquist for the standard sampling interval of 6°. High test-retest variability interferes with the ability to track visual field progression and is common to all variants of SAP (Maddess, 2014; Pearce & Maddess, 2016). Another limitation is that the different perimeters have been shown to produce quite nonlinearly related data (Wall *et al.*, 2010; Fredette *et al.*, 2015). SAP visual fields contain a mixture of locations with normal values, non-seeing locations, and locations with mildly or moderately reduced sensitivity values ranging from 0 to 43 dB. The Matrix is provided with only 15 discrete values unevenly distributed between 0 and 38 dB, thus creating an uneven distribution of values (Fredette *et al.*, 2015). To overcome this problem and find the main trend in the data researchers have used the principal curve analysis (**Figure 1.13**) (Wall *et al.*, 2010; Fredette *et al.*, 2015). The starting point of the curve is defined by the first principal component of a cloud of points and the algorithm pushes the points onto a trajectory the middle of the data so that it has the same number of points on either side of the principle curve (Hastie & Stuetzle,

38

1989).

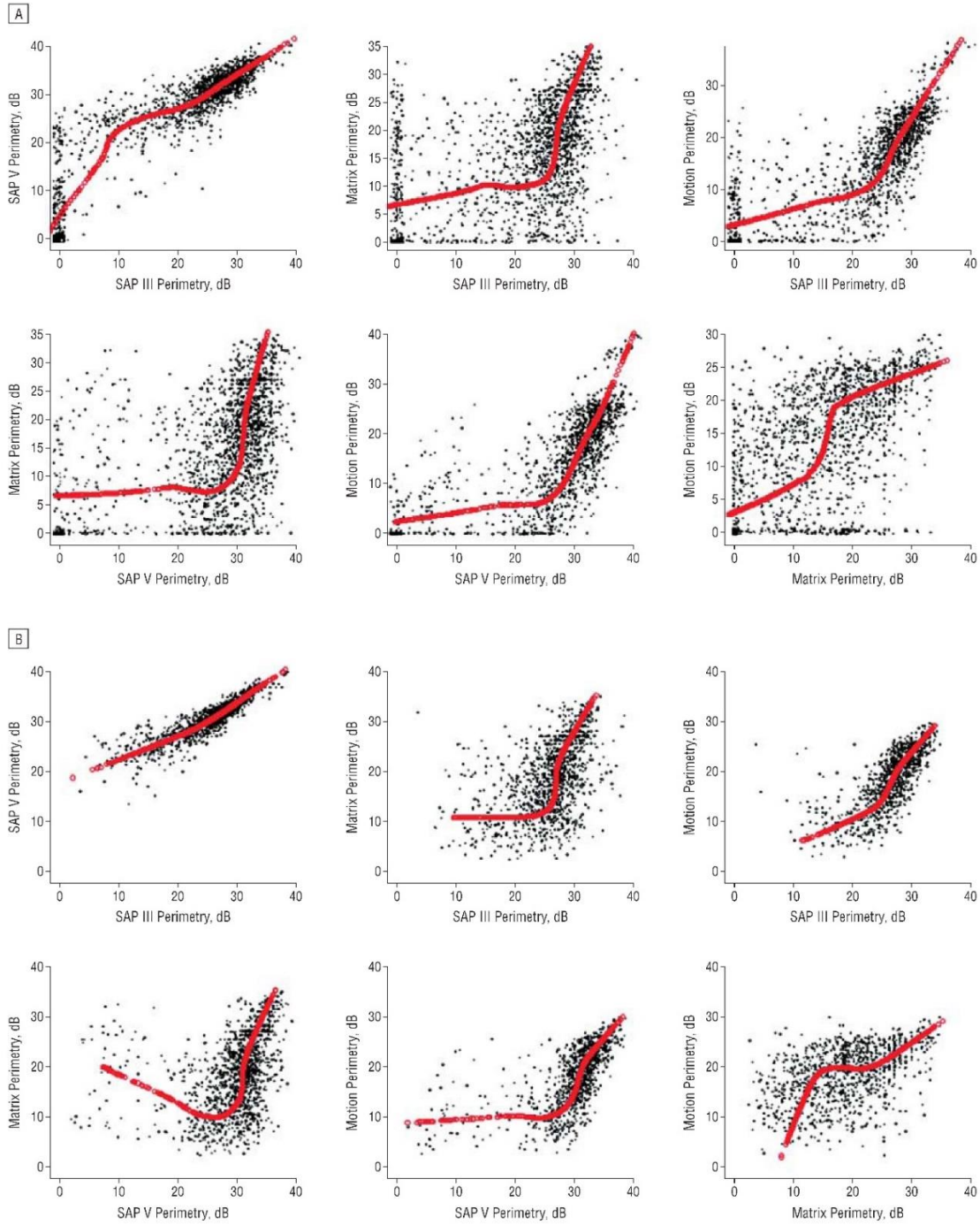

Figure 1.13. Scatter plots with principal curves (red) to compare the effective dynamic range of different perimeters. Glaucomatous patients were retested 5 times and mean thresholds plotted one test against another. (**A**) The data graphed with the 0 dB trials included. (**B**) Data with the floor effect of 0 dB thresholds removed. Matrix and Motion perimetry have similar effective dynamic ranges and the Goldmann size V has a greater dynamic range than SAP size III by about 1 log unit. Reproduced from (Wall *et al.*, 2010).

The quest and search for better or ideal perimeter has put main emphases towards the development of procedures to improve accuracy, enhance efficiency, provide comfort to both

39

the patient and the examiner, obtain informative clinical diagnostic tools for detection, differentiating different clinic-pathological conditions and provide repeatability and reproduce comparable data for follow up of the patients.

Objective Perimetric Methods

Electroretinogram: The electroretinogram (ERG) is an electrophysiological test, which records a diffuse electrical response developed by cells within the retina. This response is an algebraic summation of several component waves or impulses occurring as a result of light-induced transmembrane movement of cations and anions. The recording is made between an active electrode either in contact with the cornea or a skin electrode placed just below the lower eyelid margin, and a reference electrode placed on the forehead. The potential between the two electrodes is then amplified and displayed. Historically, Dewar recorded it for the first time in humans in 1877. The majority of investigations were limited to animals until 1941, when Riggs developed a recording electrode that was compatible for human use (Fishman, 1985).

The resting membrane potential, mechanism of impulse generation and photochemical cascade have been described above.

A light-induced closure of cGMP-gated channels decreases the inward sodium conductance across the plasma membrane resulting hyperpolarization. This negative change in intracellular electrical potential generated is measured clinically as the corneal-negative *a-wave* (photoreceptor driven) of the ERG. The hyperpolarization of photoreceptors diminishes the release of neurotransmitters at the synaptic terminals of the photoreceptors, which in turn causes depolarization of post-synaptic bipolar and horizontal cells. Subsequently, change in the extracellular potassium is sensed by the Muller cells. This resulting electrical response of the Muller cells generates corneal-positive *b-wave* (Muller & bipolar cells driven) of the clinical ERG (Kline, 1978). Although it is generated from Muller and bipolar cells, it is directly dependent on functional photoreceptors and its magnitude is an indirect and convenient measure of photoreceptor integrity. It has two subcomponents, b-1, probably represents both rod and cone activity, and b-2 mainly cone activity. This subcomponent activities are applied for distinguishing rod or cone responses with appropriate techniques (Bowling, 2016c). The change in the extracellular potassium also alters the resting membrane potentials of the retinal pigment epithelium. Secondarily, this cause transient alteration in the

40

potential and electrical changes within the Muller cells, inducing monophasic corneal-positive deflection that follows the b-wave, referred to as the *c-wave* of the clinical ERG (Steinberg *et al.*, 1970; Perlman). Oscillatory potentials occur as wavelets on the ascending limb of b-wave are generated by cells in the inner retina.

Full-field ERG: An International Society for Clinical Electrophysiology of Vision (ISCEV) standard full-field (also known as Ganzfeld, meaning *whole field* in German) ERG consists of five types of recordings taken during diffuse stimulation of the entire retina (Marmor *et al.*, 2009). It is useful to assess the generalized retinal disorders but may not detect localized pathology. The *scotopic ERG* is performed after 30 minutes of dark adaptation. It consists of rod responses elicited with a very dim flash of white or blue light, resulting a large b-wave and a small or non-recordable a-wave. Combined rod and cone responses are elicited with a very bright white flash, resulting prominent a- and b-waves. Oscillatory potentials are the third recordings in the scotopic ERG and is elicited by a bright flash of light and changing the recording parameters. The *photopic ERG* is conducted after 10 minutes of adaptation in moderately bright diffuse illumination. Cone responses are elicited with a single bright flash, resulting a- and b-waves with subsequent small oscillations. Cone flicker isolates the response of cones only and is elicited by using flickering light stimulus at a frequency of 30 Hz to which rods cannot respond (Marmor & Zrenner, 1998; Gjörloff *et al.*, 2004; Bowling, 2016c).

The limitations of traditional full-field ERG are that the stimulation response consists of unequal contributions from different areas of the retina with differing cell densities (Sutter & Tran, 1992), and lack of sensitivity in diagnosing diseases. ERG reports are reported to be normal unless more than 20% of the retina is affected (Creel, 2011). The limitations of full-field ERG inspired the search, experiments and invention of multifocal ERG.

Multifocal ERG (mfERG): Erich Sutter adapted the mathematical sequences called the binary m-sequences enabling isolation of an electroretinogram representing less than each square millimetres of retina, from a single electrical signal in response to a visual stimulus. mfERG programs measure electrical activity from more than a hundred retinal areas per eye within a few seconds. The enhanced spatial resolution enables scotomas and retinal dysfunction to be mapped and quantified (Sutter, 2010).The key feature of the modulation sequences used for the multifocal methods is that the sequences driving different test regions should be minimally and mutually correlated in time (Lee & Schetzen, 1965). There are different types of recording electrodes and the stimulus patterns. The parameters recorded are

41

amplitudes of waves, latency and implicit time. It is recommended that all the recording procedures and equipment used must follow the ISCEV guidelines (Hood *et al.*, 2008; Hood *et al.*, 2012a). **Figure 1.14** shows a normal mfERG.

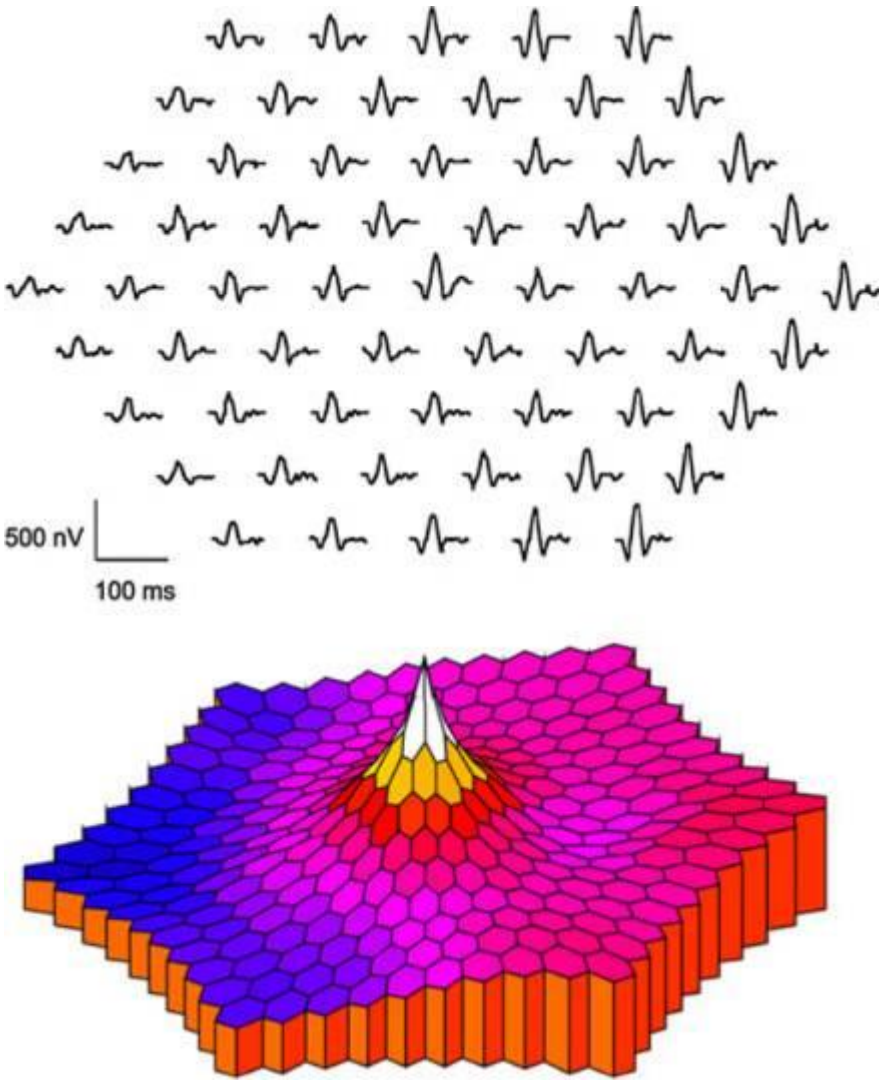

Figure 1.14. Sample of mfERG plotting with hill of vision. (Reproduced from ISCEV standard for clinical mfERG, 2011edition (Hood *et al.*, 2012b).

mfERG has been well tested and standardized by comparing with other methods of diagnostic procedures like optical coherence tomography (Birch *et al.*, 2010; Dale *et al.*, 2010). Several studies have found mf ERG very sensitive in detecting the field defects in various types of retinal diseases and disorders like retinitis pigmentosa (Dolan *et al.*, 2002; Chang *et al.*, 2011), retinal toxicity due to chloroquine and hydroxychloroquine (Lai *et al.*, 2005; Michaelides *et al.*, 2011), age-related macular degenerations (Feigl *et al.*, 2005), glaucoma

42

(Miguel-Jimenez *et al.*, 2011), birdshot retinochoroidopathy (Birch *et al.*, 2010), retinal diseases affecting photoreceptors (Greenstein *et al.*, 2004), and other retinal abnormalities (Dale *et al.*, 2010). In infants the amplitudes were significantly smaller and implicit time was significantly longer than in adults. This fact is explained by the immaturities of processing in the central retina. Infant-adult differences in the distribution of cones and bipolar calls may account for the results (Hansen *et al.*, 2009). However, some studies have reported that even mfERG has failed to reliably detect local ganglion cell damage (Hood & Greenstein, 2003; Hood, 2003).

Physiologic experiments and exploitations of clinical conditions have provided compelling evidence that retinal ganglion cells and other inner retinal structures generate the PERG (Berninger & Arden, 1988; Porciatti, 2007; Bode *et al.*, 2011). The stimulus used is a achromatic grating or checkerboard pattern, in which the bright and the dark regions reverse. PERG has a major clinical role in examining localized retinal pathology and subtle optic neuropathy. In glaucoma the amplitudes were reported to be reduced before the scotoma was detectable. It is very useful to understand the pathophysiology of various retinal and neural diseases (Berninger & Arden, 1988). Focal or foveal ERG, is used to assess the macular disease.

Visual Evoked Potential (VEP): Visual or visually evoked potential, visual evoked response (VER) or visually evoked cortical potential (VECP) are used interchangeably. These are the electrical potentials initiated by a brief visual stimulus, recorded from the scalp overlying the visual cortex. These primarily measure the functional integrity of the visual pathway, extending from retina via optic nerve to the visual cortex. The VEP waveforms are extracted from the electro-encephalogram by signal-averaging, adding the electrical for set time period (Creel, 2015). An array of electrodes are used for recording the potentials with different arrangements of placement of electrodes on the scalp, like the *10-20 International system* (Jasper, 1958), or the *Queen Square System* (Blumhardt *et al.*, 1977). The reference electrode is place on the earlobe, on the midline on the top of the head or on the forehead. The ground electrode is placed on the earlobe, mastoid process, or on the scalp. Commonly used stimuli are strobe flash, flashing light-emitting diodes (LEDs), transient and steady state pattern reversal and pattern onset/offset (Odom *et al.*, 2010). However, the most commonly used stimulus is the checkerboard pattern, which reverses every half a second. The most preferred stimulus is the pattern reversal stimulus because it has less inter-subject VEP variability than

43

with flash or pattern onset stimuli. Video monitors or CRT displays are used to display the stimuli (Creel, 2015). **Figure 1.15** shows the typical recording of VEP in a normal subject.

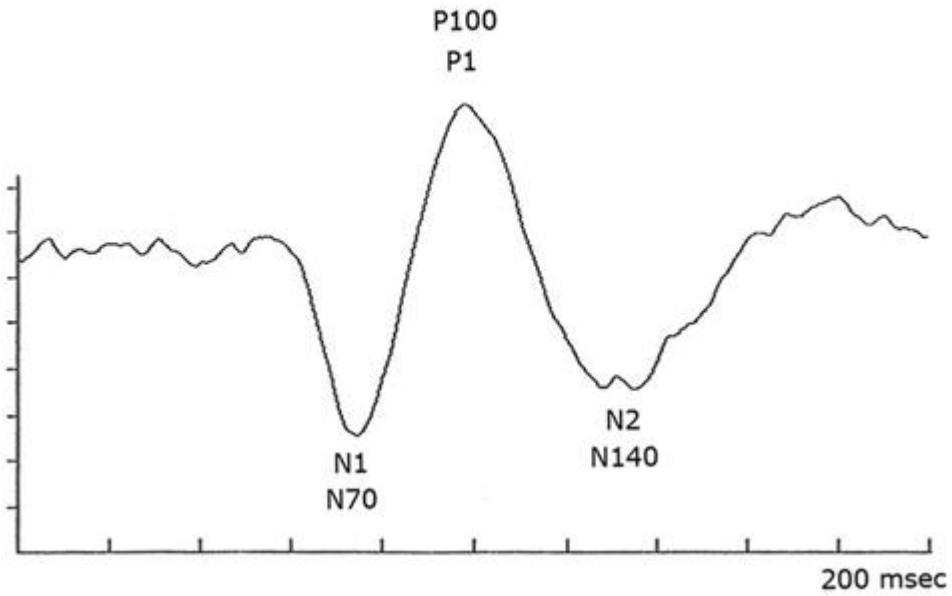

Figure 1.15. Representative normal pattern reversal VEP recorded from mid-occipital scalp using 50' checkerboard pattern stimuli. It shows a prominent negative component at a peak time of about 70 millisecond (N1), a larger amplitude positive component at 100 millisecond P1), and a more variable component at about 140 millisecond (N2). Adapted from Webvision – The organization of the retina and visual system (Creel, 2015).

Since its inception in 1930s there has been different modifications and improvements in the experimental and clinical use of VEP in various diseases (Clark & Hillyard, 1996; Di Russo *et al.*, 2002), including its comparison and combination with psychological tests in glaucoma (Abdullah *et al.*, 2014). Traditional VEPs evaluate the optic nerves and the central visual pathways as a whole. However, often the small or localised pathway dysfunction is not detected.

Multifocal VEP (mfVEP): An important development in the VEP is the introduction of multifocal VEP. Using mfVEP one can isolate smaller dysfunctional areas using hundreds of stimulations presented in the same amount of time that it would take to record a single whole VEP with traditional methods (Klistorner *et al.*, 1998). It can use the same binary m-sequences modulation as explained in mfERG (Sutter, 2010). The mf VEP is primarily generated in the V1 or striate cortex with some contribution from the extrastriate cortex (Slotnick *et al.*, 1999; Fortune & Hood, 2003; James, 2003a; Ruseckaite *et al.*, 2005). The

44

common stimulus display for the mfVEP is the dartboard or checkerboard pattern although there are different modifications to this (Goldberg *et al.*, 2002). The dartboard pattern is displayed on a monitor viewed at a distance of 32 cm and the diameter subtending an angle of 44.5^{o}. The display is cortically scaled and has 60 sectors, each sector containing 16 checks, 8 black and 8 white (Baseler *et al.*, 1994). The placement of electrodes varies. In single-channel recording, also known as bipolar recording as done in typical mfVEP, two electrodes are placed in the midline over the clacarine fissure, and third ground electrode is placed on the forehead or he earlobe. In multi-channel recording additional electrodes are placed lateral to the inion because this has been reported to improve the signal in the regions (Graham *et al.*, 2000). However, the multi-channel recording has received criticism stating that it needs developing techniques for combining the information from different channels and it is time-consuming (Hood *et al.*, 2002). The amplitudes and the waveforms are compared. The mfVEPs recorded from monocular stimulation of each eye are essentially identical for normal subjects with midline placement of electrodes. However, small amplitude asymmetry and interocular latency difference of about 4 to 5 milliseconds are found normally across the midline. Similarly, variations in the amplitude and waveform can be seen across individuals due to location of the clacarine fissure relative to the external electrodes and the differences in the local folding of the primary visual cortex (Brindley, 1972; Rademacher *et al.*, 1993). As pointed out above that automated achromatic perimetry, generally accepted as the gold standard perimetry for detecting ganglion cell damage failed to detect early or subtle visual field defects and has some limitations (described under SAP section), and mfERG failed to reliably detect local ganglion cell damage (described under mfERG section) mfVEP has been proposed as a reliable objective solution to these problems (Klistorner *et al.*; Fortune & Hood, 2003; Hood & Greenstein, 2003). mfVEP have been proposed for evaluating the asymmetry of visual function between eyes, however that should only be done if the two eyes are recorded and tested at the same time. It has been reported to correctly identify patients with glaucomatous visual field loss and shows abnormalities in many patients considered at high risk for glaucoma who still have normal visual fields, thereby identifying the early visual field loss objectively before the subjective field loss occurs (Graham *et al.*, 2000). The divided attention and ongoing mental processes did not affect the mfVEP proving it a robust objective measure of visual field function that may be useful for some patients with unreliable perimetry results (Seiple *et al.*, 2005).

45

Steady-state Multifocal Evoked Potential (ssmfVEP): Maddess et al. suggested employing steady-state stimuli rather than usual m-sequence stimuli may simplify statistical evaluation and reduce test time. It was also shown that different viewing distances could be used to detect central and peripheral visual defects without a change in SNR (Rosli *et al.*, 2009; Abdullah *et al.*, 2012). These methods were developed form the similar mfERG methods (Maddess *et al.*, 2000a, b).

1.4.4 Infrared Pupillography: Investigators have used various responses of the eyes to determine many things, from interest in sexual feelings to the relative degree of processing occurring in the brain (Stem, 2000). The pupillary reactions have been studied for centuries. Their application in physiological research as indicators of autonomic nervous activity dates back to the 18th century, and the interest of physicians still much earlier (Lowenstein & Loewenfeld, 1958). Otto Lowenstein, a German-American neuropsychiatrist, was a pioneer in the study of pupil function and later he introduced pupillography to American neuro-ophthalmology (Thompson, 2005), and he is honoured as the *Founder of Pupillography* (Trobe, 2010). The invention of personal computer-based infra-red video instruments has brought the pupillography into research and clinical practices like determining sleepiness, effects of new pharmaceutical agents, measuring pupil diameter for refractive surgery, quantitative analysis of relative afferent pupillary defects, and distinguishing pathologic from physiologic anisocoria. Most recently, this infrared tracking of pupillary size has been used to plot the visual fields by means of graded pupillary constriction as response to light stimuli (Wilhelm & Wilhelm, 2003). The investigators started using it by coupling infrared video for tracing pupillary size with an HFA. Kardon et al developed software to automatically analyse the pupil responses to focal light stimuli and display results graphically. All 76 locations of HFA program 30-2 was tested twice and relative sensitivity determined by comparing amplitude of pupillary constriction and latency at each stimulus location proving that pupil perimetry as useful objective means of assessing visual field function (Kardon *et al.*, 1991) (Chang *et al.*, 2017)

1.4.5 Multifocal Pupillographic Objective Perimetry (mfPOP): It is an objective measure of visual field defects. This method was attempted earlier by other researchers such as Sutter (Sutter, 1996), Wilhelm (Wilhelm *et al.*, 2000; Wilhelm & Wilhelm, 2003) and Tan (Tan *et al.*, 2001). But it was not successful due to low signal-to-noise ratios (SNR), this test requiring long presentation time (Maddess *et al.*, 2009). The preliminary study in mfPOP pioneered by Maddess investigated a means of concurrently assessing the visual field defects

46

of both eyes by recording the pupillary responses to multifocal stimuli. The biggest advantage is that only one pupil needs to be functional to plot both visual fields of both eyes, and it requires no electrodes for recording (Maddess *et al.*, 2009). The coloured stimuli for the technology is driven by the parvocellular pathway (Livingstone & Hubel, 1987; Maddess *et al.*, 2009; Carle *et al.*, 2013; Carle *et al.*, 2014; Carle *et al.*, 2015).

The multiple stimuli are presented dichoptically to both the eyes from two independent LCD monitors. These images are reflected by cold dichroic mirrors, which transmit only the infrared light but reflect the shorter wavelengths. There are four infrared light emitting diodes (LED) which illuminate the eyes facilitating a separate infrared video camera to monitor the pupillary size. The pupillary diameters are then extracted in real-time and retained using personal computer. To nullify the accommodative effect the viewing distance is increased to optical infinity by using plano-convex lenses. Different parts of the mfPOP is shown in **Figure 1.16**.

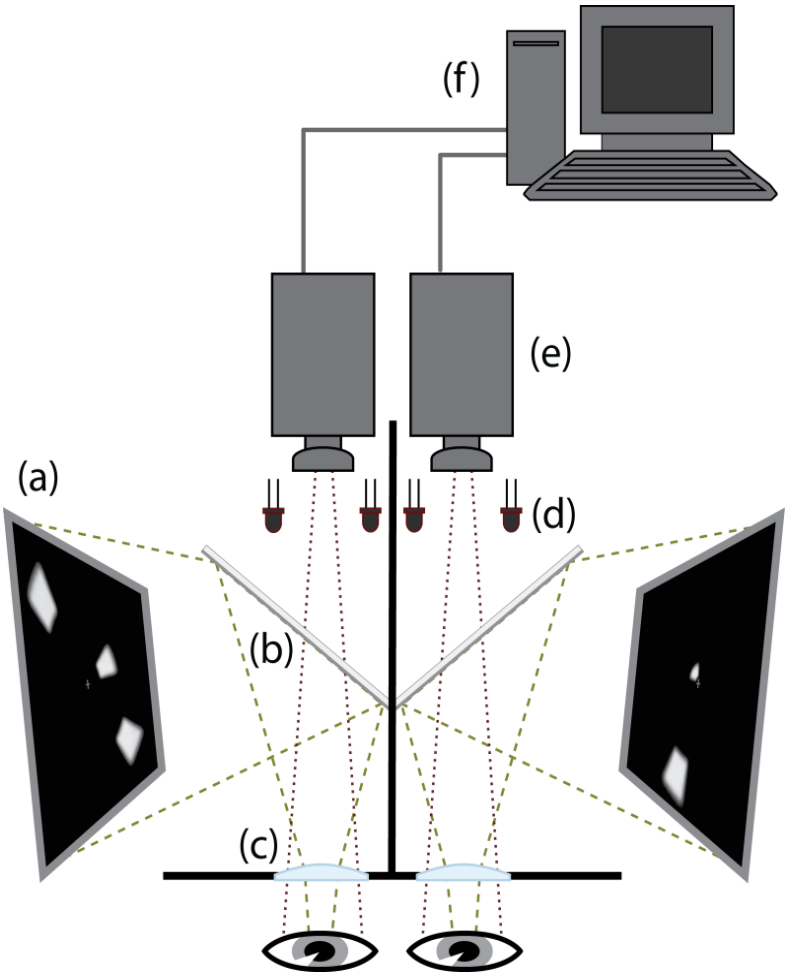

Figure 1.16. Schematic diagram of mfPOP: a = LCD monitors; b = Cold dichroic mirrors; c = Plano-convex lenses; d = Infrared emitting diodes; e = Infrared video camera; f = Personal computer
Adopted from PhD Thesis by Corinne F. Carle.

47

The stimuli are never presented in the same visual field location of both the eyes simultaneously to reduce any binocular rivalry. Both the direct and consensual pupillary responses are measured in each stimulus region from the independent recording of responses of both pupils using infrared light in both eyes. The individual regional responses, essentially the mean of many stimulus presentations in that region, are extracted from the continuous record of raw pupil diameter measurements using a least-square regression methods. Any segment of the recordings which are deemed not to contain enough useful data, due to excessive blinks or other reasons, are repeated. Practically, up to 15% of the recording sequence is tolerated, beyond which the deemed segment needs to be repeated (James, 2003b; James *et al.*, 2005). The anomalous data are removed from the record before the regression. The preselected temporal window for each response, the resulting pupillary diameter data is temporally synchronized with the stimulus-course and then regressed. This provides corrected individual responses for each region of the visual field without any overlap to other regions, and also allows for the independent estimation of variance for each regions of the visual field at every point of the response waveform (James *et al.*, 2005). Contrary to the traditional multifocal methods, it allows a section of the record to be removed without interfering the extraction of the responses.

The amplitude is significantly larger in the temporal field than in the nasal field despite the presence of the blind spot in the temporal field (Smith, 1980; Cox & Drewes, 1984; Schmid, 1995; Delgado *et al.*, 2002; Rai *et al.*, 2020d). Though the inter-individual variation is high, the intra-individual responses are consistent, which has encouraged the investigators to explore pupillography as an objective method of determining functional visual field defect. It has been found that the pupillary responses can be elicited by different stimuli, commonly change in luminance (Gamlin *et al.*, 2007; Kawasaki & Kardon, 2007), colour (Carle *et al.*, 2013; Kimura *et al.*, 2014), depth perception, motion (Barbur *et al.*, 1992) and spatial content (Ukai, 1985). The blue stimulus showed increasing gain with stimulus luminance without any evidence of saturation which was obvious with the red stimulus (Carle *et al.*, 2015). Different studies were performed in different ways. Some studies involved the use of hemi-field or whole-field stimuli, which is useful in determining the overall visual function but has minimal value in mapping of visual field defects (Chen *et al.*, 2008). So the more importance is given to focal or multifocal stimuli in picking up smaller visual field defects and mapping of visual field (Asakawa *et al.*, 2010). mfPOP is useful in assessing both the peripheral and central visual fields (Sabeti *et al.*, 2011).

48

The luminance stimuli have been used extensively. The studies have found that slower presentation rates than used in mfVEP and mfERG are required for larger mfPOP responses. However, higher luminance is also associated with higher SNR, which is not desirable, so balancing is needed between high SNR obtained at higher luminance and response saturation, as well as between testing time and variance (Maddess *et al.*, 2010). As applied in mfVEP, SNR can be improved by using sparse multifocal stimulus presentation (Maddess *et al.*, 2005). Different stimulus protocols were tested, namely Less Sparse Steady, Less Sparse Flicker, Moderate Sparse Flicker and Very Sparse Flicker. Among these protocols, the Very Sparse Flicker protocol was found to be the most effective in determining the diagnosis (Carle *et al.*, 2010).

Several comparative studies have validated the diagnostic power of mfPOP. A comparative study with mfVEP reported that mfPOP and mfVEP were equally effective in diagnosing age-related macular degeneration and type 2 diabetic retinopathy (Sabeti *et al.*, 2017). Head to head comparison of mfPOP and SAP and showing similar structural and functional relationships with regards to the RNFL thickness and visual field changes (Kolic *et al.*, 2013). Most of these studies have correlated with OCT findings too.

So far mfPOP has been applied for the diagnoses and assessment of various ophthalmological and neurological diseases. There was a significant reduction in amplitudes and significant delayed time-to-peak ($p < 0.001$), proving mfPOP as well tolerated objective method in the diagnosis and assessment of multiple sclerosis (Maddess *et al.*, 2011b; Ali *et al.*, 2014). The amplitude was found lower among the migraineur patients than in normal controls but did not reach the statistical significance, and treatment of migraine with Triptan improved the amplitudes (Ali *et al.*, 2014). Extensive studies have been conducted on the use of mfPOP in diagnosing, assessment and follow up of the glaucomatous patients, like different colour stimuli (Maddess *et al.*, 2011a), luminance and colour variant pupil perimetry in glaucoma (Ali *et al.*, 2014), blue mfPOP may have advantages over yellow in detecting early glaucoma (Carle *et al.*, 2015), etc.

mfPOP also identifies changes in the visual sensitivity according to the severity of diabetic retinopathy in type 2 diabetes (Sabeti *et al.*, 2015; Sabeti *et al.*, 2017). mfPOP identifies retinal damage and visual field defects even in the near absence of clinical diabetic retinopathy (Bell *et al.*, 2010). A comparative study of macular and widefield mfPOP found that central retinal sensitivity loss was more informative in NPDR (Sabeti *et al.*, 2012).

49

mfPOP is sensitive in the detection of exudative age-related macular degeneration (AMD) (Sabeti *et al.*, 2011; Sabeti *et al.*, 2017), and identifying ranibizumab-induced changes in the retinal function for exudative AMD (Sabeti *et al.*, 2012). These studies were the basis of the work here on mfPOP in Retinal diseases.

The studies have proven that mfPOP is a potential objective non-invasive method of testing visual function and visual field defects even prior to the visible clinical stage of the diseases.

1.5 VITREORETINAL DISEASES AND THEIR TREATMENT

Of particular interest to this thesis is the epidemiology of VR in Bhutan and that region. The Rapid Assessment of Avoidable Blindness (RAAB) survey conducted in Bhutan in 2009 reported the prevalence of blindness and visual impairment at 1.5%, 22.1% resulting from posterior segment pathology among the population aged 50 years and above (Lepcha *et al.*, 2013). The Follow-up RAAB survey conducted in 2017-2018 reported prevalence of 1.3% and that 7.7% was due to posterior segment diseases (IAPB, 2018; Lepcha *et al.*, 2019). This reduction in the prevalence of posterior segment disorders could be due to successful VR services in the country, which was established at the beginning of 2012 (by the current author). Thus far however there is no data on the pattern of VR diseases in the country. In Nepal, The 1981 Blindness Survey reported VR disorders as the third leading cause of bilateral blindness, second only to cataract and its complications (Brilliant, 1981). A more recent population based study reported VR disorders to be the second commonest cause of bilateral blindness, second only to cataract, and the most common cause among pseudophakics (Thapa *et al.*, 2011a). Population-based studies in Nepal also reported AMD was the most common VR disorder. In 2011, AMD was the most common VR disorder, followed by branch retinal vein occlusion (BRVO) among the population aged ≥ 40 years with mean age of 70.3 ± 10.2 years (Thapa *et al.*, 2011b). In 2013, AMD was the most common VR disorder, followed by diabetic retinopathy (DR), hypertensive retinopathy

50

(HTR), macular scar, BRVO, and retinal detachment (RD); mean age being 55.08 ± 11.51 years (Thapa *et al.*, 2013). In 2018, AMD was the commonest VR disorder, followed by BRVO, epiretinal membrane (ERM), DR, myopic degeneration, and macular hole (Thapa *et al.*, 2018).

This brings us to the retinal diseases covered by chapters of this thesis. I will now review those diseases and their main therapies.

1.5.1 AMD, mainly neovasuclar

AMD is the leading cause of irreversible blindness in people aged 50 years or older in the developed world (Age-Related Eye Disease Study Research, 2001; Seigel, 2002). It is caused by a combination of genetic and environmental factors (Christoforidis *et al.*, 2011). It has been reported to be more common among women compared to men of the same age (Klein *et al.*, 1997). The non-modifiable risk factor for developing AMD is increasing age above 50 years, while modifiable risk factors include smoking and high levels of the high-density lipoprotein cholesterol (Klein *et al.*, 2007; Klein *et al.*, 2010). The burden of AMD on an individual as measured by a loss of quality of life has been immense, ranging from 17 to 60% decrease in quality of life of the average patient (Brown *et al.*, 2005). An economic analysis based on losses to the gross domestic product suggested that AMD has approximately a $30 billion annual negative impact (Brown *et al.*, 2005). A streamlined version of four-step AMD severity scale is presented in Table 1 (Grp, 2001).

51

Table 1. Age-Related Eye Disease Study Age-related Macular Degeneration Levels Defined for Eyes

AMD Level	Criteria
1	Drusen maximum size < circle C-0 (63 µm diameter) and total area < circle C-1 (125 µm diameter)
2	Presence of one or more of the following:
	(a) Drusen maximum size ≥ circle C-0 but circle C-1
	(b) Drusen total area ≥ circle C-1
	(c) Retinal pigment epithelial pigment abnormalities consistent with AMD, defined as one or more of the following in the central or inner subfields:
	(1) Depigmentation present
	(2) Increased pigment ≥ circle C-1
	(3) Increased pigment present and depigmentation at least questionable
3	Presence of one or more of the following:
	(a) Drusen maximum size ≥ circle C-1
	(b) Drusen maximum size ≥ circle C-0 and total area > circle I-2 and type is soft indistinct
	(c) Drusen maximum size ≥ circle C-0 and total area > circle O-2 and type is soft distinct
	(d) Geographic atrophy within grid but none at center of macula
4 (Advanced)	Presence of one or more of the following:
	(a) Geographic atrophy in central subfield with at least questionable involvement of center of macula
	(b) Evidence of neovascular AMD
	(1) Fibrovascular/serous pigment epithelial detachment
	(2) Serous (or hemorrhagic) sensory retinal detachment
	(3) Subretinal/subretinal pigment epithelial hemorrhage
	(4) Subretinal fibrous tissue (or fibrin)
	(5) Photocoagulation for AMD
	AMD: age-related macular degeneration.

Traditionally, neovascular AMD (nAMD) was treated with laser photocoagulation. The macular photocoagulation study (MPS) reported that extrafoveal or juxtafoveal sub-retinal choroidal neovascular membrane (CNVM) treated with argon (Group, 1982) or krypton laser had better long-term visual acuity compared to patients who did not receive therapy (Group, 1990). But the biggest drawback was the immediate reduction of central visual acuity. In

52

2000, the use of Photodynamic therapy (PDT) with verteporfin was approved by FDA. Injected intravenously verteporfin was selectively absorbed by the CNVM. When verteporfin was irradiated with a 689 nm laser light it released highly-reactive oxygen species which would damage the CNVM (Donati *et al.*, 1999; Arnold *et al.*, 2001; Schlotzer-Schrehardt *et al.*, 2002). As work presented in this thesis has shown in Bhutan AMD was the fourth most common VR disease with 43.6% having late-stage disease in their first presentation (Rai *et al.*, 2020b). In Nepal AMD was the most common VR disease, 79.2% of the cases were dry type (Rai *et al.*, 2019).

1.5.2 Anti-VEGF treatments

Vascular endothelial growth factor (VEGF) is a signalling protein that stimulates the proliferation of vascular endothelium resulting in CNVM. This promotes angiogenesis and neovascularisation. This is the basis for pathogenesis of retinal and choroidal vascular diseases such as AMD (Rosenfeld *et al.*, 2006), DR and diabetic macular oedema (DMO) (Baker *et al.*, 2016), retinal vein occlusion (RVO) (Oellers *et al.*, 2016), neovascular glaucoma, retinopathy of prematurity (ROP), sickle cell retinopathy (Menaa *et al.*, 2017), and inherited retinal dystrophies (Marano *et al.*, 2000; Campochiaro, 2015). VEGF is a dimeric glycoprotein of approximately 40 kDa. In mammals, the VEGF family consists of seven members: VEGF-A (typically, and hereafter, referred to as VEGF), VEGF-B, VEGF-C, VEGF-D, VEGF-E, VEGF-F and PlGF (placental growth factor) (Penn *et al.*, 2008). The introduction of anti-VEGF in the treatment of not only nAMD, but also other diseases caused by VEGF which are mentioned above, was a revolutionary milestone (Campochiaro, 2000; Marano *et al.*, 2000; Menaa *et al.*, 2017). The different anti-VEGF agents used so far are pegaptanib (Gragoudas *et al.*, 2004), ranibizumab (Chong, 2016), bevacizumab (Shih & Lindley, 2006), aflibercept (Zhang *et al.*, 2017), and brolucizumab (Dugel *et al.*, 2019). Pegaptanib (Macugen), a 28-base ribonucleic acid aptamer, was developed to bind and block

53

the activity of extracellular VEGF, specifically the 165-amino-acid isoform ($VEGF_{165}$) for treating nAMD. It provided a statistically significant and clinically meaningful benefit in a broad spectrum of patients with nAMD (Gragoudas *et al.*, 2004). Bevacizumab is the first angiogenesis inhibitor to have been approved by the Food and Drug Administration (FDA) in February, 2004 (Steinbrook, 2006). It is a humanized monoclonal immunoglobulin G antibody with a molecular weight of 149 kDa. It is 93% human and 7% murine in protein sequence, and inhibits all active isoforms of VEGF (Shih & Lindley, 2006). Primarily it was introduced as a treatment for colorectal carcinoma with but now used as off-level treatment of vascular diseases in ophthalmology. Serious systemic toxicity was shown in clinical trials with systemic administration of bevacizumab, which is attributed to the fragment crystallizable (Fc) domain of the whole molecule (Ferrara *et al.*, 2006).

Ranibizumab is a recombinant humanized monoclonal antibody fragment containing only the antigen-binding fragment (Fab) portion. It has a molecular weight of approximately 48 kDa, and is designed to bind and inhibit all biologically active isoforms of human VEGF (Patel & Klufas, 2019). It was approved by Food and Drug Administration (FDA) on June 30, 2006 for the treatment of nAMD, manufactured by Genetech under the brand name Lucentis (Steinbrook, 2006). The systemic toxicity caused by whole molecules like bevacizumab is known to be mediated by the fragment crystallizable (Fc) domain, which can initiate immune system activation. So ranibizumab was developed to minimise the systemic toxicity when used for intraocular administration for diseases such as AMD which commonly affect elderly population who are not able to tolerate adverse effects. Ranibizumab has a shorter half-life than full-length antibodies. This limitations are reasoned to be balanced by the fact that a Fab would prevent Fc-dependent complement activation or immune cell destruction and limit systemic antibody exposure (Ferrara *et al.*, 2006; Meyer & Holz, 2011).

54

The studies have reported equivalent efficacy on visual acuity and safety between bevacizumab and ranibizumab for AMD cases (Group *et al.*, 2011; Berg *et al.*, 2015), as well as DR and DMO cases (Wells *et al.*, 2016). Cost-wise, bevacizumab costs approximately 100 times less than ranibizumab ($1,950 for a single dose of 0.5 mg ranibizumab in 0.05 ml cf. $550 for 4-ml vial containing 100 mg bevacizumab (Steinbrook, 2006). Then this 4-ml vial of bevacizumab can be prepared into small aliquots in syringes for intraocular injection at a cost of $17 to $50 per injection. Thus, the use of bevacizumab is more common in the resource limited public health centres (Steinbrook, 2006).

Aflibercept is a 115 kDa recombinant Fc fragment fusion protein consisted of parts of the extracellular domains of human VEGF receptors 1 and 2 genetically fused to the Fc portion of human IgG1 (Sivertsen *et al.*, 2018). Compared to other anyi-VEGF drugs aflibercept has a higher binding affinity for VEGF (Papadopoulos *et al.*, 2012), and longer intravitreal half-life and therefore better effects (Balaratnasingam *et al.*, 2015). The comparative efficacy of bevacizumab, ranibizumab and aflibercept was found to be equivalent, or not statistically significant for the treatment of macular edema secondary to RVO (Sangroongruangsri *et al.*, 2018). Another study reported bevacizumab as a reasonable alternative to ranibizumab and aflibercept in treating patients of nAMD, DMO, RVO and CNVM with similar efficacy with the exception that aflibercept was more effective for patients with DMO and BCVA <69 ETDRS letters at 12 months, but not significantly maintained at 24 months (Pham *et al.*, 2019).

Brolucizumab is a humanised single-chain antibody fragment inhibitor of all isoforms of VEGF-A. This single-chain antibody fragment with a 26 kDa molecular weight is the smallest functional subunit of an antibody that still retains full binding capacity to its intended target (Yannuzzi & Freund, 2019). The stability and solubility of brolucizumab allows it to achieve high doses in a single 50 microliter intravitreal injection (Tietz *et al.*,

55

2015). It was approved by FDA on 8th October, 2019 for the treatment of nAMD (NOVARTIS, 2019).

1.5.3 Diabetic eyes disease

Globally it was estimated that 285 million people had diabetes in 2010, and by 2014 the figure had increased to 442 million. Over one-third of them had signs of DR, and a third of these were afflicted with vision-threatening diabetic retinopathy (VTDR) in the form of severe non-proliferative and proliferative diabetic retinopathy (PDR) or DMO (Choi *et al.*, 2015). In Australia alone 72,000 of its 1.73 million diabetics had DMO in 2015. These figures are projected to increase by 42% by 2030 leading to 2.45 million with diabetes and 102,000 with DMO (Deloitte Access Economics, 2015). The indirect cost of vision loss associated with DMO in 2015 alone was estimated to be $2.07 billion p.a. because of loss of wellbeing, and inability to work or to not be able work to full capacity due to poor vision caused by DMO (Deloitte Access Economics, 2015). Despite improved diagnostic and management skills, diabetes remains an escalating global health challenge (Gale *et al.*, 2017). The management of DR and DMO is targeted at two levels. First, the general management of diabetes such as optimum glycaemic control, change of life style, and controlling the aggravating factors like hypertension and lipid profile. Second, the specific management of DR and DMO. Worldwide, laser is still the first line of therapy for DR and diffuse DMO as reported by different studies including the Diabetic Retinopathy Study. It is effective in improving vision and arresting further worsening of DR (Group, 1976, 1987; Shah & Chen, 2011). Laser is selectively absorbed by RPE due to its melanin content. So the RPE cells and the adjacent photoreceptors are damaged by the laser. The oxygen consumption at the outer retina is drastically reduced, so now the oxygen flux from the choriocapillaries can reach the inner retina. This extra supply of oxygen compensates for the reduced supply from the retinal circulation. Hypoxia is corrected and the production of hypoxia-induced cytokines such as

56

VEGF is normalised (Stefansson *et al.*, 1981; Budzynski *et al.*, 2008; Stefansson, 2009). The cytokines such as VEGF released by RPE is also reduced following laser therapy (Duh *et al.*, 2002; Sohn *et al.*, 2011). The commonly used pharmacological treatment is the intravitreal injection of anti-VEGF in both DR and DMO (Ip *et al.*, 2012). The details are explained above. Others include corticosteroids in the form if intravitreal injection of triamcinolone acetonite , dexamethasone implant (Callanan *et al.*, 2013), or flucinolone acetonide implant (Campochiaro *et al.*, 2012). In our Bhutan study presented here co-existent diabetes and HT was the most common associated systemic disease, and combined DR and DMO was the third most common VR disease (Rai *et al.*, 2020b). In Nepal diabetes was the second most common associated systemic disease, only next to HT, and DR was the second most common VR disease only less than AMD (Rai *et al.*, 2019).

Table 2 describes the International Clinical Diabetic Retinopathy disease severity scale adopted from the American Academy of Ophthalmology.

Table 2. International Clinical Diabetic Retinopathy Disease Severity Scale

Proposed Disease Severity Level	Findings upon Dilated Ophthalmoscopy	Derivation from ETDRS Levels	Risk Assessment	Management Options
No apparent DR	No abnormalities	Levels 10: DR absent		Optimize medical therapy: glucose, blood pressure & lipids
Mild NPDR	Microaneurysms only	Level 20: Very mild NPDR		Optimize medical therapy: glucose, blood pressure & lipids
Moderate NPDR	More than just microaneurysms but less than Severe NPDR	Levels 35,43: moderate NPDR less than 4:2:1 Level 47: moderate	One year early PDR: 5.4 – 11.9% One year high risk PDR: 1.2-3.6% One year early PDR: 26.3%	Refer to an ophthalmologist Optimize medical therapy of glucose,

57

		NPDR less than 4:2:1	One year High Risk PDR: 8.1%	blood pressure and lipids
Severe NPDR	Any of the following: 1. Extensive (>20) intraretinal hemorrhages in each of 4 quadrants 2. Definite venous beading in 2+ quadrants 3. Prominent IRMA in 1+ quadrant	53A-E: severe to very severe NPDR, 4:2:1 rule	One year risk for early PDR: 50.2% (severe NPDR) One year High Risk PDR: 14.6% (severe NPDR) – 45.0% (very severe NPDR)	Consider scatter (panretinal) laser treatment for patients with type 2 diabetes Optimize medical therapy as above
Proliferative Diabetic Retinopathy	One or more of the following: 1. Neovascularization 2. Vitreous/preretinal hemorrhage	Levels 61, 65, 71,75, 81,85: PDR, high-risk PDR, very severe or advanced PDR		Strongly consider PRP, without delay for patients with VH or neovascularization within 1 DD of the optic nerve head

DD- disc diameter; NPDR- Non proliferative diabetic retinopathy; PRP- Panretinal photocoagulation; VH- Vitreous haemorrhage;

1.5.4 Hypertensive retinopathy

Poorly controlled systemic hypertension (HT) is associated with significant morbidity and mortality. It causes cardiovascular risk by causing target-organ damage such as hypertensive retinopathy, cardiovascular disease, cerebrovascular accident, renal insufficiency, and peripheral vascular disease. So the recognition of hypertensive retinopathy (HTR) is important to prevent vision loss, and in cardiovascular and other disease risk stratification of hypertensive patients (Chatterjee *et al.*, 2002; Grosso *et al.*, 2005). There are different classification systems for HTR. In this thesis, whenever there is mention of HTR, the author has followed the Keith-Wagener-Barker classification (Grosso *et al.*, 2005). It is given in Table 3.

58

Table 3. The Keith-Wagener-Barker classification of hypertensive retinopathy based on the level of severity of the retinal findings.

Grade	Classification	Symptom
Grade I (mild)	Mild generalised retinal arteriolar narrowing	No symptom
Grade II (moderate)	Focal arteriolar narrowing and arteriovenous nipping. Moderate to marked sclerosis of the retinal arterioles. A copper wiring opacified appearance of arteriolar walls. Exaggerated arterial light reflex	Asymptomatic
Grade III (angiospastic)	Grade II plus retinal haemorrhages (dot, blot and flame-shaped), exudates and cotton wool spots. Exudates in around the fovea appear as macular star. Sclerosis and spastic lesions of retinal arterioles	Symptomatic
Grade IV (malignant)	Grade III plus optic disc swelling. This is a marker of malignant hypertension.	Reduced survival

HT is also risk factor to other ocular conditions such as anterior ischaemic optic neuropathy, retinal vein occlusion (RVO), retinal embolic phenomenon, AMD and glaucoma (Dodson & Kritzinger, 1997). In Bhutan, we found that HTR was the most common VR disease (Rai *et al.*, 2020b); in Nepal HT was the most common associated systemic disease followed by diabetes, and HTR ranked seventh among the VR diseases (Rai *et al.*, 2019).

1.5.5 The retinal Vein Occlusions

RVO is the second most common sight-threatening retinal vascular disorder after DR (Laouri *et al.*, 2011). The untreated cases result in visual impairment and significant ocular

59

complications in both BRVO (Rogers *et al.*, 2010), and CRVO cases (McIntosh *et al.*, 2010). All types of RVO cases including CRVO, HRBRVO, and BRVO are treated with similar approaches: managing the risk factors like systemic HT, diabetes and dyslipidaemia; and specific treatment of retinal disorders with laser and intravitreal injection of anti-VEGF. The mechanism of anti-VEGF is explained above. Laser works by damaging the RPE cells and surrounding photoreceptors, which in turn reduces the oxygen demand of the outer retina so there is increased oxygen flux to the inner retina from the choriocapillaries (Stefansson *et al.*, 1981; Budzynski *et al.*, 2008; Stefansson, 2009). Second, laser therapy also creates chorioretinal venous anastomosis. This chorioretinal anastomosis allows blood to bypass the occluded vein into choroidal circulation (McAllister & Constable, 1995; Fekrat *et al.*, 1998). In Nepal RVO was the third most common VR disease (Rai *et al.*, 2019); in Bhutan it was the sixth most common (Rai *et al.*, 2020b).

1.5.6 The retinal detachments

RD is defined as the separation of the neurosensory retina from the underlying RPE layers. There are four major types of RD: rhegmatogenous, tractional, exudative or serous, and combined tractional-rhegmatogenous RD, rhegmatogenous RD being the most common type (Ghazi & Green, 2002). It is potentially a blinding VR disorder with geographical variations in incidence. It is reported to have average annual incidence of approximately 12 per 100,000 population in USA (Wilkes *et al.*, 1982) and 7 to 10 per 100,000 in Europe (Laatikainen *et al.*, 1985). The Asian populations might be at higher risk for RD than Caucasian populations because of the greater prevalence of myopia is reported as high as 96.5% (Jung *et al.*, 2012; Morgan *et al.*, 2018). The annual incidence of RD was reported at 10.4 per 100,000 population in Japan (Sasaki *et al.*, 1995), 10.39 per 100,000 in Korea (Park *et al.*, 2013). In Singapore the Chinese population had the highest annual incidence, followed by Malays and Indians (Wong *et al.*, 1999). RD is managed surgically by scleral buckling or pars plana

60

vitrectomy or combination of both methods with internal tamponde with silicon oil or expansible gases such as sulphur hexafluoride (SF6), perfluoroethane (C2F6) or perfluoropropane (C3F8) (Vaziri *et al.*, 2016). RD is reported the seventh most common VR disease in Bhutan, and interestingly prevalence was found to be significantly higher among females (p=0.007) (Rai *et al.*, 2020b). In Nepal the RD was the third most common VR disease, next to AMD and DR (Rai *et al.*, 2019).

1.5.7 Complications of myopia

Uncorrected refractive error is the commonest cause of visual impairment worldwide (Pascolini & Mariotti, 2012), myopia being the major type of refractive error (Althomali, 2018). Myopia is associated with complications and VR disorders such as atrophic retinal holes and retinal detachment (RD), myopic choroidal neovascular membrane (mCNVM), degenerative changes resulting in cataract, glaucoma, and macular hole that collectively cause severe visual loss (Foster & Jiang, 2014). Retinal thinning, lattice degeneration and atrophic retinal holes are managed by barrage prophylactic laser or cryoptherapy around the lesions, which creates sterile chorioretinitis with fibrosis and stronger adhesion thereby preventing RD (Wilkinson, 2014). mCNVM is managed with intravitreal injection of anti-VEGF commonly, and also with laser photocoagulation and photodynamic thermotherapy (Wong *et al.*, 2015). Refractive errors, 92.1% being myopia, referred for retinal evaluation was the second most common reason for visiting VR subspeciality clinic, only next to HTR (Rai *et al.*, 2020b). Myopia was more common among females (p=0.01) and urbanites (p=0.02), the prevalence was the highest among urban females (20.9%) (Rai *et al.*, 2020a). Lattice degeneration was present in 13.4% of myopic eyes, retinal breaks in 1.4% and mCNVM in 0.4% (Rai *et al.*, 2020b).

61

1.5.8 Retinopathy of prematurity

ROP needs focus because its incidence is increasing all over the world because of higher incidence of premature babies born at 24 weeks or less gestational age (Isaza *et al.*, 2019). It affects infants and children causing significant public health burden because of longer life-years affected (Rahi *et al.*, 1999). ROP is treated with the laser photocoagulation of the peripheral retina, which reduces the oxygen demand. It also creates sterile chorioretinitis with fibrosis and prevent occurrence of tractional RD (Tewari *et al.*, 2019). In Bhutan 24 of 36 paediatric cases who received examination under general anaesthesia over three years were ROP cases. Further 8 of 24 ROP cases required further interventions in the form of retinal photocoagulation or major VR surgery (Rai *et al.*, 2020b; Rai *et al.*, 2020c).

1.5.9 Ocular trauma

Ocular trauma remains an important avoidable cause of visual impairment globally causing significant ocular morbidity and huge socioeconomic burden. Approximately 55 million eye injuries occur annually worldwide, 19 million of them result in permanent unilateral vision loss and 1.6 million in blindness (Negrel & Thylefors, 1998). The VR disorders resulting from eye injuries are closed- or open-globe injuries, retinal detachment, vitreous haemorrhage, subluxated or dislocated cataract or IOLs, endophthalmitis and retained intraocular foreign bodies. The management is dependent on the types of injury and the ocular tissues involved (Rejdak *et al.*, 2017). Ocular trauma was the second most presenting complaint in Nepal (Rai *et al.*, 2019). It was reported fifth most presenting in Bhutan, but the cases were associated with vision-threatening conditions such as traumatic endophthalmitis (5 of 9 endophthalmitis cases over 3 years were traumatic) (Rai *et al.*, 2020c), and retained intraocular foreign body with associated RD and traumatic cataract (Rai *et al.*, 2016). The common causes of trauma were road traffic accidents, fall from height, agricultural and sports or recreational activities related (Rai *et al.*, 2020b).

62

SUMMARY

This thesis will cover epidemiological studies of retinal disease, especially in the context of Nepal and Bhutan, and also studies of a potential new tool for diagnosis and management of retinal diseases: multifocal pupillographic objective perimetry (mfPOP). The chapters on mfPOP cover practical clinical issues, like the need for dilation, and also comparisons of mfPOP with other technologies like perimetry and optical coherence tomography. The retinal diseases examined in the mfPOP studies are AMD and DMO.

63

REFERENCES:

Abdullah SN, Aldahlawi N, Rosli Y, Vaegan, Boon MY & Maddess T. (2012). Effect of contrast, stimulus density, and viewing distance on multifocal steady-state visual evoked potentials (MSVs). *Invest Ophthalmol Vis Sci* **53,** 5527-5535.

Abdullah SN, Sanderson GF, James AC, Vaegan & Maddess T. (2014). Visual evoked potential and psychophysical contrast thresholds in glaucoma. *Doc Ophthalmol* **128,** 111-120.

Adams AJ, Rodic R, Husted R & Stamper R. (1982). Spectral sensitivity and color discrimination changes in glaucoma and glaucoma-suspect patients. *Invest Ophthalmol Vis Sci* **23,** 516-524.

Age-Related Eye Disease Study Research G. (2001). A Randomized, Placebo-Controlled, Clinical Trial of High-Dose Supplementation With Vitamins C and E, Beta Carotene, and Zinc for Age-Related Macular Degeneration and Vision Loss: AREDS Report No. 8. *Archives of ophthalmology* **119,** 1417-1436.

Agte S, Junek S, Matthias S, Ulbricht E, Erdmann I, Wurm A, Schild D, et al. (2011). Müller Glial Cell-Provided Cellular Light Guidance through the Vital Guinea-Pig Retina. *Biophysical Journal* **101,** 2611-2619.

Ahmed E. (2011). Anatomy of Visual Pathway. In *Comprehensive Manual of Ophthalmology*, pp. Page. 33-35. Japyee Brothers Medical Publishers (P) Ltd.

Alencar LM & Medeiros FA. (2011). The role of standard automated perimetry and newer functional methods for glaucoma diagnosis and follow-up. *Indian Journal of Ophthalmology* **59,** S53-S58.

Ali EN, Maddess T, James AC, Voicu C & Lueck CJ. (2014). Pupillary response to sparse multifocal stimuli in multiple sclerosis patients. *Multiple sclerosis (Houndmills, Basingstoke, England)* **20,** 854-861.

Allison T, McCarthy G, Nobre A, Puce A & Belger A. (1994). Human Extrastriate Visual Cortex and the Perception of Faces, Words, Numbers, and Colors. *Cerebral Cortex* **4,** 544-554.

Althomali TA. (2018). Relative Proportion Of Different Types Of Refractive Errors In Subjects Seeking Laser Vision Correction. *Open Ophthalmol J* **12,** 53-62.

Amunts K & Zilles K. (2015). Architectonic Mapping of the Human Brain beyond Brodmann. *Neuron* **88,** 1086-1107.

Anderson RS. (2006). The psychophysics of glaucoma: improving the structure/function relationship. *Prog Retin Eye Res* **25,** 79-97.

Arevalo JFF, C.F; Mendoza, A.J. (2006). Normal Anatomy of the Macula. In *Age-related Macular Degeneration: A Comprehensive Textbook*, First edn, ed. Alfaro DVL, P.E; Mieler, W.F; Mercado, H.Q; Jager, R.D; Tano, Y., pp. Page. 1-12. Lippincott Williams & Wilkins, USA.

Arnold J, Kilmartin D, Olson J, Neville S, Robinson K, Laird A, Richmond C, et al. (2001). Verteporfin therapy of subfoveal choroidal neovascularization in age-related macular degeneration: Two-year results of a randomized clinical trial including lesions with occult with no classic choroidal neovascularization-verteporfin in photodynamic therapy report 2. *American Journal of Ophthalmology* **131,** 541-560.

Asakawa K, Shoji N, Ishikawa H & Shimizu K. (2010). New approach for the glaucoma detection with pupil perimetry. *Clinical Ophthalmology (Auckland, NZ)* **4,** 617-623.

64

Asanuma C, Andersen RA & Cowan WM. (1985). The thalamic relations of the caudal inferior parietal lobule and the lateral prefrontal cortex in monkeys: divergent cortical projections from cell clusters in the medial pulvinar nucleus. *J Comp Neurol* **241,** 357-381.

Baez KA, McNaught AI, Dowler JG, Poinoosawmy D, Fitzke FW & Hitchings RA. (1995). Motion detection threshold and field progression in normal tension glaucoma. *Br J Ophthalmol* **79,** 125-128.

Baker CW, Jiang Y & Stone T. (2016). Recent advancements in diabetic retinopathy treatment from the Diabetic Retinopathy Clinical Research Network. *Current opinion in ophthalmology* **27,** 210-216.

Balaratnasingam C, Dhrami-Gavazi E, McCann JT, Ghadiali Q & Freund KB. (2015). Aflibercept: a review of its use in the treatment of choroidal neovascularization due to age-related macular degeneration. *Clin Ophthalmol* **9,** 2355-2371.

Ballesteros JM, Van Der List DA & Chalupa LM. (2005). Formation of eye-specific retinogeniculate projections occurs prior to the innervation of the dorsal lateral geniculate nucleus by cholinergic fibers. *Thalamus & related systems* **3,** 157-163.

Barbur JL, Harlow AJ & Sahraie A. (1992). Pupillary responses to stimulus structure, colour and movement. *Ophthalmic & physiological optics : the journal of the British College of Ophthalmic Opticians (Optometrists)* **12,** 137-141.

Baseler HA, Sutter EE, Klein SA & Carney T. (1994). The topography of visual evoked response properties across the visual field. *Electroencephalography and Clinical Neurophysiology* **90,** 65-81.

Baylor DA. (1987). Photoreceptor signals and vision. Proctor lecture. *Invest Ophthalmol Vis Sci* **28,** 34-49.

Baylor DA, Fuortes MG & O'Bryan PM. (1971). Receptive fields of cones in the retina of the turtle. *J Physiol* **214,** 265-294.

Bebie H, Fankhauser F & Spahr J. (1976). Static perimetry: strategies. *Acta Ophthalmol (Copenh)* **54,** 325-338.

Bedggood P, Tanabe F, McKendrick AM & Turpin A. (2016). Automatic identification of the temporal retinal nerve fiber raphe from macular cube data. *Biomedical Optics Express* **7,** 4043-4053.

Bell A, James AC, Kolic M, Essex RW & Maddess T. (2010). Dichoptic Multifocal Pupillography Reveals Afferent Visual Field Defects in Early Type 2 Diabetes. *Investigative Ophthalmology & Visual Science* **51,** 602-608.

Benevento LA, Rezak M & Santos A. (1977). An autoradiographic study of the projections of the pretectum in the rhesus monkey (Macaca mulatta): evidence for sensorimotor links to the thalamus and oculomotor nuclei. *Brain Res* **127,** 197-218.

Berg K, Pedersen TR, Sandvik L & Bragadottir R. (2015). Comparison of ranibizumab and bevacizumab for neovascular age-related macular degeneration according to LUCAS treat-and-extend protocol. *Ophthalmology* **122,** 146-152.

Berman N. (1977). Connections of the pretectum in the cat. *J Comp Neurol* **174,** 227-254.

Berninger TA & Arden GB. (1988). The pattern electroretinogram. *Eye* **2,** S257-S283.

Bernstein PS. The Organization of the Retina and Visual System: PART XIII: FACTS AND FIGURES CONCERNING THE HUMAN RETINA BY HELGA KOLB John A. Moran Eye Centre, USA.

65

Bhattacharyya KB. (2011). Eminent neuroscientists their lives and works. In *Eminent neuroscientists their lives and works*. Academic Publishers.

Bickford ME, Günlük AE, Guido W & Sherman SM. (1993). Evidence that cholinergic axons from the parabrachial region of the brainstem are the exclusive source of nitric oxide in the lateral geniculate nucleus of the cat. *The Journal of Comparative Neurology* **334,** 410-430.

Binder S. (2006). Human Retinal Transplantation. In *Age-related Macular Degeneration: A Comprehensive Textbook*, First edn, ed. Alfaro DVL, P. E; Mieler, W. F; Quiroz-Mercado,H; Jager, R. D; Tano, Y., pp. Page 314-327. Lippincott Williamsons & Wilkins, USA.

Birch DG, Williams PD, Callanan D, Wang R, Locke KG & Hood DC. (2010). Macular atrophy in birdshot retinochoroidopathy: an optical coherence tomography and multifocal electroretinography analysis. *Retina* **30,** 930-937.

Blumhardt LD, Barrett G & Halliday AM. (1977). The asymmetrical visual evoked potential to pattern reversal in one half field and its significance for the analysis of visual field defects. *The British Journal of Ophthalmology* **61,** 454-461.

Bode SFN, Jehle T & Bach M. (2011). Pattern Electroretinogram in Glaucoma Suspects: New Findings from a Longitudinal Study. *Investigative Ophthalmology & Visual Science* **52,** 4300-4306.

Bosworth CF, Sample PA & Weinreb RN. (1997). Perimetric motion thresholds are elevated in glaucoma suspects and glaucoma patients. *Vision research* **37,** 1989-1997.

Bowling B. (2016a). Acquired Macular Disorders. In *Kanski's Clinical Ophthalmology: A Systematic Approach*, pp. p. 580-640. Elsevier, USA.

Bowling B. (2016b). Glaucoma. In *Kanski's Clinical Ophthalmology: A Systemic Approach*, Eighth edn, ed. Bowling B, pp. Page 306-395. Elsevier, USA.

Bowling B. (2016c). Hereditary fundus dystrophies. In *Kanski's Clinical Ophthalmology: A systematic approach*, Eighth edn, pp. Page 641-680. Elsevier, USA.

Bowling B. (2016d). Neuro-ophthalmology. In *Kanski's Clinical Ophthalmology: A Systemic Approach*, Eighth edn, ed. Bowling B, pp. Page 774-851. Elsevier, USA.

Bowling B. (2016e). Retinal Vascular Disease. In *Kansk's Clinical Ophthalmology: A Systematic Approach*, Eighth edn, ed. Bowling B, pp. P. 519-577. Elsevier, USA.

Brilliant GEP, R. P.; Grasset, N. C.; Lepkowski, J. M.; Shrestha, S. R.; Konyama, K.; et al. (1981). The Epidemiology of blindness in Nepal: report of the 1981 Nepal Blindness survey In *The Sewa Foundation*, ed. Chelsea MI. Nepal.

Brindley GS. (1972). The variability of the human striate cortex. *J Physiol* **225,** 1p-3p.

Broadway DC. (2012). Visual field testing for glaucoma – a practical guide. *Community Eye Health* **25,** 66-70.

Bron AJ. (1997a). The Retina. In *Wolff's Anatomy of Eye and Orbit*, Eighth edn, pp. 454-488. Chapman & Hall, London, UK.

Bron AJ. (1997b). The Visual Pathway. In *Wolff's Anatomy of the Eye and Orbit*, Third edn, pp. Page. 589-596.

Brown GC, Brown MM, Sharma S, Stein JD, Roth Z, Campanella J & Beauchamp GR. (2005). THE BURDEN OF AGE-RELATED MACULAR DEGENERATION: A VALUE-BASED MEDICINE ANALYSIS. *Transactions of the American Ophthalmological Society* **103,** 173-186.

Brusini P, Salvetat ML, Parisi L & Zeppieri M. (2005). Probing glaucoma visual damage by rarebit perimetry. *Br J Ophthalmol* **89,** 180-184.

66

Budzynski E, Smith JH, Bryar P, Birol G & Linsenmeier RA. (2008). Effects of photocoagulation on intraretinal PO2 in cat. *Invest Ophthalmol Vis Sci* **49,** 380-389.

Burkhardt DA. (1994). Light adaptation and photopigment bleaching in cone photoreceptors in situ in the retina of the turtle. *J Neurosci* **14,** 1091-1105.

Buttner-Ennever JA, Cohen B, Horn AK & Reisine H. (1996). Pretectal projections to the oculomotor complex of the monkey and their role in eye movements. *J Comp Neurol* **366,** 348-359.

Byzov A. (1977). Model for the feedback mechanism between horizontal cells and photoreceptors of vertebrate retinas. *Neirofiziologiia= Neurophysiology* **9,** 86-94.

Callanan DG, Gupta S, Boyer DS, Ciulla TA, Singer MA, Kuppermann BD, Liu CC, et al. (2013). Dexamethasone intravitreal implant in combination with laser photocoagulation for the treatment of diffuse diabetic macular edema. *Ophthalmology* **120,** 1843-1851.

Campochiaro PA. (2000). Retinal and choroidal neovascularization. *J Cell Physiol* **184,** 301-310.

Campochiaro PA. (2015). Molecular pathogenesis of retinal and choroidal vascular diseases. *Prog Retin Eye Res* **49,** 67-81.

Campochiaro PA, Brown DM, Pearson A, Chen S, Boyer D, Ruiz-Moreno J, Garretson B, et al. (2012). Sustained Delivery Fluocinolone Acetonide Vitreous Inserts Provide Benefit for at Least 3 Years in Patients with Diabetic Macular Edema. *Ophthalmology* **119,** 2125-2132.

Carle C, James A, Kolic M, Essex R & Maddess T. (2014). *Luminance and colour variant pupil perimetry in glaucoma*, vol. 42.

Carle C, James A, Kolic M, Loh Y-W & Maddess T. (2010). High Resolution Pupillographic Objective Perimetry in Glaucoma. *Investigative Ophthalmology & Visual Science* **52,** 604-610.

Carle CF, James AC, Kolic M, Essex RW & Maddess T. (2015). Blue Multifocal Pupillographic Objective Perimetry in Glaucoma. *Invest Ophthalmol Vis Sci* **56,** 6394-6403.

Carle CF, James AC & Maddess T. (2013). The Pupillary Response to Color and Luminance Variant Multifocal Stimuli. *Investigative Ophthalmology & Visual Science* **54,** 467-475.

Casagrande VA & Kaas JH. (1994). The Afferent, Intrinsic, and Efferent Connections of Primary Visual Cortex in Primates. In *Primary Visual Cortex in Primates*, ed. Peters A & Rockland KS, pp. 201-259. Springer US, Boston, MA.

Casagrande VA, Royal DW & Sáry G. (2005). Geniculate Nucleus (LGN). *The primate visual system: a comparative approach***,** 191.

Casagrande VI, J. (2011). Processing in the Lateral Geniculate Nucleus (LGN). In *Adler's Physiology of the Eye*, Eleventh edn, ed. Kaufman PLA, A; Levin, L.A; Nilsson, S.F.E; Hoeve, J.V; Wu, S.M., pp. Page. 574-585. Saunders & Elsevier, UK, USA.

Chang LY-L, Turuwhenua J, Qu TY, Black JM & Acosta ML. (2017). Infrared Video Pupillography Coupled with Smart Phone LED for Measurement of Pupillary Light Reflex. *Frontiers in Integrative Neuroscience* **11**.

Chang S, Vaccarella L, Olatunji S, Cebulla C & Christoforidis J. (2011). Diagnostic Challenges in Retinitis Pigmentosa: Genotypic Multiplicity and Phenotypic Variability. *Current Genomics* **12,** 267-275.

Chatterjee S, Chattopadhyay S, Hope-Ross M & Lip PL. (2002). Hypertension and the eye: changing perspectives. *J Hum Hypertens* **16,** 667-675.

Chauhan BC. (2000). The value of high-pass resolution perimetry in glaucoma. *Current opinion in ophthalmology* **11,** 85-89.

67

Che XIN, Fan X-Q & Wang Z-L. (2014). Mechanism of blood-retinal barrier breakdown induced by HIV-1 (Review). *Experimental and Therapeutic Medicine* **7,** 768-772.

Chen FK, Patel PJ, Xing W, Bunce C, Egan C, Tufail AT, Coffey PJ, et al. (2009). Test-Retest Variability of Microperimetry Using the Nidek MP1 in Patients with Macular Disease. *Investigative Ophthalmology & Visual Science* **50,** 3464-3472.

Chen Y, Wyatt HJ, Swanson WH & Dul MW. (2008). Rapid Pupil-Based Assessment of Glaucomatous Damage. *Optometry and vision science : official publication of the American Academy of Optometry* **85,** 471.

Choi W, Moult EM, Waheed NK, Adhi M, Lee B, Lu CD, de Carlo TE, et al. (2015). Ultrahigh-Speed, Swept-Source Optical Coherence Tomography Angiography in Nonexudative Age-Related Macular Degeneration with Geographic Atrophy. *Ophthalmology* **122,** 2532-2544.

Chong V. (2016). Ranibizumab for the treatment of wet AMD: a summary of real-world studies. *Eye* **30,** 270-286.

Christoforidis JB, Tecce N, Dell'Omo R, Mastropasqua R, Verolino M & Costagliola C. (2011). Age related macular degeneration and visual disability. *Current drug targets* **12,** 221-233.

Clark VP & Hillyard SA. (1996). Spatial Selective Attention Affects Early Extrastriate But Not Striate Components of the Visual Evoked Potential. *Journal of Cognitive Neuroscience* **8,** 387-402.

Clarke RJ, Zhang H & Gamlin PD. (2003). Primate pupillary light reflex: receptive field characteristics of pretectal luminance neurons. *Journal of neurophysiology* **89,** 3168-3178.

Cohen AI. (1988). The retina: An approachable part of the brain. *Survey of Ophthalmology* **33,** 63-64.

Connolly M & Van Essen D. (1984). The representation of the visual field in parvicellular and magnocellular layers of the lateral geniculate nucleus in the macaque monkey. *J Comp Neurol* **226,** 544-564.

Cox TA & Drewes CP. (1984). Contraction Anisocoria Resulting From Half-Field Illumination. *American Journal of Ophthalmology* **97,** 577-582.

Creel DJ. (2011). Multifocal Electroretinograms. *Journal of Visualized Experiments : JoVE***,** 3176.

Creel DJ. (2015). Visually Evoked Potentials. In *Webvision-The Organization of the Retina and Visual System*. Webvision, USA.

Curcio CA, Sloan KR, Kalina RE & Hendrickson AE. (1990). Human photoreceptor topography. *The Journal of Comparative Neurology* **292,** 497-523.

Dacey DM, Liao H-W, Peterson BB, Robinson FR, Smith VC, Pokorny J, Yau K-W, et al. (2005). Melanopsin-expressing ganglion cells in primate retina signal colour and irradiance and project to the LGN. *Nature* **433,** 749.

Dale EA, Hood DC, Greenstein VC & Odel JG. (2010). A comparison of multifocal ERG and frequency domain OCT changes in patients with abnormalities of the retina. *Doc Ophthalmol* **120,** 175-186.

Daniel PM & Whitteridge D. (1961). The representation of the visual field on the cerebral cortex in monkeys. *The Journal of Physiology* **159,** 203-221.

Dartnall HJ, Bowmaker JK & Mollon JD. (1983). Human visual pigments: microspectrophotometric results from the eyes of seven persons. *Proceedings of the Royal Society of London Series B, Biological sciences* **220,** 115-130.

de Sousa AA, Sherwood CC, Hof PR & Zilles K. (2013). Lamination of the lateral geniculate nucleus of catarrhine primates. *Brain, behavior and evolution* **81,** 93-108.

68

Delgado MF, Nguyen NT, Cox TA, Singh K, Lee DA, Dueker DK, Fechtner RD, et al. (2002). Automated perimetry: a report by the American Academy of Ophthalmology. *Ophthalmology* **109,** 2362-2374.

Deloitte Access Economics. (2015). The economic impact of diabetic macular oedema in Australia, pp. 1 online resource (69 pages).

Demirkaya N, van Dijk HW, van Schuppen SM, Abramoff MD, Garvin MK, Sonka M, Schlingemann RO, et al. (2013). Effect of Age on Individual Retinal Layer Thickness in Normal Eyes as Measured With Spectral-Domain Optical Coherence Tomography. *Investigative Ophthalmology & Visual Science* **54,** 4934-4940.

Derrington A. (2001). The lateral geniculate nucleus. *Current Biology* **11,** R635-R637.

DeVries SH. (2000). Bipolar cells use kainate and AMPA receptors to filter visual information into separate channels. *Neuron* **28,** 847-856.

Di Russo F, Martinez A, I Sereno M, Pitzalis S & A Hillyard S. (2002). *Cortical sources of the early components of the visual evoked potential Hum*, vol. 15.

Dineen JT & Hendrickson A. (1983). Overlap of retinal and prestriate cortical pathways in the primate pretectum. *Brain Res* **278,** 250-254.

Distler C & Hoffmann KP. (1989). The pupillary light reflex in normal and innate microstrabismic cats, II: Retinal and cortical input to the nucleus praetectalis olivaris. *Vis Neurosci* **3,** 139-153.

Distler C & Hoffmann KP. (2009). The pupillary light reflex in normal and innate microstrabismic cats, II: Retinal and cortical input to the nucleus praetectalis olivaris. *Visual Neuroscience* **3,** 139-153.

Dodson PM & Kritzinger EE. (1997). Medical cardiovascular treatment trials: relevant to medical ophthalmology in 1997? *Eye (Lond)* **11 (Pt 1),** 3-11.

Dolan FM, Parks S, Hammer H & Keating D. (2002). The wide field multifocal electroretinogram reveals retinal dysfunction in early retinitis pigmentosa. *The British Journal of Ophthalmology* **86,** 480-481.

Donati G, Kapetanios AD & Pournaras CJ. (1999). Principles of treatment of choroidal neovascularization with photodynamic therapy in age-related macular degeneration. *Semin Ophthalmol* **14,** 2-10.

Dougherty RF, Koch VM, Brewer AA, Fischer B, Modersitzki J & Wandell BA. (2003). Visual field representations and locations of visual areas V1/2/3 in human visual cortex. *Journal of Vision* **3,** 1-1.

Dowling JE & Werblin FS. (1971). Synaptic organization of the vertebrate retina. *Vision research* **Suppl 3,** 1-15.

Dugel PU, Koh A, Ogura Y, Jaffe GJ, Schmidt-Erfurth U, Brown DM, Gomes AV, et al. (2019). Re: Dugel et al: HAWK and HARRIER: phase 3, multicenter, randomized, double-masked trials of brolucizumab for neovascular age-related macular degeneration (Ophthalmology. 2019 Apr 12 [Epub ahead of print]) Reply. *Ophthalmology* **126,** E96-E97.

Duh EJ, Yang HS, Suzuma I, Miyagi M, Youngman E, Mori K, Katai M, et al. (2002). Pigment epithelium-derived factor suppresses ischemia-induced retinal neovascularization and VEGF-induced migration and growth. *Invest Ophthalmol Vis Sci* **43,** 821-829.

Duke-Elder SW. (1961). The anatomy of the visual system. In *Duke-Elder's System of Ophthalmology*.

Ebrey T & Koutalos Y. (2001). Vertebrate photoreceptors. *Prog Retin Eye Res* **20,** 49-94.

69

Ellis CJ. (1981). The pupillary light reflex in normal subjects. *The British Journal of Ophthalmology* **65,** 754-759.

Ennis FA & Johnson CA. (2002). Are high-pass resolution perimetry thresholds sampling limited or optically limited? *Optometry and vision science : official publication of the American Academy of Optometry* **79,** 506-511.

Fankhauser F, Spahr J & Bebie H. (1977). Some aspects of the automation of perimetry. *Survey of Ophthalmology* **22,** 131-141.

Feigl B, Brown B, Lovie-Kitchin J & Swann P. (2005). Adaptation responses in early age-related maculopathy. *Invest Ophthalmol Vis Sci* **46,** 4722-4727.

Fekrat S, Goldberg MF & Finkelstein D. (1998). Laser-induced chorioretinal venous anastomosis for nonischemic central or branch retinal vein occlusion. *Archives of ophthalmology (Chicago, Ill : 1960)* **116,** 43-52.

Ferrara N, Damico L, Shams N, Lowman H & Kim R. (2006). Development of ranibizumab, an anti-vascular endothelial growth factor antigen binding fragment, as therapy for neovascular age-related macular degeneration. *Retina* **26,** 859-870.

Firth SI, Wang CT & Feller MB. (2005). Retinal waves: mechanisms and function in visual system development. *Cell calcium* **37,** 425-432.

Fishman GA. (1985). Basic Principles of Clinical Electroretinogram. *Retina* **5,** Page 123-126.

Fitzgibbon T & Taylor SF. (1996). Retinotopy of the human retinal nerve fibre layer and optic nerve head. *J Comp Neurol* **375,** 238-251.

Fitzpatrick D, Lund JS, Schmechel DE & Towles AC. (1987). Distribution of GABAergic neurons and axon terminals in the macaque striate cortex. *J Comp Neurol* **264,** 73-91.

Flammer J & Drance SM. (1984). Correlation between color vision scores and quantitative perimetry in suspected glaucoma. *Archives of ophthalmology (Chicago, Ill : 1960)* **102,** 38-39.

Foerster O, Gagel O & Mahoney W. (1936). Über die Anatomie, Physiologie und Pathologie der Pupillarinnervation. *Verh Dtsch Ges Inn Med* **48,** 386-397.

Fortune B & Hood DC. (2003). Conventional Pattern-Reversal VEPs Are Not Equivalent to Summed Multifocal VEPs. *Investigative Ophthalmology & Visual Science* **44,** 1364-1375.

Foster PJ & Jiang Y. (2014). Epidemiology of myopia. *Eye (Lond)* **28,** 202-208.

Fredette MJ, Giguere A, Anderson DR, Budenz DL & McSoley J. (2015). Comparison of Matrix with Humphrey Field Analyzer II with SITA. *Optometry and vision science : official publication of the American Academy of Optometry* **92,** 527-536.

Frisen L. (2002). New, sensitive window on abnormal spatial vision: rarebit probing. *Vision research* **42,** 1931-1939.

Frisen L. (2003). Spatial vision in visually asymptomatic subjects at high risk for multiple sclerosis. *J Neurol Neurosurg Psychiatry* **74,** 1145-1147.

Gale R, Scanlon PH, Evans M, Ghanchi F, Yang Y, Silvestri G, Freeman M, et al. (2017). Action on diabetic macular oedema: achieving optimal patient management in treating visual impairment due to diabetic eye disease. *Eye* **31**.

Gamlin PD, McDougal DH, Pokorny J, Smith VC, Yau K-W & Dacey DM. (2007). Human and Macaque Pupil Responses Driven by Melanopsin-Containing Retinal Ganglion Cells. *Vision research* **47,** 946-954.

70

Gamlin PDR. (2006). The pretectum: connections and oculomotor-related roles. In *Progress in Brain Research*, ed. Büttner-Ennever JA, pp. 379-405. Elsevier.

Gamlin PDR & Reiner A. (1991). The edinger-westphal nucleus: Sources of input influencing accommodation, pupilloconstriction, and choroidal blood flow. *The Journal of Comparative Neurology* **306,** 425-438.

Gastinger MJ, O'Brien JJ, Larsen NB & Marshak DW. (1999). Histamine immunoreactive axons in the macaque retina. *Investigative Ophthalmology & Visual Science* **40,** 487-495.

Ghazi NG & Green WR. (2002). Pathology and pathogenesis of retinal detachment. *Eye (Lond)* **16,** 411-421.

Giolli RA & Tigges J. (1970). The primary optic pathways and nuclei of primates. *Advances in primatology* **1,** 29-54.

Gjörloff K, Andréasson S & Ehinger B. (2004). Standardized full-field electroretinography in rabbits. *Documenta Ophthalmologica* **109,** 163-168.

Gloor BP. (2009). Franz Fankhauser: The Father of the Automated Perimeter. *Survey of Ophthalmology* **54,** 417-425.

Gloor BR. (2010). Hans Goldmann (1899-1991). *European journal of ophthalmology* **20,** 1-11.

Goga C & Türe U. (2015). The anatomy of Meyer's loop revisited: changing the anatomical paradigm of the temporal loop based on evidence from fiber microdissection. *Journal of Neurosurgery* **122,** 1253-1262.

Goldberg I, Graham SL & Klistorner AI. (2002). Multifocal objective perimetry in the detection of glaucomatous field loss11Drs Graham, and Klistorner have patents pending for techniques used by the ObjectiVision system and stock in ObjectiVision. Klistorner is a Sydney Medical Foundation research fellow. *American Journal of Ophthalmology* **133,** 29-39.

Gragoudas ES, Adamis AP, Cunningham ET, Feinsod M, Guyer DR & Neova VISO. (2004). Pegaptanib for neovascular age-related macular degeneration. *New Engl J Med* **351,** 2805-2816.

Graham SL, Klistorner AI, Grigg JR & Billson FA. (2000). Objective VEP perimetry in glaucoma: asymmetry analysis to identify early deficits. *J Glaucoma* **9,** 10-19.

Greaves D & Perkins ES. (1952). Influence of the sympathetic nervous system on the intra-ocular pressure and vascular circulation of the eye. *The British journal of ophthalmology* **36,** 258.

Greenberg A, Su D, Simonson J, Park SC, Tello C, Liebmann J & Ritch R. (2012). Efficacy Of The Amsler Grid Test In Evaluating Glaucomatous Central Visual Field Defects. *Investigative Ophthalmology & Visual Science* **53,** 177-177.

Greenstein VC, Holopigian K, Seiple W, Carr RE & Hood DC. (2004). Atypical multifocal ERG responses in patients with diseases affecting the photoreceptors. *Vision research* **44,** 2867-2874.

Gross AKW, T.G. (2011). Biochemical Cascade of Phototransduction. In *Adler's Physiology of the Eye*, eleventh edn, ed. Kaufman PLA, A; Levin, L.A; Nilsson, S.F.E; Hoeve, J.V; Wu, S.M., pp. 394-410. Saunders & Elsevier, UK, USA.

Grosso A, Veglio F, Porta M, Grignolo FM & Wong TY. (2005). Hypertensive retinopathy revisited: some answers, more questions. *Brit J Ophthalmol* **89,** 1646-1654.

Group CR, Martin DF, Maguire MG, Ying GS, Grunwald JE, Fine SL & Jaffe GJ. (2011). Ranibizumab and bevacizumab for neovascular age-related macular degeneration. *N Engl J Med* **364,** 1897-1908.

71

Group ETDRSR. (1991). Grading Diabetic Retinopathy from Stereoscopic Color Fundus Photographs—An Extension of the Modified Airlie House Classification: ETDRS Report Number 10. *Ophthalmology* **98,** 786-806.

Group MPS. (1990). Krypton laser photocoagulation for neovascular lesions of age-related macular degeneration. Results of a randomized clinical trial. Macular Photocoagulation Study Group. *Archives of ophthalmology (Chicago, Ill : 1960)* **108,** 816-824.

Group SMDS. (1982). Argon Laser Photocoagulation for Senile Macular Degeneration: Results of a Randomized Clinical Trial. *Archives of Ophthalmology* **100,** 912-918.

Group TDRSR. (1976). Preliminary report on effects of photocoagulation therapy. The Diabetic Retinopathy Study Research Group. *Am J Ophthalmol* **81,** 383-396.

Group TDRSR. (1987). Indications for photocoagulation treatment of diabetic retinopathy: Diabetic Retinopathy Study Report no. 14. *International Ophthalmology Clinics* **27,** 239-253.

Grp A-REDSR. (2001). The age-related eye disease study system for classifying age-related macular degeneration from stereoscopic color fundus photographs: The Age-Related Eye Disease Study Report Number 6. *American Journal of Ophthalmology* **132,** 668-681.

Gullapalli V, Sugino I & Zarbin M. (2008). Mueller cells and the retinal pigment epithelium. In *Albert and Jakobiec's principles and practice of ophthalmology*, pp. 1633-1639. Saunders/Elsevier, Philadelphia.

Hamill TR, Post RB, Johnson CA & Keltner JL. (1984). Correlation of color vision deficits and observable changes in the optic disc in a population of ocular hypertensives. *Archives of ophthalmology (Chicago, Ill : 1960)* **102,** 1637-1639.

Hansen RM, Moskowitz A & Fulton AB. (2009). Multifocal ERG Responses in Infants. *Investigative Ophthalmology & Visual Science* **50,** 470-475.

Harrington ME. (1997). The ventral lateral geniculate nucleus and the intergeniculate leaflet: interrelated structures in the visual and circadian systems. *Neurosci Biobehav Rev* **21,** 705-727.

Harris A, Ciulla TA, Chung H & Martin B. (1998). Regulation of retinal and optic nerve blood flow. *Archives of Ophthalmology* **116,** 1491-1495.

Hastie T & Stuetzle W. (1989). Principal curves. *J Am Statistical Soc* **84,** 502–516.

Hayreh SS. (2011a). *Structure of the Optic Nerve in Ischemic Optic Neuropathies*. Springer, Iowa, USA.

Hayreh SS. (2011b). Treatment of non-arteritic anterior ischaemic optic neuropathy. *Br J Ophthalmol* **95,** 1617-1618.

Heijl A. (2012). *The Field Analyzer Primer: Effective Perimetry*. Carl Zeiss Meditec, Inc., Dublin, California, USA.

Heijl AP, V.M. (2002). The Essentials of Perimetry. In *The Field Analyzer Primer:* , Third edn, ed. Haley MJ, pp. Page 3-13. Carl Zeiss Meditec Inc., Dublin, California.

Hitchcock PF & Hickey TL. (1980). Prenatal development of the human lateral geniculate nucleus. *J Comp Neurol* **194,** 395-411.

Hood DC, Bach M, Brigell M, Keating D, Kondo M, Lyons JS, Marmor MF, et al. (2012a). ISCEV standard for clinical multifocal electroretinography (mfERG) (2011 edition). *Doc Ophthalmol* **124,** 1-13.

72

Hood DC, Bach M, Brigell M, Keating D, Kondo M, Lyons JS, Marmor MF, et al. (2012b). ISCEV standard for clinical multifocal electroretinography (mfERG) (2011 edition). *Documenta ophthalmologica Advances in ophthalmology* **124,** 1-13.

Hood DC, Bach M, Brigell M, Keating D, Kondo M, Lyons JS & Palmowski-Wolfe AM. (2008). ISCEV guidelines for clinical multifocal electroretinography (2007 edition). *Doc Ophthalmol* **116,** 1-11.

Hood DC & Greenstein VC. (2003). Multifocal VEP and ganglion cell damage: applications and limitations for the study of glaucoma. *Progress in Retinal and Eye Research* **22,** 201-251.

Hood DC, Zhang X, Hong JE & Chen CS. (2002). Quantifying the benefits of additional channels of multifocal VEP recording. *Doc Ophthalmol* **104,** 303-320.

Hood DCO, J. G.; Chen, C. S.; Winn, B. J. (2003). The mfERG: Applications and Limitations in Neuro-ophthalmology. *Neuro-ophthalmology*.

Horn AK, Eberhorn A, Hartig W, Ardeleanu P, Messoudi A & Buttner-Ennever JA. (2008). Perioculomotor cell groups in monkey and man defined by their histochemical and functional properties: reappraisal of the Edinger-Westphal nucleus. *J Comp Neurol* **507,** 1317-1335.

Horn AK, Schulze C & Radtke-Schuller S. (2009). The Edinger-Westphal nucleus represents different functional cell groups in different species. *Ann N Y Acad Sci* **1164,** 45-50.

Hoyt WF & Luis O. (1962). Visual fiber anatomy in the infrageniculate pathway of the primate: Uncrossed and crossed retinal quadrant fiber projections studied with nauta silver stain. *Archives of Ophthalmology* **68,** 94-106.

Hutchins B & Weber JT. (1985). The pretectal complex of the monkey: A reinvestigation of the morphology and retinal terminations. *The Journal of Comparative Neurology* **232,** 425-442.

IAPB. (2017a). The International Agency for the Prevention of Blindness.

IAPB. (2017b). The WHO Global Action Plan 2014-19.

IAPB. (2018). Summary Report of Rapid Assessment of Avoidable Blindness in Bhutan - 2018.

Ichida JM & Casagrande VA. (2002). Organization of the feedback pathway from striate cortex (V1) to the lateral geniculate nucleus (LGN) in the owl monkey (Aotus trivirgatus). *J Comp Neurol* **454,** 272-283.

Ip MS, Domalpally A, Hopkins JJ, Wong P & Ehrlich JS. (2012). Long-term Effects of Ranibizumab on Diabetic Retinopathy Severity and Progression. *Archives of Ophthalmology* **130,** 1145-1152.

Isaza G, Donaldson L & Chaudhary V. (2019). Increased incidence of retinopathy of prematurity and evolving treatment modalities at a Canadian tertiary centre. *Canadian Journal of Ophthalmology* **54,** 269-274.

Isipradit S, Sirimaharaj M, Charukamnoetkanok P, Thonginnetra O, Wongsawad W, Sathornsumetee B, Somboonthanakij S, et al. (2014). The first rapid assessment of avoidable blindness (RAAB) in Thailand. *PloS one* **9,** e114245.

Jackman SL, Babai N, Chambers JJ, Thoreson WB & Kramer RH. (2011). A Positive Feedback Synapse from Retinal Horizontal Cells to Cone Photoreceptors. *PLoS Biology* **9,** e1001057.

James AC. (2003a). The pattern-pulse multifocal visual evoked potential. *Invest Ophthalmol Vis Sci* **44,** 879-890.

James AC. (2003b). The Pattern-Pulse Multifocal Visual Evoked Potential. *Investigative Ophthalmology & Visual Science* **44,** 879-890.

73

James AC, Ruseckaite R & Maddess T. (2005). Effect of temporal sparseness and dichoptic presentation on multifocal visual evoked potentials. *Vis Neurosci* **22,** 45-54.

Jasper HH. (1958). Reports of Committee on Methods of Clinical Examination Electroencephalography. *Clinical Neurophysiology* **10,** Page 370-375.

Jeffrey GL. (2011). Optic Nerve. In *Adler's Physiology of the Eye*, Eleventh edn, ed. Kaufman. P.L; Alm AL, L.A; Nilsson, S.F.E; Hoeve, J.V; Wu, S.M., pp. Page. 550-573. Sanuders & Elsevier, UK, USA.

Johnson CA. (2013). Psychophysical factors that have been applied to clinical perimetry. *Vision research* **90,** 25-31.

Johnson CA, Adams AJ, Casson EJ & Brandt JD. (1993a). Blue-on-yellow perimetry can predict the development of glaucomatous visual field loss. *Archives of ophthalmology (Chicago, Ill : 1960)* **111,** 645-650.

Johnson CA, Adams AJ, Casson EJ & Brandt JD. (1993b). Progression of early glaucomatous visual field loss as detected by blue-on-yellow and standard white-on-white automated perimetry. *Archives of ophthalmology (Chicago, Ill : 1960)* **111,** 651-656.

Johnson CA, Wall M & Thompson HS. (2011). A History of Perimetry and Visual Field Testing. *Optometry and Vision Science* **88,** E8-E15.

Joselevitch C. (2008). Human retinal circuitry and physiology. *Psychology & Neuroscience* **1,** 141-165.

Jung SK, Lee JH, Kakizaki H & Jee D. (2012). Prevalence of myopia and its association with body stature and educational level in 19-year-old male conscripts in seoul, South Korea. *Invest Ophthalmol Vis Sci* **53,** 5579-5583.

Kalaboukhova L & Lindblom B. (2003). Frequency doubling technology and high-pass resolution perimetry in glaucoma and ocular hypertension. *Acta Ophthalmologica Scandinavica* **81,** 247-252.

Kaliner E, Cohen MJ, Miron H, Kogan M & Blumenthal EZ. (2007). Retinal nerve fiber layer split bundles are true anatomic variants. *Ophthalmology* **114,** 2259-2264.

Kanagalingam S & Miller NR. (2015). Horner syndrome: clinical perspectives. *Eye and Brain* **7,** 35.

Kaneko A. (1973). Receptive field organization of bipolar and amacrine cells in the goldfish retina. *J Physiol* **235,** 133-153.

Kaneko A & Tachibana M. (1987). GABA mediates the negative feedback from amacrine to bipolar cells. *Neurosci Res Suppl* **6,** S239-251.

Kardon R. (2011). Regulation of light through the pupil. *Adler's physiology of the eye 11th ed New York/Philadelphia: Saunders, Elsevier*.

Kardon RH, Kirkali PA & Thompson HS. (1991). Automated pupil perimetry. Pupil field mapping in patients and normal subjects. *Ophthalmology* **98,** 485-495; discussion 495-486.

Kawasaki A & Kardon RH. (2007). Intrinsically photosensitive retinal ganglion cells. *Journal of neuro-ophthalmology : the official journal of the North American Neuro-Ophthalmology Society* **27,** 195-204.

Kayama Y, Shimada S, Hishikawa Y & Ogawa T. (1989). Effects of stimulating the dorsal raphe nucleus of the rat on neuronal activity in the dorsal lateral geniculate nucleus. *Brain Res* **489,** 1-11.

Kimura E, Abe S & Goryo K. (2014). Attenuation of the pupillary response to luminance and color changes during interocular suppression. *Journal of Vision* **14,** 14-14.

74

Klein R, Cruickshanks KJ, Nash SD, Krantz EM, Nieto FJ, Huang GH, Pankow JS, et al. (2010). The prevalence of age-related macular degeneration and associated risk factors. *Archives of ophthalmology (Chicago, Ill : 1960)* **128,** 750-758.

Klein R, Klein BE, Jensen SC & Meuer SM. (1997). The five-year incidence and progression of age-related maculopathy: the Beaver Dam Eye Study. *Ophthalmology* **104,** 7-21.

Klein R, Klein BE, Knudtson MD, Meuer SM, Swift M & Gangnon RE. (2007). Fifteen-year cumulative incidence of age-related macular degeneration: the Beaver Dam Eye Study. *Ophthalmology* **114,** 253-262.

Kline RPR, H.; Dowling, J. E. (1978). Generation of b-wave currents in the skate retina. In *National Academy of Sciences*, pp. Pages 5727-5731.

Klistorner AI, Graham SL, Grigg JR & Billson FA. (1998). Multifocal topographic visual evoked potential: improving objective detection of local visual field defects. *Invest Ophthalmol Vis Sci* **39,** 937-950.

Koch SMU, E.M. (2011). Development of Retinogeniculate Projections. In *Adler's Physiology of the Eye*, Eleventh edn, ed. Kaufman PLA, A; Levin, L.A; Nilsson, S.F.E; Hoeve, J.V; Wu, S.M., pp. Page. 725-731. Saunders & Elsevier, UK, USA.

Kolb H. (2007). The Organization of the Retina and Visual System. In *Webvision: The Organization of the Retina and Visual System*, ed. Kolb H, Fernandez E & Nelson R. University of Utah Health Sciences Center, Salt Lake City (UT).

Kolic M, Chain A, James A, Maddess T & Carle C. (2013). Structure and function in multifocal pupillographic objective perimetry (mfPOP). *Investigative Ophthalmology & Visual Science* **54,** 2294-2294.

Kozicz T, Bittencourt JC, May PJ, Reiner A, Gamlin PDR, Palkovits M, Horn AKE, et al. (2011). THE EDINGER-WESTPHAL NUCLEUS: A HISTORICAL, STRUCTURAL AND FUNCTIONAL PERSPECTIVE ON A DICHOTOMOUS TERMINOLOGY. *The Journal of comparative neurology* **519,** 1413-1434.

Kuchiiwa S. (1990). Morphology of the accessory ciliary ganglion of the cat. *Anatomy and Embryology* **181,** 299-303.

Kuchiiwa S, Kuchiiwa T & Nakagawa S. (1994). Localization of preganglionic neurons of the accessory ciliary ganglion in the midbrain: HRP and WGA-HRP studies in the cat. *The Journal of Comparative Neurology* **340,** 577-591.

Kuchiiwa S, Kuchiiwa T, Nakagawa S & Ushikai M. (1993). Oculomotor parasympathetic pathway to the accessory ciliary ganglion bypassing the main ciliary ganglion by way of the trigeminal nerve. *Neuroscience research* **18,** 79-82.

Kuchiiwa S, Kuchiiwa T & Suzuki T. (1989). Comparative anatomy of the accessory ciliary ganglion in mammals. *Anatomy and Embryology* **180,** 199-205.

Kuwayama Y, Grimes PA, Ponte B & Stone RA. (1987). Autonomic neurons supplying the rat eye and the intraorbital distribution of vasoactive intestinal polypeptide (VIP)-like immunoreactivity. *Experimental eye research* **44,** 907-922.

Laatikainen L, Tolppanen EM & Harju H. (1985). Epidemiology of rhegmatogenous retinal detachment in a Finnish population. *Acta Ophthalmol (Copenh)* **63,** 59-64.

Lai TY, Chan WM, Li H, Lai RY & Lam DS. (2005). Multifocal electroretinographic changes in patients receiving hydroxychloroquine therapy. *Am J Ophthalmol* **140,** 794-807.

75

Landers J, Sharma A, Goldberg I & Graham S. (2006). A comparison of diagnostic protocols for interpretation of frequency doubling perimetry visual fields in glaucoma. *J Glaucoma* **15,** 310-314.

Landers JA, Goldberg I & Graham SL. (2003). Detection of early visual field loss in glaucoma using frequency-doubling perimetry and short-wavelength automated perimetry. *Archives of ophthalmology (Chicago, Ill : 1960)* **121,** 1705-1710.

Laouri M, Chen E, Looman M & Gallagher M. (2011). The burden of disease of retinal vein occlusion: review of the literature. *Eye* **25,** 981-988.

Lascaratos J & Marketos S. (1988). A historical outline of Greek ophthalmology from the Hellenistic period up to the establishment of the first universities. *Doc Ophthalmol* **68,** 157-169.

Lee YW & Schetzen M. (1965). Measurement of the Wiener Kernels of a Non-linear System by Cross-correlation. *International Journal of Control* **2,** 237-254.

Leichnetz GR. (1990). Preoccipital cortex receives a differential input from the frontal eye field and projects to the pretectal olivary nucleus and other visuomotor-related structures in the rhesus monkey. *Vis Neurosci* **5,** 123-133.

Lepcha NT, Chettri CK, Getshen K, Rai BB, Bindiganavale Ramaswamy S, Saibaba S, Nirmalan PK, et al. (2013). Rapid Assessment of Avoidable Blindness in Bhutan. *Ophthalmic Epidemiology* **20,** 212-219.

Lepcha NT, Sharma IP, Sapkota YD, Das T, Phuntsho T, Tenzin N, Shamanna BR, et al. (2019). Changing trends of blindness, visual impairment and cataract surgery in Bhutan: 2009–2018. *PloS one* **14,** e0216398.

Leskov IB, Klenchin VA, Handy JW, Whitlock GG, Govardovskii VI, Bownds MD, Lamb TD, et al. (2000). The gain of rod phototransduction: reconciliation of biochemical and electrophysiological measurements. *Neuron* **27,** 525-537.

LeVere TE. (1978). The primary visual system of the rat: A primer of its anatomy. *Physiological Psychology* **6,** 142-169.

Ling S, Pratte MS & Tong F. (2015). Attention alters orientation processing in the human lateral geniculate nucleus. *Nat Neurosci* **18,** 496-498.

Livingstone MS & Hubel DH. (1987). Psychophysical evidence for separate channels for the perception of form, color, movement, and depth. *Journal of Neuroscience* **7,** 3416-3468.

Loewy AD & Saper CB. (1978). Edinger-Westphal nucleus: projections to the brain stem and spinal cord in the cat. *Brain Res* **150,** 1-27.

Lowenstein O & Loewenfeld IE. (1958). Electronic pupillography: A new instrument and some clinical applications. *AMA Archives of Ophthalmology* **59,** 352-363.

Lui F, Gregory KM, Blanks RH & Giolli RA. (1995). Projections from visual areas of the cerebral cortex to pretectal nuclear complex, terminal accessory optic nuclei, and superior colliculus in macaque monkey. *J Comp Neurol* **363,** 439-460.

MacLeish P & Makino C. (2011). Photoresponses of rods and cones. *Adler's physiology of the eye 11th ed New York, Philadelphia/London: Saunders/Elsevier*.

Maddess T. (1991a). Method and apparatus for use in diagnosis of glaucoma. ANU, Australia.

Maddess T. (1991b). Method and apparatus for use in diagnosis of glaucoma. ANU, USA.

Maddess T. (2014). Modeling the relative influence of fixation and sampling errors on retest variability in perimetry. *Graefe's archive for clinical and experimental ophthalmology =*

76

Albrecht von Graefes Archiv fur klinische und experimentelle Ophthalmologie **252,** 1611-1619.

Maddess T, Bedford SM, Goh XL & James AC. (2009). Multifocal pupillographic visual field testing in glaucoma. *Clin Exp Ophthalmol* **30,** 678-686.

Maddess T, Ho Y-L, Wong SSY, Kolic M, Goh X-L, Carle CF & James AC. (2010). Multifocal pupillographic perimetry with white and colored stimuli *J Glaucoma* **20,** 336-343.

Maddess T, Ho Y-L, Wong SSY, Kolic M, Goh X-L, Carle CF & James AC. (2011a). Multifocal Pupillographic Perimetry With White and Colored Stimuli. *Journal of Glaucoma* **20,** 336-343.

Maddess T, James AC & Bowman EA. (2005). Contrast response of temporally sparse and contrast reversing dichoptic multifocal evoked potentials. *Visual Neurosci* **22,** 153-162.

Maddess T, James AC, Goldberg I, Wine S & Dobinson J. (2000a). Comparing a parallel PERG, automated perimetry, and frequency-doubling thresholds. *Invest Ophthalmol Vis Sci* **41,** 3827-3832.

Maddess T, James AC, Goldberg I, Wine S & Dobinson J. (2000b). A spatial frequency-doubling illusion-based pattern electroretinogram for glaucoma. *Invest Ophthalmol Vis Sci* **41,** 3818-3826.

Maddess T, Lueck CJ, Voicu C & James AC. (2011b). Multifocal Objective Pupil Perimetry (mfpop) In Ms. *Investigative Ophthalmology & Visual Science* **52,** 267-267.

Mainster MA, Timberlake GT, Webb RH & Hughes GW. (1982). Scanning laser ophthalmoscopy. Clinical applications. *Ophthalmology* **89,** 852-857.

Malpeli JG & Baker FH. (1975). The representation of the visual field in the lateral geniculate nucleus of Macaca mulatta. *The Journal of Comparative Neurology* **161,** 569-594.

Marano F, Deutman AF, Leys A & Aandekerk AL. (2000). Hereditary retinal dystrophies and choroidal neovascularization. *Graefe's archive for clinical and experimental ophthalmology = Albrecht von Graefes Archiv fur klinische und experimentelle Ophthalmologie* **238,** 760-764.

Marc RE. (2011). The Synaptic Organisation of the Retina. In *Adler's Physiology of the Eye*, ed. Kaufman PLA, A; Levin, L.A; Nilsson, S.F.E; Hoeve, J.V; Wu, S.M., pp. Page 443-458. Saunders & Elsevier, UK, USA.

Markowitz SN & Reyes SV. (2013). Microperimetry and clinical practice: an evidence-based review. *Canadian journal of ophthalmology Journal canadien d'ophtalmologie* **48,** 350-357.

Marmor MF, Fulton AB, Holder GE, Miyake Y, Brigell M, Bach M & International Society for Clinical Electrophysiology of V. (2009). ISCEV Standard for full-field clinical electroretinography (2008 update). *Doc Ophthalmol* **118,** 69-77.

Marmor MF & Zrenner E. (1998). Standard for clinical electroretinography (1999 update). *Documenta Ophthalmologica* **97,** 143-156.

May CA. (2004). Morphology of the long and short uveal nerves in the human eye. *Journal of Anatomy* **205,** 113-120.

May PJ, Reiner AJ & Ryabinin AE. (2008a). Comparison of the distributions of urocortin-containing and cholinergic neurons in the perioculomotor midbrain of the cat and macaque. *J Comp Neurol* **507,** 1300-1316.

May PJ, Sun W & Erichsen JT. (2008b). Defining the Pupillary Component of the Perioculomotor Preganglionic Population within a Unitary Primate Edinger-Westphal Nucleus. *Progress in brain research* **171,** 97-106.

77

McAllister IL & Constable IJ. (1995). Laser-induced chorioretinal venous anastomosis for treatment of nonischemic central retinal vein occlusion. *Archives of ophthalmology (Chicago, Ill : 1960)* **113,** 456-462.

McDougal DH & Gamlin PD. (2015). Autonomic control of the eye. *Comprehensive Physiology* **5,** 439-473.

McIntosh RL, Rogers SL, Lim L, Cheung N, Wang JJ, Mitchell P, Kowalski JW, et al. (2010). Natural history of central retinal vein occlusion: an evidence-based systematic review. *Ophthalmology* **117,** 1113-1123 e1115.

McKee SP & Nakayama K. (1984). The detection of motion in the peripheral visual field. *Vision research* **24,** 25-32.

McKendrick AM. (2005). Recent developments in perimetry: test stimuli and procedures. *Clinical and Experimental Optometry* **88,** 73-80.

Medeiros FA, Sample PA & Weinreb RN. (2004). Frequency doubling technology perimetry abnormalities as predictors of glaucomatous visual field loss. *Am J Ophthalmol* **137,** 863-871.

Membrey LF, F. W. (2000). Effect of lens opacity on white-on-white perimetry, frequency doubling perimetry, and motion detection perimetry. In *Perimetry Update 2000/2001*, ed. Wall MW, J., pp. 259-266. Kugler Publications, Netherland.

Menaa F, Khan BA, Uzair B & Menaa A. (2017). Sickle cell retinopathy: improving care with a multidisciplinary approach. *J Multidiscip Healthc* **10,** 335-346.

Meyer CH & Holz FG. (2011). Preclinical aspects of anti-VEGF agents for the treatment of wet AMD: ranibizumab and bevacizumab. *Eye (Lond)* **25,** 661-672.

Michael CR. (1988). Retinal afferent arborization patterns, dendritic field orientations, and the segregation of function in the lateral geniculate nucleus of the monkey. *Proceedings of the National Academy of Sciences of the United States of America* **85,** 4914-4918.

Michaelides M, Stover NB, Francis PJ & Weleber RG. (2011). Retinal toxicity associated with hydroxychloroquine and chloroquine: risk factors, screening, and progression despite cessation of therapy. *Archives of ophthalmology (Chicago, Ill : 1960)* **129,** 30-39.

Miguel-Jimenez JM, Ortega S, Boquete L, Rodriguez-Ascariz JM & Blanco R. (2011). Multifocal ERG wavelet packet decomposition applied to glaucoma diagnosis. *Biomedical engineering online* **10,** 37.

Mikelberg FS, Yidegiligne HM, White VA & Schulzer M. (1991). Relation between Optic Nerve Axon Number and Axon Diameter to Scleral Canal Area. *Ophthalmology* **98,** 60-63.

Miller AM & Schwartz EA. (1983). Evidence for the identification of synaptic transmitters released by photoreceptors of the toad retina. *The Journal of Physiology* **334,** 325-349.

Morgan IG, French AN, Ashby RS, Guo X, Ding X, He M & Rose KA. (2018). The epidemics of myopia: Aetiology and prevention. *Prog Retin Eye Res* **62,** 134-149.

Morgenstern NA, Bourg J & Petreanu L. (2016). Multilaminar networks of cortical neurons integrate common inputs from sensory thalamus. *Nat Neurosci* **19,** 1034-1040.

Morris JS, Öhman A & Dolan RJ. (1999). A subcortical pathway to the right amygdala mediating “unseen” fear. *Proceedings of the National Academy of Sciences of the United States of America* **96,** 1680-1685.

78

Morrison JH & Foote SL. (1986). Noradrenergic and serotoninergic innervation of cortical, thalamic, and tectal visual structures in old and new world monkeys. *The Journal of Comparative Neurology* **243,** 117-138.

Moss ID, Wild JM & Whitaker DJ. (1995). The influence of age-related cataract on blue-on-yellow perimetry. *Invest Ophthalmol Vis Sci* **36,** 764-773.

Müller B & Peichl L. (1993). *Horizontal cells in the cone-dominated tree shrew retina: Morphology, photoreceptor contacts, and topographical distribution*, vol. 13.

Naber M, Frässle S & Einhäuser W. (2011). Perceptual Rivalry: Reflexes Reveal the Gradual Nature of Visual Awareness. *PloS one* **6,** e20910.

Nassi JJ & Callaway EM. (2006). Multiple Circuits Relaying Primate Parallel Visual Pathways to the Middle Temporal Area. *The Journal of neuroscience : the official journal of the Society for Neuroscience* **26,** 12789-12798.

Negrel AD & Thylefors B. (1998). The global impact of eye injuries. *Ophthalmic Epidemiol* **5,** 143-169.

Newman E & Reichenbach A. (1996). The Muller cell: a functional element of the retina. *Trends Neurosci* **19,** 307-312.

Nie F & Wong-Riley M. (1999). Nuclear respiratory factor-2 subunit protein: correlation with cytochrome oxydase and regulation by functional activity in the monkey primary visual cortex. *J Comp Neurol* **404,** 310-320.

Noback CR. (1975). The visual system of primates in phylogenetic studies. In *Phylogeny of the Primates*, pp. 199-218. Springer.

NOVARTIS. (2019). Novartis receives FDA approval for Beovu®, offering wet AMD patients vision gains and greater fluid reductions vs aflibercept. Basel, Switzerland.

O'Connell JEA. (1973). The anatomy of the optic chiasma and heteronymous hemianopia. *Journal of Neurology, Neurosurgery, and Psychiatry* **36,** 710-723.

Odom JV, Bach M, Brigell M, Holder GE, McCulloch DL, Tormene AP & Vaegan. (2010). ISCEV standard for clinical visual evoked potentials (2009 update). *Doc Ophthalmol* **120,** 111-119.

Oellers P, Grewal DS & Fekrat S. (2016). Role of aflibercept for macular edema following branch retinal vein occlusion: comparison of clinical trials. *Clin Ophthalmol* **10**.

Ogden TE. (1983). Nerve fiber layer of the macaque retina: retinotopic organization. *Investigative Ophthalmology & Visual Science* **24,** 85-98.

Ong E-L, Zheng Y, Aung T, Tan L, Cheng C-Y, Wong T-Y & How A. (2014). Performance of the Moorfields Motion Displacement Test for Identifying Eyes with Glaucoma. *Ophthalmology* **121,** 88-92.

Palkovits S, Hirnschall N, Georgiev S, Leisser C & Findl O. (2018). Test-Retest Reproducibility of the Microperimeter MP3 With Fundus Image Tracking in Healthy Subjects and Patients With Macular Disease. *Transl Vis Sci Technol* **7,** 17.

Papadopoulos N, Martin J, Ruan Q, Rafique A, Rosconi MP, Shi E, Pyles EA, et al. (2012). Binding and neutralization of vascular endothelial growth factor (VEGF) and related ligands by VEGF Trap, ranibizumab and bevacizumab. *Angiogenesis* **15,** 171-185.

Park SH, Lee JS, Heo H, Suh Y-W, Kim S-H, Lim KH, Moon NJ, et al. (2015). A Nationwide Population-Based Study of Low Vision and Blindness in South Korea. *Investigative Ophthalmology & Visual Science* **56,** 484-493.

79

Park SJ, Choi NK, Park KH & Woo SJ. (2013). Five year nationwide incidence of rhegmatogenous retinal detachment requiring surgery in Korea. *PloS one* **8,** e80174.

Pascolini D & Mariotti SP. (2012). Global estimates of visual impairment: 2010. *Br J Ophthalmol* **96,** 614-618.

Passatore M & Pettorossi VE. (1976). Efferent fibers in the cervical sympathetic nerve influenced by light. *Experimental neurology* **52,** 66-82.

Patel A, Wollstein G, Ishikawa H & Schuman JS. (2007). Comparison of Visual Field Defects Using Matrix Perimetry and Standard Achromatic Perimetry. *Ophthalmology* **114,** 480-487.

Patel SN & Klufas MA. (2019). Evidence to date: ranibizumab and its potential in the treatment of retinopathy of prematurity. *Eye Brain* **11,** 25-35.

Pearce JG & Maddess T. (2016). Retest Variability in the Medmont M700 Automated Perimeter. *Optometry and vision science : official publication of the American Academy of Optometry* **93,** 272-280.

Penn AA, Riquelme PA, Feller MB & Shatz CJ. (1998). Competition in retinogeniculate patterning driven by spontaneous activity. *Science (New York, NY)* **279,** 2108-2112.

Penn JS, Madan A, Caldwell RB, Bartoli M, Caldwell RW & Hartnett ME. (2008). Vascular endothelial growth factor in eye disease. *Prog Retin Eye Res* **27,** 331-371.

Perlman I. (2017). Electroretinogram In *Webvision: The Organization of the retina and the visual system*. Wordpress, USA.

Perlman I, Kolb H & Nelson R. (1995). S-Potentials and Horizontal Cells. In *Webvision: The Organization of the Retina and Visual System*, ed. Kolb H, Fernandez E & Nelson R. Salt Lake City (UT).

Pham B, Thomas SM, Lillie E, Lee T, Hamid J, Richter T, Janoudi G, et al. (2019). Anti-vascular endothelial growth factor treatment for retinal conditions: a systematic review and meta-analysis. *BMJ Open* **9,** e022031.

Porciatti V. (2007). The mouse pattern electroretinogram. *Documenta ophthalmologica Advances in ophthalmology* **115,** 145-153.

Provis JM, Diaz CM & Dreher B. (1998). Ontogeny of the primate fovea: a central issue in retinal development. *Progress in neurobiology* **54,** 549-580.

Pula JH & Yuen CA. (2017). Eyes and stroke: the visual aspects of cerebrovascular disease. *Stroke Vasc Neurol* **2,** 210-220.

Quigley HA. (1999). Neuronal death in glaucoma. *Progress in Retinal and Eye Research* **18,** 39-57.

Quigley HA, Addicks EM & Green WR. (1982). Optic nerve damage in human glaucoma. III. Quantitative correlation of nerve fiber loss and visual field defect in glaucoma, ischemic neuropathy, papilledema, and toxic neuropathy. *Archives of ophthalmology (Chicago, Ill : 1960)* **100,** 135-146.

Quigley HA, Dunkelberger GR & Green WR. (1989). Retinal Ganglion Cell Atrophy Correlated With Automated Perimetry in Human Eyes With Glaucoma. *American Journal of Ophthalmology* **107,** 453-464.

Rademacher J, Caviness JVS, Steinmetz H & Galaburda AM. (1993). Topographical Variation of the Human Primary Cortices: Implications for Neuroimaging, Brain Mapping, and Neurobiology. *Cerebral Cortex* **3,** 313-329.

80

Rahi JS, Gilbert CE, Foster A & Minassian D. (1999). Measuring the burden of childhood blindness. *Br J Ophthalmol* **83,** 387-388.

Rai BB, Ashby R, French A & Maddess T. (2020a). Rural-urban difference in prevalence of Myopia: retrospective analysis of myopes presenting to the retina clinic at the national referral hospital in Bhutan over 3 years. *Graefe's archive for clinical and experimental ophthalmology = Albrecht von Graefes Archiv fur klinische und experimentelle Ophthalmologie* **Online**.

Rai BB, Dorji S, Zangmo P & Tshering T. (2016). Retained intraocular metallic foreign body causing retinal detachment. *Bhutan Health Journal* **2,** 48-52.

Rai BB, Morley MG, Bernstein PS & Maddess T. (2020b). Pattern of vitreo-retinal diseases at the national referral hospital in Bhutan: a retrospective, hospital-based study. *BMC Ophthalmology* **20**.

Rai BB, Morley MM, Zangmo P, Tshering T, Khatiwara AN, Bernstein PS & Maddess T. (2020c). Surgical management of vitreo-retinal diseases at the national referral hospital in Bhutan: a retrospective study. *BMC Ophthalmol* **Under Review**.

Rai BB, Sabeti F, Carle CF, Rohan EMF, Sarac O, van Kleef J & Maddess T. (2020d). Recovery dynamics of multifocal pupillographic objective perimetry from tropicamide dilation. *Graefe's archive for clinical and experimental ophthalmology = Albrecht von Graefes Archiv fur klinische und experimentelle Ophthalmologie* **258,** 191-200.

Rai BB, Shresthra MK, Thapa R, Essex RW, Paudyal G & Maddess T. (2019). Pattern and Presentation of Vitreo-Retinal Diseases: An Analysis of Retrospective Data at a Tertiary Eye Care Center in Nepal. *Asia-Pac J Ophthalmo* **8,** 481-488.

Ramke J, Brian G, Maher L, Qalo Qoqonokana M & Szetu J. (2012). Prevalence and causes of blindness and low vision among adults in Fiji. *Clinical & Experimental Ophthalmology* **40,** 490-496.

Reede D, Garcon E, R K Smoker W & Kardon R. (2008). *Horner's Syndrome: Clinical and Radiographic Evaluation*, vol. 18.

Reese BE. (2011). Development of the Retina and Optic Pathway. *Vision research* **51,** 613-632.

Reeves AG & Posner JB. (1969). The ciliospinal response in man. *Neurology* **19,** 1145-1145.

Reh TA & Moshiri A. (2006). The development of the retina. In *Retina*, ed. Ryan SJ, pp. 3-21. Elsevier Mosby

Rejdak R, Juenemann AG & Natarajan S. (2017). Posterior Segment Ocular Trauma: Timing and Indications for Vitrectomy. *J Ophthalmol* **2017,** 5250924.

Rogers SL, McIntosh RL, Lim L, Mitchell P, Cheung N, Kowalski JW, Nguyen HP, et al. (2010). Natural History of Branch Retinal Vein Occlusion: An Evidence-Based Systematic Review. *Ophthalmology* **117,** 1094-U1099.

Rosenfeld PJ, Brown DM, Heier JS, Boyer DS, Kaiser PK, Chung CY, Kim RY, et al. (2006). Ranibizumab for neovascular age-related macular degeneration. *N Engl J Med* **355,** 1419-1431.

Rosli Y, Maddess T, Dawel A & James AC. (2009). Multifocal frequency-doubling pattern visual evoked responses to dichoptic stimulation. *Clin Neurophysiol* **120,** 2100-2108.

Ruben S & Fitzke F. (1994). Correlation of peripheral displacement thresholds and optic disc parameters in ocular hypertension. *Br J Ophthalmol* **78,** 291-294.

Ruseckaite R, Maddess T, Danta G, Lueck CJ & James AC. (2005). Sparse multifocal stimuli for the detection of multiple sclerosis. *Ann Neurol* **57,** 904-913.

81

Sabeti F. (2011). Multifocal Pupillography in Patients with Ealy Age-related Macular Degeneration. In *Neuroscience*. Australian National University, Australia.

Sabeti F, James AC, Carle CF, Essex RW, Bell A & Maddess T. (2017). Comparing multifocal pupillographic objective perimetry (mfPOP) and multifocal visual evoked potentials (mfVEP) in retinal diseases. *Scientific Reports* **7,** 45847.

Sabeti F, James AC & Maddess T. (2011). Spatial and temporal stimulus variants for multifocal pupillography of the central visual field. *Vision research* **51,** 303-310.

Sabeti F, Maddess T, Essex RW & James AC. (2012). Multifocal pupillography identifies ranibizumab-induced changes in retinal function for exudative age-related macular degeneration. *Invest Ophthalmol Vis Sci* **53,** 253-260.

Sabeti F, Nolan CJ, James AC, Jenkins A & Maddess T. (2015). Multifocal Pupillography Identifies Changes in Visual Sensitivity According to Severity of Diabetic Retinopathy in Type 2 Diabetes. *Invest Ophthalmol Vis Sci* **56,** 4504-4513.

Salvetat ML, Zeppieri M, Parisi L & Brusini P. (2007). Rarebit Perimetry in Normal Subjects: Test–Retest Variability, Learning Effect, Normative Range, Influence of Optical Defocus, and Cataract Extraction. *Investigative Ophthalmology & Visual Science* **48,** 5320-5331.

Sample PA, Martinez GA & Weinreb RN. (1994). Short-wavelength automated perimetry without lens density testing. *Am J Ophthalmol* **118,** 632-641.

Sample PA, Taylor JD, Martinez GA, Lusky M & Weinreb RN. (1993). Short-wavelength color visual fields in glaucoma suspects at risk. *Am J Ophthalmol* **115,** 225-233.

Sanchez RM, Dunkelberger GR & Quigley HA. (1986). The number and diameter distribution of axons in the monkey optic nerve. *Investigative Ophthalmology & Visual Science* **27,** 1342-1350.

Sangroongruangsri S, Ratanapakorn T, Wu O, Anothaisintawee T & Chaikledkaew U. (2018). Comparative efficacy of bevacizumab, ranibizumab, and aflibercept for treatment of macular edema secondary to retinal vein occlusion: a systematic review and network meta-analysis. *Expert Rev Clin Phar* **11,** 903-916.

Sasaki K, Ideta H, Yonemoto J, Tanaka S, Hirose A & Oka C. (1995). Epidemiologic characteristics of rhegmatogenous retinal detachment in Kumamoto, Japan. *Graefe's archive for clinical and experimental ophthalmology = Albrecht von Graefes Archiv fur klinische und experimentelle Ophthalmologie* **233,** 772-776.

Schimiti RB, Avelino RR, Kara-Jose N & Costa VP. (2002). Full-threshold versus Swedish Interactive Threshold Algorithm (SITA) in normal individuals undergoing automated perimetry for the first time. *Ophthalmology* **109,** 2084-2092; discussion 2092.

Schlotzer-Schrehardt U, Viestenz A, Naumann GOH, Laqua H, Michels S & Schmidt-Erfurth U. (2002). Dose-related structural effects of photodynamic therapy on choroidal and retinal structures of human eyes. *Graef Arch Clin Exp* **240,** 748-757.

Schmid RW, H.; Wilhelm, B.; Kriegbaum, C.; Miliczek, K.; Wannek, U. (1995). Naso-temporal differences in pupillomotor sensitivity. *IOVS* **37,** 159.

Seigel D. (2002). AREDS investigators distort findings. *Archives of ophthalmology (Chicago, Ill : 1960)* **120,** 100-101.

Seiple W, Holopigian K, Clemens C, Greenstein VC & Hood DC. (2005). The multifocal visual evoked potential: An objective measure of visual fields? *Vision research* **45,** 1155-1163.

82

Shaarawy TMS, M. B.; Hitchins, R. A.; Crowston, J. G. (2009). Electrophysiology in Glaucoma Assessment. In *Glaucoma: Medical Diagnosis and Therapy*, pp. Page 151-171. Saunders & Elsevier, U.K.

Shah CP & Chen C. (2011). Review of therapeutic advances in diabetic retinopathy. *Ther Adv Endocrinol Metab* **2,** 39-53.

Shatz C & Kirkwood P. (1984). Prenatal development of functional connections in the cat's retinogeniculate pathway. *The Journal of Neuroscience* **4,** 1378-1397.

Shih T & Lindley C. (2006). Bevacizumab: An angiogenesis inhibitor for the treatment of solid malignancies. *Clin Ther* **28,** 1779-1802.

Simons E & Smith PG. (1994). Sensory and autonomic innervation of the rat eyelid: neuronal origins and peptide phenotypes. *Journal of chemical neuroanatomy* **7,** 35-47.

Sivertsen MS, Jorstad OK, Grevys A, Foss S, Moe MC & Andersen JT. (2018). Pharmaceutical compounding of aflibercept in prefilled syringes does not affect structural integrity, stability or VEGF and Fc binding properties. *Scientific Reports* **8**.

Slotnick SD, Klein SA, Carney T, Sutter E & Dastmalchi S. (1999). Using multi-stimulus VEP source localization to obtain a retinotopic map of human primary visual cortex. *Clinical Neurophysiology* **110,** 1793-1800.

Smith SA, Ellis CJ & Smith SE. (1979). Inequality of the direct and consensual light reflexes in normal subjects. *The British Journal of Ophthalmology* **63,** 523-527.

Smith SAS, S. E. (1980). Contraction anisocoria: nasal versus temporal illumination. *Br J of Ophthalmology* **64,** Page 933-934.

Sohn HJ, Han DH, Kim IT, Oh IK, Kim KH, Lee DY & Nam DH. (2011). Changes in Aqueous Concentrations of Various Cytokines After Intravitreal Triamcinolone Versus Bevacizumab for Diabetic Macular Edema. *American Journal of Ophthalmology* **152,** 686-694.

Springer C, Bultmann S, Volcker HE & Rohrschneider K. (2005). Fundus perimetry with the Micro Perimeter 1 in normal individuals: comparison with conventional threshold perimetry. *Ophthalmology* **112,** 848-854.

Sretavan D & Shatz C. (1986). Prenatal development of retinal ganglion cell axons: segregation into eye-specific layers within the cat's lateral geniculate nucleus. *The Journal of Neuroscience* **6,** 234-251.

Steele GE & Weller RE. (1993). Subcortical connections of subdivisions of inferior temporal cortex in squirrel monkeys. *Vis Neurosci* **10,** 563-583.

Stefansson E. (2009). The Mechanism of Retinal Photocoagulation – How Does the Laser Work? In *European Ophthalmic Review*. United Kingdom.

Stefansson E, Landers MB, 3rd & Wolbarsht ML. (1981). Increased retinal oxygen supply following pan-retinal photocoagulation and vitrectomy and lensectomy. *Trans Am Ophthalmol Soc* **79,** 307-334.

Steiger H-J & Büttner-Ennever J. (1979). Oculomotor nucleus afferents in the monkey demonstrated with horseradish peroxidase. *Brain research* **160,** 1-15.

Steinberg RH, Schmidt R & Brown KT. (1970). Intracellular Responses to Light from Cat Pigment Epithelium: Origin of the Electroretinogram c-Wave. *Nature* **227,** 728-730.

Steinbrook R. (2006). The Price of Sight — Ranibizumab, Bevacizumab, and the Treatment of Macular Degeneration. *The NEW ENGLAND JOURNAL of MEDICINE* **355,** 1409-1412.

83

Stem RMR, W. J.; Quigley, K. S. (2000). Eyes: Pupillographyand Electrooculography. In *Psychophysiological Recording*. Oxford, UK.

Strasburger H, Rentschler I & Jüttner M. (2011). Peripheral vision and pattern recognition: A review. *Journal of Vision* **11,** 13-13.

Strauss OH, H. (2011). The Function of the Retinal Pigment Epithelium. In *Adler's Physiology of the Eye*, Eleventh edn, ed. Kaufman PLA, A; Levin, L. A; Nilsson, S. F. E; Hoeve, J. V; Wu, S. M., pp. Page 325-332. Saunders & Elsevier, UK; USA.

Sutter EE. (1996). The field topography of the pupillary response: Rod and cone inputs. *Investigative Ophthalmology & Visual Science* **37,** 3157-3157.

Sutter EE. (2010). Noninvasive Testing Methods: Multifocal Electrophysiology. In *Encyclopedia of the Eye*, ed. Dartt DA, pp. Page 142-160. Academic Press, Oxford.

Sutter EE & Tran D. (1992). The field topography of ERG components in man--I. The photopic luminance response. *Vision research* **32,** 433-446.

Syed MM, Lee S, Zheng J & Zhou ZJ. (2004). Stage-dependent dynamics and modulation of spontaneous waves in the developing rabbit retina. *The Journal of Physiology* **560,** 533-549.

Szabadi E. (2013). Functional neuroanatomy of the central noradrenergic system. *Journal of psychopharmacology* **27,** 659-693.

Takayama K, Ooto S, Hangai M, Arakawa N, Oshima S, Shibata N, Hanebuchi M, et al. (2012). High-resolution imaging of the retinal nerve fiber layer in normal eyes using adaptive optics scanning laser ophthalmoscopy. *PloS one* **7,** e33158.

Tan L, Kondo M, Sato M, Kondo N & Miyake Y. (2001). Multifocal pupillary light response fields in normal subjects and patients with visual field defects. *Vision research* **41,** 1073-1084.

Tehovnik EJ & Slocum WM. (2003). Microstimulation of macaque V1 disrupts target selection: effects of stimulation polarity. *Exp Brain Res* **148,** 233-237.

Tewari R, Chandra P, Agarwal R & Azad R. (2019). Posterior laser barrage in advancing retinopathy of prematurity: A prospective randomized study. *Indian J Ophthalmol* **67,** 866-870.

Thapa R, Bajimaya S, Paudyal G, Khanal S, Tan S, Thapa SS & van Rens G. (2018). Prevalence and causes of low vision and blindness in an elderly population in Nepal: the Bhaktapur retina study. *BMC Ophthalmol* **18,** 42.

Thapa SS, Berg RV, Khanal S, Paudyal I, Pandey P, Maharjan N, Twyana SN, et al. (2011a). Prevalence of visual impairment, cataract surgery and awareness of cataract and glaucoma in Bhaktapur district of Nepal: the Bhaktapur Glaucoma Study. *BMC Ophthalmol* **11,** 2.

Thapa SS, Khanal S, Paudyal I, Twyana SN, Ruit S & van Rens GH. (2011b). Outcomes of cataract surgery: a population-based developing world study in the Bhaktapur district, Nepal. *Clin Exp Ophthalmol* **39,** 851-857.

Thapa SS, Thapa R, Paudyal I, Khanal S, Aujla J, Paudyal G & Rens Gv. (2013). Prevalence and pattern of vitreo-retinal diseases in Nepal: the Bhaktapur glaucoma study. *BMC Ophthalmology* **13,** 9-9.

Thavorncharoensap M, Teerawattananon Y, Natanant S, Kulpeng W, Yothasamut J & Werayingyong P. (2013). Estimating the willingness to pay for a quality-adjusted life year in Thailand: does the context of health gain matter? *ClinicoEconomics and Outcomes Research: CEOR* **5,** 29-36.

Thompson HS. (2005). Otto lowenstein, pioneer pupillographer. *Journal of neuro-ophthalmology : the official journal of the North American Neuro-Ophthalmology Society* **25,** 44-49.

84

Tick S, Rossant F, Ghorbel I, Gaudric A, Sahel J-A, Chaumet-Riffaud P & Paques M. (2011). Foveal Shape and Structure in a Normal Population. *Investigative Ophthalmology & Visual Science* **52,** 5105-5110.

Tietz J, Spohn G, Schmid G, Konrad J, Jampen S, Maurer P, Schmidt A, et al. (2015). Affinity and Potency of RTH258 (ESBA1008), a Novel Inhibitor of Vascular Endothelial Growth Factor A for the Treatment of Retinal Disorders. *Investigative Ophthalmology & Visual Science* **56**.

Traquair HM. (1927). *An Introduction to Clinical Perimetry*. London.

Traschütz A, Zinke W & Wegener D. (2012). Speed change detection in foveal and peripheral vision. *Vision research* **72,** 1-13.

Trobe J. (2010). Otto Lowenstein, MD, PhD: Founder of Pupillography. In *Neuro-ophthalmology Virtual Education Library: NOVEL*. Spencer S. Eccles Health Sciences Library, University of Utah., USA.

Ukai K. (1985). Spatial pattern as a stimulus to the pupillary system. *J of Optical Society of America* **2,** Page 1094-1100.

Ulldemolins AR, Lansingh VC, Valencia LG, Carter MJ & Eckert KA. (2012). Social inequalities in blindness and visual impairment: a review of social determinants. *Indian J Ophthalmol* **60,** 368-375.

Van Essen DC, Newsome WT & Maunsell JH. (1984). The visual field representation in striate cortex of the macaque monkey: asymmetries, anisotropies, and individual variability. *Vision research* **24,** 429-448.

Vaziri K, Schwartz SG, Kishor KS & Flynn HW, Jr. (2016). Tamponade in the surgical management of retinal detachment. *Clin Ophthalmol* **10,** 471-476.

Verdon-Roe GM, Westcott MC, Viswanathan AC, Fitzke FW & Garway-Heath DF. (2006). Exploration of the Psychophysics of a Motion Displacement Hyperacuity Stimulus. *Investigative Ophthalmology & Visual Science* **47,** 4847-4855.

Vrabec F. (1966). The temporal raphe of the human retina. *Am J Ophthalmol* **62,** 926-938.

Wall M. (1995a). Idiopathic intracranial hypertension. *Semin Ophthalmol* **10,** 251-259.

Wall M. (1995b). Optic disk edema with cotton-wool spots. *Surv Ophthalmol* **39,** 502-508.

Wall M, Brito, C., Kutzko, K. (1997). Motion Perimetry: Properties and results. Perimetry Update 1996/1997. In *International Perimetric Society* ed. Wall M, pp. 21-33.

Wall M, Chauhan B, Frisen L, House PH & Brito C. (2004). Visual field of high-pass resolution perimetry in normal subjects. *J Glaucoma* **13,** 15-21.

Wall M & Ketoff KM. (1995). Random dot motion perimetry in patients with glaucoma and in normal subjects. *Am J Ophthalmol* **120,** 587-596.

Wall M & May DR. (1987). Threshold Amsler Grid Testing in Maculopathies. *Ophthalmology* **94,** 1126-1133.

Wall M & Montgomery EB. (1995). Using motion perimetry to detect visual field defects in patients with idiopathic intracranial hypertension: a comparison with conventional automated perimetry. *Neurology* **45,** 1169-1175.

Wall M, Woodward KR, Doyle CK & Zamba G. (2010). The effective dynamic ranges of standard automated perimetry sizes III and V and motion and matrix perimetry. *Archives of ophthalmology (Chicago, Ill : 1960)* **128,** 570-576.

85

Walsh FB & Hoyt WF. (2008). *Walsh and Hoyt's clinical neuro-ophthalmology: the essentials*. Lippincott Williams & Wilkins.

Walters NB, Egan GF, Kril JJ, Kean M, Waley P, Jenkinson M & Watson JDG. (2003). In vivo identification of human cortical areas using high-resolution MRI: An approach to cerebral structure–function correlation. *Proceedings of the National Academy of Sciences* **100,** 2981-2986.

Wang J, O'Sullivan ML, Mukherjee D, Puñal VM, Farsiu S & Kay JN. (2017). Anatomy and spatial organization of Müller glia in mouse retina. *Journal of Comparative Neurology* **525,** 1759-1777.

Wang JJ, Zhu M & Le YZ. (2015). Functions of Muller cell-derived vascular endothelial growth factor in diabetic retinopathy. *World J Diabetes* **6,** 726-733.

Wang M & Wong WT. (2014). Microglia-Müller Cell Interactions in the Retina. *Advances in experimental medicine and biology* **801,** 333-338.

Wang X, Iannaccone A & Jablonski MM. (2005). Contribution of Müller cells toward the regulation of photoreceptor outer segment assembly. *Neuron glia biology* **1,** 1-6.

Warwick R. (1954). The ocular parasympathetic nerve supply and its mesencephalic sources. *J Anat* **88,** 71-93.

Wassle H, Grunert U, Rohrenbeck J & Boycott BB. (1989). Cortical magnification factor and the ganglion cell density of the primate retina. *Nature* **341,** 643-646.

Wassle H, Grunert U, Rohrenbeck J & Boycott BB. (1990). Retinal ganglion cell density and cortical magnification factor in the primate. *Vision research* **30,** 1897-1911.

Watanabe S-I, Koizumi A, Matsunaga S, Stocker JW & Kaneko A. (2000). GABA-Mediated Inhibition Between Amacrine Cells in the Goldfish Retina. *Journal of neurophysiology* **84,** 1826-1834.

Watson C & Vijayan N. (1995). The sympathetic innervation of the eyes and face: A clinicoanatomic review. *Clinical Anatomy* **8,** 262-272.

Webb WG. (2017). 4 - Neuronal Function in the Nervous System. In *Neurology for the Speech-Language Pathologist (Sixth Edition)*, ed. Webb WG, pp. 74-92. Mosby.

Wells JA, Glassman AR, Ayala AR, Jampol LM, Bressler NM, Bressler SB, Brucker AJ, et al. (2016). Aflibercept, Bevacizumab, or Ranibizumab for Diabetic Macular Edema: Two-Year Results from a Comparative Effectiveness Randomized Clinical Trial. *Ophthalmology* **123,** 1351-1359.

White AJR, Sun H, Swanson WH & Lee BB. (2002). An Examination of Physiological Mechanisms Underlying the Frequency-Doubling Illusion. *Investigative Ophthalmology & Visual Science* **43,** 3590-3599.

Wikiwand. (2018). The Optic Radiations and Meyer's loop in The Visual System.

Wilhelm H, Neitzel J, Wilhelm B, Beuel S, Ludtke H, Kretschmann U & Zrenner E. (2000). Pupil perimetry using M-sequence stimulation technique. *Investigative Ophthalmology & Visual Science* **41,** 1229-1238.

Wilhelm H & Wilhelm B. (2003). Clinical applications of pupillography. *Journal of neuro-ophthalmology : the official journal of the North American Neuro-Ophthalmology Society* **23,** 42-49.

Wilkes SR, Beard CM, Kurland LT, Robertson DM & O'Fallon WM. (1982). The incidence of retinal detachment in Rochester, Minnesota, 1970-1978. *Am J Ophthalmol* **94,** 670-673.

86

Wilkinson CP. (2014). Interventions for asymptomatic retinal breaks and lattice degeneration for preventing retinal detachment. *Cochrane Database Syst Rev***,** CD003170.

Wong EN, Morgan WH & Chen FK. (2017). Intersession test-retest variability of 10-2 MAIA microperimetry in fixation-threatening glaucoma. *Clin Ophthalmol* **11,** 745-752.

Wong RO. (1999). Retinal waves and visual system development. *Annual review of neuroscience* **22,** 29-47.

Wong TY, Ohno-Matsui K, Leveziel N, Holz FG, Lai TY, Yu HG, Lanzetta P, et al. (2015). Myopic choroidal neovascularisation: current concepts and update on clinical management. *Br J Ophthalmol* **99,** 289-296.

Wong TY, Tielsch JM & Schein OD. (1999). Racial difference in the incidence of retinal detachment in Singapore. *Archives of ophthalmology (Chicago, Ill : 1960)* **117,** 379-383.

Xu H-Z & Le Y-Z. (2011). Significance of Outer Blood–Retina Barrier Breakdown in Diabetes and Ischemia. *Investigative Ophthalmology & Visual Science* **52,** 2160-2164.

Yannuzzi NA & Freund KB. (2019). Brolucizumab: evidence to date in the treatment of neovascular age-related macular degeneration. *Clin Ophthalmol* **13,** 1323-1329.

Zatic T, Bendelic E, Paduca A, Rabiu M, Corduneanu A, Garaba A, Novac V, et al. (2015). Rapid assessment of avoidable blindness and diabetic retinopathy in Republic of Moldova. *Br J Ophthalmol* **99,** 832-836.

Zhang Y, Chioreso C, Schweizer ML & Abramoff MD. (2017). Effects of Aflibercept for Neovascular Age-Related Macular Degeneration: A Systematic Review and Meta-Analysis of Observational Comparative Studies. *Investigative Ophthalmology & Visual Science* **58,** 5616-5627.

87

Graefe's Archive for Clinical and Experimental Ophthalmology (2020) 258:191–200
https://doi.org/10.1007/s00417-019-04523-8

NEUROPHTHALMOLOGY

Recovery dynamics of multifocal pupillographic objective perimetry from tropicamide dilation

Bhim Bahadur Rai[1] · Faran Sabeti[1,2] · Corinne F. Carle[1,3] · Emilie M. F. Rohan[1] · Özge Saraç[1,4] · Joshua van Kleef[1] · Ted Maddess[1]

Received: 18 June 2019 / Revised: 14 October 2019 / Accepted: 23 October 2019 / Published online: 13 November 2019
© Springer-Verlag GmbH Germany, part of Springer Nature 2019

Abstract

Purpose To study the pupillary system by combining mydriasis and multifocal pupillographic objective perimetry (mfPOP). In particular, we explored how the dynamics of recovery differ for concurrently measured direct and consensual sensitivity, response delay, and signal-to-noise ratios (SNRs) for binocular mydriasis.

Methods We recruited 26 normal participants, all with brown irides. The dichoptic mfPOP stimuli concurrently assessed 44-region/eye and both pupils. Two pre-dilation tests were followed by pairs of repeated tests at 1, 2, 4, 6, 8, 12, 24, and 48 h following dilation of both pupils with 1% tropicamide. Three subjects were retested with only the right pupil dilated. Linear models determined the independent effects of mydriasis upon the per-region and pupil measures over time.

Results Post-dilation, the per-region delays initially decreased by 16.3 ± 6.02 ms (mean ± SE) ($p < 0.0001$, cf. baseline of 471.1 ± 4.36 ms), then increased to slower than baseline by 17.42 ± 5.57 ms after 4 h ($p < 0.002$), recovering to baseline at 8 h. By comparison, per-region sensitivities (constriction amplitudes) were still reduced by − 6.20 ± 0.70 μm at 8 h ($p < 0.0001$, cf. baseline of 21.1 ± 0.55 μm), recovered at 24 h, but rebounded at 48 h ($p = 0.005$). The SNRs for sensitivities and delays both recovered by 8–12 h. Across all the data, sensitivities reduced by 2.67 ± 0.25 μm/decade of age, and delay increased by 15.4 ± 1.98 ms/decade (both $p < 0.00001$). Data from 3 of the 26 subjects who repeated the testing for monocular dilation found that consensual response sensitivities were larger than direct for 8 h ($p < 0.018$).

Conclusions The per-region sensitivities were affected for longer than SNRs or delays. Strong early SNRs indicated proportionately lower pupil noise for larger pupil diameters. Following mydriasis with tropicamide 1%, the constriction amplitude measurements with mfPOP should be considered only after 48 h, but time-to-peak can be measured after 8–12 h.

Keywords Anisocoria · Multifocal · Objective perimetry · Pupillography · Rebound miosis · Tropicamide

Introduction

The multifocal pupillographic objective perimetry (mfPOP) method attempts to provide objective, non-invasive, non-contact perimetry. Recent publications [1–3] illustrate the utility of the developing method for both glaucoma and retinal diseases. The responses to mfPOP's transient stimuli have been shown to be substantially cortically driven [3, 4], and its ability to measure changes to both sensitivity and response delay means that it has utility in diseases such as multiple sclerosis [5]. Since both eyes are stimulated, and both pupils recorded concurrently, mfPOP allows direct and consensual responses of both eyes to be measured at 44 or more visual field locations/eye. This has helped explain paradoxical contraction anisocoria that can occur for stimulation of the temporal hemifield [6]. Comparing mfPOP results for dilating one or both pupils provides an avenue for studying these properties of the pupillary system and also the recently characterised pupillary gain control mechanism [7].

Heavily pigmented irides absorb mydriatic agents resulting smaller mydriatic effects due to loss of free drug to the pigment cells. The absorbed drug is then released slowly onto the

✉ Bhim Bahadur Rai
bhim.rai@anu.edu.au

1 Division of Neuroscience, John Curtin School of Medical Research, Australian National University, Building 131 Garran Road, Canberra, ACT 2601, Australia

2 School of Optometry, University of Canberra, Bruce, ACT, Australia

3 ANU Medical School, ANU, Canberra, ACT, Australia

4 Department of Ophthalmology, Ankara Atatürk Training and Research Hospital, Yildirim Beyazit University, Ankara, Turkey

muscarinic receptors resulting in longer duration of dilation [8]. Similar effects were seen while using the dapiprazole to reverse the mydriatic effects of tropicamide [9]. Some studies have however reported no significant difference in pupillary dilatation with tropicamide between light and dark coloured irides [10], including age [11]. Some have reported that mydriasis was independent of iris pigmentation [12].

Acetylcholine and norepinephrine are the principal neurotransmitters initiating parasympathetic and sympathetic effects upon the irides [8–12], which act upon the cholinergic and adrenergic receptors respectively [13]. Commonly used mydriatics comprise two groups. First, the *parasympatholytics*, like tropicamide, inhibit the constriction of sphincter pupillae and ciliary muscles causing mydriasis and cycloplegia. Second, the *sympathomimetics*, like phenylephrine, potentiate the action of dilator pupillae producing mydriasis without cycloplegia [14, 15]. Phenylephrine is short-acting but is effective only when used in combination with parasympatholytics. It might also cause transient corneal oedema and may cause acute systemic hypertension [16]; hence, tropicamide is the most commonly used mydriatic in ophthalmology [14]. Therefore, we chose tropicamide for our study. It is both an anticholinergic and an antimuscarinic agent. Maximal mydriasis is seen within 30 min and is reported to last for between 6 and 24 h [17, 18].

Here we study differences in the dynamics of recovery from mydriasis of per-region measures including sensitivity, delay, and signal-to-noise ratios for both sensitivity and delay. Both the direct and consensual versions of these measures were quantified concurrently for both eyes. While the results are intended to identify the clinically useful post-dilation periods for the various measures, the study also has the potential to provide basic information about the operation of the pupillary system as well.

Methods

Subjects

We screened normal volunteer subjects for ophthalmological or neurological diseases that would potentially affect visual acuity, colour vision, or pupillary function. This included slit lamp examinations and measured IOP by Goldmann applanation tonometry. We measured best-corrected visual acuity (BCVA, ETDRS Chart 2), visual fields with the FDT Matrix (Carl Zeiss Meditec Inc., Dublin, CA), pachymetry (Pachmate DGH 55, DGH Technology Inc., USA), and did keratometry (Topcon OM-4 Keratometer Topcon OM-4, Japan). Macular and retinal nerve fibre layer (RNFL) scanning was done with optical coherence tomography (OCT Spectralis, Heidelberg Engineering GmbH, Germany). *Exclusion criteria* included BCVA worse than 6/9.5, abnormal IOP, visual fields, or macular or RNFL scans. Twenty-six normal voluntary participants were recruited. Seventeen (65.4%) of the participants were male. Their ages ranged from 22 to 55 years, mean and median: 40.5 years and 45 years. Persons with brown irides were selected because they tend to absorb (see "Introduction") and then later release tropicamide resulting in longer dilation duration [8]. Thus, by selecting darker irides, we were conservatively selecting eyes with longer dilation effects.

Multifocal pupillographic objective perimetry

Presentation of stimuli and real-time monitoring of the pupillary diameter with infra-red video cameras was done using a FDA-cleared prototype of the objectiveFIELD mfPOP device (Konan Medical USA, Irvine, CA). mfPOP concurrently presents independent multifocal stimuli to both eyes while measuring direct and consensual responses from every visual field location stimulated [19]. Any vergence deficit was corrected before starting the tests. The maximal luminance of the stimuli was 150 cd/m^2 presented on a 10 cd/m^2 background. Figure 1a shows the 44 stimulus regions per eye arranged in a dartboard layout pattern. Figure 1b shows an example of the luminance-balanced yellow-on-yellow stimuli described previously [21], yielding 176 simultaneous measured direct and consensual responses (Fig. 1c). The colour spectra, CIE coordinates, and relative cone excitations of the yellow stimuli are given elsewhere [20]. Compared to blue stimuli, or white stimuli containing blue, the yellow stimuli are less affected by lens brunescence [20] and visual attention [4]. Our LCD displays could not generate bright enough red stimuli. One transiently presented (30 ms) stimulus was presented on average every 4 s to each test region, total 22 stimuli/s. Each test was run as 9 segments, each of 40-s duration, delivered with short breaks between them. A 750-ms section of data was deleted for each blink. Stimuli were presented at optical infinity to minimise accommodative responses. The participants fixated a red cross in the centre of the viewing field. Fixation and blinks were monitored online, and data obtained during those periods was removed. The regressive response estimation method means that as long as all the 40-s segments have at least 85% of their data then the analysis may proceed. Segments with less than 85% data are therefore re-recorded [19].

Avoiding confounding factors

The test room was isolated to reduce external disturbances to the minimum possible and had dim office lighting of 100 Lux measured at the mfPOP device. Two pre-dilatation mfPOP tests were done, 5 min apart, without exposing the subject to other tests in the preceding 24 h and participants did not drink caffeinated beverages within that period. We enrolled only the

Graefes Arch Clin Exp Ophthalmol (2020) 258:191–200

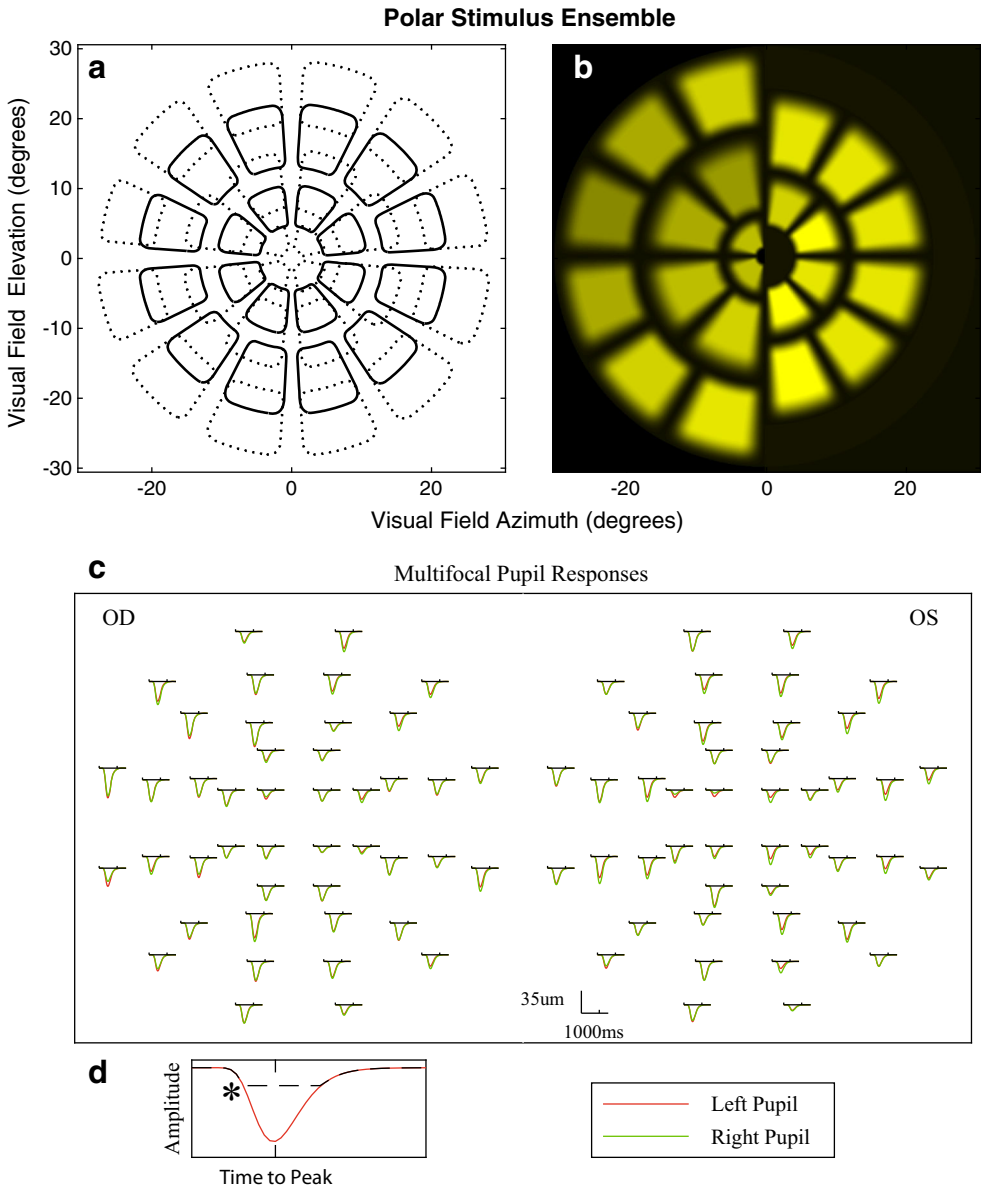

Fig. 1 Multifocal stimuli arranged in a dartboard layout pattern presenting 44 stimulus regions per eye. **a** The 44-region layout consisted of five rings with yellow stimuli. Any stimuli which potentially partially overlapped are never presented simultaneously. No stimuli encroached upon the horizontal and vertical midlines. **b** Example of luminance balancing [20] yellow stimulus components with half the regions activated. The differences in luminance are slightly exaggerated to make them more visible. The concept is to make response amplitudes more similar across the field. **c** Layout of the 176 response waveforms measured from right (OD) and left (OS) eyes. Their locations correspond to the stimulus locations in the visual field. Each waveform is the mean of responses to 90 stimuli presented to each corresponding area. Direct and consensual responses are very similar (red and green waveforms, legend). Responses are somewhat larger from the superior-temporal visual field. Downward deflection of the waveforms represents pupillary constriction. **d** A schematic representation of amplitude of constriction and time-to-peak. The horizontal dashed line illustrates a potentially truncated (clipped) response waveform during extreme dilation. The truncated waveform would have the effect of artificially shortening the time-to-peak (asterisk)

participants with brown irides to prevent the disparities in the effects of the drug.

Test procedures

Following the eye exams and baseline mfPOP tests, both pupils were dilated with 1% tropicamide eye drops. Sometimes tropicamide is combined with phenylephrine; however, the same degree of mydriasis, cycloplegia, and recovery time is achieved by two drops of 1% tropicamide at an interval of 5 min [22], so we adopted this method. Post-dilatation time was counted from instillation of the first drop. After 5 min, the second drop was instilled in each eye. After each instillation, the subject closed their eyes for 1 min to ensure uniform absorption of tropicamide across subjects. mfPOP testing was repeated twice pre-dilation, and then at each of 1, 2, 4, 6, 8, 12, 24, and 48 h post-dilation. The whole sequence was repeated on three of the subjects, but in those pairs of repeats, only the pupil of the right eye was dilated.

Analysis

Data analysis used MATLAB (2016b, The MathWorks, Natick, MA). The response waveforms for each of the 44 test regions/eye were extracted from raw pupillary responses using a multiple regression method [23–25]. The response waveforms (Fig. 1c) were effectively the average response of each retinal region to 90 repeated presentations, and these were fitted to a log-normal function [26], allowing per-region constriction amplitude (sensitivity) and time-to-peak (delay) be measured. The term *per-region* refers to those measures that were determined for every stimulus region of each eye

and pupil providing 176 sensitivities, delays, and SE for each for every recording. The regressive method also generated standard errors for all the estimated constriction amplitudes and delays [19, 27]. Per-region signal-to-noise ratios (SNRs) were determined by the ratio of the measured parameter (amplitude or time-to-peak) on its standard error, i.e. *t* statistics. Blinks were removed from the record before the regression [23–25]. For some analyses, the mean diameters were normalised to a 3.5-mm pupil size to produce *standardised amplitudes*, as done in all our other mfPOP studies to reduce the effects of age. These can be converted to decibel sensitivities [19, 27].

Main outcome measures

The different parameters that we measured were the amplitude of constriction, time-to-peak or delays, SNRs, and pupillary diameters for binocular dilation. All these parameters were measured before and after the pupillary dilation with two repeats each, at each time period mentioned above. We also measured the effects of age (change per decade), test repeats (repeat 1 cf. repeat 2), and genders on different parameters. Some auxiliary outcomes for monocular dilation of some for 3 of the same subjects are also given for interest.

Results

All 26 participants completed 24 h of post-dilatation mfPOP tests, and 16 of them were also tested at 48 h post-dilatation. We analysed the 176 per-region values/subject and repeat for the following: standardised amplitude of constriction, time-to-peak constriction (delay), and SNR measured as *t* statistics. We also examined pupil diameter.

Visual field asymmetries

Figure 2 shows by-region plots of means (across subjects, repeats, and pupils) of the amplitude of constriction (left column) and time-to-peak (right column) as the pupils recovered from mydriasis (rows). These regional means were estimated using linear models fitted to the per-region responses for each post-installation time. The linear models included adjustment for age, sex, and repeat. Before fitting, data from right eye regions was flipped to correspond to left eyes, yielding the temporal field on the left.

For pre-dilation tests, the largest mean amplitudes of constriction were found in the supero-temporal quadrant, and the weakest ones in infero-nasal quadrant (Fig. 2a, cf. Fig. 1c). In the first hour following mydriasis, the amplitude of constriction was typically < 1 μm (Fig. 2c). This increased steadily with time towards normal pre-dilation strength (Fig. 2e, g, i).

Pre-dilation times-to-peak were shorter in supero-temporal and infero-nasal regions of the visual fields (Fig. 2b). Delays were least in the first hour as shown in Fig. 2d. Delays were longest at 4 h post-dilation (Fig. 2f), becoming not significantly different than baseline from about 8 h post-dilation (cf. Fig. 2b, h, j).

The linear models of Fig. 2 were adjusted for age, sex, and repeat, and the significance of those parameters required correction for multiple comparisons. We therefore created pooled models where the input for each post-dilation time was the mean across eyes and regions for each subject. These models thus quantified the magnitude and significance of the difference between the average pre-dilation condition and the average at each post-dilation time, for each per-region measure. We fitted similar models to pupil diameter (Table 1).

Table 1 shows that the main effect of interest, beyond those of post-dilation time itself (see below), was the age dependence, which was significant at $p \leq 0.0001$ for all four variables examined. The mean diameter increased by 0.21 ± 0.051 mm per decade of age. Constriction amplitude and SNR declined with age by 2.67 ± 0.25 μm/decade and 0.62 ± 0.044 t-units/decade, respectively. Time-to-peak increased significantly with age at 15.4 ± 1.98 ms/decade. Figures 3, 4, and 5 present the adjusted effects of recovery time from these pooled linear models. Before that, however, we quantify the constriction asymmetries suggested by Fig. 2.

So far we have presented additive models; however, one may transform the constriction amplitudes to decibels and then fit multiplicative attenuations of constriction amplitudes at each post-dilation time. Of most interest was whether the asymmetries between the quadrants of the field (Fig. 2a, c, e, g, i) are in fixed proportions at all post-dilation times. To quantify this, we fitted models containing decibel attenuations for each post-dilation time, and also for the mean constriction for every quadrant (9 × 4 values), or just 4 average the attenuations for each quadrant (4 values) across post-dilation time. An *F* change test showed the simple model was as good, as exemplified by the r^2 values of 0.699 and 0.703 for the simple and complex models. Both models were adjusted for age, sex, and repeat and agreed with Table 1. Table 2 summarises the per-quadrant results.

Thus, at all post-dilation times, quadrants 1 and 3 responded equally, while quadrant 4 responded only 0.807× as much, and quadrant 2 responded 1.455× as much.

Recovery of pupil diameter from mydriasis

Figure 3a shows the time course of recovery of the diameters of right pupil (RP) and left pupil (LP) when both pupils were dilated (OU-dil). At 24 h, the pupil size was smaller than the pre-dilation indicating *rebound miosis*, which did not recover to pre-dilation size until 48 h. We examined these effects in detail on the 16 subjects who completed the pre-dilation, 24-

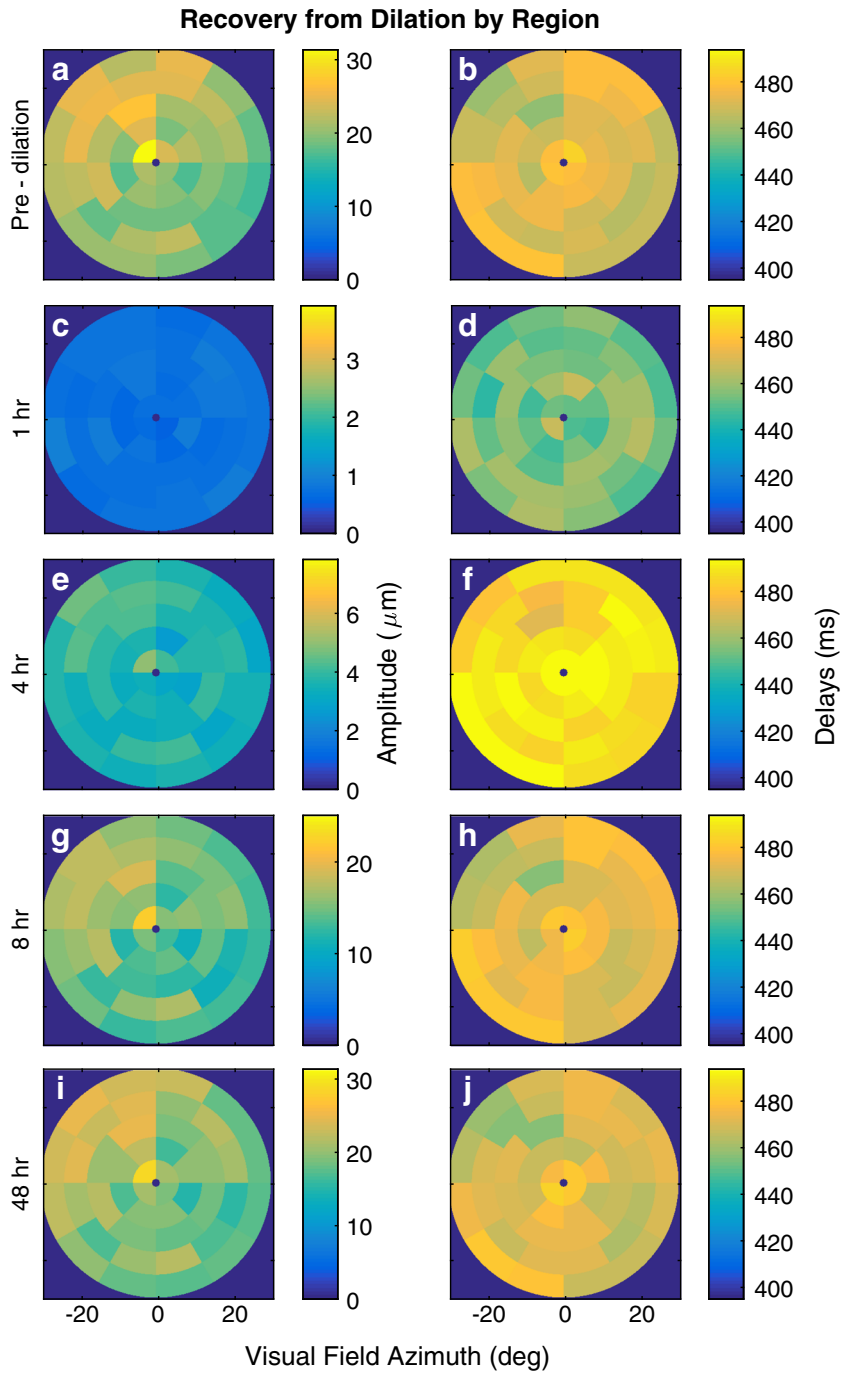

Fig. 2 Regional mean effects on amplitude of constriction shown in the left column and delays (time-to-peak) in the right column. The pre-dilation plots on top are followed by other plots going down in order of post-dilation time period in hours. Right eye data was flipped right-to-left before averaging making all the data left eye equivalent. Thus, the temporal visual field is represented on the left side of each panel. The per-region values are adjusted for age, sex, and repeat

and 48-h tests, using paired *t* tests on the means across repeats and pupils for each subject. The 24-h diameter was less than pre-dilation by 208.1 ± 64.3 μm ($p = 0.005$). The 48-h diameter was less than pre-dilation by 130.9 ± 42.8 μm ($p = 0.008$), but the difference between 24 and 48 h (77.2 ± 54.6 μm) was not significant. Figure 3b compares recovery from mydriasis for the cases of OU and OD dilation (OD-dil) in three subjects, who were a subset of those in Fig. 3a. When only the right pupil was dilated, the diameter of the left pupil (dark-red, LP OD-dil) was smaller than the pre-dilation from 1 to 8 h when they became equal. From 1 to 6 h post-dilation, the left pupil diameters were between 253.2 and 389.6 μm smaller (all $p \leq 0.024$, pooled linear model).

Recovery of per visual field per-region constriction amplitudes and their SNRs

The per-region amplitude of constriction was least in the first hour post-dilation, < 1 μ (Fig. 4a). Amplitudes increased towards baseline after the first hour but the pooled linear models

Table 1 Age, sex, and repeat effects

	Pupil diameter (baseline = 4.16 mm)			
	Difference	Std error	*t* stat	*p* value
Female factor	− 0.41	0.08	− 4.93	< 0.00001
Second repeat	− 0.05	0.07	− 0.70	0.49
mm/decade	0.21	0.05	4.00	0.0001
	Regional constriction amplitude (baseline = 21.1 μm)			
	Difference	Std error	*t* stat	*p* value
Female factor	− 0.16	0.40	− 0.41	0.68
Second repeat	0.62	0.34	1.83	0.07
μm/decade	− 2.67	0.25	− 10.72	< 0.0001
	Regional time-to-peak (baseline = 471.1 ms)			
	Difference	Std error	*t* stat	*p* value
Female factor	− 3.75	3.15	− 1.2	0.23
Second repeat	− 8.50	2.68	− 3.18	0.002
ms/decade	15.4	1.98	7.77	< 0.0001
	Regional signal-to-noise ratio (baseline = 4.12)			
	Difference	Std error	*t* stat	*p* value
Female factor	0.02	0.07	0.32	0.75
Second repeat	0.10	0.06	1.65	0.10
SNR/decade	− 0.63	0.04	− 14.13	< 0.0001

Each factor is a difference relative to the model constant value in parentheses, which was the value at pre-dilation baseline. The age effects were relative to the mean age in decades

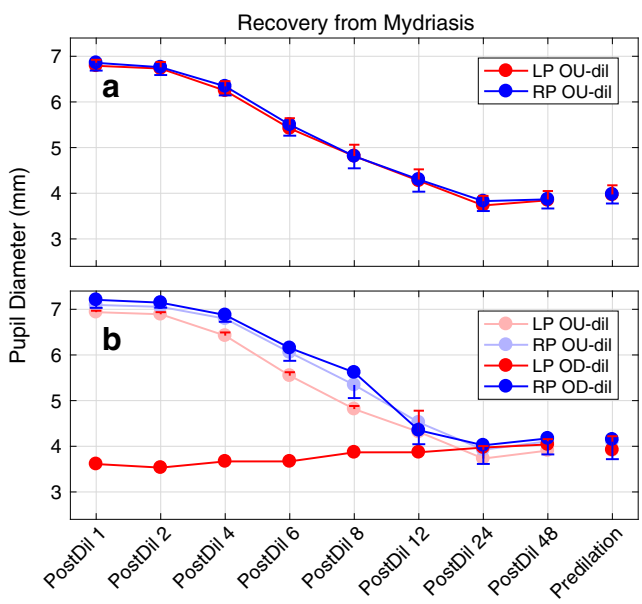

Fig. 3 Dynamics of recovery of right pupil (RP) and left pupil (LP) diameters. **a** Binocular dilation (OU-dil). **b** For dilation of the right pupil only (OD-dil). The undilated left pupil (LP OD-dil) shows miosis from the first hour until 8 h post-dilation while right pupil was dilated. Error bars represent standard errors, some being smaller than the symbols. To reduce clutter, only the lower or upper error bars of representative data are presented. For the same reason, no error bars are given for the OD dilation, but they are given in Fig. 7. Error bars are SE from the age- and sex-adjusted pooled linear models

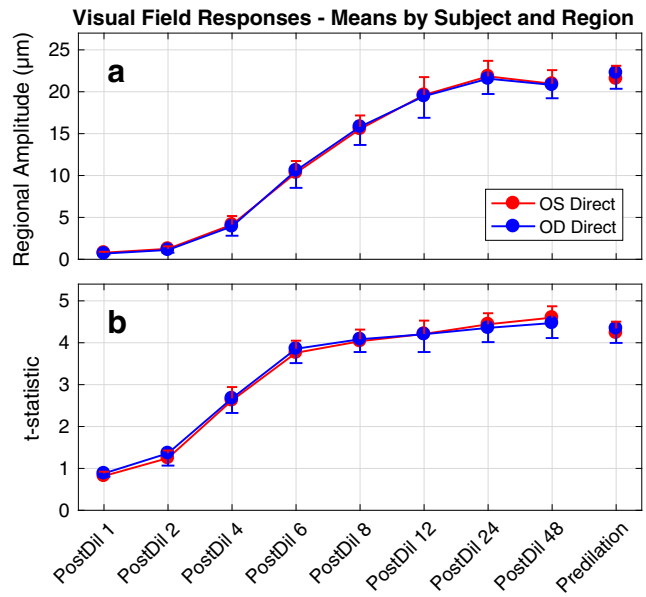

Fig. 4 Dynamics of recovery of measured per-region constriction amplitudes and SNRs. **a** Mean per-region amplitudes of constriction as measured by the direct responses of the right (OD) and left (OS) pupils (legend). Amplitude peaked at 24 h post-dilation, after which it rebounded at 48 h. **b** Mean per-region SNR of the amplitudes as measured as *t* statistics

indicated significant response suppression even at 12 h post-dilation (− 2.4 ± 0.07 μm, $p = 0.0004$, off a mean baseline constriction of 21.1 ± 0.70 μm). The constriction amplitudes appeared to rebound but there were no significant differences between baseline, 24 h, and 48 h. Interestingly, the per-region SNR improved more quickly achieving 87.9% of baseline levels by 8 h, while constriction had only recovered to

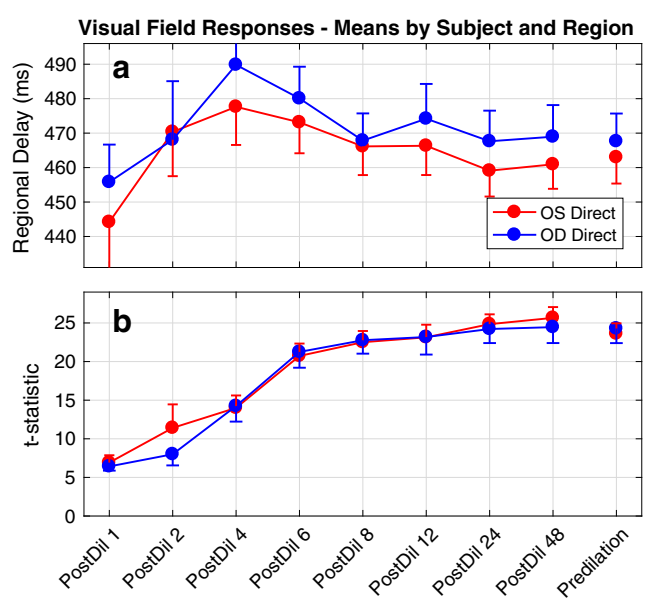

Fig. 5 Direct responses of time-to-peak with binocular pupil dilation. **a** Time-to-peak was maximal at 4 h and did not recover to baseline until 12 h after dilation. **b** Mean per-region SNR as measured by *t* statistics

Table 2 Summary of per-quadrant results

Name	dB	SE dB	Fold change	*t* stat
Constant	18.6*	0.19		99.9
Quadrant 2	1.63*	0.14	1.455×	11.4
Quadrant 3	0.00	0.14	1.000×	0.0
Quadrant 4	− 0.93*	0.14	0.807×	6.5

Constant is the dB constriction for the conditions: pre-dilation time, quadrant 1, for males of the mean age

*Indicates significant at $p < 0.0001$, note the *t* statistics (t-stat)

46.7% of baseline by that time (Fig. 4b). This means that the SE in the fitted values remained smaller for longer, *that is there was proportionately less noise in the pupil responses between 4 and 8 h*.

Recovery of regional times-to-peak and their SNRs

The mean per-region time-to-peak for regional responses appeared to be longer for right pupils than left but the small mean difference of 3.29 ± 2.67 ms was not significant (Fig. 5a). A pooled linear model indicated that the average per-region delays were longer than baseline at 4 and 6 h by 17.4 ± 5.57 ms (mean ± SE, $p < 0.002$) and 11.0 ± 5.57 ms ($p < 0.05$) (cf. Fig. 2f). Delay recovered to baseline by 8 h. There were no significant differences in delay between pre-dilation, 24 h, and 48 h. Figure 5b shows that delay SNRs recovered similarly to contraction amplitudes, being not significantly different from baseline from 6 h onwards.

We had hypothesised that at extreme dilations, the pupil response might be truncated producing a falsely early estimate of time to peak (Fig. 1d). We therefore examined the mean constriction response waveforms of 9 subjects who had complete data sets for all test periods in both repeats (1 h was not measurable due to the pupil tracking system having difficulty with pupils > 7 mm, 18 of 52 repeats failed). The resulting 9 plots are each the mean of 3168 per-region results (Fig. 6). The 1-h post-dilation waveforms appear quite normal, i.e. not truncated, but have shorter times to peak as shown by every test region by Fig. 2d.

Recovery of per-region responses from monocular versus binocular dilation

We compared the mean per-region amplitude of constriction and delay following monocular and binocular dilation in three subjects. When only the right pupil was dilated, the consensual responses driven by the right retina were larger than the direct responses of the left retina for 8 h (3.55 ± 0.38 μm, $p < 0.018$, Bonferroni corrected) due to more light input through the dilated right pupil. Paradoxically, these differences remained near constant

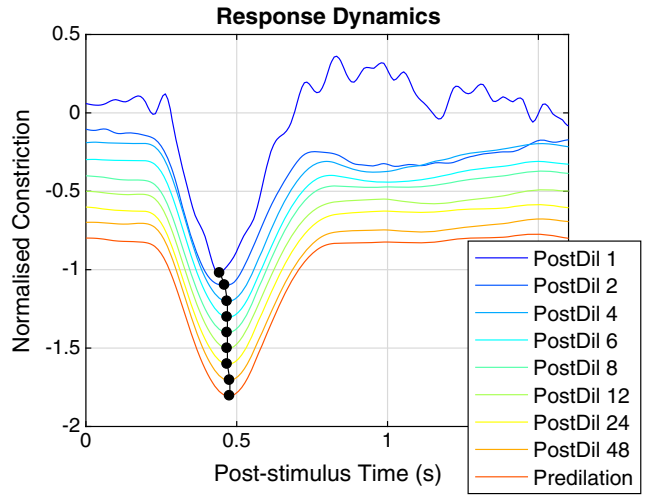

Fig 6 Normalised mean pupil response waveforms for each post-dilation time and pre-dilation. The waveforms are offset in steps of 0.1. The means are computed across regions, eyes, pupils, and subjects ($N = 3168$ waveforms/trace). The dotted black line indicates that the time-to-peak is initially quicker and then gets slower (cf. Fig. 1)

despite right pupil size shrinking by a factor of 2 over that period (Fig. 2a). Due to the small *N* of 3, we examined the effect sizes measured as Hodges' *g* (Cohen's *d* corrected for small *N*) for PostDil 1 to PostDil 8. They were as follows: 1.47, 1.99, 1.39, 1.01., and 0.85, which are in the large to huge effect size range. Additionally, the direct responses of the left pupil (indicating left retinal responses, Fig. 7a saturated red) were lower compared to baseline for the first 8 h: range − 2.31 to − 3.26 μm (all $p \leq 0.026$). The consensual responses (from the right retina, saturated blue) had higher than baseline sensitivities for 6 h (range 2.05 to 2.43 μm, all $p \leq 0.046$). The first four delays were between 12.8 and 21.8 ms quicker than baseline ($p \leq 0.006$, mean SE 4.5 ms), but not for the same subjects tested twice with both pupils dilated (Fig. 7, unsaturated lines and dots). Effect sizes for the first 5 direct versus consensual delays were 0.23 or less.

Discussion

Visual field asymmetries

The mean amplitudes of constriction to the 44 region/eye stimuli were stronger in the supero-temporal visual field (Fig. 2, left column, Table 2). This agrees with findings by our group in 24 experiments on 1480 eyes [6], and other researchers [28–30], and has also been reported for multifocal ERGs [31]. These gradients appear to reflect retinal ganglion cell densities of humans [32]. This is supported by the finding here that these relative gradients of retinal sensitivity did not appear to change with degree of dilation.

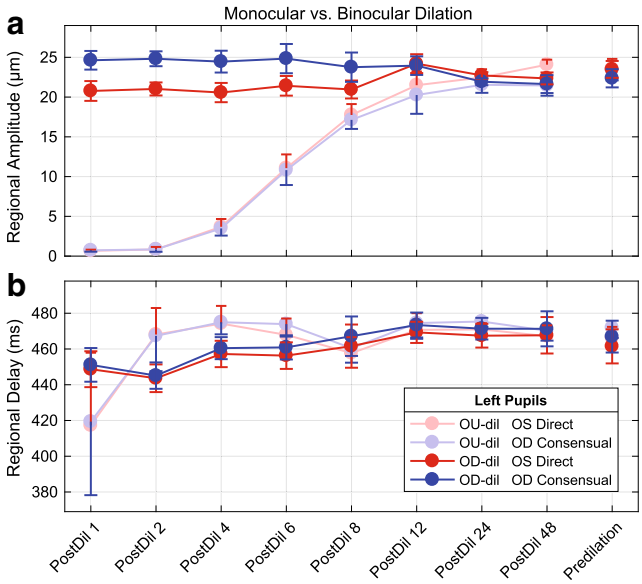

Fig. 7 Retinal responses measured via the left pupil comparing monocular and binocular dilation (n = 3 subjects). **a** Mean constriction response across the 44 regions per eye and subjects. Pre-region response amplitude peaked at 24 h and did not recover to baseline until 48 h after dilation. The consensual OD response was significantly larger than the direct OS response for 8 h. **b** Mean response delay across the 44 regions per eye and subjects. Error bars are SE

Recovery dynamics

An interesting feature of the study was the different rates at which particular measures recovered to baseline levels. This was quantified as the differential effect of post-dilation time relative to baseline using the pooled linear models. The time courses for these measures are illustrated in Figs. 4 and 5. Constriction amplitudes required 24 h to be not significantly different to baseline levels (but see "Rebound miosis" below). By contrast, the average SNR in the per-region constriction amplitudes was recovered by 12 h. The per-region times-to-peak were recovered by 8 h as did the SNRs in those values. The mfPOP method has been shown to be effective in multiple sclerosis [5] where the primary diagnostic variable is response delay. Therefore, in such diseases, testing could perhaps commence 8 to 12 h after mydriasis.

The relatively rapid recovery of the SNRs may have to do with there being proportionately less pupil response noise early in recovery. The standard deviation in pupil noise is reported to be largest for pupil sizes of about 5 mm and is less for both smaller and larger diameters [33], and that is regardless of how the diameter is set: including accommodation, light level, or tropicamide. Thus, it is quite possible that noise is lower in the early phases of recovery when the pupil diameter was large. The drop-off in constriction size with dilation is reported to be quite linear for tropicamide, but is nonlinear for phenylephrine: responses remaining relatively larger for pupil sizes > 6 to 7 mm [34]. It might therefore be worthwhile investigating the recovery of SNRs comparing tropicamide and phenylephrine.

Rebound miosis

Rebound miosis has been described to occur 1 day after use of 10% phenylephrine eye drops, a phenomenon originally observed by Saint-Martin in 1929 and more recently by Haddad et al. [35]. It has been attributed to damage the dilator pupillae by high concentrations as it was found to be dose-dependent and supported by iris pigments being released into aqueous humor [36]. However, in our study, we have noticed rebound miosis with 1% tropicamide (Fig. 3a). It was maximum at 24 h post-dilation (p = 0.005). It reduced after 24 h but remained significant even at 48 h (p = 0.008). A possible mechanism is that acetylcholine accumulates and is unused in post-ganglionic parasympathetic nerve endings when the muscarinic receptors are engaged with tropicamide, and then once the tropicamide is cleared, there is increased acetylcholine action on sphincter pupillae producing rebound miosis.

Monocular and binocular dilation

When only the right pupil was dilated, the mean per-region *consensual* constrictions of the right retina (as measured by the left pupil) became significantly larger than the *direct* responses of the left retina until 8 h post-dilation (Fig. 7a). We have proposed a model to explain reports of contraction anisocoria in which consensual responses can be larger, at least in the temporal field [6]. That is in part due to differing rates of response saturation (i.e. reaching a maximal plateau value) in the direct and consensual pathways as a function of stimulus intensity.

For cone-driven responses, one would expect that the contrast of the stimuli would determine the pre-region response size and this is unchanged by dilation, but this does not explain the consensual > direct outcome. The results might suggest a response that is partially dependent on absolute light level. That cannot be a large effect however because the direct/consensual differences remained near constant for 8 h, while right pupil area reduced 4-fold (Fig. 3a). Note that the left pupil was also significantly smaller than baseline for the first 6 h (Fig. 3b). Responses to absolute light level could be mediated by melanopsin containing retina ganglion cells [37], but our stimuli are too transient and dim to drive melanopsin [1]. That being said, normal primate retinal ganglion cells encode some information on absolute light level [38], albeit with low gain. It is worth noting that near constant initial consensual

responses were probably not due to saturation alone, because mean responses up to 50 to 100 μm are quite possible with mfPOP stimuli [1, 6] (see their Fig. 2a and b). It is possible that a combination of saturation [6] and gain control [7] could explain the small but near constant direct/consensual differences. That could be tested by presenting all the stimuli but changing the luminance of one test region on different runs to record the shape of the stimulus-response function. The times-to-peak possibly showed early anomalies for monocular dilation but these were not very significant and need to be repeated. Interestingly, binocular times-to-peak at 4 h were significantly longer by about 15 ms than baseline (Figs. 2f, 5a, and 7b).

A potential limitation of the study was that 18 of 52 repeats in the first hour following mydriasis were missed because the pupil tracking system failed to track the pupils with diameters > 7 mm.

Conclusions

The recovery dynamics were clearly different for different measures. Following mydriasis with tropicamide, mfPOP measurement of constriction amplitudes may be considered only after 48 h, but after 8–12 h for times-to-peak or SNRs. While rebound miosis is expected for phenylephrine, the observed rebound for tropicamide at 24 h was less expected. The latter may provide a useful tool for dissecting gain control in the pupil system. For example, measuring the stimulus-response function of selected regions during a test would illuminate aspects of gain control and saturation in the pupil system. The suggestion of lower pupil noise in early recovery was interesting. Comparing monocular and binocular recovery for tropicamide and phenylephrine mydriasis may also be informative.

Funding information This research was supported by the Australian Research Council through the ARC Centre of Excellence in Vision Science (CE0561903), intramural funding from the ANU, and an ANU PhD scholarship to BB Rai.

Compliance with ethical standards

Conflict of interest Authors FS, CFC, JvK, and TM could possibly receive royalty income from patents assigned to Konan Medical USA Inc. for a possible product based upon the mfPOP methods. The other authors declare that they have no conflict of interest.

Ethical approval and informed consent All procedures performed in studies involving human participants were in accordance with the ethical standards of the Australian National University and ACT Health and with the 1964 Helsinki declaration and its later amendments or comparable ethical standards. Informed consent was obtained from all individual participants included in the study.

References

1. Carle CF, James AC, Kolic M, Essex RW, Maddess T (2015) Blue multifocal pupillographic objective perimetry in glaucoma. Invest Ophthalmol Vis Sci 56:6394–6403
2. Sabeti F, Nolan C, Essex R, Kolic M, James AC, Maddess T (2015) Multifocal pupillography identifies changes in visual sensitivity according to severity of diabetic retinopathy in type 2 diabetes. Invest Ophthalmol Vis Sci 56:4504–4513
3. Sabeti F, James AC, Carle CF, Essex WR, Bell A, Maddess T (2017) Comparing multifocal pupillographic objective perimetry (mfPOP) and multifocal visual evoked potentials (mfVEP) in retinal diseases. Sci Rep 7:45847
4. Rosli Y, Carle CF, Ho Y, James AC, Kolic M, Rohan EMF, Maddess T (2018) Retinotopic effects of visual attention revealed by dichoptic multifocal pupillography. Sci Rep 8:2991
5. Ali EN, Maddess T, James AC, Voicu C, Lueck CJ (2014) Pupillary response to sparse multifocal stimuli in multiple sclerosis patients. Mult Scler J 20:854–861
6. Carle CF, Maddess T, James AC (2011) Contraction anisocoria: segregation, summation, and saturation in the pupillary pathway. Invest Ophthalmol Vis Sci 52(5):2365–2371
7. Carle CF, James AC, Rosli Y, Maddess T (2019) Localization of neuronal gain control in the pupillary response. Front Neurol 10(203):1–9
8. Salazar M, Shimada K, Patil PN (1976) Iris pigmentation and atropine mydriasis. J Pharmacol Exp Ther 197(1):79–88
9. Anicho UM, Cooper J, Feldman J, Jaanus SD, Dignam K (1999) The clinical efficacy of paremyd with and without dapiprazole in subjects with light and dark brown irides. Optom Vis Sci 76(2):94–101
10. Richardson RW (1982) Comparing the mydriatic effect of tropicamide with respect to iris pigmentation. J Am Optom Assoc 53(11):885–887
11. Cooper J, Feldman JM, Jaanus SD, Appleman W, Appel S, Horn D (1996) Pupillary dilation and funduscopy with 1.0% hydroxyamphetamine plus 0.25% tropicamide (Paremyd) versus tropicamide (0.5 or 1.0%) as a function of iris and skin pigmentation, and age. J Am Optom Assoc 67(11):669–675
12. Dillon JR, Tyhurst CW, Yolton RL (1977) The mydriatic effect of tropicamide on light and dark irides. J Am Optom Assoc 48(5):653–658
13. Becker DE (2012) Basic and clinical pharmacology of autonomic drugs. Anesth Prog 59(4):159–169
14. Ihekaire DE (2012) The comparative efficacy of cycloplegic drugs—tropicamide and cyclopentolate. Int J Sci Res Educ 5(3):223–246
15. Bradley MM, Miccoli L, Escrig MA, Lang PJ (2008) The pupil as a measure of emotional arousal and autonomic activation. Psychophysiol 45(4):602–607
16. Wilensky JT, Woodward HJ (1973) Acute systemic hypertension after conjunctival instillation of phenylephrine hydrochloride. Am J Ophthalmol 76(1):156–157
17. Drugs.com (2017) Tropicamide: FDA prescription information. www.drugs.com/pro/tropicamide.html. Accessed 15 Dec 2017
18. Montgomery DM, MacEwan C (1989) Pupil dilation with tropicamide. The effects of acuity, accommodation and refraction. 3(Pt 6). https://doi.org/10.1038/eye.1989.129
19. Maddess T, Bedford SM, Goh XL, James AC (2009) Multifocal pupillographic visual field testing in glaucoma. Clin Exp Ophthalmol 30:678–686
20. Carle CF, James AC, Kolic M, Essex RW, Maddess T (2014) Luminance and colour variant pupil perimetry in glaucoma. Clin Exp Ophthalmol 42(9):815–824

21. Carle CF, James AC, Maddess T (2013) The pupillary response to color and luminance variant multifocal stimuli. Invest Ophthalmol Vis Sci 54:467–475
22. Molinari JF (1983) A clinical comparison of mydriatics. J Am Optom Assoc 54(9):781–784
23. Ruseckaite R, Maddess T, Danta G, Lueck CJ, James AC (2005) Sparse multifocal stimuli for the detection of multiple sclerosis. Ann Neurol 57(6):904–913
24. James AC (2003) The pattern-pulse multifocal visual evoked potential. Invest Ophthalmol Vis Sci 44(2):879–890
25. James AC, Ruseckaite R, Maddess T (2005) Effect of temporal sparseness and dichoptic presentation on multifocal visual evoked potentials. Vis Neurosci 22(1):45–54
26. Carle CF, James AC, Kolic M, Loh YW, Maddess T (2011) High-resolution multifocal pupillographic objective perimetry in glaucoma. Invest Ophthalmol Vis Sci 52(1):604–610
27. Bell A, James AC, Kolic M, Essex RW, Maddess T (2010) Dichoptic multifocal pupillography reveals afferent visual field defects in early type 2 diabetes. Invest Ophthalmol Vis Sci 51(1):602–608
28. Cox TA, Drewes CP (1984) Contraction anisocoria resulting from half-field illumination. Am J Ophthalmol 97(5):577–582
29. Schmid R, Wilhelm H, Wilhelm B, Kriegbaum C, Miliczek K, Wannek U (1995) Naso-temporal differences in pupillomotor sensitivity. Invest Ophthalmol Vis Sci 37:159
30. Smith SA, Smith SE (1980) Contraction anisocoria: nasal versus temporal illumination. Br J Ophthalmol 64:933–934
31. Sutter EE, Tran D (1992) The field topography of ERG components in man—I. The photopic luminance response. Vis Res 32(3):433–446
32. Curcio CA, Allen KA (1990) Topography of ganglion cells in human retina. J Comp Neurol 300(1):5–25
33. Usui S, Stark L (1978) Sensory and motor mechanisms interact to control amplitude of pupil noise. Vis Res 18(4):505–507
34. Miller D, Stark L (1964) Effect of mydriatic drugs on pupil dynamics. Res Lab Elec MIT Q Prog Rep 74:265–269
35. Haddad NJ, Moyer NJ, Riley FC (1970) Mydriatic effect of phenylephrine hydrochloride. Am J Ophthalmol 729–733
36. Aggarwal JL, Beveridge B (1971) Liberation of iris pigment in anterior chamber after instillation of 10% phenylephrine hydrochloride solution. Br J Ophthalmol 55:544–549
37. Dacey DM, Liao HW, Peterson BB, Robinson FR, Smith VC, Pokorny J, Yau KW, Gamlin PD (2005) Melanopsin-expressing ganglion cells in primate retina signal colour and irradiance and project to the LGN. Nature 433(7027):749–754
38. Purpura K, Tranchina D, Kaplan E, Shapley RM (1990) Light adaptation in the primate retina: analysis of changes in gain and dynamics of monkey retinal ganglion cells. Vis Neurosci 4(1):75–93

Publisher's note Springer Nature remains neutral with regard to jurisdictional claims in published maps and institutional affiliations.

Chapter 3

Multifocal Pupillographic Objective Perimetry as a biomarker for anti-VEGF injection requirements in neovascular Age-related Macular Degeneration.

1

ABSTRACT

Purpose: To evaluate Multifocal Pupillographic Objective Perimetry (mfPOP) as a biomarker for anti-VEGF injection requirements in neovascular AMD (nAMD).

Methods: We recruited newly diagnosed unilateral or bilateral nAMD patients. Detailed clinical workup and diagnostic procedures including mfPOP, perimetry, OCT, and macular photography were performed. For the current study we are correlating only the mfPOP findings and the requirements for anti-VEGF injection. Two mfPOP variants with maximal eccentricities of 15 and 30 degrees were used to measure visual-field function. Each presented 44 interleaved stimuli/eye arranged in 5 rings presented pseudorandomly. Practitioner directed intravitreal injection anti-VEGF was administered with follow-up of 14 to 28 monthly visits. Post hoc visual field data analysis used MATLAB (2016b, The MathWorks, Natick, MA). Most analysis was with respect to stimulus ring and month.

Results: Twenty-three eyes of 18 patients were included, the majority being females (14 cases, 77.8%). Central sensitivity decreased in eyes requiring treatment, or kept decreasing until the anti-VEGF was needed, while peripheral regions often showed hypersensitivity. In the untreated fellow eyes the median sensitivity of the central ring-1 declined at -0.17 ± 0.07 dB/month ($p=0.033$). Among the treated eyes, the sensitivity started to plateau after 5-6 months, and among less responsive eyes, the sensitivity approached but remained below normal. Central ring-1 of eyes needing treatment was less sensitive than in the untreated eyes by -2.23 ± 0.051 dB ($p<0.0002$). The slope of sensitivity for outer rings-3 to 5 was significant at -0.76 ± 0.18 dB/month ($p=0.002$). Time-to-peak was delayed before, or progressively delayed until treatment was required. Treated eyes showed quicker responses in ring-1 by 13.08 ± 3.77 ms than untreated eyes ($p=0.001$). Similarly, rings-3 to 5 in the treated eyes were quicker by 7.81 ± 2.10 ms ($p=0.001$). Treated and fellow eyes showed that sensitivity

correlated positively in rings-2 to 4, with the least correlation in ring-1. Temporal cross-correlation showed a treatment effect lag of 2 months for sensitivity and 1 month for time-to-peak. Based on peripheral sensitivity and delay we have identified two categories of patients: positive types with peripheral hypersensitivity and longer delay, and negative types with peripheral hyposensitivity and shorter delay than normal controls. When these groups were analysed separately mfPOP showed an ability to predict the need for treatment. Among the positive eyes the peripheral sensitivity increased on average by 9.88 ± 4.41 dB (p=0.042) a month before the treatment day. Following 3 injections it returned to normal level. Similarly, the time-to-peak increased at 3.49 ± 1.75 ms per month (p=0.049) until the treatment was given. For the negative eyes, the peripheral sensitivity dropped until the treatment was needed, and the time-to-peak was shorter a month before the treatment by 9.38 ± 3.59 (p=0.013), and a month following treatment it improved towards normal value (shorter by 8.50 ± 2.71 ms, p=0.004).

Conclusions: We observed decreased central sensitivity in the macular regions affected by AMD, coincident with peripheral hypersensitivity mostly. In the untreated fellow eyes, the central sensitivity decreased and time-to-peak increased progressively until treatment was needed. Among the less responsive eyes, the sensitivity and time-to-peak improved but remained below normal levels, and there was treatment effect lag of 2 months for sensitivity and 1 month for time-to-peak. The rings-3 and 4 showed the best correlation between the treated and untreated fellow eyes. The central and the peripheral regions responded differently both in terms on sensitivity and time-to-peak. We further noticed that based on the peripheral response the eyes could be divided into positive and negative groups. The predictive value of mfPOP improved after the positive and negative eyes were analysed separately. Diagnostic sensitivity and delay changes could precede active disease by 1 to 3 months on either positive or negative ways. Following treatment the responses improved

towards normal values. Supported by our findings we conclude that mfPOP as a potential biomarker to predict the need for anti-VEGF injections in nAMD.

Key words: AMD, anti-VEGF, mfPOP, multifocal pupillography, retinal sensitivity, time-to-peak

INTRODUCTION

Age-related macular degeneration (AMD), accounting for 8.7% of blindness worldwide (Wong *et al.*, 2014) and a global prevalence of more than 170 million (Pennington & DeAngelis, 2016), is the leading cause of irreversible blindness in people aged 50 years or older (Age-Related Eye Disease Study Research, 2001; Seigel, 2002). It's aetiology includes a combination of genetic and environmental factors (Christoforidis *et al.*, 2011), and is more common among women than men of same age (Klein *et al.*, 1997). There is a non-modifiable risk factor with increasing age above 50 years, and modifiable risk factors include smoking and high blood levels of high-density lipoprotein cholesterol (Klein *et al.*, 2007; Fan *et al.*, 2017). The burden of AMD on an individual, measured by loss of quality of life (QoL), is immense, ranging from a 17 to 60% decrease in an average patient (Brown *et al.*, 2005). An economic analysis based on losses to the gross domestic product suggested that AMD has approximately a $30 billion annual negative impact (Brown *et al.*, 2005).

Complete clinical examination including best corrected visual acuity (BCVA), contrast sensitivity, and optical coherence tomography (OCT) (Jager *et al.*, 2008) must be performed to ascertain if the injection of anti-vascular endothelial growth factor (anti-VEGF) is indicated. Fundus fluorescein angiography (FA) (Novotny & Alvis, 1961), fundus photography, and OCT Angiography (OCTA) may also be informative (Gao *et al.*, 2016). Additionally, OCTA identifies non-exudative macular neovascularisation (neMNV), which neither show leaks nor exudates on structural OCT (Choi *et al.*, 2015). Thus, choroidal neovascularisation membrane (CNVM) and neMNV are difficult to identify with OCT and FA (Palejwala *et al.*, 2015) and asymptomatic CNVM in intermediate AMD can occur (Roisman *et al.*, 2016). Though very precise and accurate, the suitability of the above mentioned diagnostic methods are time consuming.

A rapid non-invasive, non-contact functional method, indicating the need for anti-VEGF treatment would be useful. Multifocal Pupillographic Objective Perimetry (mfPOP) may be such a method. The mean effect of neovascular AMD (nAMD) on regional pupil constriction amplitudes and time-to-peak constriction reflects the severity of the disease, and reports suggest mfPOP can detect functional loss in early AMD (Sabeti *et al.*, 2011; Sabeti *et al.*, 2013). We have also reported that mfPOP identifies ranibizumab-induced changes in retinal function in nAMD. Peripheral mfPOP hypersensitivity indicated better outcomes for anti-VEGF treatment (Sabeti *et al.*, 2012). Recently, another study by this group has reported that retinal thickness (OCT) outside 8° was significantly associated with high contrast visual acuity and macular sensitivity (Matrix 10-2 perimetry), indicating outer macular thickness as a useful prognostic indicator in nAMD (Sabeti *et al.*, 2020). The current longitudinal study was conducted to validate the effectiveness of mfPOP as an indicator for need of anti-VEGF injection in nAMD.

METHODS

Subjects

Patients diagnosed with nAMD were invited to participate in the study through treating physicians, ophthalmologists and optometrists. All participants gave informed written consent. The *inclusion criteria* included patients with newly diagnosed (mainly) unilateral or bilateral nAMD, aged 50 years or above, indication of treatment with anti-VEGF agents and BCVA of ≥ 20 letters (6/12). The *exclusion criteria* included nAMD in fellow eye already receiving anti-VEGF, or having received it within last 6 months as injection into eye or systemically for other diseases, and study eye having received anti-VEGF at any time. Exclusion criteria also included retinal laser within 6 months, or retinal haemorrhage greater than 50% of the lesion area. We also excluded cases with ocular co-morbidities known to

affect retinal function such as glaucoma, optic neuropathy, diabetes, and maculopathy other than AMD. Diseases affecting pupillary or iris functions such as posterior synechiae, oculomotor dysfunction, cataract surgery within last 6 months or likely to require surgery within 2 years of study period, were also excluded. Normative mfPOP data was based on a separate study of 133 subjects each tested twice, 2 weeks apart (Carle *et al.*, 2020).

Study Design

The prospective longitudinal study was conducted with monthly patient follow ups over 14 to 28 months. The ophthalmological tests and diagnostic procedures were performed in each visit (see below) and if indicated the intravitreal injection of anti-VEGF injection was administered, i.e. management was *pro re nata* (PRN).

Ophthalmic examinations

A number of other eye tests followed mfPOP testing on the same day. Visual fields were mapped with a Matrix 10-2 test (Carl Zeiss Meditec Inc., Dublin, CA), using the Alternative fixation method for persons with central field loss. We measured the best corrected visual acuity (BCVA) with an ETDRS Chart 2 and low contrast visual acuity with a low contrast (10%) Chart 3. Corneal curvature was measured with auto-refractometer (ARK-1s NIDEK co. Ltd, AICHI Japan), pachymetry with Pachmate DGH 55 (DGH Technology Inc., USA) to allow calibration of OCT measurements. Intraocular pressure (IOP) was measured with Goldmann applanation tonometry. Both the pupils were dilated under 1% tropicamide eye drops for the remaining eye examinations. We performed slit-lamp examination of the anterior and posterior segments. Any cataracts were graded using the Lens Opacities Classification System III (LOCS III) (Chylack *et al.*, 1993). An 8×8 grid macular scan, retinal nerve fibre layer (RNFL) analysis around the optic nerve head, and autofluorescence were performed with Spectralis Optical Coherence Tomography (Heidelberg Engineering

GmbH, Germany). Coloured macular fundus photographs were taken with a Canon Digital Retinal Camera (CR-2, Canon Inc., Tokyo, Japan). FA were used to classify eyes as: predominantly classic choroidal neovascularization (P), minimally classic choroidal neovascularization (M), and occult choroidal neovascularization (O).

Multifocal Pupillographic Objective Perimetry

The participants were prevented from drinking caffeinated beverages within an hour before or during the test. Presentation of stimuli and monitoring of the pupillary diameter with infrared video cameras were performed using a FDA-cleared prototype of the objectiveFIELD mfPOP device (Konan Medical USA, Irvine, CA). mfPOP concurrently presents independent multifocal stimuli to both eyes while measuring direct and consensual pupil responses from every visual field location stimulated (Maddess *et al.*, 2009). Vergence deficits were corrected before beginning the tests. The maximal luminance of the stimuli was 150 cd/m^2 presented on a 10 cd/m^2 background. Two stimulus protocols were used: P131, that covers the central 30°, and P129, that covers the central 60° of visual field, each with 44 stimuli per eye (**Fig. 1A**). The stimuli were luminance balanced (**Fig. 1B**) (Carle *et al.*, 2014) and employed the clustered volleys method (Carle *et al.*, 2013; Sabeti *et al.*, 2014).

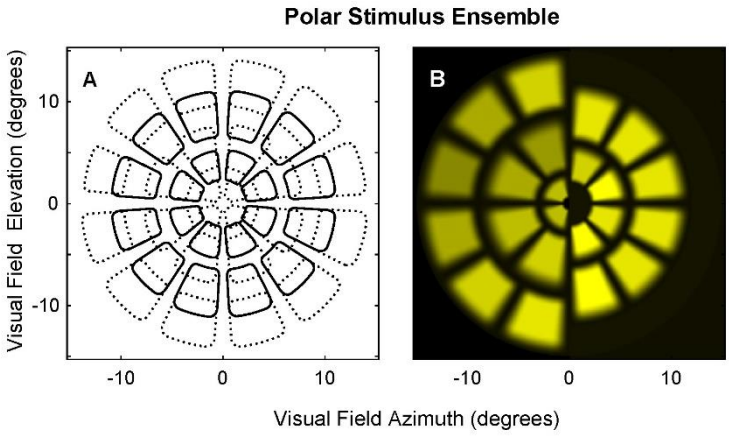

Figure 1. Multifocal stimuli arranged in a dartboard layout pattern presenting 44 stimulus regions per eye. **(A)** The 44-region layout consists of five interleaved rings of yellow stimuli. Overlapping stimuli are never presented simultaneously. No stimuli encroach upon the horizontal and vertical midlines. **(B)** Example of luminance balancing (Carle *et al.*, 2014) yellow stimulus components with half the regions activated. The differences in luminance are slightly exaggerated to make them more visible. The concept is to make response amplitudes homogeneous across the entire field. Both plots show the macular P131 stimulus that extends to ±15 deg eccentricity. The wide-field P129 stimulus is a two-times scaled version of P131 extending to ±30 deg with the same number of yellow stimuli (not shown in Figure).

Analysis

Data analysis was performed using in-house developed MATLAB scripts (2016b, The MathWorks, Natick, MA). The response waveforms for each of the 44 test regions per eye were extracted from raw pupillary responses using multiple regression, with blinks removed from the pupil data before regression (James, 2003; James *et al.*, 2005; Ruseckaite *et al.*, 2005). Temporal impulse responses at each retinal region were fitted to a log-normal function (Carle *et al.*, 2011), allowing per-region estimation of constriction amplitude (sensitivity) and time-to-peak. The regressive method also generated standard errors for the estimated sensitivities and times-to-peak (Maddess *et al.*, 2009; Bell *et al.*, 2010). To reduce the effects of age and standardize sensitivities, the mean diameters were standardised to a 3.5 mm pupil size, as in previous studies. Thus, we were examining relative pupil amplitudes rather than absolute size, as is commonly done (Bremner, 2012; Maddess, 2012). To further account for age and sex effects, the sensitivity and delay of age- and sex-matched normal responses were subtracted from the values obtained in the test, to form the deviations as in standard perimetry (Anderson and Patella, 1999). Normative values were from a normative model developed in a separate, unpublished, study where 204 subjects each performed two repeats (over two weeks) of both the mfPOP test variants used here (P129 and P131).

To find the mfPOP characteristics among the responders and non-responders to anti-VEGF treatment we sometimes examined different treatment-patterns across consecutive months,

where within a pattern, “1” indicated a treatment in a month, and “0”, no treatment. Thus, we identified patterns such as [1 0 0 0], and [0 0 0 1] within the sequences of 14 to 28 months of treatments. The pattern [1 1 1 1] would indicate a relative non-responder, while [1 0 0 0] indicates a possible good responder. We then quantified changes in the sensitivity (constriction amplitude) and time-to-peak across collections of these patterns, typically investigating ring-median responses. We never took more than 3 treatment-pattern sequences from any eye. This meant that in cases where 3 occurrences of a pattern occurred within an eye, the responses examined were from the first 3 instances of that treatment-pattern from that eye.

We also performed some analyses across large numbers of months, sometimes dividing eyes into those that required more treatment than average, and those that required less treatment than average. Analysis typically involved fitting linear models to compare a treatment day with other days in a particular treatment-pattern, or slopes indicating rates of change by month.

We further performed two forms of correlation analysis across time. The first involved correlation between ring-median responses of different cases like treated eyes vs. non-treated fellow eyes. This allowed us to examine the question of how responses of the peripheral field rings of untreated eyes correlated with the same or more central rings of the fellow treated eyes. We also examined lagged effects between treatment and responses in later months using the cross-correlation and by fitting a time invariant linear model with relatively short memory of 2- months, to account for the effects of auto-correlation in the response. These were estimated with the Matlab function *impulseest*.

Anti-VEGF treatments

This study was originally part of a registered clinical trial, **R**anibizumab vs. **A**flibercept for **A**MD using **M**ultifocal pupillometric objective **P**erimetry (RAAMP). It was designed to compare treatment with ranibizumab and aflibercept under PRN management. The clinical trial registration number was ACTRN12614000497606, and ethical approval number ETH.11.13.319. It was a randomised blinded trial. Thus the lead physician (typically RWE) examined the patient and records from that day (BCVA, OCT, etc) and then determined if an injection was required based on renewed or continuing disease activity. These definitions of active lesions requiring treatment were followed:-

1. Intra- or sub- retinal fluid attributable to leak from choroidal neovascularisation,
2. New macular haemorrhage
3. Serous or fibrovascular pigment epithelial detachment which is not stable. This could be: increasing in size since last review, or decreasing in size in response to previous injection at last review. In the second setting injections will be indicated monthly until the volume of the retinal pigment epithelium (RPE) detachment (RPED) stabilises.

Treatment was advised with the above lesion activity unless in the opinion of the assessing clinician further treatment was futile such as the case of RPE tear.

The assessing doctor and some other staff were blinded to which drug the patients were assigned to as per the block randomisation. An ophthalmic registrar then administered any required treatment. If the fellow eye subsequently developed nAMD requiring anti-VEGF therapy then it received the same medication as the study eye. Due to limited patient numbers we are treating treatment with either drug as treatment. Here we take advantage of the

opportunities afforded by the large numbers of repeat mfPOP tests performed up to 28 months.

While we do not present the OCT data in this chapter it is important to recall that the specialist (RWE) inspected new OCT scans on each visit to determine the need for treatment and any progression of the neo-vascular AMD

RESULTS

The study included 23 eyes of 18 patients. Majority of the patients were female (14 cases, 77.8%, **Table 1**). Of the 18 patients, 13 received anti-VEGF injection in one eye, and 5 received injection in both the eyes. Among those patients treated bilaterally, 3 cases received injection from the beginning in both the eyes, and the other 2 cases began receiving injection in the fellow eyes at later visits after an untreated fellow eye developed active nAMD. Of those 2 patients, one case received injections of ranibizumab and the other received injections of aflibercept. Nine patients had smoked for 12.8 ± 15.9 years (mean ± SD), but had quit 18.4 ± 16.3 years before the study. Subject 85704 was diagnosed with mild Type 2 Diabetes at month 8 and continued in the study.

Table 1. Subject demographics. For Hypertension (HT) and the FA data (FAos, FAod) a '.' indicates none. For the FA the definitions of P, O, and M are given in the Methods, (16) and (22) indicate the study month in which that fellow eye developed new nAMD. The high (VAos, VAod) and low contrast (LcVAos, LcVAod) best corrected acuities are given in letter scores. For reference 85 is 6/6, 76 is 6/9, 59 is 6/20.

Subject	*Age*	*Sex*	*HT*	*VAos*	*VAod*	*LcVAos*	*LcVAod*	*FAos*	*FAod*
85700	67	F	.	85	76	78	64	.	O
85701	82	F	.	81	80	74	61	O	O(22)
85703	69	M	.	89	69	79	68	.	O
85704	81	F	Y	48	79	37	67	P	O
85705	87	M	.	84	73	76	62	.	P
85706	79	F	Y	78	60	69	52	O(16)	O
85707	87	F	.	82	29	77	18	.	P
85708	81	F	Y	78	80	64	70	O	.
85711	73	F	Y	56	83	42	73	O	.
85712	83	M	.	77	88	65	78	O	.
85713	78	F	Y	79	87	62	76	O	.
85714	96	F	Y	19	43	10	25	O	P
85716	82	F	Y	76	77	55	61	M	.
85717	75	M	Y	78	59	59	28	M	M
85718	75	F	.	73	69	60	49	P	P
85719	66	F	Y	77	28	56	17	O	.
85721	83	F	Y	86	79	78	66	.	P
85724	88	F	Y	70	79	77	64	.	O

We studied more than 12 treatment-patterns of interest. **Figure 2** introduces this process. The pattern [0 0 0 1] included 12 instances where the injection anti-VEGF was not required for initial monthly 3 visits but was required on visit 4 (Fig. 2A). The pattern [1 1 1 1] included 44 instances where the treatment was required in every monthly visit (Fig. 2B). Each region of each panel represents the median sensitivity deviation in decibels (dB) at that region across the instances of the required pattern. A deviation of "0" indicates the sensitivity is equal to that expected for a subject of that age and sex. Inspection of the calibration bar shows that the background grey in each panels represents (on average) no sensitivity difference from normal with darker shades representing reduced sensitivity, and lighter shades hypersensitivity.

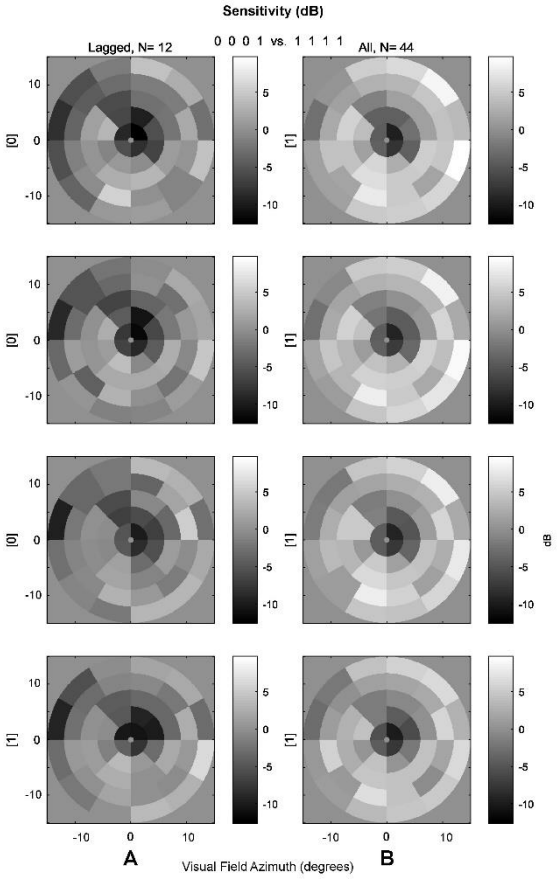

Figure 2. Outcomes for two treatment-patterns: **(A)** [0 0 0 1], and **(B)** [1 1 1 1]. "0" indicates treatment not given and "1" indicates treatment given. Each row is a consecutive month and the y-axis labels indicate treatment given or not given. No eye contributed more than their first three matching sequences. The data are median decibel sensitivity deviations relative to normal at each region. The background grey indicates 0 difference from normal sensitivity. **(A)** sensitivity for the two central rings of stimuli declines (ring-1, 2), especially on the treatment day. Some outer rings show hypersensitivity (ring-3 to 5). The word "lagged" in column title was the name for the pattern [0 0 0 1], implying later treatment. **(B)** central sensitivity is consistently low, peripheral sensitivity appears higher than for the less-treated eyes. The word "All" in the column title indicates treatment on all four visits.

In Figure 2A the sensitivity for the central two rings of stimuli layout was lower than normal and appeared to decline, particularly on the treatment day. It is important to point out that the injection was administered after the mfPOP test on the day. The outer rings indicate hypersensitivity of 2 to 5 dB. The Figure 2B shows sensitivity deviations for subjects under treatment-pattern [1 1 1 1], representing eyes that were ascertained by the clinician to be not

responding to the treatment. In this case, the central sensitivity was consistently lower than normal, while the peripheral regions appeared hypersensitive compared to the less-treated eyes, with deviations up to 9 dB. Note that the same calibration scale is used for all 8 panels.

The time-to-peak was also analysed for the above treatment-patterns (**Fig. 3**). In Figure 3A representing the treatment-pattern [0 0 0 1], the time-to-peak became longer with subsequent monthly visits in the lead up to a required treatment. In the eyes with treatment-pattern [1 1 1 1], the times-to-peak were consistently shorter than normal in the central regions. By contrast, in peripheral rings the time-to-peak was longer than normal (Fig. 3B). Similar findings were observed with the wider-field stimulus protocol P129 (not shown).

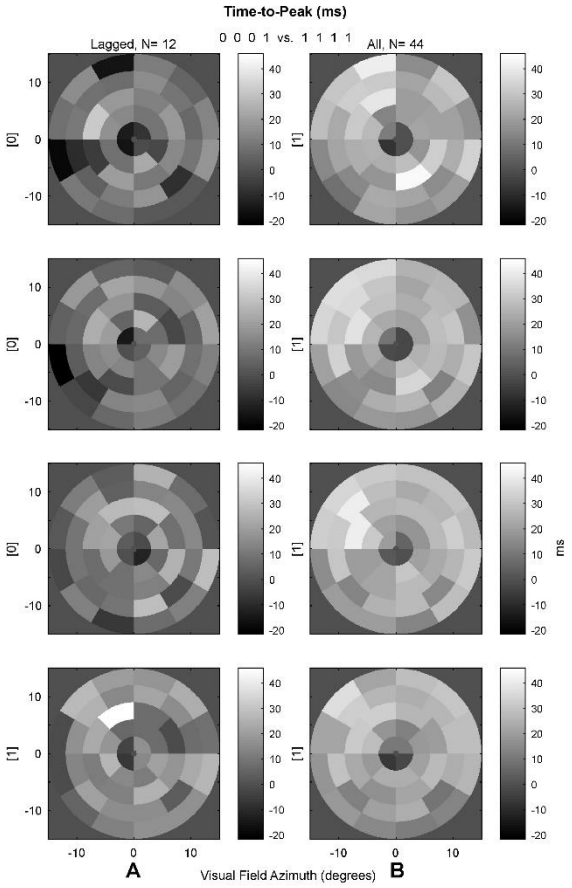

Figure 3. Regional delay deviations for the same eyes as Fig. 1. **(A)** Delays appear to become longer in the time leading up to treatment. **(B)** Central delays are consistently shorter than normal by around 10 to 20 ms,

The initial findings described above strongly indicate that the central and peripheral regions behave differently both in terms of sensitivity and time-to-peak. We therefore, simplified our presentation and analysis by combining, through taking the median, the regions within each of the five rings. As before, we then took medians across instances unless otherwise indicated. This allowed us to plot months by rings. **Figure 4** shows the data of Figure 2 replotted in this way. It shows more clearly that, in the treatment-pattern [0 0 0 1], the sensitivity of the central regions kept decreasing until the treatment was required in the fourth visit, while some peripheral regions showed hypersensitivity (Fig. 4A). However, these

trends were not significant, for reasons that will become clear later. For the treatment-pattern [1 1 1 1] the sensitivity increased over visits but remained below normal (Fig. 4B). The peripheral regions showed hypersensitivity consistently. The slope of rings-3 to 5 (averaged to reduce multiple comparisons) of the sensitivity was significant at -0.76 ± 0.18 dB/month (p= 0.002, n=12). The times-to-peak by rings for both the treatment patterns (Figs. 4C & 4D) were consistent with the findings of Figure 3.

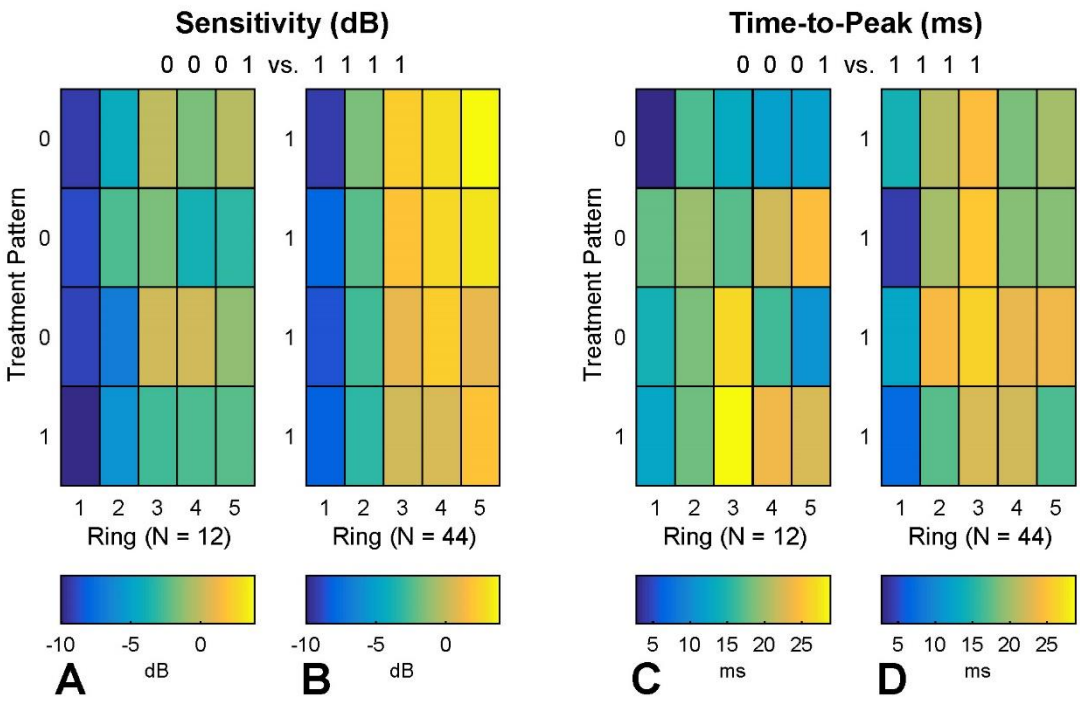

Figure 4. The ring-medians deviations for the same data as in Figure 2 and 3 above: ring-1 is the median result of the central 4 regions, ring-5 for the outer 12 regions, 0 again indicates normal sensitivity or delay. **(A)** The slope of rings-3 to 5 of the sensitivity data was significant at -0.76 ± 0.18 dB/month, p= 0.002. **B to D** correspond to Fig 2B, and Fig. 3 A, B.

We next examined the treatment-patterns [0 0 1 0 0] and [0 0 1 1 1] and their associated temporal profiles for sensitivity **(Fig. 5)**. For the first pattern, the less-treated eyes showed improvement in the ring-1 sensitivity in the post-treatment month with peripheral hypersensitivity (Fig. 5A). The less responsive eyes in the second treatment-pattern showed

gradual improvement in the central sensitivity (Fig. 5B). However, these trends did not reach significance. We will come back to analysis of treatment-patterns later.

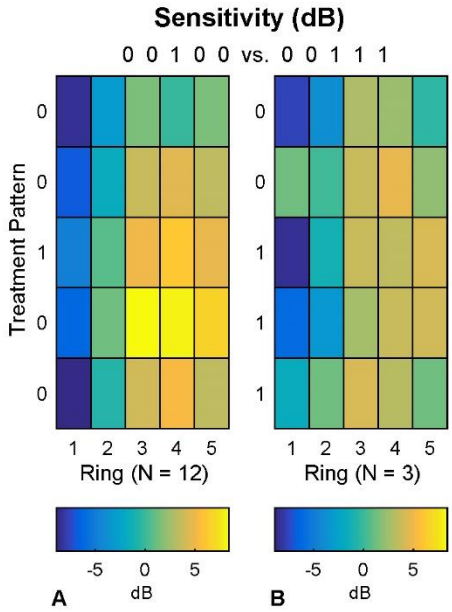

Figure 5. Sensitivity deviations for 12 instances with treatment-patterns [0 0 1 0 0], compared to 3 instances with pattern [0 0 1 1 1]. **(A)** The less-treated eyes seem to show improved ring-1 sensitivity in the post treatment month, and peripheral hypersensitivity. **(B)** The less responsive eyes seem to show gradual improvement of central sensitivity. These trends were not significant.

We next analysed data that included 14 pairs of treated and untreated fellow eyes that extended across 15 months. By untreated eyes we mean eyes that were judged by the clinician not to need treatment. Most subjects began treatment in one eye so there was a good pool of these pairs of treated/untreated eyes. In the untreated fellow eyes the ring-1 median sensitivity declined at -0.17 ± 0.07 dB/month ($p=0.033$) **(Fig. 6A)**. Among the treated eyes, the sensitivity initially improved and that plateaued after about 5 to 6 months of treatment (Fig. 6B). Ring-1 of the treated eyes was less sensitive than in the untreated eyes by -2.23 ± 0.051 dB ($p<0.0002$, $n=14$). A similar result was found for another stimulus protocol P129 (not shown) with a difference of -2.57 ± 0.57 ($p<0.0002$).

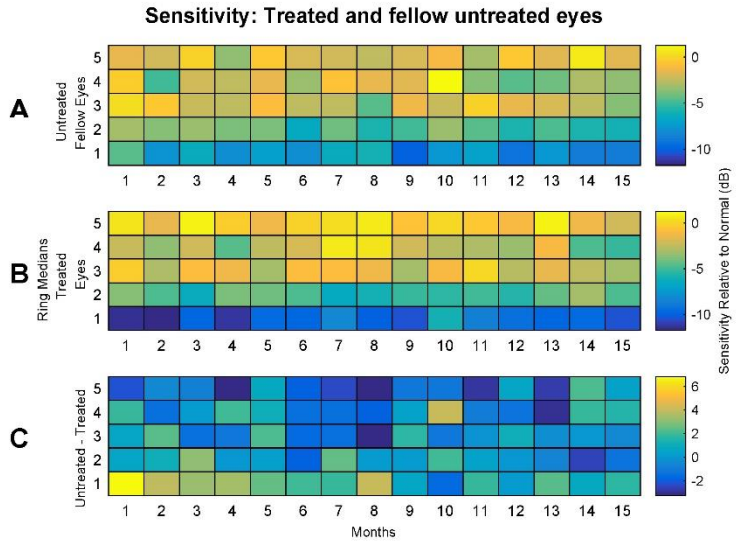

Figure 6. Median sensitivity deviations in 14 pairs of treated and untreated fellow eyes relative to normal values. (**A**) For the untreated eyes -1 medians declined at -0.17 ± 0.07 dB/month (p=0.033). (**B**) Treated eyes appeared to plateau after about 5 to 6 months of treatment. Ring-1 was less sensitive than the untreated eyes by -2.23 ± 0.051 dB (p<0.0002). (**C**) shows the differences between untreated and treated eyes.

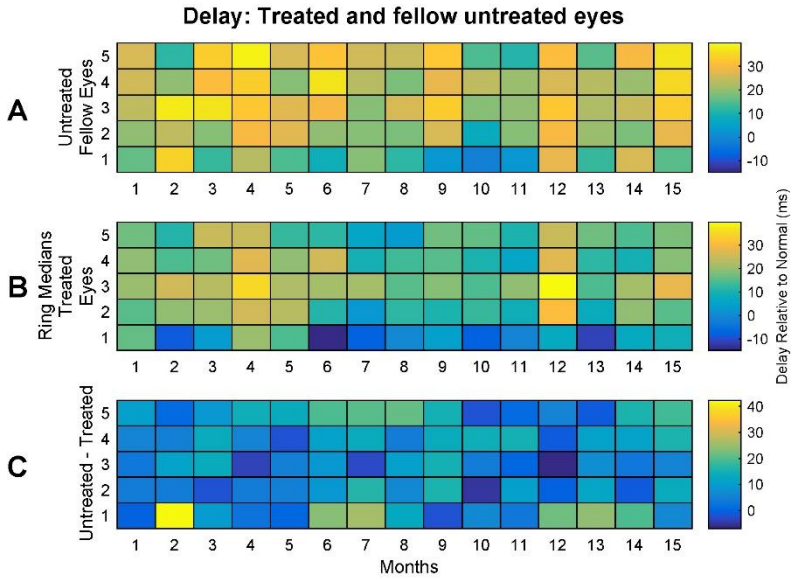

Figure 7. Response Time-to-peak deviations in treated cf. untreated eyes. (**A**) the untreated eyes being slower than normal by about 20 ms. **(B)** ring-1 of treated eyes was 13.08 ± 3.77 ms quicker than untreated eyes (p=0.001). Similarly rings-3 to 5 were also quicker by 7.81 ± 2.10 ms (p=0.001). **(C)** shows the differences between untreated and treated eyes.

We analysed the times-to-peak as we did for the sensitivity for the same treated and untreated fellow eyes. The treated eyes showed quicker responses in ring-1 by 13.08 ± 3.77 ms than untreated eyes (p=0.001) (**Fig. 7B**). Similarly, rings-3 to 5 in the treated eyes (averaged together) were also quicker by 7.81 ± 2.10 ms (p=0.001). Overall the untreated eyes were slower than normal eyes by about 20 ms (Fig. 7A).

We also followed up the patients who had been receiving treatment in one eye for whom their fellow eye required an alteration in treatment during the study. **Figure 8** shows the treatment-patterns for two such subjects. Subject 1 received treatment in one eye every month for 5 months, then on alternate months until 18 months. From the 19th month, again the subject needed treatment every month until the study was completed. The fellow eye started receiving monthly treatment from the 16th month until the end of the study. Subject 2 received treatment in one eye monthly for 4 months, and again in 9th and 10th months. The fellow eye needed monthly treatment from the 16th month, for 3 months.

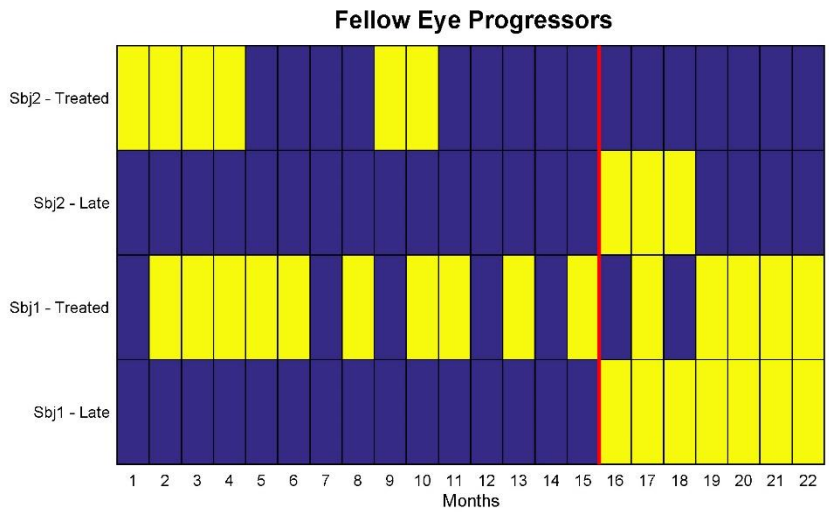

Figure 8. Two subjects required anti-VEGF injection in the fellow eyes: O(16) and O(22) of Table 1. As per the study design both began with one eye being treated. After 15 or more months, however, the two subjects required treatment in their previously untreated eye. We have aligned the treatment sequence for the new eye at 15 months (red line). Note that Subject 1's treated eye had 4 injections over 5 months before relative month 1.

We next show the sensitivity and time-to-peak data for these two subjects. **Figure 9** shows the findings for sensitivity for stimulus protocol P131. For subject 1 the sensitivity in the ring-1 of the treated eyes improved over time (Fig. 9C). The peripheral rings showed hypersensitivity as indicated previously. The sensitivity in the fellow eye dropped until the 16th month when the treatment was required (Fig. 9D). In subject 2, the sensitivity in the central ring was low initially but with the treatment the sensitivity improved (Fig. 9A).

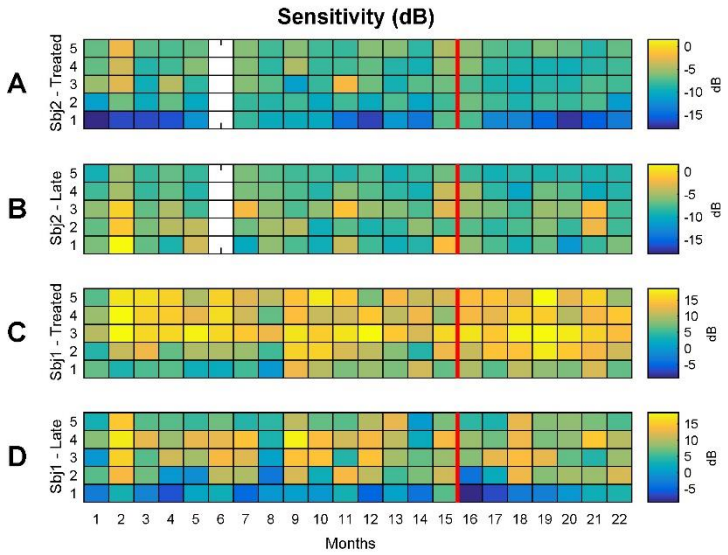

Figure 9. Sensitivity deviation results for the subjects of Figure 8. **(D)** For subject 1 there is a distinct drop in ring-1 sensitivity on the month the surgeon decided that treatment was necessary (after the red line). This is not seen for subject 2. **(A)** Subject 2 was treated less and their ring-1 sensitivity appears to drop by month 20. Both subjects possibly show increased hypersensitivity the month before treatment. The white rectangles for month 6 of Subject 2 represent a missed visit.

Figure 10 shows time-to-peak data for the same subjects as Figure 9 for stimulus protocol P131. The time-to-peak in the peripheral rings of both the treated and fellow eyes increased at the month 16th indicating the need for the treatment, concordant with the drop in sensitivity (Fig. 9B, 9D). Similar findings were observed with the stimulus protocol P129 as shown in **Figure 11**. The results shown use data where direct and consensual responses are combined using a weight based on the per-region signal to noise ratio (more reliable data contributes relatively more). This introduces the possibility that a treatment effect is carried to the pupil of the fellow eye. We therefore separately examined only direct (and only consensual) responses and the outcomes were the same as Figures 10 and 11 (data not shown).

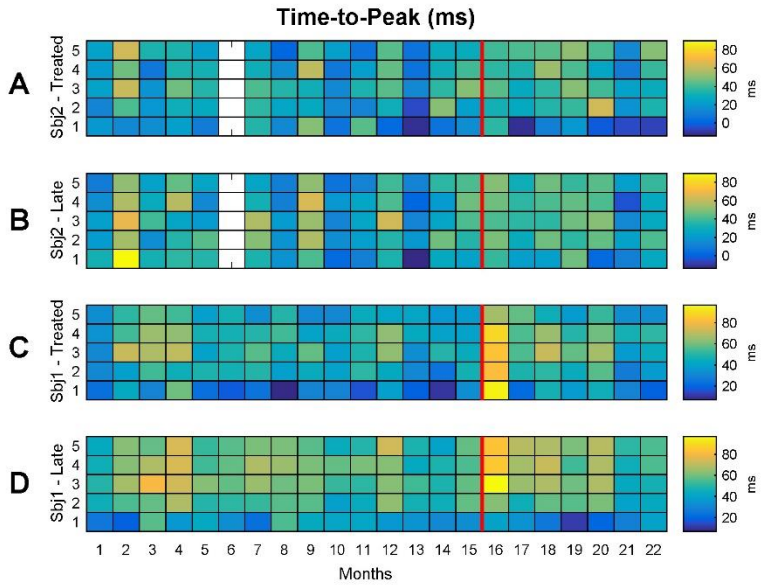

Figure 10. The P131 response delay deviations relative for the two subjects of Figs. 8 and 9. Note that Subject 1 shows an increase in peripheral delay at month 16 *in both eyes* (C & D).

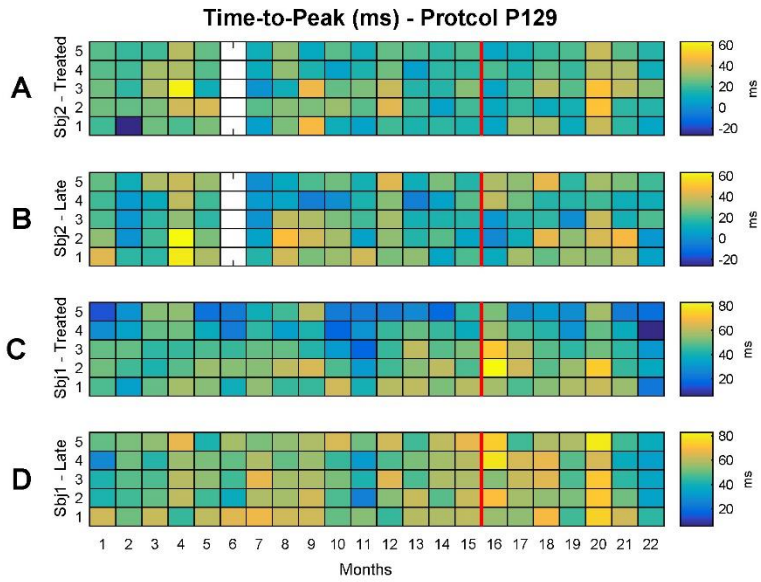

Figure 11. The P129 response delay deviation results for the subjects of Figure 10. A similar binocular increase in delay is seen at month 16 for Subject 1.

The times-to-peak of Figure 11 fluctuate from month to month in a correlated way between eyes. We therefore examined the ring-wise correlations in the time-to-peak between eyes that received treatment early, and the fellow eyes that received treatment at the later stage, as shown in Figure 10 for stimulus protocol P131 (**Fig. 12)**. The correlation between eyes was most positive in rings-3 and 4, and smallest in the central ring-1 (Fig. 12A). The p-values were mostly significant in ring-2 through to ring-5. Ring-1 did not show any significant p-values (Fig. 12B).

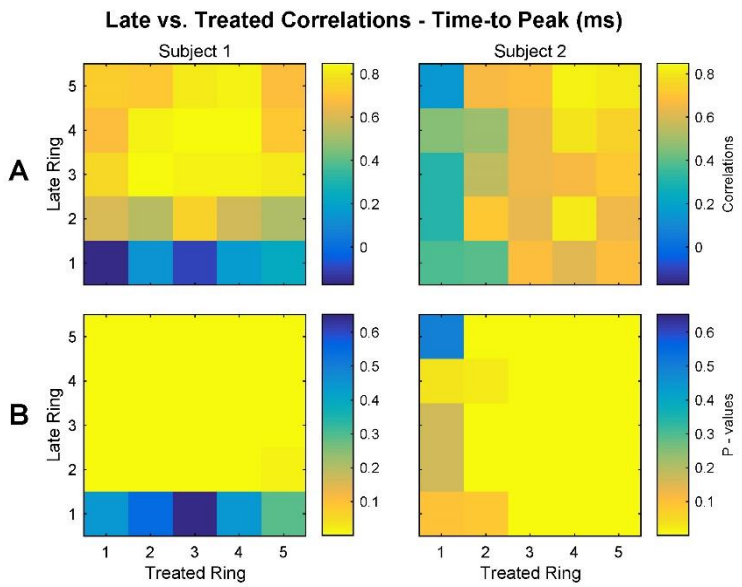

Figure 12. Correlations by ring of the delay results of Figure 10. **(A)** The rings-3 and 4 appear to be the most correlated rings, and ring-1 the least. **(B)** shows the p-values for the two subjects.

The results for the two subjects of Figures 11 and 12 raised the question of whether there are correlations between rings of all treated and untreated eyes. We therefore examined correlations in the cases from Figures 6 and 7 for which we had at least 15 months data. For some analyses we divided the data for treated eyes into the 7 least treated and 7 most treated eyes, the cut-off being a treatment rate below 75% of visits. **Figure 13** shows the results for P129 to illustrate how far into the periphery the effects of correlations between treated and untreated eyes extend. For both sensitivity (Fig. 13A-C), and delay (Fig. 13D-F) plots, regions with orange to yellow tones are significant at $p < 0.05$. The results for P131 were similar, with correlations being overall lower for sensitivity and higher for time-to-peak. Correlations were higher for the pairings of untreated vs. less-treated eyes. Correlations between ring-1 of each were low, especially for pairs containing a more-treated eye.

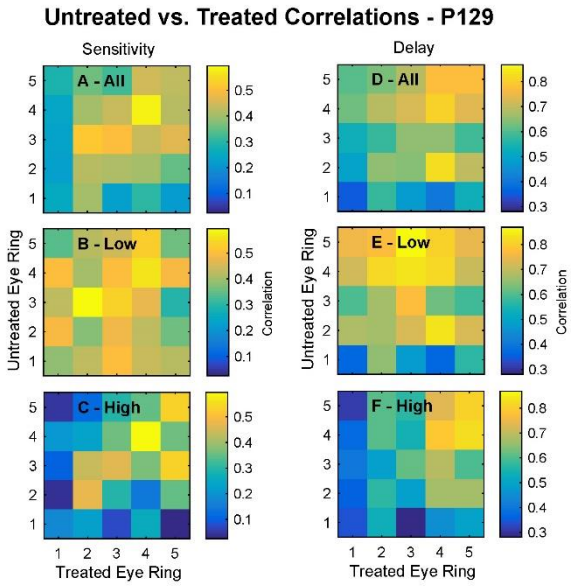

Figure 13. Representing 14 eyes pairs of treated and untreated of Figure 7 & 8. Low and High are for the pairs of eyes from 7 most and least treated eyes with at least 75% of visits received treatment.

The results raise the possibility that correlations might be partly a treatment effect. We therefore examined the cross-correlation in time between treatments and responses from treated eyes. The findings are shown in **Figure 14**. We examined the presence of response auto-correlation using the Durban-Watson statistic and found that most of the 9 data sets used had significant auto-correlation. Accordingly, we used a model that account for the effects of auto-correlation, specifically a simple linear model relating the response (output) to the treatment (input) over the last 2-3 months. We used the 5 data sets that were treated < 75% of the time and for which we had 28 months of data. This produced a cross-kernel with 2 significant lags (months), with lag 1 almost always being larger than lag 0, in agreement with Figure 14.

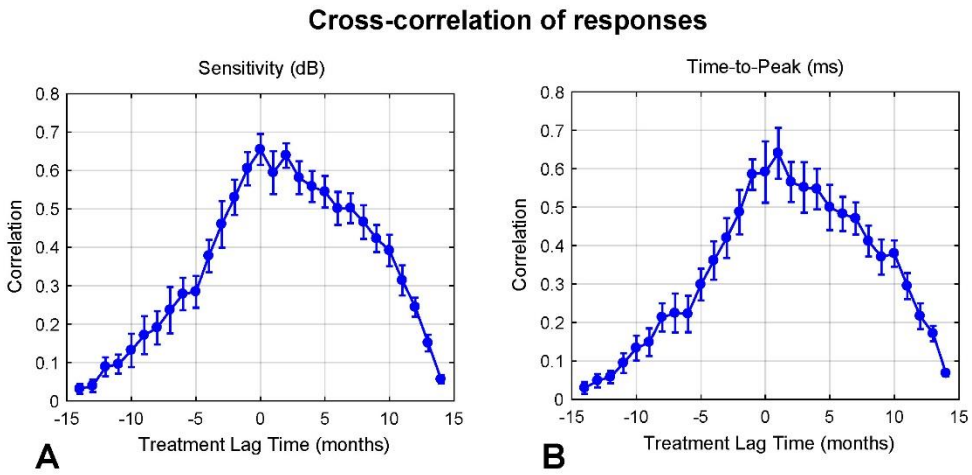

Figure 14. Cross-correlation results for P131. Correlation with a lag of +1 or more months is likely to indicate a treatment effect, i.e. there is a response to treatment in the following 1 to 2 months. **(A)**: Sensitivity shows a secondary peak at 2 months and delay at 1 month. Data are for the 9 treated eyes treated on 70% or fewer visits for 15 months. **(B)**: Delay. Error bars are SE

In fact Figure 14 values are the means of the absolute value of the cross-correlation function.

We took this approach because the sign of the mean outer-ring deviations from normal (rings-3 to 5) predicted the sign of the cross-correlation peak in 18/18 cases examined, as shown in **Figure 15**.

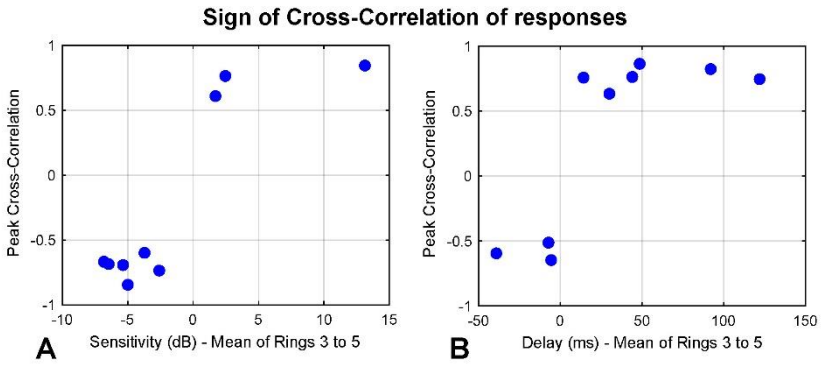

Figure 15. The sign of the outer ring mean data determine sign of the cross-correlation peak, where 0 indicates normal responses. **(A)**: Sensitivity, **(B)**: Delay. Negative delays are faster than normal.

The effects seen in Figure 15 suggest that either treatment drives outer-ring responses towards normality, from a positive or negative starting point, or it drives the outer-ring responses away from normality, off their baseline, or both. Signs of both can be seen in **Figure 16**, where data from the seven less-treated eyes are shown. Panels A-G show the delay relative to normal value by rings, treatment and visits up to 15 months, for five illustrative subjects. The figure shows subjects can have faster or slower than average delays in their outer rings. As Figure 15 shows, this corresponds to more or less sensitivity than a normal subject, in the outer rings. *Thus, it appears subjects fall into two categories of what could be called positive or negative depending whether their outer-region sensitivities or delays are larger or smaller respectively, than normal.* We realised these sub-groups had a large effect on our treatment-pattern analysis because we were pooling data from these groups, resulting in very high outer-ring variance. We therefore undertook separate treatment-pattern analyses for the positive and negative sub-groups.

Treatment-patterns of subjects from positive and negative sub-groups

To quantify these data we created linear models where the treatment month was taken as the reference (constant) and the other two months were fitted as contrasts to the treatment month. This analysis allowed us to assess the significance of the differences of those months. There are two model versions: the first where data from ring-1 was fitted, and second, where the averaged data across rings-3 to 5 were fitted. The titles of the resulting figures thus contain the label: ring-1 or rings-3 to 5, to indicate the type of model. In each figure below the month(s) that are significantly different to the treatment month are flagged with a * on the right-hand side of the figures. We also sometimes fitted a slope across the months of the treatment-patterns.

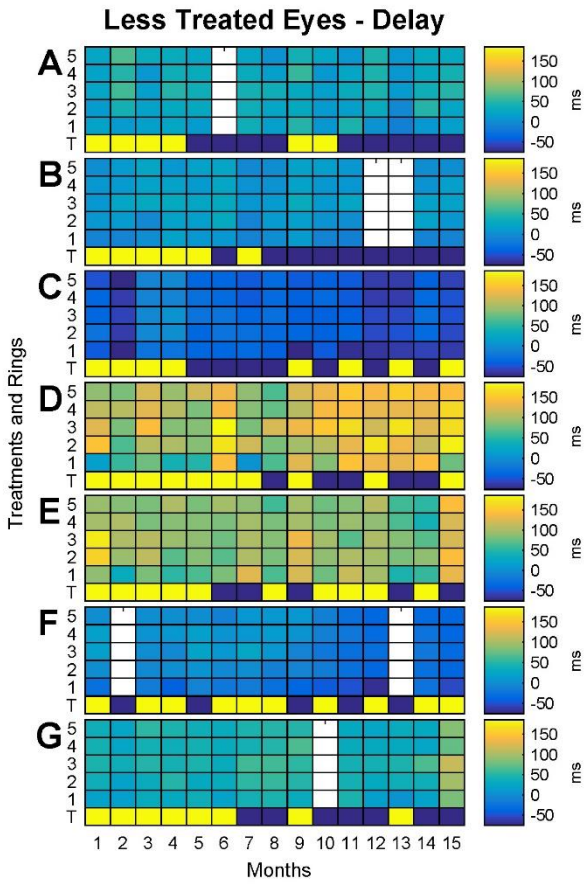

Figure 16. A-G are delay (relative to normal) data from the treated eye of different subjects. Most had three treatments initially and then were on PRN management out to month 15. They are the seven less-treated eyes of Figures 14 and 15. The bottom row of each plot (marked T) records treatment (yellow), or no treatment (dark blue). White rectangles represent missed visits. Note that the mfPOP testing was done before the treatment and so any treatment effect will be seen in the following month.

Figure 17 shows the group of eyes with peripheral hypersensitive responses. In 12 eyes, the first month sensitivities for ring-1 are significantly different from the treatment month, increasing on average by 9.88 ± 4.41 dB (p=0.042). Thus, the data appear to successfully flag the need for treatment the month before a clinician makes that decision. Subjects 1 and 2 of Figure 9 also show this effect. So in these 12 instances the eyes became hypersensitive in the month before the disease activity, meaning they needed treatment. The subjects received three monthly anti-VEGF injections and their ring-1 sensitivity returned to near normal. It is interesting to note that this data was obtained using stimulus P129 where ring-1 covers the

equivalent rings-1 and 2 for P131, which had a similar, but not significant, trend for its ring-1.

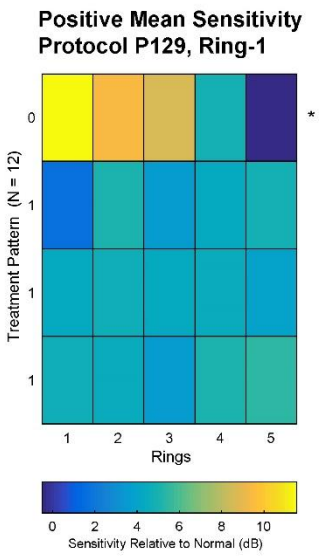

Figure 17. Sensitivities for 12 hypersensitive instances obtained with the wide-field P129 stimulus. These subjects responded relatively poorly and therefore had the treatment-pattern [0 1 1 1]. The sensitivity in the first month for ring-1 is significantly higher than for the first two treatment months by 9.88 ± 4.41 dB (p=0.042). These 12 instances became significantly hypersensitive in the month before disease activity, potentially indicating treatment. After three anti-VEGF injections, the ring-1 sensitivity returned to near normal. The * on the right hand side of figure indicates significance.

Figure 18 shows nine subjects with peripheral hyposensitive responses that received the treatment-pattern [0 1 0 0]. A linear model fit to ring-1 data for protocol P131 shows that the sensitivity for the first month was significantly higher than the treatment day by 2.69 ± 1.23 dB (p=0.040), but with the progress of the disease, this improvement in sensitivity collapsed, leading to treatment. So, in this case, the significant changes occur on the day treatment was judged to be needed. **Figure 19** shows another example of a subject with peripheral hyposensitivity. The treatment-pattern [0 0 0 1] spans the 3 months before the treatment was required. Here the visits 1 and 2 months before treatment are the fitted factors. In these eight cases only the month before treatment is significantly hypersensitive compared to the

treatment month, in this case by 3.56 ± 1.61 dB (p=0.040). Thus, like Figure 17 the data appear to predict the need for treatment in the subsequent month.

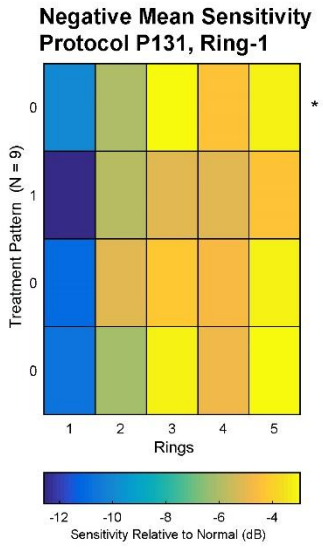

Figure 18. Sensitivity for nine cases with peripheral P131 hyposensitive responses for the treatment-pattern [0 1 0 0], apparent good responders. The fit shows ring-1 sensitivity of the first month was significantly higher than the treatment month by 2.69 ± 1.23 dB (p=0.040).

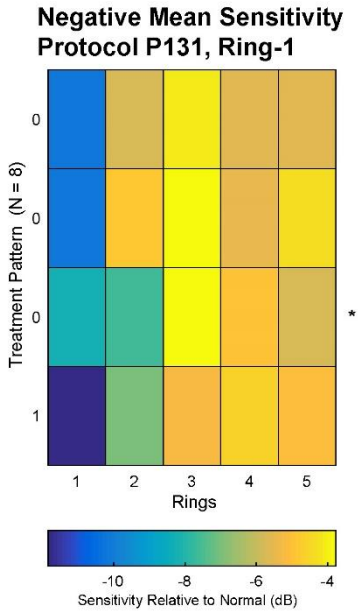

Figure 19. Sensitivity for cases with peripheral hyposensitive responses for a treatment-pattern examining the lead-up to a treatment after no treatments for 3 months: [0 0 0 1]. In these eight cases only the month before the treatment ring-1 was significantly hypersensitive by 3.56 ± 1.61 dB (p=0.040).

Similarly, we analysed times-to-peak taking into consideration whether the peripheral delays were longer or shorter than normal values. **Figure 20** shows P131 data for eight subjects with longer than normal peripheral delays in rings-3 to 5 with the same treatment pattern as Figure 19, [0 0 0 1]. The peripheral delay becomes longer as the treatment day approaches. Two months before treatment the delay becomes shorter and moves towards normal values by 14.0 ± 5.23 ms (p=0.009). Even within one month of treatment the delay became shorter by 8.52 ± 5.23 ms but this was not significant (p=0.108). On fitting the delay slope we found that over the 3 pre-treatment months, delay rose at 3.49 ± 1.75 ms per month (p=0.049). Overall, hyper- and hypo-sensitive peripheral delays appeared to predict the need for treatment.

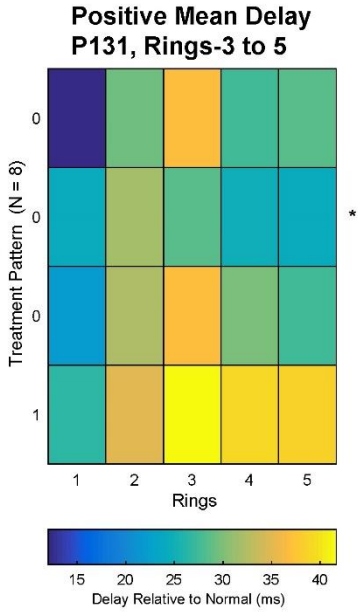

Figure 20. Times-to-peak for eyes showing longer than normal peripheral delays for the same treatment pattern as Fig. 19. Rings-3 to 5 of eight cases are analysed. The peripheral delay grows as treatment day approaches, being 14.0 ± 5.23 ms quicker (p=0.009) (and so closer to normal) two months out from treatment. One month out, delays were also shorter by 8.52 ± 5.23 ms, but this was not significant (p-0.108). Fitted as a slope, delay rose from month 1 at 3.49 ± 1.75 ms per month (p=0.049).

A second category in terms of time-to-peak was those cases with shorter than normal peripheral delays. Fourteen cases in this category are shown in **Figure 21**. Here the months before and after treatment are fitted for rings-3 to 5 of protocol P129. Both are significantly quicker responses than the treatment month, which had become more delayed than normal. For the first month the delay was shorter by 9.38 ± 3.59 (p=0.013), and for month 3 the delay was shorter by 8.50 ± 2.71 ms (p=0.004). Ring-1, month 1, responses appear to be slower than the first treatment day, but not significantly.

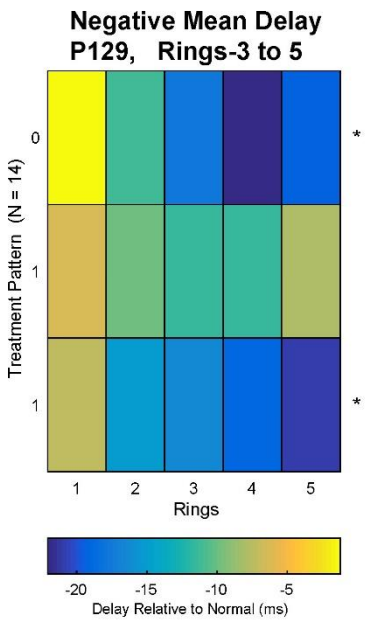

Figure 21. Time-to-peak for 14 treatment instances showing shorter than normal peripheral delays. Here the months before and after treatment are fitted for rings-3 to 5 of P129. Both are significantly quicker than the treatment month, which had become more delayed than normal. For month 1 and 3 the delays were shorter by 9.38 ± 3.59 and 8.50 ± 2.71 ms, (p=0.013 and p=0.004) respectively. Ring-1, month 1, appears to be more delayed than treatment day but this was not significant.

DISCUSSION

A number of publications now support the diagnostic power of mfPOP in AMD (Sabeti *et al.*, 2011; Rosli *et al.*, 2012; Sabeti *et al.*, 2013). It also has the potential to detect ranibizumab-induced changes in nAMD (Sabeti *et al.*, 2012). Importantly in that study eyes with peripheral hypersensitivity appeared to predict eyes that respond well to ranibizumab. Comparative studies of mfPOP with other established diagnostic methods have found it comparable to multifocal visual evoked potentials (mfVEP) (Sabeti *et al.*, 2017), Humphrey Matrix and short-wavelength automated perimetry (Sabeti *et al.*, 2015a). Clinical guidelines for the use of mfPOP in the clinical setting following mydriasis are provided (Rai *et al.*, 2020). In the current study on nAMD patients we evaluated whether mfPOP test results could be used to easily and rapidly obtain biomarkers that would indicate the need for anti-VEGF injections in follow-up visits. We discuss the responses, namely sensitivity and time-to-peak, first when all eyes are analysed together, secondly as relative to the median values and finally the positive and negative types of eyes are analysed separately. The final category of data showed significant ability of mfPOP to predict the need for treatment.

Sensitivity

In the treatment-pattern [0 0 0 1], the central rings showed progressive deterioration in sensitivity until in the fourth visit requiring treatment (Fig. 2A). The peripheral rings showed hypersensitivity, which is consistent with the findings reported in previous studies where mfPOP had shown hypersensitivity peripheral to the retinal regions affected by AMD, diabetic retinopathy (DR) and diabetic macular oedema (DMO) (Sabeti *et al.*, 2015b; Sabeti *et al.*, 2017). Similar hypersensitive regions peripheral to the affected retinal regions were also reported with mfVEP (Sabeti *et al.*, 2017) in the same subjects that were tested with mfPOP. Both mfPOP and mfVEP showed suppression of sensitivity in cases with more advanced disease, or as the disease worsened to clinically significant AMD similar to the

findings of our current study. So we may conclusively say that those retinal regions affected by advanced AMD or early AMD worsening to more advance AMD, show suppressed sensitivity, and that peripheral hypersensitivity shows potential as a biomarker for future development of AMD or worsening disease condition (Sabeti *et al.*, 2017).

Some cautions must be taken in interpreting peripheral hypersensitivity because previous studies have reported that the supero-temporal regions showed higher sensitivity in normal-control subjects. In our case, we have used luminance-balanced stimuli layout to minimise this effect (Carle *et al.*, 2011; Rai *et al.*, 2020). Among the less responsive eyes, the central macular regions initially showed suppressed sensitivity with peripheral hypersensitivity, but with subsequent treatment, there was a gradual improvement in the central sensitivity (Fig. 5B). This again supports the observation that central macular regions affected by disease show suppressed sensitivity while peripheral regions not affected by the disease can show significant hypersensitivity, before the disease may advances into those regions. It has been reported that, along with improvements in the central retinal thickness (CRT) following treatment with ranibizumab, peripheral hypersensitivity also improves (Sabeti *et al.*, 2012).

Among the treated eyes, despite often being clinically nonresponsive types, sensitivity seemed to plateau after 5 to 6 months of treatment (Fig. 6B). At the same time, the median sensitivity in ring-1 declined significantly in their untreated fellow eyes. This may be due to poor ocular bio-availability of anti-VEGF in ocular tissues of the untreated fellow eyes from the treated eyes, because most of the anti-VEGF circulating in the blood are metabolised before it reaches the fellow eyes (Semeraro *et al.*, 2015). We have noticed that both the sensitivity and time-to-peak behave differently in the central and the peripheral regions. Using the median of the central and the peripheral regions we observed that the central sensitivity in the treatment-pattern [0 0 0 1] kept decreasing until the treatment was administered, while the peripheral regions were progressively more hypersensitive than the

median values (Fig. 2A, 4A). Among the non-responder eyes in treatment-pattern [1 1 1 1], the sensitivity increased with the treatment over visits but remained below normal with peripheral region showing hypersensitivity. From these findings we infer that among the non-responder eyes, despite lack of clinically obvious improvement, in OCT thickness and visual acuity, with anti-VEGF treatment, there is still a constant improvement in the micro-vasculature including retinal and choroidal circulation and anatomical integrity of the macula. Despite lack of clinical improvement, like resorption of sub- or intraretinal fluid or haemorrhage or settling of a detached retinal pigment epithelium (RPE), there is improvement in the retinal and choroidal microvascular structure such as decreases in dark halo, secondary to choriocapillary dropouts around CNV, regression of peripheral anastomosis and larger choroidal vessels that developed as a pathogenesis of the nAMD and reduction in the choroidal thickness (Lipecz *et al.*, 2019). In our study, the improved sensitivity may reflect the functional improvement due to reversal of the microvascular changes with anti-VEGF treatment before the structural improvements. This idea is also supported by the haemodynamic theory of AMD development (Gelfand & Ambati, 2016; Lipecz *et al.*, 2019).

In this study, we have provided evidence for the existence of two types of peripheral sensitivity responses relative to normal controls. The positive patients had peripheral sensitivity higher than normal (hypersensitive type), and negative patients showing peripheral sensitivity lower than normal (hyposensitive type). For positive patients, sensitivity increased in the month preceding the appearance of active disease (Fig. 17). After receiving three monthly anti-VEGF injections the sensitivity returned to near normal value. Thus in positive eyes the hypersensitivity prior to treatment was an indication of worsening disease, thereby needing treatment. For negative patients, there was mainly a drop in sensitivity with increased disease activity (Fig. 18), but increased sensitivity could predate activity by a

month (Fig. 19). Our previous study has reported that peripheral hypersensitivity as a biomarker for favourable outcomes with the anti-VEGF treatment (Sabeti *et al.*, 2012).

Time-to-peak

We observed that for nAMD patients, the central time-to-peak in the very first visit was shorter than normal, and got progressively slower with subsequent visits until the anti-VEGF injection was needed. The prolongation of the time-to-peak might have been synchronous with the worsening of the disease. This prolonged time-to-peak suggested the worsening nAMD to the clinical stage where the anti-VEGF injection was indicated. This supports the conclusions of previous studies (Sabeti *et al.*, 2011; Maddess *et al.*, 2013; Sabeti *et al.*, 2015b). Similar to sensitivity, times-to-peak behaved differently in the central vs. peripheral regions. As with sensitivities, we analyzed the median of the central and peripheral regions for different treatment-patterns. In treatment-pattern [0 0 0 1], time-to-peak for the central 4 regions increased consistently over the visits until the treatment was administered (Figs. 3A, 4C). A previous study also reported that asymmetry in local delay deviations produced higher sensitivity and specificity than the sensitivity deviations (Sabeti *et al.*, 2015b). The findings of the cross-correlations of responses (Fig. 14, 15) flagged the possibility of existence of two patterns of responses. Similar to the sensitivity, time-to-peak can be used to delineate two types of patients. In positive patients, there was increase in peripheral delays up to three months (Fig. 20) before active disease was detected through conventional methods, and large increases in delay accompanied disease activity. For negative patients, peripheral delays in rings-3 to 5 were shorter by 1-2 months before the treatment was administered (Fig. 21). Correspondingly these patients showed increased macular delay (ring-1) in the month before disease activity.

Systemic side effects and thromboembolic phenomena such as cerebral vascular accidents or myocardial infarction have been reported following intravitreal injection of anti-VEGF (El-Sanhouri *et al.*, 2008; Costagliola *et al.*, 2012; Semeraro *et al.*, 2015) indicating significant amount of anti-VEGF reaches systemic circulation following intravitreal injection. It is reported that the systemic exposure in nAMD, DMO and retinal vein occlusion (RVO) cases was highest with bevacizumab, followed by aflibercept and least with ranibizumab (Zehetner *et al.*, 2015; Avery *et al.*, 2017). In our study, we did not encounter such systemic side effects.

There are some studies reporting that the fellow eyes would benefit from the anti-VEGF injection administered to an eye. The intravitreal injection of ranibizumab and bevacizumab administered in one eye, in cases of bilateral DMO, improved the macular thickness and DMO in the untreated fellow eyes. The result was more significant with bevacizumab than ranibizumab (Bakbak *et al.*, 2016). Michalska-Malecka et al. reported that intravitreal injection of ranibizumab reduced the central retinal thickness (CRT) of both the treated and untreated fellow eyes and also indicated differences in gene expression of mononuclear cells in peripheral blood before and after the treatment (Michalska-Malecka *et al.*, 2016). In the untreated fellow eyes, the ring-1 median sensitivity declined significantly (Fig. 6A). For 14 pairs of treated and untreated eyes, in at least two untreated fellow eyes the AMD worsened and required anti-VEGF injections at the later visits despite the eyes under treatment continued to receive it. This was possibly because the anti-VEGF circulating in the blood are metabolised significantly before it reaches the fellow eyes attaining a therapeutic level (Semeraro *et al.*, 2015). Likewise the time-to-peak was slower in the untreated eyes by 13.08 ± 3.77 ms in the ring-1 regions (p=0.001), and by 7.81 ± 2.10 ms in the rings 3 to 5 regions (p=0.001). Similar observations were made in both the stimulus protocols. This supports the

idea that anti-VEGF injected in one eye does not reach the therapeutic level in the fellow eyes due to metabolism (Semeraro *et al.*, 2015; Avery *et al.*, 2017). The time-to-peak between the treated and the untreated fellow eyes correlated positively and significantly in ring-3 and 4 with the least correlation in ring-1. This is consistent with the macular regions being involved (and peripheral regions not) in nAMD, explaining why they behave differently both in terms of sensitivity and time-to-peak. The difference is also partly influenced by the treatment lag period, which was 2 months for sensitivity and 1 month for time-to-peak.

Limitations of the study

The lack of structure-function correlation is a major limitation. The study has limited number of participants: 23 eyes of 18 patients. However, we have large amount of pooled data across up to 28 visits, subjects, visits, eyes, direct and consensual responses, and two stimulus protocols. We have considered the retinal function purely based on the mfPOP characteristics. The macular structural changes that might influence retinal function, are not discussed here, but will be discussed in a separate article.

CONCLUSIONS

The mfPOP method is informative because of its ability to detect local pathologies at various macular locations compared to the BCVA, which remains largely unaffected in early AMD or even in advanced case if the central fovea remains spared (Maddess & Daria, 2017). We observed that the central sensitivities decreased progressively until the anti-VEGF injection was administered. There was peripheral hypersensitivity which improved with the progression of the disease. Amongst the less-responding eyes, as defined by the ongoing monthly need of anti-VEGF treatment and based on OCT thickness, the sensitivity started to plateau after 5 to 6 months of treatment. The time-to-peak increased progressively until treatment was required. In most cases, the anti-VEGF injected intravitreally in one eye did

not benefit the fellow eye because it did not reach the therapeutic level in the fellow eye due to metabolism and clearance from systemic circulation. The treatment drives subsequent responses towards normality either from a positive, or negative, starting point. We have noticed that central and peripheral regions reflected different responses. Based on the peripheral responses we have recognised two categories of patients. The positive ones show higher peripheral sensitivity and longer peripheral delays than normal controls. The negative patients show lower peripheral sensitivity and shorter delays than normal controls. These changes in responses predate 1 to 3 months before the treatment is indicated clinically or with other diagnostic methods. The findings support that mfPOP may be a potential biomarker for need of anti-VEGF injection in nAMD.

REFERENCES

Age-Related Eye Disease Study Research G. (2001). A Randomized, Placebo-Controlled, Clinical Trial of High-Dose Supplementation With Vitamins C and E, Beta Carotene, and Zinc for Age-Related Macular Degeneration and Vision Loss: AREDS Report No. 8. *Archives of ophthalmology* **119,** 1417-1436.

Avery RL, Castellarin AA, Steinle NC, Dhoot DS, Pieramici DJ, See R, Couvillion S, et al. (2017). Systemic Pharmacokinetics and Pharmacodynamics of Intravitreal Aflibercept, Bevacizumab, and Ranibizumab. *Retina (Philadelphia, Pa)* **37,** 1847-1858.

Bakbak B, Ozturk BT, Gonul S & Gedik S. (2016). The effect of intravitreal bevacizumab and ranibizumab on macular edema of the contralateral eye: A comparative study of two anti-VEGFs. *Oman J Ophthalmol* **9,** 44-48.

Bell A, James AC, Kolic M, Essex RW & Maddess T. (2010). Dichoptic Multifocal Pupillography Reveals Afferent Visual Field Defects in Early Type 2 Diabetes. *Investigative Ophthalmology & Visual Science* **51,** 602-608.

Bremner FD. (2012). Pupillometric evaluation of the dynamics of the pupillary response to a brief light stimulus in healthy subjects. *Invest Ophthalmol Vis Sci* **53,** 7343-7347.

Brown GC, Brown MM, Sharma S, Stein JD, Roth Z, Campanella J & Beauchamp GR. (2005). THE BURDEN OF AGE-RELATED MACULAR DEGENERATION: A VALUE-BASED MEDICINE ANALYSIS. *Transactions of the American Ophthalmological Society* **103,** 173-186.

Carle C, James A, Kolic M, Essex R & Maddess T. (2013). Getting the timing right: Clustered volley stimulus presentation for multifocal pupil perimetry in glaucoma. *Investigative Ophthalmology & Visual Science* **54**.

Carle CF, James AC, Kolic M, Essex RW & Maddess T. (2014). Luminance and colour variant pupil perimetry in glaucoma. *Clin Exp Ophthalmol* **42,** 815-824.

Carle CF, Maddess T & James AC. (2011). Contraction anisocoria: segregation, summation, and saturation in the pupillary pathway. *Invest Ophthalmol Vis Sci* **52,** 2365-2371.

Carle CF, Maddess T, Kolic M, Essex RW & van Kleef JP. (2020). Normative data for wide-field an macular multifocal pupilographic objective perimetry tests. *In preparation*.

Choi W, Moult EM, Waheed NK, Adhi M, Lee B, Lu CD, de Carlo TE, et al. (2015). Ultrahigh-Speed, Swept-Source Optical Coherence Tomography Angiography in Nonexudative Age-Related Macular Degeneration with Geographic Atrophy. *Ophthalmology* **122,** 2532-2544.

Christoforidis JB, Tecce N, Dell'Omo R, Mastropasqua R, Verolino M & Costagliola C. (2011). Age related macular degeneration and visual disability. *Current drug targets* **12,** 221-233.

Chylack LT, Wolfe JK, Singer DM, Leske MC, Bullimore MA, Bailey IL, Friend J, et al. (1993). The Lens Opacities Classification System-Iii. *Archives of Ophthalmology* **111,** 831-836.

Costagliola C, Agnifili L, Arcidiacono B, Duse S, Fasanella V, Mastropasqua R, Verolino M, et al. (2012). Systemic thromboembolic adverse events in patients treated with intravitreal anti-VEGF drugs for neovascular age-related macular degeneration. *Expert Opin Biol Ther* **12,** 1299-1313.

El-Sanhouri A, Puklin C, Patel C, Iezzi R, Murphy G, Abrams G & Mahmoud T. (2008). Systemic Side Effects and Risks Associated With Bilateral Anti-VEGF Injections. *Investigative Ophthalmology & Visual Science* **49**.

Fan Q, Maranville JC, Fritsche L, Sim X, Cheung CMG, Chen LJ, Gorski M, et al. (2017). HDL-cholesterol levels and risk of age-related macular degeneration: a multiethnic genetic study using Mendelian randomization. *Int J Epidemiol* **46,** 1891-1902.

Gao SS, Jia Y, Zhang M, Su JP, Liu G, Hwang TS, Bailey ST, et al. (2016). Optical Coherence Tomography Angiography. *Investigative Ophthalmology & Visual Science* **57,** OCT27-OCT36.

Gelfand BD & Ambati J. (2016). A Revised Hemodynamic Theory of Age-Related Macular Degeneration. *Trends Mol Med* **22,** 656-670.

Jager RD, Mieler WF & Miller JW. (2008). Age-Related Macular Degeneration. *New England Journal of Medicine* **358,** 2606-2617.

James AC. (2003). The Pattern-Pulse Multifocal Visual Evoked Potential. *Invest Ophthalmol Vis Sci* **44,** 879-890.

James AC, Ruseckaite R & Maddess T. (2005). Effect of temporal sparseness and dichoptic presentation on multifocal visual evoked potentials. *Visual neuroscience* **22,** 45-54.

Klein R, Klein BE, Jensen SC & Meuer SM. (1997). The five-year incidence and progression of age-related maculopathy: the Beaver Dam Eye Study. *Ophthalmology* **104,** 7-21.

Klein R, Klein BE, Knudtson MD, Meuer SM, Swift M & Gangnon RE. (2007). Fifteen-year cumulative incidence of age-related macular degeneration: the Beaver Dam Eye Study. *Ophthalmology* **114,** 253-262.

Lipecz A, Miller L, Kovacs I, Czako C, Csipo T, Baffi J, Csiszar A, et al. (2019). Microvascular contributions to age-related macular degeneration (AMD): from mechanisms of choriocapillaris aging to novel interventions. *Geroscience* **41,** 813-845.

Maddess T. (2012). Pupil dynamics and response amplitude: only size matters. *Invest Ophthalmol Vis Sci* **53**.

Maddess T, Baker L, James A, Coombes C, Cheung V, Melody Chiou M, Kolic M, et al. (2013). Clinical Utility of Multifocal Pupillographic Objective Perimetry in Type 1 Diabetes. *Investigative Ophthalmology & Visual Science* **54,** 218-218.

Maddess T, Bedford SM, Goh XL & James AC. (2009). Multifocal pupillographic visual field testing in glaucoma. *Clin Exp Ophthalmol* **30,** 678-686.

Maddess T & Daria VR. (2017). To BCVA, or not to BCVA, that is the question. *Clin Exp Ophthalmol* **45,** 437-439.

Michalska-Malecka K, Kabiesz A, Kimsa MW, Strzalka-Mrozik B, Forminska-Kapuscik M, Nita M & Mazurek U. (2016). Effects of intravitreal ranibizumab on the untreated eye and systemic gene expression profile in age-related macular degeneration. *Clin Interv Aging* **11,** 357-365.

Novotny HR & Alvis DL. (1961). A method of photographing fluorescence in circulating blood in the human retina. *Circulation* **24,** 82-86.

Palejwala NV, Jia Y, Gao SS, Liu L, Flaxel CJ, Hwang TS, Lauer AK, et al. (2015). DETECTION OF NONEXUDATIVE CHOROIDAL NEOVASCULARIZATION IN AGE-RELATED MACULAR DEGENERATION WITH OPTICAL COHERENCE TOMOGRAPHY ANGIOGRAPHY. *Retina (Philadelphia, Pa)* **35,** 2204-2211.

Pennington KL & DeAngelis MM. (2016). Epidemiology of age-related macular degeneration (AMD): associations with cardiovascular disease phenotypes and lipid factors. *Eye Vis (Lond)* **3,** 34.

Rai BB, Sabeti F, Carle CF, Rohan EMF, Sarac O, van Kleef J & Maddess T. (2020). Recovery dynamics of multifocal pupillographic objective perimetry from

tropicamide dilation. *Graefe's archive for clinical and experimental ophthalmology = Albrecht von Graefes Archiv fur klinische und experimentelle Ophthalmologie* **258,** 191-200.

Roisman L, Zhang Q, Wang RK, Gregori G, Zhang A, Chen CL, Durbin MK, et al. (2016). Optical Coherence Tomography Angiography of Asymptomatic Neovascularization in Intermediate Age-Related Macular Degeneration. *Ophthalmology* **123,** 1309-1319.

Rosli Y, Bedford SM, James AC & Maddess T. (2012). Photopic and scotopic multifocal pupillographic responses in age-related macular degeneration. *Vision Res* **69,** 42-48.

Ruseckaite R, Maddess T, Danta G, Lueck CJ & James AC. (2005). Sparse multifocal stimuli for the detection of multiple sclerosis. *Annals of Neurology* **57,** 904-913.

Sabeti F, James AC, Carle CF, Essex RW, Bell A & Maddess T. (2017). Comparing multifocal pupillographic objective perimetry (mfPOP) and multifocal visual evoked potentials (mfVEP) in retinal diseases. *Scientific Reports* **7,** 45847.

Sabeti F, James AC, Essex RW & Maddess T. (2013). Multifocal pupillography identifies retinal dysfunction in early age-related macular degeneration. *Graefe's archive for clinical and experimental ophthalmology = Albrecht von Graefes Archiv fur klinische und experimentelle Ophthalmologie* **251,** 1707-1716.

Sabeti F, Lane J, Rohan EMF, Essex RW, McKone E & Maddess T. (2020). Central versus peripheral macular structure and function and acuity in age-related macular degeneration. *Clinical and Experimental Ophthalmology* **Under Review**.

Sabeti F, Maddess T, Essex RW & James AC. (2011). Multifocal pupillographic assessment of age-related macular degeneration. *Optometry and vision science : official publication of the American Academy of Optometry* **88,** 1477-1485.

Sabeti F, Maddess T, Essex RW & James AC. (2012). Multifocal pupillography identifies ranibizumab-induced changes in retinal function for exudative age-related macular degeneration. *Invest Ophthalmol Vis Sci* **53,** 253-260.

Sabeti F, Maddess T, Essex RW, Saikal A, James AC & Carle CF. (2014). Multifocal pupillography in early age-related macular degeneration. *Optometry and vision science : official publication of the American Academy of Optometry* **91,** 904-915.

Sabeti F, Mallikarjunan R, Nolan C, Carle CF, James A & Maddess T. (2015a). A comparative analysis of changes in visual field sensitivity in type 2 diabetes. *Investigative Ophthalmology & Visual Science* **56,** 4685-4685.

Sabeti F, Nolan CJ, James AC, Jenkins A & Maddess T. (2015b). Multifocal Pupillography Identifies Changes in Visual Sensitivity According to Severity of Diabetic Retinopathy in Type 2 Diabetes. *Invest Ophthalmol Vis Sci* **56,** 4504-4513.

Seigel D. (2002). AREDS investigators distort findings. *Archives of ophthalmology (Chicago, Ill : 1960)* **120,** 100-101.

Semeraro F, Morescalchi F, Duse S, Gambicorti E, Cancarini A & Costagliola C. (2015). Pharmacokinetic and Pharmacodynamic Properties of Anti-VEGF Drugs After Intravitreal Injection. *Curr Drug Metab* **16,** 572-584.

Wong WL, Su X, Li X, Cheung CM, Klein R, Cheng CY & Wong TY. (2014). Global prevalence of age-related macular degeneration and disease burden projection for 2020 and 2040: a systematic review and meta-analysis. *Lancet Glob Health* **2,** e106-116.

Zehetner C, Kralinger MT, Modi YS, Waltl I, Ulmer H, Kirchmair R, Bechrakis NE, et al. (2015). Systemic levels of vascular endothelial growth factor before and after intravitreal injection of aflibercept or ranibizumab in patients with age-related macular degeneration: a randomised,prospective trial. *Acta Ophthalmologica* **93,** 154-159.

Chapter 4

Correlation between macular structure and function with multifocal pupillographic objective perimetry in early-stage type 2 diabetic macular oedema.

1

ABSTRACT

Purpose: In type 2 diabetes patients without and with mild diabetic macular oedema (DMO) to correlate macular thickness and Matrix 10-2 perimetry, with macular sensitivity and delay as measured by multifocal pupillographic objective perimetry (mfPOP), commercially known as the ObjectiveField Analyser (OFA).

Methods: We recruited 33 type 2 diabetic patients ages 59.2 ± 10.5 years, 17 were males (51.5%). To allow point to point comparisons Macular 8×8 OCT thickness grid data, and OFA sensitivity and delay, were mapped onto the Matrix 10-2 pattern. We then applied scatter plots and principal curve analysis to find out the main trends and correlations between variables. Macular regions were next grouped into 8 (4 inner and 4 outer) groups. Means within these groups were sorted according to retinal thickness, and that sort order was applied to the other measures. This allowed structure-function correlations to be computed relative to the degree of oedema wherever it occurred. A generalised linear mixed-effects determined which variables contribute to clinical diagnosis of DMO.

Results: The mean sensitivity difference compared to normal in diabetic patients was negative and the mean delay difference positive indicating drop in sensitivity and prolonged delay. Both differences increased with duration of diabetes. Peripheral hypersensitivity and shorter delay than normal were seen with shorter diabetes duration. The principal curve analysis showed good correlation between OFA and Matrix values, with initial hypersensitivity shifting to hyposensitivity with increasing macular thickness. For DMO patients outer macular thickness was correlated significantly with inner and outer OFA sensitivity and delay, all $p<0.0012$, but inner thickness was not correlated with any functional measurement. The same was true for diabetic patients without DMO where the median p-value was 0.001. Inner and outer OFA delays were marginally correlated with Matrix

sensitivity (p=0.052 to p=0.065). A Mixed-effects Logistic regression determined outer thickness and OFA sensitivity (p=0.043), male gender (p=0.313) and time in the study (p=0.001), contributed independently to the odds of a clinical diagnosis of DMO.

CONCLUSIONS

The mean sensitivity difference decreased, and mean delay difference increased in diabetic patients compared to normal in later-stage disease. Outer macular thickness correlated significantly with inner and outer OFA sensitivity and delay, while the inner macular thickness did not. As a clinical end-point outer thickness and functional measures may be a better indication of eye health in retinal disease than provided by the visual acuity or central functional measures.

Key words: diabetic macular oedema; multifocal pupillography; objective perimetry; retinal function; structure and function correlation.

INTRODUCTION

Globally 442 million people had diabetes in 2014, over one-third of them had diabetic retinopathy (DR), and a third of these were afflicted with vision-threatening DR in the form of severe non-proliferative or proliferative DR, or diabetic macular oedema (DMO) (Lee *et al.*, 2015). In Australia alone 72,000 of the 1.73 million diabetics had DMO in 2015. These figures are projected to increase by 42% by 2030 leading to 2.45 million with diabetes and 102,000 with DMO (Deloitte Access Economics, 2015). The indirect cost of vision loss associated with DMO in 2015 alone was estimated to be $2.07 billion because of loss of wellbeing and persons who could not work, or could not work to full capacity, due to poor vision caused by DMO (Deloitte Access Economics, 2015). Despite improved diagnosis and management, diabetes remains an escalating global health challenge (Gale *et al.*, 2017).

The concept of *Metabolic Memory* (Engerman & Kern, 1987) recommended intensive control of blood glucose level to reduce the risk of diabetic micro- and macro-vascular and other diabetes-related complications, and that HbA1c values from 2 to 3 years earlier contribute most to the risk of progression of retinopathy (Lind *et al.*, 2010). Those findings were supported by the Diabetes Complications and Control Trial (DCCT *et al.*, 1993), the Epidemiology of Diabetes Interventions and Complications trial (Nathan *et al.*, 2003), and the United Kingdom Prospective Diabetes Study (Stratton *et al.*, 2001). Different mechanisms are involved in metabolic memory including: mitochondrial DNA damage, protein kinase C activation, the polyol pathway, increased production of advanced glycation end products (AGEs), AGE receptor overexpression, increased anion peroxidase formation and glycation of mitochondrial and other cellular protein and lipids, all resulting in diabetic complications (Testa *et al.*, 2017). The key factor in preventing vision-threatening diabetic eye disease is earliest possible diagnosis of DR and DMO with timely treatment (Ranchod & Fine, 2009). However, to effect early diagnosis conventional perimetry, functional end points

like BCVA, and structural end points like macular thickness by OCT, are possibly not sensitive enough to pick up early focal pathology (Maddess & Daria, 2017). The micro-perimeters (Laishram *et al.*, 2017) and mfPOP (Sabeti *et al.*, 2017) potentially provide the crucial ability to diagnose early focal lesions. A cross-sectional study by the Maddess Group has shown reduced sensitivity with some peripheral hypersensitivity, and asymmetry in local delay deviations between eyes with mfPOP are correlated with the severity of type 2 diabetes (T2D) (Sabeti *et al.*, 2015). mfPOP has also detected afferent visual field defects in early T2D (Bell *et al.*, 2010), and focal functional damage as measured by Matrix perimetry preceded structural change among diabetes (Rai *et al.*, 2020b). Surprisingly, BCVA was mainly determined by off-axis thickness, and not central thickness (Rai *et al.*, 2020b). Another study (in preparation) by the Maddess group reported that the outer macular thickness might be more useful prognostic indicator among the patients of advanced AMD (Maddess *et al.*, 2020).

The present longitudinal study was conducted to validate any mfPOP characteristics which could identify the eyes at risk of developing or progression of DMO, and to compare that data with: macular thickness, mfPOP sensitivity and delay, and Matrix perimetry data.

METHODS

Subjects

T2D patients with and without early-stage DMO were recruited through treating physicians, ophthalmologists, and optometrists. Informed written consent was given by all participants as per the ANU Human Experimentation Ethics Committee approval number ETH.2010/194 and Human Research Ethics Committee, ACH Health approval number ETH.7.07.667. The diabetes participants were categorised into two groups: with and without DMO. Normative

mfPOP data was based on a separate study of 133 subjects each tested twice, 2 weeks apart (Carle *et al.*, 2020).

Study Design

This was a prospective longitudinal case series study. The participants with DMO were followed at intervals of about every three months, while those without DMO were followed up every six months, both groups for up to one to two years.

Ophthalmic examination

The other eye tests followed the mfPOP testing on the same day. A 10-2 perimetry test was done with the FDT Matrix (Carl Zeiss Meditec Inc., Dublin, CA). We measured best corrected visual acuity (BCVA) with an ETDRS Chart 2, corneal curvature with auto-refractometer (ARK-1s NIDEK co. Ltd, AICHI Japan), intraocular pressure (IOP) with Goldmann applanation tonometry, and pachymetry with a Pachmate DGH 55 (DGH Technology Inc., USA). Both the pupils were then dilated with 1% tropicamide eye drops for rest of the eye examination. We evaluated the anterior and posterior segments under slit-lamp (BQ 900, Haag Streit, Switzerland). Any cataract was graded using the Lens Opacities Classification System III (LOCS III) (Chylack *et al.*, 1993). An 8×8 grid macular scan and a retinal nerve fibre layer (RNFL) analysis was done with an Optical Coherence Tomograph (OCT, Spectralis, Heidelberg Engineering GmbH, Germany). Standard 5-photo/eye fundus photographs were taken with a Canon Digital Retinal Camera CR-2, Canon Inc., Tokyo, Japan). The blood pressure and glycosylated haemoglobin (HbA1c) values were recorded.

The *inclusion criteria* were T2D patients with or without early-stage DMO. The *exclusion criteria* included best corrected visual acuity (BCVA) less than 6/12 in both eyes (except participant mf87155 had 6/48 in the left eye), colour blindness, history of eye or head trauma, neurological disorders and treatment received in the form of retinal laser, intravitreal anti-

VEGF injections or vitreoretinal surgery. If the patients received treatment during study period further follow up was discontinued but the data collected prior to the treatment was used for analysis.

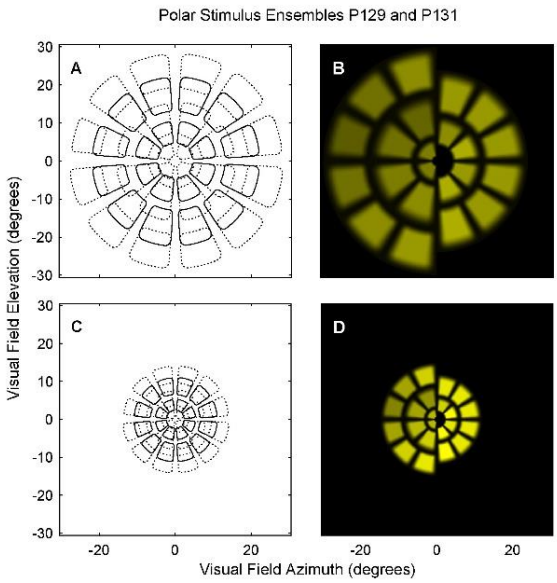

Figure 1. Multifocal stimuli arranged in a dartboard layout pattern presenting 44 stimulus regions per eye. (**A**) Protocol P129 is a wide-field stimulus covering central 60° (extending to ±30° eccentricity) (**C**) Protocol P131 covering central 30° (extending to ±15° eccentricity) of the visual field, both with 44-region layout consisting of five interleaved rings of yellow stimuli. Overlapping stimuli are never presented simultaneously. No stimuli encroach upon the horizontal and vertical midlines. (**B**) & (**D**) illustrate the luminance balancing for P129 and P131 respectively (Carle *et al.*, 2014) with half the regions activated on the left and right sides. The differences in luminance are slightly exaggerated to make them more visible. The concept is to make response amplitudes homogeneous across the entire field.

Multifocal Pupillographic Objective Perimetry

Presentation of stimuli and monitoring of the pupillary diameter with infra-red video cameras was done using a FDA cleared prototype mfPOP machine, the objectiveFIELD Analyser (OFA) (Konan Medical USA, Irvine, CA). The equipment presents dichoptic multifocal stimuli to both eyes concurrently, measuring direct and consensual responses from every visual field location corresponding to each retinal area stimulated (Maddess *et al.*, 2009). Any vergence deficit was corrected before starting the tests. The background illumination was 10 cd/m^2. The luminance of the stimuli was 80 - 150 cd/m^2 (Carle *et al.*, 2015) in a Yellow-on-

Yellow stimulus patterns with luminance balance flickering dartboard layout in 44 regions per eye. Two stimulus protocols were used: P129, which covers the central 60 º (**Fig. 1A**), and P131, which covers the central 30 º of visual field (**Fig. 1C**), each with 44 stimuli per eye. In this chapter we only present data for the P131 protocol because of the good overlap with the OCT and Matrix 10-2 data (see below). The stimuli were luminance balanced for both the protocols (**Fig. 1B, 1D**) (Carle *et al.*, 2014) and employed the clustered volleys method (Carle *et al.*, 2013; Sabeti *et al.*, 2014) (**Fig. 2**).

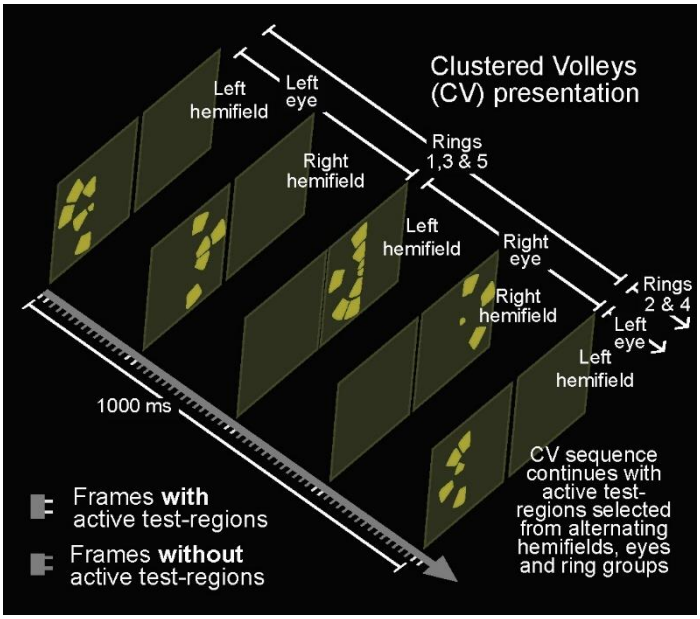

Figure 2. Clustered volleys stimulus presentation. Only frames where stimuli are activated are shown. The clustered volleys stimulus presentation restricts stimuli to within a single hemifield and eye at a time. The sets of hemifield stimuli were drawn from either the two rings of stimuli shown by solid lines in Fig. 1A,C or the 3 rings of stimuli shown by dotted lines in Fig. 1A,C. Altogether there were 8 possible hemifield/eye sets, and these were cycled through in round-robin fashion, with active some regions being displayed for 33 ms every 0.25 s. On each of these active frames the probability of each of the 10 or 12 regions/hemifield being shown was 50%. Thus, while stimuli arrived in volleys their arrival at any one region was random, and stimulation at every region was independent of every other region, allowing the multifocal method to operate. The volleys kept the pupillary gain high and even.

Analysis

Data analysis was performed using in-house developed MATLAB scripts (2016b, The MathWorks, Natick, MA). The response waveforms for each of the 44 test regions per eye

were extracted from raw pupillary responses using multiple regression, with blinks removed from the pupil data before regression (James, 2003; James *et al.*, 2005; Ruseckaite *et al.*, 2005). Temporal impulse responses at each retinal region were fitted to a log-normal function (Carle *et al.*, 2011), allowing per-region estimation of constriction amplitude (sensitivity) and time-to-peak (delay). The regressive method also generated standard errors for the estimated sensitivities and delays (Maddess *et al.*, 2009). To reduce the effects of age and pupil size the mean diameters were standardised to a 3.5 mm pupil size. Thus, we were examining relative pupil amplitudes rather than absolute size. Use of relative pupil size to estimate sensitivity is commonly done (Bremner, 2012; Maddess, 2012). For mfPOP the standardised data were then mapped to relative sensitivity in decibels. The per-region times-to-peak and there SE were also recorded.

The 8×8 grid macular thickness OCT scanning was done with a 7° tilt. This is the default angle for the Heidelberg and we wished our study to be relevant to standard clinical practice. Each grid square measured 3° on a size, which overlapped well with the Matrix 10-2 array of 2° square stimuli (**Fig. 3A**). For comparison with visual field data the thickness map was flipped to fit the visual field projection. The overlaps facilitated the point-by-point comparison of the 44 macular thickness measures with the 44 functional regions assessed by Matrix 10-2. Similarly, the 44 regions of the pupillary responses were also mapped to the 44 regions of the Matrix 10-2 array (**Fig. 3B**). Mapping on the Matrix grid was based upon the propositions of overlapping areas (Ruseckaite *et al.*, 2006). Overall the best grid to map onto to allow direct comparison between the three diagnostic modalities was the 10-2 pattern.

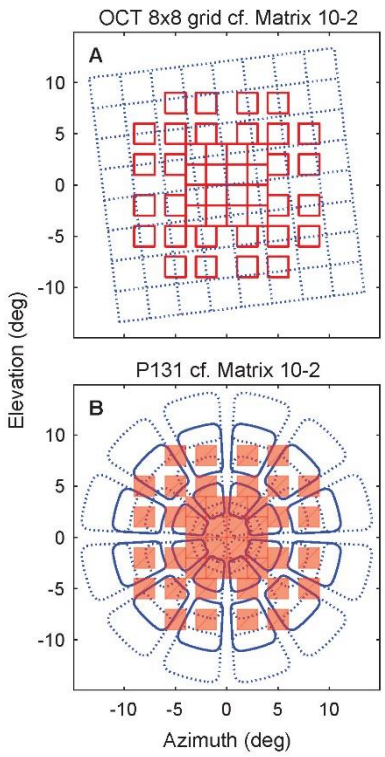

Figure 3. Overlapping of the structural and functional measures. (**A**) Overlap of the Spectralis OCT 8×8 grid macular thickness of 3×3° regions, set at 7° tilt with the Matrix 10-2 grid of 44 2×2° square stimuli. The thickness map was flipped over first to fit the visual field projection. (**B**) Overlap of the 44 stimulus regions of the P131 test (extending to ±15° eccentricity of visual field) with the 44 regions of Matrix 10-2.

Scatter plots and principal curves

Having got the OCT, mfPOP and Matrix data all on the same grid we first did scatter plots with principal curve analysis (Pcurve). Different perimeters have been shown to produce quite nonlinearly related data (Wall *et al.*, 2010; Fredette *et al.*, 2015). Additionally, noise in the data of any particular device means that scatter plots examining the relationship between data of different devices can be quite diffuse. To find the main trend in the data researchers have used principal curve analysis (Wall *et al.*, 2010; Fredette *et al.*, 2015). The starting point of Pcurve is to find the first principal component of a cloud of points, and then to iteratively push the points from that line onto a curved trajectory that has the same number of points on either side in the direction normal to the trajectory (Hastie & Stuetzle, 1989). Thus, one

winds up with the same number of points as in the original cloud, but now moved onto the principal curve to show the main trend in the cloud. Like previous authors (Wall *et al.*, 2010; Fredette *et al.*, 2015) we used the Princurve package of R version 2.15.0 (Free Software Foundation, Boston MA).

Correlations

An issue for any analysis of DMO is that it can be distributed asymmetrically across the retina, posing a problem for comparing different eyes. To deal with this issue we averaged results from groups of field regions beginning with the OCT thickness data. We then sorted those smaller number of average retinal thickness data and applied that sort-order to the mfPOP and Matrix data clustered in the same way. We then computed correlations between these sorted measures. Thus we were examining the OCT data from the thickest regions with the mfPOP and Matrix data from the same regions, wherever they occurred across the field/retina. Correlation matrices, and their p–values were calculated using the *corrcoeff* function of Matlab.

Logistic regression

We investigated which variables were predictive of clinically diagnosed DMO as opposed to simple diabetes with no DMO. For some models we examined the data from the inner and outer retina/field. Obviously, the main predictor variable should be retinal thickness as determined by OCT. The question was, in a multiple-regression, setting would any other variables add extra predictive power? That is would there be any independent variable(s) that had power to predict DMO over simple diabetes without DMO? The data set had data from both eyes and in some cases multiple visits/subjects. We therefore fitted a generalised linear mixed-effects model (*fitglme* in Matlab) to account for the effects of multiple comparisons of eyes and repeats being nested within subjects. We used a logit link-function to fit a logistic

regression, where the fitted quantities were the log(Odds), which we converted back to Odds. In some cases the odds were an N-fold effect for some factor, like Male gender. In other cases the odds were per unit of the fitted quantity, like age.

Normative OCT data

Figure 4 shows our normative macular thickness Spectralis OCT data mapped into the visual field. All the data was mapped as left eye equivalent, hence the thicker peripheral data on the right correspond to the effect of the optic disc as it would appear projected into visual space when looking at the left eye of a patient. To generate the normative data we computed the median retinal thickness at each region of the diabetic patients, i.e. no DMO patients. The resulting data appeared very close to those reported for similar aged normal subjects using the Spectralis (Yamashita *et al.*, 2013; Hashemi *et al.*, 2017). The normative data was used to calculate the difference in macular thickness grid of the patients.

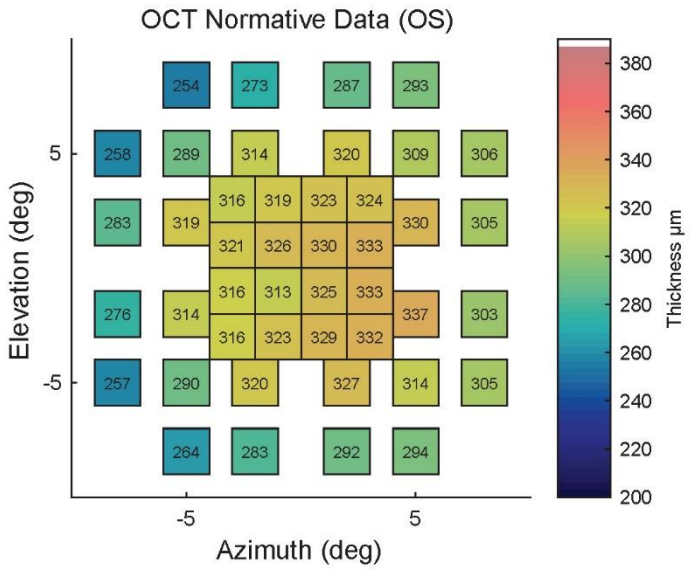

Figure 4. Normative macular thickness Spectralis OCT data mapped into the visual field. All data were mapped as left eye equivalent, and then later flipped to right-eyed data for presentation purposes as necessary.

RESULTS

Demographics

A total of 33 T2D patients qualified for the study and were included for analysis. Seventeen of them were males (51.5%). The mean age at presentation was 59.2 ± 10.5 years. Nineteen had DMO in at least one eye. The demographic details of the participants are shown in **Table 1**.

Table 1. Demographic characteristics of patients

Subject	Age (years)	Gender	Diabetes duration (years)	Diabetes macular oedema	Retinopathy grading		HbA1c	Blood pressure		Visual Acuity (Log MAR)		Intraocular pressure	
					OS	OD		Systolic	Diastolic	OS	OD	OS	OD
mf87150	44	F	2.5	no	1	0	-	142	114	0	0	18	16
mf87156	57	F	3	no	1	1	7	136	79	0.4	0	13	13
mf87159	55	M	0.5	no	1	1	7.1	140	98	0	0	22	21.5
mf87168	79	M	11	no	1	1	7	120	68	-0.1	-0.1	18	17
mf87170	52	F	2	no	1	1	7.6	142.5	88	0	0.1	16.5	17.5
mf87171	65	F	12	no	1	1	7.3	141.3	79.3	0	0	20.3	19.7
mf87173	70	M	10	no	1	1	5.7	121.5	81.5	0	0	19.5	19.5
mf87175	60	M	0.5	no	1	1	6.3	127	86	0	0	14	14
mf87176	70	F	9.5	no	2	2	7.2	131	79	-0.1	-0.1	22	25
mf87178	45	F	5	no	1	1	8.1	147	92	0	0.1	21	21
mf87179	62	M	17	no	1	1	5.7	100	63	0	0	13	12
mf87180	69	M	5	no	1	1	5.8	127	73	0	0	16.5	16.5
mf87182	70	M	2	no	1	1	8.3	147	80	0.2	0.1	16	16
mf87184	60	F	34	no	1	1	6.2	126	76	0.1	0.1	19	20
mf87151	60	F	18.3	yes	3	3	6.5	147.5	63	0	0.1	13	14
mf87152	63	M	30.5	yes	5	5	8.4	149	85	0.3	0.2	12	12
mf87153	37	M	23	yes	4	4	8.1	114	77	0.1	0.1	17	18
mf87154	52	M	1	yes	4	1	8.5	140	90	0	0	14	14
mf87155	66	F	10	yes	3	4	8.4	144	84	0.9	0.2	12	12
mf87157	62	F	8	yes	3	1	6.7	119.8	80	0	0	18.8	18.3
mf87158	63	M	11	yes	1	3	6.9	142.2	85.3	0	-0.1	16.8	16.8
mf87160	58	F	27	yes	5	5	6.7	150	85	0.1	0.2	23	22
mf87161	27	M	20	yes	5	4	9.5	137	71	-0.1	-0.1	13	14
mf87162	55	M	9	yes	4	4	9	116	79	0.1	-0.1	13	13
mf87163	62	F	13	yes	5	5	9.8	149.5	94.5	0.3	0.2	13.5	12.5
mf87164	67	M	4	yes	2	1	6.6	136.7	92	0	0	18	18.3
mf87167	67	F	22.8	yes	4	4	9.2	141.7	77.3	0.1	0	20.7	20.7
mf87169	54	M	10	yes	3	1	8.3	129.3	78.3	0	0.1	18	16.3
mf87172	65	F	1	yes	3	3	6.6	105.8	59.5	0	0	18.3	18.3
mf87174	55	F	17	yes	4	4	9.1	137	83.7	-0.1	0	18.7	19
mf87177	67	M	13	yes	1	2	6.3	143	85.8	0	0	16	15.8
mf87183	67	M	20	yes	3	3	8.9	127	74	-0.1	0	18	18
mf87190	48	F	5	yes	3	3	10.2	101	67	-0.1	0	12	12

Diabetic retinopathy gradings: 0 = Normal; 1 = Diabetic with no signs (normal retina); 2 = Diabetic with pathology not consistent with retinopathy; 3 = Minimal NPDR (microaneurysm only); 4 = Mild NPDR (microaneurysms + Exudates + Retinal ahemmorhages + Cotton-wool spots); 5 = Moderate NPDR (equal to or more than standard 2A photograph); 6 = Severe NPDR (4-2-1 rule); 7 = Proliferative DR.

Summary data from each test modality

Before comparing the data from the different instruments we first examined data produced by each method.

Figure 5 shows the basic outcomes for the 33 subjects for the central retina from the Spectralis OCT. The maximum central thickness was within 350 µm, and the total volume was within normal limits (Fig. 5A). The majority of the patients had macular thickness between 200 to 300 µm (Fig. 5B). The minimum and maximum macular thickness did not vary much and aligned within 200 to 350 µm (Fig. 5C, D).

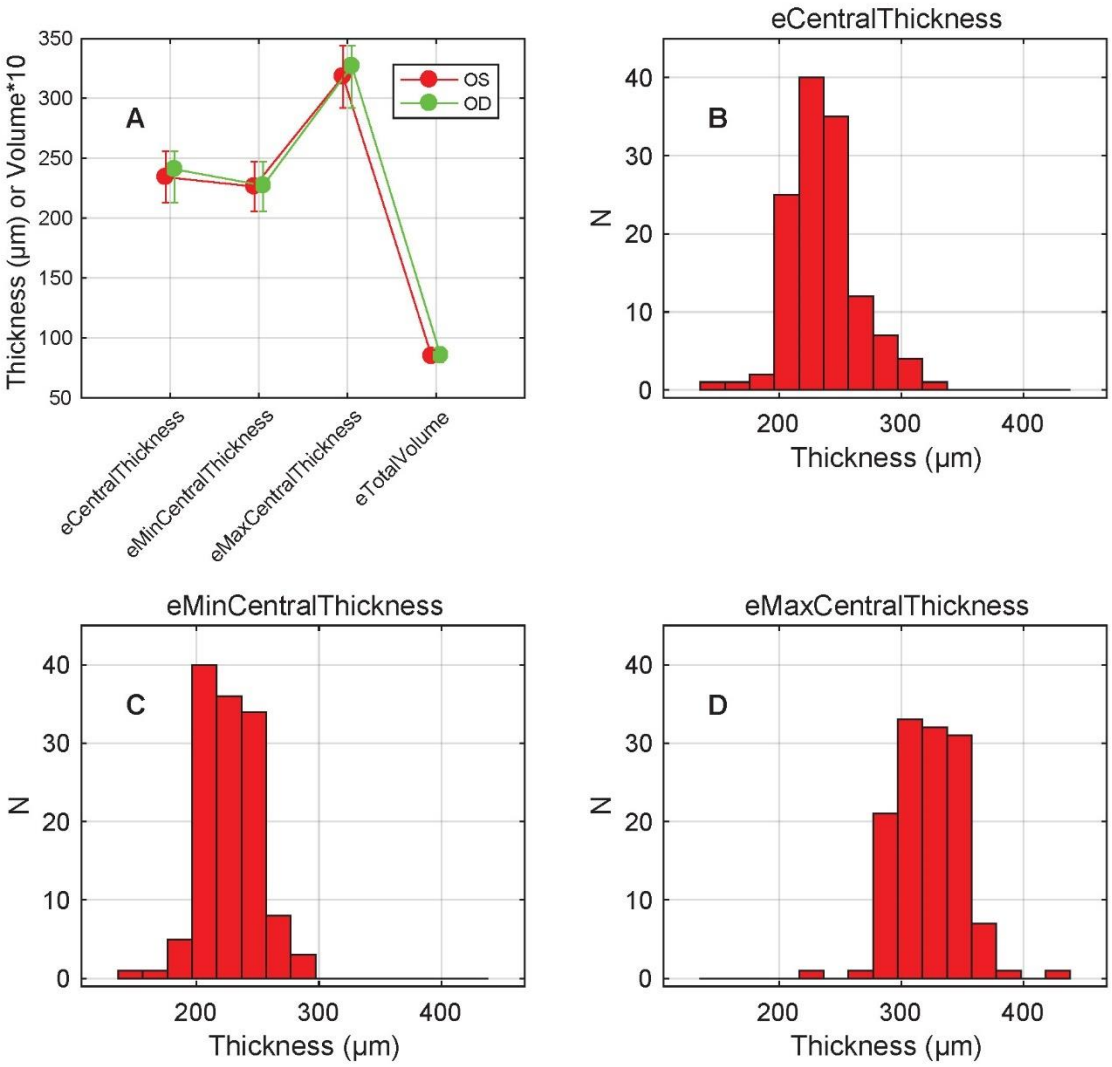

Figure 5. Summary of data from the Spectralis OCT showing patient distributions according to the macular thickness. (**A**) Shows the average, minimum and maximum macular thickness for the central ETDRS region, and the total volume (multiplied by 10 to align the volume values with thickness values). The abscissa labels are the names used in the Spectralis XML files. Points for OS and OD are displaced left-right to make them more visible. The distributions of the 3 thickness variables of A are shown in B to D. (**B**) Shows the central macular thickness and the number of ETDRS regions in each thickness group across eyes and patients. (**C**) Shows the minimum thickness and the number of regions in each group. (**D**) Shows the maximum thickness with the number of regions in each group.

Summary data for the Matrix 10-2 are shown in **Figure 6.** Many fields showed considerable damage in terms of their Mean Defects, and Pattern Standard Deviations (Fig. 6A,C,D), and

there was a preponderance of superior field defects (Fig. 6B). The rates of fixation errors, false positives and negatives were low (Fig. 6D).

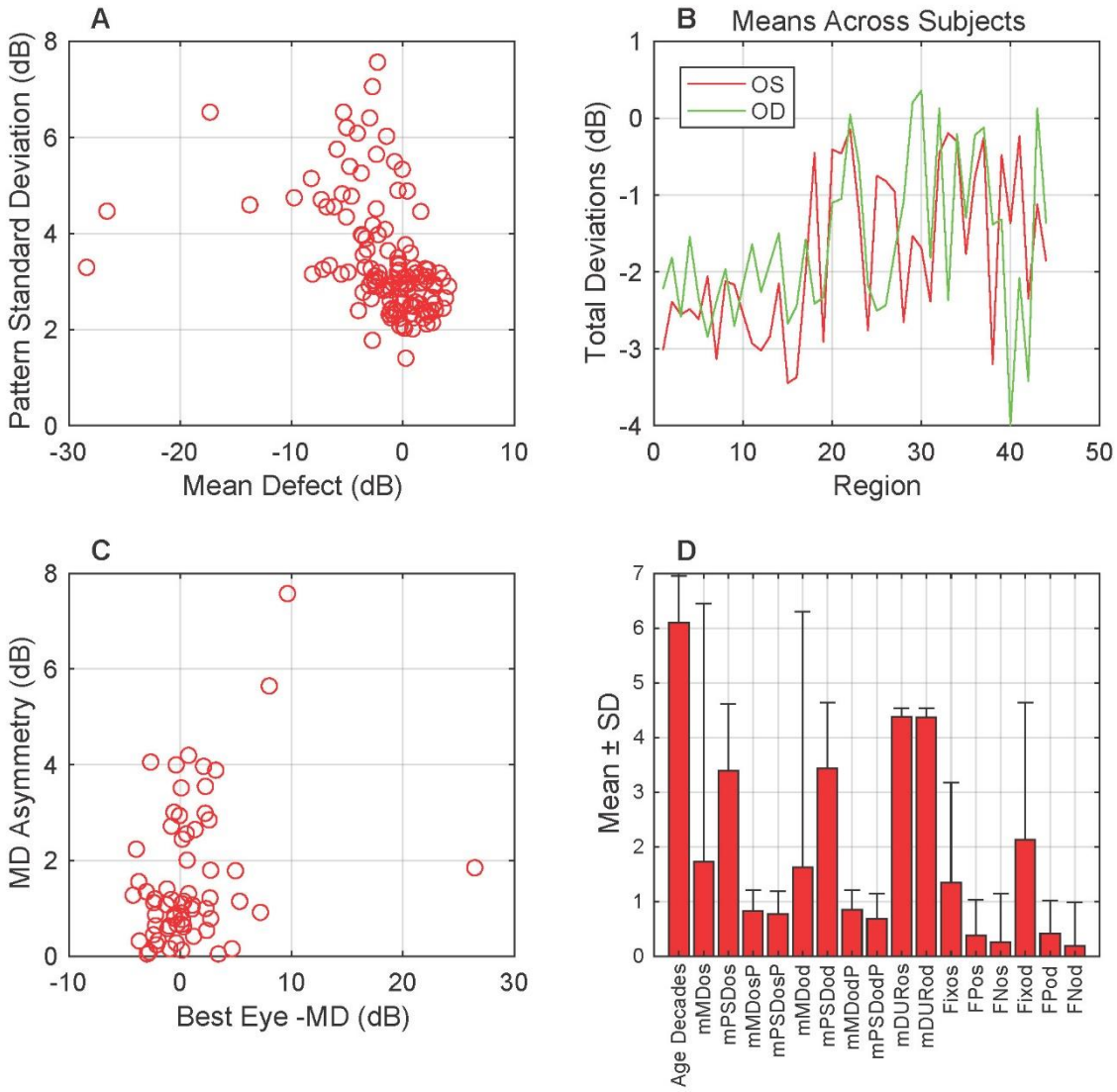

Figure 6. Summary of statistics from the Matrix perimeter showing that the fields were reliable and some showed considerable damage. (**A**) a scatter plot of the Matrix Pattern Standard Deviations (PSD) on the Mean Defects (MD) from the 33 pairs of eyes. (**B**) Means across subjects and eyes (of the OS equivalent data). The Matrix data are saved in order from superior to inferior. Therefore, the data show superior defects on average. (**C**) We took the absolute value of the differences in MD from the two eyes and plotted them on the minus the maximum MD of the two eyes. Thus better eyes get worst for left to right. Thus, pairs of eyes are somewhat more asymmetric as the better eye declines. (**D**) plots of the summary statistics from the Matrix fields. For the abscissa labels a leading 'm' indicates 'mean', a trailing 'P' indicates the p-values. Leading Fix, FP and FN indicate the percentage rates of fixation errors, false positives and negatives.

Like the Matrix data we considered the differences from normative data for mfPOP, for both sensitivity and time-to-peak. As an initial exercise we plotted the mean sensitivity difference (across test regions and eyes) between the patients and age and sex-matched normative data against the duration of diabetes (**Fig. 7A**). Negative values indicate a drop sensitivity relative to normal. Positive values indicate hyper-sensitivities, which we have reported before in early-stage retinal disease (see Discussion). It seemed clear that more of the diabetics (blue, Diab) showed hyper-sensitivities than the DMO patients (red, DMO). We labelled some of the symbols with the age of the subject. It seemed that years of disease was more important that age in determining position on the plot.

The differences in the mean delays were positive indicating prolonged times-to-peak for the patients compared to controls (**Fig. 7B**). Negative mean delays indicated faster than normal responses. These were more common in the patients with fewer years of diabetes. The age labels allow some subjects to be identified on both Figure 7A and 7B. It seems that faster responses are associate with normal to hyper-sensitive responses. Faster responses and hypersensitivity may be less common earlier in the disease. The observed delays are not simple neuropathy of the iris however because large and reproducible local differences are observed from region to region (see Discussion).

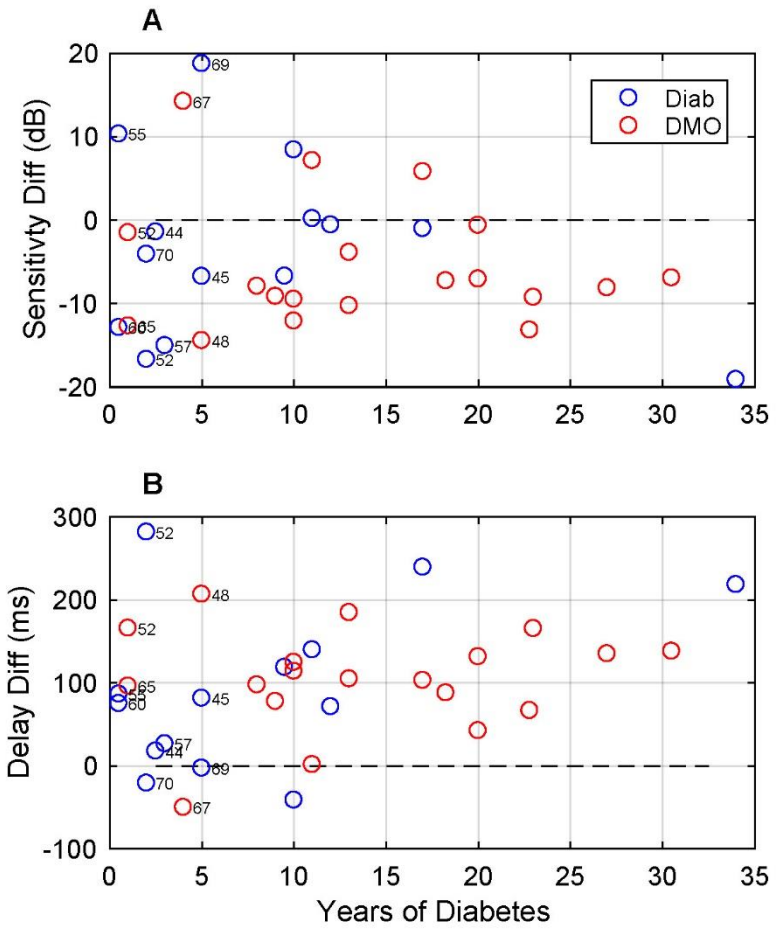

Figure 7. OFA data showing the mean sensitivity and delay differences compared to normal in the diabetes patients without and with DMO. Some of the patients are labelled with their age so that the same patients can be identified in both plots. (**A**) Mean sensitivity differences are negative indicating drop in sensitivity among the patients. The number of patients with drop in sensitivity increases with the duration of diabetes. In the beginning some cases have shown retinal hypersensitivity. (**B)** Positive mean delay differences indicate the time-to-peak was prolonged relative to normal. The number of patients with prolonged delay increases with the duration of diabetes.

Comparing data types

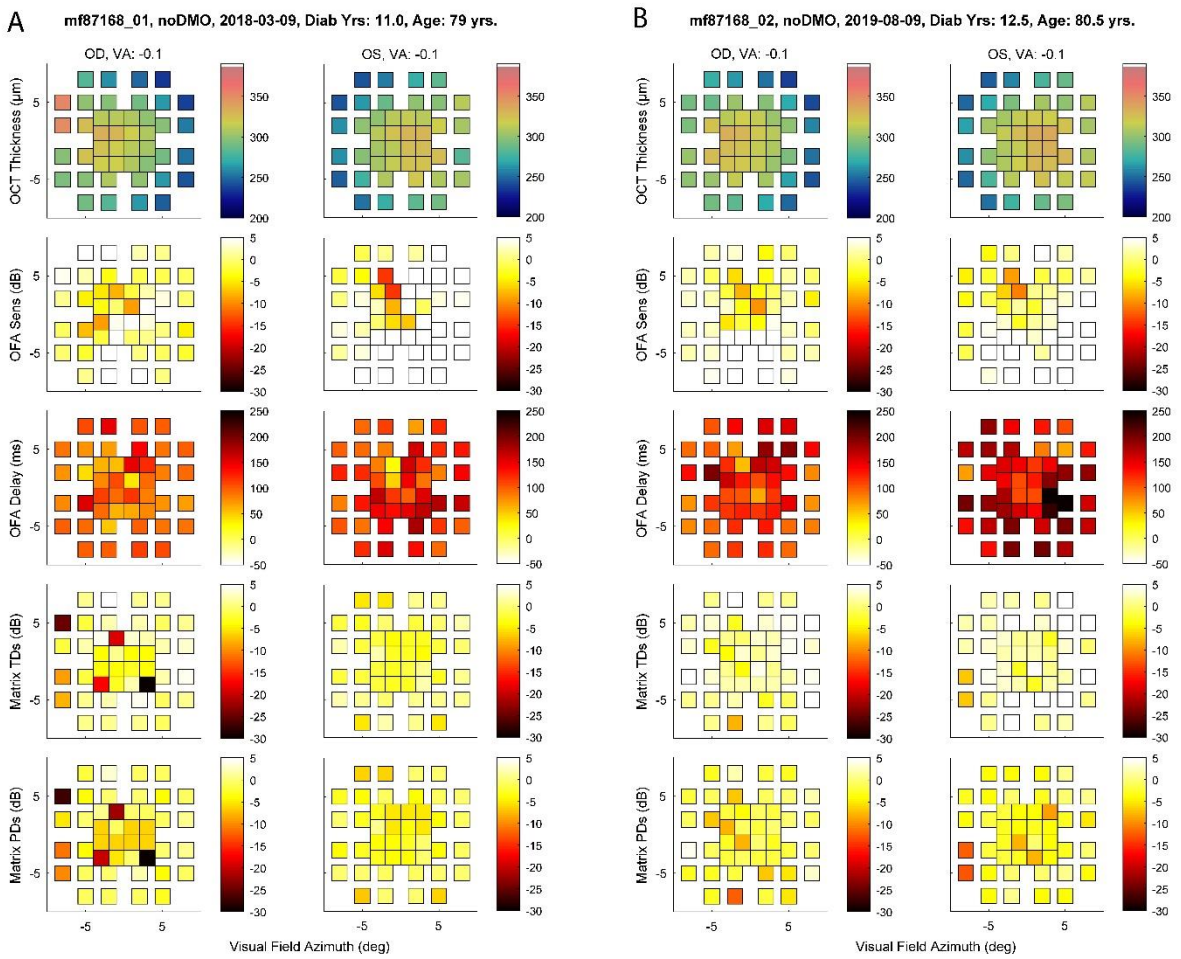

Figure 8. Illustration of data mapped to the 10-2 format for OCT, OFA and Matrix Total Deviations (TDs) and Pattern Deviations (PDs) for two visits (**A,B**) by a diabetic patient whose initial age was 79 years. The pairs of columns in A and B are for OD and OS, the rows are identified by the numerals i to v. **i**) The OCT data are very consistent between visits. **ii**) The OFA sensitivities (OFA Sens) are consistent between visits with some superior loss and peripheral hypersensitivity. **iii)** Delays appear to have grown on the second visit. **iv & v)** The Matrix TD and PD data are variable between visits thus in this case the OFA showed more consistent sensitivity results than the Matrix 10-2 perimeter. The Matrix TDs showed some peripheral hypersensitivity.

Figure 8 is pair of data sets from one 79 year-old that illustrate several points. The full set of these plots for all subjects and visits is supplied in the Appendix to this chapter. Here the data (Fig. 8A,B) were taken 17 months apart (dates in the titles). The OCT data of Figure 8i

(denoting the 4 panels of row i) appear little changed. The OFA sensitivity data (Fig. 8ii) are remarkably consistent centrally, and show some hypersensitivity peripherally. The delay data (Fig. 8iii) seem to show worsening delay in OS on the second visit especially in the inferio-temporal field, which may be correlated with a slight increase in thickness. The Matrix fields (Fig. 8iv,v) are less consistent, especially OD. The Total Deviations (Fig. 8iv) show some peripheral hyper-sensitivity (the PDs, Fig. 8v, would not be expected to show that), which roughly matches the OFA sensitivities. Many of these features are found in the other sets of fields.

Scatter plots and principal curve analysis

The scatter plots and the fitting of the principal curve were performed for the patients with and without DMO separately to see if there any differences (**Fig. 9A,B**). We have presented together them for ease of comparison. Very similar plots have been presented by Wall et al. (2010) for Standard Perimetry (for both Goldmann Size 3 and 5), Matrix, and motion perimetry. We observed a quantised distribution of the values measured by the Matrix perimeter (Fig **9A,B**:ii,v,xi,vii,viii,ix). This is expected for the Matrix (Wall *et al.*, 2010; Fredette *et al.*, 2015). With increasing delay, the OFA and Matrix sensitivity tended to drop (**Fig 9A,B**:i,ii). The trends for OFA sensitivity and OCT macular thickness were interesting. For the DMO group the Pcurve data suggest that thinner than normal retina was associated with hypersensitivity, moving to depressed sensitivity for thicker retina (**Fig. 9B**:vi,xi). For diabetes the trend seemed to be reversed with thicker retina being associate with hypersensitivity (**Fig. 9A**:vi,xi). Decreasing macular thickness seemed to trend towards longer delays (Fig. 9A,B:iii,x). The Matrix and OFA sensitivities are quite correlated although the PCurve is biased by the bulk of the data being at smaller values (**Fig. 9**:v,viii).

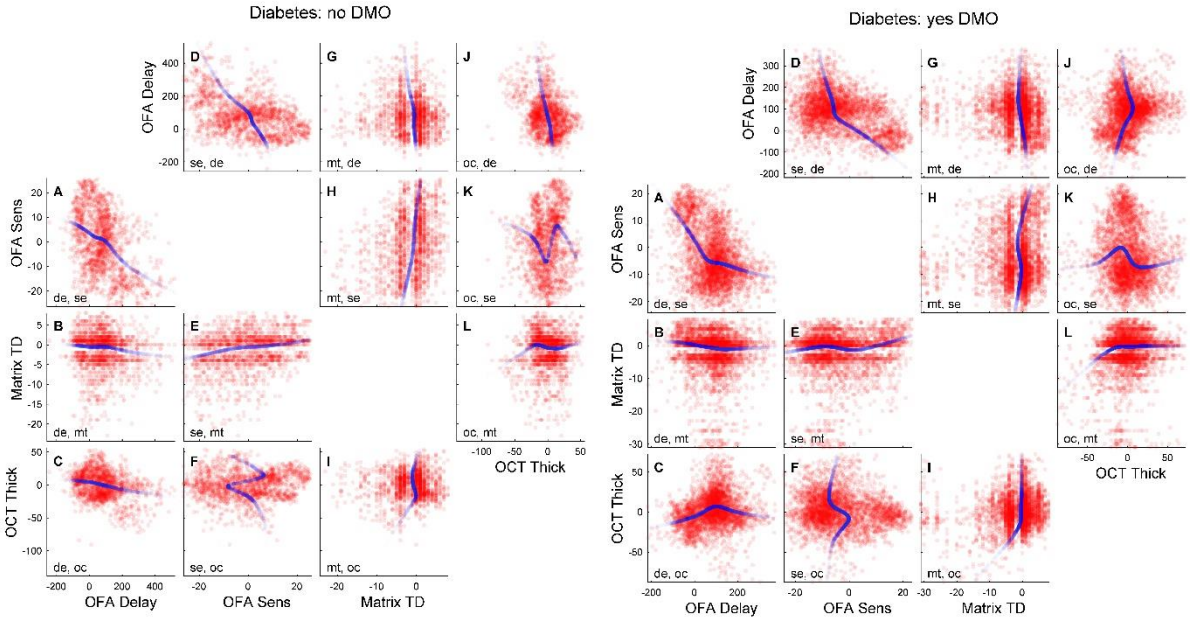

Figure 9. Scatter plots and principal curves. The mapping of all 4 data types onto the 10-2 pattern allows scatter plots to be drawn in which each dot represents a visual field region. The individual dots are translucent to allow the density of the points to be seen. The blue dots are the Principal Curves (PCurve) illustrating the main trends. **A** and **B** each show 12 plots for the Diabetes and DMO patients, and the two are presented together to permit easy comparisons. Each column of A and B is for one of the 4 data types from left to right: OFA delay (de), OFA sensitivity (Sens, se), Matrix Total Deviations (TD, mt), and OCT Thickness (Thick, oc). At bottom left of each panel is a two-part mnemonic to help recall the meaning of the x and y axes of a given panel. Thus "de, oc" (in A,B:iii) indicates OCT thickness plotted on OFA delay. The rows of A and B are in the same order as the columns, thus the panels of A and B each have the form of a correlation matrix, thus all the unique information is captured by either the lower or upper triangular part of A or B, but showing both allows pairs of plots with transposed axes to be seen. Plots of a variable on itself on the diagonals are not shown. Each panel of A contains 1848 = 44 × 2 × 21 points, and B 3784 = 44 × 2 × 43 points.

Analysis by visual field groups

DMO patients often have their greatest oedema in particular quadrants, distributed more or less centrally. This makes it hard to compare data between eyes. We therefore grouped regions into 8 groups of regions, four inner and four outer macular groups (**Fig. 10**). We computed the means of the thickness, OFA sensitivity and delay, and Matrix data in each group, to yield 8 points per eyes/subject/repeat (a repeat is a repeated visit). The OCT thickness was that relative to normative data (Fig. 4). As a next step we sorted the OCT thickness data across the groups within each eye (for each repeat). We then sorted the group means from other data types by the thickness order. In this way sensitivity and delay data for the thinnest to thickest groups of regions could be compared.

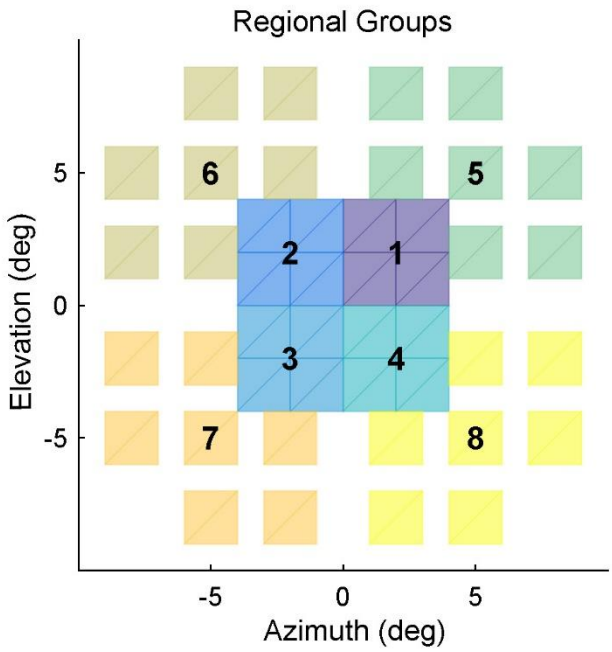

Figure 10. The macular regional groups. The macular regions were grouped into 8 groups denoted here by colour coding and number. Groups 1 to 4 represent inner macula, and groups 5 to 8 represent outer macula.

In a simpler analysis we sorted the OCT data and then applied that sort order for each eye to the other 3 data types for all 8 groups/eye. As we have reported in a study of AMD this strategy was not well-based because different things can be happening in the inner and outer

groups (Rai *et al.*, 2020a). To examine this, we also separately sorted the inner and outer groups and applied those sort orders to the inner and outer data from the other modalities.

Table 2 shows the correlations between the groups of 8 for the first analysis. The mean of the values corresponding to the two thickest groups were computed and were then used to calculate the correlations. OCT thickness was correlated with OFA sensitivity and delay but not Matrix sensitivity. The significant correlations are in bold fonts and are all p<0.0032. Matrix sensitivity was marginally correlated with OFA delay; the correlation of -0.169 was at p=0.120.

Table 2. DMO patients' data sorted across groups by OCT thickness.

	OCT	Odelay	Osens	Matrix
OCT	1	**0.315**	**-0.317**	-0.095
Odelay	**0.315**	1	**-0.585**	-0.169
Osens	**-0.317**	**-0.585**	1	0.135
Matrix	-0.095	-0.169	0.135	1

N.B. Correlations are between for data from the thickest 2 of 8 groups for each eye of the DMO patients. OCT: thickness; Odelay: OFA delay; Osens: OFA sensitivity, Matrix: Matrix total deviations. The significant correlations are shown in bold, marginally significant in normal font, and non-significant correlations in grey.

In the next step, the groups for each data type were separately sorted according to the OCT thickness relative to normative data within the 4 inner, and the 4 outer groups (Fig. 10). First, we have analysed the data for the patients with DMO (**Table 3, Fig. 11**). As before the means of the values for the two thickest groups were included to calculate the correlations. The significant correlations are in bold fonts and are all p<0.0012. The correlation of -0.206 between Inner-Matrix and the Outer-OFA delay was at p=0.057; and between Inner-Matrix and Inner-delay was -0.210 (p=0.052). Those marginal correlations are shown in normal typeface. Non-significant correlations are shown in light grey. The main result can be seen in the first and fifth columns showing the correlation between outer and inner OCT thickness

(oOCT and iOCT) and the other variables. iOCT was not correlated with any of the other variables, while oOCT was correlated with inner and outer OFA delay and sensitivity data. Inner Matrix data was marginally correlated with outer OFA delay. Interestingly, inner and outer OCT data were relatively poorly correlated with each other (r=0.636), while inner and outer OFA and Matrix data were well correlated, all r > 0.9.

Table 3. DMO patients comparing inner vs. outer group data.

		Outer Groups				Inner Groups			
		OCT	Odelay	Osens	Matrix	OCT	Odelay	Osens	Matrix
Outer	OCT	1	**0.366**	**-0.345**	-0.016	**0.636**	**0.449**	**-0.343**	-0.004
	Odelay	**0.366**	1	**-0.616**	-0.160	0.081	**0.916**	**-0.650**	-0.153
	Osens	**-0.345**	**-0.616**	1	0.177	-0.110	**-0.611**	**0.941**	0.125
	Matrix	-0.016	-0.160	0.177	1	-0.018	-0.210	0.100	**0.938**
Inner	OCT	**0.636**	0.081	-0.110	-0.018	1	0.152	-0.118	0.090
	Odelay	**0.449**	**0.916**	**-0.611**	-0.210	0.152	1	**-0.622**	-0.206
	Osens	**-0.343**	**-0.650**	**0.941**	0.100	-0.118	**-0.622**	1	0.067
	Matrix	-0.004	-0.153	0.125	**0.938**	0.090	-0.206	0.067	1

N.B.- Odelay: OFA delay; Osens: OFA sensitivity; Matrix: Matrix total deviations. Significant correlations are shown in bold, marginally significant in normal, and insignificant correlations in grey fonts.

Similarly, we have analysed the data for the diabetes without DMO (**Table 4**). Significant correlations are bolded and the median p-value was 0.001 (least significant p=0.048). The correlation between oOCT thickness and Inner-OFA delay of -0.284 had a p-value of 0.065.

Figure 11 illustrates the sorting process among the diabetic patients with DMO. **Figure 11A** shows the sorted outer group thickness data for each eyes/subject/repeat. **Figures 11B to C** show the other data types sorted by the thickness order. That is, the different rows for each data set is according to the macular thickness, arranged from the thickest to the thinnest. We found good correlation between the sensitivity and delay with the macular thickness in the outer 4 groups.

Table 4. Diabetics comparing inner vs. outer group data.

		Outer Groups				Inner Groups			
		OCT	Odelay	Osens	Matrix	OCT	Odelay	Osens	Matrix
Outer	OCT	1	**-0.359**	0.012	0.045	**0.818**	-0.284	-0.014	-0.015
	Odelay	**-0.359**	1	**-0.502**	-0.131	**-0.348**	**0.959**	**-0.546**	0.011
	Osens	0.012	**-0.502**	1	**0.379**	0.102	**-0.443**	**0.967**	0.232
	Matrix	0.045	-0.131	**0.379**	1	0.220	-0.162	**0.342**	**0.872**
Inner	OCT	**0.818**	**-0.348**	0.102	0.220	1	**-0.307**	0.130	0.151
	Odelay	-0.284	**0.959**	**-0.443**	-0.162	**-0.307**	1	**-0.490**	-0.039
	Osens	-0.014	**-0.546**	**0.967**	**0.342**	0.130	**-0.490**	1	0.179
	Matrix	-0.015	0.011	0.232	**0.872**	0.151	-0.039	0.179	1

N.B.- Odelay: OFA delay; Osens: OFA sensitivity; Matrix: Matrix total deviations. Significant correlations are shown in bold, marginally significant in normal, and insignificant correlations in grey fonts.

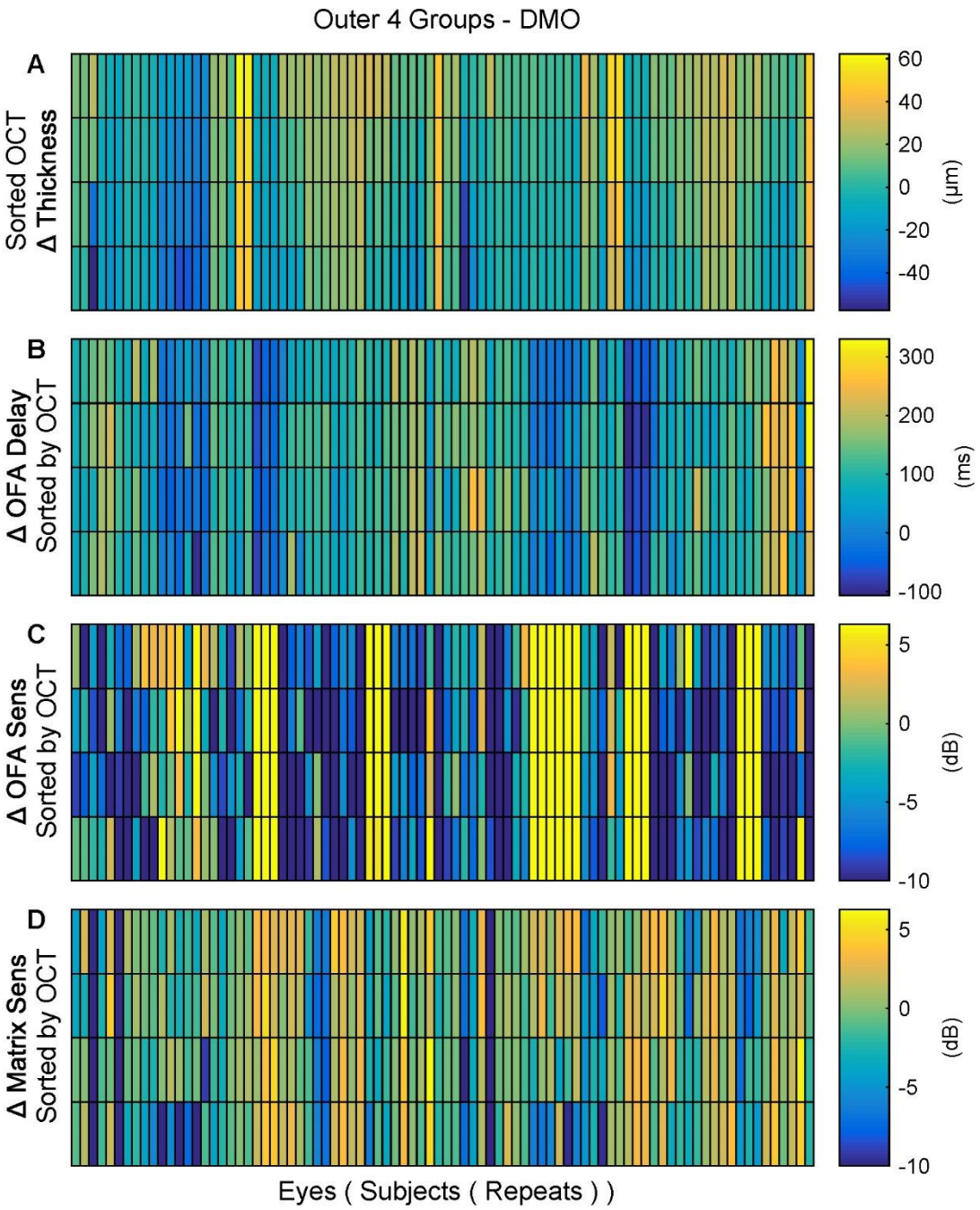

Figure 11. The results for sorting of the Outer 4 groups. The x-axis is Eyes/Subjects/Repeats. Thus, the left half are for left eyes, and the right half for right eyes. Then from left to right the eyes are grouped by subjects with any repeats concatenated. (**A**) Retinal thicknesses were differences relative to the normative data arranged thickest to the thinnest (Fig. 4). (**B**) OFA delay seems to show some inverse correlation with thickness. (**C**) Generally we see reduced sensitivity with thickness, with some cases showing hypersensitivity. (**D**) Correlation with OFA and Matrix sensitivity seems modest but it is necessary to compute them.

Independent Determinants of DMO

We used a mixed-effects logistic regression to determine which data can contribute to a clinical diagnosis of DMO, comparing the diabetes and DMO patients. Surprisingly outer OCT thickness, but not inner thickness, and OFA sensitivity contribute independently to the clinical diagnosis. Each repeat visit (i.e. time in the study) and being male also increased the odds of DME. Recall that some subjects returned for up to 6 visits over 3 years. The results are shown in **Table 5**.

Table 5. Mixed-effects Logistic regression model summary

	Odds	log(Odds)	SE	t	p	Lower	Upper
(Intercept)	0.072	-2.625	0.834	-3.149	**0.0021**	-4.276	-0.974
Visits	2.923	1.073	0.305	3.512	**0.0006**	0.468	1.677
Male	3.742	1.320	0.605	2.180	**0.0313**	0.121	2.518
oOCT	1.042	0.041	0.016	2.582	**0.0111**	0.010	0.072
oOdelay	1.002	0.002	0.008	0.203	0.8391	-0.014	0.017
oOFAsens	1.094	0.090	0.075	1.191	0.2359	-0.059	0.239
oMatrix	1.085	0.081	0.127	0.642	0.5222	-0.170	0.332
iOFAdelay	0.996	-0.004	0.008	-0.588	0.5579	-0.020	0.011
iOFAsens	0.849	-0.164	0.080	-2.044	**0.0432**	-0.323	-0.005
iMatrix	0.869	-0.140	0.115	-1.220	0.2251	-0.368	0.087

N.B.- oOCT: outer OCT; oOdelay: outer OFA delay; oOFAsens: outer OFA sensitivity; oMatrix: outer Matrix; iOFAdelay: inner OFA delay; iOFAsens: inner OFA sensitivity; iMatrix: inner Matrix. Significant correlations are shown in bold, marginally significant in normal, and insignificant correlations in grey fonts.

Interestingly, our initial model included both iOCT and oOCT. It showed that both were significant determinants of the odds having DMO, but they had opposite effects. iOCT decreased the odds and oOCT increased it (not shown). The iOCT effect was smaller and less significant (cf. p=0.003 and p=0.024). We took out iOCT to see the effect. The main effect was to make inner OFA sensitivity significant (p=0.043) as shown in Table 5. Time in the study (Visits) also increased the odds significantly per visit. Recall that some subjects returned for up to 6 visits over 3 years. Male gender was also significant in this group. We

also investigated what happened if we removed oOCT, leaving no OCT data. Inner OFA sensitivity remained significant (p=0.045). In both models increased OFA sensitivity relative to normal increased the odds for each dB, by about 1/0.85 = 18% per dB.

DISCUSSION

DMO is a major cause of blindness and visual impairment and has a hugely negative impact on the socio-economy worldwide (Lee *et al.*, 2015), including Australia (Deloitte Access Economics, 2015). To this time, it has been challenging to find a suitable functional assessment tool to diagnose the condition at the earliest stages, to provide better management. So far, treatment is administered mainly based upon macular structural changes (OCT) and a single functional end point: BCVA. In the current study we have applied mfPOP (OFA) for macular functional assessment alongside the Matrix perimetry, structural changes. All but one subject had normal BCVA.

We recruited T2D patients without or with early-stage DMO so their macular thickness was normal or near normal because one of the objectives was to determine if the functional damage preceded major structural changes.

We observed that the mean sensitivity difference compared to normal in the diabetes patients without and with DMO was reduced, at least later in the disease (Fig. 7). In cases with shorter duration of diabetes there was an initial stage of hypersensitivity, which gradually progressed to hyposensitivity with duration and severity of the disease, see also Fig 8B:ix. We have reported similar findings with mfPOP earlier (Sabeti *et al.*, 2015; Sabeti *et al.*, 2017; Rai *et al.*, 2020b). In fact, another study reported that extrafoveal hypersensitivity among the AMD cases was a good prognostic biomarker for improvement with ranibizumab therapy (Sabeti *et al.*, 2012). Such peripheral hypersensitivity, or hypersensitivity peripheral to the border of a defined lesion, was also shown by the multifocal electroretinogram (mfERG) among diabetic and AMD patients (Sabeti *et al.*, 2017). We saw increased per-region delays among the diabetes compared to normal, which was expected because retinal diseases cause afferent sensitivity defects (Bell *et al.*, 2010), and asymmetry in local delay was found to be

consistent with retinal disease severity (Sabeti *et al.*, 2015). Just like OFA, mfERG has shown that the delays not only precede the onset and progression of retinopathy, but also predict the location of future retinopathy up to 3 years before the visible changes occur (Ozawa *et al.*, 2015). Our study of AMD with mfPOP identified two types of patients based on the peripheral responses: positive type showing hypersensitivity and prolonged delay, and negative type with hyposensitivity and delay shorter than normal, which is described in the Chapter 3 of this thesis.

Principal curve analysis was first used by Wall et al. in 2010 (Figure 1 of that study) to compare results between different perimeters. We have similarly used scatter plots to compare different variables between three modalities: macular thickness by OCT, functional assessment with Matrix, and OFA in terms of sensitivity and delay (Fig. 9). Then, we used the principal curve analysis to find out the main relationship trends. The first point that we noticed was the uneven distribution of the values measured by the Matrix perimeter, which resulted in discrete segregation of the dots in the scatter plots. This was also observed by other researchers and occurs because the Matrix decibel distribution is spaced at discrete intervals, sometimes quite widely spaced, compared to other perimetric methods (Patel *et al.*, 2007; Fredette *et al.*, 2015). There was no simple correlation between the macular thickness and OFA sensitivity. Instead sensitivity fluctuated between hyper- and hypo-sensitivity, possibly related to progress of the disease. We have noted similar findings in our previous publication (Rai *et al.*, 2020b). Taken together the results indicate that the functional change precedes structural change in diabetic patients with and without DMO, and that in diabetes several stages of change may be identified before structural change (Sabeti *et al.*, 2015). Macular thickness and the delay were correlated positively and more consistently. This agrees with the previous findings that the increased delay or asymmetry in local delay was found consistent with the severity of retinal disease (Sabeti *et al.*, 2015). OFA sensitivity and

delay were well correlated showing a drop in sensitivity with increases in delay. This may again be related to increasing severity of the disease. The Matrix and OFA sensitivities correlated well although the principal curve was biased by the bulk of the data being at smaller values.

We have noticed that the results of OFA was often more consistent than that of the Matrix. This would need to be confirmed using head-to-head testing by both methods within 2 weeks or so to isolate short-term change. Both the hyposensitivity and increased delay were seen to agree with the macular thickness in the follow up eye tests, but the Matrix perimeter showed improved function in terms of total and pattern deviations despite persistent macular structural thickening. This may be explained due to the learning curve effect involved, or inattentiveness of the patients, with the Matrix perimeter (Fredette *et al.*, 2015). The OFA does not have a learning curve effect because it is an objective method. The other factor may be that the OFA defines hypersensitivity as a larger than normal response, whereas the Matrix uses tiny contrast thresholds to indicate high sensitivity, requiring subjects to notice miniscule differences in contrast, +6 dB being a change in contrast of 1 part in 1000. Thus, the OFA might be expected to characterise hypersensitivity better than the Matrix. Note also that the same sort of hypersensitivities are observed in diabetes and AMD patients when tested with OFA and mfVEPs on the same day. Those mfVEP hypersensitivities are observed on EEG electrodes recording the extra-striate cortex (Sabeti *et al.*, 2017), which is known to synapse with the pretectal olivary nucleus (Gamlin, 2006).

On computing the regional group-means of the macular thickness, OFA sensitivity and delay and Matrix data in each of outer and inner macular groups (Fig. 10) we found that the inner macular thickness was not correlated with any other variables (Table 3), while outer macular thickness was correlated with inner and outer OFA sensitivity and delay. Previously, we have reported that in AMD the BCVA was mainly determined by the off-axis macular thickness

and average Matrix 10-2 sensitivity loss, and not the central thickness (Rai *et al.*, 2020b). This may be due to the fact that the density of the ganglion cells are reported to be maximum in the off-axis fovea, and not in the centre (Curcio & Allen, 1990). The disorganisation of the retinal inner layers (DRIL), including the retinal ganglion cell (RGC) layer, serves as prognostic biomarker in DMO: patients without baseline DRIL have better responses to treatment and better visual recovery than patients with DRIL (Zur *et al.*, 2020). Another study reported that presence of RGC layer cysts in DMO has poorer prognosis than those without RGC layer cysts (Ceklic *et al.*, 2019).

The reduction in the thickness of the RGC layer and inner plexiform layer measured by Spectral Domain OCT and microperimetry, was found significantly correlated to the visual improvement following anti-VEGF treatment of DMO (Xu *et al.*, 2019). RGC loss and neuronal damage are present in diabetic subjects even without DR (Ng *et al.*, 2016). These studies indicate that involvement of RGC layer in DMO is significant pathophysiological process that affect the retinal function, indicated by drop in sensitivity and prolonged delays in the current study. Another study (in preparation) by the Maddess Group on the advanced AMD has reported that the retinal thickness outside 8 degrees was significantly associated with the high contrast visual acuity and macular sensitivity suggesting that the outer macular thickness as useful prognostic indicator (Sabeti *et al.*, 2020). Therefore, in contradiction to the general theory that the central macular structural integrity is vital for normal retinal function, the off-centre macular structural integrity may be more crucial. Perhaps healthier parts of the retina peripheral to the fovea provide better prognostic indicators for the fovea.

Our mixed-effects logistic regression analysis determined that outer macular thickness and OFA sensitivity contributed independently to a clinical diagnosis of DMO. Outer thickness, number of visits or duration in study, and male gender increased the odds of having DMO. Male gender with increased odds of getting DMO could be because it is reported that T2D is

more common in men than women (Nordstrom *et al.*, 2016), and DR is more common among men due genetic susceptibility and other factors (Ozawa *et al.*, 2015).

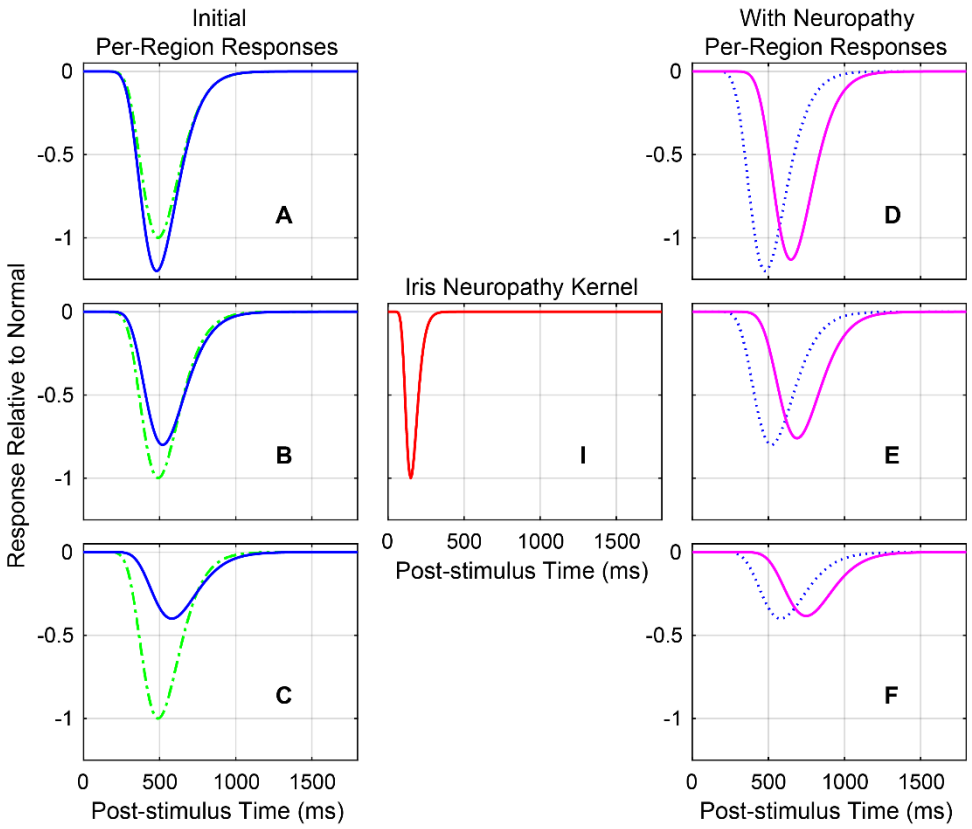

Figure 12. A simple model of the effects of iris neuropathy. **A to C**, show normal per-region pupil responses as dashed green lines. A peak value of -1 indicates normal constriction amplitudes. The blue curves are meant to be OFA responses of a patient. **A** shows a somewhat faster and larger than normal response as may occur in a less affected part of the retina. **B and C** are slower and less sensitive responses. These curves might represent neural responses at the level of the Edinger–Westphal nucleus. The red waveform of **I** represents the filter characteristic (kernel) of an iris experiencing neuropathy. The blue dotted lines of **D to F** are reproductions of the blue responses of A to C. The magenta waveforms are the convolution of the (blue) responses with the Iris kernel capturing the smoothing effect of the neuropathy. The effect is to stretch the response waveforms out in time and possibly reduce the amplitude (in this example the waveforms maintain their area).

A noticeable feature of many of the OFA delay plots is just how long some of the delays are. This is not strictly due to neuropathy of the iris because there are per-region changes, that are often reproducible, and localised to inner and outer macula (Fig. 10). Thus these per-region differences seem to reflect localised function change. This has been reported before in early-

stage T2D (Bell *et al.*, 2010; Sabeti *et al.*, 2015). It is possible, however, that neuropathy contributed to the very long delays seen, effectively stretching them out. If the iris itself was becoming slower the effect would be to low-pass filter (smooth) the responses. **Figure 12** illustrates how this could work, modelling the effect of neuropathy as a linear filtering (convolution) with the characteristic of a slower iris (Fig. 12I). The effect is to stretch out, or magnify, the delays caused by per-region functional changes (Fig. 12D,E,F).

Future directions and limitations

Having demonstrated that DMO was associated with peripheral functional change, as measured by OFA but not Matrix, we would like to gather more repeats from a larger number so subjects so we can see how OFA tracts disease progression. As part of that we would also like to characterise test-retest variability by retesting subjects about 2 weeks apart (Artes *et al.*, 2002; Maddess, 2014). This would allow us to determine the level for significant change. We would make these measurements with OCT, OFA and Matrix. We would also determine peripheral neuropathy as a possible correlate of iris neuropathy. We would also measure Advanced Glycation Endproducts (AGEs) as a measure of longer term diabetic tissue damage. We have begun collecting these data now.

This study was limited by a small number of participants and some patients having fewer follow up visits because their further visit was terminated because they started receiving treatment, or they dropped out from the study, or they entered the study late.

CONCLUSIONS

OFA is proving to be a useful tool for functional assessment of retinal function, detecting drop in sensitivity and increased delay even prior to the detectable structural changes. That being said earlier in the disease hypersensitivity appears to be an indicator of earlier functional change. Its values correlated well with that of the Matrix, and were possibly

superior in terms of reproducibility and consistency. The outer macular regions were more correlated with OFA sensitivity and delay than the inner regions. Thus, the outer macular integrity may be more prognostically valuable than inner retinal condition for the optimal functioning of the macula. Mixed-effects logistic regression determined that the outer macular thickness and OFA sensitivity contributed independently to a clinical diagnosis of DMO, and outer thickness, increased number of visits or duration in study, and male gender increased the odds of developing DMO.

REFERENCES

Artes P, Iwase A, Ohno Y, Kitazawa Y & Chauhan B. (2002). Properties of perimetric threshold estimates from full threshold, SITA Standard, and SITA Fast Strategies. *Invest Ophth Vis Sci* **43,** 2654-2659.

Bell A, James AC, Kolic M, Essex RW & Maddess T. (2010). Dichoptic multifocal pupillography reveals afferent visual field defects in early type 2 diabetes. *Invest Ophthalmol Vis Sci* **51,** 602-608.

Bremner FD. (2012). Pupillometric evaluation of the dynamics of the pupillary response to a brief light stimulus in healthy subjects. *Invest Ophthalmol Vis Sci* **53,** 7343-7347.

Carle C, James A, Kolic M, Essex R & Maddess T. (2013). Getting the timing right: Clustered volley stimulus presentation for multifocal pupil perimetry in glaucoma. *Investigative Ophthalmology & Visual Science* **54**.

Carle CF, James AC, Kolic M, Essex RW & Maddess T. (2014). Luminance and colour variant pupil perimetry in glaucoma. *Clin Exp Ophthalmol* **42,** 815-824.

Carle CF, James AC, Kolic M, Essex RW & Maddess T. (2015). Blue multifocal pupillographic objective perimetry in glaucoma. *Invest Ophth Vis Sci* **56,** 6394-6403.

Carle CF, James AC, Kolic M, Loh YW & Maddess T. (2011). High-resolution multifocal pupillographic objective perimetry in glaucoma. *Invest Ophthalmol Vis Sci* **52,** 604-610.

Carle CF, Maddess T, Kolic M, Essex RW & van Kleef JP. (2020). Normative data for wide-field an macular multifocal pupilographic objective perimetry tests. *In preparation*.

Ceklic L, Huf W, Ebneter A, Wolf S, Zinkernagel MS & Munk MR. (2019). The impact of ganglion cell layer cysts in diabetic macular oedema treated with anti-vascular endothelial growth factor. *Acta Ophthalmol* **97,** e1041-e1047.

Chylack LT, Wolfe JK, Singer DM, Leske MC, Bullimore MA, Bailey IL, Friend J, Mccarthy D & Wu SY. (1993). The Lens Opacities Classification System-Iii. *Archives of Ophthalmology* **111,** 831-836.

Curcio CA & Allen KA. (1990). Topography of ganglion cells in human retina. *J Comp Neurol* **300,** 5-25.

DCCT, Nathan DM, Genuth S, Lachin J, Cleary P, Crofford O, Davis M, Rand L & Siebert C. (1993). The effect of intensive treatment of diabetes on the development and progression of long-term complications in insulin-dependent diabetes mellitus. *N Engl J Med* **329,** 977-986.

Deloitte Access Economics. (2015). The economic impact of diabetic macular oedema in Australia, pp. 1 online resource (69 pages).

Engerman RL & Kern TS. (1987). Progression of incipient diabetic retinopathy during good glycemic control. *Diabetes* **36,** 808-812.

Fredette MJ, Giguere A, Anderson DR, Budenz DL & McSoley J. (2015). Comparison of Matrix with Humphrey Field Analyzer II with SITA. *Optom Vis Sci* **92,** 527-536.

Gale R, Scanlon PH, Evans M, Ghanchi F, Yang Y, Silvestri G, Freeman M, Maisey A & Napier J. (2017). Action on diabetic macular oedema: achieving optimal patient management in treating visual impairment due to diabetic eye disease. *Eye* **31**.

Gamlin PD. (2006). The pretectum: connections and oculomotor-related roles. *Prog Brain Res* **151,** 379-405.

Hashemi H, Khabazkhoob M, Yekta A, Emamian MH, Nabovati P & Fotouhi A. (2017). The Distribution of Macular Thickness and Its Determinants in a Healthy Population. *Ophthalmic Epidemiol* **24,** 323-331.

Hastie T & Stuetzle W. (1989). Principal curves. *J Am Statistical Soc* **84,** 502–516.

James AC. (2003). The Pattern-Pulse Multifocal Visual Evoked Potential. *Investigative Ophthalmology & Visual Science* **44,** 879-890.

James AC, Ruseckaite R & Maddess T. (2005). Effect of temporal sparseness and dichoptic presentation on multifocal visual evoked potentials. *Vis Neurosci* **22,** 45-54.

Laishram M, Srikanth K, Rajalakshmi AR, Nagarajan S & Ezhumalai G. (2017). Microperimetry - A New Tool for Assessing Retinal Sensitivity in Macular Diseases. *Journal of Clinical and Diagnostic Research* **11,** Nc08-Nc11.

Lee R, Wong TY & Sabanayagam C. (2015). Epidemiology of diabetic retinopathy, diabetic macular edema and related vision loss. *Eye and Vision* **2,** 17.

Lind M, Oden A, Fahlen M & Eliasson B. (2010). The shape of the metabolic memory of HbA1c: re-analysing the DCCT with respect to time-dependent effects. *Diabetologia* **53,** 1093-1098.

Maddess T. (2012). Pupil dynamics and response amplitude: only size matters. *Invest Ophthalmol Vis Sci* **53**.

Maddess T. (2014). Modelling the relative influence of fixation and sampling errors on test-retest-variability in perimetry. *Graefes Archive Ophthalmol* **DOI 10.1007/s00417-014-2751-y**.

Maddess T, Bedford SM, Goh XL & James AC. (2009). Multifocal pupillographic visual field testing in glaucoma. *Clin Exp Ophthalmol* **30,** 678-686.

Maddess T & Daria VR. (2017). To BCVA, or not to BCVA, that is the question. *Clinical & Experimental Ophthalmology* **45,** 437-439.

Maddess T, Lane J, Rohan EMF, Essex RW, McKone E & Sabeti F. (2020). Central versus peripheral macular structure and function and acuity in age-related macular degeneration. In *ARVO*, pp. e-3007. Baltimaore.

Nathan DM, Lachin J, Cleary P, Orchard T, Brillon DJ, Backlund JY, O'Leary DH, Genuth S, Diabetes C, Complications T, Epidemiology of Diabetes I & Complications Research G. (2003). Intensive diabetes therapy and carotid intima-media thickness in type 1 diabetes mellitus. *N Engl J Med* **348,** 2294-2303.

Ng DS, Chiang PP, Tan G, Cheung CG, Cheng CY, Cheung CY, Wong TY, Lamoureux EL & Ikram MK. (2016). Retinal ganglion cell neuronal damage in diabetes and diabetic retinopathy. *Clin Exp Ophthalmol* **44,** 243-250.

Nordstrom A, Hadrevi J, Olsson T, Franks PW & Nordstrom P. (2016). Higher Prevalence of Type 2 Diabetes in Men Than in Women Is Associated With Differences in Visceral Fat Mass. *Journal of Clinical Endocrinology & Metabolism* **101,** 3740-3746.

Ozawa GY, Bearse MA, Jr. & Adams AJ. (2015). Male-female differences in diabetic retinopathy? *Curr Eye Res* **40,** 234-246.

Patel A, Wollstein G, Ishikawa H & Schuman JS. (2007). Comparison of visual field defects using matrix perimetry and standard achromatic perimetry. *Ophthalmology* **114,** 480-487.

Rai BB, Essex RW, Sabeti F, Rohan E, vanKleef J, Carle CF & Maddess T. (2020a). Multifocal Pupillographic Objective Perimetry as a biomarker for anti-VEGF injection requirements in neovascular Age-related Macular Degeneration. *In preparation*.

Rai BB, Maddess T, Carle CF, Rohan EMF, van Kleef JP, Essex RW, Nolan CJ & Sabeti F. (2020b). Comparing retinal thickness and Matrix 10-2 functional testing in diabetic macular edema. In *IOVS-ARVO*, pp. e-4866. Baltimore.

Ranchod TM & Fine SL. (2009). Primary treatment of diabetic macular edema. *Clinical Interventions in Aging* **4,** 101-107.

Ruseckaite R, Maddess T, Danta G, Lueck CJ & James AC. (2005). Sparse multifocal stimuli for the detection of multiple sclerosis. *Annals of Neurology* **57,** 904-913.

Ruseckaite R, Maddess T & James AC. (2006). Frequency doubling illusion VEPs and automated perimetry in multiple sclerosis. *Documenta Ophthalmol* **113,** 29-41.

Sabeti F, James AC, Carle CF, Essex RW, Bell A & Maddess T. (2017). Comparing multifocal pupillographic objective perimetry (mfPOP) and multifocal visual evoked potentials (mfVEP) in retinal diseases. *Sci Rep* **7,** 45847.

Sabeti F, Lane J, Rohan EMF, Essex RW, McKone E & Maddess T. (2020). Central versus peripheral macular structure and function and acuity in age-related macular degeneration. **In preparation**.

Sabeti F, Maddess T, Essex RW & James AC. (2012). Multifocal pupillography identifies ranibizumab-induced changes in retinal function for exudative age-related macular degeneration. *Invest Ophthalmol Vis Sci* **53,** 253-260.

Sabeti F, Maddess T, Essex RW, Saikal A, James AC & Carle CF. (2014). Multifocal pupillography in early age-related macular degeneration. *Optom Vis Sci* **91,** 904-915.

Sabeti F, Nolan CJ, James AC, Jenkins A & Maddess T. (2015). Multifocal pupillography identifies changes in visual sensitivity according to severity of diabetic retinopathy in type 2 diabetes. *Invest Ophthalmol Vis Sci* **56,** 4504-4513.

Stratton IM, Kohner EM, Aldington SJ, Turner RC, Holman RR, Manley SE & Matthews DR. (2001). UKPDS 50: risk factors for incidence and progression of retinopathy in Type II diabetes over 6 years from diagnosis. *Diabetologia* **44,** 156-163.

Testa R, Bonfigli AR, Prattichizzo F, La Sala L, De Nigris V & Ceriello A. (2017). The "Metabolic Memory" Theory and the Early Treatment of Hyperglycemia in Prevention of Diabetic Complications. *Nutrients* **9**.

Wall M, Woodward KR, Doyle CK & Zamba G. (2010). The effective dynamic ranges of standard automated perimetry sizes III and V and motion and matrix perimetry. *Arch Ophthalmol* **128,** 570-576.

Xu Y, Qu Y, Suo Y, Gao J, Chen X, Liu K & Xu X. (2019). Correlation of retinal layer changes with vision gain in diabetic macular edema during conbercept treatment. *BMC Ophthalmol* **19,** 123.

Yamashita T, Tanaka M, Kii Y, Nakao K & Sakamoto T. (2013). Association between retinal thickness of 64 sectors in posterior pole determined by optical coherence tomography and axial length and body height. *Invest Ophthalmol Vis Sci* **54,** 7478-7482.

Zur D, Iglicki M, Sala-Puigdollers A, Chhablani J, Lupidi M, Fraser-Bell S, Mendes TS, Chaikitmongkol V, Cebeci Z, Dollberg D, Busch C, Invernizzi A, Habot-Wilner Z, Loewenstein A & Group tIR. (2020). Disorganization of retinal inner layers as a biomarker in patients with diabetic macular oedema treated with dexamethasone implant. *Acta Ophthalmologica* **98,** e217-e223.

ORIGINAL CLINICAL STUDY

OPEN

Pattern and Presentation of Vitreo-Retinal Diseases: An Analysis of Retrospective Data at a Tertiary Eye Care Center in Nepal

Bhim B. Rai, MD, Mohan K. Shresthra, PhD†, Raba Thapa, MD†, Rohan W. Essex, MD‡, Govinda Paudyal, MD†, and Ted Maddess, PhD**

Purpose: We examined patients presenting in a tertiary eye hospital in Nepal, focusing on information relevant to screening and management programs for vitreo-retinal (VR) disease.

Design: Retrospective, cross-sectional study.

Methods: We reviewed all patients presenting for the first time to the VR-clinic over 1 year. We quantified patient demography, symptoms and duration, systemic diseases, ophthalmological examinations, diagnostic investigations, and final diagnoses.

Results: Of the 1905 cases, 1148 were male (60.3%). The 25th percentile of ages was 29 and 38 years for male and female, respectively; thus, female presented later ($P < 0.0001$). Hypertension was the commonest systemic disease (40.8%), followed by diabetes (32.5%). Age-related macular degeneration (AMD) and diabetic retinopathy (DR) affected 447 eyes (11.8%) and 416 eyes (10.9%), respectively. Male and female AMD and DR patients did not differ in age or disease duration. Similarly, age or disease duration for DR did not correlate with severity. Asymmetry of disease severity between eyes with AMD and DR was largest in patients with 1 normal eye. Presenting acuity was asymmetric between eyes ($P < 0.0001$) with people more often reporting once their right eyes had acuity of 6/18 or worse.

Conclusions: The screening of blood pressure and glucose levels combined with fundus photography could prevent many from progressing to life-changing visual impairment and blindness. Later reporting by females began at childbearing age; therefore, education and ocular screening could be usefully coupled in reproductive health programs. Clubbing VR disease screening with other established health programs like diabetes control program, hypertension clinics, school health program, and so on, would provide economical and sustainable approach.

Key Words: AMD, diabetic retinopathy, retinal diseases, laterality, sex differences

(*Asia Pac J Ophthalmol (Phila)* 2019;8:481–488)

From the *John Curtin School of Medical Research, Australian National University, ACT, Australia; †Tilganga Institute of Ophthalmology, Kathmandu, Nepal; and ‡ANU Academic Unit of Ophthalmology, ANU Medical School; Department of Ophthalmology, Canberra Hospital, ACT Health, Australia.

Submitted April 24, 2019; accepted June 18, 2019.
Funding: The study did not receive any funding.
The authors have no conflicts of interest to declare.
Supplemental Digital Content is available for this article.

Address Correspondence and Reprint Requests to: Dr Govinda Paudyal, Tilganga Institute of Ophthalmology, Kathmandu 44600, Nepal. E-mail: govinda.paudyal@tilganga.org

Copyright © 2019 Asia-Pacific Academy of Ophthalmology. Published by Wolters Kluwer Health, Inc. on behalf of the Asia-Pacific Academy of Ophthalmology. This is an open access article distributed under the terms of the Creative Commons Attribution-Non Commercial-No Derivatives License 4.0 (CCBY-NC-ND), where it is permissible to download and share the work provided it is properly cited. The work cannot be changed in any way or used commercially without permission from the journal.

ISSN: 2162-0989
DOI: 10.1097/01.APO.0000604400.50700.2d

Downloaded from https://journals.lww.com/apjoo by BhDMf5ePHKav1zEoum1tQfN4a+kJLhEZgbsIHo4XMi0hCywCX1AWnYQp/IlQrHD3i9dFgv3yuisNQsGwJy4BZ3d22GEwCDONSwtwUFuNK4= on 12/05/2019

Vitreo-retinal (VR) diseases are common causes of visual impairment and blindness. Population-based studies have reported the overall prevalence of VR disorders to be 8.56% (range 10.4%–21.02%) among the population aged 40 years and older.[1,2] The 1981 Nepal Blindness Survey reported VR disorders as the third leading cause of bilateral blindness, second only to cataract and its complications.[3] A more recent Nepalese population-based study reported VR disorders to be the second commonest cause of bilateral blindness, second only to cataract, and the most common cause among pseudophakics.[4]

A population-based study in Bhutan reported that 22.1% of visual impairment and blindness was due to VR pathologies among the population aged 50 years or older.[5] A similar survey in Bangladesh reported VR diseases as the second leading cause of bilateral blindness accounting for 13.3%,[6] and in India 17.1% among persons aged 30 years or older.[7] By contrast, a Nigerian study reported a prevalence of 8.1%, with AMD, DR, retinal vein occlusion (RVO), and retinal detachment (RD) as the most common retinal diseases.[8] An Ethiopian study reported RD as the commonest cause of both bilateral (59.4%) and unilateral (41.2%) blindness.[9] The Tehran study reported VR prevalence of 8.56% with acquired retinopathies and peripheral lesions as the most common retinal diseases.[2]

In developed countries, AMD affects nearly 10% of those older than 65 years, and 25% of those older than 75 years,[10] including Australia.[11] In the United States, >8 million people have intermediate AMD and nearly 2 million have advanced AMD.[12] In the UK, the prevalence of late AMD was 2.4% among the population aged 50 years and older, 4.8% for 65 years or older, and 12.2% for 80 years or older.[13]

DR often affects adults of working age.[14] The American National Health and Nutritional Examination Survey 2005–2008 reported that 28.5% of diabetic patients had some degree of DR, and 4.4% had vision-threatening DR.[15] In 2012, global prevalence was 34.6% for any DR, 6.96% for proliferative DR (PDR), 6.81% for diabetic macular edema, and 10.2% for vision-threatening DR.[16] India and China are confronting a growing epidemic of diabetes and DR.[17–19]

The current study focuses on the features of VR diseases presenting to a tertiary eye care center in Nepal. Surprisingly the results indicate that analysis of the disease laterality is sometimes required. The study provides clear recommendations for improving care that are applicable outside Nepal, and the work provides a baseline for planned comparison studies.

METHODS

Setting

This study was conducted at the Tilganga Institute of Ophthalmology (TIO), Kathmandu, Nepal. The TIO is a tertiary

eye care center with subspeciality clinics providing services for ophthalmological patients from all over Nepal, India, and Bhutan. All subspeciality clinics in the TIO, including the VR clinic, run from morning till afternoon, and an extended paying clinic operates in the evening. Despite this availability of extended facilities, 1843 cases (96.7%) presented to the routine public VR clinic. Only 36 cases (1.9%) presented to the paying clinic, whereas 26 cases (1.4%) reported to the emergency department.

Study Design and Ethics

The study has been approved by the TIO-Institutional Review Committee (TIO-IRC) vide letter number: Ref: 10/2018. The need for consent was waived by TIO-IRC because the retrograde study collected de-identified data from patient files.

Study Population

This study covers all cases presenting to the VR clinic for the first time over 1 year. Patients who presented for repeat or follow-up visits were not included. The study ran from January 1, 2010 to December 31, 2010. A key objective of this study is to provide a baseline reference for planned follow-up studies that will use similar analyses. A further benefit of recording this hospital-based study is that there are population-based studies of disease prevalence from both Nepal[4,20] and Bhutan[5] from 2009/2010 with which this study can be compared, adding extra value for both the region and similar countries.

Data Collection and Analysis

Detailed demographic information, presenting complaints, treatment history, and associated systemic diseases were noted. Best corrected visual acuity (BCVA), refractive status, Goldmann applanation tonometry, findings of slit-lamp examination, 90D biomicroscopy, fundoscopy, and diagnostic investigations performed were recorded. Diagnoses were noted separately for right and left eyes. Data collection was supervised by the head of the VR unit to ensure high quality and uniform practice. Hypertensive retinopathy was graded according to Keith-Wagener-Barker classification system,[21] and DR was classified as per the modified Airlie House and Abbreviated Early Treatment Diabetic Retinopathy Study (ETDRS) classification of DR.[22]

The data were analyzed using SPSS (version 20.0, IBM, New York, NY) and MATLAB (2016b, The MathWorks, Natick, MA). Comparisons of the expected and observed frequency of sex or eye-wise effects were done using Chi-squared tests. To compare the 10th, 25th, 50th, 75th, and 90th percentiles of the distributions of Figure 1B for male and female, we applied a sampling-with-replacement-based bootstrap analysis[23] to estimate the population means and the standard errors (SE) of the means of those percentiles. We employed 10,000 bootstrap cycles to insure the estimated means and SE converged to within 2 decimal places on 5 independent cross-validations. We then applied *t* tests employing the estimated means and SE.

RESULTS

We will first give an overview of the general presentation of the 1905 cases. We will then present the ocular disease data as: the nonretinal diseases involving posterior segment other than retina, and the main analysis of the retinal diseases. Background data are presented in 5 Supplementary tables, http://links.lww.com/APJO/A56.

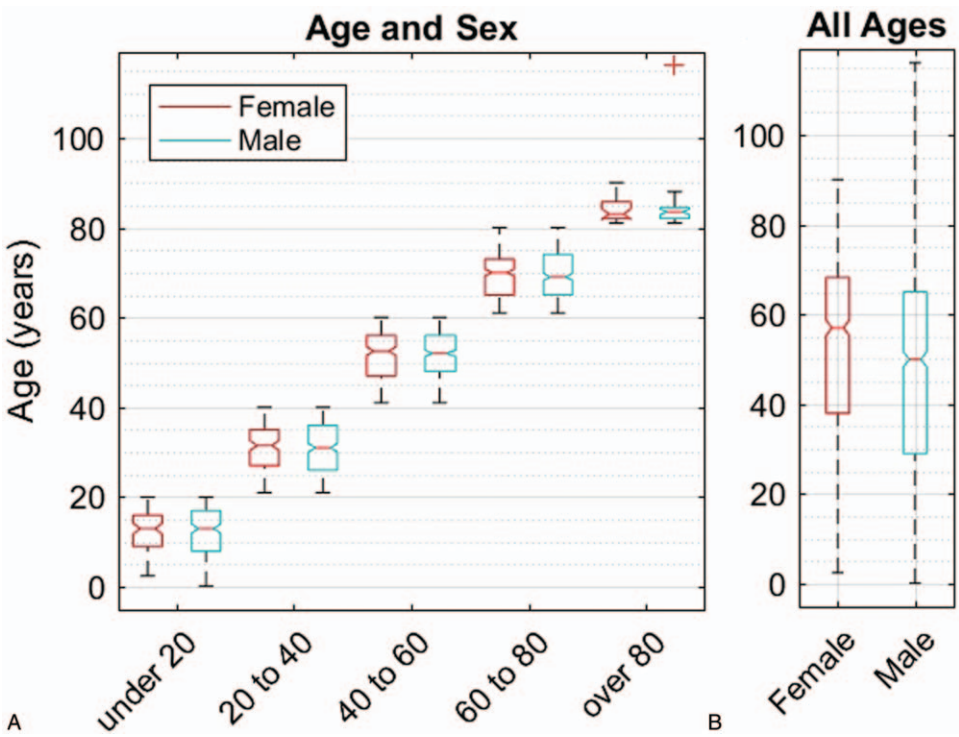

FIGURE 1. Age and sex boxplot. A, Presenting ages of the 1905 patients in cohorts of 20 years. The boxes indicate 25th, 50th, and 75th percentile of the age distributions. The red + represents a 116-year-old male outlier. B. The overall distribution of ages. A bootstrap analysis showed that the 10th, 25th, 50th, and 75th percentiles for female were all significantly older than for male (Text).

© 2019 Asia-Pacific Academy of Ophthalmology.

General Presentation

The 1905 new cases presenting to the VR clinic were split as: 1148 male (60.3%) and 757 female (39.7%). Demographic data are shown in Table 1. Figure 1A gives a breakdown of the presenting ages in 20-year cohorts for each sex. Figure 1B shows that, for the whole cohort. The 25th percentile was 29 years for male and 38 years for female. A bootstrap analysis revealed that the 10th, 25th, 50th and 75th percentiles were all significantly older for female than male by 3.95, 9.28, 7.25, and 3.08 years (ie, median is 5.6 years). The 10th percentile difference was significant at $P < 0.003$, and the others at $P = 0.0001$. It is noted that the 25th percentiles for the males were lower in the 20-year cohorts of Figure 1A as well.

A total of 802 cases (42.1%) were from the Kathmandu valley, 1038 cases (54.5%) were from Nepal outside the Kathmandu valley, and 65 cases (3.4%) were from other countries. A total of 1574 cases (82.6%) reported to the hospital as primary cases, whereas 331 cases (17.4%) were referred from other hospitals or health care centers.

The commonest presenting complaint was poor vision accounting for 1142 cases (59.9%), followed by trauma in 227 (11.9%), loss of vision in 155 (8.1%), floaters in 91 (4.8%), and vision not improving after cataract surgery in 44 (2.3%). All presenting complaints are summarized in Table 2. A total of 565 cases (30.5%) presented within a month of the onset of their symptoms, whereas 500 (27.0%) presented only after 12 months. In 53 cases, we could not affirm the time (Supplemental Digital Content 1, Table S1, http://links.lww.com/APJO/A56).

Hypertension was the commonest systemic disease associated in 250 cases (40.8%), followed by diabetes in 199 cases (32.5%) and combined diabetes and hypertension in 124 cases (20.2%) (Fig. 2). The other systemic diseases found in 40 cases (6.5%) are summarized in Supplemental Digital Content 1, Table S2, http://links.lww.com/APJO/A56. The duration of systemic disease association was found to be <5 years in 42.8% of cases, 5 to 10 years in 33.2%, and >10 years in 24.0%.

We quantified interventions done at other centers before patients reported to our clinic, including surgical, laser, or ophthalmic injections. These cases included cataract surgery in 55 (2.9%), VR surgery in 27 (1.5%), retinal laser in 27 (1.5%), and primary repair of corneoscleral tear or eyelid lacerations in 20 (1.1%). All previous interventions are summarized in Table 2.

Hematological testing was the most commonly diagnostic test performed in 584 cases (23.1%), followed by optical coherence tomography in 516 (20.4%), B-scan in 436 (17.2%), fundus fluorescence angiography in 89 (3.5%), and visual fields in 39 (1.5%). Diagnostic investigation was not indicated or not done in 687 cases (27.1%). Supplemental Digital Content 1, Table S4, http://links.lww.com/APJO/A56 summarizes the diagnostic procedures.

TABLE 1. Demographic Characteristics of Patients

Parameters	Female Patients	Male Patients
No. patients	757	1148
Mean age, y	52.3	47.1
Median age, y	57	50
Standard deviation	20.5	22.2
Minimum age, y	2.5	0.17
Maximum age, y	90	116

TABLE 2. Presenting Symptoms

Presenting Complaints	Frequency	%
Poor vision	1142	59.9
Trauma	227	11.9
Loss of vision	155	8.1
Floaters	91	4.8
Vision not improving after cataract surgery	44	2.3
Sudden loss of vision	43	2.3
Routine eye check-up	41	2.2
Night blindness	34	1.8
Foreign body sensation	20	1.0
Pain	18	0.9
Flashes of light	8	0.4
Black spot in visual field	8	0.4
White eye	5	0.3
Others	69	3.6
Total	1905	100

BCVA was 6/18 or better in the right eye in 660 cases (34.8%), and in left eyes in 1025 cases (54.1%). In 751 cases (39.4%) right eyes, and 355 cases (18.6%) left eyes, the BCVA was 6/18 to 6/60. Figure 3 illustrates how surprisingly asymmetric these values were ($P < 0.0001$, see legend). These findings prompted us to explore our data to see whether any other such asymmetries occurred. Cases with BCVA <6/60 or no perception of light (NPL) were more common on the left, but not significantly so. NPL was found in 37 (1.8%) right eyes and 44 (2.3%) left eyes.

Nonretinal Diseases

Before detailing the VR diseases, we quickly summarize the other issues discovered. Posterior vitreous detachment was the commonest nonretinal disease with 79 cases (35 OS). There were 51 cases of endophthalmitis (24 OS): 33 (64.7%) were post-traumatic, 13 (25.5%) postoperative, and 5 (9.8%) endogenous in origin. The other diseases involving posterior segment other than the retina are enumerated in Supplemental Digital Content 1, Table S5, http://links.lww.com/APJO/A56.

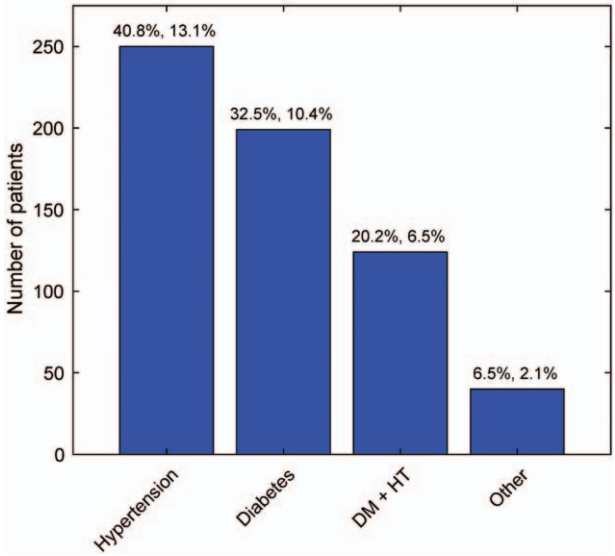

FIGURE 2. Systemic disease prevalence. The breakdown of the commonest systemic diseases found in 613 (32.2%) of the 1905 patients. The values at the top of the columns give the percentage of the systemic disease patients (left), and the percentage of all patients (right). DM indicates diabetes mellitus; HT, hypertension.

© 2019 Asia-Pacific Academy of Ophthalmology.

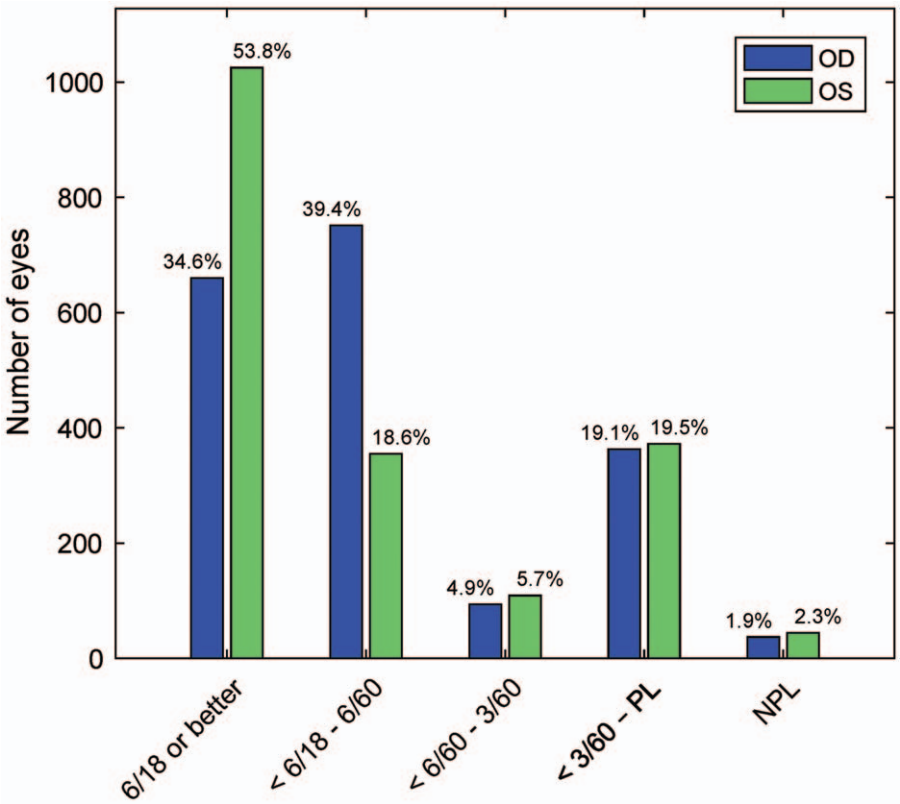

FIGURE 3. Presenting BCVA. The presenting BCVAs provided significant asymmetries between eyes ($P < 0.0001$, Bonferroni corrected) in the 2 groups with acuities of 6/60 or better (chi-square = 158 for "6/18 or better", and 283 for "6/18 to 6/60"). BCVA indicates best corrected visual acuity; NPL, no perception of light; PL, perception of light.

Most of the trauma-related conditions involved the left eyes, but this bias did not reach statistical significance. When pooled together, atrophic bulbi, phthisis, and absolute eyes were more common in left eyes: 16 (0.8%) compared with only 8 right eyes (0.4%, $P = 0.05$, chi-square). Dislocated cataract was similar in left eyes: 14 (0.8%) compared with 10 right eyes (0.5%, $P = 0.25$, chi-square). Dislocated intraocular lens into the vitreous cavity was also seen in 7 left eyes (0.4%) and 3 right eyes (0.2%, $P = 0.10$, chi-square). Retained intraocular foreign body involved 7 left and 4 right eyes ($P = 0.15$, chi-square). Open- and close-globe injuries affected both eyes equally. The fundus was not visible in 6 left eyes (0.3%), and 7 right eyes (0.4%).

Retinal Diseases

The commonest retinal disease was AMD, affecting 223 right eyes (11.7%) and 224 left eyes (11.8%), followed by DR involving 208 left, and 208 right eyes (10.9%). RD was the third commonest, affecting 112 right eyes (5.9%) and 126 left eyes (6.6%), of which 71% were rhegmatogenous, 17.2% exudative, and 11.8% tractional RD. There were 150 cases of branch RVO (BRVO), 80 in right and 70 in left eyes. Myopic degeneration affected 63 right and 54 left eyes, and retinitis pigmentosa (RP) was seen in 56 right and 57 left eyes. Other retinal diseases diagnosed were hypertensive retinopathy in total of 87 eyes, central serous chorioretinopathy in 77 eyes, central RVO in 65 eyes, macular scar in 53 eyes, macular hole in 55 eyes, retinal vasculitis in 46 eyes, and others detailed in Table 3. 94.8% of full-thickness macular hole and 84.6% lamellar macular hole were unilateral. The fundus was found to be normal in 623 left eyes (32.7%) and 593 right eyes (31.1%). The types of AMD and the severity of DR are shown in Table 4.

Among the AMD patients, dry AMD was the commonest type (79.2%), followed by wet AMD (15.9%), retinal pigment epithelium (RPE) change (4%), and familial drusen (0.9%). In contrast to the results of all patients (Fig. 1), there was no statistical difference in the number of male (122) and female (100) AMD patients. The male and female AMD patients also did not differ significantly in age: male 71.0 ± 9.48 years, female 68.8 ± 10.3 years (mean $\pm$ SD years). Among these patients, 81.7% of the AMD was bilateral and 18.3% unilateral. As might be expected, patients with unilateral disease were significantly younger than those with bilateral disease: 67.0 ± 13.1 cf. 70.7 ± 8.93 years ($P = 0.031$, t test).

In part because of the higher rate of smoking by male in Nepal (32.8% among male cf. 15.8% among female),[24] we decided to examine wet AMD eyes relative to fellow eyes. 2 patients had familial bilateral drusen, and for this analysis they were classed as having dry AMD. 4 patients had nonvisible fundus (mainly due to cataract) and were eliminated from the analysis. The age of male whose worst eye had wet AMD was not different from female: 66.0 ± 15.3 versus 65.8 ± 13.7 years. There were 40 males whose worst eye had wet AMD, versus 15 females, which was marginally significant ($P = 0.063$, t test, correcting for the relative abundance of males in the study population). Interestingly, patients whose worst eye had dry AMD were older than those with a worst eye having wet AMD [69.5 ± 14.8 versus 65.9 ± 10.5 years ($P = 0.045$)]. Overall, there was a suggestion that males develop wet AMD earlier, and in relatively greater numbers compared with females. This might have been an effect of smoking, but further investigation is needed.

We also examined severity and laterality by scoring normal fundus to wet AMD on a scale of 1 to 3 (normal, dry, wet) and then

© 2019 Asia-Pacific Academy of Ophthalmology.

TABLE 3. Diseases Involving Retina

	Right Eye			Left Eye		
Diagnosis	**N**	**% Across Retinal Diseases**	**% Across All Diseases**	**N**	**% Across Retinal Diseases**	**% Across All Diseases**
AMD	223	13.5	11.7	224	13.6	11.8
Diabetic retinopathy	208	12.6	10.9	208	12.6	10.9
Retinal detachment	112	6.8	5.9	126	7.6	6.6
BRVO	80	4.8	4.2	70	4.2	3.7
Myopic degeneration	63	3.8	3.3	54	3.3	2.8
Retinitis pigmentosa	56	3.4	2.9	57	3.5	3
Hypertensive retinopathy	45	2.7	2.4	42	2.5	2.2
CSCR	44	2.7	2.3	33	2	1.7
CRVO	33	2	1.7	32	1.9	1.7
Macular scar	31	1.9	1.6	22	1.3	1.2
Macular hole	30	1.8	1.6	25	1.5	1.3
Retinal vasculitis	23	1.4	1.2	23	1.4	1.2
Chorio-retinal scar	22	1.3	1.2	20	1.2	1
Epiretinal membrane	20	1.2	1	19	1.2	1
Macular dystrophy	16	1	0.8	15	0.9	0.8
Irido-chorio-retinal coloboma	15	0.9	0.8	18	1.1	0.9
Retinal break	13	0.8	0.7	12	0.7	0.6
Status post RD surgery	9	0.5	0.5	4	0.2	0.2
Central retinal artery occlusion	8	0.5	0.4	5	0.3	0.3
Stargardt disease	5	0.3	0.3	8	0.5	0.5
Retinal hemorrhage	4	0.2	0.2	10	0.6	0.5
Cone dystrophy	3	0.2	0.2	3	0.2	0.2
Normal fundus	593	35.8	31.1	622	37.7	32.6
Total	1656	100.1	86.9	1652	100	86.7

AMD indicates macular degeneration; BRVO, branch retinal vein occlusion; CRVO, central retinal vein occlusion; CSCR, central serous chorioretinopathy; RD, retinal detachment.

examining the absolute value of the difference in scores between eyes. 6 patients had bilateral wet AMD OU. For the 186 patients whose best eye had dry AMD, only 30 had a worst eye with wet AMD. Patients whose best eye was normal were even more heterogeneous. Of those 36 patients, 17 had a fellow eye that was dry, and 19 had a fellow eye that was wet. Thus, the pattern of progression seemed to follow relative heterogeneity earlier, progressing to more bilateral disease later, rather than simple bilateral disease at each stage.

Among DR eyes, moderate nonproliferative DR (NPDR) was the commonest (34.6%), followed by severe NPDR (26.2%), proliferative diabetic retinopathy (PDR) (25.2%), and mild NPDR (13.9%). A total of 230 eyes had clinically significant macular edema (CSME): 50.9% involving left eyes and 49.1% right eyes. Like the AMD patients, the DR group contained more males (123) than females (91), but this was not significant. Their ages also did not differ at 58.7 ± 9.91 years for males, and 58.3 ± 11.21 years for females. Their durations of diabetes did not differ at 11.5 ± 6.79 and 10.4 ± 6.96 years, respectively. 9 patients had a nonvisible fundus in 1 eye and were removed from further analysis. We examined the laterality of DR in the remaining 205 patients.

We scored the 5 DR diagnostic-categories/severities from normal fundus to PDR as 1 to 5. As with AMD, the pattern of progression seemed to follow relative heterogeneity earlier, progressing to more bilateral disease later. As with AMD, we then binned subjects according to the diagnosis in their least affected eye. To quantify the degree of laterality, we took the absolute value of the difference of these severity steps in each pair of eyes. A box plot of the results is shown in Figure 4A. Basically, as with AMD, eyes tended to become more similar as severity of the best

TABLE 4. Types of AMD and Severity of DR

	Right Eye		Left Eye		Total	
AMD	**N**	**%**	**N**	**%**	**N**	**%**
Dry	175	78.5	179	79.9	354	79.2
Wet	37	16.6	34	15.2	71	15.9
RPE change	9	4	9	4	18	4
Familial drusen	2	0.9	2	0.9	4	0.9
Total	223	100	224	100	447	100
DR						
Mild NPDR	33	15.9	25	12	58	13.9
Moderate NPDR	68	32.7	76	36.5	144	34.6
Severe NPDR	57	27.4	52	25	109	26.2
PDR	50	24	55	26.4	105	25.2
Total	208	100	208	100	416	100

AMD indicates macular degeneration; DR, diabetic retinopathy; NPDR, nonproliferative diabetic retinopathy; RPE, retinal pigment epithelium; PDR, proliferative diabetic retinopathy.

© 2019 Asia-Pacific Academy of Ophthalmology.

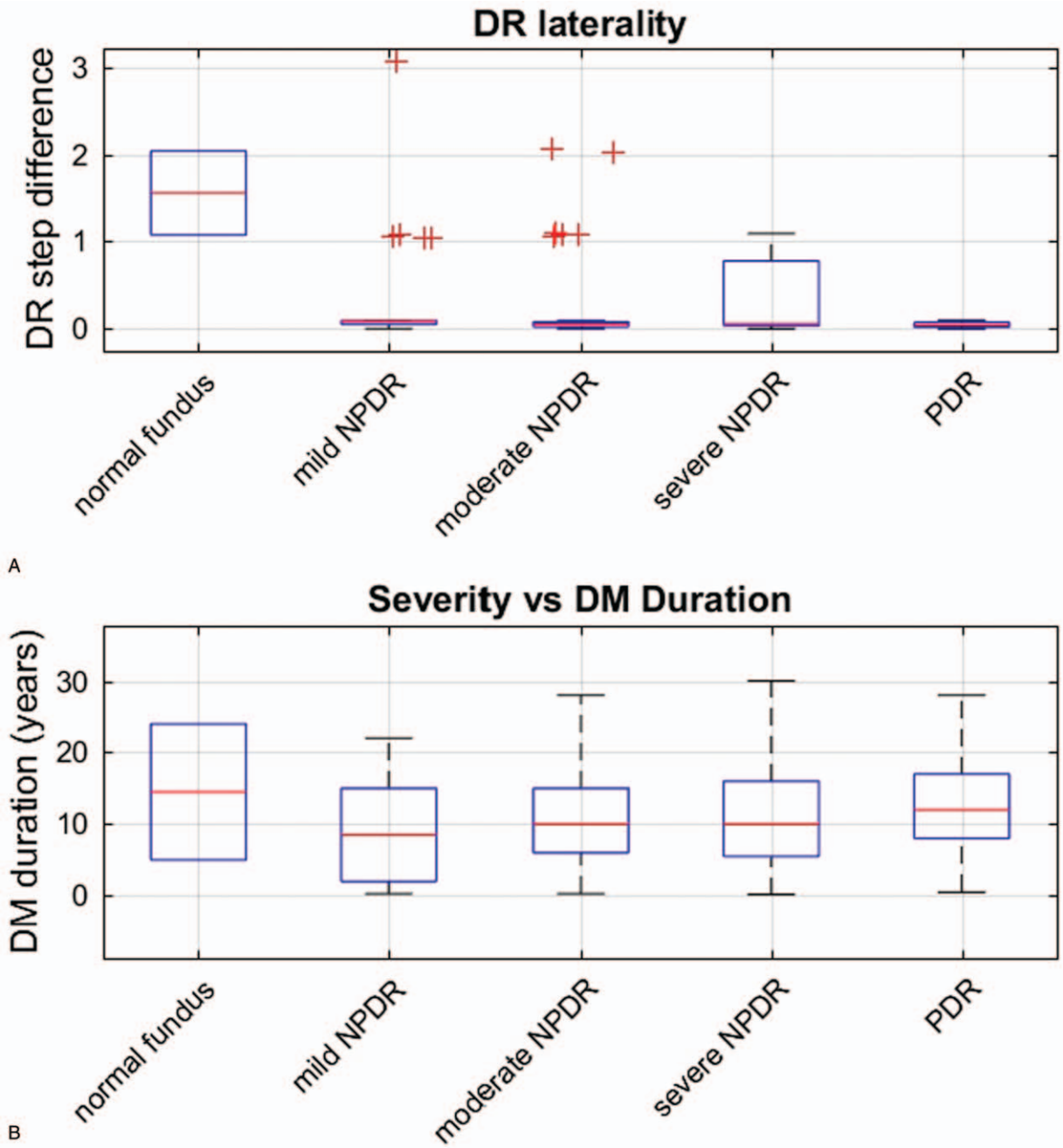

FIGURE 4. DR laterality and DM duration. Laterality and duration disease grouped by the 205 DR patients' better eye (abscissa). A, The absolute value of the difference between DR-severity steps in the 2 eyes when the severity levels (normal to PDR) are scored as 1 to 5. Generally the DR became more bilaterally symmetric. A small amount of uniformly distributed noise (0–0.03) was added to the data to make the outliers more distinct (red+). B, Diabetes duration as a function of the best eye. Duration did not seem to strongly determine severity. DM indicates diabetes mellitus; DR, diabetic retinopathy; NPDR, nonproliferative DR; PDR, proliferative diabetic retinopathy.

eye increased. As shown in Figure 4B, severity of DR was not correlated with duration of disease.

DISCUSSION

The visual handicap experienced by individuals suffering from unilateral eye disease, such as macular hole, is reported to be strongly influenced by ocular dominance.[25] Ocular-dominance and handedness are associated, with about 65% of right-handers, and 43% of left-handers, being right eye-dominant.[26] Some of our data (Fig. 3) suggested that eye dominance played a role in patients reporting to the hospital, with the predominantly right-handed subjects only reporting that their right eye had BCVA worse than 6/18 once. This type of asymmetry has been reported before.[25] AMD and DR were very homogenous with respect to age and sex; however, when the best eye was normal, the range of severity in the fellow eye was surprisingly broad (eg, Fig. 4). Taking together the results might mean that if their nondominant eye is affected, then patients tended not to notice their sight threatening disease, indicating an excellent argument for more screening. Given the subjects only reporting (Fig. 3), we subsequently analyzed other data by eye (Tables 3 and 4, and Supplemental Digital Content 1, Table S4, http://links.lww.com/APJO/A56) to elucidate any eye-wise biases; however, few were found.

© 2019 Asia-Pacific Academy of Ophthalmology.

The preponderance of males in the total group was 60.3%, and for subgroup of AMD and DR patients combined it was 56.5%, marginally more than for females ($P = 0.052$). This agrees with the findings of some hospital-based studies on VR diseases,[9,27] but differs from a Nepalese population-based study from the same era, in which only 45.5% were male,[20] and 1 in India with only 45% male.[1] Our results could be due to women being reserved due to social norms and therefore not coming forward for medical check-ups. Here the 25th percentile of ages reporting was nearly 10 years higher for female ($P < 0.0001$, t test 9.27 years; 95% confidence level (CL) 6.05 and 12.5 years). The mean and median ages of male and female (49 years and 54 years, respectively) tally well with other studies of VR diseases.[1,9] Reported ages ranged from 2 months to 116 years.

Only 41 cases (2.2%) presented for routine check-up. Chronic retinal diseases like AMD, DR, RD, RVO, RP, and so on, ranked high in the diagnostic list, but only 2.2% of cases were found to present for routine check-up, indicating that there is a need to emphasize patient education and counseling about the importance of regular check-ups and follow-ups.

A total of 565 cases (30.5%) presented within a month, 507 cases (27.1%) between 1 to 6 months, 280 cases (15.1%) between 6 to 12 months, and 500 cases (27.0%) presented after 12 months from the onset of the symptoms. The delayed presentation time might be because of illiteracy and ignorance (the overall literacy rate of Nepal for population aged 5 years and above was 65.9% in 2011, 75.1% for male and 57.4% for female).[28] Remote areas and associated poor accessibility to modern medical services encourage people initially to rely on traditional methods of healing.

Systemic disease association was not found in 1292 of the 1905 cases. As shown in Fig. 2 (and Supplemental Digital Content 1, Table S2, http://links.lww.com/APJO/A56), among the 613 remaining cases, the commonest associated diseases were hypertension (40.8%), diabetes (32.5%), and both (20.2%). This agrees with the Tehran eye study which reported hypertension (21.14%), followed by diabetes (15.99%).[2] By contrast, a Nigerian study found diabetes to be more common (14.6%) than hypertension (13.2%).[27] Other systemic diseases were found in 40 of our cases (6.5%, Supplemental Digital Content 1, Table S2, http://links.lww.com/APJO/A56). The duration of systemic disease association was <5 years in 210 cases (42.8%), 5 to 10 years in 163 cases (33.2%), and >10 years in 118 cases (24.0%).

The commonest VR disease was AMD affecting 11.8%, followed by DR at 10.9%; matching another Nepalese study which reported that AMD was the commonest VR disease at 28.3%, followed by DR at 17.9%.[20] This does not match with a Nigerian hospital study, which reported DR (24.9%) as the commonest VR disease, followed by hypertensive retinopathy (13.3%) and AMD (10.7%).[27] In our case, 208 of 324 (64.2%) confirmed diabetic cases had some form of DR, which did not tally with population-based studies (10.5%).[1] In our study, 117 left eyes and 113 right eyes of 323 patients had CSME but a population-based study in Nepal found it in only 2 of 305 diabetic cases.[20] This disparity could be explained by the early onset of macular edema causing a high percentage of CSME patients presenting to the TIO.

RD was the third commonest VR disease in our study, affecting 112 right eyes (5.9%) and 126 left eyes (6.6%), whereas a Nepalese population-based study reported population prevalence of 0.10%.[20] A hospital-based study in Ethiopia reported RD as the second commonest VR disease at 24.5%.[9] Of 65 cases of full-thickness macular hole in our study, 33 cases (50.8%) affected right eyes, whereas others have reported 48% of right eyes affected.[25] In our study, 94.8% of the full-thickness macular hole and 84.6% of the lamellar macular hole were unilateral, which are similarly reported in other studies, and are basically the consequence of factors affecting the macula locally.[25] When such unilateral macular diseases affect the dominant eyes of the individuals, they cause greater functional visual impairment.[25]

In eastern Asia, pathological myopia is a major issue found in 80% to 90% of school-leavers, and 10% to 20% of those completing secondary school,[29] and contributes to RD numbers. The prevalence of myopia varies from 0.8% to 53.4%, depending on geographical area, age, occupation, and ethnicity.[30–32] In Nepal, Sherpa children had a prevalence of 2.9% as compared with 21.7% for Tibetan children.[33] A myriad of myopic complications like atrophic retinal holes and RD, choroidal neovascular membranes, degeneration, cataract, and glaucoma, cause visual loss warranting attention.[34] Thapa et al[20] reported the population prevalence of macular hole as 0.20% in Nepal. Asymptomatic macular holes occur at a prevalence of 6.26% among high myopes with >-20 diopters.[35]

Limitations

19 patients were excluded due to incomplete data. AMD was not classified as per the Age-Related Eye Disease Study (AREDS) classification system. Only the final diagnoses, but not ocular comorbidities, have been considered for analysis, which might have altered the reported disease patterns. The ocular dominance and handedness were not recorded in the case records of the study population, but based on the literature reviewed and cited above, we speculated that if only the nondominant eye was affected, this might cause the patients to present late. In future studies it would be valuable to record the dominant eye. Similarly, the reviewed medical records of the diabetic patients under study did not differentiate the type of diabetes, which we will consider in follow-up studies.

CONCLUSIONS

We found that without screening programs, patients often fail to notice developing visual impairment until the disease progresses to advanced stage, especially in their nondominant eye. In Nepal, and perhaps in similar countries, females report later for care than men. That was true from childbearing age, so education and screening could be usefully coupled for reproductive health programs. This study indicates that low-cost screening and management programs for retinal disease could be of immense value in developing countries. The high prevalence of hypertension and diabetes among retinal disease patients suggest that a simple screening of blood pressure and glucose levels combined with fundus photography could prevent many from progressing to life-changing visual impairment and blindness. We recommend that coordinating with other established health programs would provide economical and sustainable screening methods such as diabetes control program for screening DR, hypertension clinics for screening hypertensive retinopathy, reproductive health program for VR diseases affecting female of childbearing age, comprehensive school health program for pathological myopia and hereditary diseases among school children, and counseling

© 2019 Asia-Pacific Academy of Ophthalmology.

and rehabilitation centers for counseling people affected with permanent visual impairment or blindness, and other hereditary diseases.

REFERENCES

1. Nirmalan PK, Katz J, Robin AL, et al. Prevalence of vitreoretinal disorders in a rural population of southern India: the Aravind Comprehensive Eye Study. *Arch Ophthalmol*. 2004;122:581–586.
2. Hatef E, Fotouhi A, Hashemi H, et al. Prevalence of retinal diseases and their pattern in Tehran: the Tehran eye study. *Retina*. 2008;28:755–762.
3. Brilliant GE, Pokhrel RP, Grasset NC, et al. The Epidemiology of blindness in Nepal: report of the 1981 Nepal Blindness survey Nepal; 1981.
4. Thapa SS, Berg RV, Khanal S, et al. Prevalence of visual impairment, cataract surgery and awareness of cataract and glaucoma in Bhaktapur district of Nepal: The Bhaktapur Glaucoma Study. *BMC Ophthalmology*. 2011;11:2.
5. Lepcha NT, Chettri CK, Getshen K, et al. Rapid assessment of avoidable blindness in Bhutan. *Ophthal Epidemiol*. 2013;20:212–219.
6. Wadud Z, Kuper H, Polack S, et al. Rapid assessment of avoidable blindness and needs assessment of cataract surgical services in Satkhira District, Bangladesh. *Br J Ophthalmol*. 2006;90:1225–1229.
7. Dandona L, Dandona R, Naduvilath TJ, et al. Is current eye-care-policy focus almost exclusively on cataract adequate to deal with blindness in India? *Lancet*. 1998;351:1312–1316.
8. Nwosu SN. Prevalence and pattern of retinal diseases at the Guinness Eye Hospital, Onitsha, Nigeria. *Ophthal Epidemiol*. 2000;7:41–48.
9. Teshome T, Melaku S, Bayu S. Pattern of retinal diseases at a teaching eye department, Addis Ababa, Ethiopia. *Ethiop Med J*. 2004;42:185–193.
10. Smith W, Assink J, Klein R, et al. Risk factors for age-related macular degeneration: Pooled findings from three continents. *Ophthalmology*. 2001;108:697–704.
11. Mitchell P, Bressler N, Doan QV, et al. Estimated Cases of Blindness and Visual Impairment from Neovascular Age-Related Macular Degeneration Avoided in Australia by Ranibizumab Treatment. *PLoS One*. 2014;9:e101072.
12. Ratnapriya R, Chew EY. Age-related macular degeneration—clinical review and genetics update. *Clin Genet*. 2013;84:160–166.
13. Owen CG, Jarrar Z, Wormald R, et al. The estimated prevalence and incidence of late stage age related macular degeneration in the UK. *Br J Ophthalmol*. 2012;96:752–756.
14. Zheng Y, He M, Congdon N. The worldwide epidemic of diabetic retinopathy. *Indian J Ophthalmol*. 2012;60:428–431.
15. Zhang X, Saaddine JB, Chou CF, et al. Prevalence of diabetic retinopathy in the United States, 2005–2008. *JAMA*. 2010;304:649–656.
16. Yau JW, Rogers SL, Kawasaki R, et al. Global prevalence and major risk factors of diabetic retinopathy. *Diabetes Care*. 2012;35:556–564.
17. Wang FH, Liang YB, Zhang F, et al. Prevalence of diabetic retinopathy in rural China: the Handan Eye Study. *Ophthalmology*. 2009;116:461–467.
18. Gadkari SS, Maskati QB, Nayak BK. Prevalence of diabetic retinopathy in India: The All India Ophthalmological Society Diabetic Retinopathy Eye Screening Study 2014. *Indian J Ophthalmol*. 2016;64:38–44.
19. Raman R, Ganesan S, Pal SS, et al. Prevalence and risk factors for diabetic retinopathy in rural India. Sankara Nethralaya Diabetic Retinopathy Epidemiology and Molecular Genetic Study III (SN-DREAMS III), report no 2. *BMJ Open Diabetes Res Care*. 2014;2. e000005.
20. Thapa SS, Thapa R, Paudyal I, et al. Prevalence and pattern of vitreo-retinal diseases in Nepal: the Bhaktapur glaucoma study. *BMC Ophthalmol*. 2013;13:9.
21. Downie LE, Hodgson LA, Dsylva C, et al. Hypertensive retinopathy: comparing the Keith-Wagener-Barker to a simplified classification. *J Hypertens*. 2013;31:960–965.
22. Wu L, Fernandez-Loaiza P, Sauma J, et al. Classification of diabetic retinopathy and diabetic macular edema. *World J Diabetes*. 2013;4:290–294.
23. Efron B. Bootstrap methods: another look at the jackknife. *Ann Statist*. 1979;1:1–26.
24. Sreeramareddy CT, Ramakrishnareddy N, Harsha Kumar H, et al. Prevalence, distribution and correlates of tobacco smoking and chewing in Nepal: a secondary data analysis of Nepal Demographic and Health Survey-2006. *Subst Abuse Treat*. 2011;6:33.
25. Waheed K, Laidlaw DAH. Disease laterality, eye dominance, and visual handicap in patients with unilateral full thickness macular holes. *Br J Ophthalmol*. 2003;87:626–628.
26. McManus IC, Porac C, Bryden MP, et al. Eye-dominance, writing hand, and throwing hand. *Laterality*. 1999;4:173–192.
27. Eze BI, Uche JN, Shiweobi JO. The burden and spectrum of vitreo-retinal diseases among ophthalmic outpatients in a resource-deficient tertiary eye care setting in South-Eastern Nigeria. *Middle East Afr J Ophthalmol*. 2010;17:246–249.
28. NPHC. National Population and Housing Census 2011 (National Report). In: Commission, N.P., editor. Kathmandu, Nepal 2012.
29. Morgan IG, Ohno-Matsui K, Saw SM. Myopia. *Lancet*. 2012;379:1739–1748.
30. Saw SM, Katz J, Schein OD, et al. Epidemiology of myopia. *Epidemiol Rev*. 1996;18:175–187.
31. Nepal BP, Koirala S, Adhikary S, et al. Ocular morbidity in schoolchildren in Kathmandu. *Br J Ophthalmol*. 2003;87:531–534.
32. Adhikari S, Nepal BP, Shrestha JK, et al. Magnitude and determinants of refractive error among school children of two districts of Kathmandu, Nepal. *Oman J Ophthalmol*. 2013;6:175–178.
33. Garner LF, Owens H, Kinnear RF, et al. Prevalence of myopia in Sherpa and Tibetan children in Nepal. *Optom Vis Sci*. 1999;76:282–285.
34. Tano Y. Pathologic myopia: where are we now? *Am J Ophthalmol*. 2002;134:645–660.
35. Coppé AM, Ripandelli G, Parisi V, et al. Prevalence of asymptomatic macular holes in highly myopic eyes. *Ophthalmology*. 2005;112:2103–2109.

© 2019 Asia-Pacific Academy of Ophthalmology.

Pattern and presentation of vitreo-retinal diseases: an analysis of retrospective data at a tertiary eye care centre in Nepal

Bhim B. Rai,[1] Mohan K. Shresthra,[2] Raba Thapa,[2] Rohan W. Essex,[3] Govinda Paudyal,[2] and Ted Maddess[1]

[1]John Curtin School of Medical Research, Australian National University, ACT, Australia.

[2]Tilganga Institute of Ophthalmology, Kathmandu, Nepal.

[3]ANU Academic Unit of Ophthalmology, ANU Medical School; Department of Ophthalmology, Canberra Hospital, ACT Health, Australia.

Corresponding Author

Dr. Bhim Bahadur Rai

Neuroscience, John Curtin School of Medical Research, ANU,

Canberra, ACT 2607.

bhim.rai@anu.edu.au

Mobile number: +61 431520440

Table S1 Symptom onset-Presentation interval (months)

Duration of symptoms	Frequency	Valid Percent
0 – 1	565	30.5
> 1 – 6	507	27.4
> 6 – 12	280	15.1
> 12	500	27.0
Total	**1852**	**100.0**
Data not found	53	
	1905	

Table S2 Systemic diseases associated

Diseases	Frequency	Percent
Hypertension (HT)	250	40.8
Diabetes (DM)	199	32.5
DM + HT	124	20.2
Asthma / COPD	15	2.4
Chronic renal failure	6	1
Tuberculosis	6	1
Hepatitis B	4	0.7
Leukemia	4	0.7
Arthritis	3	0.5
Brain tumor	2	0.3
HIV / AIDS	2	0.3
Others*	8	1.3
Total	**613**	**100**
Not found	1292	
	1905	

*Others included malaria, filariasis, thyroiditis, cardiac disease, Parkinson's disease, preterm baby, connective tissue disorder.

Table S3 Prior interventions (surgical/Laser)

Intervention	Frequency	Percent
No Intervention	1769	92.9
Cataract surgery	55	2.9
VR surgery	27	1.5
Retinal laser	27	1.5
Primary repair: Corneo-scleral and eyelids	20	1
Intravitreal Avastin	2	0.2
Anterior chamber wash	2	0.2
Glaucoma surgery	1	0.1
Retrobulbar Methyl-prednisolone	1	0.1
Retinal laser + Inj. Avastin	1	0.1
Total	1905	100

Table S4 Diagnostic procedures

Diagnostic tests	Frequency	Percent
Hematological tests	584	23.1
Optical Coherence Tomography	516	20.4
B-scan	436	17.2
Fundus Fluorescence Angiography	89	3.5
Visual field	39	1.5
Chest X-ray	36	1.4
Mantoux test	30	1.2
Electroretinogram	25	1.0
Colour vision	14	.6
CT scan head & orbit	14	.6
Vitreous culture/sensitivity	12	.5
Biometry	10	.4
A-scan	8	.3
Examination Under Aaesthesia	7	.3
Visual Evoked Potential	5	.2
Others	7	.3
No investigation	687	27.1
Total test frequency	**2532**	**100.0**

Table S5 Diseases involving posterior segment other than retina

	Right Eye			Left Eye		
Diagnosis	N	Percent across non-retinal diseases	Percent across all diseases	N	Percent across non-retinal diseases	Percent across all diseases
Posterior vitreous degeneration	44	17.7	2.3	35	14.1	1.8
Endophthalmitis	27	10.8	1.5	24	9.6	1.2
Optic atrophy	26	10.4	1.4	25	10	1.3
Vitreous degeneration	23	9.2	1.2	25	10	1.3
Asteroid hyaloisis	13	5.2	0.7	13	5.2	0.7
Close-Globe Injuries	12	4.8	0.6	10	4	0.6
Choroidal involvement	10	4	0.5	10	4	0.6
Dislocated cataract	10	4	0.5	14	5.5	0.8
Optic disc involvement	10	4	0.5	14	5.6	0.7
Open globe injury	9	3.6	0.5	8	3.2	0.4
Phthisis/Atrophic/Absolute	8	3.2	0.4	16	6.4	0.8
No fundal view	7	2.8	0.4	6	2.4	0.3
Glaucomatous optic atrophy	5	2	0.3	3	1.2	0.2
RIOFB	4	1.6	0.2	7	2.8	0.4
Dislocated IOL in vitreous	3	1.2	0.2	7	2.8	0.4
Others	38	15.3	1.9	36	14.5	1.8
Total	**249**	**99.8**	**13.1**	**253**	**101.3**	**13.3**

Rai *et al. BMC Ophthalmology* (2020) 20:51
https://doi.org/10.1186/s12886-020-01335-x

BMC Ophthalmology

RESEARCH ARTICLE Open Access

Pattern of vitreo-retinal diseases at the national referral hospital in Bhutan: a retrospective, hospital-based study

Bhim B. Rai[1,2*], Michael G. Morley[3], Paul S. Bernstein[4] and Ted Maddess[1]

Abstract

Background: Knowing the pattern and presentation of the diseases is critical for management strategies. To inform eye-care policy we quantified the pattern of vitreo-retinal (VR) diseases presenting at the national referral hospital in Bhutan.

Methods: We reviewed all new patients over three years from the retinal clinic of the Jigme Dorji Wangchuck National Referral Hospital. Demographic data, presenting complaints and duration, treatment history, associated systemic diseases, diagnostic procedures performed, and final diagnoses were quantified. Comparisons of the expected and observed frequency of gender used Chi-squared tests. We applied a sampling with replacement based bootstrap analysis (10,000 cycles) to estimate the population means and the standard errors of the means and standard error of the 10th, 25th, 50th, 75th and 90th percentiles of the ages of the males and females within 20-year cohorts. We then applied t-tests employing the estimated means and standard errors. The 2913 subjects insured that the bootstrap estimates were statistically conservative.

Results: The 2913 new cases were aged 47.2 ± 21.8 years. 1544 (53.0%) were males. Housewives (953, 32.7%) and farmers (648, 22.2%) were the commonest occupations. Poor vision (41.9%), screening for diabetic and hypertensive retinopathy (13.1%), referral (9.7%), sudden vision loss (9.3%), and trauma (8.0%) were the commonest presenting symptoms. Coexistent diabetes and hypertension were the most common associated systemic diseases. Haematological tests (blood sugar, HbA1c and lipid profile, 31.8%), OCT (27.4%), refraction (9.9%), B-scan (8.7%), fundus photography (8.0%) were the most commonly performed diagnostic tests. Hypertensive retinopathy (18.9%) was the commonest VR disease, followed by refractive errors referred for retinal evaluation (16.7%), diabetic retinopathy with macular oedema (15.8%), and AMD (11.0%). Retinal detachment was more prevalent in females (83 vs. 41, $p = 0.007$). Rare vision-threatening diseases like seasonal hyper-acute pan-uveitis also presented.

Conclusions: The developing VR service in Bhutan is challenged by the spectrum of diseases, limited human resources (e.g. one retinal surgeon during the study), and accessibility to tertiary eye-care services, all amidst difficult terrain. Sustained effort and robust coordination among the eye-care professionals, government and non-governmental organisations are critical for optimising VR services, especially as rates of diseases such as diabetes and hypertension grow.

Keywords: AMD, Blindness, Diabetic macular oedema, Diabetic retinopathy, Pattern and presentation, Retinal diseases, SHAPU

* Correspondence: bhim.rai@anu.edu.au
[1]John Curtin School of Medical Research, Australian National University, Canberra, ACT 2601, Australia
[2]Department of Ophthalmology, JDW National Referral Hospital, Thimphu, Bhutan
Full list of author information is available at the end of the article

© The Author(s). 2020 **Open Access** This article is distributed under the terms of the Creative Commons Attribution 4.0 International License (http://creativecommons.org/licenses/by/4.0/), which permits unrestricted use, distribution, and reproduction in any medium, provided you give appropriate credit to the original author(s) and the source, provide a link to the Creative Commons license, and indicate if changes were made. The Creative Commons Public Domain Dedication waiver (http://creativecommons.org/publicdomain/zero/1.0/) applies to the data made available in this article, unless otherwise stated.

Background

Bhutan has 73% of its land under forest cover and its terrain can be challenging. At the same time legislation does not permit the import of used vehicles or machinery, so aspects of Bhutan's infrastructure can be modern. Taken together Bhutan's fairly unique aspects have implications for the health of its population of 735,553 [1]. Here we concentrate on VR diseases.

Traditional healing methods were predominant in Bhutan until the 1960s [2]. A hierarchical system of healthcare centres is now established in the country: basic health units (BHU) equipped with X-Ray facilities at the village or block level, district hospitals at district level, and regional referral hospitals in each of the eastern, central and western regions. At each level there is emphasis on health advocacy to the public and collaboration among departments [2]. The first national ophthalmologist, Dr. Kunzang Getshen joined the civil service in 1987 and is honoured as the *Father of Ophthalmology* in Bhutan. Eye-care services improved rapidly under his leadership.

The Rapid Assessment of Avoidable Blindness (RAAB) survey conducted in 2009 and 2018 respectively reported 22.1% [3] and 7.7% [4] of visual impairment and blindness in Bhutan was due to posterior segment pathologies among the population aged ≥50 years. There has, however, never been a study conducted on the pattern of VR diseases in Bhutan. Within the region, a population-based study in India reported the overall prevalence of VR disorders to be 8.56% among the population aged 40 years and above [5]. The 1981 Nepal Blindness Survey reported VR disorders as the third leading cause of bilateral blindness, second only to cataract and its complications [6]. A population-based study in Nepal in 2013 reported VR disorders to be the second commonest cause of bilateral blindness, second only to cataract, and the most common cause among pseudophakics [7]. A more recent population-based study in Nepal reported that retinal disorders as the second most common cause of bilateral low vision, and the most common cause for blindness [8]. A RAAB survey in Bangladesh reported VR disease as the second leading cause of bilateral blindness [9].

Knowing the disease pattern and prevalence is important for planning national strategies and formulating action plans to control blindness effectively. The current study of 2913 cases was conducted to better understand the pattern and presentation of VR diseases presenting at the apex national referral hospital, and to provide baseline data for formulating action plans to control VR diseases in the country. The study has implications for other developing countries.

Methods

Study design

This was a retrospective cross-sectional case series study; approved by the Research Ethics Board of Health (REBH), Ministry of Health, Royal Government of Bhutan, Thimphu, Bhutan, and adhered to the principle of Declaration of Helsinki. The consent was waived by REBH because this retrospective study collected only the de-identified data.

Setting

The Jigme Dorji Wangchuck National Referral Hospital (JDWNRH) is the apex national referral hospital located in Thimphu, the capital city. It provides subspeciality services in Cornea and anterior segment, Paediatric ophthalmology and strabismus, Glaucoma, Oculoplasty, Vitreo-retina. Currently, every BHU and district hospital provides primary eye-care services administered by ophthalmic technicians or optometrists. The regional referral hospitals are manned by teams of ophthalmologists, optometrists and ophthalmic nurses. The VR services in the country are provided only at the JDWNRH. All the VR patients across the country are referred to JDWNRH for management. Therefore, the pattern and presentation of the VR diseases at this hospital represents the VR diseases from the entire citizenry. JDWNRH also serves as the main clinical centre for the postgraduate medical students, interns and optometric and paramedic students. The current study was conducted at the VR Subspeciality Clinic (VRSC), Ophthalmology Department, JDWNRH, Thimphu, Bhutan.

Participants

All new patients presenting to the VRSC over 3 years (01 May 2013 until 30 April 2016) were included in this study.

Clinical examination and data collection

The data collected included the demographic information, presenting complaints and their duration, medical or surgical treatments received before presenting to the VRSC, and associated systemic diseases with their durations. Best corrected visual acuity (BCVA) at presentation was measured using a Snellen chart: Tumbling E for illiterate patients or the Sheridan Gardeners 3 m vision chart for children. Intraocular pressure was measured by Goldmann applanation tonometry or an iCare tonometer, and the anterior and posterior segments were examined under slit-lamp biomicroscopy (BM 900, Haag-Streit, Switzerland) and 90D bio-microscopy. The funduscopic findings were confirmed by binocular indirect ophthalmoscope (Model 125, Welch Allyn, USA). Macular and retinal nerve fibre (RNFL) scans were measured using a Spectral Domain OCT (Cirrus-HD 4000, Carl Zeiss Germany). Fundus photographs were taken by a VISUCAM-524 (Carl Zeiss, Germany). In case of children, the diagnoses were confirmed by examination under anaesthesia (EUA) if necessary, following a proper pre-anaesthetic check-up (PAC).

Hypertensive retinopathy (HTR) was graded using the Keith-Wagener-Barker classification system [10]. Diabetic retinopathy (DR) was classified as per the modified Airlie House or Abbreviated ETDRS classification [11]. Clinically significant macular oedema (CSMO) was defined as: 1) retinal oedema at or within 500 μm of the centre of the macula; 2) hard exudates at or within 500 μm of the centre of the macula if associated with retinal thickening (including outside 500 μm); 3) retinal thickening of one disc diameter (1500 μm) or larger, any part of which is within one disc diameter of the centre of the macula [12]. Age-related macular degeneration (AMD) was classified by the clinical Classification of Age-related Macular Degeneration method [13]. Screening for retinopathy of prematurity (ROP) was done for infants born at gestational age ≤ 32 weeks and birth weight ≤ 1500 g, and those who were given oxygen therapy in the neonatal period [14].

Statistical analysis

The data were analysed using MATLAB (2016b, The MathWorks, Natick, MA). Comparisons of the expected and observed frequency of gender used Chi-squared tests. We applied a sampling with replacement based bootstrap analysis [15] to estimate the population means and the standard errors of the means and SE of the 10th, 25th, 50th, 75th and 90th percentiles of the ages of the males and females within 20-year cohorts (Fig. 1a), and the whole cohort (Fig. 1b). We employed 10,000 bootstrap cycles to insure the estimated means and SE converged to within 2 decimal places on 5 independent cross-validations. We then applied t-tests employing the estimated means and SE. The 2913 subjects insured that the bootstrap estimates were statistically conservative.

Results

We saw 2913 new cases at the VRSC during the study period, and 1544 (53.0%) were males. The mean age was 47.21 ± 21.8 years (range 20 days to 91 years). Among the 1369 female patients the mean age was 45.7 ± 21.9 years with median age of 49 years, while among male patients the mean age was 48.6 ± 21.6 years with median age of 51 years. One thousand eight hundred forty-five cases (63.3%) were from urban areas, and only 1068 cases (36.7%) were from the rural settings.

The breakdown of occupation and education is given in Table 1, and the reported reasons for seeking a consultancy is given in Table 2.

Two hundred thirty-two cases (8.0%) reported with trauma, mainly with wooden sticks, farming tools, falls, animal-related injuries, road traffic accident (RTA), domestic assaults and fights. The mode of trauma is given in Table 3. There were four cases of retained intraocular foreign body (RIOFB), one of them also had RD secondary to RIOFB.

The interval between symptom onset and the presentation is shown in Fig. 2. Four hundred forty-five cases (18.4%) presented within 3 days of the onset of the

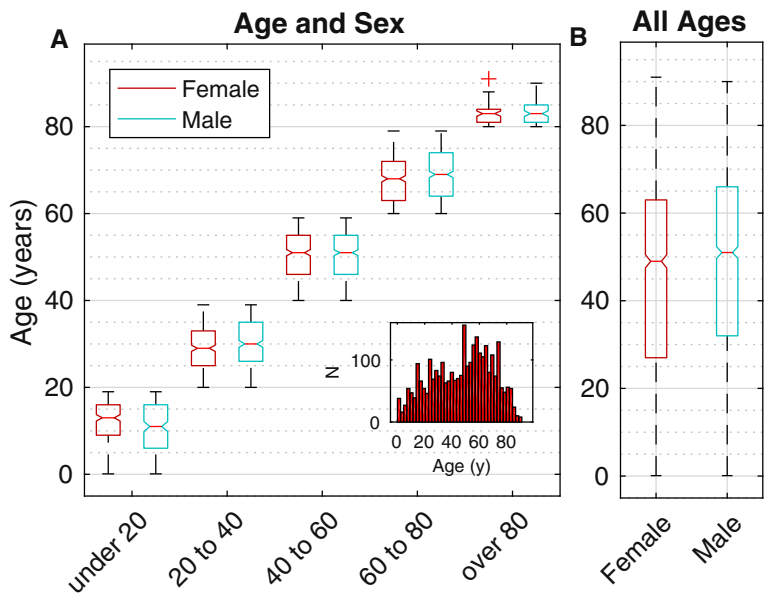

Fig. 1 Age and Sex Boxplots. **a** Presenting ages of the 2913 patients in cohorts of 20 years. The boxes indicate 25th, 50th and 75th percentile of the age distributions. The red + represents a 91 year old female outlier. The inset shows a histogram of all the ages. A bootstrap analysis showed that overall the females presented significantly earlier than males in most cohorts. **b** In the overall distribution of ages females presented earlier than males at the 25th, 50th and 75th percentiles

Table 1 Breakdown of Occupation and Education distributions of patients

Occupation	Frequency	%	Education level	Frequency	Percentage
Housewife	953	32.7	Primary	570	19
Farmer	648	22.2	Graduate	363	12.5
Student	396	13.6	High School	350	12
Government employee	315	10.8	Postgraduate	86	3
Private sector employee	274	9.4	Intermediate	30	1
Religious personnel	136	4.7	Nursery	2	0.1
Retired personal	80	2.7	Did not attend modern school	1512	51.9
Corporate employee	41	1.4			
Others	70	2.4			
Total	2913	100	Total	2913	100

symptoms. 492 (20.3%) presented between 0.1 to 0.5 months, 727 cases (30.1%) presented between 0.5 to 2 months, 183 cases (7.8%) presented between 2 to 4 months, 141 cases (5.8%) presented between 4 to 12 months, and 430 cases (17.8%) presented after 12 months.

One thousand three hundred eighty cases (47.4%) had associated systemic diseases. Coexistent diabetes (DM) and hypertension (HT) was the commonest issue, found in 500 patients (35.9%), followed by HT in 473 cases (34.0%), and DM in 342 cases (24.6%) (Fig. 3). Note those percentages are of the systemic disease patients. Those percentages and those of the total population are given atop each column of Fig. 3. Brain tumours and other intracranial pathologies grouped together as intracranial space occupying lesion (ISOL) were diagnosed in 15 cases (1.1%). Chronic kidney disease (CKD) was seen in 8 patients (0.6%), and another 8 patients (0.6%) had rheumatic arthritis (RA) or rheumatoid heart disease (RHD). Seven patients (0.5%) had pulmonary tuberculosis (PTB). Other systemic diseases are detailed in Additional file 1: Table S1. The prevalence of coexistent DM and HT was 17.1% across all the patients in the study. The prevalence of other systemic diseases was 16.2% for HT, 11.7% for DM, 0.5% for ISOL, 0.3% for CKD, 0.3% for RA or RHD, 0.2% for PTB and 1.3% for other systemic diseases.

Table 2 Presenting symptoms

Presenting symptoms	Number of patients	% across symptoms
Poor vision	1222	41.9
Screening for diabetic & hypertensive retinopathy	381	13.1
Cases referred to retina clinic	282	9.7
Sudden loss of vision	271	9.3
Trauma	232	8
Vision not improving after cataract surgery	145	5
Floater	135	4.6
Headache	76	2.6
Discomfort eye	47	1.6
Flashes of light	30	1
Night blindness	23	0.8
Premature baby	13	0.4
Painful eye	11	0.4
Watering eye	9	0.3
Chloroquine treatment	6	0.2
White eye (leukocoria)	6	0.2
Others[a]	24	0.8
Total	2913	100

[a]Diplopia, proptosis, squint, black spot in visual field, foreign body sensation, Transient ischaemic attack, ENT surgery, Itching, Discharge, Fainting, Drooping eye lids

Table 3 Mode of Injury

Mode	Frequency	Percentage
Road Traffic Accident	21	9.1
Fall from height	19	8.2
Assault/fight	18	7.8
Wood/stick related	14	6
Sports/Recreation related	13	5.6
Stone	5	2.2
Blast injury (bottle/firecrackers)	5	2.2
Iron rod	4	1.7
Animal related	3	1.3
Electric wire	2	0.9
Hammer/Chisel injury	2	0.9
Others	8	3.4
Unknown	118	50.8
Total	232	100

We analysed the management interventions done before the patients presented to the VRSC. Cataract surgery with intraocular lens implantation was the commonest intervention done in 146 cases (50.3% across all interventions). Retinal detachment (RD) surgery was done in 44 cases (15.1%) in India and Nepal, retinal laser in 38 cases (13.1%), corneal tear repair in 11 cases (3.8%) and brain tumour operation in 8 cases (2.8%). Other interventions are given in Additional file 2: Table S2.

We analysed BCVA by eye to see if the ocular dominance affected the patient presentation to the hospital, but there was none (Fig. 4). The BCVA data were not available for 41 patients who were infants and others who were not responsive.

The intraocular pressure (IOP) level ranged from hypotony (≤4 mmHg) to 74 mmHg in a case of neovascular glaucoma. IOP was not measured in 62 cases who were infective, toddlers in whom the measurement of IOP was not felt necessary, or patients with prosthesis or phthisis bulbi. The distribution of the IOP levels is shown in Additional file 3: Figure S1.

A diagnostic investigation was done in 2855 cases (98.0%) of total patients, while it was not felt necessary or not done in 58 cases (2.0%). Haematological test (blood sugar, glycosylated haemoglobin (HbA1c), and lipid profile) was the most common test done in 1313 cases (31.8%), followed by OCT in 1131 cases (27.4%), refraction in 410 cases (9.9%), B-scan of eye in 358 cases (8.7%), fundus photography in 328 cases (8.0%), MRI of brain and/or orbit in 155 cases (3.8%) and visual field test (Humphrey and FDT) in 144 cases (3.5%). The chest X-ray in 67 cases (1.6%) and Mantoux skin test in 66 cases (1.6%) were performed in cases of retinal vasculitis. EUA with PAC was done in 36 cases (0.9%), mainly for ROP cases. The other diagnostic tests performed were FFA, electroretinogram, vitreous culture and sensitivity, X-ray skull/orbit, CT-scan, orthoptic tests, etc. shown in Additional file 4: Table S3.

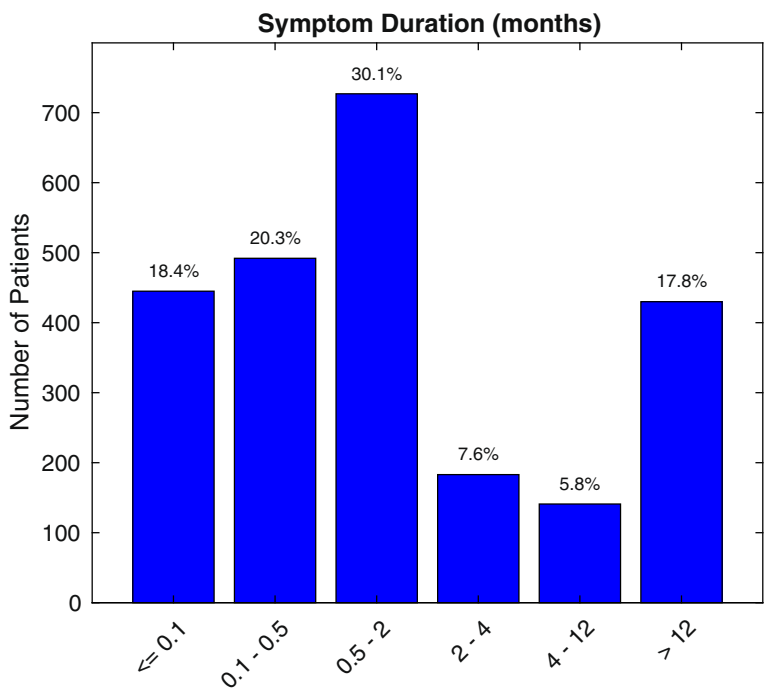

Fig. 2 Interval between the symptom onset and presentation to the Vitreo-retinal Subspecialty Clinic (VRSC)

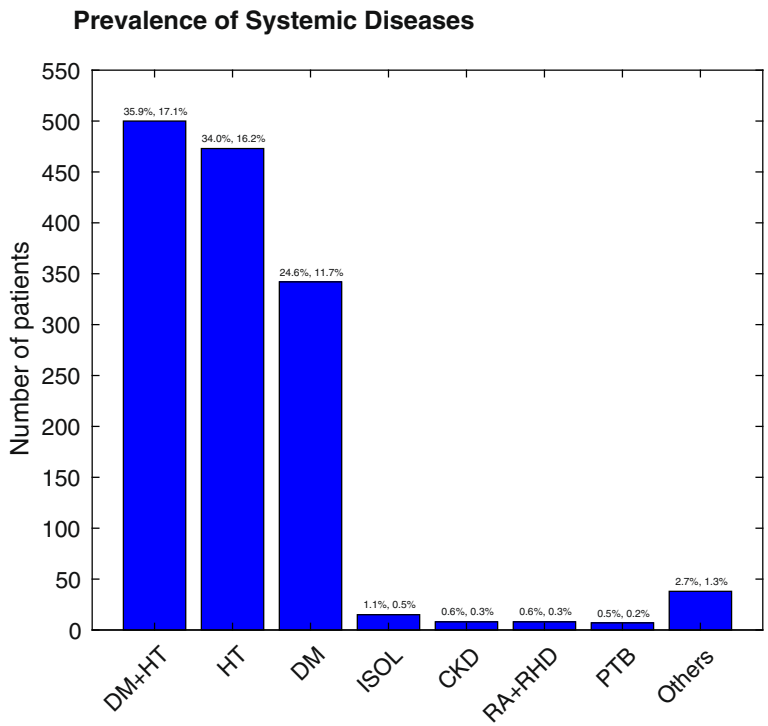

Fig. 3 Prevalence of Systemic Diseases. Breakdown of the commonest systemic diseases found in 1380 (47.4%) of the 2913 patients. The values at the top of the columns give the percentages of the systemic disease patients (left), and the percentage of all patients (right). Others included pregnancy induced hypertension, thyroid disorders, systemic lupus erythematosus, meningitis/encephalitis, anaemia, human immunodeficiency virus, Marfans syndrome, etc

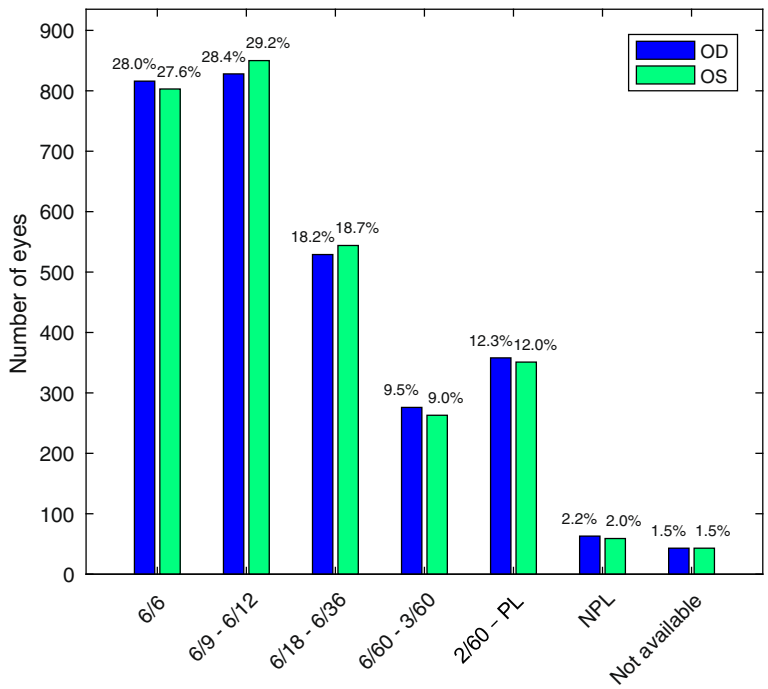

Fig. 4 Best Corrected Visual Acuity at presentation. BCVAs between eyes were not different significantly. The BCVA data was not available in 1.5% of cases

Fundus was normal in 1394 eyes and not visible in 65 eyes. These eyes were excluded for ranking the VR diseases based only on the primary diagnoses. HTR was the commonest VR disease involving 827 eyes (18.9% of all the diagnoses), followed by refractive errors referred for retinal evaluation affecting 728 eyes (16.7%), DR and CSMO in 690 eyes (15.8%), AMD in 482 eyes (11.0%), optic nerve involvement in 223 eyes (5.1%), retinal vein occlusion (RVO) in 123 eyes (2.8%), RD in 110 eyes (2.5%), glaucoma in 104 eyes (2.4%), posterior vitreous detachment (PVD) in 98 eyes (2.2%), macular scar in 88 eyes (2.0%) and macular hole in 84 eyes (1.9%). Other VR diseases are shown in Table 4.

We included the primary, secondary and tertiary diagnoses for the detailed description of each VR disease. A total of 840 eyes had HTR (with or without DM), of which 389 eyes (46.3%) had stage 1, 366 eyes (43.6%) had stage 2, 67 eyes (8.0%) had stage 3 and 18 eyes (2.1%) had stage 4 retinopathy. Case-wise, 253 females with mean age of 57.5 ± 14.4 years and 217 males with mean age of 55.0 ± 13.9 years had HT ($p = 0.2$). The classification DR and CSMO, and AMD is presented in Table 5. Seven hundred twenty-two eyes were affected by diabetes: 333 eyes (46.1%) had mild non-proliferative diabetic retinopathy (NPDR), 162 eyes (22.4%) had moderate NPDR, 75 eyes (10.4%) had severe and 2 eyes

Table 4 VR disease ranking based on Primary Diagnoses

Diseases	Right Eye	Left Eye	Total Eyes	% across total
Hypertensive retinopathy	409	418	827	18.9
Refractive errors referred for retinal evaluation	367	361	728	16.7
Diabetes retinopathy/CSMO	344	346	690	15.8
Age-related macular degeneration	242	240	482	11.0
Optic nerve involvement	94	129	223	5.1
Retinal vein occlusion	67	56	123	2.8
Retinal detachment	54	56	110	2.5
Glaucoma	48	56	104	2.4
Posterior vitreous detachment	48	50	98	2.2
Macular scar	51	37	88	2.0
Macular hole	49	35	84	1.9
Retinitis pigmentosa	41	42	83	1.9
Vitreous haemorrhage	39	41	80	1.8
Retinal vasculitis	30	32	62	1.4
Vitreous opacities/degeneration	29	28	57	1.3
Amblyopia	19	30	49	1.1
Retinopathy of prematurity	24	24	48	1.1
Chorioretinal scar	16	18	34	0.8
Central serous chorioretinopathy	15	19	34	0.8
Status post RD surgery	15	18	33	0.8
Hereditary maculopathy	11	11	22	0.5
Traumatic macular oedema	9	12	21	0.5
Poserior dislocated/subluxated cataract/IOL	11	8	19	0.4
Endophthalmitis	9	7	16	0.4
Panuveitis	6	10	16	0.4
Vitreo-macular traction	7	6	13	0.3
Retinal breaks	6	6	12	0.3
Others[a]	101	100	201	4.6
Total	2171	2196	4367	100

[a]Acute retinal necrosis, choroidopathy, Cystoid macular oedema, Cytomegalo virus retitinits, Chorioretinal coloboma, Central retinal artery occlusion, Coats disease, Cone dystrophy, ERM, Irido-chorio-retinal coloboma, Macular/retinal haemorrhage other than DR/AMD, myelinated nerve fibre, Nephrotic maculopathy, Open-globe injury, Optic nerve head nevus, Phthisis bulbi, Physiological cupping, Prosthesis, Retained intraocular foreign body, Localised retinal oedema/haemorrhage, Retinal telangiectasia, Retinoblastoma, Solar retinopathy, Tilted disc

Table 5 Classifications of diabetic retinopathy and macular oedema and AMD

Disease	Classification	Number of eyes	% across types
Diabetes retinopathy and macular oedema	Mild NPDR	333	46.1
	Moderate NPDR	162	22.4
	Severe NPDR	75	10.4
	Very severe NPDR	2	0.3
	Proliferative DR	71	9.8
	CSMO	79	10.9
	Total	722	100
Age-related macular degeneration	Early	247	51.2
	Intermediate	25	5.2
	Late	210	43.6
	Total	482	100

(0.3%) had very severe NPDR. Seventy-one eyes (9.8%) had proliferative DR (PDR) and 79 eyes (10.9%) had CSMO. Four hundred eighty-two eyes were affected by AMD: 247 eyes (51.2%) had early, 25 eyes (5.2%) had intermediate and 193 eyes (43.6%) had late AMD. Late AMD consisted of neovascular (nAMD) (139 eyes), disciform scar (49 eyes), polypoidal choroidal vasculopathy (PCV) (17 eyes) and geographic atrophy (5 eyes).

Of a total of 110 RD cases, 86 cases were rhegmatogenous (RRD), 13 cases were exudative (ERD) and 11 cases were tractional (TRD). The prevalence of RD was significantly higher among females: 41 males and 83 females ($p = 0.007$).

One hundred and four eyes (2.4%) presented with glaucoma, including 48 glaucomatous OA and 3 neovascular glaucoma.

Eighty-eight eyes had macular scar (including 11 eyes with toxoplasmic macular scar) caused by diseases other than AMD. There were 87 cases of macular hole (MH): 76 cases (87.4%) were full-thickness MH, 9 cases (10.3%) were lamellar MH and 2 cases (2.3%) were impending MH. Sixty-two cases (89.9%) of full-thickness MH were unilateral, while 7 cases (10.1%) were bilateral. Among lamellar MH, 5 cases were unilateral and 2 cases were bilateral. Both cases of impending MH were unilateral. Sixteen cases presented with endophthalmitis, commonest being traumatic involving 7 eyes, followed by postoperative in 6 eyes and 3 endogenous. Two of the endogenous cases were diagnosed to be seasonal hyperacute pan-uveitis (SHAPU) clinically [16].

Discussion

We found that the majority of the patients were male. This finding agrees with other hospital-based studies on VR diseases [17, 18]. The females presented earlier than males. This might be because of the health advocacy routinely given to the women of child-bearing age in the reproductive health unit, and the eye-care education given by the eye-care professionals in the primary through to the tertiary health centres. This may also explain why housewives were the commonest group to seek consultation in the VRSC. The educational profile of the citizenry is a yardstick of development of Bhutan. Bhutan is a developing country where the majority of the patients, especially senior citizens, have not attended modern schooling. This is because the modern education was only introduced in Bhutan in the 1960s [19]. This study found that the majority of the patients were from urban areas, where educational attainment is higher and access to care is easier. Note however that the patients who came from the rural settings, but who had been living in the towns and cities for 6 months or more with their relatives, were been categorised as urban people.

Patients presenting for screening for DR and HTR were second only to poor vision as a complaint. They had either HT or DM or both. This again could be the positive impact of health advocacy. The third highest presenting complaint was referral from other health centres or inferred from other departments in the JDWNRH, reflecting the positive collaboration among the health care staff across different departments and health centres and the value of multi-disciplinary approach to health care system emphasized in the country. Sudden loss of vision was also a frequent cause for presentation. This is because of the high prevalence of HT and DM (Fig. 3) and resulting HTR, DR, CSMO, RVO and vitreous haemorrhage (VH) (Table 4). Ocular trauma was common and was mainly related to agricultural activities, domestic animals and RTA. This resulted severe ocular complications such as retained IOFB, including secondary RD [20]. This is because working with hammer and chisel, and other agricultural tools is commonly practised in Bhutan. The agriculture, livestock and forest sectors provide livelihood for about 57% of the total population [21]. The agricultural sector contributed 16.18% of the GDP of Bhutan in 2013 [21, 22]. RTA is common in Bhutan: in 2013–14 alone there were 1866 accidents resulting 1143 injuries and 157 deaths [23]. Considering the population of less than a million, this death toll due to RTA is significant [1]. Vision not improving after cataract operation was a major concern because of the patients' dissatisfaction. The retinal examination revealed the causes of poor visual outcome were AMD, macular scar, RVO, optic atrophy (OA), DR, CSMO and cystoid macular oedema (CMO).

Eighteen percent of patients presented within 3 days from the onset of the symptoms despite that the patients outside Thimphu have to travel for a day to reach JDWNRH. They were the cases of acute conditions which cause sudden loss of vision like trauma, RVO, RD, VH, central serous chorio-retinopathy (CSCR), and

endophthalmitis. Thirty percent of cases presented between 15 days to 2 months as these were the cases of acute and chronic diseases like AMD, CSMO, MH, DR, PVD, refractive errors, etc. because these conditions are not so acute, and the patients plan and decide to seek the consultation. Eighteen percent presented only after 12 months as these were the cases like HTR, DR and peripheral retinal lesions like chorioretinal scars, which are less symptomatic or asymptomatic conditions.

In our study, 47.4% of the patients had associated systemic disease. Coexistent DM and HT was the commonest (35.9%), isolated HT (34.0%) and DM (24.6%) being the second and third commonest. This finding differs from most of the other hospital-based studies on retinal diseases, which have found either HT or DM as the commonest [17, 18, 24]. The high prevalence of HT among the patients presenting to VRSC could be attributed to high altitude. The southern belt has a median altitude of 300 m, while the highest peak Gangkhar Puensum in the north is at 7570 m, and human settlement is found as high as 5250 m in Lhedi village in Lunana [25]. There is evidence that for every 100 m increase in altitude there is corresponding 2% increase in the prevalence of HT [26]. At the VRSC we also saw a spectrum of other systemic diseases (Additional file 1: Table S1). We and others have noticed that patients tend to present earlier when their dominant eye is affected [27], this most often means when their right eye is affected. Given that handedness and eye dominance are correlated [28], we analysed BCVA of right and left eyes separately (Fig. 4), but we did not find any between-eye disparity. In our similar study of VR diseases in Nepal [29] we noticed that those patients tended not to report vision problems until the acuity of their dominant eye, generally their right eye, was worse than 6/18. This resulted in a highly significant bias in the BCVA between eyes of those patients.

Blood tests for sugar, lipid profile and HbA1c were the commonest investigation done because of high prevalence of diseases with bio-markers in blood like DM, HT, RVO, VH, etc. in our study. These were also done as part of pre-operative workups. OCT was the second commonest test done (Additional file 4: Table S3) because of its utility for AMD, CSMO, RVO, CSCR, MH, macular dystrophies, CMO, myopic choroidal neovascular membrane, glaucoma, trauma, etc. OCT has become an indispensable ancillary test in the diagnosis and management of diseases involving retina and/or choroid. Substantial information is gained about the pathologic and structural changes of the ocular conditions and so OCT is commonly applied in the VRSC [30]. Refraction was third commonest test done because in our study refractive error was the second commonest disease only next to HTR. B-scans were the fourth common test done. It was applied mainly to confirm RD, VH, PVD, vitreous opacities/degenerations and in 65 cases of poor ocular media clarity. Fundus photography was done in cases of DR as baseline work up, documentation, classification using the Modified Airlie House Classification System [11], and also as a tool for evaluating the progression of the retinopathy. These were also taken in cases of RD, chorioretinal coloboma, OA, papilloedema, retinal myelinated nerve fibre, etc. The photographs also served as important tool for explaining the diseases to the patients. The visual field testing was done in VRSC because doubtful cases of glaucoma were referred to VRSC to rule out other neurological and VR diseases.

Chest X-Ray and Mantoux tests were mostly done in cases of retinal vasculitis, popularly known as Eales' disease, to see if tuberculosis was the causative factor. Immunological, molecular biological and biochemical studies have indicated the role of human leucocyte antigen, retinal autoimmunity, *Mycobacterium tuberculosis* genome, and free radical-mediated damage in the etiopathogenesis of the disease [31]. EUA with PAC was done for screening, diagnosing and delivering laser therapies for ROP. The target infants were selected as per the ROP screening guidelines [14].

MRI of the brain and orbit was sought frequently because the cases of trauma and intracranial pathologies are referred to VRSC for ruling out raised intracranial tension, manifested clinically as papilloedema, headache, vomiting and partial or total OA [32]. Often we did MRI for confirmation or ruling out the pathology. MRI was performed in cases of optic neuritis to confirm the retrobulbar neuritis and rule out multiple sclerosis [33].

HTR was the commonest VR disease in our clinic. Partly this high prevalence of HT and HTR could be due to high altitude of Bhutan [26]. In our study 31.4% of DR had vision-threatening DR (VTDR), including severe and very severe DR, PDR and CSMO. This finding agrees with previous literature stating that a third of the DR are VTDR. It is estimated that this figure will escalate in future due to the increasing prevalence of diabetes, aging population, and growing life expectancy [34].

Our study found that 43.6% of AMD patients had late or advanced disease, whereas the literature supports that only 10% of AMD are late AMD, mainly nAMD and accounts for 90% of blindness from AMD [35]. This disparity could be due to that our study being a hospital-based and mostly the advanced AMD cases presented for treatment, and also we have included 17 eyes with PCV in late AMD group considering PCV as a subset of nAMD [36].

Interestingly, we found that the prevalence of RD was significantly higher among females ($p = 0.007$). However, the literature states that the prevalence of RD is more common among males [37–39].

We found that 87.4% of MH were full-thickness and 89.9% of these were unilateral in agreement with another

study [27]. Post-traumatic endophthalmitis was the commonest type and the trauma occurred during the agricultural activities, which is the major source of income for the Bhutanese population [21, 22]. We also diagnosed three cases of endogenous endophthalmitis, two of them as SHAPU based on the clinical findings of childhood presentation, sudden onset of redness, leukocoria, profound loss of vision, minimal pain and hypotony [40].

A similar hospital-based study was conducted by some of the present authors on the pattern and presentation of VR diseases at a tertiary eye care centre in Nepal. It also reported that the majority of the patients were male (60.3% cf. 53.0% in Bhutan) [29]. Interestingly, in Nepal females presented almost a decade later than the age- and sex-matched males ($p < 0.0001$), where as in Bhutan the females presented earlier. HT was the most common systemic disease in Nepal, followed by DM. In Bhutan coexistent DM and HT was the most common, followed by HT and DM. In both the studies poor vision was the most common presenting complaint, trauma being second in Nepal but only fifth in Bhutan. In Nepal AMD was the most common VR disease, followed by DR, RVO, RP, and HTR. In Bhutan HTR was the most common VR disease. AMD ranked fourth, DR ranked third, RVO sixth, while RP ranked twelfth [29]. Population-based studies in Nepal also reported AMD was the most common VR disorder. In 2011, AMD was the most common VR disorder, followed by BRVO among the population aged ≥40 years with mean age of 70.3 ± 10.2 years [41]. In 2013, AMD was the most common VR disorder, followed by DR, HTR, macular scar, BRVO, and RD; mean age being 55.08 ± 11.51 years [7]. In 2018, AMD was the commonest VR disorder, followed by BRVO, ERM, DR, myopic degeneration, and macular hole [8].

There are some limitations in this study. JDWNRH is the single apex referral centre in Bhutan treating the vast majority of the VR diseases in the country. Therefore, the pattern of VR in this hospital may represent VR diseases in the entire citizenry. However, the difficult terrain, poor public transport and limited human resource limit the accessibility of the service. The patient registry is maintained in the out-patient department by each unit and department, but Bhutan is unique for having the patients responsible for bringing their own medical records, often in a handwritten notebook.

Conclusions

The disease pattern reflects the economy and geographic location of a country, and the activities and life style of the population. Any action plan to control the diseases and the rehabilitation of those who are affected should be based on the disease pattern. Bhutan needs to focus on non-communicable diseases like HT and DM and their complications. There is a need to promote safer agricultural activities and stricter legislation of the traffic rules to safeguard the population. The third front is to tackle is the specific eye diseases like refractive error, AMD and glaucoma, and rare but dreadful conditions like SHAPU.

Supplementary information

Supplementary information accompanies this paper at https://doi.org/10.1186/s12886-020-01335-x.

Additional file 1: Table S1. Systemic Diseases associated.

Additional file 2: Table S2. Prior Interventions done before presenting to VRSC, JDWNRH.

Additional file 3: Figure S1. Intraocular pressure. The readings ranged from 4 mmHg to 74 mmHg. The histogram is split into two parts to show the detail of the long tail of high IOPs above 20 mmHg corresponding the eyes above the 95th percentile of all IOPs.

Additional file 4: Table S3. Diagnostic Investigations.

Abbreviations

AMD: Age-related Macular Degeneration; BCVA: Best Corrected Visual Acuity; BRVO: Branch Retinal Vein Occlusion; CKD: Chronic Kidney Disease; CMO: Cystoid Macular Oedema; CRVO: Central Retinal Vein Occlusion; CSCR: Central Serous Chorio-retinopathy; CSMO: Clinically Significant Macular Oedema; DM: Diabetes Mellitus; DR: Diabetic Retinopathy; ERG: Electroretinogram; ETDRS: Early Treatment Diabetic Retinopathy Study; FFA: Fundus Fluorescence Angiography; HT: Hypertension; HTR: Hypertensive retinopathy; IOL: Intra-ocular Lens; IOP: Intraocular pressure; ISOL: Intracranial Space Occupying Lesions; MH: Macular Hole; nAMD: Neovascular AMD; NPDR: Non-proliferative Diabetic Retinopathy; NPL: No Perception of Light; OA: Optic Atrophy; OCT: Optical Coherence Tomography; PCV: Polypoidal Choroidal Vasculopathy; PDR: Proliferative Diabetic Retinopathy; PTB: Pulmonary Tuberculosis; PVD: Posterior Vitreous Detachment; RA: Rheumatic Arthritis; RD: Retinal Detachment; RHD: Rheumatoid Heart Disease; RIOFB: Retained Intra-ocular Foreign Body; ROP: Retinopathy Of Prematurity; RP: Retinitis Pigmentosa; RPE: Retinal Pigment Epithelium; RVO: Retinal Vein Occlusion; S/P: Status Post; SHAPU: Seasonal Hyper-Acute Pan-Uveitis

Acknowledgements

None.

Authors' contributions

BBR conceived of the study, collected data, did analysis and drafted the manuscript. PSB guided BBR and reviewed the manuscript. MGM guided BBR and reviewed the manuscript. TM did much of the analysis, reviewed the manuscript and guided BBR closely. All authors read, reviewed and approved the final manuscript.

Funding

None.

Availability of data and materials

The data have not been placed in any online data storage. The datasets generated and analysed during the study are available upon request from the first author.

Ethics approval and consent to participate

This study was approved by the Research Ethics Board of Health (REBH), Ministry of Health, Royal Government of Bhutan, Thimphu, Bhutan, and adhered to the principle of Declaration of Helsinki. The consent was waived by REBH because this retrospective study collected only the de-identified data.

Consent for publication

Not applicable.

Competing interests

The authors declare that they have no competing interests.

Author details
[1]John Curtin School of Medical Research, Australian National University, Canberra, ACT 2601, Australia. [2]Department of Ophthalmology, JDW National Referral Hospital, Thimphu, Bhutan. [3]Ophthalmic Consultants of Boston, Harvard Medical School, Boston, MA, USA. [4]Moran Eye Centre, University of Utah, Salt Lake City, UT, USA.

Received: 1 August 2019 Accepted: 6 February 2020
Published online: 13 February 2020

References

1. Population and Housing Census of Bhutan 2017. National Report. 2017 [cited 2019 January]. Available from: http://www.nsb.gov.bt/publication/files/PHCB2017_national.pdf.
2. The Kingdom of Bhutan Health System Review. 2017 [cited 2019 January]. Available from: apps.searo.who.int/PDS_DOCS/B5319.pdf.
3. Lepcha NT, Chettri CK, Getshen K, Rai BB, Ramaswamy SB, Saibaba S, et al. Rapid assessment of avoidable blindness in Bhutan. Ophthalmic Epidemiol. 2013;20(4):212–9.
4. Lepcha NT, Sharma IP, Sapkota YD, Das T, Phuntsho T, Tenzin N, et al. Changing trends of blindness, visual impairment and cataract surgery in Bhutan: 2009–2018. PLoS One. 2019;14(5):e0216398.
5. Nirmalan PK, Katz J, Robin AL, Tielsch JM, Namperumalsamy P, Kim R, et al. Prevalence of vitreoretinal disorders in a rural population of southern India: the Aravind comprehensive eye study. Arch Ophthalmol. 2004;122(4):581–6.
6. Brilliant GE, Pokhrel RP, Grasset NC, Lepkowski JM, Shrestha SR, Kea K. The Epidemiology of blindness in Nepal: report of the 1981 Nepal Blindness survey Nepal; 1981.
7. Thapa SS, Thapa R, Paudyal I, Khanal S, Aujla J, Paudyal G, et al. Prevalence and pattern of vitreo-retinal diseases in Nepal: the Bhaktapur glaucoma study. BMC Ophthalmol. 2013;13:9.
8. Thapa R, Bajimaya S, Paudyal G, Khanal S, Tan S, Thapa SS, et al. Prevalence and causes of low vision and blindness in an elderly population in Nepal: the Bhaktapur retina study. BMC Ophthalmol. 2018;18(1):42.
9. Wadud Z, Kuper H, Polack S, Lindfield R, Akm MR, Choudhury KA, et al. Rapid assessment of avoidable blindness and needs assessment of cataract surgical services in Satkhira District, Bangladesh. Br J Ophthalmol. 2006; 90(10):1225–9.
10. Downie LE, Hodgson LAB, D'Sylva C, McIntosh RL, Rogers SL, Connell P, et al. Hypertensive retinopathy: comparing the Keith-Wagener-barker to a simplified classification. J Hypertens. 2013;31(5):960–5.
11. Wu L, Fernandez-Loaiza P, Sauma J, Hernandez-Bogantes E, Masis M. Classification of diabetic retinopathy and diabetic macular edema. World J Diabetes. 2013;4(6):290–4.
12. Mathew C, Yunirakasiwi A, Sanjay S. Updates in the management of diabetic macular edema. J Diabetes Res. 2015;2015:794036.
13. Ferris FL, Wilkinson CP, Bird A, Chakravarthy U, Chew E, Csaky K, et al. Clinical classification of age-related macular degeneration. Ophthalmology. 2013;120(4):844–51.
14. Jefferies A. Retinopathy of prematurity: recommendations for screening. Paediatr Child Health. 2010;15(10):667–74.
15. Efron B. 1977 Rietz lecture - bootstrap methods - another look at the jackknife. Ann Stat. 1979;7(1):1–26.
16. Upadhyay MP, Rai NC, Ogg JE, Shrestha BR. Seasonal hyperacute panuveitis of unknown etiology. Ann Ophthalmol. 1984;16(1):38–44.
17. Eze BI, Uche JN, Shiweobi JO. The burden and Spectrum of Vitreo-retinal diseases among ophthalmic outpatients in a resource-deficient tertiary eye care setting in south-eastern Nigeria. Middle East Afr J Ophthalmol. 2010; 17(3):246–9.
18. Teshome T, Melaku S, Bayu S. Pattern of retinal diseases at a teaching eye department, Addis Ababa, Ethiopia. Ethiop Med J. 2004;42(3):185–93.
19. Bhutan - Education [Internet]. 2019 [cited 2019 January]. Available from: https://www.nationsencyclopedia.com/Asia-and-Oceania/Bhutan-EDUCATION.html.
20. Rai BB, Dorji S, Zangmo P, Tshering T. Retained intraocular metallic foreign body causing retinal detachment. Bhutan Health J. 2016;2(1):48–52.
21. Climate-Smart Agriculture in Bhutan. International Centre for Tropical Agriculture (CIAT). 2017 [cited 2019 Janauary]. Available from: http://sdwebx.worldbank.org/climateportal/doc/agricultureProfiles/CSA-in-Bhutan.pdf.
22. Gulati AB, Chandra S. Economic reforms and food security: the impact of trade and technology in South Asia. 1st ed. New York: Food Products Press; 2005.
23. Wangdi C, Gurung MS, Duba T, Wilkinson E, Tun ZM, Tripathy JP. Burden, pattern and causes of road traffic accidents in Bhutan, 2013-14: a police record review. Int J Inj Control Saf Promot. 2017;25(1):65–9.
24. Hatef E, Fotouhi A, Hashemi H, Mohammad K, Jalali KH. Prevalence of retinal diseases and their pattern in Tehran: the Tehran eye study. Retina (Philadelphia, Pa). 2008;28(5):755–62.
25. Lamsang T. His Majesty in Lunana. Thimphu: The Bhutanese; 2016. 29/10/2016
26. Mingji C, Onakpoya IJ, Perera R, Ward AM, Heneghan CJ. Relationship between altitude and the prevalence of hypertension in Tibet: a systematic review. Heart. 2015;101(13):1054.
27. Waheed K, Laidlaw DAH. Disease laterality, eye dominance, and visual handicap in patients with unilateral full thickness macular holes. Br J Ophthalmol. 2003;87(5):626–8.
28. McManus IC, Porac C, Bryden MP, Boucher R. Eye-dominance, writing hand, and throwing hand. Laterality. 1999;4(2):173–92.
29. Rai BB, Shrestha MK, Thapa R, Essex RW, Paudyal G, Maddess T. Pattern and presentation of Vitreo-retinal diseases: an analysis of retrospective data at a tertiary eye-care Centre in Nepal; 2019.
30. Murthy RK, Haji S, Sambhav K, Grover S, Chalam KV. Clinical applications of spectral domain optical coherence tomography in retinal diseases. Biom J. 2016;39(2):107–20.
31. Biswas J, Ravi RK, Naryanasamy A, Kulandai LT, Madhavan HN. Eales' disease - current concepts in diagnosis and management. J Ophthalmic Inflamm Infect. 2013;3(1):11.
32. Dunn LT. Raised intracranial pressure. J Neurol Neurosurg & Psychiatry. 2002;73(suppl 1):i23.
33. Hoorbakht H, Bagherkashi F. Optic neuritis, its differential diagnosis and management. Open Ophthalmol J. 2012;6:65–72.
34. Lee R, Wong TY, Sabanayagam C. Epidemiology of diabetic retinopathy, diabetic macular edema and related vision loss. Eye Vis (Lond). 2015;2:17.
35. Chakravarthy U, Wong TY, Fletcher A, Piault E, Evans C, Zlateva G, et al. Clinical risk factors for age-related macular degeneration: a systematic review and meta-analysis. BMC Ophthalmol. 2010;10:31.
36. Hatz K, Prunte C. Polypoidal choroidal vasculopathy in Caucasian patients with presumed neovascular age-related macular degeneration and poor ranibizumab response. Br J Ophthalmol. 2014;98(2):188–94.
37. Wong TY, Tielsch JM, Schein OD. Racial difference in the incidence of retinal detachment in Singapore. Arch Ophthalmol. 1999;117(3):379–83.
38. Mitry D, Charteris DG, Yorston D, Siddiqui MA, Campbell H, Murphy AL, et al. The epidemiology and socioeconomic associations of retinal detachment in Scotland: a two-year prospective population-based study. Invest Ophthalmol Vis Sci. 2010;51(10):4963–8.
39. Park SJ, Choi NK, Park KH, Woo SJ. Five year nationwide incidence of rhegmatogenous retinal detachment requiring surgery in Korea. PLoS One. 2013;8(11):e80174.
40. Malla OK. Endophthalmitis probably caused by Tussock moth. Report of the Proceedings of the first National Seminar on Prevention of Blindness. Nepal; 1978:44.
41. Thapa SS, Khanal S, Paudyal I, Twyana SN, Ruit S, van Rens GH. Outcomes of cataract surgery: a population-based developing world study in the Bhaktapur district, Nepal. Clin Exp Ophthalmol. 2011;39(9):851–7.

Publisher's Note

Springer Nature remains neutral with regard to jurisdictional claims in published maps and institutional affiliations.

Ready to submit your research? Choose BMC and benefit from:

- fast, convenient online submission
- thorough peer review by experienced researchers in your field
- rapid publication on acceptance
- support for research data, including large and complex data types
- gold Open Access which fosters wider collaboration and increased citations
- maximum visibility for your research: over 100M website views per year

At BMC, research is always in progress.

Learn more biomedcentral.com/submissions

BMC

Supplementary data

Table S1. Systemic Diseases associated

Systemic diseases	Disease frequency	% among diseases
Coexistent DM & HT	500	35.9
Hypertension (HT)	473	34
Diabetes Mellitus (DM)	342	24.6
Brain tumour*/Epilepsy, 10+2	12	0.9
Chronic Kidney Disease	8	0.6
Rheumatic Arthritis/RHD	8	0.6
Pulmonary Tuberculosis	7	0.5
Pregnancy-induced Hypertension	6	0.4
Dysthyroidism	5	0.4
Systemic Lupus Erythematosus	5	0.4
Encephalitis/Meningitis	3	0.2
Anaemia	3	0.2
HIV infection	2	0.1
Marfans syndrome	2	0.1
Others**	12	0.9
Total systemic diseases	**1388**	**100**
Patients without systemic diseases	1533	52.6
Patients with systemic disease	1380	47.4
Total patients in the study	**2913**	**100**

*Tumour, craniopharyngioma, Empty sella syndrome, hydrocephalus, pituitary cyst and macroadenoma.
**Carcinoma lung, Congestive cardiac failure, Chronic obstructive pulmonary disease, Cerebrovascular accident, Downs syndrome, Deep vein thrombosis, Hepatitis B, Pheochromocytoma, Masquerade syndrome, Myesthenia gravis, Non-Hodgkin's lymphoma, Syphilis.

Table S2. Prior Interventions done before presenting to VRSC, JDWNRH

Interventions	Number of eyes	% across interventions
Cataract operation + IOL	146	49.2
Retinal detachment surgery	44	14.8
Retinal laser	37	12.5
Corneal tear repair	15	5.1
Brain tumor operation	8	2.7
Scleral tear repair	8	2.7
Lensectomy	5	1.7
Lid Tear Repair	5	1.7
Pterygium excision with graft	5	1.7
Anti-VEGF injection	4	1.4
Cancer Chemotherapy	3	1.0
Trabeculectomy	3	1.0
Pars plana vitrectomy	2	0.7
Renal transplant	2	0.7
Others*	10	3.4
Total interventions done	**297**	**100**
No. of patients without intervention	2627	90.2
No. of patients with intervention	286	9.8
Total patients	**2913**	**100**

*Conjunctival tear repair, Cryotherapy, Hemodialysis, Injection methyl prednesolone, Injection Vancomycin + Ceftazidime + Dexamethasone, Laser peripheral iridotomy, Lasik, Macular hole surgery, Parotid gland operation, Radiotherapy.

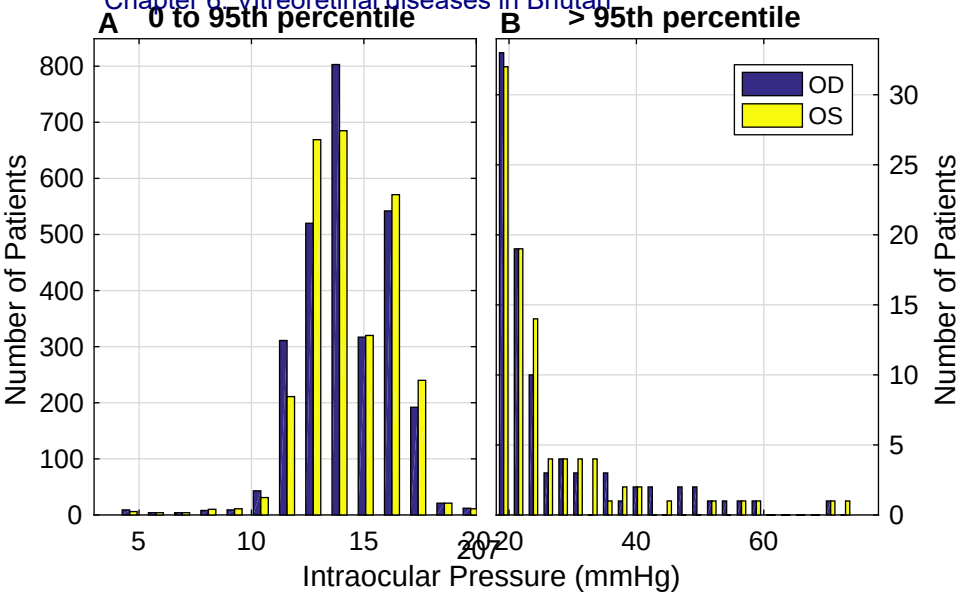
A
0 to 95th percentile
B
> 95th percentile
OD
OS
Number of Patients
Number of Patients
Intraocular Pressure (mmHg)
0
100
200
300
400
500
600
700
800
5
10
15
20
20
40
60
0
5
10
15
20
25
30

Table S3. Diagnostic Investigations

Tests	Test frequency	% across tests
*Haematological tests	1,313	31.8
Optical Coherence Tomography	1,131	27.4
Refraction	411	9.9
B-scan	358	8.7
Fundus photography	331	8.0
MRI Brain/Orbit	155	3.8
Visual Field (HVF+FDT)	144	3.5
Chest X-Ray	67	1.6
Mantoux test	66	1.6
Examination Under Anaesthesia	36	0.9
X-ray skull	26	0.6
Fundus Fluorescein Angiography	23	0.6
CT-scan	22	0.5
Vitreous culture/sensitivity	16	0.4
Orthoptic test	14	0.3
Electroretinogram	12	0.3
Others**	7	0.2
Total tests done	**4,132**	**100**
No. of patients with diagnostic tests done	2,855	98.0
No. of patients without any test	58	2.0
Total patients	**2,913**	**100**

*Blood sugar, lipid profile & HbA1c; **Cytology, Diplopia charting, Lacrimal syringing

Graefe's Archive for Clinical and Experimental Ophthalmology
https://doi.org/10.1007/s00417-020-04891-6

RETINAL DISORDERS

Rural-urban differences in myopia prevalence among myopes presenting to Bhutanese retinal clinical services: a 3-year national study

Bhim Bahadur Rai[1,2] · Regan S. Ashby[3] · Amanda N. French[4] · Ted Maddess[1]

Received: 21 April 2020 / Revised: 19 July 2020 / Accepted: 10 August 2020
© Springer-Verlag GmbH Germany, part of Springer Nature 2020

Abstract

Purpose To determine the prevalence and demographic characteristics of myopia among patients presenting to the national vitreo-retinal (VR) services in Bhutan.

Methods The records of the VR clinic at the apex national referral centre, providing the only VR services in the country, were reviewed to identify all new myopia patients over three years. Thus, we surveyed all referrals nationally. The patients were categorised into urban and rural females and males. We assessed myopia prevalence in each group by occupational and educational categories. We examined univariate prevalence data and a multivariate logistic regression (MLR) identified independent factors.

Results Of 2913 cases 1544 (53.0%) were males. Females presented earlier (mean ±SD): overall 45.7 ± 21.9 cf. 48.6 ± 21.6 years, $p = 0.003$, and among myopes 23.9 ± 13.5 cf. 27.6 ± 18.6 years, $p = 0.032$. Myopia constituted 92.1% of refractive error, an overall prevalence of 12.3%. Myopia was more common among females ($p = 0.01$) and urbanites ($p = 0.02$). Myopia prevalence was highest among urban females (20.9%), followed by urban males (11.9%), rural females (6.8%), and rural males (5.2%). Logistic regression revealed that the odds of having myopia were increased by being a student (4.96 ×) or professional (1.96 ×), and decreased by rural living (1.75 ×), all $p \leq 0.038$.

Conclusions This is the first study on myopia in Bhutan. As observed throughout East and Southeast Asia, the prevalence of myopia was higher in females and urbanites and positively associated with formal education. Given known risk factors, these prevalences may be driven by educational pressures and reduced time spent outdoors.

Key messages

- Myopia prevalence is increasing in the East and Southeast Asia and educational attainment, time spent outdoors, and genetics are suggested causal factors.
- Univariate prevalence data and multivariate logistic regression identified similar independent factors among the myopes presenting to the national retinal services in Bhutan.
- The odds of developing myopia were increased by being a student (4.96×) or professional (1.96×), and were decreased by rural living (1.75×).
- Being female had marginally significant increased odds of 1.56×, but age was not significant.

✉ Bhim Bahadur Rai
bhim.rai@anu.edu.au

[1] John Curtin School of Medical Research, Australian National University, Canberra, ACT 2601, Australia

[2] Jigme Dorji Wangchuck National Referral Hospital, Thimphu, Bhutan

[3] Faculty of Science & Technology, University of Canberra, Kirinari Street, Bruce, ACT 2617, Australia

[4] Faculty of Science & Technology, University of Technology, Sydney, NSW, Australia

Published online: 17 August 2020

Keywords Avoidable blindness · Myopia · Myopic CNVM · Prevalence of myopia · Refractive error · Retinal break · Rhegmatogenous retinal detachment

Introduction

Uncorrected refractive error is the most common cause of visual impairment, accounting for 43% of the 285 million visually impaired individuals worldwide in 2010 [1]. Myopia constitutes 91.8% of clinically significant refractive errors, and is a major cause of avoidable blindness in the world [2]. Globally, there were 1406 million people with myopia (22.9% of the world population) in 2000, with projects of a rise to 4758 million (49.8% of the world population) by 2050 [3]. The complications of high-end myopia include the following: atrophic retinal holes and retinal detachment (RD), myopic choroidal neovascular membrane (mCNVM), degenerative changes resulting in cataract, glaucoma, and macular hole that collectively cause severe visual loss [4–7]. The estimated global economic cost due to uncorrected refractive errors causing visual impairment and resultant productivity loss is USD 91.3 billion [8], and the cost to establish and maintain refractive facilities is USD 20 billion [5].

The current myopia epidemic appears to be driven by environmental risk factors, including intensive education and limited time outdoors [9], and genetic factors [10]. Educational attainment and near-work activities have been reported by several studies, but not all, to be associated with development of myopia [11, 12], and are suggested to promote compensatory elongation of the eyeball [13]. More recent work has shown that more time outdoors during childhood reduces the likelihood of developing myopia, irrespective of the amount of near work undertaken [14]. This protection has been hypothesised to be driven by the light-stimulated release of dopamine in the retina [15, 16], a hypothesis supported by animal work [17].

Overall, the greater educational load and reduced time spent outdoors by individuals in urban areas relative to their rural neighbours has been proposed to explain their higher prevalence rates [18].

So far, no survey has been conducted on refractive errors in Bhutan. Refractive error, mainly myopia, was the second commonest VR disease (16.7%), only next to hypertensive retinopathy (18.9%) in our study of the pattern of all vitreoretinal (VR) diseases in Bhutan [19]. The present study investigated the proportion of patients with moderate to high myopia attending the national tertiary referral VR sub-speciality clinic (VRSC) and to determine whether there is a difference in the proportion presenting with myopia according to rural and urban location, gender, education, and occupation. Given the Bhutanese system, this represented all referrals to VR services in the country over 3 years.

Methods

Ethics, consent, and study design

The retrospective study was approved by the Research Ethics Board of Health (REBH), Ministry of Health, Royal Government of Bhutan, and was conducted as per the REBH guidelines and tenets of the Declaration of Helsinki.

Setting and recruitment

The study was conducted in the VRSC, Ophthalmology Department, Jigme Dorji Wangchuck National Referral Hospital (JDWNRH), Thimphu, Bhutan. The JDWNRH is the apex national referral hospital, and so all retinal patients (both direct and referred) in Bhutan attended JDWNRH during the 3-year study period, which extended from 01.05.2013 to 30.04.2016. JDWNRH also serves as the main clinical centre for postgraduate medical students, interns, and optometric and paramedic students. All new patients presenting to the VRSC were included. The myopes were mostly those with moderate (− 3 D to − 6 D) to high (≥ 6 D) myopia because they were referred to VRSC for complications secondary to myopia including lattice degeneration, retinal holes, and mCNVM.

Definitions

In Bhutan, urban areas were those regions that were under the jurisdiction of City Corporations, municipalities, or town committees, locally termed as *Thromde*, collectively. Other regions were classified as rural areas [20].

Bhutan's education system embraces both monastic and modern education. Monastic education dates back to 746 AD, and was predominant until the early 1960s. It remains an important alternative education system. The first modern school was established in 1914, but it was only with the launch of first national Five-Year Plan in 1961 that the modern education system was expanded. Modern formal education starts as pre-school for children aged 6 years, progressing to year 1 to 6 as *Primary School*. Most children aged 3–5 years attend Early Childhood Care and Development (*ECCD*) programmes, but they are not compulsory. Years 7 to 10 are termed *High School*. Years 11 and 12 are termed *Intermediate Level*, following which most successful students align with professional training. Here, *Graduates* refer to persons holding Bachelor degrees. *Postgraduates* include individuals

having postgraduate diplomas, master degrees, MPhil, or PhD degrees [21].

Clinical examination and data collection

Demographic information included age and gender, rural or urban setting, educational attainment, and occupation. Details of the pattern and presentation of VR diseases including symptoms, clinical examinations, and diagnostic tests undertaken for this study are published elsewhere [19]. Myopia, and hyperopia, was determined by clinical refraction sometimes assisted by autorefraction. Cycloplegic drops were used for refraction for all children, and young adults up to 18 years to rule out pseudomyopia due to accommodation during refraction. Anterior and posterior segments of myopes were examined under a slit-lamp (BM 900, Haag-Streit, Switzerland) and 90D bio-microscopy. Funduscopic findings were confirmed by indirect ophthalmoscope (12500, Welch Allyn, USA) under mydriasis. Diagnosis of mCNVM was confirmed with Spectral Domain OCT (Cirrus-HD 4000, Carl Zeiss, Germany). Fundus photography (VISUCAM-524, Carl Zeiss, Germany) was undertaken when indicated.

Statistical analysis

The data were analysed with MATLAB (2016b, The MathWorks, Natick, MA). Comparisons of the expected and observed frequency of males or females and comparisons of prevalences such as in urban or rural settings were examined by Chi-squared tests. Further details are given in an allied review of retinal disease in Bhutan [19]. A mixed effects logistic regression was performed using the 'fitglme' function of Matlab.

Results

A total of 2913 new cases of all types presented to VRSC over the 3-year study period. The majority of patients were male (1,544, 53.0%; females 1369, 47.0%). The mean age of presentation across all patients was 47.2 ± 21.8 years (range 20 days to 91 years). Table 1 shows the demographic characteristics of the patients.

Among all presenting cases, 1845 (63.3%) were from urban areas and 1068 cases (36.7%) from rural settings. On average, urban females presented earliest, followed by urban males, rural females, and rural males (Fig. 1a). The 25th percentile age for urban females was 23 years, 29 years for males from urban, 37 years for females from rural, and 40 years for males from rural areas. We did not find any significant differences in self-reported symptom duration (Fig. 1b).

The best corrected visual acuity (BCVA) at presentation for the right and left eyes were homogenous (Fig. 2). Thus, we did not see an effect of ocular dominance on patient presentation, which we reported in a similar study in Nepal [22]. There it appeared that there was a significant tendency for patients to report visual symptoms when they impaired their dominant eye. The majority (64%) of patients had BCVA of 6/18 or better. In 1.4% of the patients (infants, toddlers, and incoherent patients), the vision was not taken.

There were 751 eyes with refractive errors, of which 692 eyes (92.1%) were myopic and only 59 eyes (7.9%) were hyperopic. All the myopic cases were bilateral, except in 8 cases, we could not confirm bilateralism. Three of these cases had undergone RD surgery, two cases had rhegmatogenous RD (RRD), and other three cases had ocular media opacity making it difficult to evaluate the posterior segments. The overall prevalence of myopia (POM) in the study group was 12.3%. The POM was further categorised based on an individual's gender and whether they were from urban or rural areas. The POM was highest among urban females (20.9%), followed by urban males (11.9%), rural females (6.8%), and finally rural males (5.2%) (Table 2). Among urbanites, myopia was significantly more common among females relative to males ($p < 0.01$), but among the rural population, there was no difference between genders ($p = 0.4$).

When viewed by occupation, Table 3 shows that the highest POM was found among all students (44.9%, broken down by educational level in Table 4, followed by prisoners (25.0%), employees of corporations (17.1%), children not attending formal education (15.6%), and clerical persons (15.4%). The POM was significantly higher among the urban students than their rural compatriots ($p < 0.0001$). The same trend was seen for private employees ($p < 0.0001$) and housewives ($p = 0.019$). The difference in POM between urban and rural settings was not significant among government employees ($p = 0.105$) or farmers ($p = 0.773$). Interestingly, the

Table 1 Demographic characteristics of patients

Category of patients	Number of patients	Presentation age (mean ± SD)	Minimum age	Median age	Maximum age
All patients, years	2913	47.2 ± 21.8	0.1	50	91
Males only, years	1544	48.6 ± 21.6	0.1	51	90
Females only, years	1369	45.7 ± 21.9	0.1	49	91

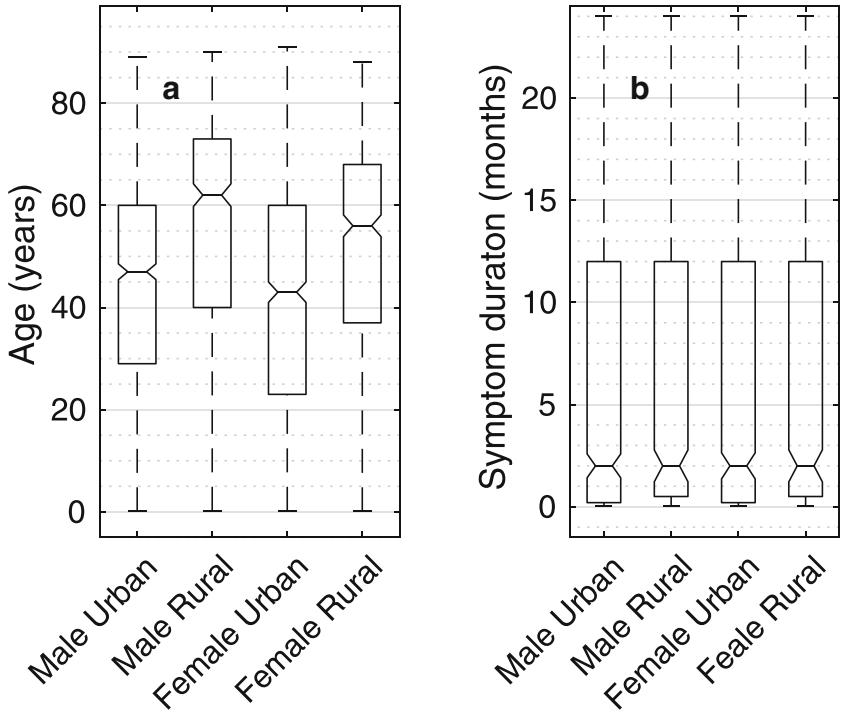

Fig. 1 Age and sex boxplots for presentation to the VRSC: **a** presentation based on age in years. **b** Presentation based on duration of symptoms

POM was higher among the rural clerics than the urban ones ($p = 0.018$) (but see Discussion).

Among all 2913 patients, 1512 (51.9%) did not receive a modern education. A total of 570 cases (19.6%) completed only Primary school, 350 cases (19.5%) completed High School, 363 cases (12.5%) were Graduates, 86 (3.0%) were Postgraduates, 30 cases (1.0%) completed Intermediate, and 2 children were Pre-schoolers.

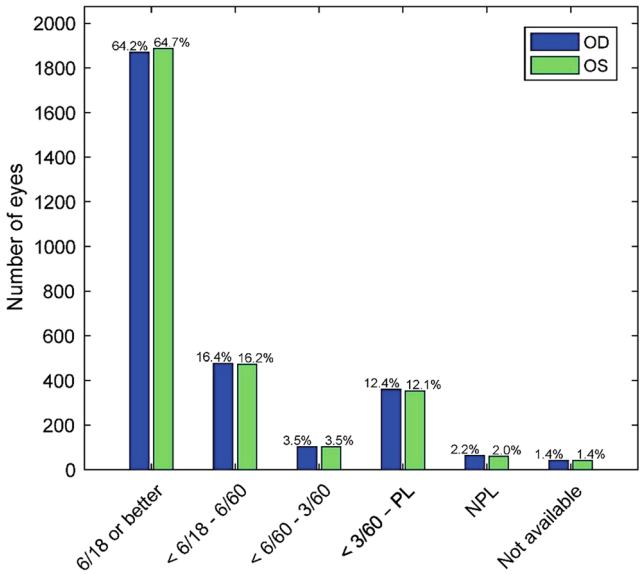

Fig. 2 Best corrected visual acuity (BCVA) at presentation. The BCVAs between eyes were not significantly different. BCVA data was not available in 41 patients (1.4%)

The overall POM among those patients who were attending or attained only a primary school level of education was 26.1%, and within this group, prevalence was higher among females ($p = 0.006$). Within this sub-group, the urban POM was higher (32.0% cf. 13.1%, $p < 0.0001$), and again was higher among females ($p = 0.01$). There was no gender bias in POM among more educated groups. Among the graduates, the overall POM was 21.8%, with 21.4% among urban and 24.4% among rural patients. By contrast, POM was low among those patients who did not attain any education: overall 2.5%, urban 3.0%, and rural 2.1%. Other details are shown in Table 4.

Thus far, the analyses have been univariate. To identify independent factors, we fitted a multivariate mixed effects logistic regression model, fitting the log-odds of various predictor variables that might determine myopia. Our normal control subjects were persons who had been referred to the national retinal progamme, but on examination were found to be normal. Restricting the age of the control and myopic subjects to under 40 years gave reasonable age matching providing 171 controls and 306 myopes (overall 21.7 ± 9.72 years). We reduced the number of Occupations (Table 3) to four roughly equal-sized groups. We aggregated Private, Corporate, Government, and Clerical persons into the category: Professional. There were large numbers of Students and Housewives so we retained those categories. This left Child, Infant, Farmer, and Prisoner in an Other category. Educational attainment was grouped in into Low, Medium, and High by aggregating: Nil+Primary, High School+Intermdiate, and Graduate+Post graduate. Education was fitted nested within

Table 2 Prevalence of myopia

Parameters	Urban female	Urban male	Rural female	Rural male
Number of myopic cases	176	119	36	28
Group population	842	1003	527	541
Prevalence %	20.9	11.9	6.8	5.2

the nuisance variable subject, where we used Age+Sex+Occupation as a proxy for subject. The results of the model are shown in Table 5.

In agreement with the univariate results, Students were about 5 × more likely to be myopic than controls (Table 5, Odds column), and Rural persons and Other about 4 × and 2 × less likely. Female was marginally significant ($p = 0.065$) with odds of 1.56 ×. Together the four Occupation factors were significant at $p = 0.0005$. Age was not significant. We fitted Age with the mean subtracted so that Age had little effect upon the Intercept. The fitglme process rolled the Professional category into the Intercept, hence its myopic tendency of 1.93 ×. Given that Age was unlikely to contribute much to the intercept, we have labelled it: "Intercept (Professional)". Our mixed effects model showed unsurprising correlations between more professional occupations and education level, and also education level with gender and age (not shown).

The most common complication associated with myopia was lattice degeneration with a prevalence of 13.4% (93 of 692 myopic eyes). We found 10 eyes with retinal breaks: 4 of these were atrophic retinal holes secondary to myopic degeneration (prevalence of 0.6%), while another 6 eyes had other associated clinical findings such as retinal tractional band due to proliferative retinopathy (PDR), retinal vasculitis, or proliferative vitreo-retinopathy (PVR) besides myopic degeneration. Therefore, we could not ascertain if the retinal break formation was definitely secondary to myopic degeneration. If we include these eyes, the prevalence of retinal holes among the myopic eyes rises to 1.4%. mCNVM was diagnosed in 3 eyes, 0.4% of myopic eyes developing it. There were 86 cases of RRD in the study patients. Due to a lack of data, we could not conclude if these were associated with atrophic retinal holes due to myopia. Posterior vitreous degeneration (PVD) was found in 1.6% (11 eyes) of the myopic eyes. The ocular co-morbidities associated with myopia were hypertensive retinopathy (8 eyes), diabetic retinopathy (6 eyes), and retinitis pigmentosa (2 eyes).

Discussion

The majority of the patients (63.3%) were from urban areas, which was unexpected in Bhutan, where 66% of its population lives in rural areas [23]. This could be due in part to a confounding factor in the study: rural patients, but whom had been living in the urban areas with their relatives for six months or more, were categorised as urban patients. Alternatively, the lower number of rural patients may reflect lower prevalence of high myopia in rural areas, which is consistent with previous findings [24, 25]. Females presented earlier than males, again possibly due to urban females more commonly having high myopia. This finding somewhat contradicted our previous findings that female VR patients

Table 3 Correlation between occupation and myopia

Occupation	Prevalence			*p* value (urban vs. rural)
	Overall	Urban	Rural	
Students	44.9	50.3	23.8	< 0.0001
Prisoners	25.0	25.0	*	*
Corporate employees	17.1	19.4	*	*
Children not attending formal education	15.6	27.8	*	*
Clerical persons	15.4	11.2	23.4	0.018
Private employees	13.1	14.5	5.0	< 0.0001
Govt. employees	12.7	13.1	10.0	0.105
Housewives	6.2	7.3	5.0	0.019
Farmers	1.7	1.8	1.6	0.773
Retired persons	1.3	1.4	*	*
Infants	*	*	*	*
Dependents	*	*	*	*

*No patient in the sub-group, vision not taken, or not comparable due to lack of data

Table 4 Correlation between educational attainment and myopia

Education attainment	Overall patients		Urban patients		Rural patients	
	Myopic cases	Prevalence	Myopic cases	Prevalence	Myopic cases	Prevalence
No formal education	38	2.5	22	3	16	2.1
Primary school	149	26.1	126	32	23	13.1
High school	76	21.7	64	21.7	12	21.8
Intermediate	8	26.7	6	23.1	2	50
Graduate	79	21.8	68	21.4	11	24.4
Postgraduate	9	10.5	9	11.5	0	0

in Nepal presented almost a decade later than males [22]. This may be a positive result of the health advocacy and education given to the public in Bhutan. In particular, this advocacy is efficiently delivered through the Reproductive, Maternal and Neonatal Health Program [26]. The levels of education attained by the study cohort agreed with the literacy status of Bhutan, which is reported at 81.7% in urban and 58.3% in the rural areas [23], some persons achieving literacy through monastic education rather than formal schooling.

Following good practice, cycloplegic refraction was performed for all children and young adults up to 18 years of age to rule out pseudomyopia due to accommodation during refraction [27, 28]. The BCVA at presentation for the right and left eyes was homogenous, indicating ocular dominance might not have affected the timing of presentation to the hospital. In a similar study conducted in Nepal, we found that patients whose non-dominant eyes were affected presented later [22], in other words they seemed to less often notice visual impairment of their non-dominant eye. We found that myopia constituted 92.1% of the refractive errors detected, agreeing with other studies [2, 29]. The overall POM in our study among the clinical population presenting to the VRSC was 12.3%. This included mainly moderate to high myopic cases, which were referred to the VRSC for retinal evaluation to rule out complications secondary to myopia. It may be expected that this is a high estimate of the population prevalence, given the use of a clinical sample in this study. Other studies have reported that the prevalence of myopia varies from 0.8 to 96.5%, depending on geographical area, age, occupation, and ethnicity [30–32]. In Nepal, Sherpa children had a prevalence of 2.9% as compared with 21.7% for Tibetan children [33]. Thus, this study reports a comparatively low prevalence of myopia within this clinical sample. Uncorrected refractive errors, mainly myopia, pose a huge socioeconomic burden worldwide in the form of: visual impairment and blindness, resultant productivity loss by the patients and family members working as carers, the cost of maintaining refractive facilities, and poor academic performance by students at schools.

Table 5 Mixed-effect Logistic Regression results for a diagnosis of myopia vs. no myopia

Variable	Log-odds	SE	Odds	t	p
Intercept (professional)	0.66	0.33	1.93 ×	2.01	0.045
Occupation: student	1.60	0.61	4.96 ×	2.63	0.009
Occupation: other	− 1.35	0.49	0.26 ×	− 2.74	0.006
Occupation: housewife	− 0.34	0.38	0.71 ×	− 0.89	0.374
Age: zero-mean	− 0.05	0.03	0.95 ×	− 1.40	0.161
Female	0.44	0.24	1.56 ×	1.85	0.065
Rural	− 0.57	0.27	0.57 ×	− 2.09	0.038

The Intercept includes the effects of Age and the Professional occupational category. The ages fitted had their mean subtracted (hence "zero-mean") therefore the Intercept is mainly due to the Professional category

The concept of light-stimulated release of dopamine in the retina when exposed to bright light levels outdoors thereby preventing or arresting myopia [9, 14, 15], as supported by animal work [17], has drawn attention. Our findings provide some further support of this theory. For example, urban females had the highest POM (Table 2). This group of people mostly spend their time indoors at home or in offices [34]. They are not exposed to sunlight as much as rural people who are constantly exposed to sunlight while working on farms, cattle grazing, or travelling on foot. This may also explain why the POM was lowest among the rural males (and lower than rural females) because they are more actively engaged in outdoor games and sports, and other activities. Myopia was highest among occupational groups who spend more time indoors including students, prisoners, corporate employees, and clerical persons.

Within each occupation, the urban sub-group had a significantly higher prevalence than their rural counterparts: students ($p < 0.0001$), private employees ($p < 0.0001$), and housewives ($p = 0.019$). High POM among the students could be a significant reason for school dropouts in Bhutan. A comprehensive School Eye Check-up Program performs annual refraction and provides free spectacles to those children who

cannot afford to buy them, but the spectacles are commonly lost or broken. Thus uncorrected refractive error causing visual impairment remains a common cause of poor academic performance in Bhutan. In 2018, dropout rates were 0.0 to 8.5% depending on the year of schooling [35]. In eastern Asia, pathological myopia is reported as a major issue found in 80–90% of school-leavers and 10–20% of those completing secondary school [7, 36].

Among farmers, the urban-rural difference was not significant ($p = 0.773$) perhaps because in both the regions, the farmers worked in open fields and are exposed to sunlight. Interestingly, among clerics, myopia was more common in the rural sub-group ($p = 0.018$). In Bhutan religious retreats and medication centres, public facilities where the clerics and even general public can perform meditation and enchant prayers peacefully are available mainly in remote areas. There, the clerics practice meditation for months and even years remaining indoors to develop peaceful and positive mental states or *virtuous minds* [37]. This might explain why myopia was more common among rural clerics. Also, rural clerics were younger (24.9 ± 7.8 years, cf. 43.0 ± 29.1 years) so they might have been studying more to achieve higher qualifications.

The univariate data reviewed above were largely confirmed by a multivariate logistic regression (Table 5). Basically, the categories Student, Professional, or Female increased the odds of being myopic, while living in a rural area or being the Other category decreased the odds of myopia, all by between about 2 × and 5 ×. The Other category contained farmers, infants, and pre-school children.

Overall, our findings indicated that exposure to sunlight is necessary for the normal growth of the eye to attain emmetropia, thereby supporting the dopamine theory [14, 15]. In our study, we did not find a strong association between educational attainment and occurrence of myopia as suggested by most other studies [11, 12]. For example, Primary students had higher prevalence (26.1%) than Graduates (21.8%). Farmers, and those who did not attend schooling, had the least myopia (2.5%). Individuals with higher education might have myopia because they spend less time outdoors [7]. Randomised clinical trials of developmental myopia have reported that limited time outdoors is a larger causative factor than genetics [9].

The prevalence of lattice degeneration among the general population is reported at 6–8%, and approximately 30% among phakic RD patients [38, 39]. We found that 13.4% of presenting myopic eyes had lattice degeneration. Cases of lattice degeneration should be followed up closely because the incidence of RD in one eye is reported to be 2–5% over 7 years among the patients with bilateral lattice degeneration [40]. If the fellow eye did not have RD, the risk of RD is less than 1% over 11 years [39]. The literature reports that asymptomatic retinal breaks/holes occur in 6% of eyes in both clinical and autopsy studies [41]; but in our study, we found it only in 1.4% of myopic eyes. The risk of RD due to retinal break is reported as high as 15% if the RD had occurred in one eye previously even if the retinal breaks were asymptomatic [41]. Retinal breaks are associated statistically with RD at variable periods later on, so treatment with laser or cryoptherapy has been proposed even in asymptomatic cases [38]. In our study, we did prophylactic (barrage) laser therapy.

mCNVM occurs in approximately 5-10% of highly myopic patients, and 0.04–0.05% of the general population [42, 43]. The prevalence of mCNVM in our study was 0.4% across all ranges of myopia. It may occur at any degree of myopia and also in eyes without any typical myopic degenerative changes [44, 45]. It is a common vision-threatening complication of myopia and different treatment modalities like laser photocoagulation, photodynamic thermotherapy (PDT), and intravitreal injection of anti-vascular endothelial growth factors (anti-VEGF) are recommended [42, 46]. We have recently submitted a study of all surgical procedures during the course of the present study, which has the same authors as our study of retinal diseases in Bhutan [19], plus 3. That companion study gives the details of all surgical procedures, and indicates that the above cases were treated with anti-VEGF injections. Techniques for following up RRD and related foveal ischemia, and prognostic indicators, are improving with the advent of OCT angiography [47].

The study considered only moderate and high myopes referred to the VRSC for retinal evaluation to rule out complications secondary to myopia, excluding cases of simple myopia. However, this study is also based on a clinical sample, which would generally be expected to inflate the prevalence estimates in comparison with a population-representative sample. Thus, the prevalence reported in this study does not necessarily reflect the overall prevalence of myopia in Bhutan. The refraction of patients was not recorded; however, in being referred to the VRSC, the patients were clearly moderate to high myopes. Remoteness and need to travel might have prevented some myopes from the rural regions seeking VR consultation affecting the difference in the urban-rural prevalence of myopia.

Conclusions

Visual impairment due to uncorrected refractive errors, mainly myopia, is highly prevalent worldwide and is a major public health issue, especially in developing countries where access to refractive correction may be limited. The current study indicates that the prevalence of myopia, in a clinically selective population, is relatively low in Bhutan but nevertheless has similar demographic characteristics to other parts of Asia, including a higher prevalence in females, those from urban locations, and those who spend greater time indoors and in

education. Thus, the myopia epidemic is relatively less developed in Bhutan, than urban areas of East Asia; however, similar trends demonstrate the impact of lifestyle on the development of myopia. With increased schooling, urbanisation, and less time spent outdoors, the prevalence would be expected to increase. This offers an opportunity to promote protective lifestyle features such as greater time spent outdoors to keep the prevalence of myopia low and prevent pathological implications of high myopia. Complications of myopia like mCNVM, macular hole, and RRD if not treated in time will lead to irreversible blindness. These devastating complications can be avoided with simple refractive error checks including vision screening in schools. It is equally important to ensure that the patients use prescribed spectacles. Many patients are limited by poverty and so governments should provide free spectacles, or at least subsidise the cost. This may also improve the performance of students.

Availability of data and material The data and material are available from the corresponding author

Funding information The study was financially supported by the John Curtin School of Medical Research at the Australian National University.

Compliance with ethical standards

Conflict of interest The author declare that they have no conflict of interest.

Ethical approval, informed consent, and consent for publication The study was approved by the Research Ethics Board of Health (REBH), Ministry of Health, Royal Government of Bhutan, and was conducted as per the REBH guidelines and tenets of the Declaration of Helsinki. The consent was waived by REBH as the retrospective study collected only the de-identified data.

References

1. Pascolini D, Mariotti SP (2012) Global estimates of visual impairment: 2010. Br J Ophthalmol 96(5):614–618
2. Althomali TA (2018) Relative proportion of different types of refractive errors in subjects seeking laser vision correction. Open Ophthalmol J 12:53–62
3. Holden BA, Fricke TR, Wilson DA, Jong M, Naidoo KS, Sankaridurg P, Wong TY, Naduvilath TJ, Resnikoff S (2016) Global prevalence of myopia and high myopia and temporal trends from 2000 through 2050. Ophthalmology 123(5):1036–1042
4. Tano Y (2002) Pathologic myopia: where are we now? Am J Ophthalmol 134(5):645–660
5. Fricke TR, Holden BA, Wilson DA, Schlenther G, Naidoo KS, Resnikoff S, Frick KD (2012) Global cost of correcting vision impairment from uncorrected refractive error. Bull World Health Organ 90(10):728–738
6. Coppé AM, Ripandelli G, Parisi V, Varano M, Stirpe M (2005) Prevalence of asymptomatic macular holes in highly myopic eyes. Ophthalmology 112(12):2103–2109
7. Foster PJ, Jiang Y (2014) Epidemiology of myopia. Eye (Lond) 28(2):202–208
8. Smith TS, Frick KD, Holden BA, Fricke TR, Naidoo KS (2009) Potential lost productivity resulting from the global burden of uncorrected refractive error. Bull World Health Organ 87(6):431–437
9. Morgan IG, French AN, Ashby RS, Guo X, Ding X, He M, Rose KA (2018) The epidemics of myopia: Aetiology and prevention. Prog Retin Eye Res 62:134–149
10. Tedja MS, AEG H, Meester-Smoor MA, Kaprio J, Mackey DA, Guggenheim JA, Hammond CJ, Verhoeven VJM, Klaver CCW, Consortium C (2019) IMI - Myopia genetics report. Invest Ophthalmol Vis Sci 60(3):M89–M105
11. Dirani M, Shekar SN, Baird PN (2008) The role of educational attainment in refraction: the Genes in Myopia (GEM) twin study. Invest Ophthalmol Vis Sci 49(2):534–538
12. Verhoeven VJ, Buitendijk GH, Rivadeneira F, Uitterlinden AG, Vingerling JR, Hofman A, Klaver CC (2013) Education influences the role of genetics in myopia. Eur J Epidemiol 28(12):973–980
13. Czepita DA, Zejmo M (2011) Environmental factors and myopia. Ann Acad Med Stetin 57(3):88–92 discussion 92
14. French AN, Ashby RS, Morgan IG, Rose KA (2013) Time outdoors and the prevention of myopia. Exp Eye Res 114:58–68
15. Rose KA, Morgan IG, Ip J, Kifley A, Huynh S, Smith W, Mitchell P (2008) Outdoor activity reduces the prevalence of myopia in children. Ophthalmology 115(8):1279–1285
16. Feldkaemper M, Schaeffel F (2013) An updated view on the role of dopamine in myopia. Exp Eye Res 114:106–119
17. Ashby R (2016) Animal studies and the mechanism of myopia-protection by light? Optom Vis Sci 93(9):1052–1054
18. Pan CW, Ramamurthy D, Saw SM (2012) Worldwide prevalence and risk factors for myopia. Ophthalmic Physiol Opt 32(1):3–16
19. Rai BB, Morley MG, Bernstein PS, Maddess T (2020) Pattern of vitreo-retinal diseases at the national referral hospital in Bhutan: a retrospective, hospital-based study. BMC Ophthalmol 20(1):51
20. MoWHS (2011) Thromde Rules, 2011 of The Kingdom of Bhutan - ministry of works and human settlement. Royal Government of Bhutan. www.mowhs.gov.bt/wp-content/uploads/2010/11/tmodeA57-2-2012. Accessed 20 Oct 2019
21. Education Mo (2014) Bhutan Education Blueprint 2014-2024: Rethinking education. Royal Government of Bhutan. https://www.globalpartnership.org/sites/default/files/bhutan_education. Accessed 20 Oct 2019
22. Rai BB, Shresthra MK, Thapa R, Essex RW, Paudyal G, Maddess T (2019) Pattern and presentation of vitreo-retinal diseases: an analysis of retrospective data at a tertiary eye care center in Nepal. Asia-Pacific J Ophthalmol 8(6):481–488
23. Bhutan NSBo (2017) Bhutan Living Standards Survey Report 2017. http://www.nsb.gov.bt/publication/files/pub2yo10667rb.pdf. Accessed 25 June 2019
24. He M, Zheng Y, Xiang F (2009) Prevalence of myopia in urban and rural children in mainland China. Optom Vis Sci 86(1):40–44
25. Pan C-W, Wu R-K, Li J, Zhong H (2018) Low prevalence of myopia among school children in rural China. BMC Ophthalmol 18(1):140–140
26. Ministry of Health B (2018) Reproductive, maternal and neonatal health program. http://www.health.gov.bt/departments/dept-of-public-health/ncdd/reproductive-maternal-and-neonatal-health-program/. Accessed 7 July 2019
27. Morgan IG, Iribarren R, Fotouhi A, Grzybowski A (2015) Cycloplegic refraction is the gold standard for epidemiological studies. Acta Ophthalmol 93(6):581–585
28. Hashemi H, Khabazkhoob M, Asharlous A, Soroush S, Yekta A, Dadbin N, Fotouhi A (2016) Cycloplegic autorefraction versus subjective refraction: the Tehran Eye Study. Br J Ophthalmol 100(8):1122–1127
29. Wu P-C, Huang H-M, Yu H-J, Fang P-C, Chen C-T (2016) Epidemiology of myopia. Asia-Pacific J Ophthalmol 5(6):386–393

30. Saw SMKJ, Schein OD, Chew SJ, Chan TK (1996) Epidemiology of Myopia. Epidemiol Rev 18(2):175–187
31. Adhikari S, Nepal BP, Shrestha JK, Khandekar R (2013) Magnitude and determinants of refractive error among school children of two districts of Kathmandu, Nepal. Oman J Ophthalmol 6(3):175–178
32. Jung SK, Lee JH, Kakizaki H, Jee D (2012) Prevalence of myopia and its association with body stature and educational level in 19-year-old male conscripts in seoul, South Korea. Invest Ophthalmol Vis Sci 53(9):5579–5583
33. Garner LF, Owens H, Kinnear RF, Frith MJ (1999) Prevalence of myopia in Sherpa and Tibetan children in Nepal. Optom Vis Sci 76(5):282–285
34. JICA (2017) Survey of Country Gender Profile (Kingdom of Bhutan). Japan International Cooperation Agency. Accessed 8/4/2020 2020
35. Education Mo (2018) Annual Education Statistics 2018. Royal Government of Bhutan. http://www.education.gov.bt/wp-content/downloads/publications/aes/Annual-Education-Statistics-Book-2018.pdf. Accessed 12 Sept 2019
36. Morgan IG, Ohno-Matsui K, Saw SM (2012) Myopia. Lancet 379(9827):1739–1748
37. Travel B (2019) Meditation and Retreat https://www.bhutan.travel/activities/meditation-retreat. Accessed 11 Sept 2019
38. Wilkinson CP (2014) Interventions for asymptomatic retinal breaks and lattice degeneration for preventing retinal detachment. Cochrane Database Syst Rev 9:CD003170
39. Byer NE (1989) Long-term natural history of lattice degeneration of the retina. Ophthalmology 96(9):1396–1401 discussion 1401-1392
40. Folk JC, Arrindell EL, Klugman MR (1989) The fellow eye of patients with phakic lattice retinal detachment. Ophthalmology 96(1):72–79
41. Wilkinson CP, Rice TA (1997) Retinal Detachment, vol Year Book. Mosby, St Louis
42. Avila MP, Weiter JJ, Jalkh AE, Trempe CL, Pruett RC, Schepens CL (1984) Natural history of choroidal neovascularization in degenerative myopia. Ophthalmology 91(12):1573–1581
43. El Matri L, Chebil A, Kort F (2015) Current and emerging treatment options for myopic choroidal neovascularization. Clin Ophthalmol 9:733–744
44. Leveziel N, Yu Y, Reynolds R, Tai A, Meng W, Caillaux V, Calvas P, Rosner B, Malecaze F, Souied EH, Seddon JM (2012) Genetic factors for choroidal neovascularization associated with high myopia. Invest Ophthalmol Vis Sci 53(8):5004–5009
45. Ikuno Y, Jo Y, Hamasaki T, Tano Y (2010) Ocular risk factors for choroidal neovascularization in pathologic myopia. Invest Ophthalmol Vis Sci 51(7):3721–3725
46. Wong TY, Ohno-Matsui K, Leveziel N, Holz FG, Lai TY, Yu HG, Lanzetta P, Chen Y, Tufail A (2015) Myopic choroidal neovascularisation: current concepts and update on clinical management. Br J Ophthalmol 99(3):289–296
47. Lee JY, Kim JY, Lee SY, Jeong JH, Lee EK (2020) Foveal microvascular structures in eyes with silicone oil tamponade for rhegmatogenous retinal detachment: a swept-source optical coherence tomography angiography study. Sci Rep 10(1):2555

Publisher's note Springer Nature remains neutral with regard to jurisdictional claims in published maps and institutional affiliations.

New Frontiers in Ophthalmology

Research Article ISSN: 2397-2092

Surgical management of vitreoretinal diseases in Bhutan: A 3-year national study

Bhim B Rai[1,3]*, Michael G Morley[2], Pema Zangmo[3], Thukten Tshering[3], Abi N. Khatiwara[3], Paul S Bernstein[4] and Ted Maddess[1]

[1]John Curtin School of Medical Research, Australian National University, Canberra, ACT, Australia

[2]Ophthalmic Consultants of Boston, Harvard Medical School, Boston, MA, USA

[3]Department of Ophthalmology, JDW National Referral Hospital, Thimphu, Bhutan

[4]Moran Eye Centre, University of Utah School of Medicine, Salt Lake City, Utah, USA

Abstract

Purpose: To describe the pattern of vitreoretinal surgeries performed in Bhutan. This first national study informs policy making and resource development.

Methods: We reviewed the surgical registers of the three hospitals in Bhutan providing VR operations or interventional procedures for VR diseases over three years. Patient demography, indications and types of vitreoretinal surgeries were logged and quantified. Comparisons of the expected and observed frequency used Chi-squared tests.

Results: A total of 214 patients received vitreoretinal surgeries, 36 paediatric cases received examination under anaesthesia for diagnostic confirmation followed by vitreoretinal surgery or retinal laser. Additionally, 381 cases received intravitreal anti-vascular endothelial growth factor injections in the operating theatres as mandated in Bhutan. The mean age was 56.2 ± 22.3 years. The majority, 375 cases (59.4%) were males ($p<0.001$). The common indications for VR surgery were retinal detachment (45.1%), vitreous haemorrhage (13.6%), and macular hole (7.7%). Retinal detachment surgery was the most common surgery performed, followed by silicon oil removal with cataract surgery. The common indications for anti-vascular endothelial growth factor injection were neovascular age-related macular degeneration (168 cases, 44.12%), retinal vein occlusion (132 cases, 34.6%), and diabetic macular oedema and retinopathy (50 cases, 13.1%).

Conclusion: Performing high-tech vitreoretinal surgeries in a resource-limited setting is challenging. With an ever-increasing load of vitreoretinal diseases such as retinal detachment, age-related macular degeneration and macular hole, and the complications of systemic diseases such as retinal vein occlusion, vitreous haemorrhage, and diabetic macular oedema and retinopathy, there is a need to improve vitreoretinal services in Bhutan.

Introduction

The origin of vitreoretinal surgery dates back to the early 1970s, when Machemer first introduced pars plana vitrectomy (PPV) using a 17 Gauge (G) cutter [1,2]. The cutter size was improved 20G by O'Mally and Heintz [3], 23G [4], 25G [5,6] and now 27G [7] for sutureless micro-incision vitrectomy. The invention of chandelier endoillumination further enhanced vitrectomy precision [8]. Sterile air was the first tamponade agent used by Ohm in 1911, but it was only in 1938 when Rosengren successfully treated retinal detachment (RD) with diathermy and air tamponade and coined the term *tamponade* [9]. Now we have newer tamponade agents such as silicon oil, sulphur hexafluoride (SF6), perfluoroethane (C2F6), and perfluoropropane (C3F8) [10]. Introduction of the wide-angle viewing systems was an important milestone: giving a panoramic view of the retina, essential for meticulous and successful VR surgery [11]. Application of these modern techniques is a relatively new in Bhutan.

Bhutan's first and only VR surgeon (BBR) completed his Fellowship in 2011 through the Himalayan Cataract Project (HCP) Scholarship program. With additional support from the HCP VR sub-speciality Clinic (VRSC) was established in 2012 at the Jigme Dorji Wangcheck National Referral Hospital (JDWNRH), Thimphu, Bhutan. The concept of *right referrals* was the cornerstone for success of the planned national VR services, therefore he established two extension VR clinics in the Eastern and Central Regional Referral Hospitals (RRHs), which were visited by his VR-team periodically. Additionally, he trained the optometrists and ophthalmic technicians posted in the feeder District Hospitals and Basic Health Units in remote areas through nationwide workshops on screening for diabetic eye diseases and other VR disorders. Another hurdle was to convince doctors treating systemic diseases affecting the eyes, such as diabetes and hypertension, to refer their potential VR patients to local optometrists and ophthalmic technicians for screening and making right referrals to the new national VR service. It is also critical to understand that proliferative diabetic retinopathy has concurrent involvement of other organs such as kidney associated with glycosuria and albuminuria [12]. With right referrals, health advocacy, and multidisciplinary coordination a successful national VRSC was established.

The authors have published articles on the pattern of VR diseases in Bhutan [13] and Nepal [14]. The current work is a complementary

***Correspondence to:** Bhim Bahadur Rai, John Curtin School of Medical Research, Australian National University, Canberra, ACT 2601, Australia, E-mail: bhim.rai@anu.edu.au

***Key words:** vitreoretinal surgery, retinal surgery in Bhutan, retinal detachment, vitreous haemorrhage, anti-VEGF, macular hole*

Received: July 05, 2020; **Accepted:** September 02, 2020; **Published:** September 09, 2020

study reporting on the pattern of VR surgeries and other VR procedures performed in Bhutan over study period. Since this is the first study on VR surgeries in Bhutan the results have impact for policy making and management of VR diseases in Bhutan and other developing countries. It also provides a baseline for future studies.

Materials and methods

Participants

All the patients who received VR operations or interventional procedures for VR diseases in the OT at the JDWNRH and Eastern and Central RRHs over three years, which extended from 01 May 2013 to 30 April 2016, were included in this study.

Setting

The study was conducted at the VRSC, Ophthalmology Department, JDWNRH, Thimphu, Bhutan, and includes the patients managed by the same VR surgeon in the Eastern and Central RRHs. The JDWNRH is the apex national referral hospital in the country. All the VR patients requiring surgery and laser therapy across the country are referred there for management, except when the VR-team visited the Eastern and Central RRHs. JDWNRH also serves as the main clinical centre for the postgraduate medical students, interns, and optometric and paramedic students.

Study design and ethics

This was a retrospective study, approved by the Research Ethics Board of Health (REBH), Ministry of Health, Royal Government of Bhutan, Thimphu, Bhutan. This study adhered to the principles of the Declaration of Helsinki. Consent was waived by REBH because this retrospective study collected only de-identified data.

Clinical examination and data collection

The details of medical history taking, clinical examinations, equipment and diagnostic procedures are given in a previous publication [13]. The surgical registers maintained in the VR OT were reviewed for the study period. The data collected included demographic information such as age and gender, indications for VR surgery, and types of surgical procedures performed.

In case of children, the diagnoses were sometimes confirmed by examination under anaesthesia (EUA), following a proper pre-anaesthetic check-up (PAC). If indicated, other procedures such as retinal laser in cases of retinopathy of prematurity (ROP) were delivered in the same sitting. However, if major surgical procedure was indicated a subsequent procedure was planned.

In the VR surgery the OT Constellation Vision System vitrector (Alcon Company, Texas, USA) was used. A green laser system (OcuLight Green, IRIDEX, Germany) was used for endolaser (EL) and indirect ophthalmoscopic delivery laser procedures in the VR OT.

Quantification and statistical analysis

The data were analysed using MATLAB (2016b, The MathWorks, Natick, MA), including tabulating and checking frequencies of cases and creating figures and tables. Comparisons of the expected and observed frequency of gender used Chi-squared tests. Further details are given in an allied review of retinal disease in Bhutan [13] (Figure 1).

Results

Demography

A total of 214 patients received VR surgeries, and 36 paediatric cases received EUA followed by VR surgery or retinal laser. Additionally, 381 patients received anti-VEGF injections in the OT over the study period. The mean age at presentation was 56.2 ± 22.3. The majority (374) were males, and 256 cases females (40.6%) ($p<0.001$). Figure 1 shows the distributions of the ages of the patients by gender (Table 1).

VR surgeries

RD was the commonest VR disease indicated for VR surgery, accounting for 55 cases (23.4%). This was followed by cases who had already received RD surgery but needed secondary surgeries such as silicon oil (SO) removal following successful surgery, or as part of procedure for alleviating complications secondary to RD surgery. Thus, status post RD surgery as an indication was seen in 51 cases (21.7%), and in total 106 cases (45.1%) were operated for RD as an indication. Vitreous haemorrhage (VH), secondary to trauma, diabetic retinopathy (DR), retinal vein occlusion (RVO), and other retinal vasculitis, was seen in 32 cases (13.6%). Other indications were full-thickness macular hole (MH) in 18 cases (7.7%), dislocated cataract in 16 cases (6.8%), vitreomacular traction (VMT) or fibrovascular membrane (FVM) in 11 cases (4.7%), dislocated and decentered intraocular lens (IOL) in 9 cases (3.8%), endophthalmitis in 9 cases (3.8%), congenital cataract in 8 cases (3.4%), ROP in 8 cases (3.4%), ectopia lentis such as Marfan's syndrome in 5 cases (2.1%). In the subgroup of 9 cases of endophthalmitis 5 were traumatic, 2 cases following penetrating keratoplasty, 1 case after cataract operation with IOL implantation and 1 case of endogenous endophthalmitis. There were four cases of retained intraocular foreign body (RIOFB). One of them also had rhegmatogenous RD secondary to the RIOFB and had successful RIOFB removal and RD surgery. Other indications are shown in Table 2.

RD surgery was the most common VR surgery performed in 52 cases (22.9%). The procedures involved PPV, fluid-air exchange (FAE), EL and injection of SO for internal tamponade (5 cases received C3F8). Scleral band buckling (SBB) and membrane peeling were performed

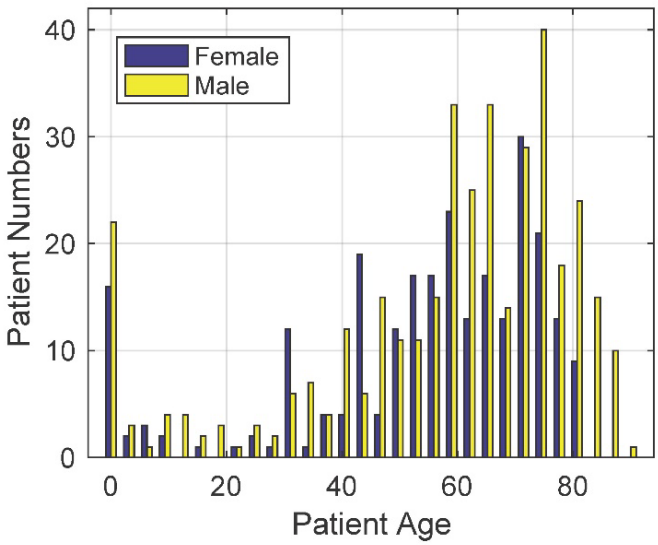

Figure 1. Age distributions of the patients in the study by gender

in 27 and 25 of the RD cases respectively. Silicon oil removal (SOR) combined with small incision cataract surgery (SICS) and intraocular lens (IOL) implantation was the second most common VR surgery performed in 45 cases (19.8%). PPV combined with lensectomy and IOL implantation was done in 28 cases (12.3%). In these cases, manual SICS was done additionally if rigid IOL implantation was planned. PPV combined with MP and EL was done 21 cases (9.3%). MH surgery was done in 18 cases (7.9%). This procedure involved PPV with internal limiting membrane (ILM) peeling with intravitreal injection of SF6 gas. PPV with removal of dislocated cataract or IOL was done in 16 cases (7.0%). Dislocated cataracts were mostly removed using the fragmatome procedure, a functional extension of the Constellation Vision System. Rigid IOLs were removed through the sclero-corneal tunnel incision. PPV (core vitrectomy) with intravitreal injections of antibiotics, with or without steroids, was done in 12 cases (5.3%). These were the cases of postoperative and traumatic endophthalmitis. Along with vitreous biopsy procedure for culture, and sensitivity tests for microbiology were also done. PPV with IOL reposition or exchange was done in 9 cases (4.0%). These cases had fully dislocated IOL into the vitreous cavity, or symptomatic subluxated or decentered IOLs affecting vision. PPV with other procedures was done in another 9 cases (4.0%). Retinal laser under general anaesthesia (EUA) was done in 8 cases (3.5%) of ROP. The details of the surgeries are summarised in Table 3. Four cases (1.8%) of retained intraocular foreign body (RIOFB) were operated. PPV was done and RIOFBs were removed manually with intraocular forceps or magnet through the extended PPV port, or corneo-scleral tunnel incision. One of the four RIOFB cases also had associated RD, which was managed with proper RD surgery procedure following removal of the RIOFB.

Table 1. Demographic characteristics of patients by basic surgery category. p-values indicate the significance of the difference in gender frequencies compared to 50%.

	N	Age	Males	Females	*p*
Vitreo-retinal (VR) surgery	214	49.5 ± 21.0	122	92	0.147
EUA* ± VR surgery /retinal laser	36	1.21 ± 2.27	22	14	0.346
Injection anti-VEGF**	381	65.2 ± 13.4	230	151	0.004

*EUA = Examination under anaesthesia; VEGF** = Vascular endothelial growth factor.

Table 2. Indications for Vitreo-retinal surgery

Indications	Number of cases	Percentage
Retinal Detachment (RD)	55	23.4
Status post RD Surgery	51	21.7
Vitreous haemorrhage*	32	13.6
Full-thickness macular hole	18	7.7
Dislocated Cataract	16	6.8
Vitreo-macular traction + Fibrovascular membrane	11	4.7
Dislocated and decentered Intraocular lens	9	3.8
Post-operative endophthalmitis	9	3.8
Congenital Cataract	8	3.4
Retinopathy of prematurity	8	3.4
Traumatic Endophthalmitis	5	2.1
Ectopia Lentis	5	2.1
Retained intraocular foreign body	4	1.7
Others**	4	1.7
Total	235	100.0

*VH=Traumatic, Diabetic retinopathy, RVO, Retinal vasculitis
**Others=Epiretinal membrane, vitreous opacities with pupillary and anterior hyaloid membranes, masquerades syndrome

Table 3. Types of Vitreo-retinal surgery

Type	Number of cases	Percentage
RD Surgery (±SBB+PPV±MP +FAE+EL+SOI or C3F8)	52	22.9
SOR+SICS+IOL	45	19.8
PPV+Lensectomy/SICS+IOL	28	12.3
PPV+MP+EL	21	9.3
Macular Hole Surgery (PPV+ILM peeling+SF6)	18	7.9
PPV+Removal of dislocated cataract/IOL	16	7.0
PPV+Intra-vitreal injection of antibiotics	12	5.3
PPV+IOL reposition/exchange	9	4.0
PPV+other procedures	9	4.0
Retinal laser for ROP	8	3.5
PPV+MP+SICS+IOL+EL+SOI	5	2.2
PPV+RIOFB removal	4	1.8
Total	**227**	**100.0**

Eleven cases excluded due to insufficient data. C3F8: perfluoropropane; EL: endolaser; FAE: Fluid-air exchange; ILM: internal limiting membrane; IOL: intraocular lens; MP: membrane peeling; PPV: pars plana vitrectomy; RIOFB: retained intraocular foreign body; ROP: retinopathy of prematurity; SBB: scleral band buckling; SF6: sulphur hexafluoride; SICS: small incision cataract surgery; SOI: silicon oil injection; SOR: silicon oil removal.

Examinations under anaesthesia

A total of 36 cases, mainly paediatric, received EUA following PCA. Within this subgroup, the majority were cases of ROP (24 cases). Eight of the 24 ROP cases required further surgical interventions in the form of retinal lasers, or RD surgery. The option of administering anti-VEGF was contemplated over laser therapy, but due to limited resources and limited funding laser therapy was commonly performed. There were 2 cases each of tractional RD and retinoblastoma. The retinoblastoma cases were referred to an advanced cancer centre in India. There was one case each of Coat's disease, retinitis pigmentosa (RP), traumatic retinal haemorrhage, congenital glaucoma, and Marfan's syndrome. Three cases undergoing EUA had normal retinas. The types of cases receiving EUA are shown in Supplementary Table S1.

Indications of intravitreal anti-VEGF injections among 381 patients who received it in the OT (as mandated in Bhutan) during the study period are shown in Table S2. Neovascular AMD (nAMD) was the most common indication for the injection (168 cases, 44.2%). Others included RVO (132 cases, 34.6%), DMO/DR (50 cases, 13.1%), myopic choroidal neovascular membrane (mCNVM) (11 cases, 0.03%), and polypoidal choroidal vasculopathy (PCV) (6 cases, 0.02%). Within the RVO subgroup, branch retinal vein occlusion (BRVO) was the most common subgroup with 70 cases (53.0% of RVO cases), followed by central retinal vein occlusion (CRVO) in 55 cases (41.7%) and hemi-retinal BRVO (HRBRVO) in 7 cases 5.3%).

Discussion

Our study on the pattern and presentation of VR diseases in Bhutan found that majority of patients were males [13]. This could explain why the majority of patients in this study receiving surgical management were also males. A meta-analysis of eye surgeries in developing countries reported that females receive fewer surgical services than males [15].

Here RD was the most common indication for VR surgery even though RD was reported by our prevalence study as being the seventh most common VR disease in Bhutan [13]. What caused this? The VRSC was established in Bhutan in early 2012 when the first national VR surgeon (BBR) joined the National Health Service. Before that VR

cases, including RD, were referred to India or Nepal. Most patients were reluctant to leave Bhutan for surgery, and consequently received no treatment, or employed traditional medicine sometimes resulting in irreversible loss of vision and even the loss of eyes. Therefore, after establishment of the VR service the number of RD cases was relatively large, and RD surgery was the most common VR surgery performed. That being said other relevant studies have reported higher prevalence of RD in Nepal [14], and more among Chinese than Indians in Singapore [16].

Before the national VR service Bhutanese patients returning home after surgery often had limited understanding of their condition and their post-operative care, due to language and cultural differences. Some of them had SO in their eyes for years, which converted into complications like secondary cataract, glaucoma, corneal decompensation, and failure of retinal attachment. Thus, SOR combined with SICS and IOL implantation was the second most common surgery performed over the study period. BBR preferred to use SO over expansible gases as the tamponade to manage RD because it is more likely to: produce reattachment, better postoperative visual acuity, and fewer postoperative complications [17,18]. Although the optimal timing for the SOR remains debatable, 3 to 6 months are commonly recommend for sustained retinal attachment [19,20]. Some retinal experts suggest SOR should be performed no longer than 6 months after its injection, and the best timing being 2 to 3 months post-injection [21], possibly avoiding complications such as keratopathy, glaucoma and visual loss [22].

VH secondary to DR, RVO, trauma and other retinal vasculitis, was the second commonest indication for VR surgery because of the high prevalence of HTR, DR, RVO and retinal vasculitis in Bhutan [13], as in nearby Nepal [14]. This demanded PPV to clear obstructive VH, with or without EL, to be performed commonly both for therapeutic and diagnostic purposes. For the same reason surgical procedures for FVM, VMT and tractional RD were also commonly performed because many of these were caused by highly prevalent DR, HTR and RVO [13]. There were eighteen cases of full-thickness MH received surgery during the study period although there were 76 eyes diagnosed with the condition [13]. This low surgical rate might be due to poor functional outcomes despite good success of MH surgery in general [23,24], which was explained to the patients and their party during counselling sessions before surgery. Another reason could be extended waiting times for surgery due to restricted availability of consumables required for MH.

Trauma was the fifth most common cause of injury requiring VR surgery in Bhutan [13], which resulted in cases of traumatic endophthalmitis and dislocated or subluxated cataract or IOL. Therefore, PPV with intravitreal injections of antibiotics with and without steroids to manage endophthalmitis, and PPV for retrieval, explant, reposition and exchange of IOL were performed commonly. Similarly, PPV for extraction of dislocated and subluxated cataract were commonly performed. Traumatic cases with associated RIOFB were managed with PPV and removal of foreign body with intraocular forceps through extended PPV port or corneoscleral tunnel. One such case developed RD secondary to RIOFB, which was managed with PPV with RIOFB removal combined with RD surgery. The case developed secondary cataract requiring SICS with IOL implantation successfully [25].

Although the number of ROP cases needing intervention was small (8) we feel this condition needs more attention. Firstly, the incidence of ROP is increasing world-wide [26-28], due to the increasing incidence of infants born at 24 weeks or earlier [26]. Increased oxygen use has improved survival rates and reduced cerebral palsy, but has increased the incidence of ROP [27]. The number of life-years affected by ROP is large [29]. Thus, it was estimated in 1996 that the global financial cost of childhood blindness in terms of lost earning capacity was between US$6 trillion and $27 trillion, surpassing the cost of adult blindness [30]. The generational cost-savings for society is approximately $516 million [31]. Finally, ROP management falls in the grey area between the VR specialist and the paediatric ophthalmologist, so there is a risk to proper follow up. Strong partnering between paediatric ophthalmologists, VR specialists, parents and neonatologists is therefore recommended, along with proper follow up mechanisms.

nAMD was the most common indication for anti-VEGF injection because AMD is the fourth most common VR disease in Bhutan [13]. Considering HTR and diabetes as risk factors for RVO [32], and both being common among the Bhutanese population, RVO cases received the second highest number of anti-VEGF injections. Although DR and DMO were the third most common VR diseases in Bhutan, and second most common in a related Nepal study [14], only a small proportion received anti-VEGF injection. Majority of such cases were managed with retinal laser. Only a small percentage of anti-VEGF injections was given to mCNVM cases because the prevalence of mCNVM among the myopes in Bhutan was only 0.4% [33]. Other studies have reported that mCNVM occurs in approximately 5-10% of highly myopic patients, and 0.04-0.05% of the general population [34,35].

This study is limited by the number of patients receiving VR surgery. Considering the national population of less than a million [36] the case number reported here is considerable. Unfortunately, we do not have data on visual acuity or outcomes of the surgery. Eleven operative cases were excluded due to incomplete data.

Conclusions

While VR services in Bhutan have advanced greatly in the last decade there is room for improvement, especially for common VR diseases such as AMD, DR, DMO, RVO, and myopic degenerations resulting in vision threatening atrophic retinal hole, mCNVM, and rhegmatogenous RD. Unfortunately, VR diseases secondary to systemic diseases such as hypertension and diabetes remain common [13]. There is an urgent need for collaboration between ophthalmologists, physicians, nutritionists, the patients and public to ameliorate these diseases. Yet another major priority is tackling ROP. A strong partnership between paediatric ophthalmologists, VR specialists, neonatologists, and parents is recommended.

Declarations

Funding

The study was supported by the John Curtin School of Medical Research at the Australian National University.

Conflict of interest

Author BBR declares that he has no conflict of interest. Author MGM declares that he has no conflict of interest. Author PZ declares that she has no conflict of interest. Author TT declares that he has no conflict of interest. Author ANK declares that he has no conflict of interest. Author PSB declares that he has no conflict of interest. Author TM declares that he has no conflict of interest.

Availability of data and materials

The data and materials are available with the first author BBR.

Ethical approval and standards

The study has been approved by the Research Ethics Board of Health (REBH), Ministry of Health, Royal Government of Bhutan, Thimphu, Bhutan, dated 06/12/2016 through approval number REBH/Approval/2016/083. All procedures performed in studies involving human participants were in accordance with the ethical standards of the REBH and in line with the principles of the Declaration of Helsinki.

Authors' contributions

BBR conceived of the study, collected data, did analysis and wrote the manuscript. MGM guided BBR and reviewed the manuscript. PZ collected data and reviewed the manuscript. TT collected data and reviewed the manuscript. ANK collected data and reviewed the manuscript. PSB guided BBR and reviewed the manuscript. TM helped with the analysis, reviewed the manuscript, and guided BBR closely. All authors read, reviewed, and approved the final manuscript.

References

1. Machemer R (1972) A new concept for vitreous surgery. 2. Surgical technique and complications. *Am J Ophthalmol* 74: 1022-1033. [Crossref]
2. Machemer R, Norton EW (1972) A new concept for vitreous surgery. 3. Indications and results. *Am J Ophthalmol* 74: 1034-1056. [Crossref]
3. O'Mally C, Heintz RM (1975) Vitrectomy with an alternative instrument system. *Ann of Ophthalmol* 7: 585-588. [Crossref]
4. Eckardt C (2005) Transconjunctival sutureless 23-gauge vitrectomy. *Retina* 25: 208-211. [Crossref]
5. de Juan E, Hickingbotham D (1990) Refinements in microinstrumentation for vitreous surgery. *Am J Ophthalmol* 109: 218-220. [Crossref]
6. Fujii GY, de Juan E, Humayun MS, Pieramici DJ, Chang TS, et al. (2002) A new 25-gauge instrument system for transconjunctival sutureless vitrectomy surgery. *Ophthalmology* 109: 1807-1812. [Crossref]
7. Oshima Y, Wakabayashi T, Sato T, Ohji M, Tano Y (2010) A 27–gauge instrument system for transconjunctival sutureless microincision vitrectomy surgery. *Ophthalmology* 117: 93-102.e102. [Crossref]
8. Oshima Y, Awh CC, Tano Y (2007) Self-retaining 27-gauge transconjunctival chandelier endoillumination for panoramic viewing during vitreous surgery. *Am J of Ophthalmol* 143: 166-167.e161. [Crossref]
9. Rosengren B (1938) Results of treatment of detachment of the retina with diathermy and injection of air into the vitreous. *Acta Ophthalmol* 16: 573-579.
10. Vaziri K, Schwartz SG, Kishor KS, Flynn HW Jr. (2016) Tamponade in the surgical management of retinal detachment. *Clin Ophthalmol* 10: 471-476.
11. de Oliveira PR, Berger AR, Chow DR (2016) Vitreoretinal instruments: vitrectomy cutters, endoillumination and wide-angle viewing systems. *Intl J Retina Vitreous* 2: 28.
12. Thapa R, Bajimaya S, Sharma S, Rai BB, Paudyal G (2014) Systemic association of newly diagnosed proliferative diabetic retinopathy among type 2 diabetes patients presented at a tertiary eye hospital of Nepal. *Nepal J Ophthalmol* 7: 26-32. [Crossref]
13. Rai BB, Morley MG, Bernstein PS, Maddess T (2020) Pattern of vitreo-retinal diseases at the national referral hospital in Bhutan: a retrospective, hospital-based study. *BMC Ophthalmol* 20: 51. [Crossref]
14. Rai BB, Shrestha MK, Thapa R, Essex RW, Paudyal G, et al. (2019) Pattern and Presentation of Vitreo-retinal Diseases: an analysis of retrospective data at a tertiary eye-care centre in Nepal. *Asia-Pacific J Ophthalmol* 8: 481-488. [Crossref]
15. Lewallen S, Courtright P (2002) Gender and use of cataract surgical services in developing countries. World Health Organization. https://www.who.int/bulletin/archives/80(4)300.pdf. Accessed November 5 2019
16. Wong TY, Tielsch JM, Schein OD (1999) Racial difference in the incidence of retinal detachment in Singapore. *Arch Ophthalmol* 117: 379-383.
17. Group TSS (1992) Vitrectomy with silicone oil or sulfur hexafluoride gas in eyes with severe proliferative vitreoretinopathy: results of a randomized clinical trial. Silicone Study Report 1. *Arch Ophthalmol* 110: 770-779. [Crossref]
18. Abrams GW, Azen SP, McCuen BW, Flynn HW Jr, Lai MY, et al. (1997) Vitrectomy with silicone oil or long-acting gas in eyes with severe proliferative vitreoretinopathy: results of additional and long-term follow-up. Silicone Study report 11. *Arch Ophthalmol* 115 (3):335-344. [Crossref]
19. Falkner CI, Binder S, Kruger A (2001) Outcome after silicone oil removal. *Br J Ophthalmol* 85: 1324-1327. [Crossref]
20. Casswell AG, Gregor ZJ (1987) Silicone oil removal. II. Operative and postoperative complications. *Br J Ophthalmol* 71: 898-902. [Crossref]
21. Jiang Y, Li X (1997) The best timing of silicone oil removal. *Zhonghua Yan Ke Za Zhi* 33: 39-41. [Crossref]
22. Hocaoglu M, Karacorlu M, Ersoz MG, Sayman Muslubas I, Arf S (2019) Vitrectomy with silicone oil tamponade for retinal detachment associated with giant retinal tears: Favourable outcomes without adjuvant scleral buckling. *Acta Ophthalmol* 97: E271-E276. [Crossref]
23. Zhao PP, Wang S, Liu N, Shu ZM, Zhao JS (2018) A review of surgical outcomes and advances for macular holes. *J Ophthalmol* 7389412.
24. Haritoglou C, Gass CA, Schaumberger M, Ehrt O, Gandorfer A, et al. (2001) Macular changes after peeling of the internal limiting membrane in macular hole surgery. *Am J Ophthalmol* 132: 363-368. [Crossref]
25. Rai BB, Dorji S, Zangmo P, Tshering T (2016) Retained intraocular metallic foreign body causing retinal detachment. *Bhutan Health J* 2: 48-52.
26. Isaza G, Donaldson L, Chaudhary V (2019) Increased incidence of retinopathy of prematurity and evolving treatment modalities at a Canadian tertiary centre. *Canadian J of Ophthalmol* 54: 269-274. [Crossref]
27. Holmstrom G, Tornqvist K, Al-Hawasi A, Nilsson A, Wallin A, et al. (2018) Increased frequency of retinopathy of prematurity over the last decade and significant regional differences. Acta Ophthalmol 96: 142-148. [Crossref]
28. Freitas AM, Morschbacher R, Thorell MR, Rhoden EL (2018) Incidence and risk factors for retinopathy of prematurity: a retrospective cohort study. *Int J Retina Vitreous* 4: 1-8.
29. Rahi JS, Gilbert CE, Foster A, Minassian D (1999) Measuring the burden of childhood blindness. *Br J Ophthalmol* 83: 387-388. [Crossref]
30. Decarlo DK, McGwin G Jr, Bixler ML, Wallander J, Owsley C (2012) Impact of pediatric vision impairment on daily life: results of focus groups. *Optom Vis Sci* 89: 1409-1416. [Crossref]
31. Dave HB, Gordillo L, Yang Z, Zhang MS, Hubbard GB, 3rd, et al. (2012) The societal burden of blindness secondary to retinopathy of prematurity in Lima, Peru. *Am J Ophthalmol* 154: 750-755.
32. Kolar P (2014) Risk factors for central and branch retinal vein occlusion: a meta-analysis of published clinical data. *J Ophthalmol* 2014: 724780. [Crossref]
33. Rai BB, Ashby R, French A, Maddess T (2020) Rural-urban differences in Myopia prevalence among myopes presenting to Bhutanese retinal clinical services: a 3-year national study. *Graef Arch Clin Exp Ophthalmol*. [Crossref]
34. Avila MP, Weiter JJ, Jalkh AE, Trempe CL, Pruett RC, et al. (1984) Natural history of choroidal neovascularization in degenerative myopia. *Ophthalmology* 91: 1573-1581.
35. El Matri L, Chebil A, Kort F (2015) Current and emerging treatment options for myopic choroidal neovascularization. *Clin Ophthalmol* 9: 733-744. [Crossref]
36. Population and Housing Census of Bhutan 2017 (2017) National Report. http://www.nsb.gov.bt/publication/files/PHCB2017_national.pdf. Accessed 2019 January

Copyright: ©2020 Rai BB. This is an open-access article distributed under the terms of the Creative Commons Attribution License, which permits unrestricted use, distribution, and reproduction in any medium, provided the original author and source are credited.

Surgical management of vitreoretinal diseases in Bhutan: a 3-year national study.

Supplementary Tables: 2

TABLE S1. Examinations under Anaesthesia (EUA)

Types of cases	**Number of cases**		**Percentage**
Retinopathy of Prematurity	24		66.7
Tractional reinal detachment	2		5.6
Retinoblastoma	2		5.6
Coat's disease	1		2.8
Congenital glaucoma	1		2.8
Marfan's syndrome	1		2.8
Retinal haemorrhage	1		2.8
Retinitis pigmentosa	1		2.8
Normal fundus	3		8.3
Total	**36**		**100**

TABLE S2. Indications for anti-VEGF Injection

Indications	*Number of cases*	*Percentage*
Neovascular AMD	168	44.2
Retinal Vein Occlusion	132	34.6
Diabetic Macular Oedema	50	13.1
Myopic CNVM	11	0.03
Polypoidal Choroidal Vasculopathy	6	0.02
Neovascular Glaucoma	4	0.01
*Others**	10	0.03
Total	381	100.00

2 cases of injection were excluded as the indications were not recorded.

*Others include Cystoid macular oedema, Central serous chorioretinopathy and Vitreomacular traction

Rai *et al. BMC Ophthalmology* (2020) 20:404
https://doi.org/10.1186/s12886-020-01675-8

BMC Ophthalmology

RESEARCH ARTICLE Open Access

Retinal laser services in Bhutan: a 3-year national survey

Bhim B. Rai[1,2*], Michael G. Morley[3], Pema Zangmo[2], Thukten Tshering[2], Abi N. Khatiwara[2], Paul S. Bernstein[4] and Ted Maddess[1]

Abstract

Background: We conducted this study to report on the indications and types of retinal laser therapy (RLT) performed in Bhutan, knowing which is critical for proper planning and successful delivery of the services.

Methods: We reviewed the laser registers maintained in the laser rooms and vitreoretinal (VR) operating theatres (including paediatric cases managed under anaesthesia) over three years at the national and the two regional referral hospitals (RRHs). Intraoperative laser treatments (endolaser) were excluded. Patient demography, indications and types of RLT were recorded and quantified. Comparisons of the expected and observed frequencies used Chi-squared tests.

Results: A total of 685 patients, including 8 cases of bilateral retinopathy of prematurity (ROP) received RLT. The majority of patients (411 cases, 60.0%, $p < 0.0001$) were males. The mean age was 54.1 ± 14.1 years, median 56 years. The most common indications for RLT were diabetic retinopathy (DR) and diabetic macular oedema (DMO) (542 cases, 66.0%), followed by retinal vein occlusion (RVO) (91 cases, 13.3%). Pan-retinal photocoagulation was the most common type of RLT performed (337 cases, 49.2%), followed by modified grid laser (207 cases, 30.2%), sectoral laser (41 cases, 6.0%), and prophylactic laser photocoagulation (33 cases, 4.8%).

Conclusions: The majority of patients were within working-age. Common indications for RLT were preventable such as DR, DMO and RVO, indicating need to control systemic diseases such as diabetes, hypertension, and dyslipidaemia. Currently, regular RLT is provided only at the national referral hospital in Thimphu, and periodically in the eastern and central RRHs when the retinal specialist visits. There is need to extend the retinal services to the eastern and central RRHs to improve accessibility and patient coverage in these regions challenged with difficult terrain and poor public transport system.

Keywords: Laser therapy, Laser services in Bhutan, pan-retinal photocoagulation, Photocoagulation, Retinal laser

Background

The therapeutic benefits of laser were first reported in 1954 [1]. This prompted the invention of xenon-arc laser in 1956 for prophylaxis of retinal detachment (RD), but it was limited by poor focus [2]. The first ophthalmic laser was developed in 1960 using a ruby laser [3] marking a big leap forward in the history of retinal laser therapy (RLT) with its blue and green light emissions [4]. Another milestone was the invention of the 532 nm frequency-doubled neodymium-doped yttrium aluminium garnet (Nd:YAG) laser [5]. The macular laser treatment is not considered a standard treatment of care anymore, and has been replaced by intravitreal anti-vascular endothelial growth factor (anti-VEGF) treatment in many places. However, it may probably still be

* Correspondence: bhim.rai@anu.edu.au
[1]John Curtin School of Medical Research, Australian National University, Canberra, ACT 2601, Australia
[2]Department of Ophthalmology, JDW National Referral Hospital, Thimphu, Bhutan
Full list of author information is available at the end of the article

© The Author(s). 2020 **Open Access** This article is licensed under a Creative Commons Attribution 4.0 International License, which permits use, sharing, adaptation, distribution and reproduction in any medium or format, as long as you give appropriate credit to the original author(s) and the source, provide a link to the Creative Commons licence, and indicate if changes were made. The images or other third party material in this article are included in the article's Creative Commons licence, unless indicated otherwise in a credit line to the material. If material is not included in the article's Creative Commons licence and your intended use is not permitted by statutory regulation or exceeds the permitted use, you will need to obtain permission directly from the copyright holder. To view a copy of this licence, visit http://creativecommons.org/licenses/by/4.0/. The Creative Commons Public Domain Dedication waiver (http://creativecommons.org/publicdomain/zero/1.0/) applies to the data made available in this article, unless otherwise stated in a credit line to the data.

considered as a treatment option if anti-VEGF treatment is not available or limited for socio-economic reasons. It is reported that anti-VEGFs have significantly superior efficacy to laser photocoagulation in diabetic macular oedema (DMO) [6, 7], retinal vein occlusion (RVO) [8], and retinopathy of prematurity (ROP) [9]. In Bhutan, RLT was still considered for retinal disorders such as DMO, diabetic retinopathy (DR), RVO, retinal breaks, ROP, and retinal vasculitis (RV) for economic reasons. The different types of RLT are focal, grid, modified grid, sectoral, scatter, and pan-retinal photocoagulation (PRP).

The aim of the current study was to report on the number, indications and types of RLT, including prophylactic laser photocoagulation (PLP) performed in the whole of Bhutan. This is a complementary article to other studies published by the same authors: first, the pattern of vitreoretinal (VR) diseases in Bhutan, which describes about the ocular comorbidities, associated systemic diseases, clinical data, diagnostic tests performed, and treatment strategies [10]; second, rural-urban difference in myopia prevalence in Bhutan, which gives additional information on patient demography [11]; and third, the surgical management of VR diseases in Bhutan [12]. Since this is the first study of RLT in Bhutan, the results have impacts for policy making on the management of VR diseases in Bhutan and other developing countries. It also serves as a baseline study for future research.

Methods

Study design

This retrospective study was approved by the Research Ethics Board of Health (REBH), Ministry of Health, Royal Government of Bhutan, and adhered to the principles of Declaration of Helsinki. Consent was waived by the REBH because only de-identified data were collected.

Setting

The study was conducted mainly at the VR Subspeciality Clinic (VRSC), Ophthalmology Department, Jigme Dorji Wangchuck National Referral Hospital (JDWNRH), Thimphu, and includes cases receiving RLT in the Eastern Regional Referral Hospital (ERRH) in Monggar, and Central Regional Referral Hospital (CRRH) in Gelephu. The JDWNRH is the apex national referral hospital with tertiary eye-care services in the pyramidal health infrastructure system, supported by the ERRH and CRRH, District Hospitals and Basic Health Units (BHUs) in more remote regions. JDWNRH serves as the main centre providing VR services and as a clinical centre for postgraduate medical students, interns, and optometric and paramedic students.

Participants

All the patients who received RLT and PLP for VR diseases in Bhutan: JDWNRH, ERRH and CRRH in the study period (01 May 2013 until 30 April 2016) were included. We have reported by the number of patients, not the laser sessions. For example, the PRP per case was usually covered in two sessions, but we counted as one case only. Intraoperative laser treatments such as endolaser during retinal detachment repair or during diabetic vitrectomy were excluded.

Clinical examination and data collection

The details of medical history taking, clinical examinations, equipment and diagnostic procedures are given in a previous publication [10]. The laser registers maintained in the laser room (LR) in the VR operating theatre (OT) of JDWNRH, ERRH and CRRH were reviewed. Demographic information such as age and gender, number, indications for RLT, and types of RLT were collected.

In paediatric cases, the diagnoses were confirmed by examination under anaesthesia (EUA), following a proper pre-anaesthetic check-up (PAC). If indicated, the RLT was delivered in the same sitting.

Laser specifications: machine, mode of delivery and types of laser therapies

The majority of patients received RLT in the LR of the out-patient department using a Nd:YAG (VISULAS 532 s, Zeiss Medical Technology, U.K.) frequency doubled laser system. The conventional single-spot slit-lamp delivery method was applied, except in extreme peripheral lesions, where the binocular indirect ophthalmoscopic (BIOM) method was used. For paediatric cases, the green diode laser system (OcuLight Green, IRIDEX, Germany) was used with the BIOM technique. PRP was performed for: generalised retinal involvement such as diabetic retinopathy (DR) and central retinal vein occlusion (CRVO); sectoral laser in branch retinal vein occlusion (BRVO), and hemiretinal BRVO (HRBRVO); and scatter laser in RV. PLP was performed for retinal breaks such as retinal tear and atrophic retinal hole, retinal thinning, chorio-retinal (CR) colobomata, and localised tractional band or tractional retinal detachment (TRD). Confluent laser burns of 2–3 rows around the lesions were performed. Focal laser was delivered for focal pathology such as focal DMO, or lysis of posterior hyaloid membrane in subhyaloid macular haemorrhage. Modified grid or grid focal laser was performed in diffuse DMO. In ROP, the avascular zone including a small rim of normal retina was covered to prevent future TRD.

Table 1 Demographic characteristics of patients

Category of patients	Number of patients	Presentation age (mean ± SD)	Minimum age	Median age	Maximum age
All patients, years	685	54.1 ± 14.1	0.2	56	87
Patients treated in LR[a], years	677	54.8 ± 12.9	10	56	87
Patients treated in OT[b], years	8	0.28 ± 0.09	0.2	0.25	0.4

[a]*LR* Laser Room, [b]*OT* Operating Theatre under general anaesthesia

Statistical analysis

The data were analysed using MATLAB (2016b, The MathWorks, Natick, MA). Comparisons of the expected and observed frequency of gender used Chi-squared test.

Results

Demography

A total of 685 patients received RLT over the study period. The mean age was 54.1 ± 14.1 years (range 0.2 to 87 years), median 56 years. The majority of patients (411 cases, 60.0%, $p < 0.0001$) were males. The infants who received RLT for ROP ranged from 0.2 to 0.4 years. Other demographic details are shown in Table 1.

Indications of retinal laser therapy

DR and DMO were the most common indications for RLT, accounting for 542 cases (66.0% of total laser cases) as shown in Table 2. The second most common indication was for RVO in 91 cases (13.3%). Within the sub-group of RVO, BRVO was the most common diagnosis in 49 cases (53.8% of RVO cases), followed by CRVO in 32 cases (35.2%), and HRBRVO in 10 cases (11.0%). There were 47 cases (6.9%) who received PLP. Retinal breaks in the form of retinal tear due to trauma or traction, and atrophic retinal hole secondary to myopic degeneration were encountered in 36 cases (5.3%) who received RLT. RV was also a common indication seen in 17 cases (2.5%). Eight cases of ROP received RLT bilaterally under general anaesthesia in the VR OT. There were 6 cases of CR coloboma and 4 cases of Coats' disease. There were 24 miscellaneous cases over the study period. Table 2.

Types of retinal laser therapy

The different types of RLT performed were PRP, sectoral involving one quadrant of the retina, scatter, PLP, focal, grid, modified grid (grid + focal), and peripheral laser for ROP (Table 3). PRP was the most common type of RLT performed in 337 cases (49.2%) of severe, very severe and proliferative DR, and CRVO. Modified grid laser (combined grid and focal) was the second most common RLT accounting for 207 cases (30.2%) of diffuse DMO associated with focal leakage secondary to microaneurysms. The sectoral laser performed in cases of BRVO and some cases of extensive RV was the third most common type in 41 cases (6.0%). PLP was performed in 33 cases (4.8%); the common indications were retinal breaks, localised tractional bands or localised TRD, and CR colobomata. Twenty-three cases (3.4%) of DMO with no obvious identified leakage site received grid laser. Focal laser was performed in 16 cases (2.3%) of DMO with localised leakage. There were 8 cases of ROP who received RLT bilaterally following PAC and EUA in the VR OT.

Discussion

Globally, the mortality from non-communicable diseases represented 72.3% of total deaths in 2016 [13]. In Bhutan, the World Health Organization (WHO) reported that 28% of total mortality in Bhutan was due to

Table 2 Indications of Laser therapies

Indications	Number	Percentage
Diabetic retinopathy / macular oedema	452	66.0
Retinal Vein Occlusion	91	13.3
Localised TRD[a] / FV[b]	47	6.9
Retinal breaks (Tear / hole)	36	5.3
Retinal Vasculitis	17	2.5
Retinopathy of prematurity	8	1.2
Chorio-retinal coloboma	6	0.9
Coats' disease	4	0.6
Others	24	3.5
Total	**685**	**100.0**

[a]*TRD* Tractional Retinal Detachment, [b]*FVT* Fibro-Vascular Traction

Table 3 Types of retinal laser therapy

Types	Number	Percentage
Pan-retinal photocoagulation	337	49.2
Modified Grid (grid + focal)	207	30.2
Sectoral	41	6.0
Prophylactic / barrage	33	4.8
Grid	23	3.4
Scatter	20	2.9
Focal	16	2.3
Laser for ROP cases	8	1.2
Total	**685**	**100.00**

cardiovascular disease, and another 17% due to other non-communicable diseases in 2016 [14]. The risk factors included harmful use of alcohol, high salt intake, unhealthy diet, physical inactivity, and tobacco use [15]. The prevalence of diabetes and hypertension was 8.2 and 26.0% respectively among the urban Bhutanese men and women, and 54.1% of the diabetes population had hypertension [16]. In our study on pattern of VR diseases in Bhutan the coexistent diabetes and hypertension was the commonest systemic disease associated, followed by isolated hypertension and diabetes [10]. The global prevalence of diabetes is reported at 9.3%, with higher prevalence in the high-income (10.4%) than low-income (4.0%) countries [17].

Although the RLT was an established first line therapy for a number of vascular disorders such as DR and DMO [18], RVO [19], RV [20], ROP [21], and Coats' disease [22], now it is replaced by anti-VEGF injection in developed countries. In Bhutan it is still performed to treat above mentioned diseases for economic reasons.

Our study of the pattern and presentation of VR diseases in Bhutan [10] and a similar study in Nepal [23] reported that the majority of patients were males (60.3 and 53.0% respectively). That trend was followed here for patients receiving RLT, 60.0% of whom were males.

DR/DMO as the most common VR disorder requiring RLT was expected because it was the third most common VR disease in Bhutan [10]. PRP for DR, and focal, grid, and modified grid for DMO were commonly performed in the developing countries for economic reasons. It is still effective in improving vision and arresting progression of DR [18]. RVO was the second most common indication for RLT because RVO, and its risk factors such as hypertension and diabetes, are common in Bhutan [10]. In DR/DMO and RVO works by reducing the oxygen demand of the outer retina [24].

We successfully performed PLP in cases of localised TRD and rhegmatogenous RD. This is supported by a study reporting on the efficacy of PLP in such cases [25]. Another effective use of laser is for retinal breaks, lattice degeneration and retinal thinning, preventing occurrence of vision-threatening secondary RD [26]. Similarly, we applied PLP for myopic degeneration and retinal tears due to trauma or tractional force. Comparatively, there were very less cases of retinal break availing PLP. This could partly be explained by the low prevalence of myopia in Bhutan [11]. With increasing prevalence of myopia, including pathological myopia, in South-East Asia [27], and high prevalence of myopia, especially among urbanites in Bhutan [11], there is a growing need for screening and treating such complications to prevent vision threatening complications such as RD.

RV was a common indication for RLT in Bhutan [10]. It is popularly known as Eales' disease and is associated with *Mycobacterium tuberculosis* infection as its etiopathogenesis [20]. Tuberculosis is still reported to be common in Bhutan, with a total incidence of 149 cases per 100,000 population in 2018 [28]. Some of the patients receiving RLT for RV were Indian nationals working as labourers in Bhutan, and tuberculosis is reported to be common in India [29].

During early development, the retina lacks blood vessels and depends on the primary vitreous for oxygen and nutrients [30]. The vascularisation of the retina commences at 12 weeks and is nearly completed by 36–40 weeks gestation [21]. This process is dependent on hypoxia-induced production of VEGF [31]. Upon premature delivery, the developing retina faces abrupt withdrawal of maternal IGF-1, and faces a relatively hyperoxic external environment. This down regulates VEGF and erythropoietin, resulting in cessation of vascularisation and vaso-obliteration, leaving the peripheral retina avascular. However, increased metabolic activity of the maturing retina becomes hypoxic, upregulating the whole process and leading to retinal neovascularisation and ROP development [21, 32]. The Early Treatment for ROP (ETROP) has reported favourable outcomes with early treatment and has provided new treatment guidelines [33]. The BEAT-ROP study reported treatment with anti-VEGF is superior to the laser treatment because the anterior segment development is present when treated with anti-VEGF and prevents development of very high myopia [9]. We treated the ROP with RLT due to economic constraints.

CR coloboma is a risk for developing RD and higher recurrence after surgery [34]. We performed PLP successfully, which is reported effective to reduce RD [34].

Coats' disease, characterised by abnormal telangiectasia, retinal exudation, and serous RD, is a vision-threatening disorder that has poor visual prognosis [35]. We managed them with RLT, although other treatment modalities have been advised including anti-VEGF [36].

PRP was the most common RLT performed in our study because VR diseases requiring PRP such as DR and CRVO were very common in Bhutan [10], and in Nepal too [23]. Similarly, modified grid laser was the second most common laser procedure performed because DR and DMO were common [10]. RLT is still the most common and standard treatment for DR and DMO in developing countries for economic reasons [37]. Sectoral RLT was also commonly performed because of higher prevalence of BRVO, HRBRVO, and RV involving extensive retina [10].

The study has some limitations. This is a retrospective and the first exploratory study on retinal laser services in Bhutan. We do not have the data on visual acuities and outcomes of the RLT procedures. Regular RLT was performed only at the JDWNRH, with only periodic visits

to the ERRH and CRRH by the retinal specialist for delivering the services. This might have left out some patients in the eastern and central regions despite a good patient referral system.

Conclusions

Despite being a small country with a population of less than a million [38], Bhutan faces a wide spectrum of VR disorders [10]. Systemic diseases such as diabetes and hypertension which are risk factors for VR disorders are common and increasing [10]. Although the surgical management of VR diseases in Bhutan utilizes diversified treatment approaches [12], the range of RLT performed in this study through the national VR service is still in the early stages of development. Currently, the VR services are mainly provided at the JDWNRH in Thimphu, with periodic visits by the VR team to the ERRH and CRRH. There is need to expand the VR service to the ERRH and CRRH to cover the eastern and central regions which are particularly challenging because of difficult terrain and poor transport services.

Abbreviations

BCVA: Best corrected visual acuity; BRVO: Branch retinal vein occlusion; CRVO: Central retinal vein occlusion; DMO: Diabetic macular oedema; DR: Diabetic retinopathy; EUA: Examination under anaesthesia; HTR: Hypertensive retinopathy; IOL: Intra-ocular lens; OCT: Optical coherence tomography; PPV: Pars plana vitrectomy; PAC: Pre-anaesthetic checkup; RD: Retinal detachment; ROP: Retinopathy of prematurity; RNFL: Retinal nerve fibre layer; RV: Retinal vasculitis; RVO: Retinal vein occlusion; VEGF: Vascular endothelial growth factor

Acknowledgements

None.

Authors' contributions

BBR conceived of the study, collected data, did analysis and drafted the manuscript. PSB guided BBR and reviewed the manuscript. MGM guided BBR and reviewed the manuscript. PZ collected data, assisted in analysis and reviewed the manuscript. TT collected data, assisted in analysis and reviewed the manuscript. ANK collected data, assisted in analysis and reviewed the manuscript. TM helped with the analysis, reviewed the manuscript and guided BBR closely. All authors read, reviewed and approved the final manuscript.

Funding

The study was supported by the John Curtin School of Medical Research at the Australian National University.

Availability of data and materials

The data have not been placed in any online data storage. The datasets generated and analysed during the study are available upon request from the first author.

Ethics approval and consent to participate

Ethical approval for this study was approved by the Research Ethics Board of Health (REBH), of the Ministry of Health, Royal Government of Bhutan, Thimphu, Bhutan (REBH/Approval/2016/083, dated 6th December, 2016), and adhered to the principles of the Declaration of Helsinki. The REBH granted the administrative permission to access to the data used in our research. The need for consent by individual participants was waived by REBH because this retrospective study collected only de-identified data.

Consent for publication

Not Applicable.

Competing interests

None.

Author details

[1]John Curtin School of Medical Research, Australian National University, Canberra, ACT 2601, Australia. [2]Department of Ophthalmology, JDW National Referral Hospital, Thimphu, Bhutan. [3]Ophthalmic Consultants of Boston, Harvard Medical School, Boston, MA, USA. [4]Moran Eye Centre, University of Utah School of Medicine, Salt Lake City, UT, USA.

Received: 29 June 2020 Accepted: 5 October 2020
Published online: 08 October 2020

References

1. Meyer-Schwickerath G. Light coagulation; a method for treatment and prevention of the retinal detachment. Albrecht von Graefes Archiv Ophthalmol. 1954;156(1):2–34.
2. Meyer-Schwickerath G. Prophylactic treatment of retinal detachment by light-coagulation. Trans Ophthalmol Soc U K. 1956;76:739–50.
3. Kapany NS, Peppers NA, Zweng HC, Flocks M. Retinal photocoagulation by lasers. Nature. 1963;199:146–9.
4. L'Esperance FA Jr. An opthalmic argon laser photocoagulation system: design, construction, and laboratory investigations. Trans Am Ophthalmol Soc. 1968;66:827–904.
5. Jalkh AE, Pflibsen K, Pomerantzeff O, Trempe CL, Schepens CL. A new solid-state, frequency-doubled neodymium-YAG photocoagulation system. Arch Ophthalmol. 1988;106(6):847–9.
6. Regnier S, Malcolm W, Allen F, Wright J, Bezlyak V. Efficacy of anti-VEGF and laser photocoagulation in the treatment of visual impairment due to diabetic macular edema: a systematic review and network meta-analysis. Plos One. 2014;9(7):e102309.
7. Muston D, Korobelnik JF, Reason T, Hawkins N, Chatzitheofilou I, Ryan F, et al. An efficacy comparison of anti-vascular growth factor agents and laser photocoagulation in diabetic macular edema: a network meta-analysis incorporating individual patient-level data. BMC Ophthalmol. 2018;18(1):340.
8. Tan MH, McAllister IL, Gillies ME, Verma N, Banerjee G, Smithies LA, et al. Randomized controlled trial of intravitreal ranibizumab versus standard grid laser for macular edema following branch retinal vein occlusion. Am J Ophthalmol. 2014;157(1):237–47 e1.
9. Geloneck MM, Chuang AZ, Clark WL, Hunt MG, Norman AA, Packwood EA, et al. Refractive outcomes following bevacizumab monotherapy compared with conventional laser treatment: a randomized clinical trial. JAMA Ophthalmol. 2014;132(11):1327–33.
10. Rai BB, Morley MG, Bernstein PS, Maddess T. Pattern of vitreo-retinal diseases at the national referral hospital in Bhutan: a retrospective, hospital-based study. BMC Ophthalmol. 2020;20(1):51.
11. Rai BB, Ashby RS, French AN, Maddess T. Rural-urban differences in myopia prevalence among myopes presenting to Bhutanese retinal clinical services: a 3-year national study. Graefes Archive Cln Exp Ophthalmol. 2020;258. https://doi.org/10.1007/s00417-020-04891-6.
12. Rai BB, Morley MG, Zangmo P,Tshering T, Khatiwara AN, Bernstein PS, Maddess T. Surgical management of vitreo-retinal diseases in Bhutan: a 3-year national study. New FrontOphthalmol. 2020;6:1–5. https://doi.org/10.15761/NFO.1000251.
13. Collaborators GBDCoD. Global, regional, and national age-sex specific mortality for 264 causes of death, 1980-2016: a systematic analysis for the global burden of disease study 2016. Lancet. 2017;390(10100):1151–210.
14. WHO. Noncommunicable Diseases/Country Profiles. 2016 [cited 2020 01 September]. Available from: https://www.who.int/nmh/countries/btn_en.pdf?ua=1.
15. Pelzom D, Isaakidis P, Oo MM, Gurung MS, Yangchen P. Alarming prevalence and clustering of modifiable noncommunicable disease risk factors among adults in Bhutan: a nationwide cross-sectional community survey. BMC Public Health. 2017;17.
16. Giri BR, Sharma KP, Chapagai RN, Palzom D. Diabetes and hypertension in urban bhutanese men and women. Indian J Community Med. 2013;38(3):138–43.
17. Saeedi P, Petersohn I, Salpea P, Malanda B, Karuranga S, Unwin N, et al. Global and regional diabetes prevalence estimates for 2019 and projections for 2030 and 2045: Results from the International Diabetes Federation Diabetes Atlas, 9(th) edition. Diabetes Res Clin Pract. 2019;157:107843.

18. Group TDRSR. Indications for photocoagulation treatment of diabetic retinopathy: diabetic retinopathy study report no. 14. Int Ophthalmol Clin. 1987;27(4):239–53.
19. Fekrat S, Goldberg MF, Finkelstein D. Laser-induced chorioretinal venous anastomosis for nonischemic central or branch retinal vein occlusion. Arch Ophthalmol. 1998;116(1):43–52.
20. Biswas J, Ravi RK, Naryanasamy A, Kulandai LT, Madhavan HN. Eales' disease - current concepts in diagnosis and management. J Ophthalmic Inflamm Infect. 2013;3(1):11.
21. Houston SK, Wykoff CC, Berrocal AM, Hess DJ, Murray TG. Laser treatment for retinopathy of prematurity. Lasers Med Sci. 2013;28(2):683–92.
22. Kodama A, Sugioka K, Kusaka S, Matsumoto C, Shimomura Y. Combined treatment for Coats' disease: retinal laser photocoagulation combined with intravitreal bevacizumab injection was effective in two cases. BMC Ophthalmol. 2014;14:36.
23. Rai BB, Shresthra MK, Thapa R, Essex RW, Paudyal G, Maddess T. Pattern and presentation of Vitreo-retinal diseases: an analysis of retrospective data at a tertiary eye Care Center in Nepal. Asia-Pac J Ophthalmo. 2019;8(6):481–8.
24. Stefansson E. The mechanism of retinal photocoagulation – how does the laser work? United Kingdom: European Ophthalmic Review; 2009. p. 76–9. https://doi.org/10.17925/EOR.2009.02.01.76.
25. Shukla D, Maheshwari R, Kim R. Barrage laser photocoagulation for macula-sparing asymptomatic clinical rhegmatogenous retinal detachments. Eye (Lond). 2007;21(6):742–5.
26. Mastropasqua L, Carpineto P, Ciancaglini M, Falconio G, Gallenga PE. Treatment of retinal tears and lattice degenerations in fellow eyes in high risk patients suVering retinal detachment: a prospective study. Br J Ophthalmol. 1999;83:1046–9.
27. Morgan IG, French AN, Ashby RS, Guo X, Ding X, He M, et al. The epidemics of myopia: Aetiology and prevention. Prog Retin Eye Res. 2018;62:134–49.
28. WHO. Bhutan: Tuberculosis profile 2018. Geneva: WHO; 2018. updated 28.01. 2020. Available from: http://www.who.int/tb/data/.
29. Chakraborty AK. Epidemiology of tuberculosis: current status in India. Indian J Med Res. 2004;120(4):248–76.
30. Goldberg MF. Persistent fetal vasculature (PFV): an integrated interpretation of signs and symptoms associated with persistent hyperplastic primary vitreous (PHPV). LIV Edward Jackson memorial lecture. Am J Ophthalmol. 1997;124(5):587–626.
31. Shweiki D, Itin A, Soffer D, Keshet E. Vascular endothelial growth factor induced by hypoxia may mediate hypoxia-initiated angiogenesis. Nature. 1992;359(6398):843–5.
32. Smith LE. Through the eyes of a child: understanding retinopathy through ROP the Friedenwald lecture. Invest Ophthalmol Vis Sci. 2008;49(12):5177–82.
33. Jones JG, MacKinnon B, Good WV, Hardy RJ, Dobson V, Palmer EA, et al. The early treatment for ROP (ETROP) randomized trial: study results and nursing care adaptations. Insight. 2005;30(2):7–13.
34. Gopal L, Badrinath SS, Sharma T, Parikh SN, Shanmugam MS, Bhende PS, et al. Surgical management of retinal detachments related to coloboma of the choroid. Ophthalmology. 1998;105(5):804–9.
35. Shields JA, Shields CL, Honavar SG, Demirci H, Cater J. Classification and management of coats disease: the 2000 proctor lecture. Am J Ophthalmol. 2001;131(5):572–83.
36. Sigler EJ, Randolph JC, Calzada JI, Wilson MW, Haik BG. Current management of coats disease. Surv Ophthalmol. 2014;59(1):30–46.
37. Kozak I, Oster SF, Cortes MA, Dowell D, Hartmann K, Kim JS, et al. Clinical evaluation and treatment accuracy in diabetic macular edema using navigated laser photocoagulator NAVILAS. Ophthalmology. 2011;118(6): 1119–24.
38. NSB. Population and Housing Census of Bhutan 2017 Thimphu, Bhutan: National Statistics Bureau of Bhutan; 2017 [updated 2019 January; cited 2019. Available from: http://www.nsb.gov.bt/publication/files/PHCB2017_national.pdf.

Publisher's Note

Springer Nature remains neutral with regard to jurisdictional claims in published maps and institutional affiliations.

Ready to submit your research? Choose BMC and benefit from:

- fast, convenient online submission
- thorough peer review by experienced researchers in your field
- rapid publication on acceptance
- support for research data, including large and complex data types
- gold Open Access which fosters wider collaboration and increased citations
- maximum visibility for your research: over 100M website views per year

At BMC, research is always in progress.

Learn more biomedcentral.com/submissions

BMC

Chapter 10

Summary and Recommendations

1

Overall summary

My thesis comprised of two parts: epidemiological studies on vitreoretinal (VR) diseases in Bhutan and Nepal, and the functional assessment of retina among the patients of diabetic macular oedema, and neovascular age-related macular degeneration (nAMD) using the multifocal pupillographic objective perimeter (mfPOP). A separate chapter provides guidelines for the use of mfPOP in the clinical settings following pupillary dilation with tropicamide eye drops.

Need for epidemiological studies

The implementation of eye care programs in the developing countries faces many challenges such as limited human resources, lack of sustained medical supplies, and poor transport services. Proper planning for the maximum use of limited resources is very critical for successful implementation of national programs for control and prevention of visual disorders. VR disorders are prevalent in the developing countries like Bhutan and Nepal. There was, however, limited data available upon which national action plans could be framed. So one of the objectives of this thesis was to provide robust data on the pattern and presentation of VR diseases, for formulating effective national strategies to control blindness. In producing this thesis we have published five epidemiological studies on VR diseases in Bhutan and Nepal, including the rural-urban difference in myopia prevalence in Bhutan, and the factors determining myopia development. The epidemiological chapters cover 1905 new VR disease patients in Nepal, and 2913 in Bhutan. Those studies identified the common and preventable VR diseases including: diabetic retinopathy and macular oedema, nAMD, high myopia, hypertensive retinopathy, retinal vein occlusion, retinal breaks, retinal vasculitis, retinopathy of prematurity, etc. In Nepal, females presented later than males by 9 years ($p<0.0001$), age or disease duration for diabetic retinopathy did not correlate with severity,

presenting visual acuity (VA) was asymmetric between eyes ($p<0.0001$), and patients often only reported once their right (dominant) eyes had VA of 6/18 or worse. In Bhutan, females presented earlier ($p=0.003$). Myopia constituted 92.1% of refractive error with a myopia prevalence (MP) of 12.3%, more common among females ($p=0.01$) and urbanites ($p=0.02$). MP was highest among urban females (20.9%), followed by urban males (11.9%), rural females (6.8%), and rural males (5.2%). Logistic regression revealed that the odds of having myopia were increased by being a student (4.96 ×) or professional (1.96 ×), and decreased by rural living (1.75 ×), all $p \leq 0.038$.

Functional assessment of retina with mfPOP

The above mentioned diseases are treatable with complete recovery if managed early. To improve management, we addressed the knowledge gap in developing countries by advancing a potentially reliable objective diagnostic method: an FDA-cleared prototype of mfPOP, the ObjectiveFIELD Analyser (OFA) (Konan Medical USA, Irvine, CA).

In nAMD, the per-region central OFA sensitivities decreased and delays increased with disease severity in patients tested monthly for up to 2 years (Chapter 6). Central sensitivity of eyes needing anti-VEGF treatment was lower than in the untreated eyes by -2.23 ± 0.051 dB ($p<0.0002$). Based on the peripheral macular responses we have noticed 2 types of patients: *positive* with peripheral hypersensitivity and longer delays than normal, and *negative* with peripheral hyposensitivity and shorter delays. Among the positive eyes the peripheral sensitivity increased on average by 9.88 ± 4.41 dB/month ($p=0.042$), and the delay increased at 3.49 ± 1.75 ms/month ($p=0.049$) before the clinical decision to treat. For the negative eyes, the peripheral sensitivity dropped, and the delay was shorter a month before the treatment by 9.38 ± 3.59 ($p=0.013$), and a month following treatment it improved (shorter by 8.50 ± 2.71 ms, $p=0.004$). Treatment drove subsequent responses towards normality either from the

positive or negative patient condition. Importantly, changes occurred 1-3 months before treatment was indicated clinically or by other diagnostic methods. For both groups the reported linear trends were found for the limited period of the study, longer-term outcomes will require further study. For example, do positive patients develop into negative patients over time?

We followed Type 2 diabetes patients for up to 34 months. Reduced mean sensitivities and longer delays were seen compared to normal. Peripheral hypersensitivity and shorter delays were associated with shorter diabetes duration. Principal curve analysis showed correlation between OFA and Matrix values. Outer macular thickness correlated significantly with inner and outer OFA sensitivity and delay, all $p<0.0012$ in patients with DMO, and median $p=0.001$ without DMO, while the inner thickness was not correlated with any functional measures. A mixed-effects logistic regression determined that outer thickness and OFA sensitivity contributed independently to a clinical diagnosis of DMO. Outer thickness, number of visits and male gender increased the odds of having DMO.

From a practical standpoint dilation with tropicamide 1% affected per-region sensitivities for more hours than either delays or signal-to-noise ratios (SNRs). So sensitivity measurements should be considered only after 48 hours, but delays or SNRs can be measured after 8–12 hours following mydriasis with tropicamide.

Recommendations

Based on our epidemiological and retinal functional assessment studies we recommend the following practices for enhanced eye care services in the developing countries. The Nepal study showed that females presented almost a decade later than the males, which may be detrimental to their health. It may be a cultural barrier, which needs to be lifted through health advocacy in the rural regions. Many VR diseases were secondary to the systemic

diseases such as diabetes and hypertension. So it is critical to observe healthy life styles in the community through physical activity, reducing intake of unhealthy food, and screening for non-communicable diseases. Disease severity among diabetes and AMD patients was not correlated with the duration of symptoms. This may be a warning bell that the general population is not aware enough to notice their vision being affected in the initial stage of the diseases unless their dominant eye is affected or the disease is so advanced as to be not amenable to treatment. So regular screening at the community level for VR diseases such as diabetic retinopathy and macular oedema, AMD, hypertensive retinopathy, refractive errors, etc. may prevent vision-threatening complications. The myopia prevalence study indicated that exposure to sunlight in the school-age population is critical to prevent or even reverse development of myopia. It may be worth incorporating outdoor physical activities into the school curriculum. In Bhutan, there is a need to extend their VR unit and services to the eastern and central regions for improved accessibility and coverage.

OFA may be a reliable objective method to diagnose and manage VR diseases such as nAMD and DMO early and prevent complications. A major advantage of OFA is that it is an objective method and does not have the disadvantage of learning curve effects, which is pertinent with other perimetric methods. The OFA values may be more reproducible than the Matrix values. Other studies from the Maddess lab indicate that OFA is more reproducible than HFA in glaucoma. The current studies indicate that changes to retinal functions such as sensitivity and delay precede structural changes indicated by OCT or clinically evident disease. So including functional assessment by OFA or other methods may be more useful in planning the treatment than merely basing the treatment plan on structural changes and visual acuity. That functional assessment should go beyond BCVA or other central measures to include more peripheral macular areas. Being portable and relatively low-cost it is suitable for use in developing countries.

Future directions

We have demonstrated that DMO was associated with peripheral macular functional change, as measured by OFA but not Matrix. We would like to gather more repeats from a larger number of subjects to see how OFA tracts disease progression. As part of that we would also like to characterise test-retest variability by retesting subjects about 2 weeks apart. This would allow us to determine the level for significant change. We would make these measurements with OCT, OFA and Matrix. We would also determine peripheral neuropathy as a possible correlate of iris neuropathy. This may also help us to find a lead in the management of diabetic foot and related complications, and correlate if compromised retinal function in absence of structural change (OCT) is due to retinal neuropathy which precedes clinical retinopathy. We would also measure Advanced Glycation Endproducts (AGEs) as a measure of longer term diabetic tissue damage, and include HbA1c to see if the metabolic memory shows correlation with retinal function. We have begun these studies recently.

We are currently conducting the so-called macular pigment optical density (MPOD) study on AREDS 1-3 AMD patients to correlate macular OCT, macular pigment optical density, macular function measured with OFA and Matrix 10-2, cone contrast sensitivity, and clinical features. Five other studies of new 80-second OFA tests are planned in a range of diseases such as glaucoma, multiple sclerosis, concussion injury among athletes, type 1 diabetes among children aged 12-17 years and young adults, and Alzheimer's disease. The first three studies have begun. The *fenofibrate and microvascular events in type 1 diabetes eye* (FAME 1) study, a multi-centred, double-blind, and placebo-controlled clinical trial to evaluate the efficacy of fenofibrate on retinopathy and its safety in adults with type 1 diabetes, is under way and we are participating with OFA added to their standard measures. Recently, our research clinic bought an OCT-angiography upgrade for our Spectralis OCT, which opens new horizons for research. I am fascinated by the mystery of varying functional outcomes

among the macular hole patients despite successful anatomical closure with surgery. I expect to conduct a study to correlate OCT (papillomacular bundle), OCT-A and retinal function before and after the surgery to formulate working guidelines for macular hole surgery. We will tap into a large macular-hole study of A/Prof Rohan Essex for this. I am also excited that we will be working with a new much more portable version of OFA manufactured recently by the Konan Medical USA, Irvine, CA in the New Year.

Appendix: Set of plots of data mapped to the 10-2 format

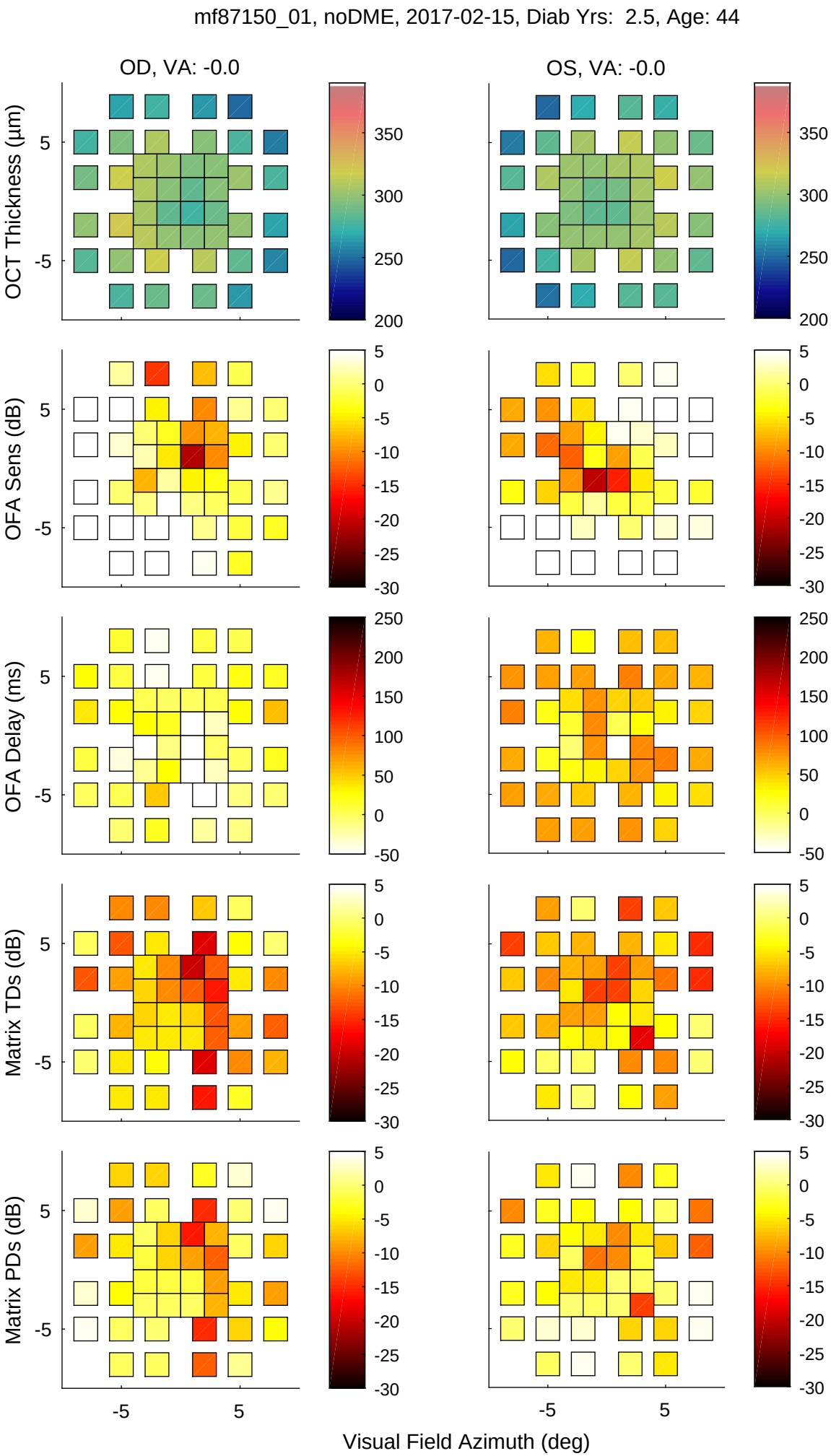
mf87150_01, noDME, 2017-02-15, Diab Yrs: 2.5, Age: 44
OD, VA: -0.0
OS, VA: -0.0
OCT Thickness (µm)
OFA Sens (dB)
OFA Delay (ms)
Matrix TDs (dB)
Matrix PDs (dB)
Visual Field Azimuth (deg)

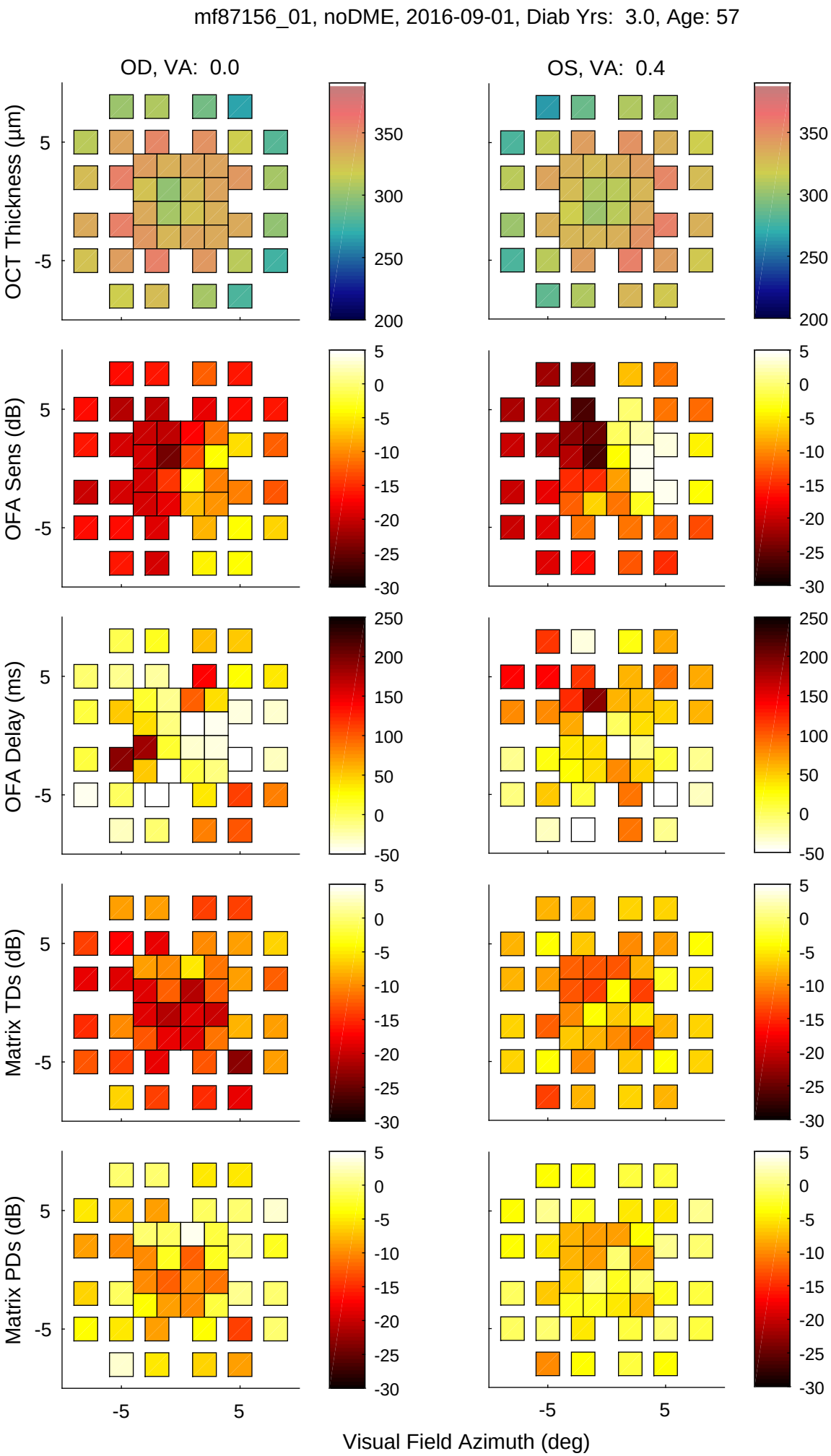
mf87156_01, noDME, 2016-09-01, Diab Yrs: 3.0, Age: 57
OD, VA: 0.0
OS, VA: 0.4
OCT Thickness (µm)
OFA Sens (dB)
OFA Delay (ms)
Matrix TDs (dB)
Matrix PDs (dB)
Visual Field Azimuth (deg)

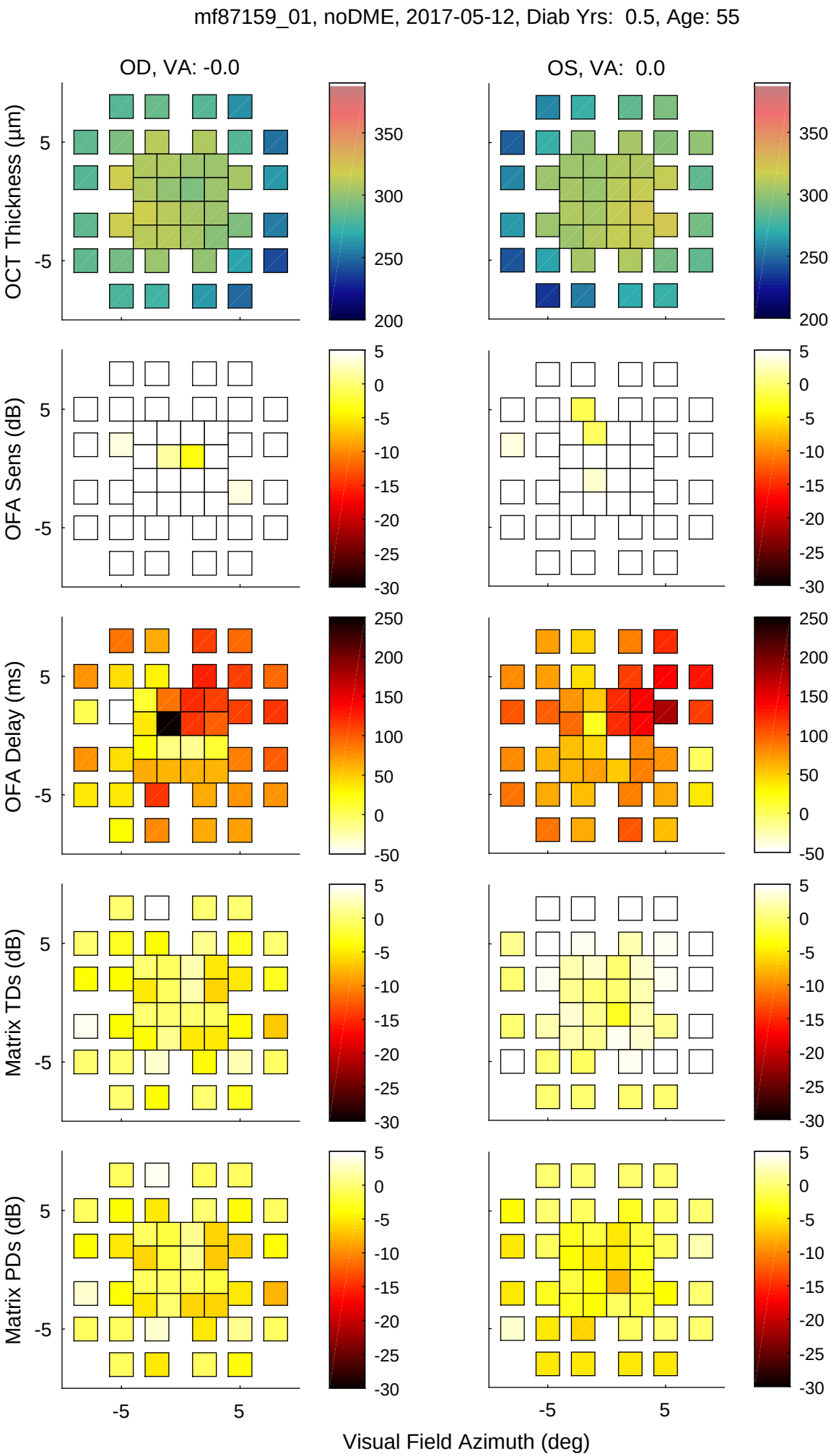
mf87159_01, noDME, 2017-05-12, Diab Yrs: 0.5, Age: 55
OD, VA: -0.0
OS, VA: 0.0
OCT Thickness (µm)
OFA Sens (dB)
OFA Delay (ms)
Matrix TDs (dB)
Matrix PDs (dB)
Visual Field Azimuth (deg)

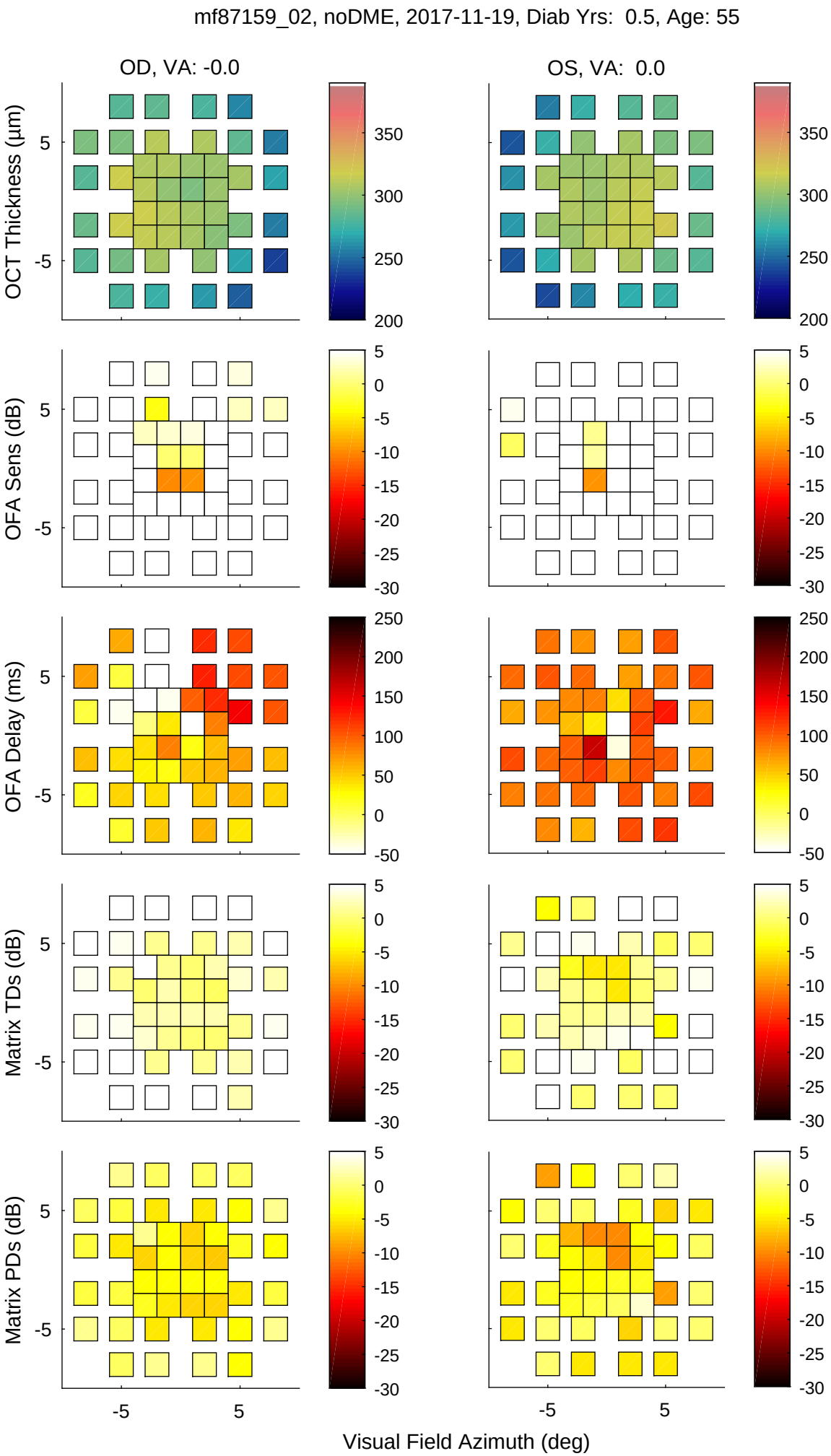
mf87159_02, noDME, 2017-11-19, Diab Yrs: 0.5, Age: 55
OD, VA: -0.0
OS, VA: 0.0
OCT Thickness (µm)
OFA Sens (dB)
OFA Delay (ms)
Matrix TDs (dB)
Matrix PDs (dB)
Visual Field Azimuth (deg)

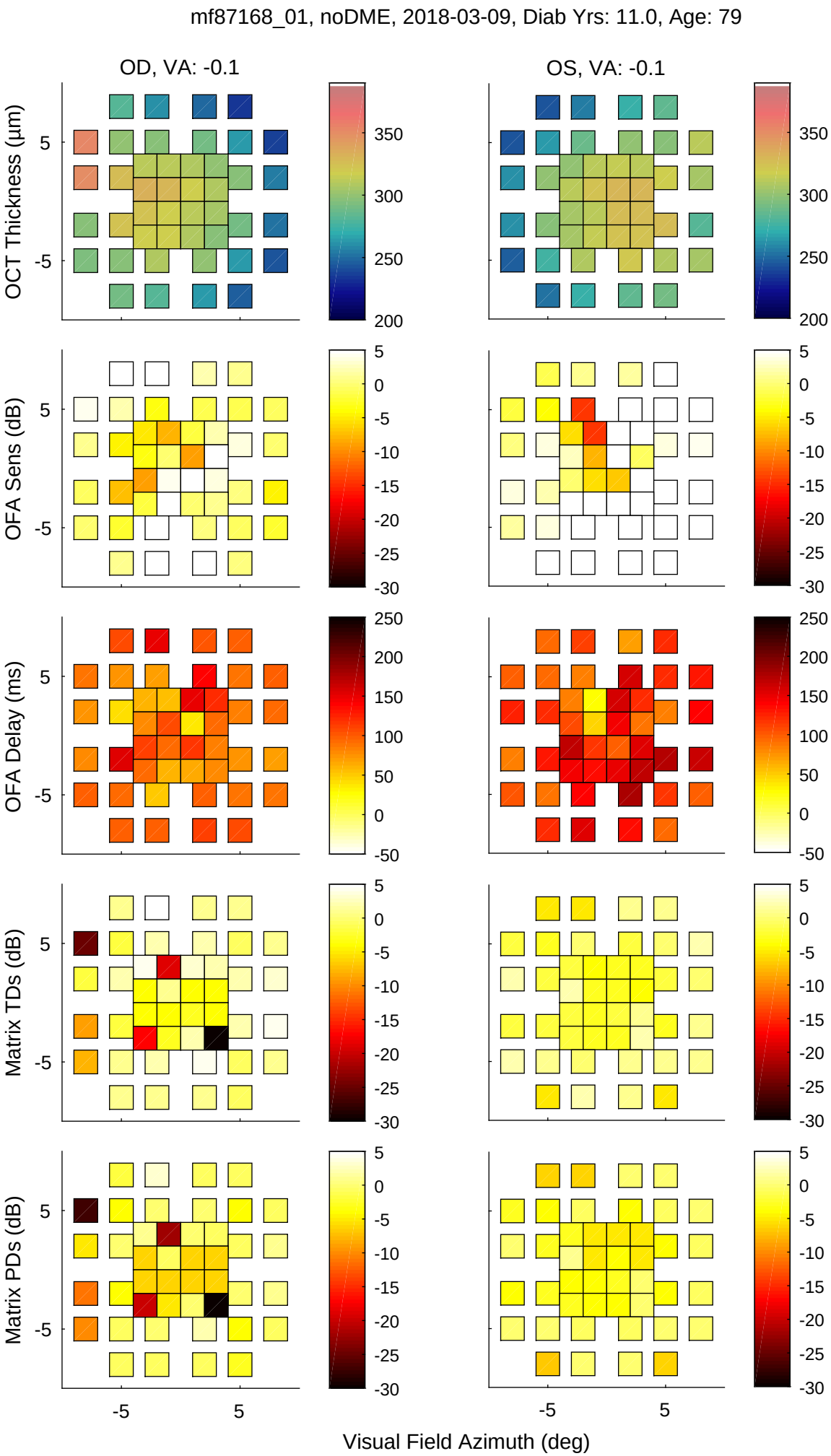
mf87168_01, noDME, 2018-03-09, Diab Yrs: 11.0, Age: 79
OD, VA: -0.1
OS, VA: -0.1
OCT Thickness (µm)
OFA Sens (dB)
OFA Delay (ms)
Matrix TDs (dB)
Matrix PDs (dB)
Visual Field Azimuth (deg)

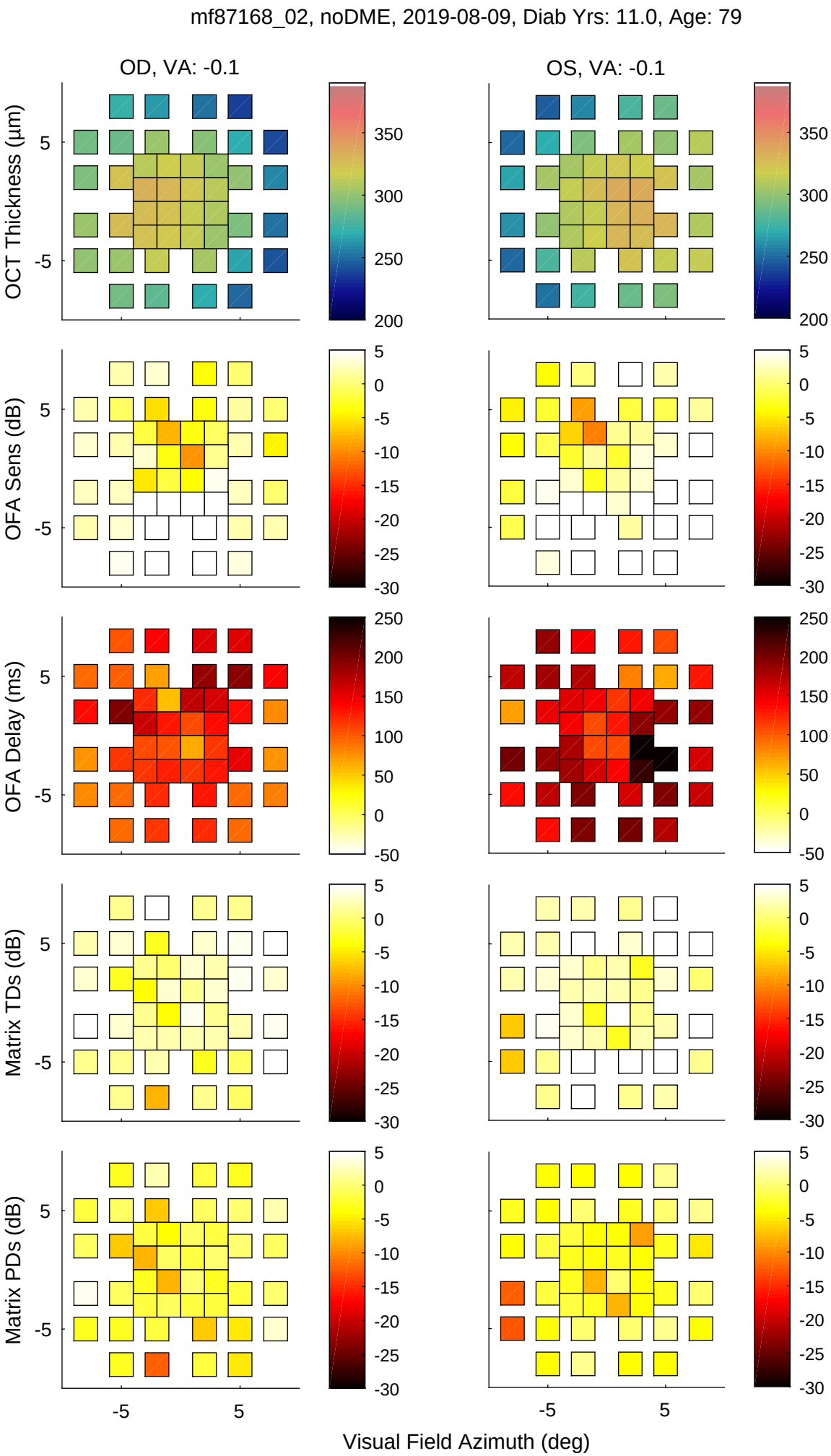
mf87168_02, noDME, 2019-08-09, Diab Yrs: 11.0, Age: 79
OD, VA: -0.1
OS, VA: -0.1
OCT Thickness (µm)
OFA Sens (dB)
OFA Delay (ms)
Matrix TDs (dB)
Matrix PDs (dB)
Visual Field Azimuth (deg)

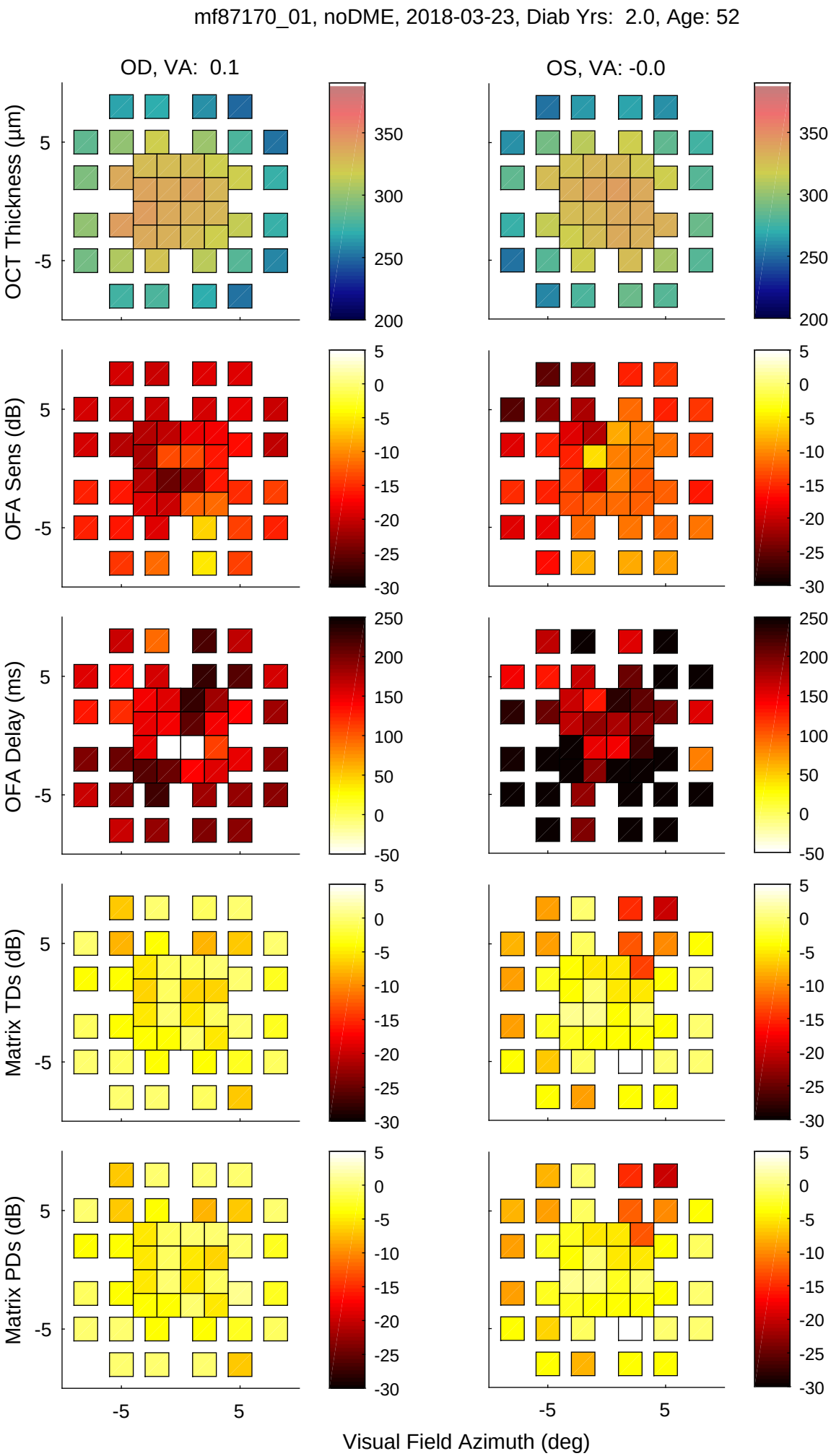
mf87170_01, noDME, 2018-03-23, Diab Yrs: 2.0, Age: 52
OD, VA: 0.1
OS, VA: -0.0
OCT Thickness (µm)
OFA Sens (dB)
OFA Delay (ms)
Matrix TDs (dB)
Matrix PDs (dB)
Visual Field Azimuth (deg)

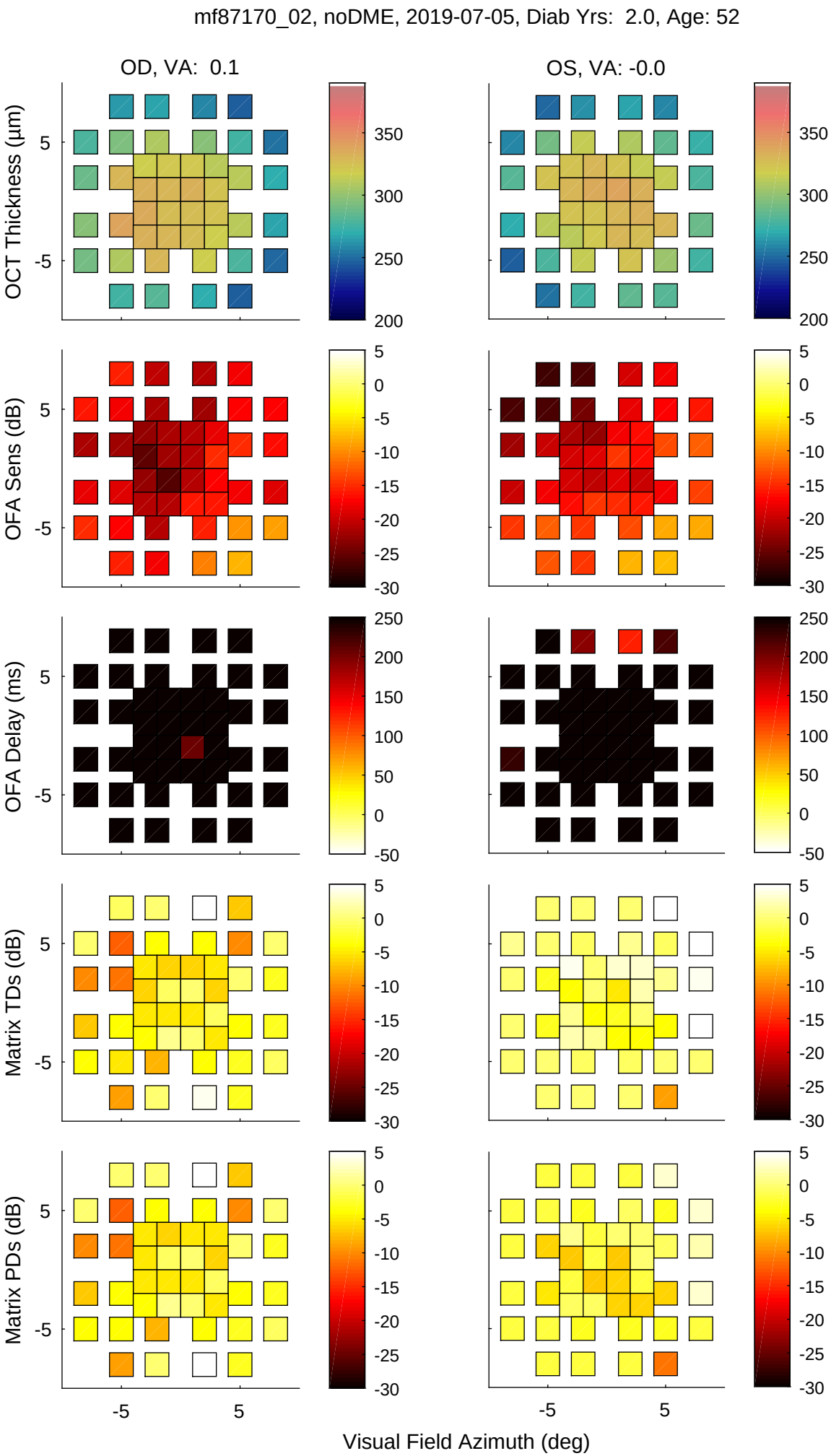
mf87170_02, noDME, 2019-07-05, Diab Yrs: 2.0, Age: 52
OD, VA: 0.1
OS, VA: -0.0
OCT Thickness (µm)
OFA Sens (dB)
OFA Delay (ms)
Matrix TDs (dB)
Matrix PDs (dB)
Visual Field Azimuth (deg)

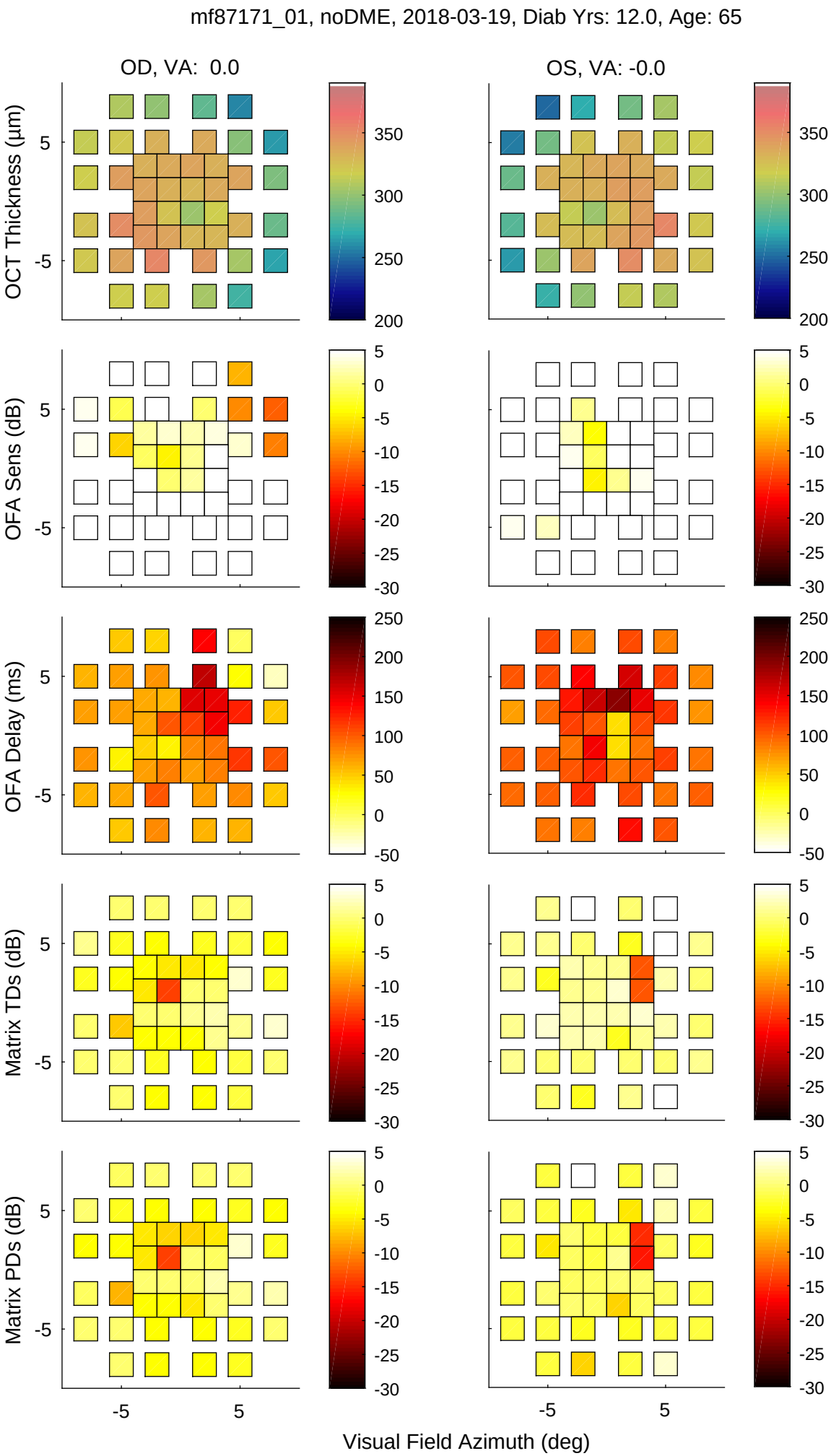
mf87171_01, noDME, 2018-03-19, Diab Yrs: 12.0, Age: 65
OD, VA: 0.0
OS, VA: -0.0
OCT Thickness (µm)
OFA Sens (dB)
OFA Delay (ms)
Matrix TDs (dB)
Matrix PDs (dB)
Visual Field Azimuth (deg)

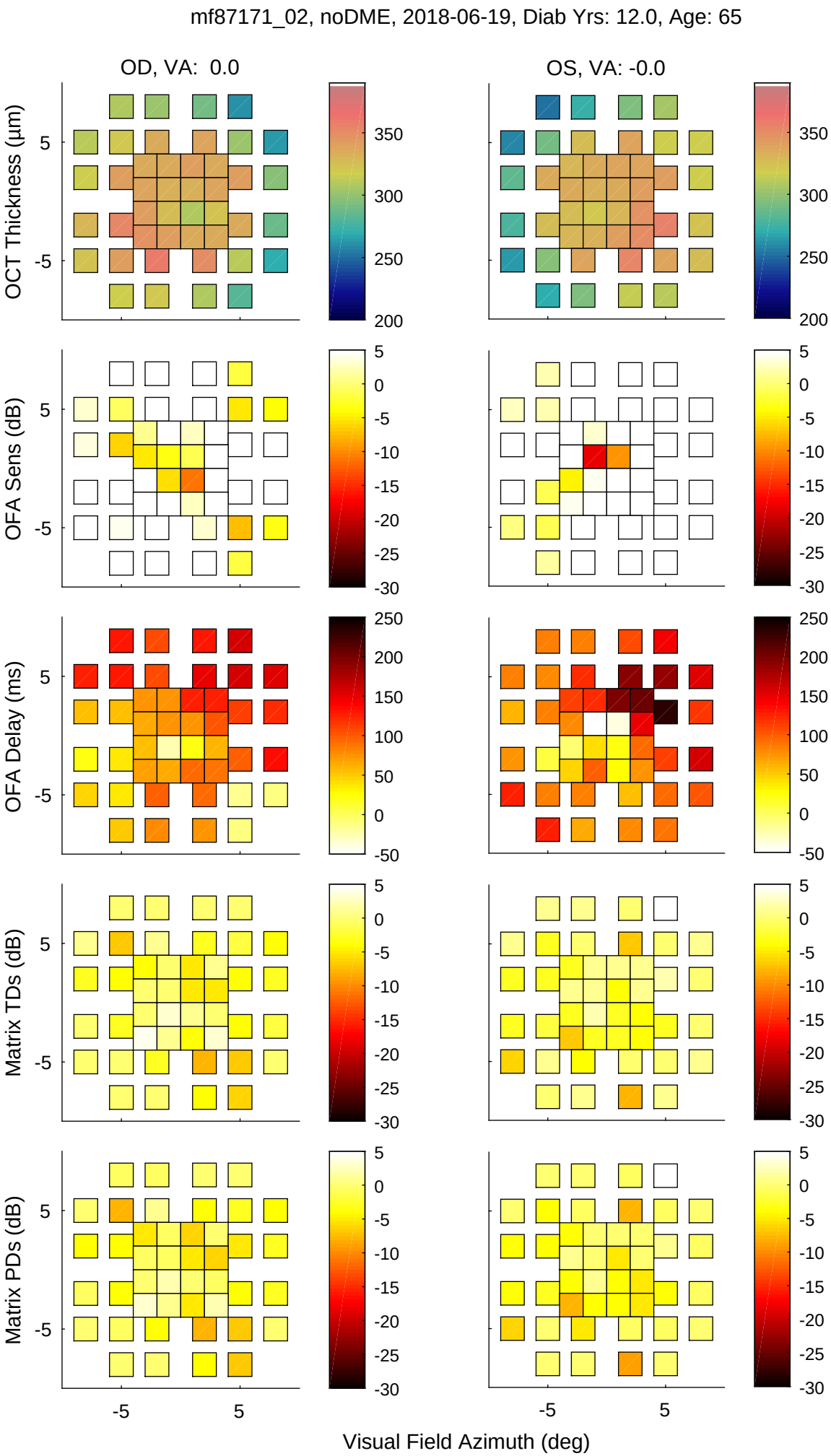
mf87171_02, noDME, 2018-06-19, Diab Yrs: 12.0, Age: 65
OD, VA: 0.0
OS, VA: -0.0
OCT Thickness (µm)
OFA Sens (dB)
OFA Delay (ms)
Matrix TDs (dB)
Matrix PDs (dB)
Visual Field Azimuth (deg)

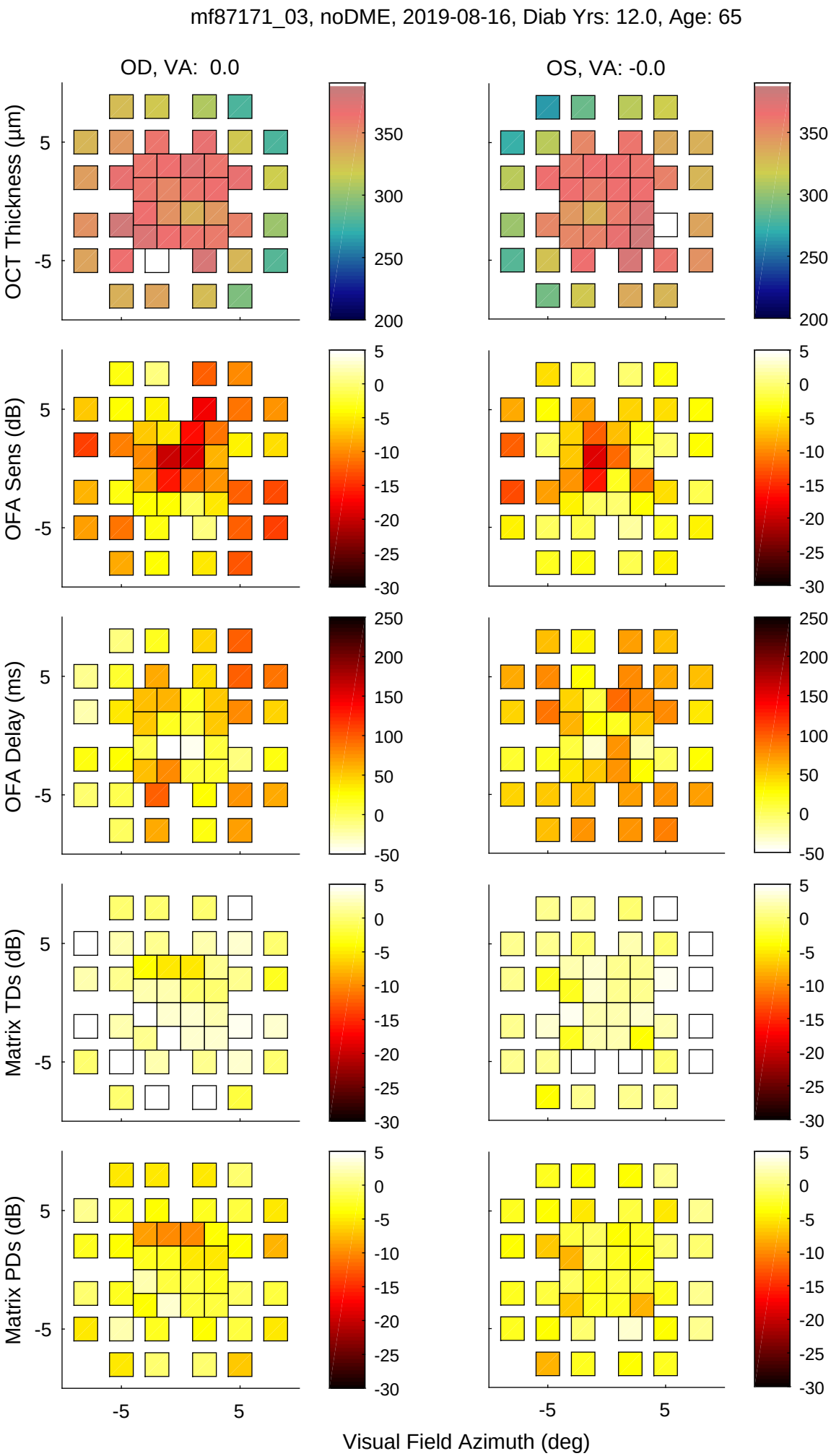
mf87171_03, noDME, 2019-08-16, Diab Yrs: 12.0, Age: 65
OD, VA: 0.0
OS, VA: -0.0
OCT Thickness (µm)
OFA Sens (dB)
OFA Delay (ms)
Matrix TDs (dB)
Matrix PDs (dB)
Visual Field Azimuth (deg)

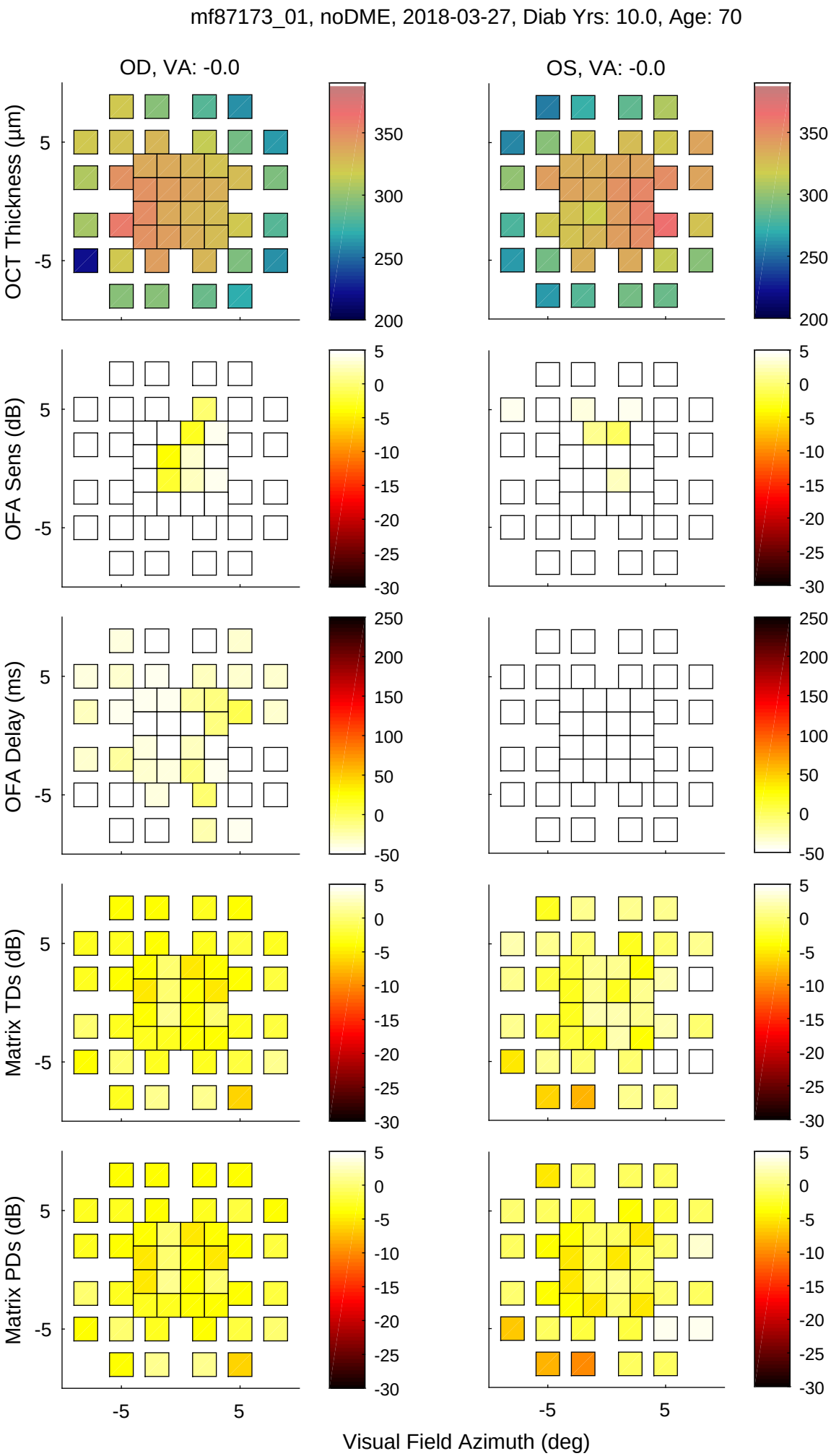
mf87173_01, noDME, 2018-03-27, Diab Yrs: 10.0, Age: 70
OD, VA: -0.0
OS, VA: -0.0
OCT Thickness (µm)
OFA Sens (dB)
OFA Delay (ms)
Matrix TDs (dB)
Matrix PDs (dB)
Visual Field Azimuth (deg)

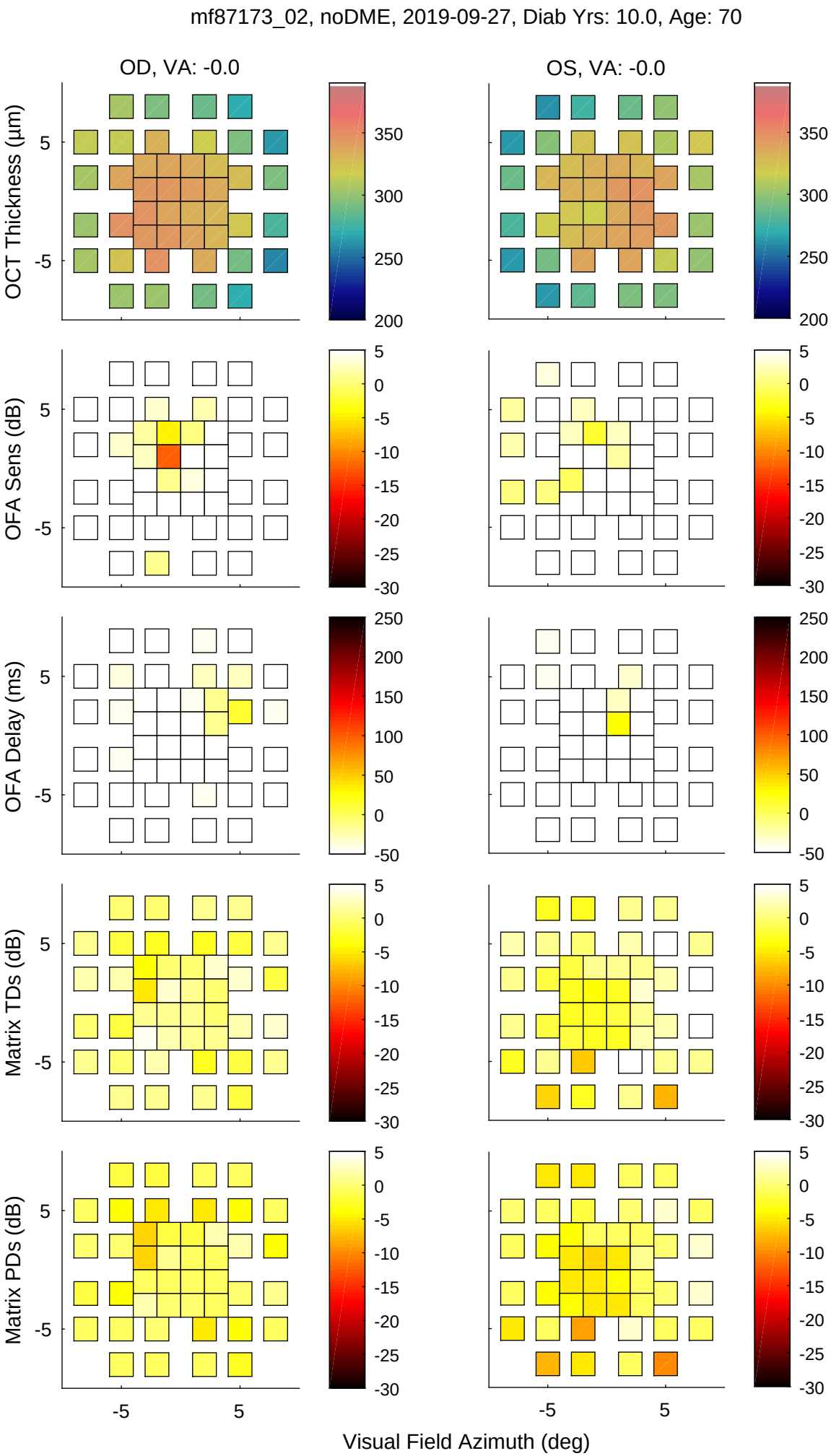
mf87173_02, noDME, 2019-09-27, Diab Yrs: 10.0, Age: 70
OD, VA: -0.0
OS, VA: -0.0
OCT Thickness (µm)
OFA Sens (dB)
OFA Delay (ms)
Matrix TDs (dB)
Matrix PDs (dB)
Visual Field Azimuth (deg)

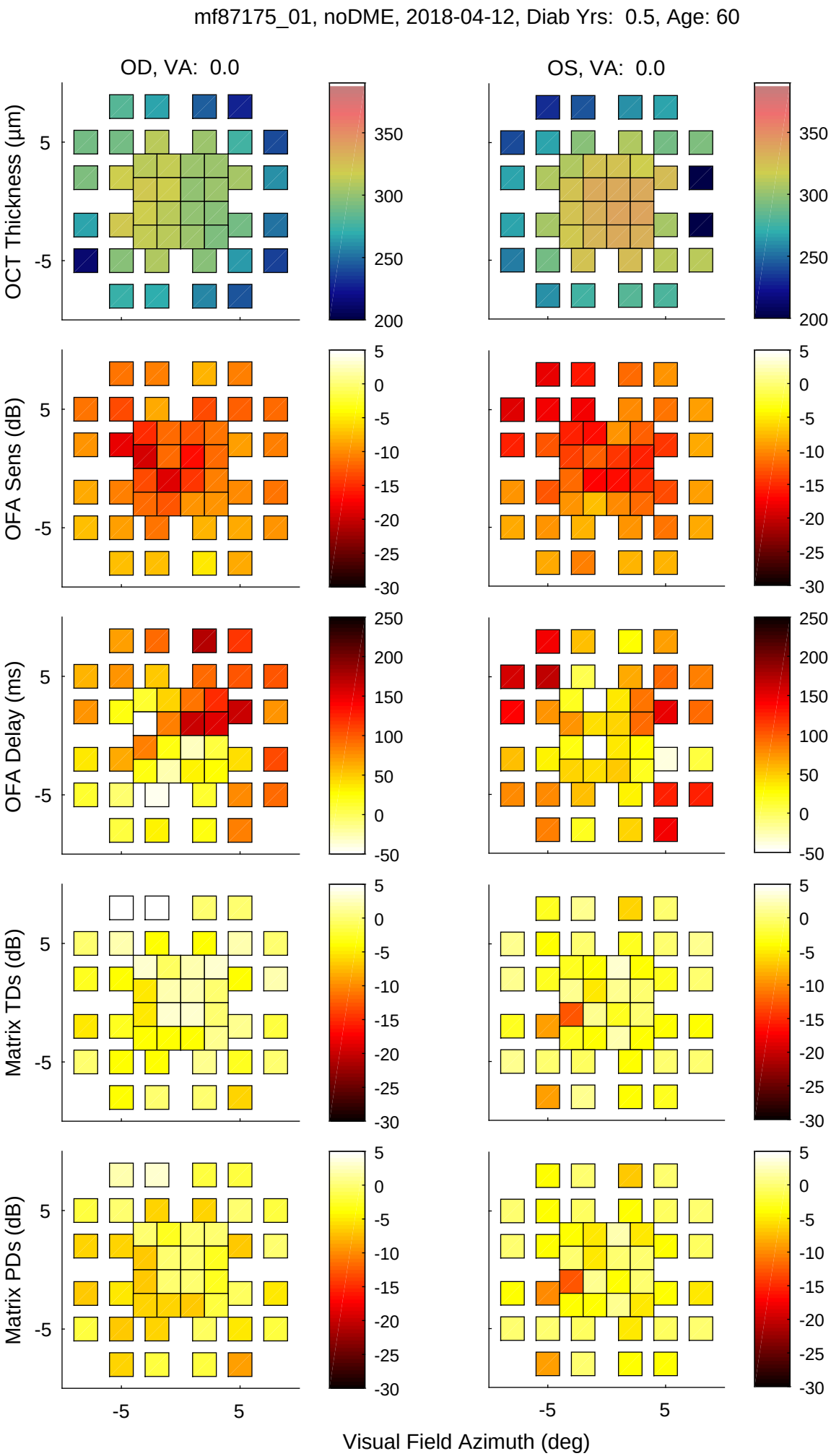
mf87175_01, noDME, 2018-04-12, Diab Yrs: 0.5, Age: 60
OD, VA: 0.0
OS, VA: 0.0
OCT Thickness (µm)
OFA Sens (dB)
OFA Delay (ms)
Matrix TDs (dB)
Matrix PDs (dB)
Visual Field Azimuth (deg)

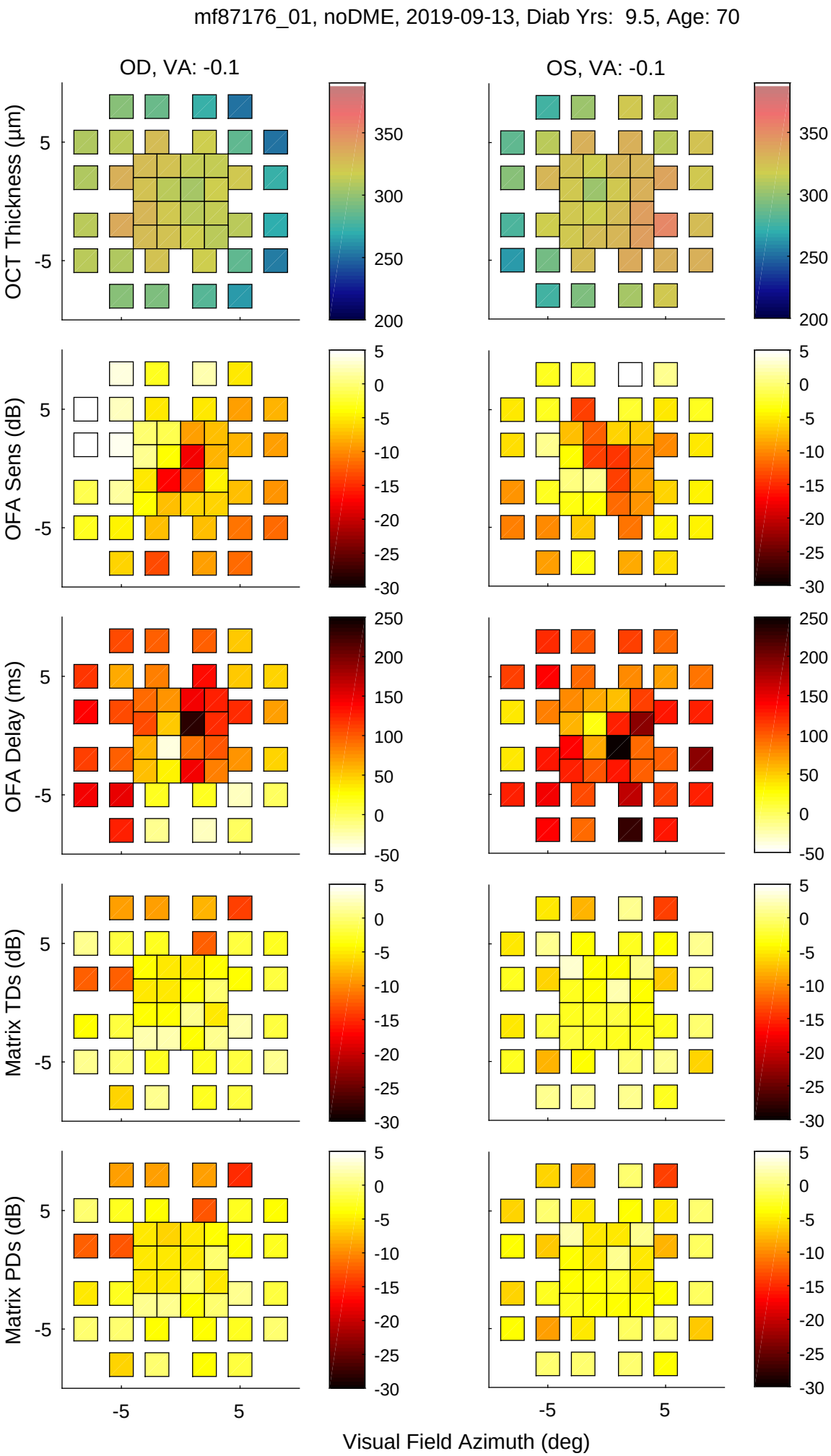
mf87176_01, noDME, 2019-09-13, Diab Yrs: 9.5, Age: 70
OD, VA: -0.1
OS, VA: -0.1
OCT Thickness (µm)
OFA Sens (dB)
OFA Delay (ms)
Matrix TDs (dB)
Matrix PDs (dB)
Visual Field Azimuth (deg)

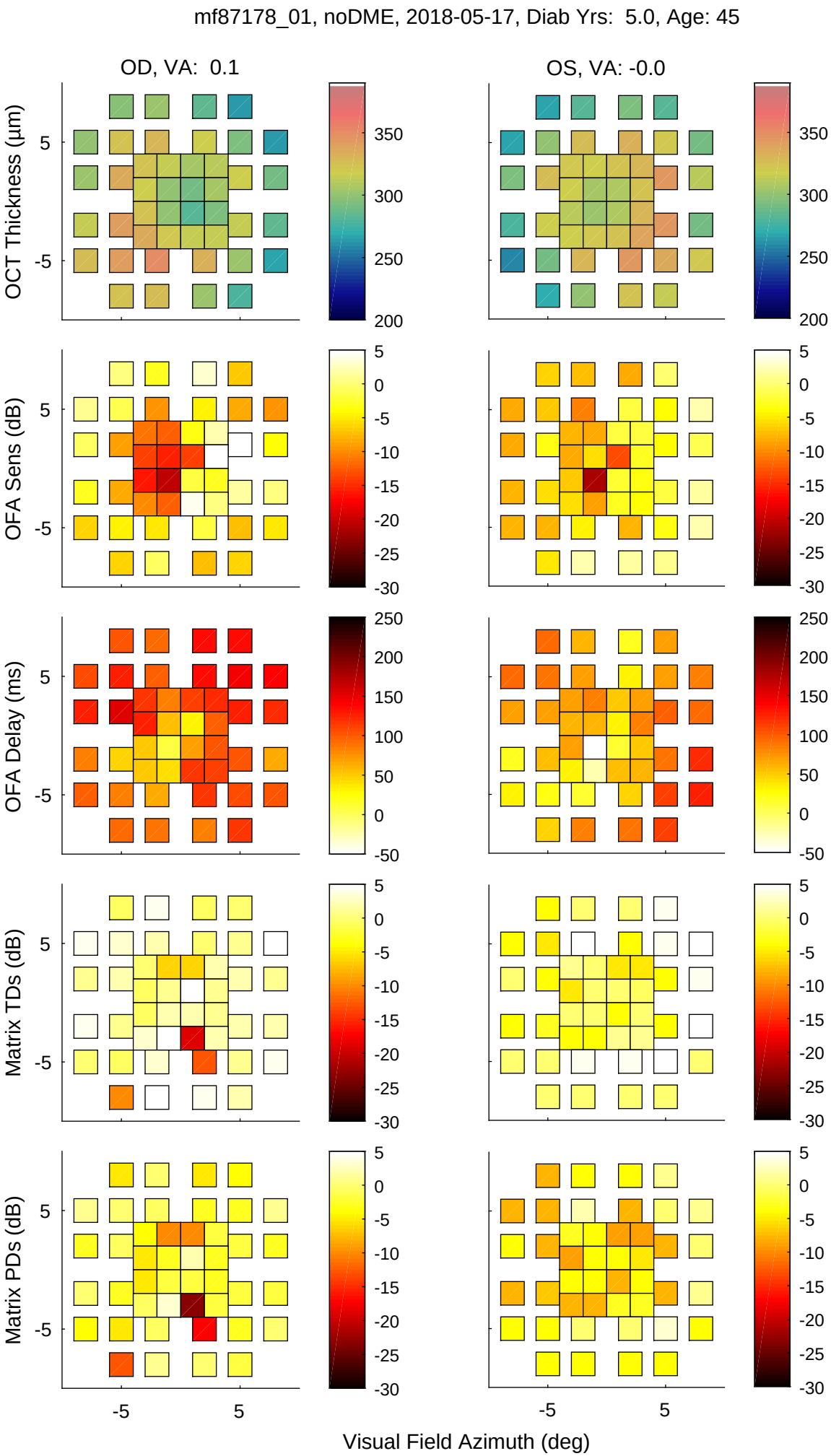
mf87178_01, noDME, 2018-05-17, Diab Yrs: 5.0, Age: 45
OD, VA: 0.1
OS, VA: -0.0
OCT Thickness (µm)
OFA Sens (dB)
OFA Delay (ms)
Matrix TDs (dB)
Matrix PDs (dB)
Visual Field Azimuth (deg)

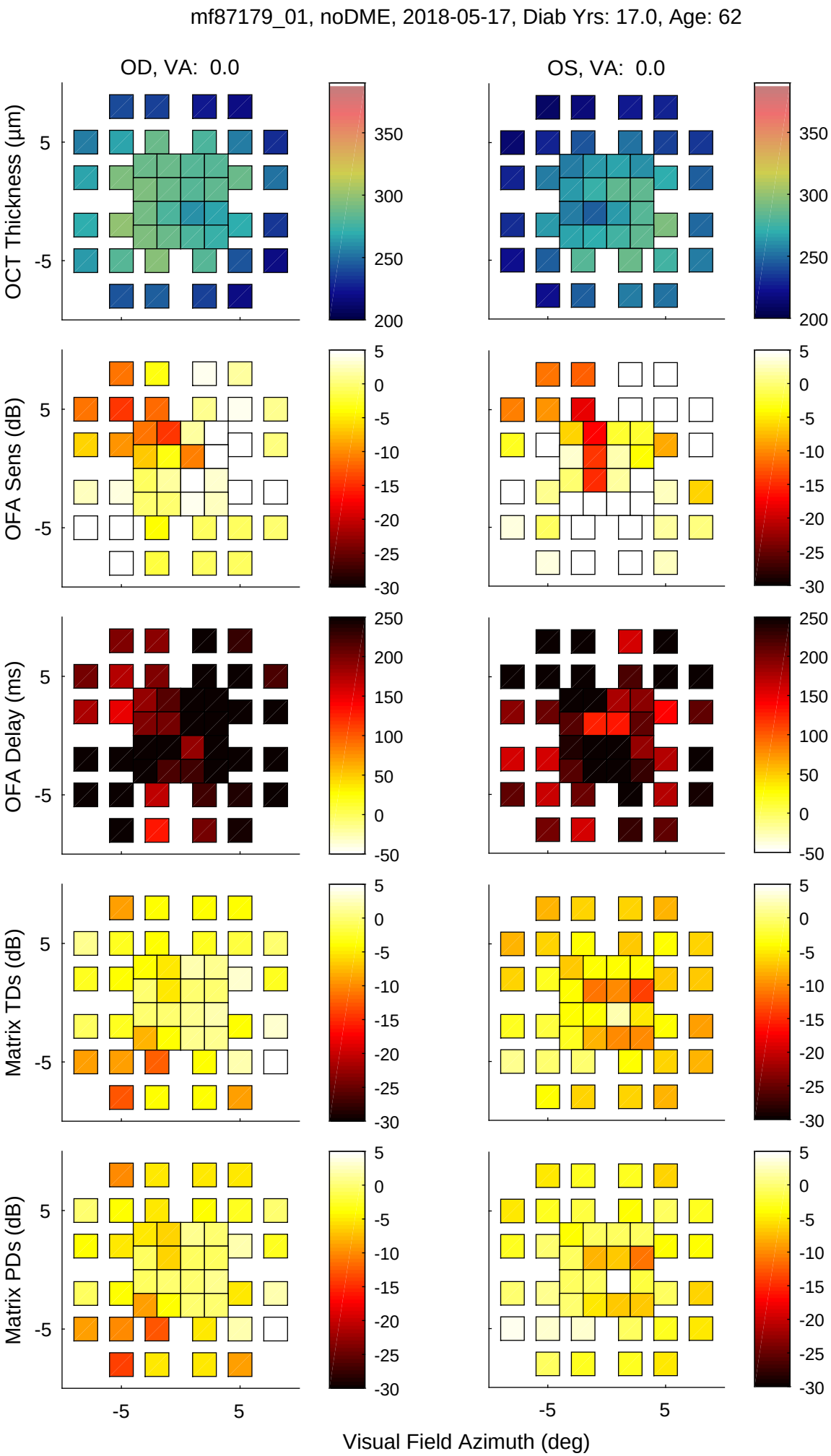
mf87179_01, noDME, 2018-05-17, Diab Yrs: 17.0, Age: 62
OD, VA: 0.0
OS, VA: 0.0
OCT Thickness (µm)
OFA Sens (dB)
OFA Delay (ms)
Matrix TDs (dB)
Matrix PDs (dB)
Visual Field Azimuth (deg)

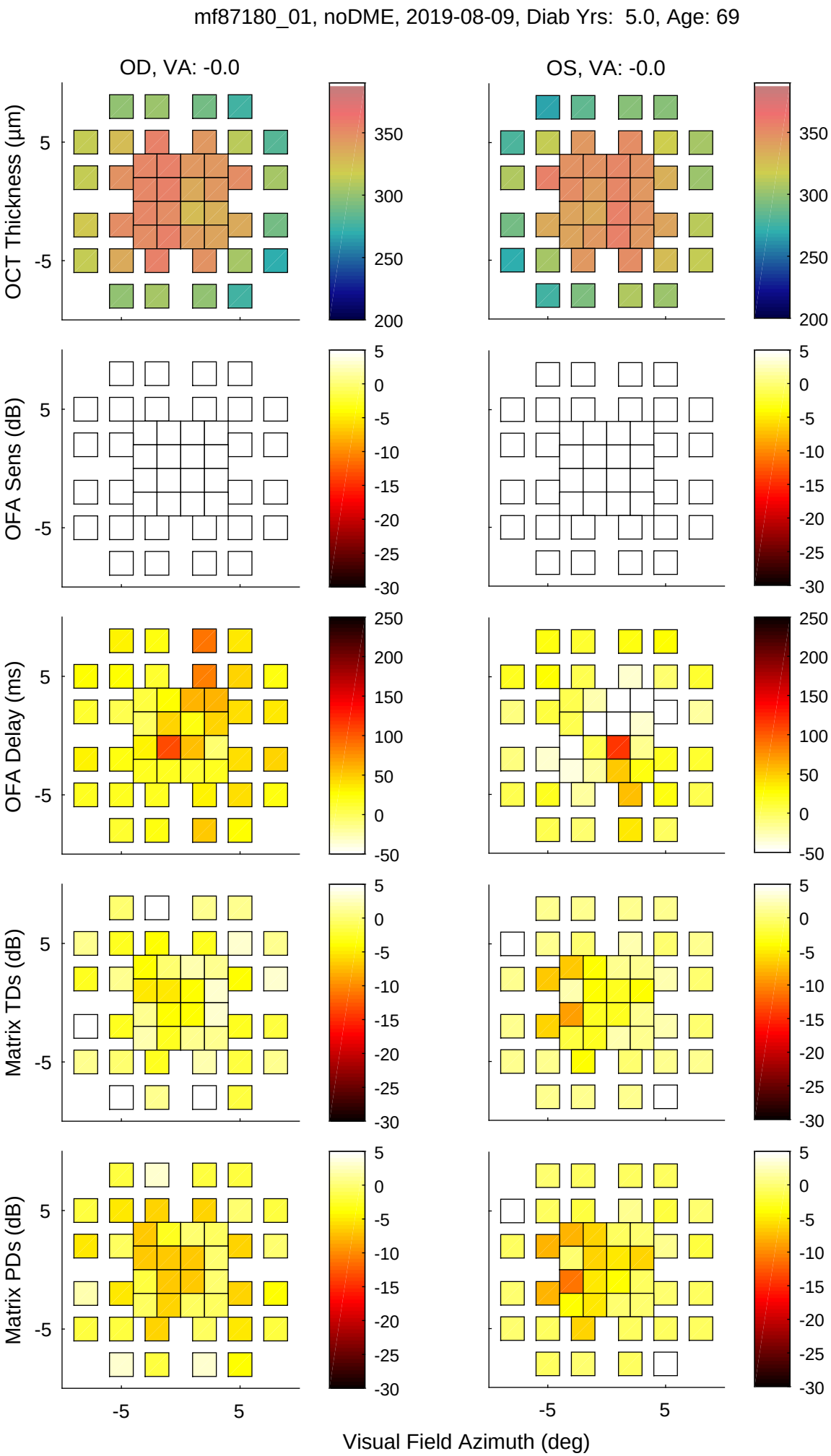
mf87180_01, noDME, 2019-08-09, Diab Yrs: 5.0, Age: 69
OD, VA: -0.0
OS, VA: -0.0
OCT Thickness (µm)
OFA Sens (dB)
OFA Delay (ms)
Matrix TDs (dB)
Matrix PDs (dB)
Visual Field Azimuth (deg)

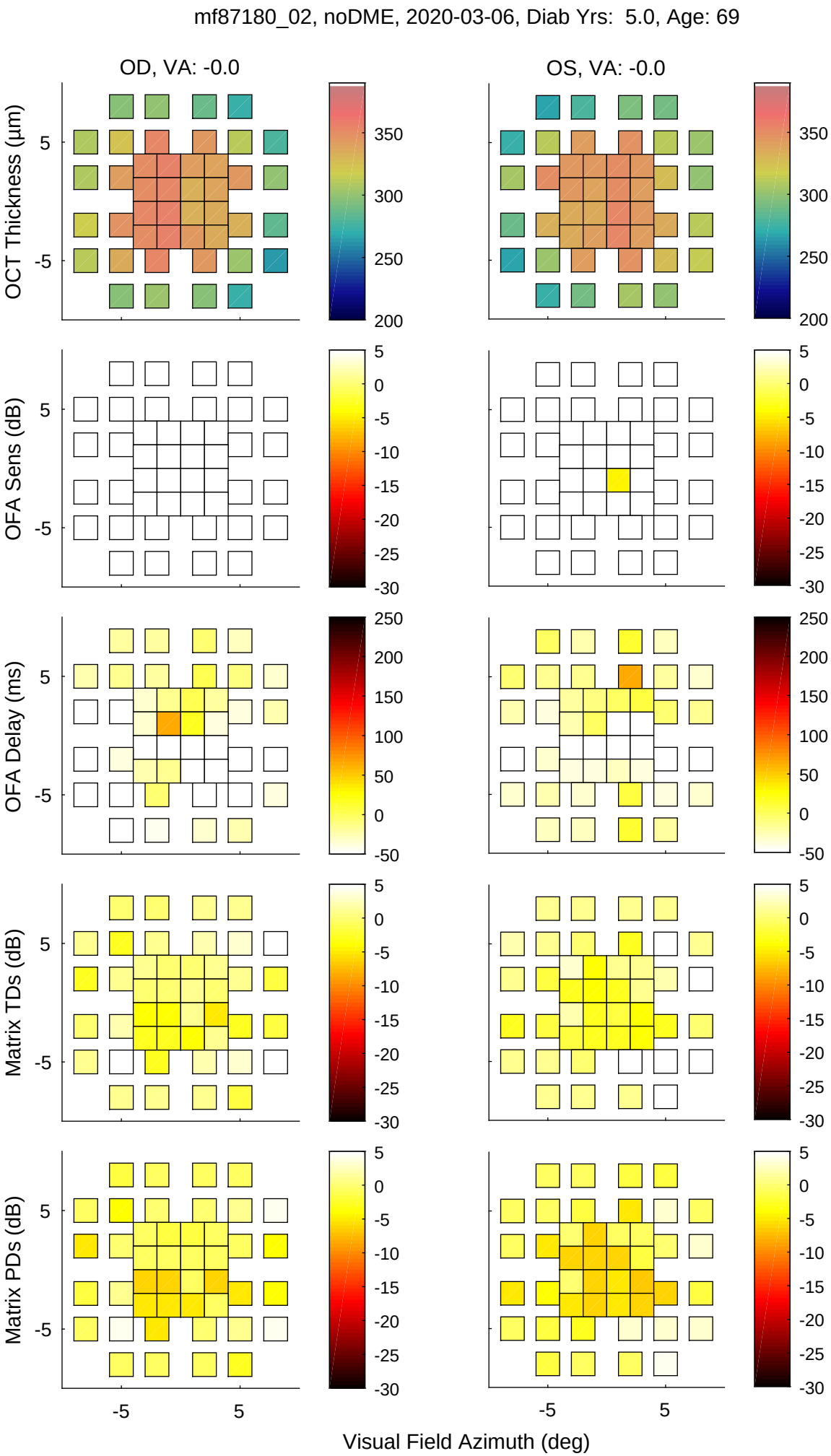
mf87180_02, noDME, 2020-03-06, Diab Yrs: 5.0, Age: 69
OD, VA: -0.0
OS, VA: -0.0
OCT Thickness (µm)
OFA Sens (dB)
OFA Delay (ms)
Matrix TDs (dB)
Matrix PDs (dB)
Visual Field Azimuth (deg)

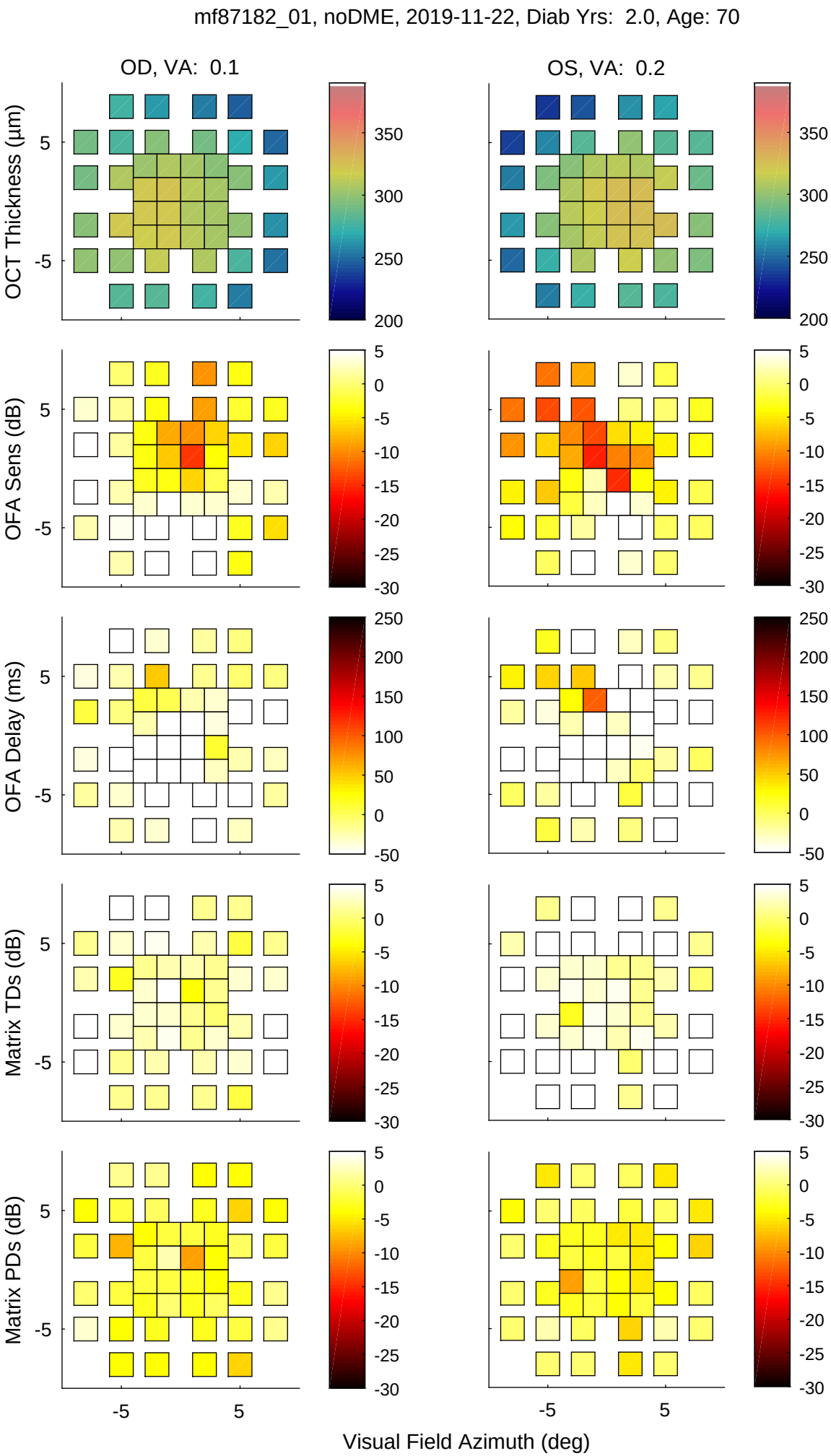
mf87182_01, noDME, 2019-11-22, Diab Yrs: 2.0, Age: 70
OD, VA: 0.1
OS, VA: 0.2
OCT Thickness (µm)
OFA Sens (dB)
OFA Delay (ms)
Matrix TDs (dB)
Matrix PDs (dB)
Visual Field Azimuth (deg)

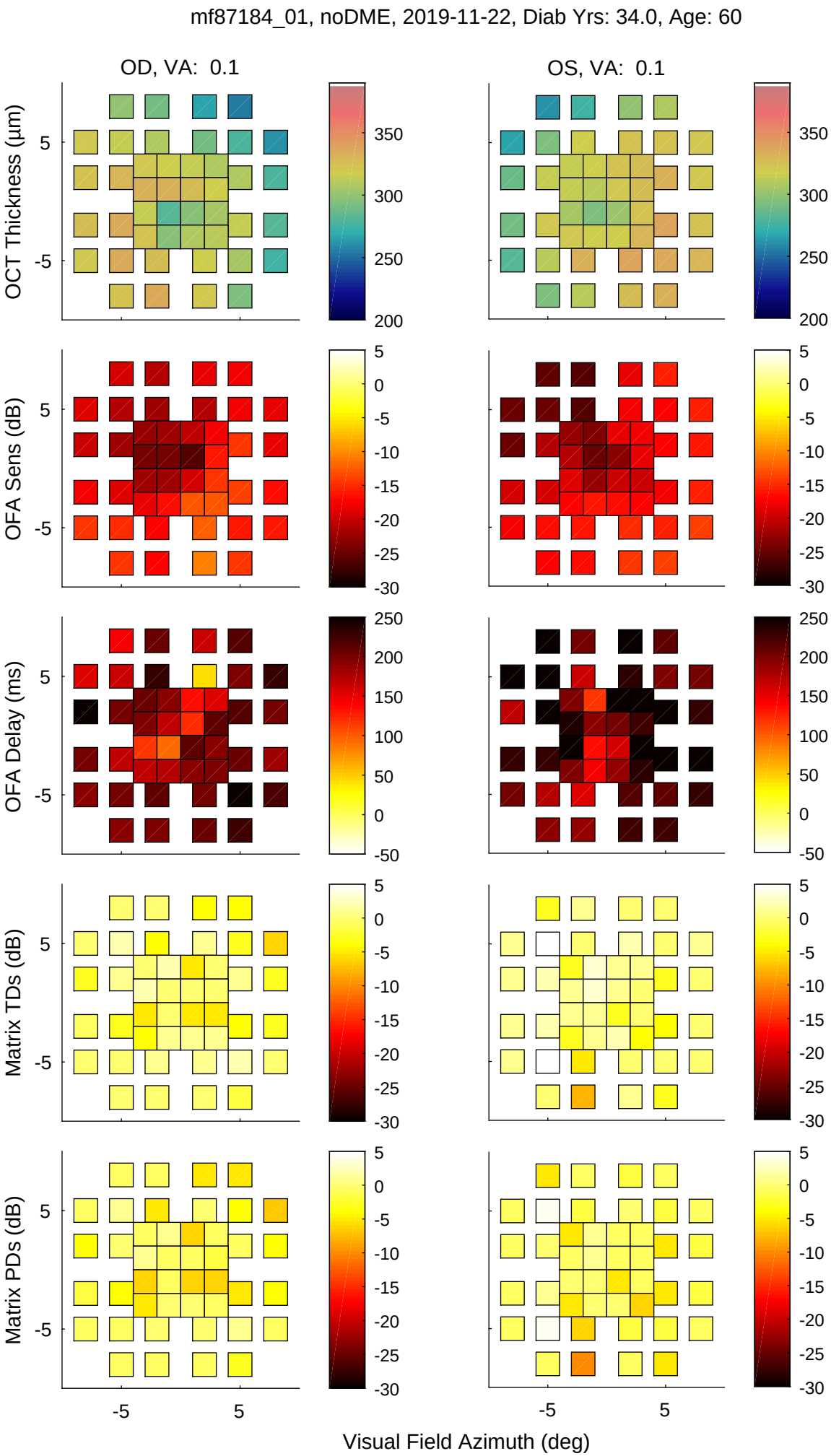
mf87184_01, noDME, 2019-11-22, Diab Yrs: 34.0, Age: 60
OD, VA: 0.1
OS, VA: 0.1
OCT Thickness (µm)
OFA Sens (dB)
OFA Delay (ms)
Matrix TDs (dB)
Matrix PDs (dB)
Visual Field Azimuth (deg)

mf87151_01, yesDME, 2017-10-30, Diab Yrs: 18.3, Age: 60

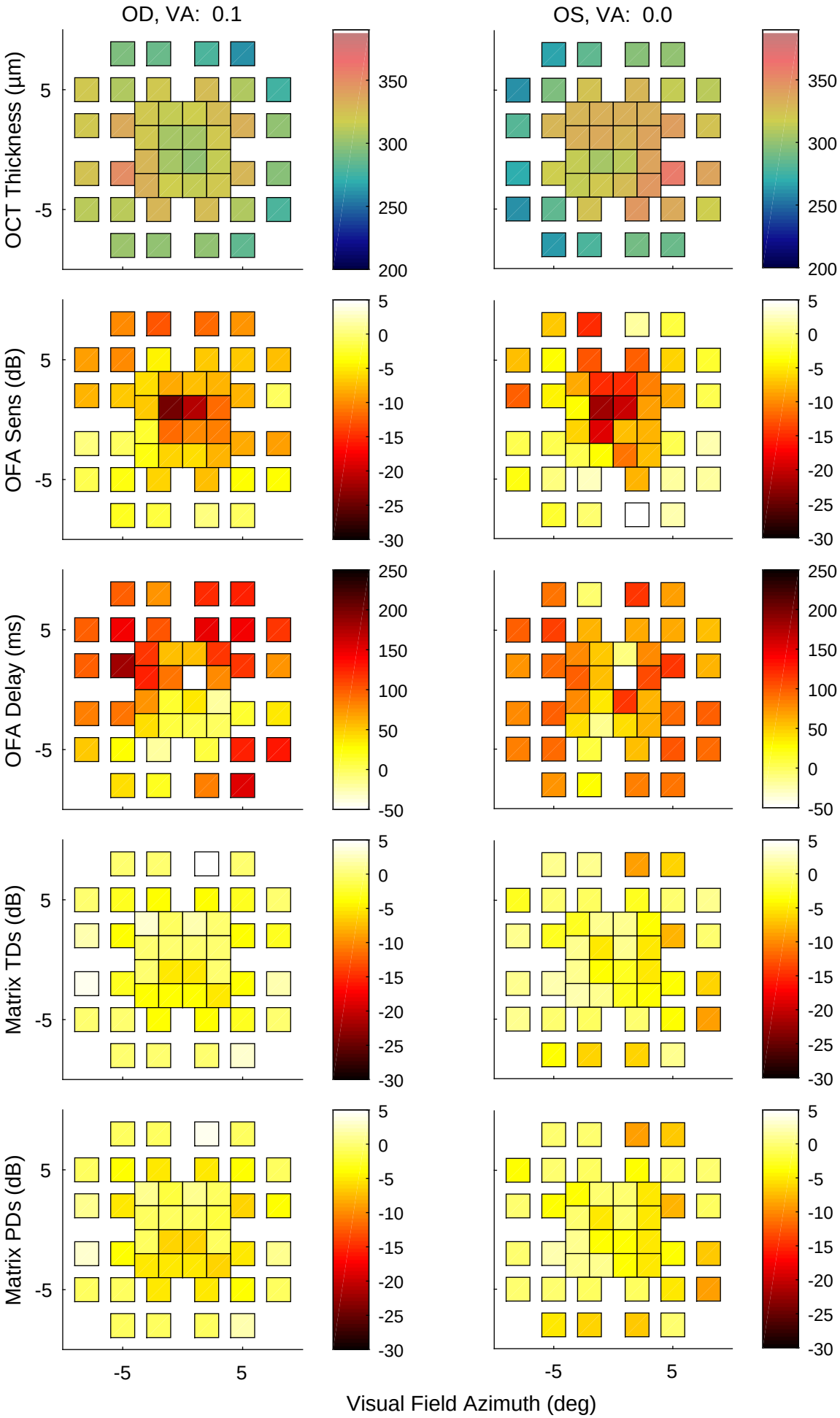

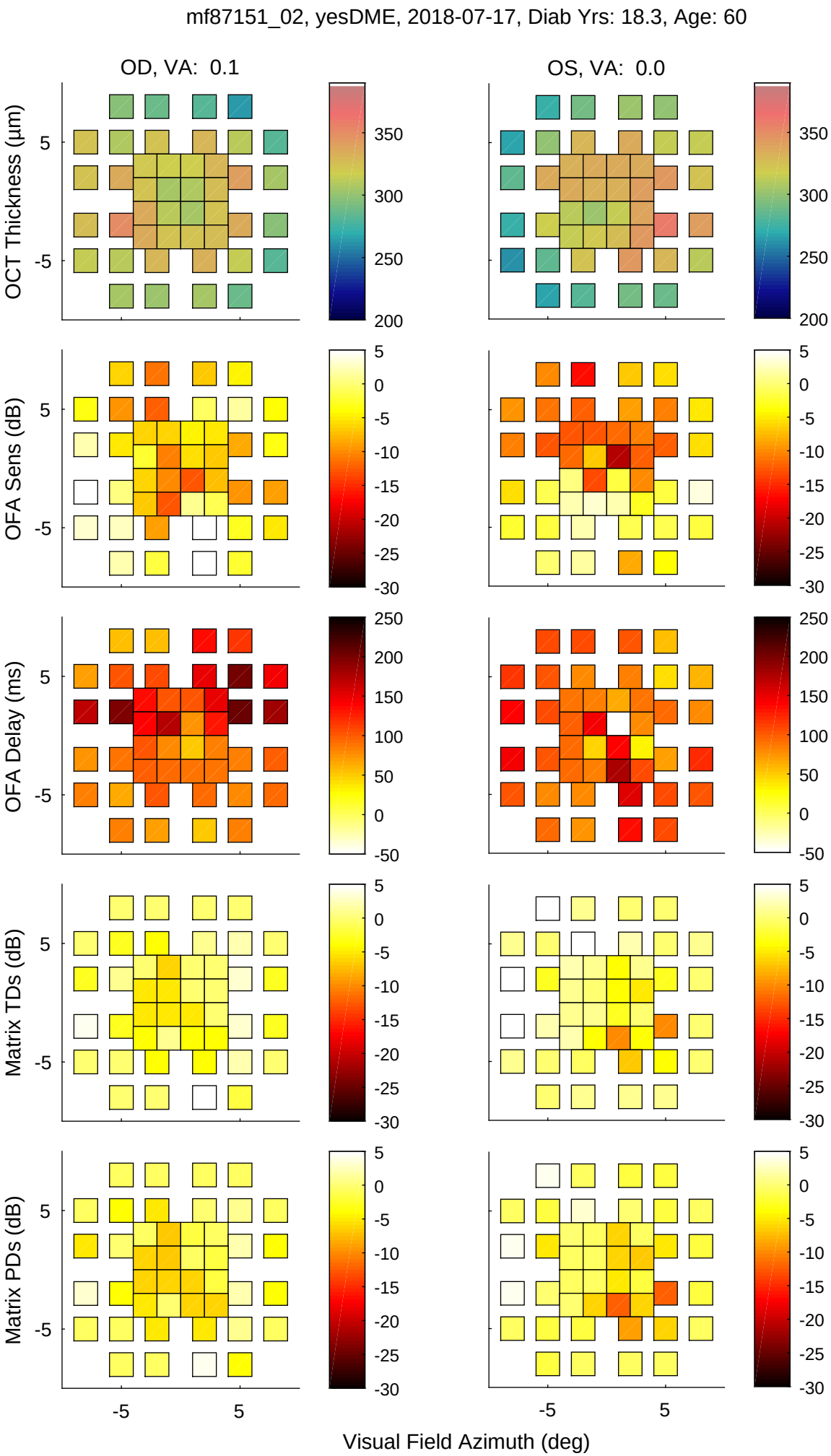
mf87151_02, yesDME, 2018-07-17, Diab Yrs: 18.3, Age: 60
OD, VA: 0.1
OS, VA: 0.0
OCT Thickness (µm)
OFA Sens (dB)
OFA Delay (ms)
Matrix TDs (dB)
Matrix PDs (dB)
Visual Field Azimuth (deg)

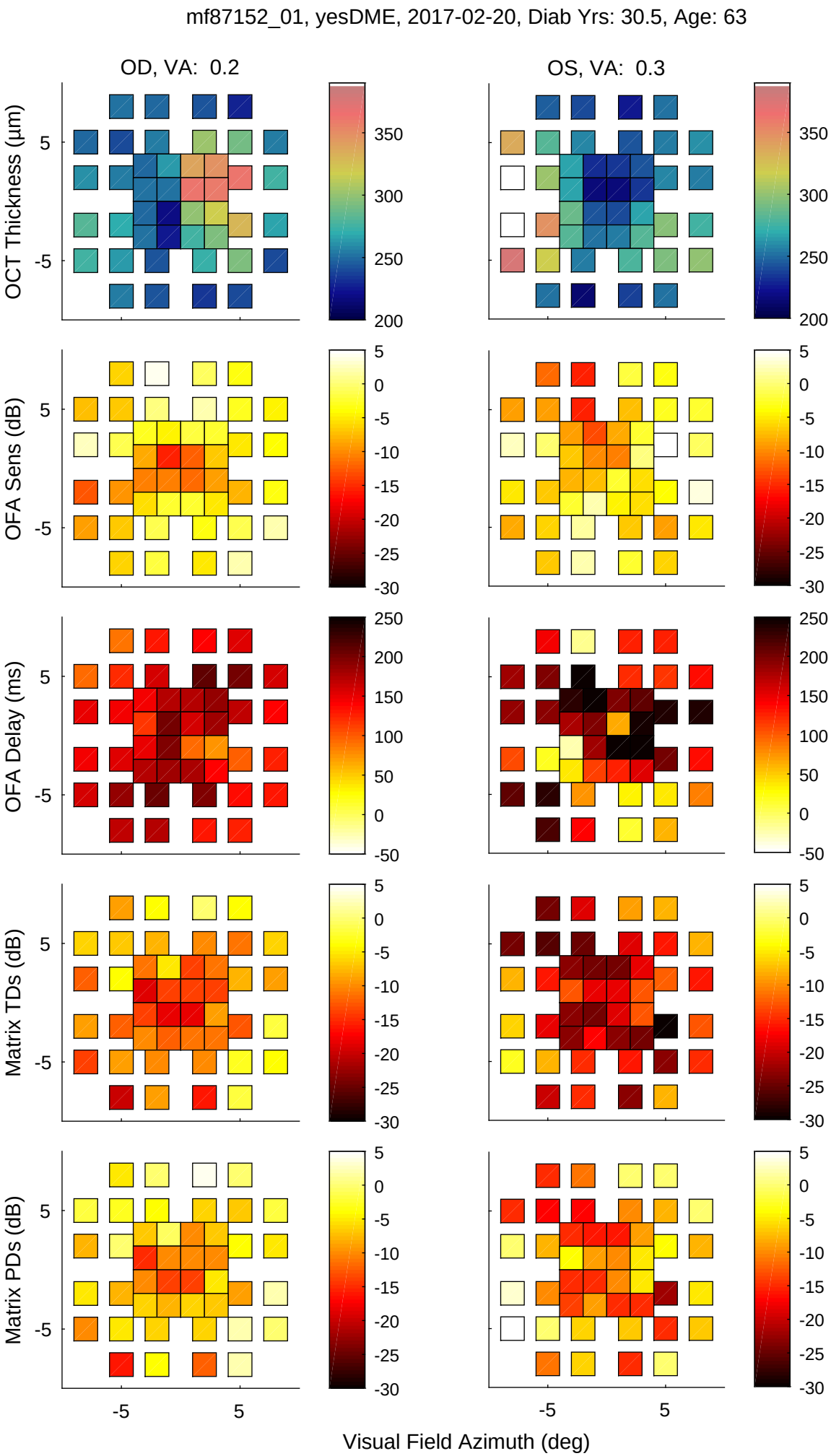
mf87152_01, yesDME, 2017-02-20, Diab Yrs: 30.5, Age: 63
OD, VA: 0.2
OS, VA: 0.3
OCT Thickness (µm)
OFA Sens (dB)
OFA Delay (ms)
Matrix TDs (dB)
Matrix PDs (dB)
Visual Field Azimuth (deg)

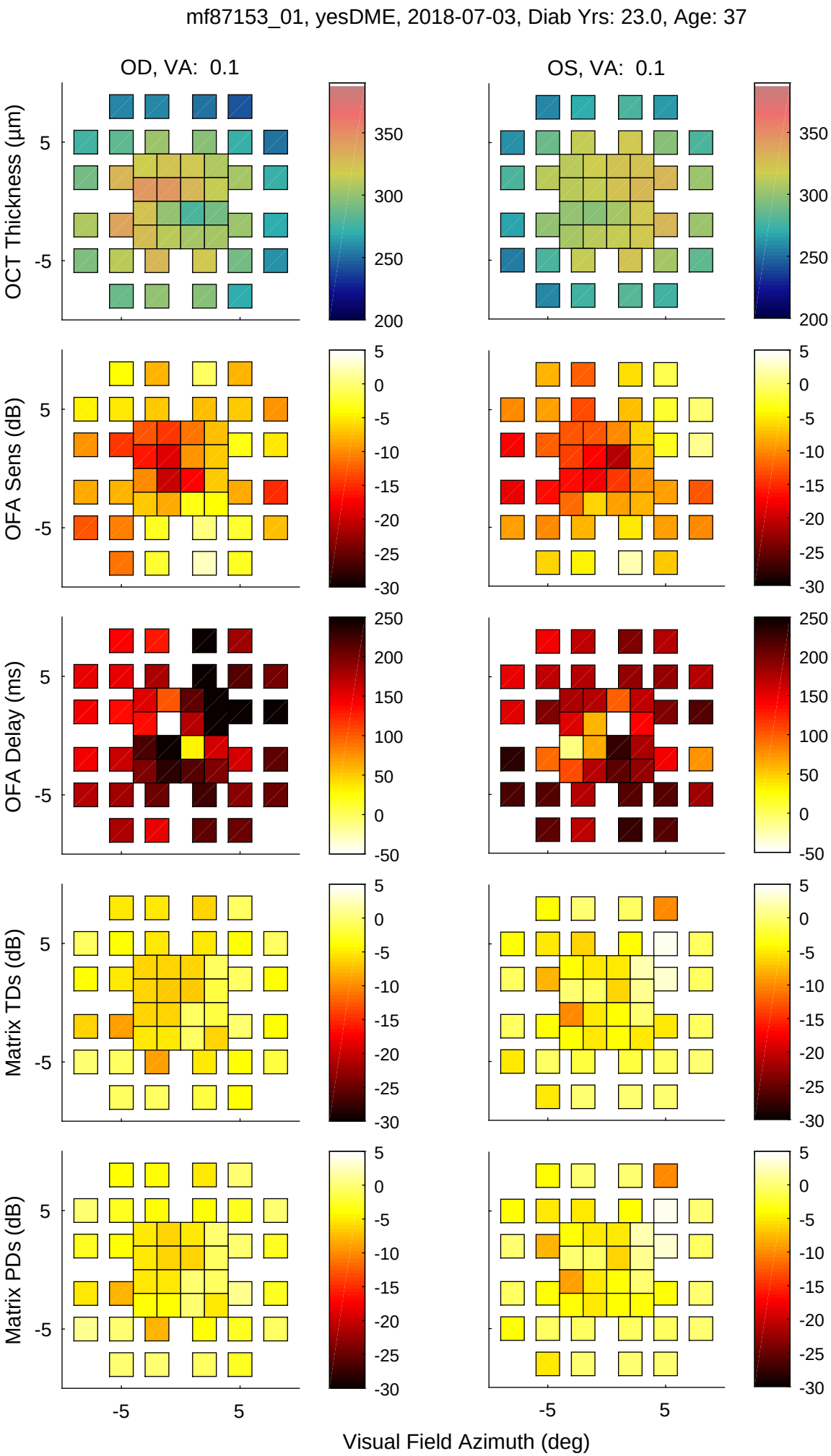
mf87153_01, yesDME, 2018-07-03, Diab Yrs: 23.0, Age: 37
OD, VA: 0.1
OS, VA: 0.1
OCT Thickness (µm)
OFA Sens (dB)
OFA Delay (ms)
Matrix TDs (dB)
Matrix PDs (dB)
Visual Field Azimuth (deg)

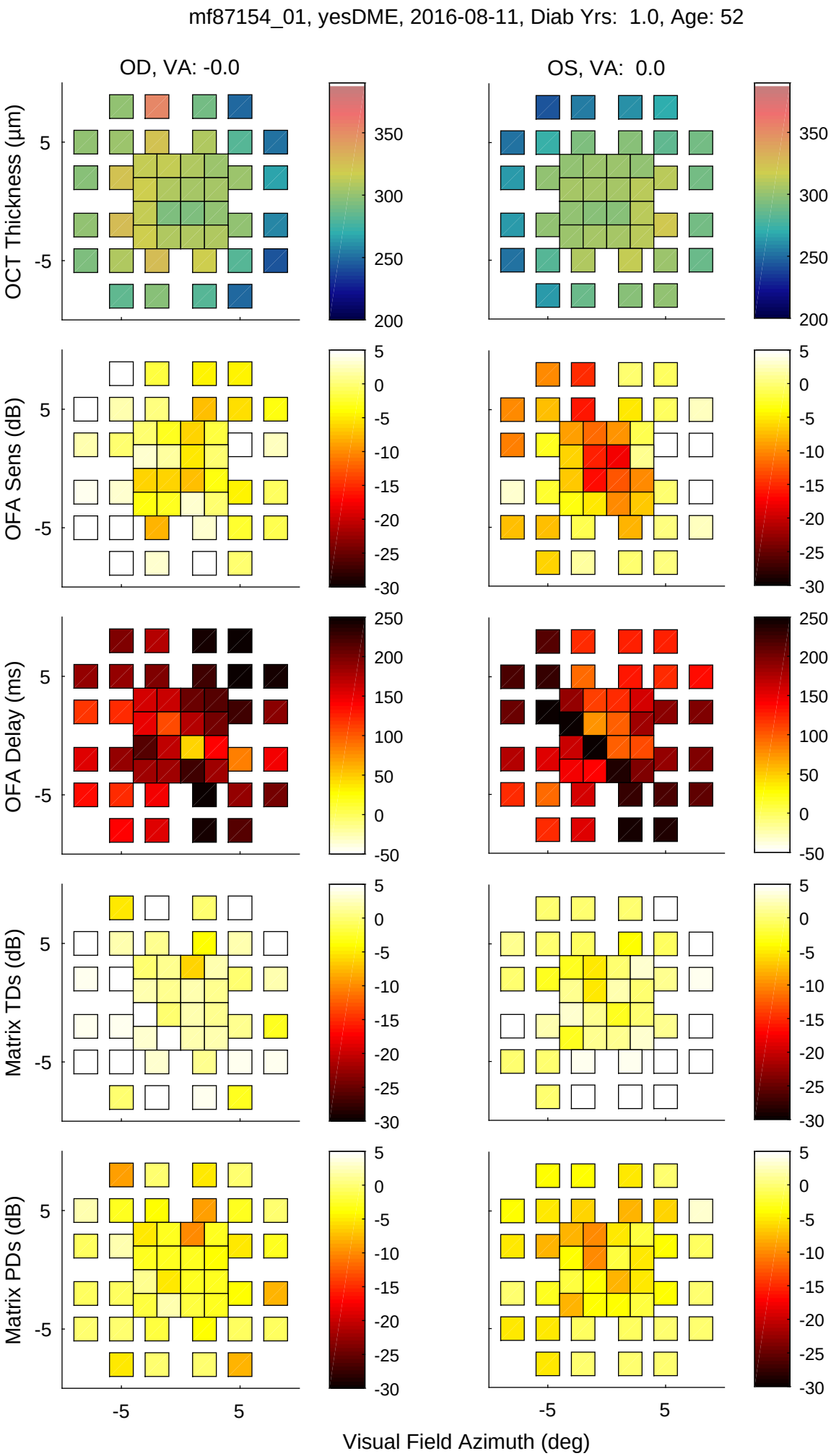
mf87154_01, yesDME, 2016-08-11, Diab Yrs: 1.0, Age: 52
OD, VA: -0.0
OS, VA: 0.0
OCT Thickness (µm)
OFA Sens (dB)
OFA Delay (ms)
Matrix TDs (dB)
Matrix PDs (dB)
Visual Field Azimuth (deg)

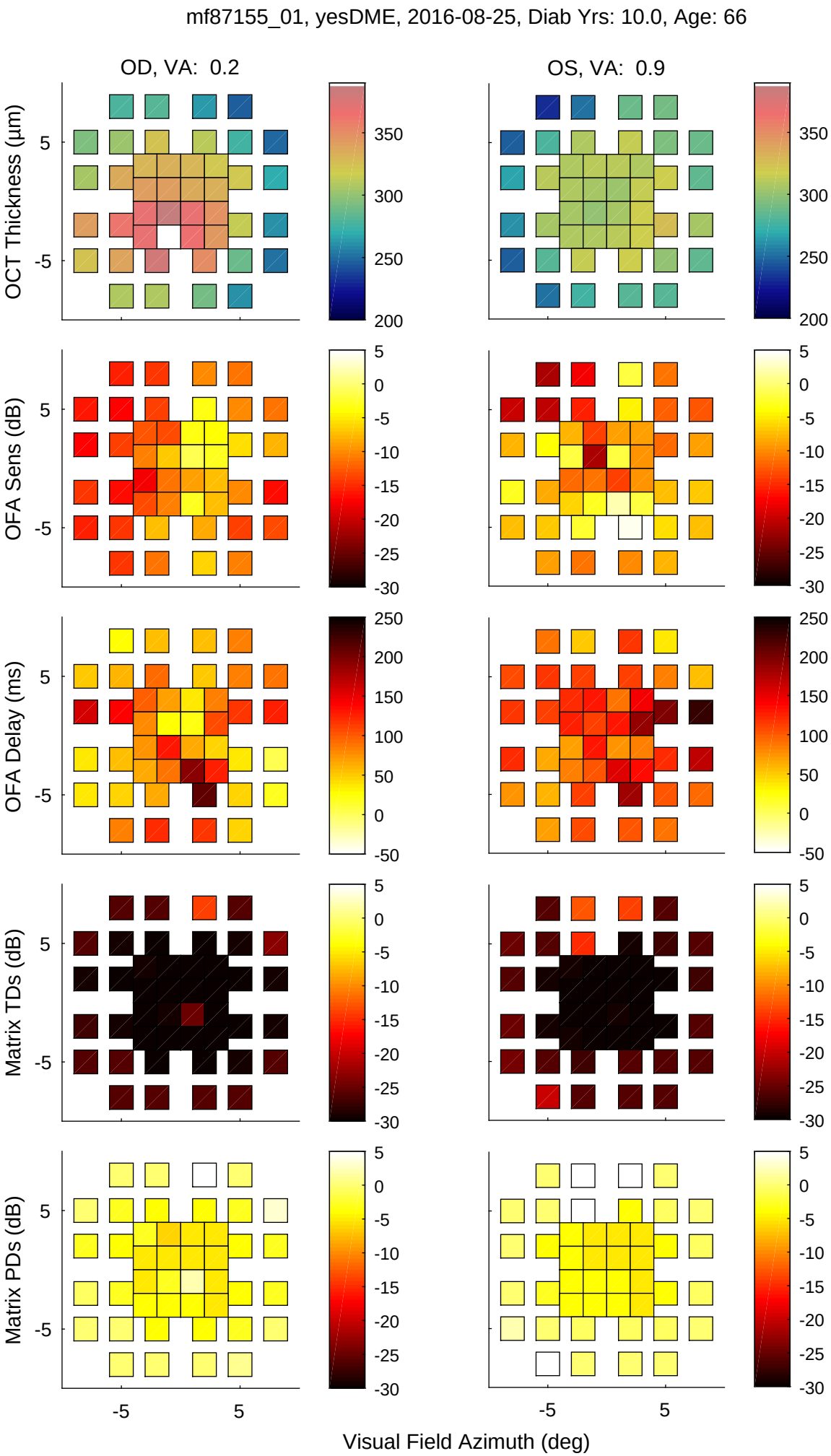
mf87155_01, yesDME, 2016-08-25, Diab Yrs: 10.0, Age: 66
OD, VA: 0.2
OS, VA: 0.9
OCT Thickness (µm)
OFA Sens (dB)
OFA Delay (ms)
Matrix TDs (dB)
Matrix PDs (dB)
Visual Field Azimuth (deg)

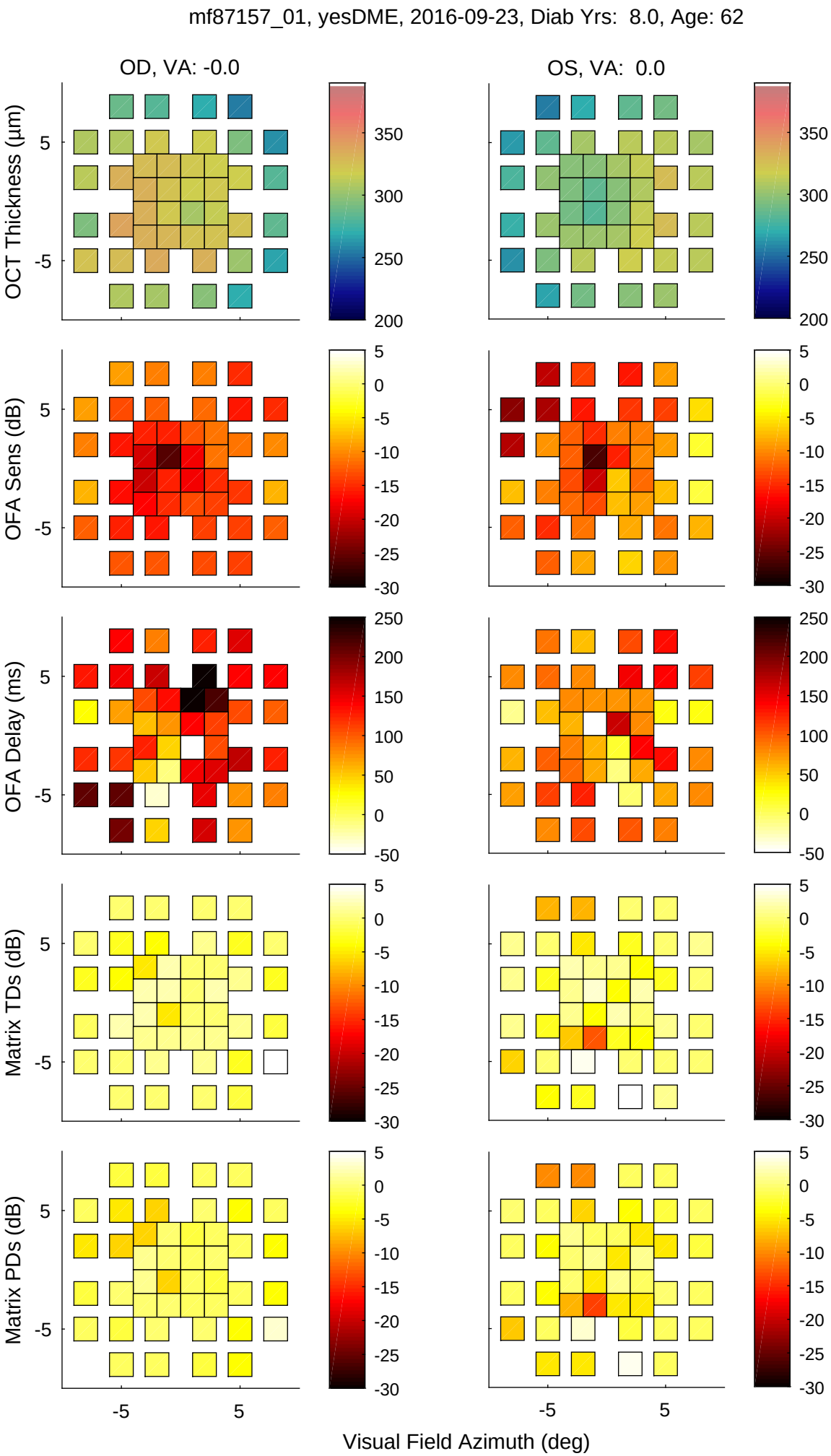
mf87157_01, yesDME, 2016-09-23, Diab Yrs: 8.0, Age: 62
OD, VA: -0.0
OS, VA: 0.0
OCT Thickness (µm)
OFA Sens (dB)
OFA Delay (ms)
Matrix TDs (dB)
Matrix PDs (dB)
Visual Field Azimuth (deg)

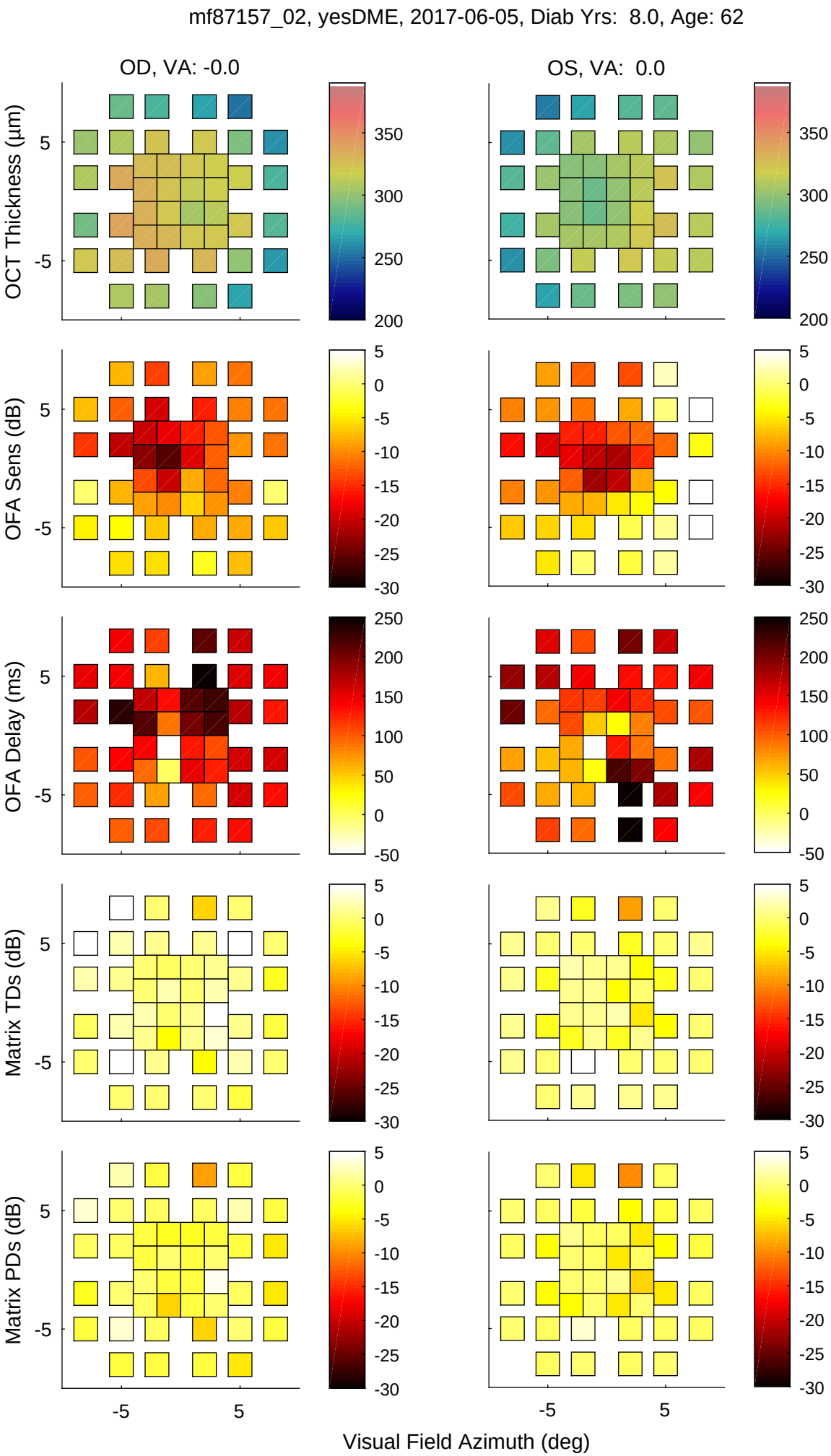
mf87157_02, yesDME, 2017-06-05, Diab Yrs: 8.0, Age: 62
OD, VA: -0.0
OS, VA: 0.0
OCT Thickness (µm)
OFA Sens (dB)
OFA Delay (ms)
Matrix TDs (dB)
Matrix PDs (dB)
Visual Field Azimuth (deg)

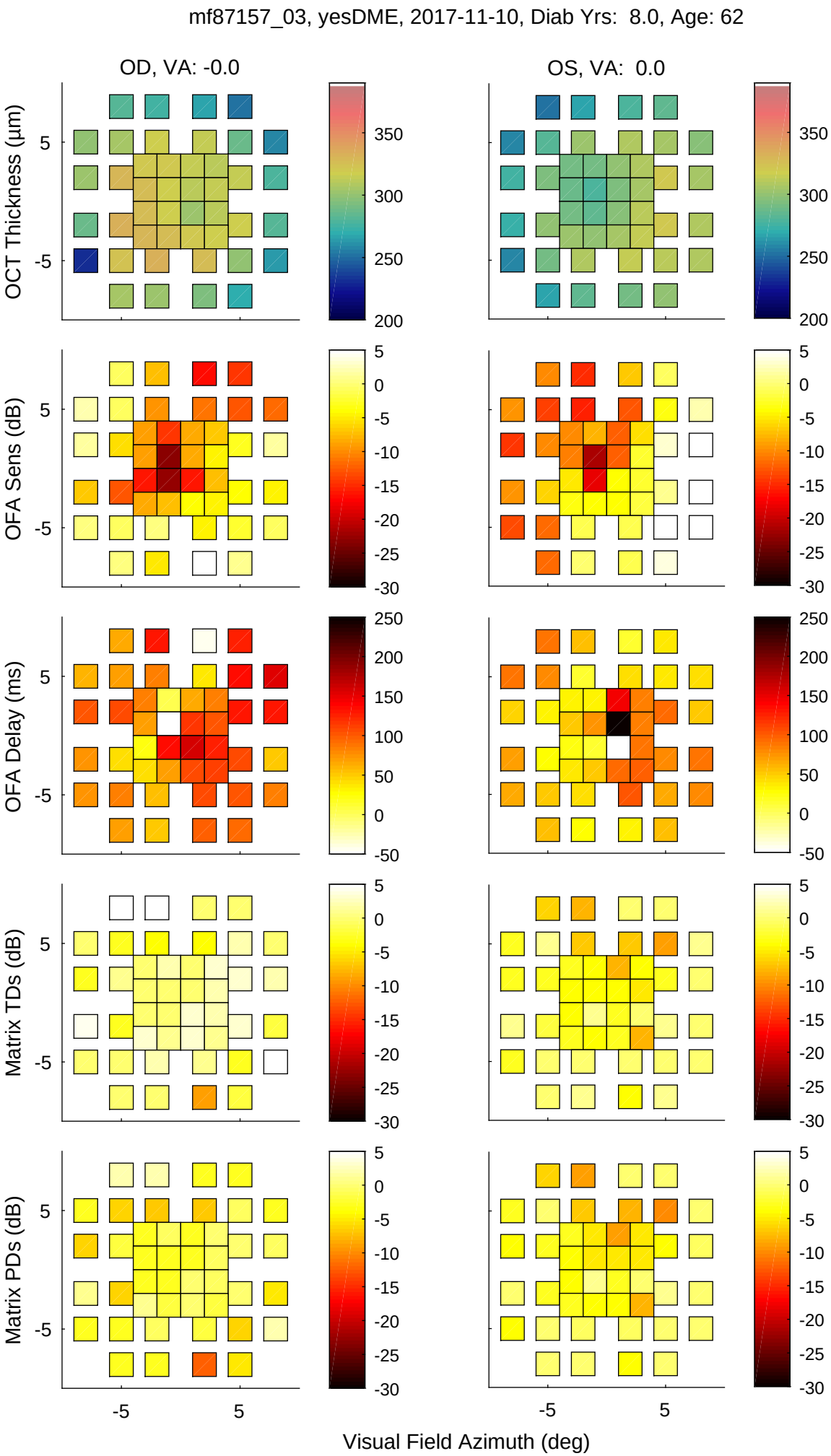
mf87157_03, yesDME, 2017-11-10, Diab Yrs: 8.0, Age: 62
OD, VA: -0.0
OS, VA: 0.0
OCT Thickness (µm)
OFA Sens (dB)
OFA Delay (ms)
Matrix TDs (dB)
Matrix PDs (dB)
Visual Field Azimuth (deg)

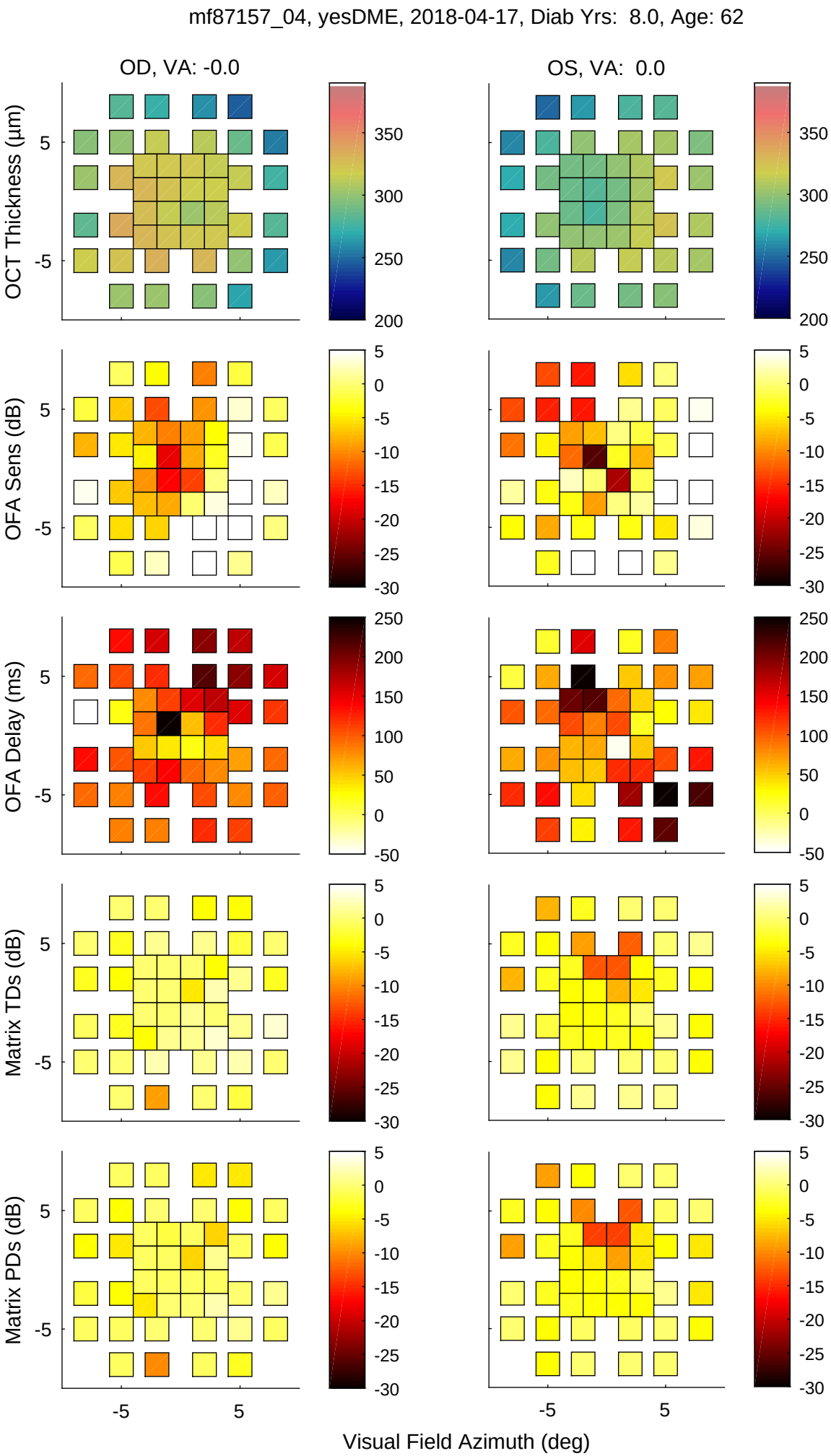
mf87157_04, yesDME, 2018-04-17, Diab Yrs: 8.0, Age: 62
OD, VA: -0.0
OS, VA: 0.0
OCT Thickness (µm)
OFA Sens (dB)
OFA Delay (ms)
Matrix TDs (dB)
Matrix PDs (dB)
Visual Field Azimuth (deg)

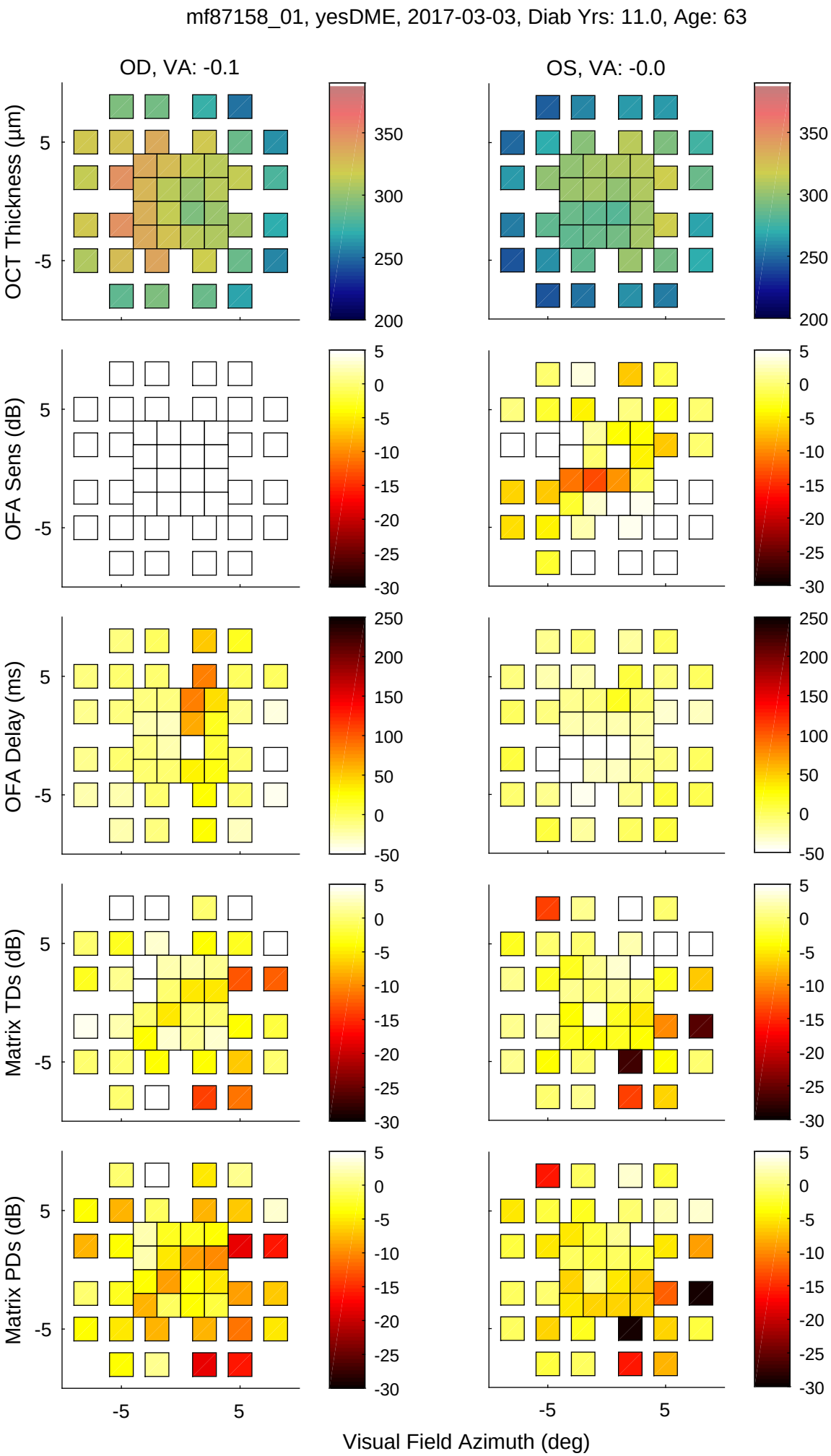
mf87158_01, yesDME, 2017-03-03, Diab Yrs: 11.0, Age: 63
OD, VA: -0.1
OS, VA: -0.0
OCT Thickness (µm)
OFA Sens (dB)
OFA Delay (ms)
Matrix TDs (dB)
Matrix PDs (dB)
Visual Field Azimuth (deg)

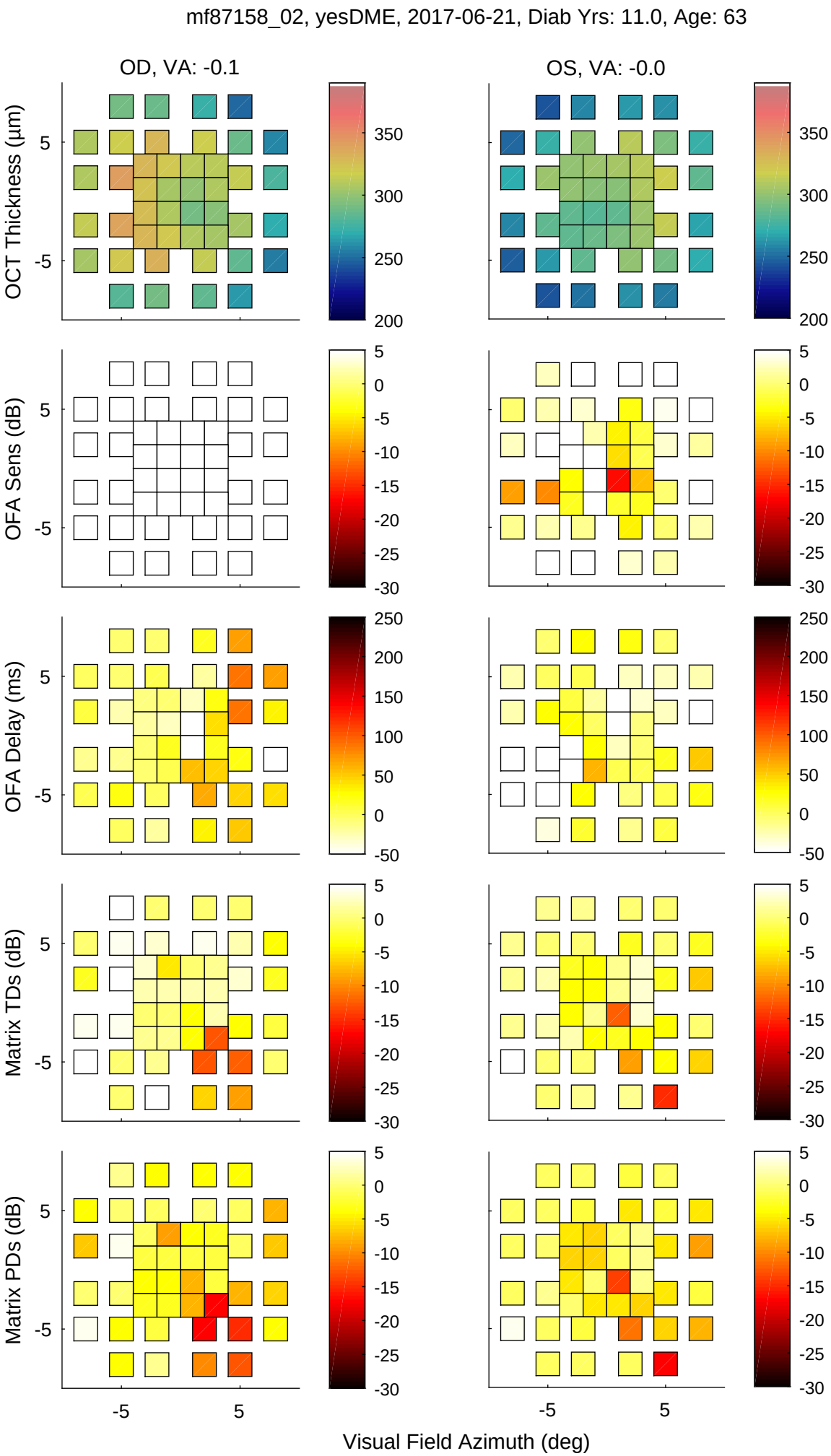
mf87158_02, yesDME, 2017-06-21, Diab Yrs: 11.0, Age: 63
OD, VA: -0.1
OS, VA: -0.0
OCT Thickness (µm)
OFA Sens (dB)
OFA Delay (ms)
Matrix TDs (dB)
Matrix PDs (dB)
Visual Field Azimuth (deg)

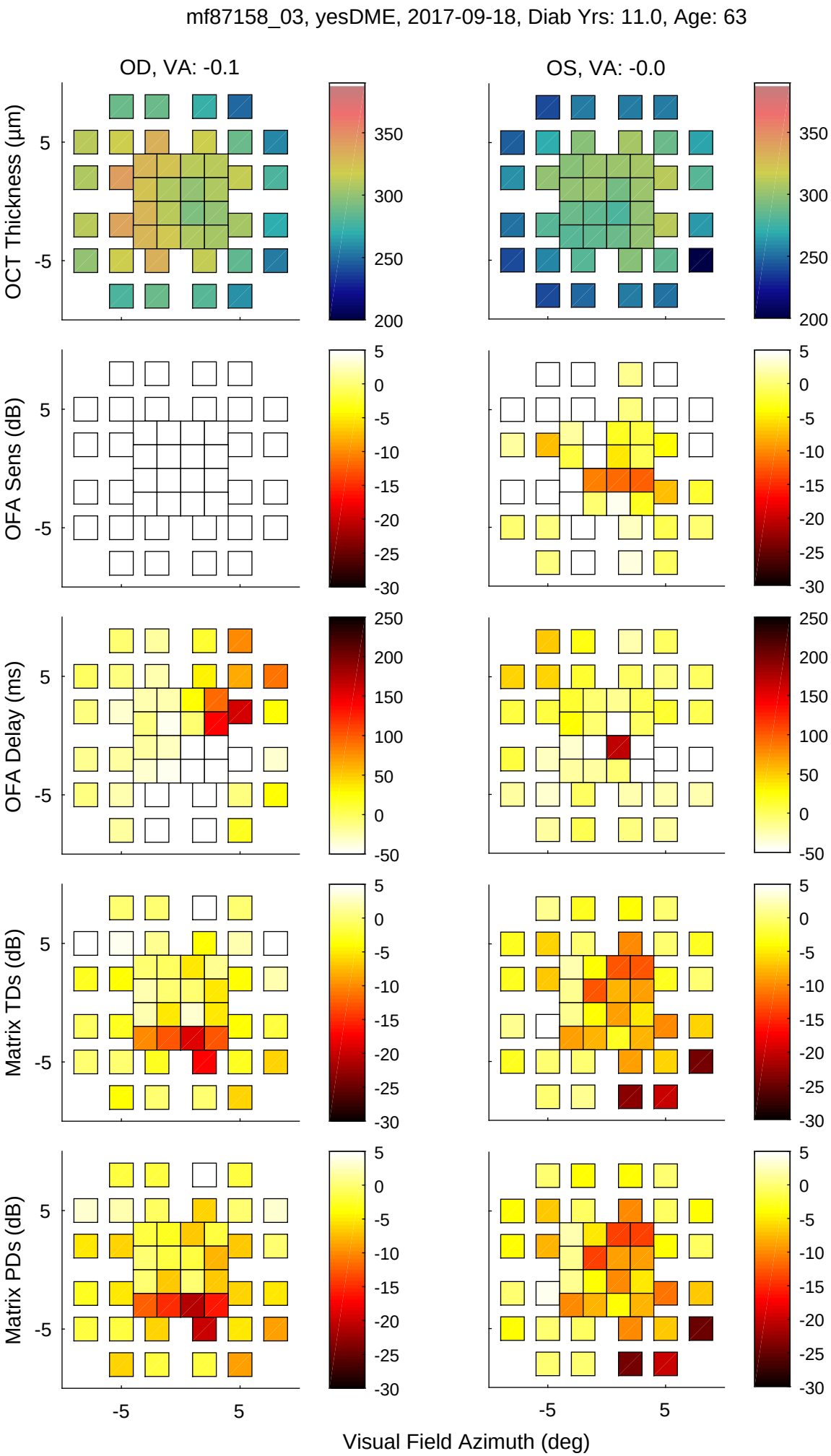
mf87158_03, yesDME, 2017-09-18, Diab Yrs: 11.0, Age: 63
OD, VA: -0.1
OS, VA: -0.0
OCT Thickness (µm)
OFA Sens (dB)
OFA Delay (ms)
Matrix TDs (dB)
Matrix PDs (dB)
Visual Field Azimuth (deg)

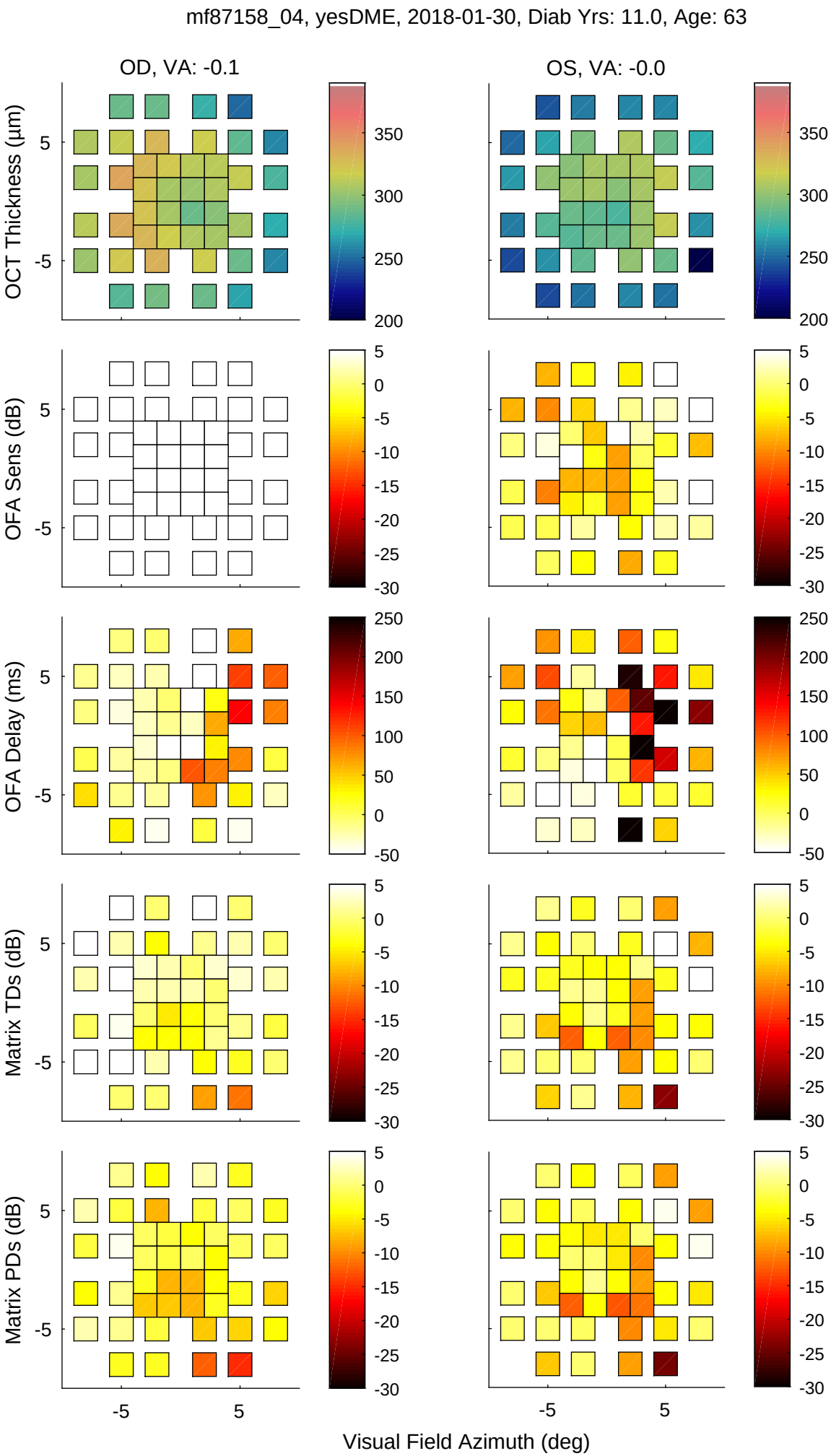
mf87158_04, yesDME, 2018-01-30, Diab Yrs: 11.0, Age: 63
OD, VA: -0.1
OS, VA: -0.0
OCT Thickness (µm)
OFA Sens (dB)
OFA Delay (ms)
Matrix TDs (dB)
Matrix PDs (dB)
Visual Field Azimuth (deg)

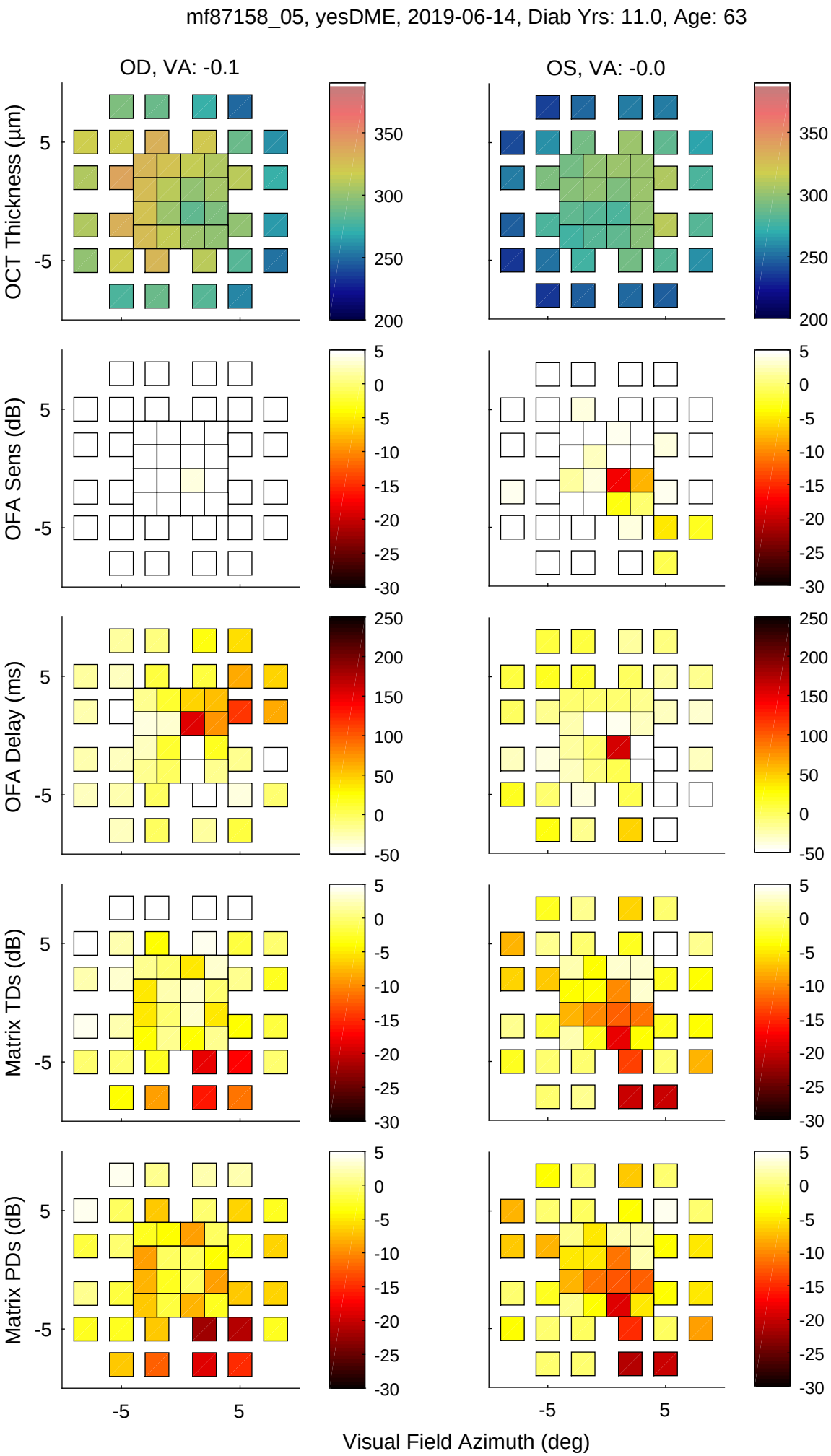
mf87158_05, yesDME, 2019-06-14, Diab Yrs: 11.0, Age: 63
OD, VA: -0.1
OS, VA: -0.0
OCT Thickness (µm)
OFA Sens (dB)
OFA Delay (ms)
Matrix TDs (dB)
Matrix PDs (dB)
Visual Field Azimuth (deg)

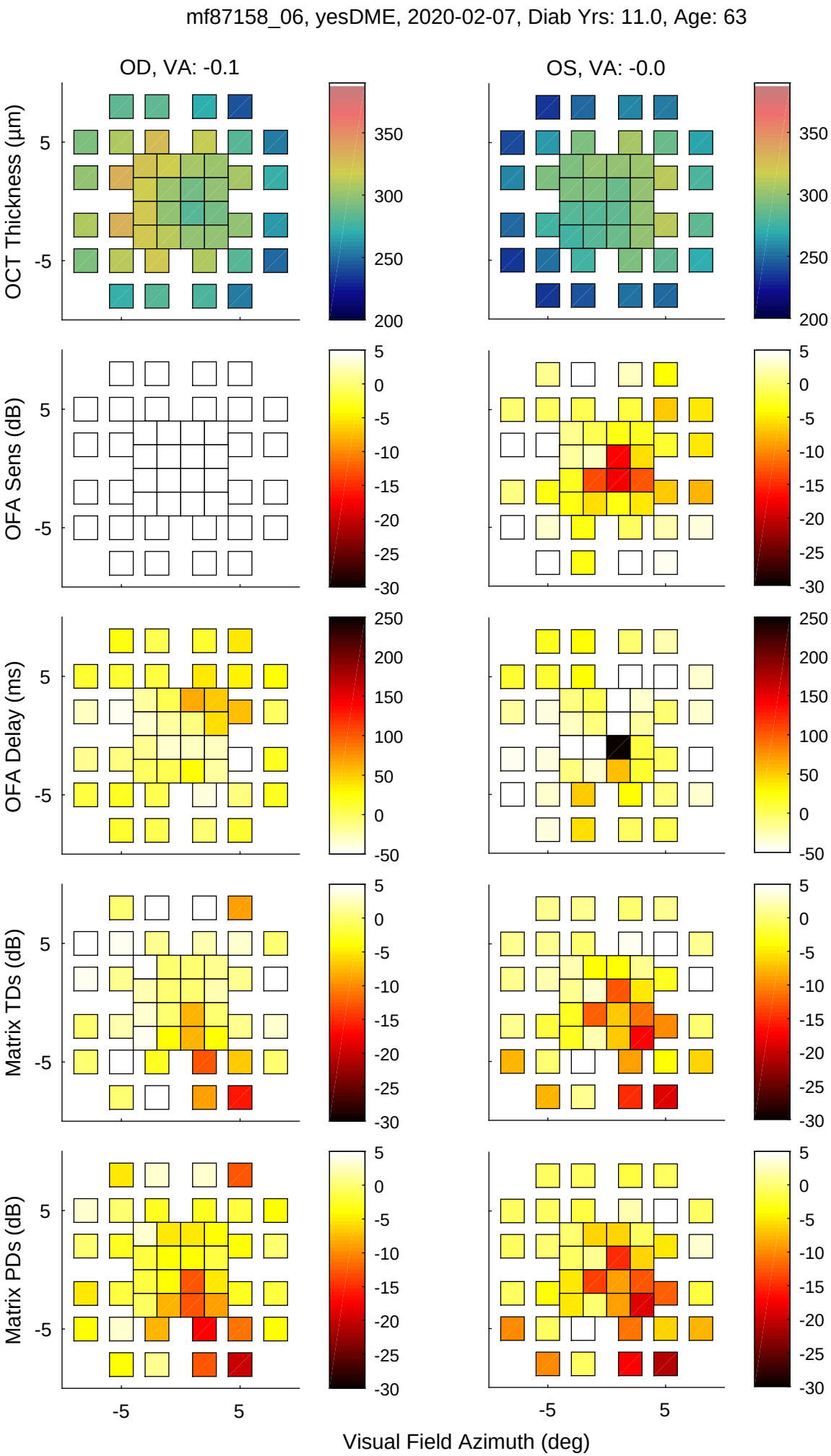
mf87158_06, yesDME, 2020-02-07, Diab Yrs: 11.0, Age: 63
OD, VA: -0.1
OS, VA: -0.0
OCT Thickness (µm)
OFA Sens (dB)
OFA Delay (ms)
Matrix TDs (dB)
Matrix PDs (dB)
Visual Field Azimuth (deg)

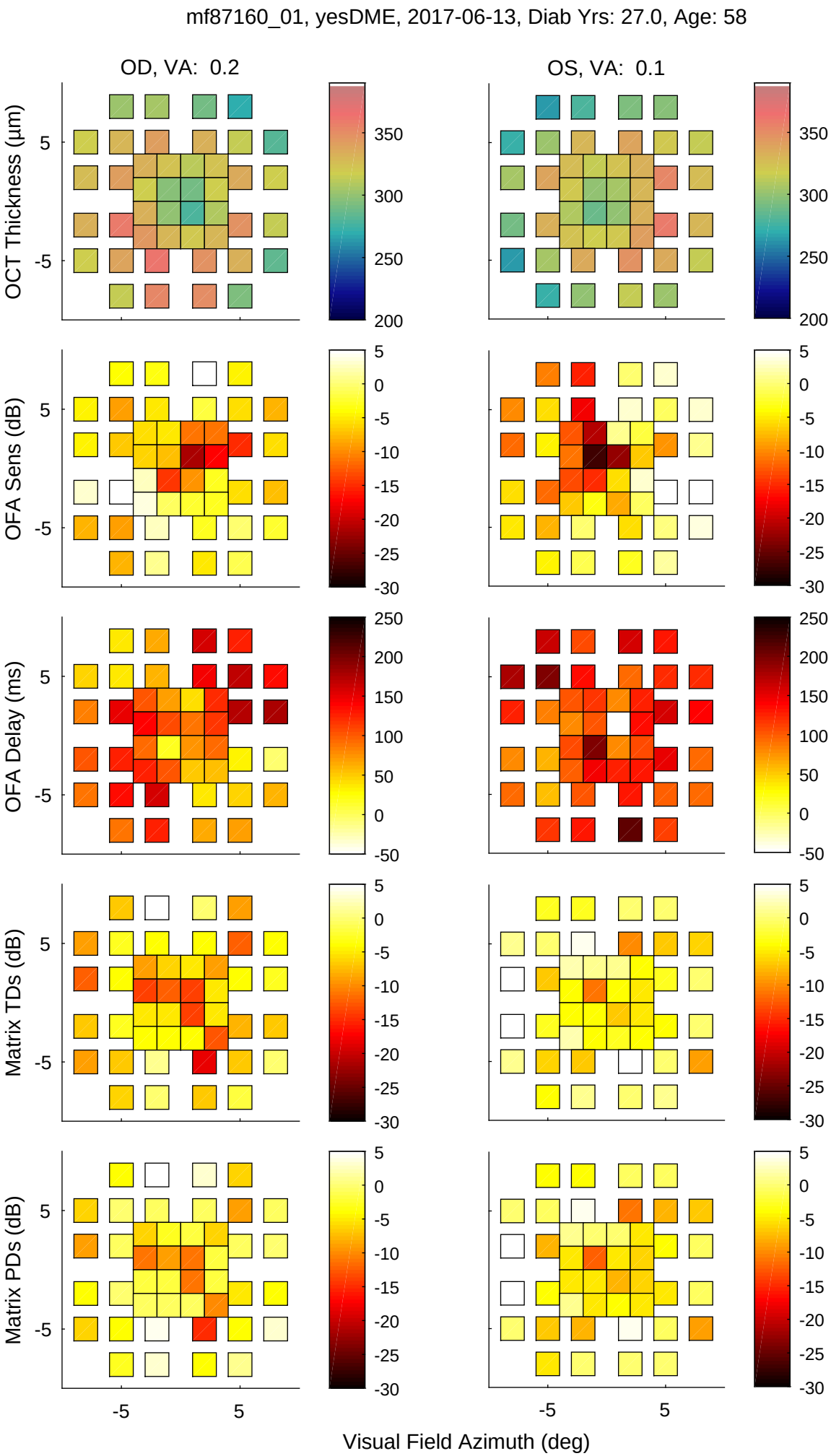
mf87160_01, yesDME, 2017-06-13, Diab Yrs: 27.0, Age: 58
OD, VA: 0.2
OS, VA: 0.1
OCT Thickness (µm)
OFA Sens (dB)
OFA Delay (ms)
Matrix TDs (dB)
Matrix PDs (dB)
Visual Field Azimuth (deg)

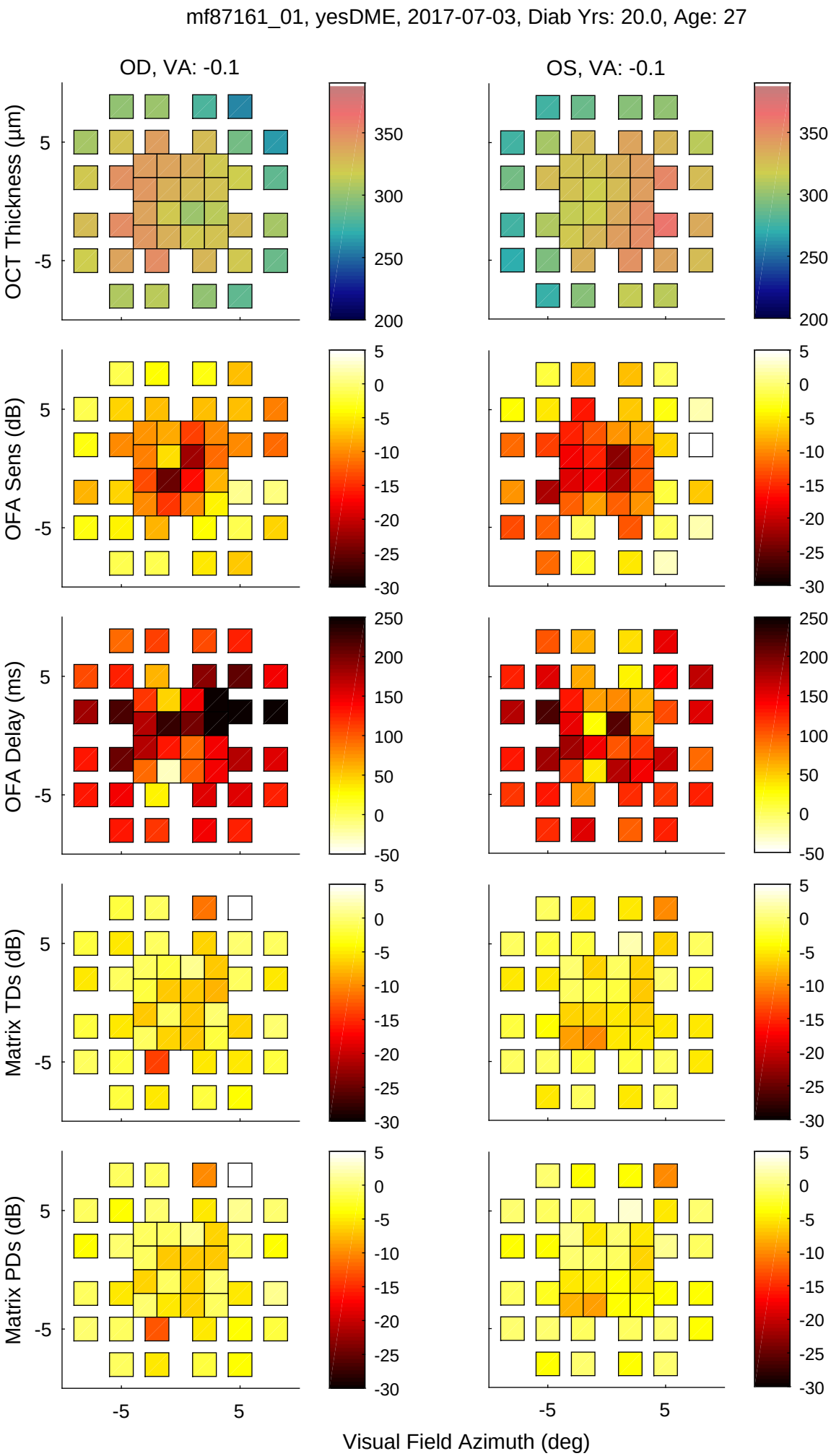
mf87161_01, yesDME, 2017-07-03, Diab Yrs: 20.0, Age: 27
OD, VA: -0.1
OS, VA: -0.1
OCT Thickness (µm)
OFA Sens (dB)
OFA Delay (ms)
Matrix TDs (dB)
Matrix PDs (dB)
Visual Field Azimuth (deg)

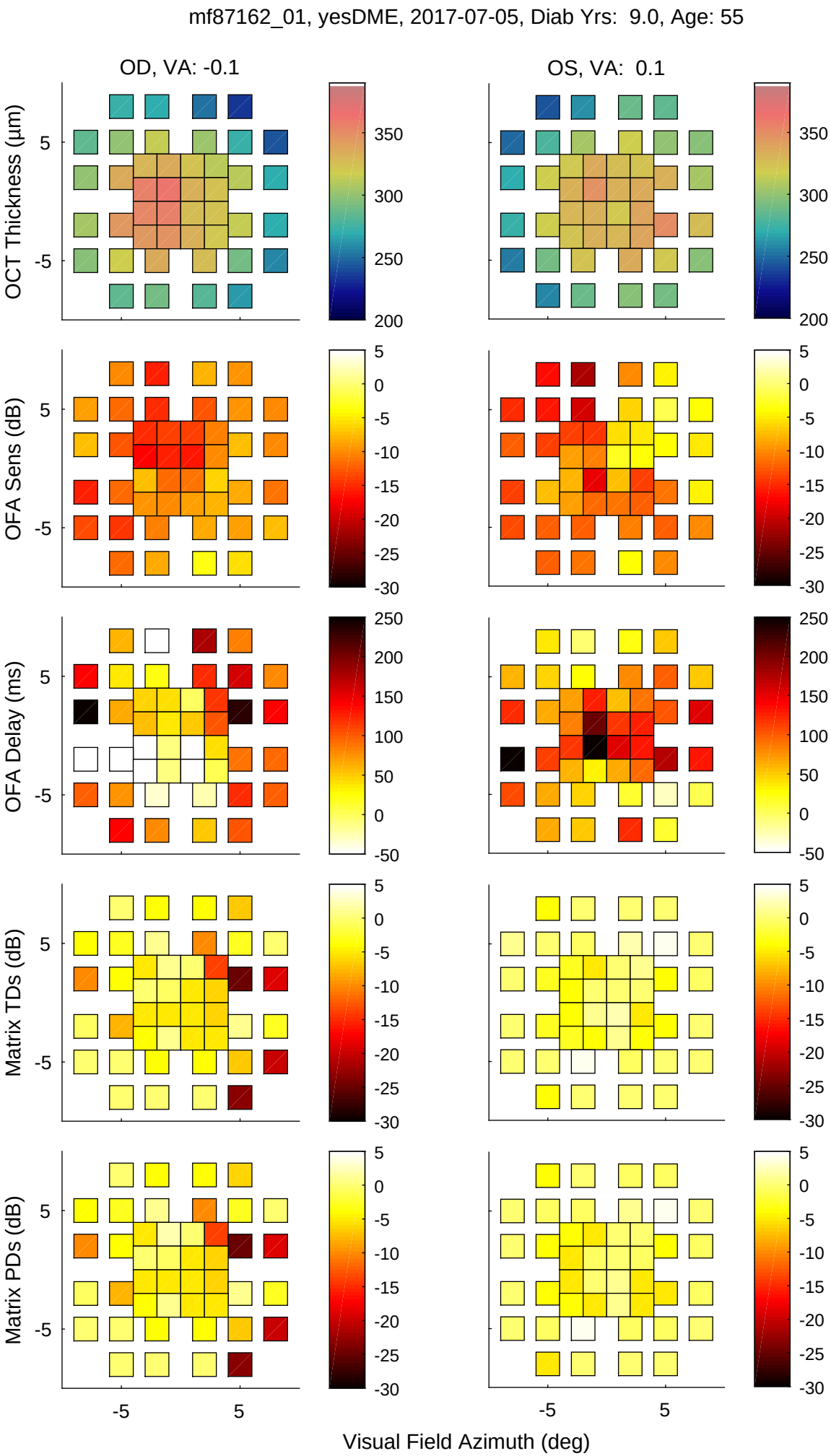
mf87162_01, yesDME, 2017-07-05, Diab Yrs: 9.0, Age: 55
OD, VA: -0.1
OS, VA: 0.1
OCT Thickness (µm)
OFA Sens (dB)
OFA Delay (ms)
Matrix TDs (dB)
Matrix PDs (dB)
Visual Field Azimuth (deg)

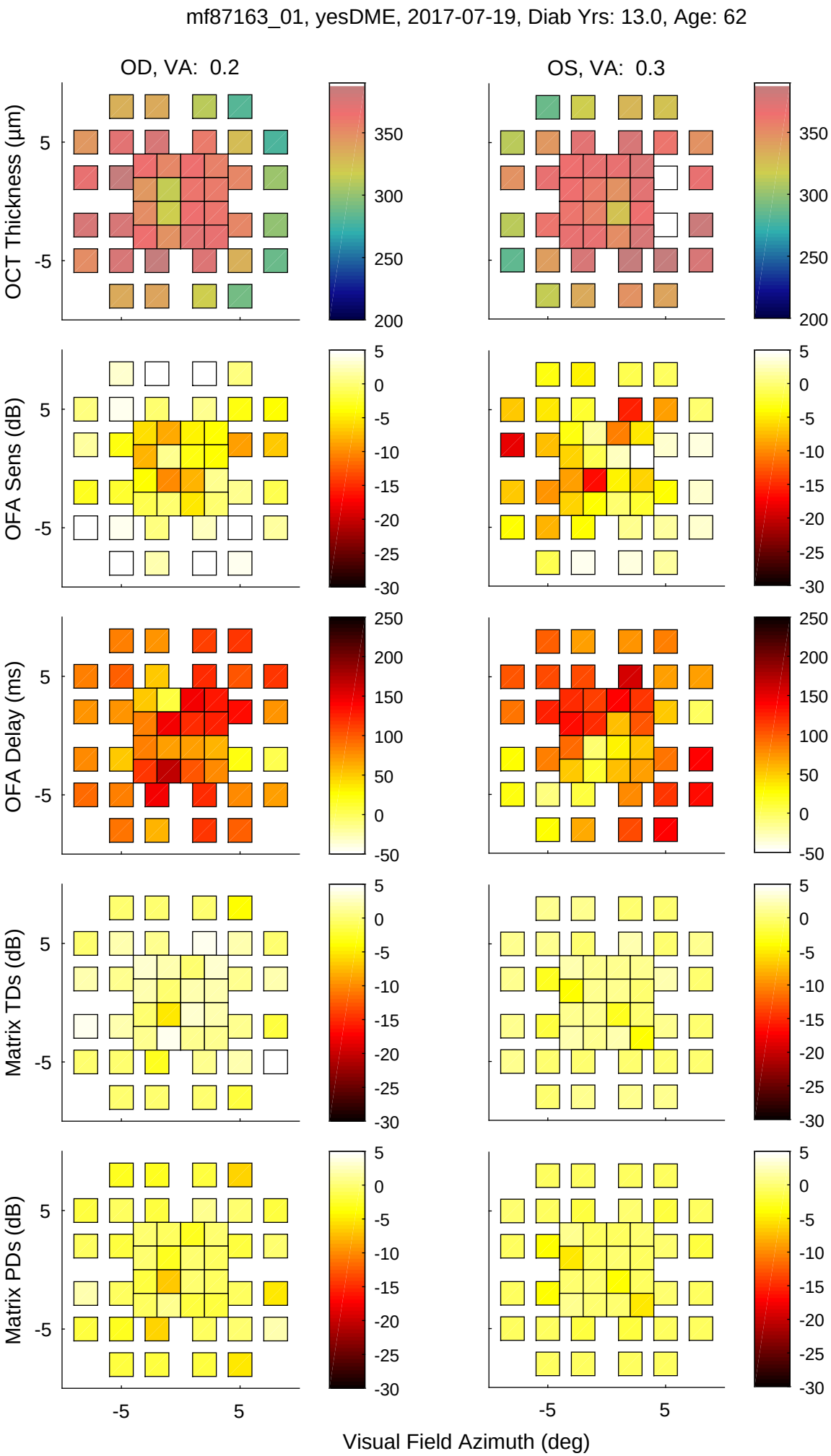
mf87163_01, yesDME, 2017-07-19, Diab Yrs: 13.0, Age: 62
OD, VA: 0.2
OS, VA: 0.3
OCT Thickness (µm)
OFA Sens (dB)
OFA Delay (ms)
Matrix TDs (dB)
Matrix PDs (dB)
Visual Field Azimuth (deg)

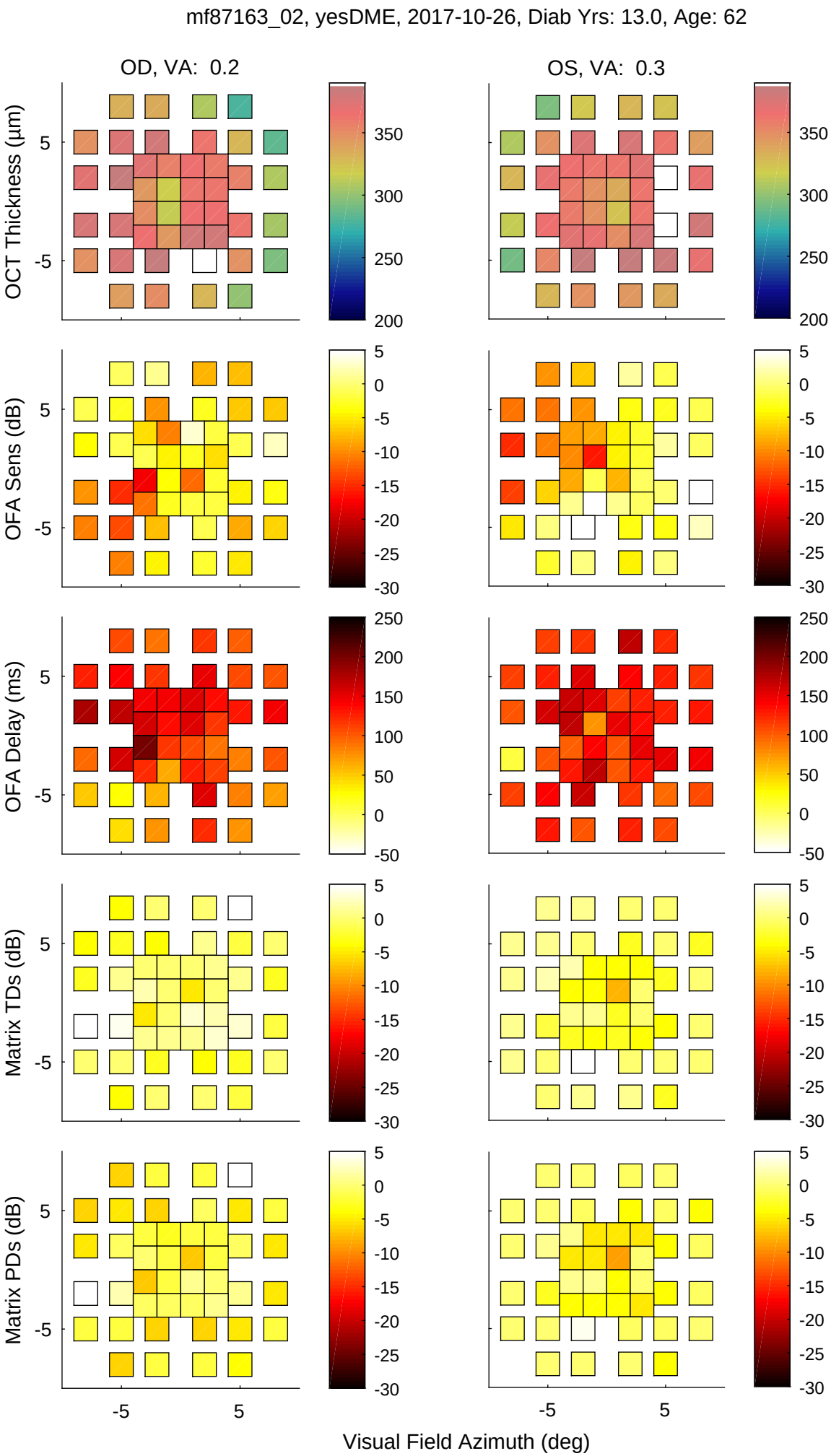
mf87163_02, yesDME, 2017-10-26, Diab Yrs: 13.0, Age: 62
OD, VA: 0.2
OS, VA: 0.3
OCT Thickness (µm)
OFA Sens (dB)
OFA Delay (ms)
Matrix TDs (dB)
Matrix PDs (dB)
Visual Field Azimuth (deg)

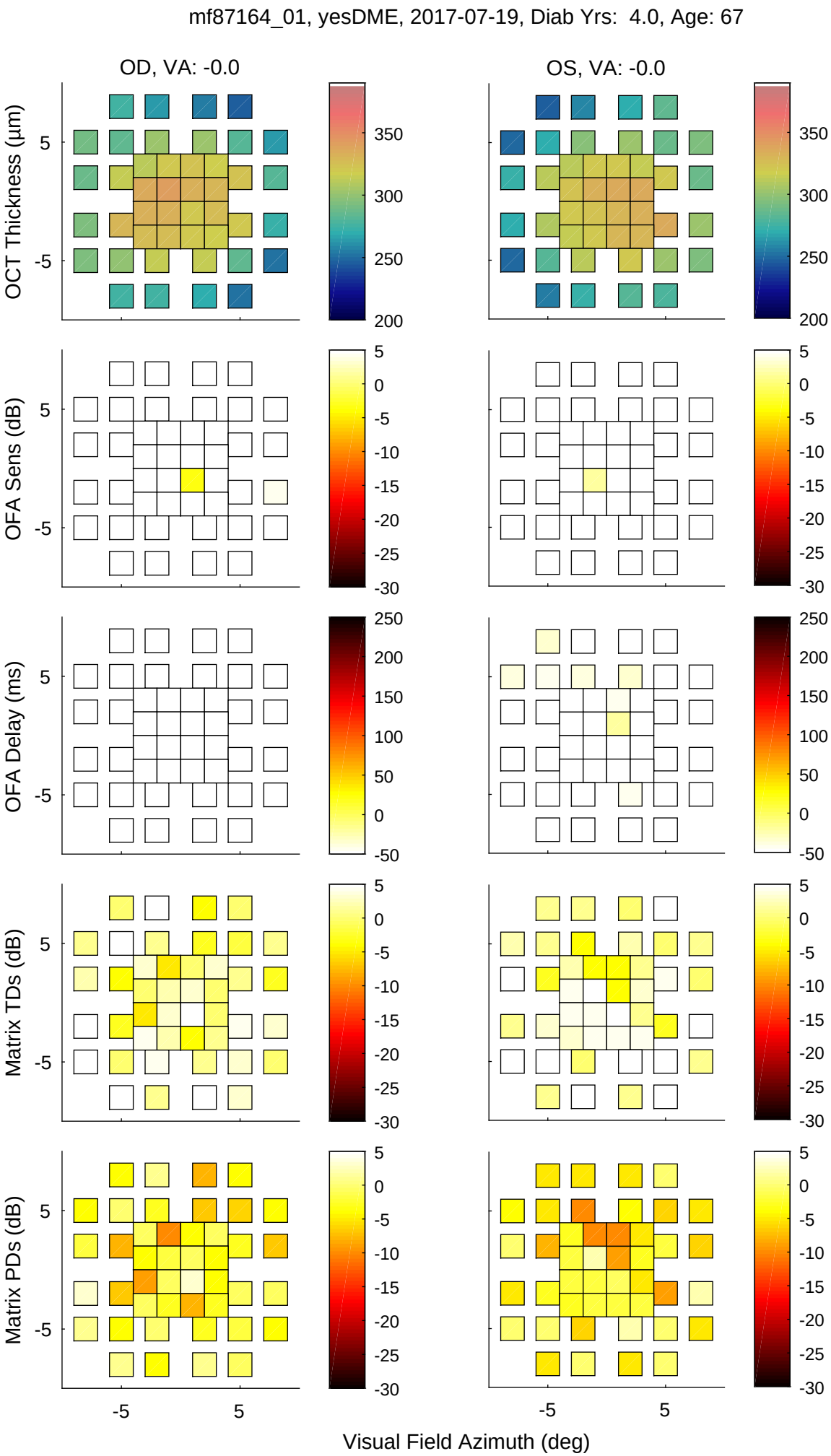
mf87164_01, yesDME, 2017-07-19, Diab Yrs: 4.0, Age: 67
OD, VA: -0.0
OS, VA: -0.0
OCT Thickness (µm)
OFA Sens (dB)
OFA Delay (ms)
Matrix TDs (dB)
Matrix PDs (dB)
Visual Field Azimuth (deg)

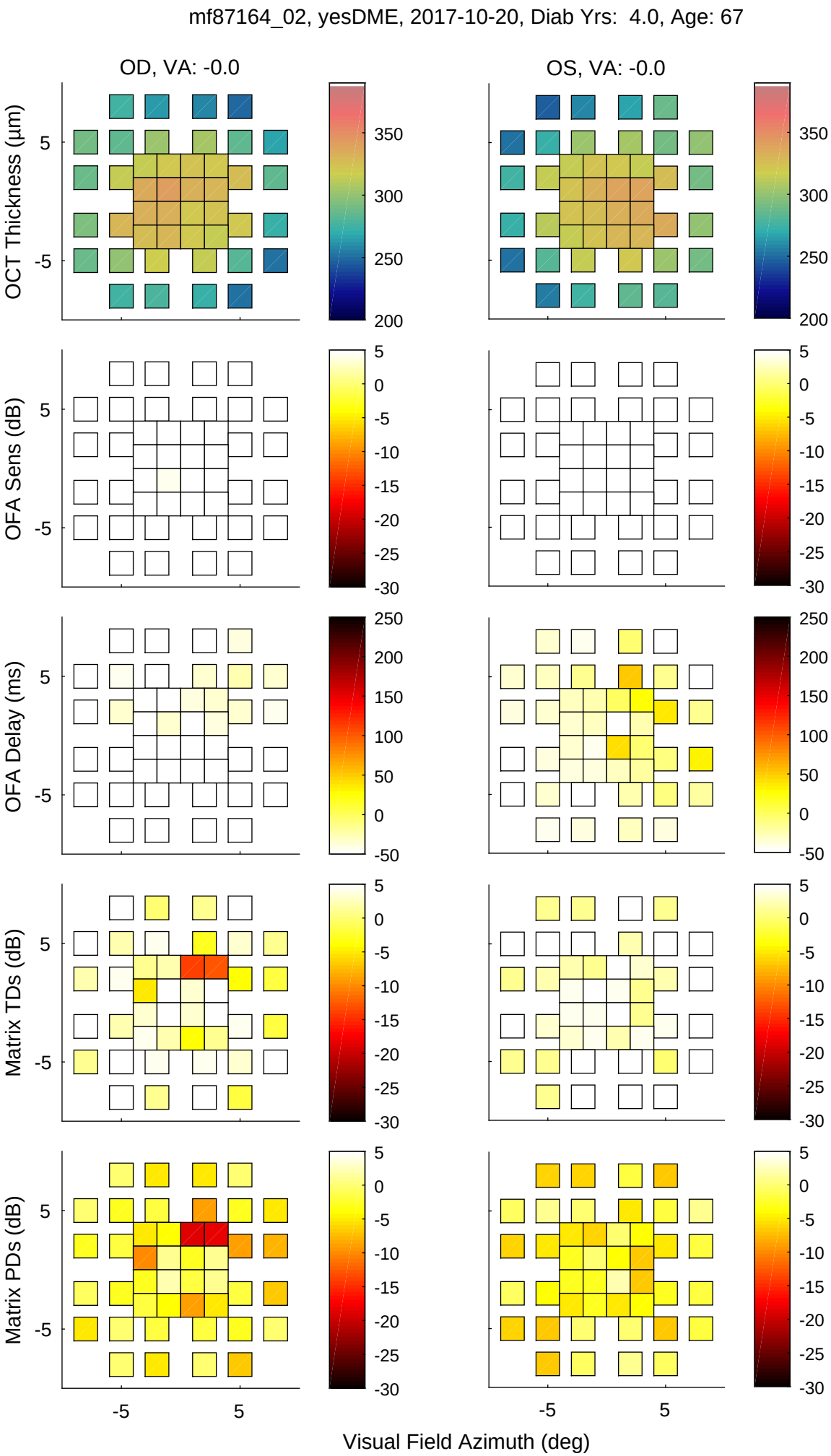
mf87164_02, yesDME, 2017-10-20, Diab Yrs: 4.0, Age: 67
OD, VA: -0.0
OS, VA: -0.0
OCT Thickness (µm)
OFA Sens (dB)
OFA Delay (ms)
Matrix TDs (dB)
Matrix PDs (dB)
Visual Field Azimuth (deg)

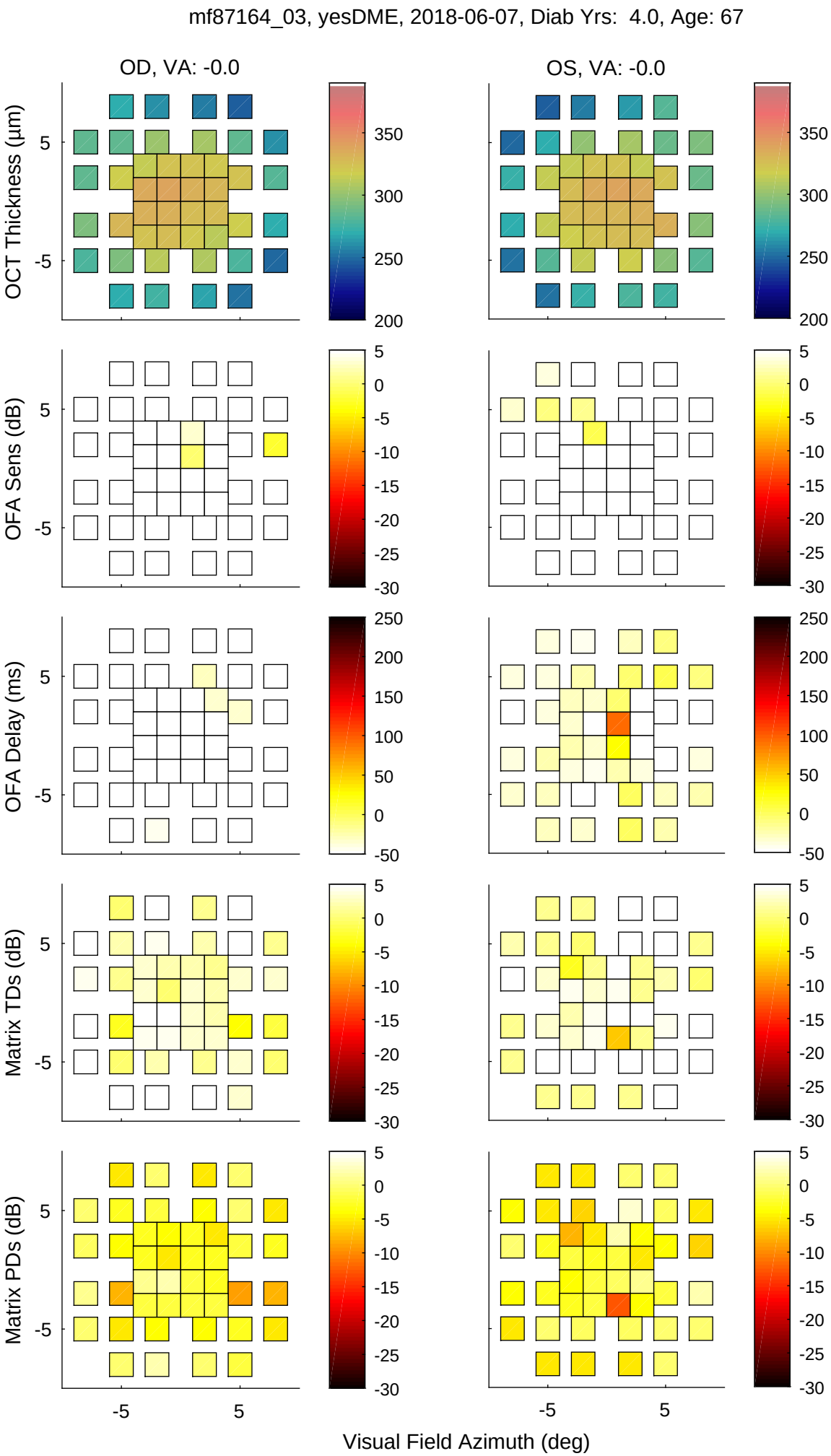
mf87164_03, yesDME, 2018-06-07, Diab Yrs: 4.0, Age: 67
OD, VA: -0.0
OS, VA: -0.0
OCT Thickness (µm)
OFA Sens (dB)
OFA Delay (ms)
Matrix TDs (dB)
Matrix PDs (dB)
Visual Field Azimuth (deg)

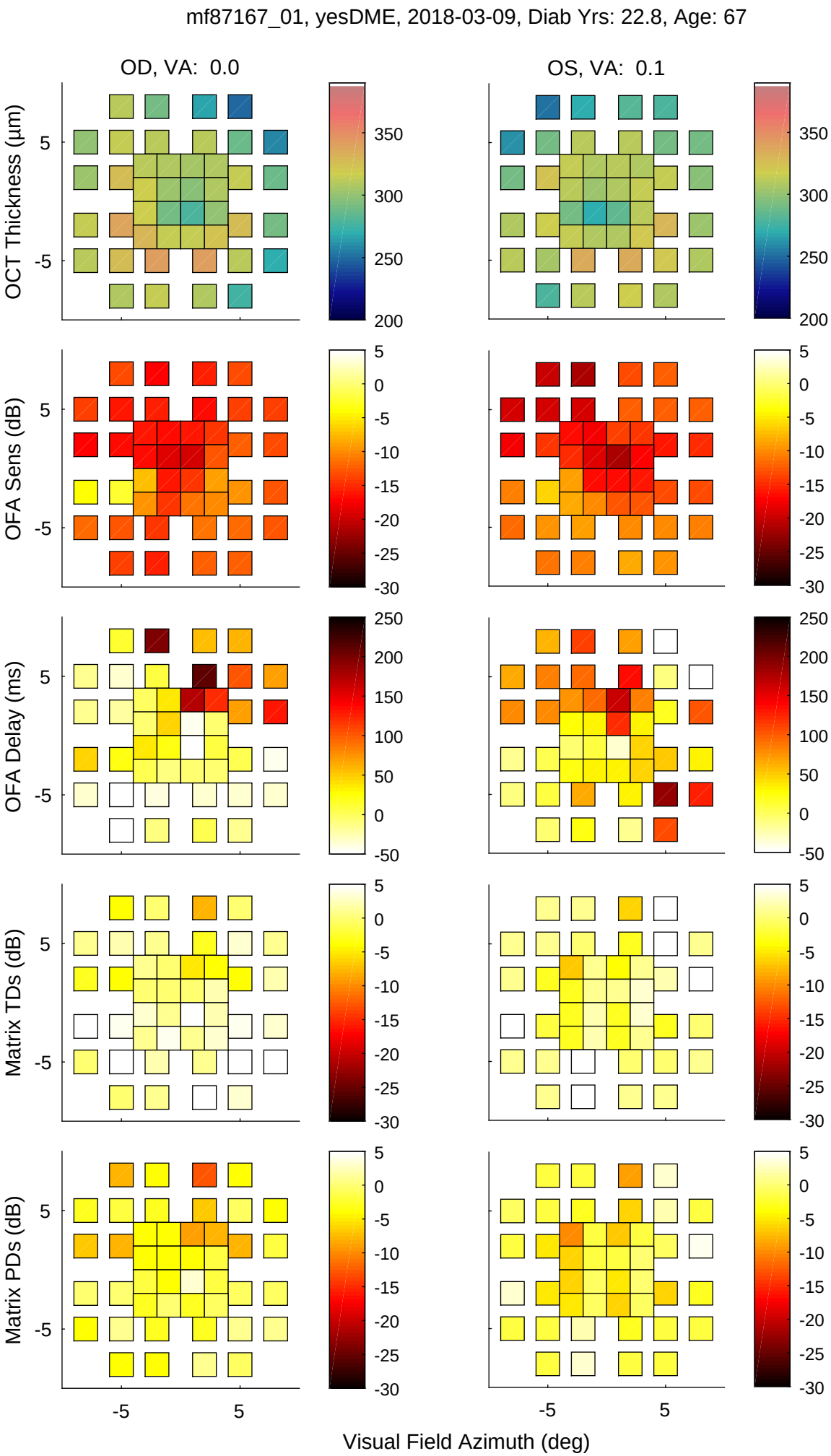
mf87167_01, yesDME, 2018-03-09, Diab Yrs: 22.8, Age: 67
OD, VA: 0.0
OS, VA: 0.1
OCT Thickness (µm)
OFA Sens (dB)
OFA Delay (ms)
Matrix TDs (dB)
Matrix PDs (dB)
Visual Field Azimuth (deg)

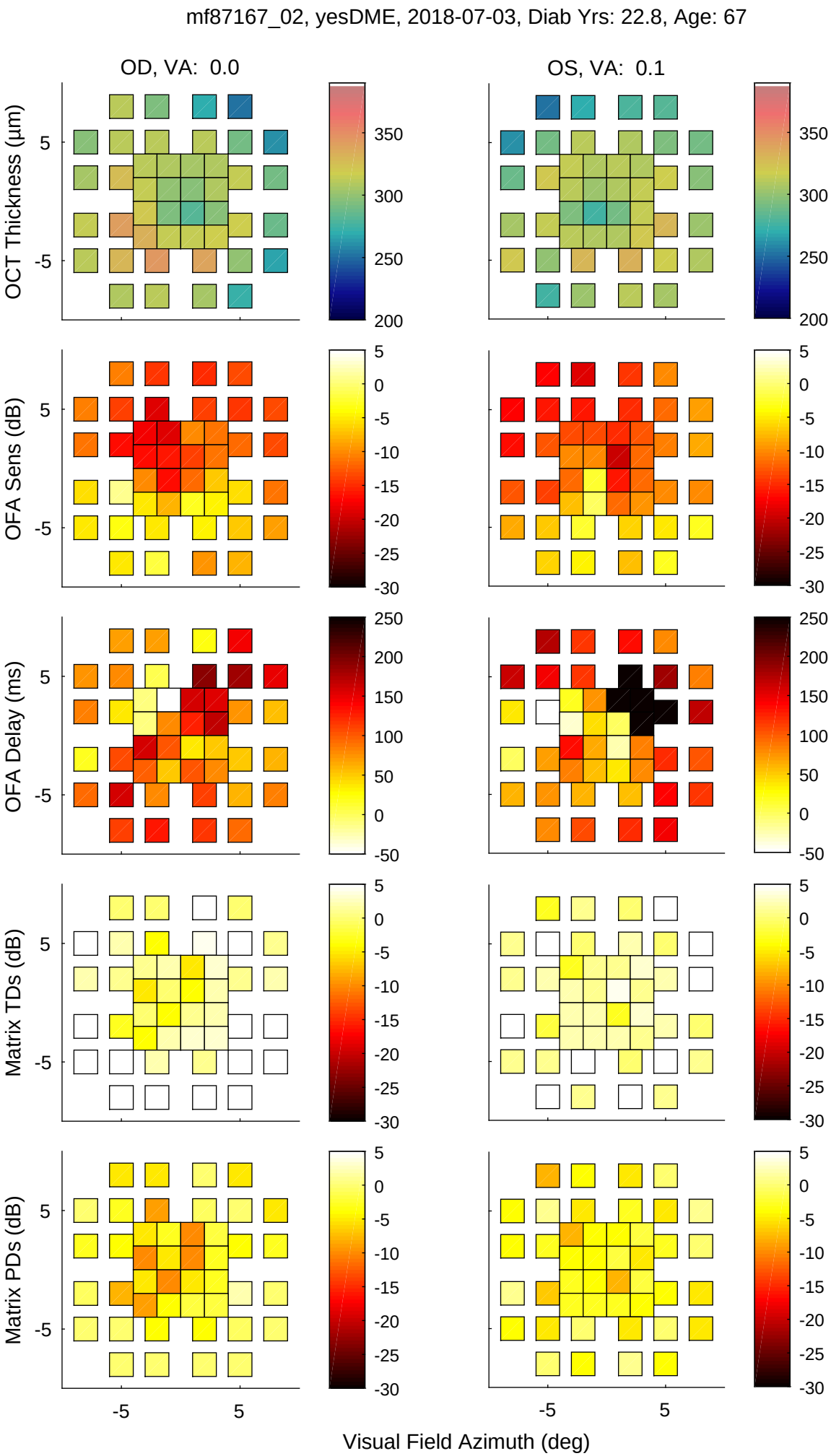
mf87167_02, yesDME, 2018-07-03, Diab Yrs: 22.8, Age: 67
OD, VA: 0.0
OS, VA: 0.1
OCT Thickness (µm)
OFA Sens (dB)
OFA Delay (ms)
Matrix TDs (dB)
Matrix PDs (dB)
Visual Field Azimuth (deg)

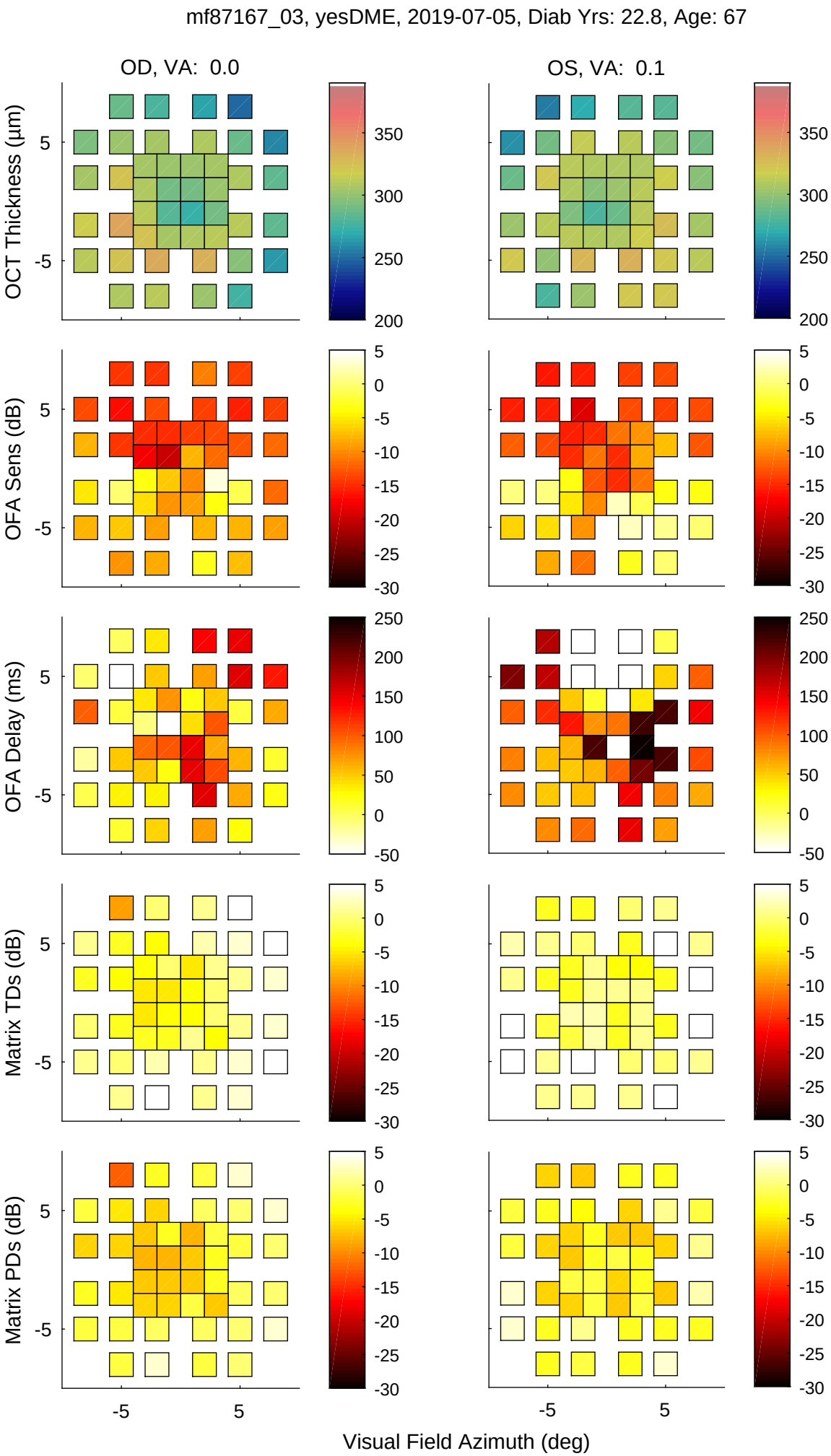
mf87167_03, yesDME, 2019-07-05, Diab Yrs: 22.8, Age: 67
OD, VA: 0.0
OS, VA: 0.1
OCT Thickness (µm)
OFA Sens (dB)
OFA Delay (ms)
Matrix TDs (dB)
Matrix PDs (dB)
Visual Field Azimuth (deg)

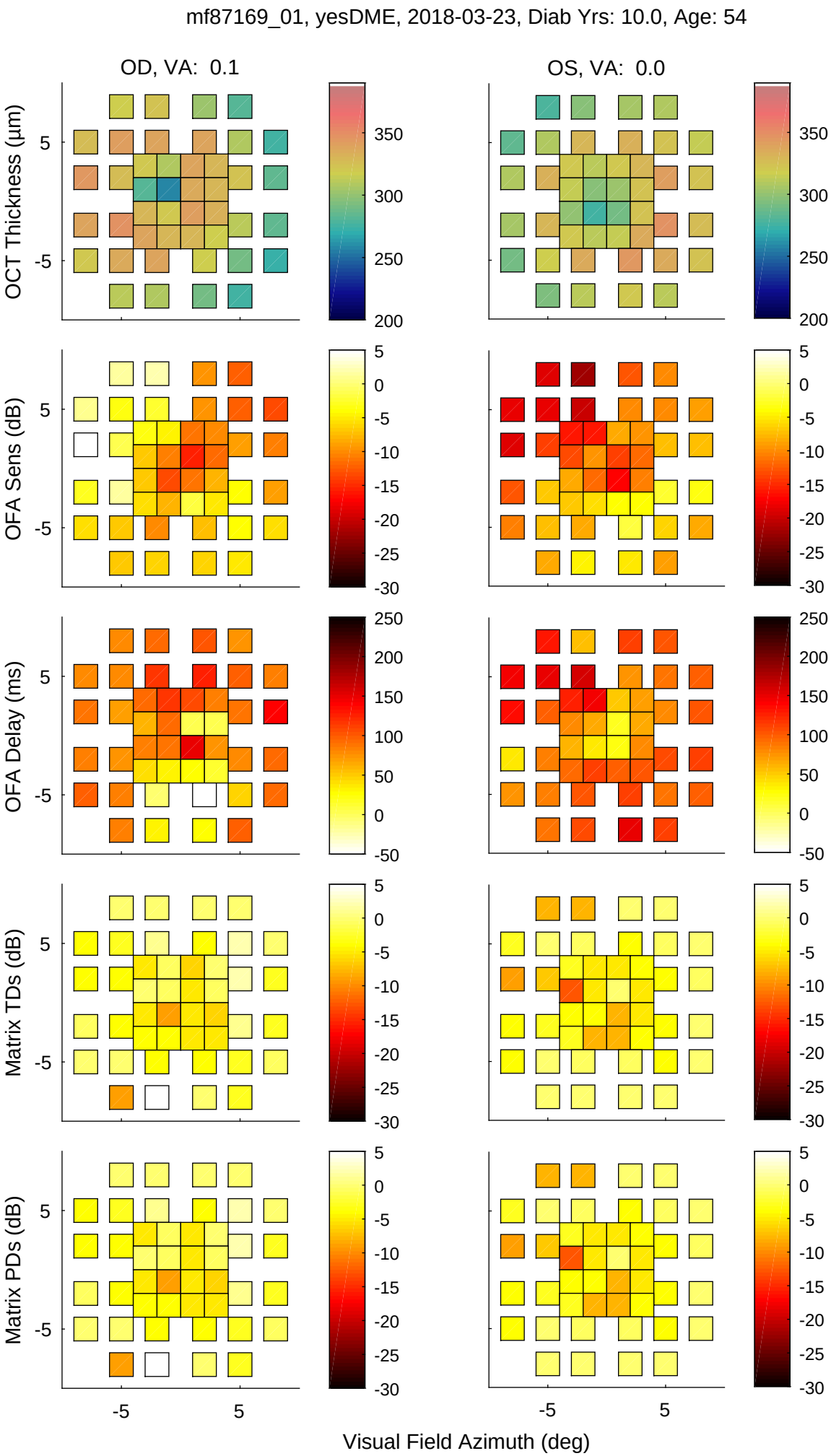
mf87169_01, yesDME, 2018-03-23, Diab Yrs: 10.0, Age: 54
OD, VA: 0.1
OS, VA: 0.0
OCT Thickness (µm)
OFA Sens (dB)
OFA Delay (ms)
Matrix TDs (dB)
Matrix PDs (dB)
Visual Field Azimuth (deg)

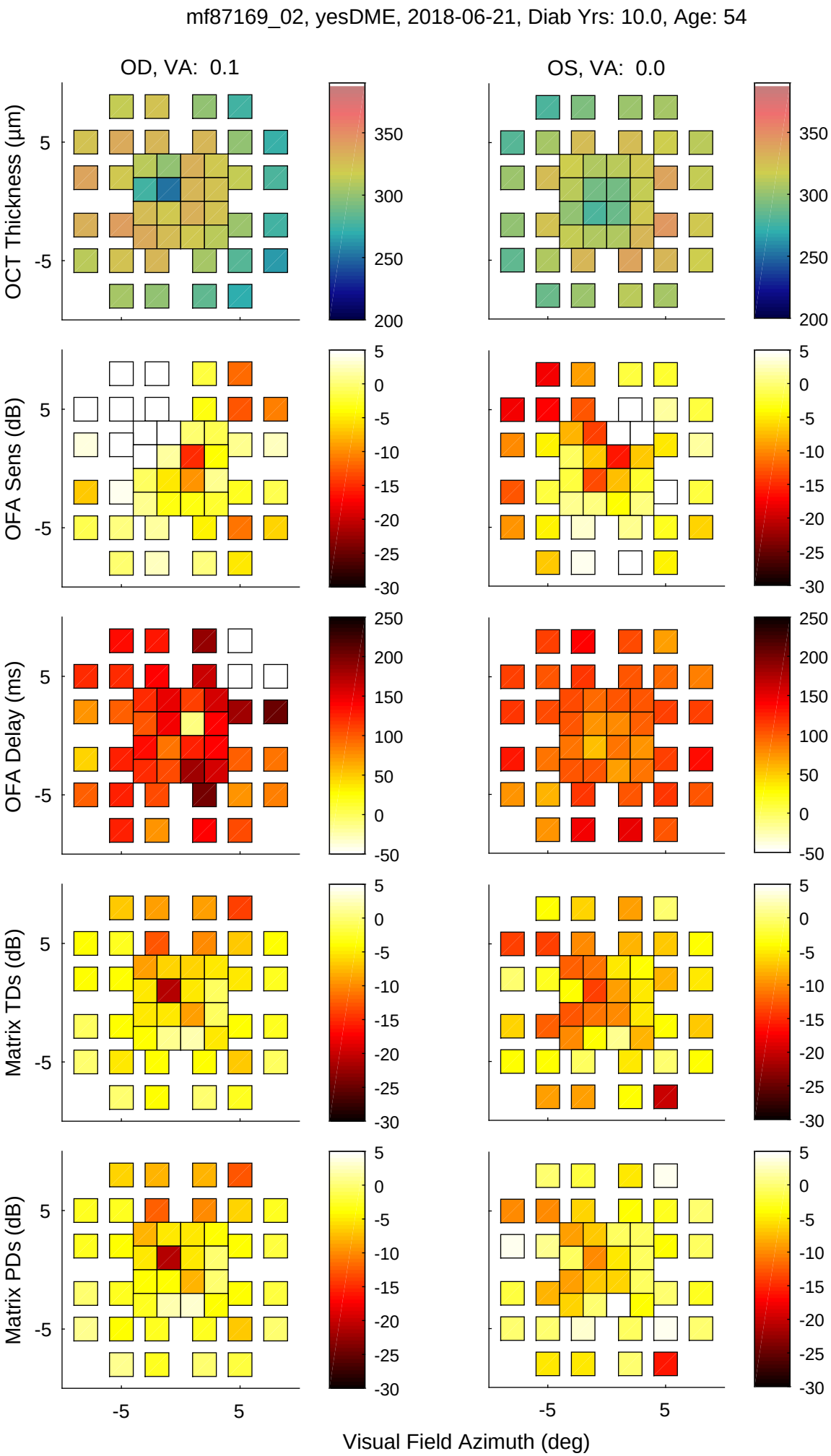
mf87169_02, yesDME, 2018-06-21, Diab Yrs: 10.0, Age: 54
OD, VA: 0.1
OS, VA: 0.0
OCT Thickness (µm)
OFA Sens (dB)
OFA Delay (ms)
Matrix TDs (dB)
Matrix PDs (dB)
Visual Field Azimuth (deg)

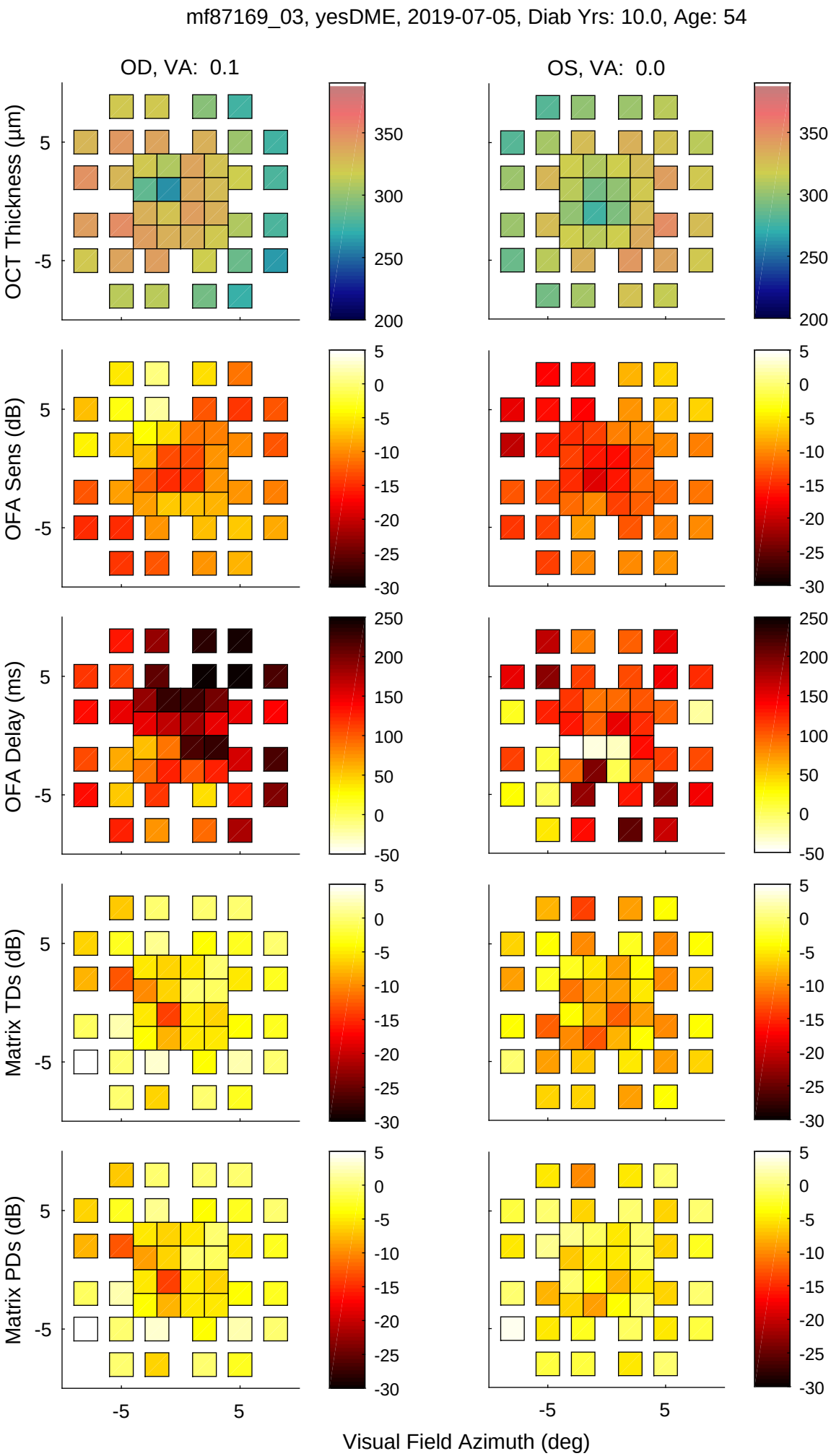
mf87169_03, yesDME, 2019-07-05, Diab Yrs: 10.0, Age: 54
OD, VA: 0.1
OS, VA: 0.0
OCT Thickness (µm)
OFA Sens (dB)
OFA Delay (ms)
Matrix TDs (dB)
Matrix PDs (dB)
Visual Field Azimuth (deg)

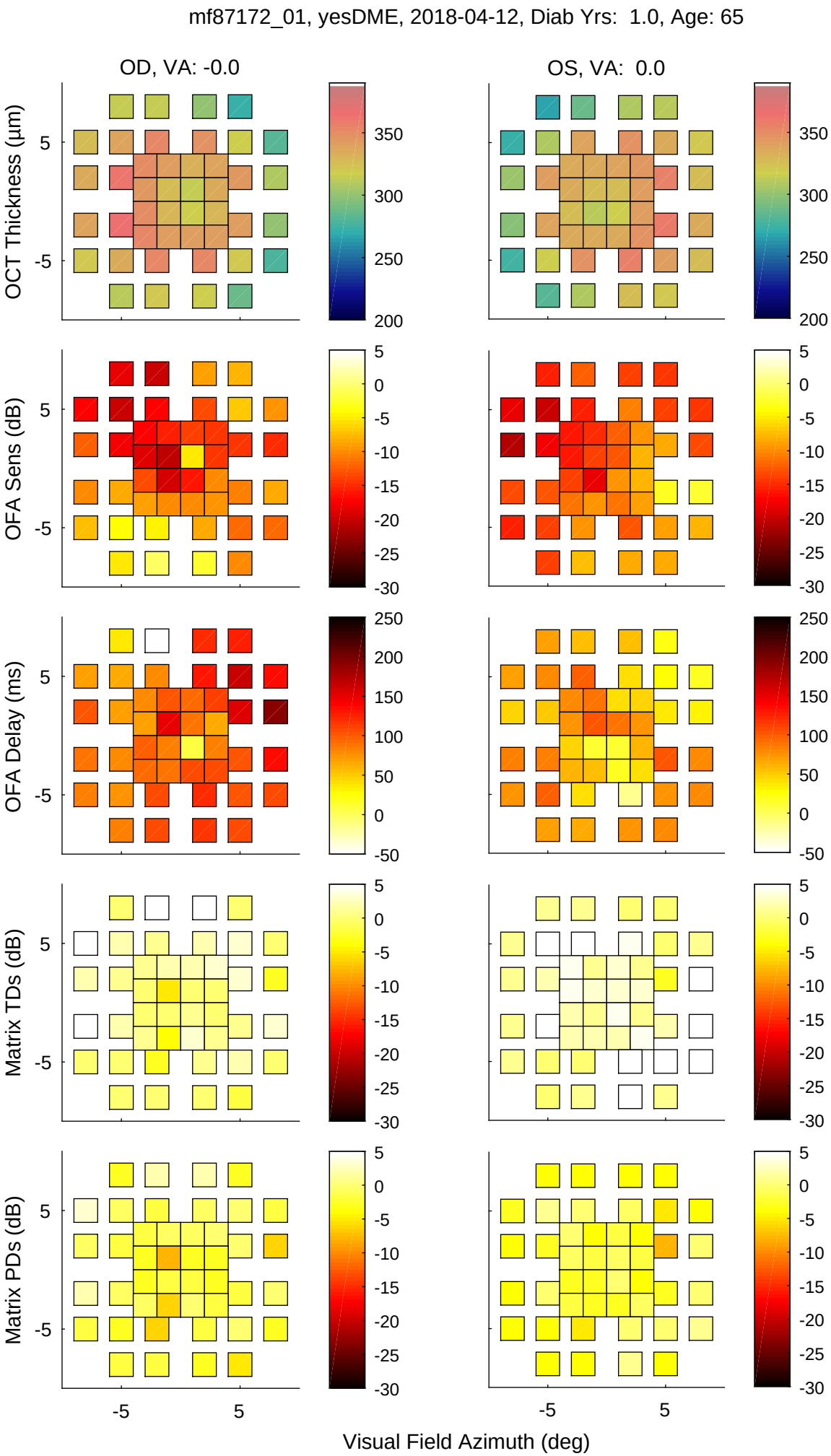
mf87172_01, yesDME, 2018-04-12, Diab Yrs: 1.0, Age: 65
OD, VA: -0.0
OS, VA: 0.0
OCT Thickness (µm)
OFA Sens (dB)
OFA Delay (ms)
Matrix TDs (dB)
Matrix PDs (dB)
Visual Field Azimuth (deg)

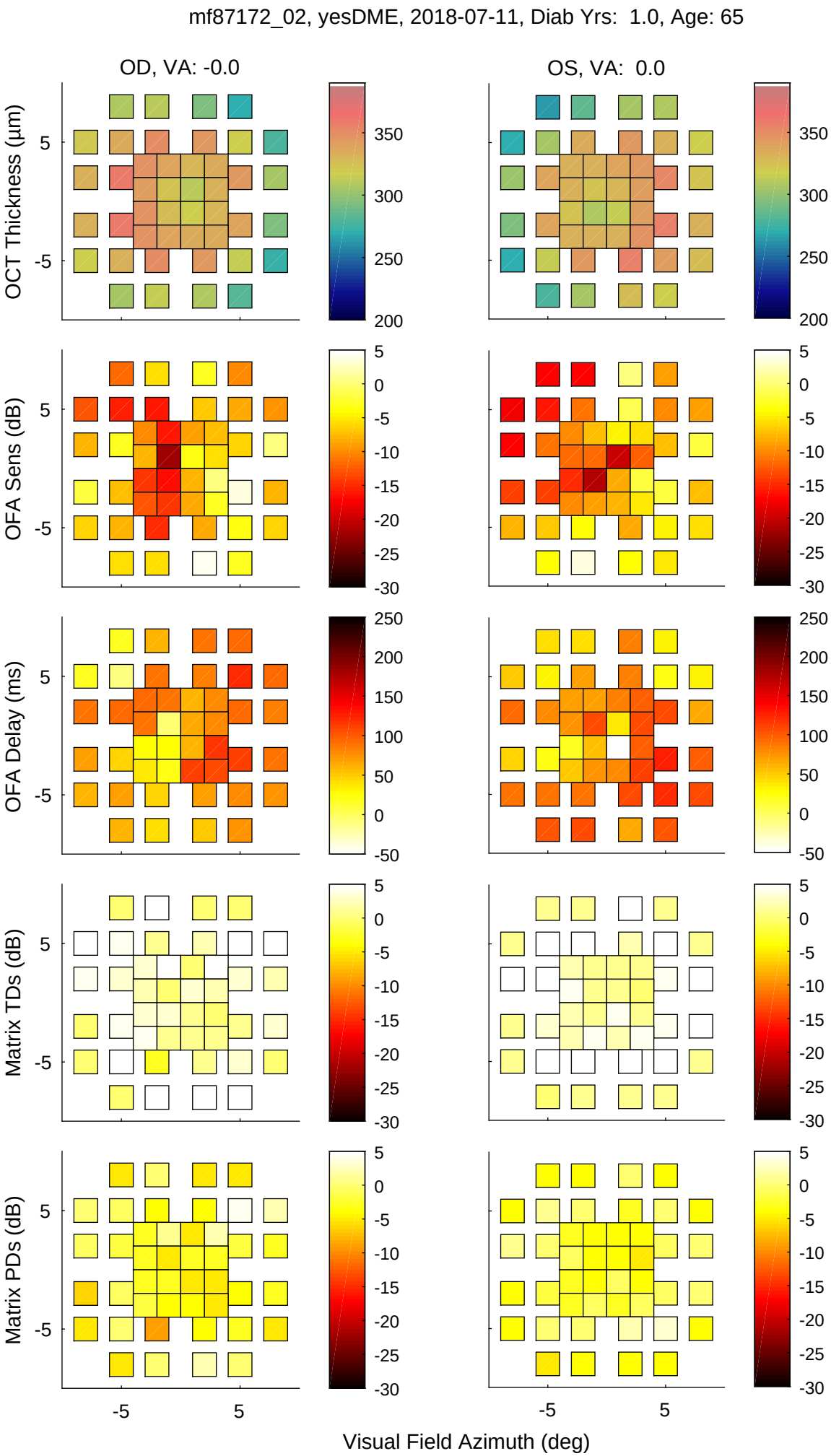
mf87172_02, yesDME, 2018-07-11, Diab Yrs: 1.0, Age: 65
OD, VA: -0.0
OS, VA: 0.0
OCT Thickness (µm)
OFA Sens (dB)
OFA Delay (ms)
Matrix TDs (dB)
Matrix PDs (dB)
Visual Field Azimuth (deg)

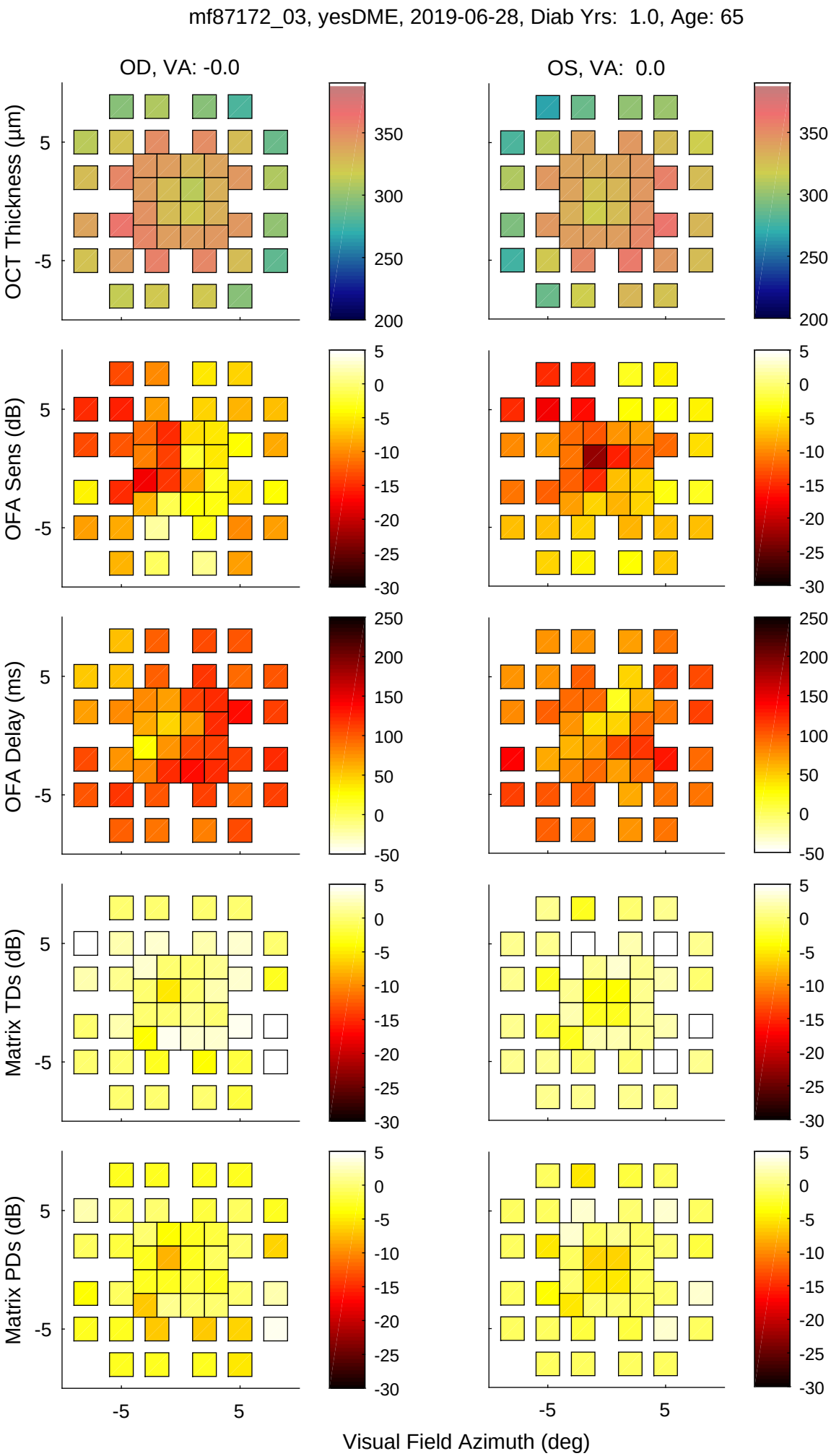
mf87172_03, yesDME, 2019-06-28, Diab Yrs: 1.0, Age: 65
OD, VA: -0.0
OS, VA: 0.0
OCT Thickness (µm)
OFA Sens (dB)
OFA Delay (ms)
Matrix TDs (dB)
Matrix PDs (dB)
Visual Field Azimuth (deg)

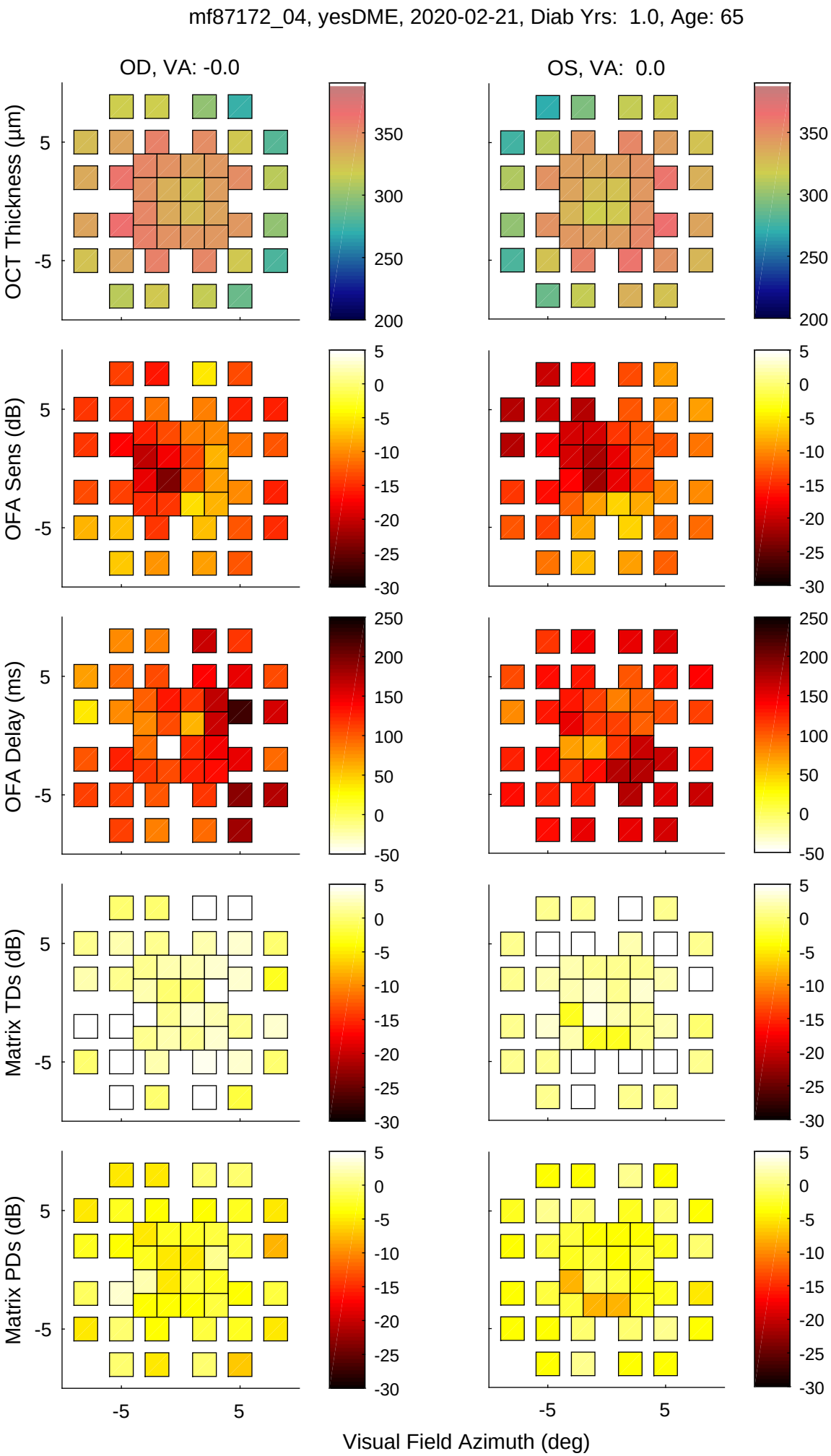
mf87172_04, yesDME, 2020-02-21, Diab Yrs: 1.0, Age: 65
OD, VA: -0.0
OS, VA: 0.0
OCT Thickness (µm)
OFA Sens (dB)
OFA Delay (ms)
Matrix TDs (dB)
Matrix PDs (dB)
Visual Field Azimuth (deg)

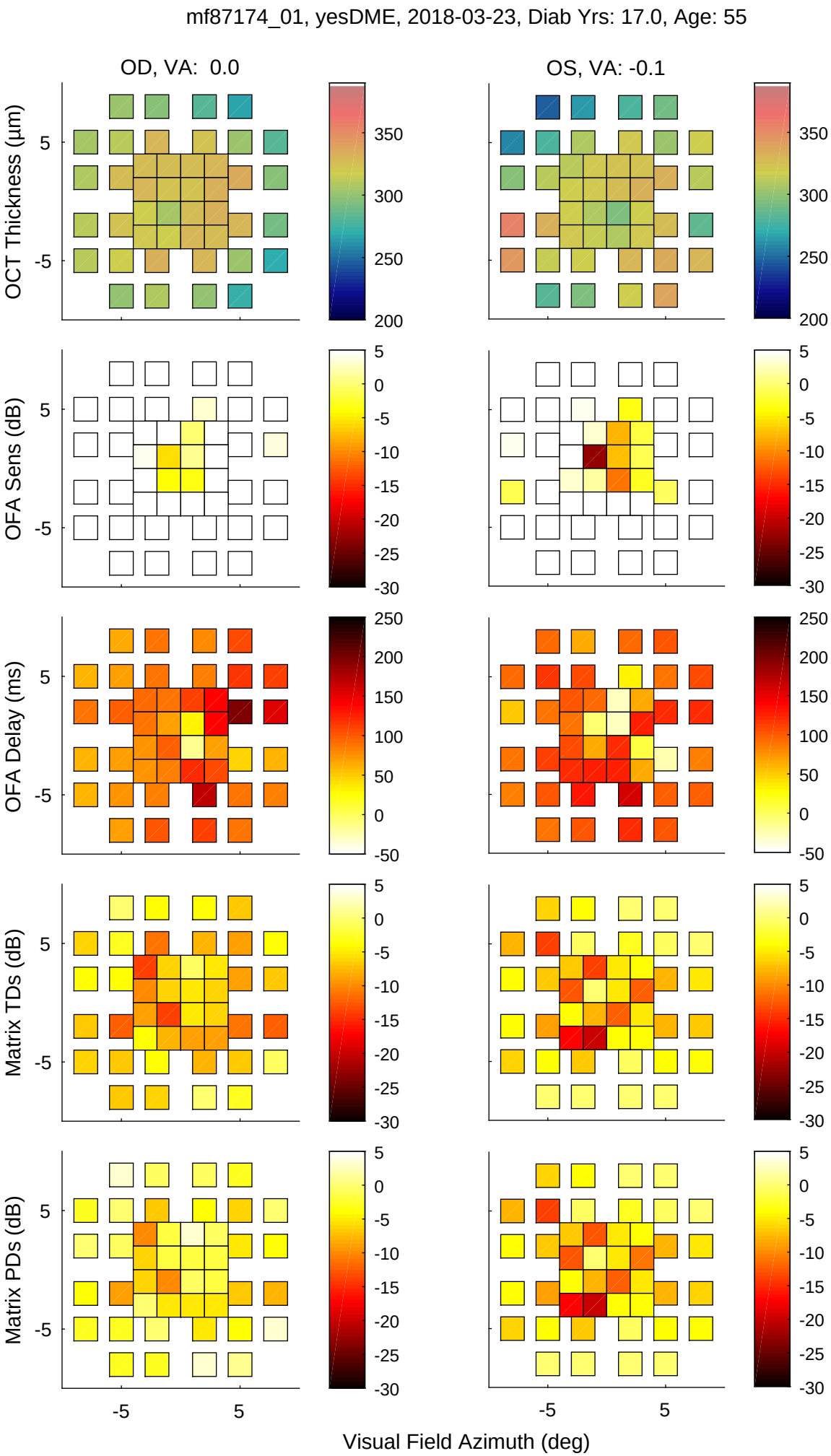
mf87174_01, yesDME, 2018-03-23, Diab Yrs: 17.0, Age: 55
OD, VA: 0.0
OS, VA: -0.1
OCT Thickness (µm)
OFA Sens (dB)
OFA Delay (ms)
Matrix TDs (dB)
Matrix PDs (dB)
Visual Field Azimuth (deg)

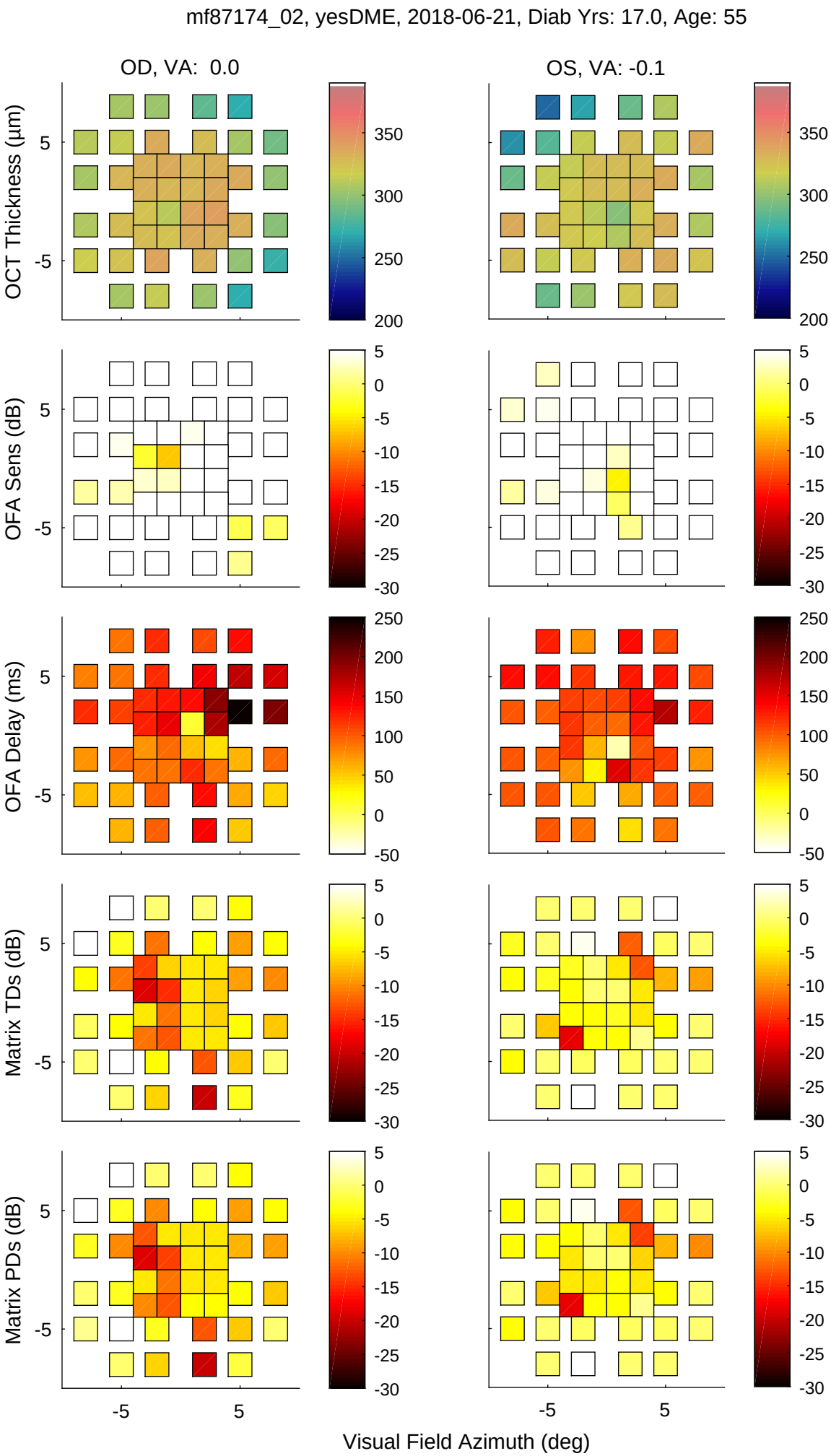
mf87174_02, yesDME, 2018-06-21, Diab Yrs: 17.0, Age: 55
OD, VA: 0.0
OS, VA: -0.1
OCT Thickness (µm)
OFA Sens (dB)
OFA Delay (ms)
Matrix TDs (dB)
Matrix PDs (dB)
Visual Field Azimuth (deg)

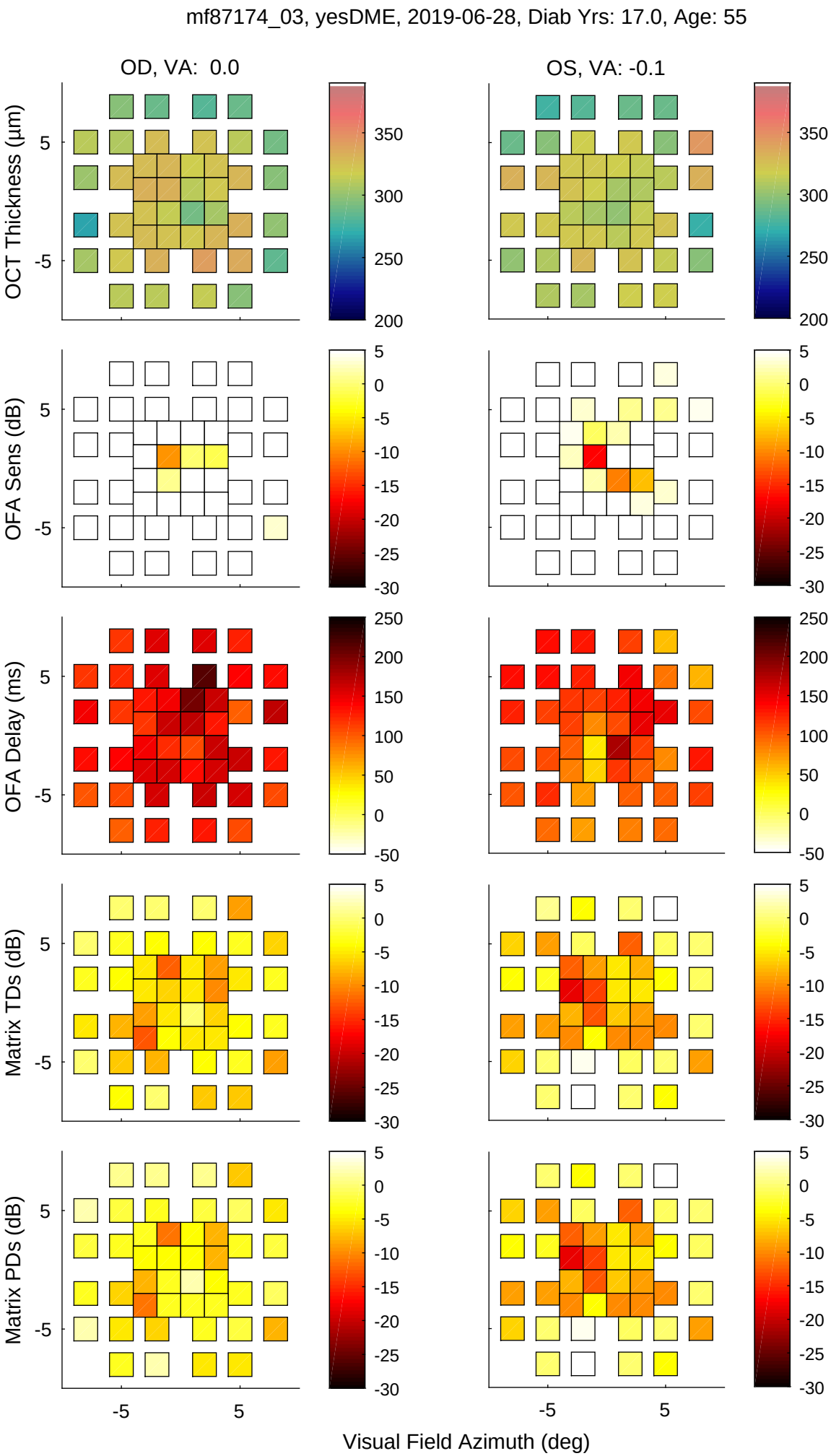
mf87174_03, yesDME, 2019-06-28, Diab Yrs: 17.0, Age: 55
OD, VA: 0.0
OS, VA: -0.1
OCT Thickness (µm)
OFA Sens (dB)
OFA Delay (ms)
Matrix TDs (dB)
Matrix PDs (dB)
Visual Field Azimuth (deg)

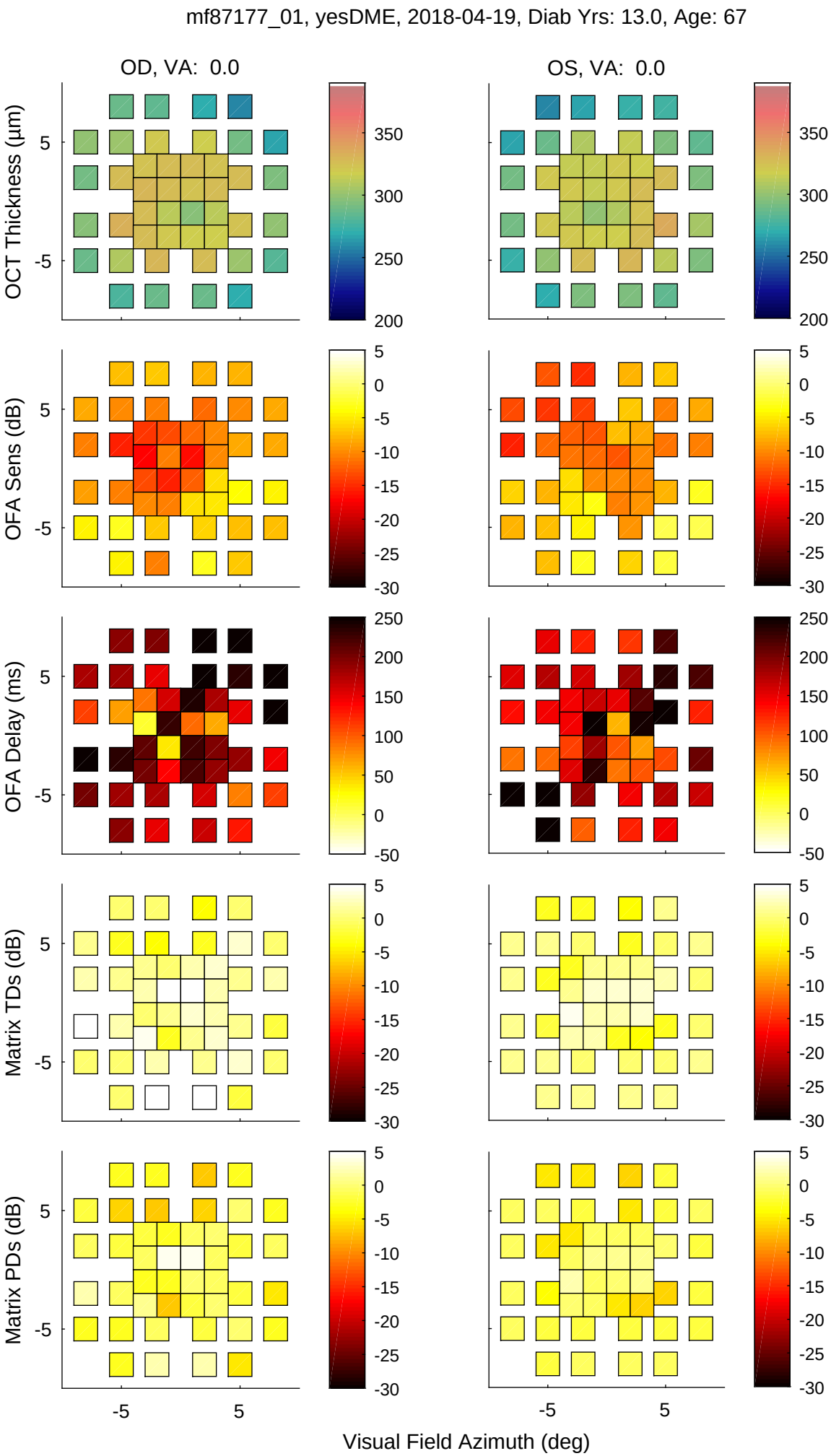
mf87177_01, yesDME, 2018-04-19, Diab Yrs: 13.0, Age: 67
OD, VA: 0.0
OS, VA: 0.0
OCT Thickness (µm)
OFA Sens (dB)
OFA Delay (ms)
Matrix TDs (dB)
Matrix PDs (dB)
Visual Field Azimuth (deg)

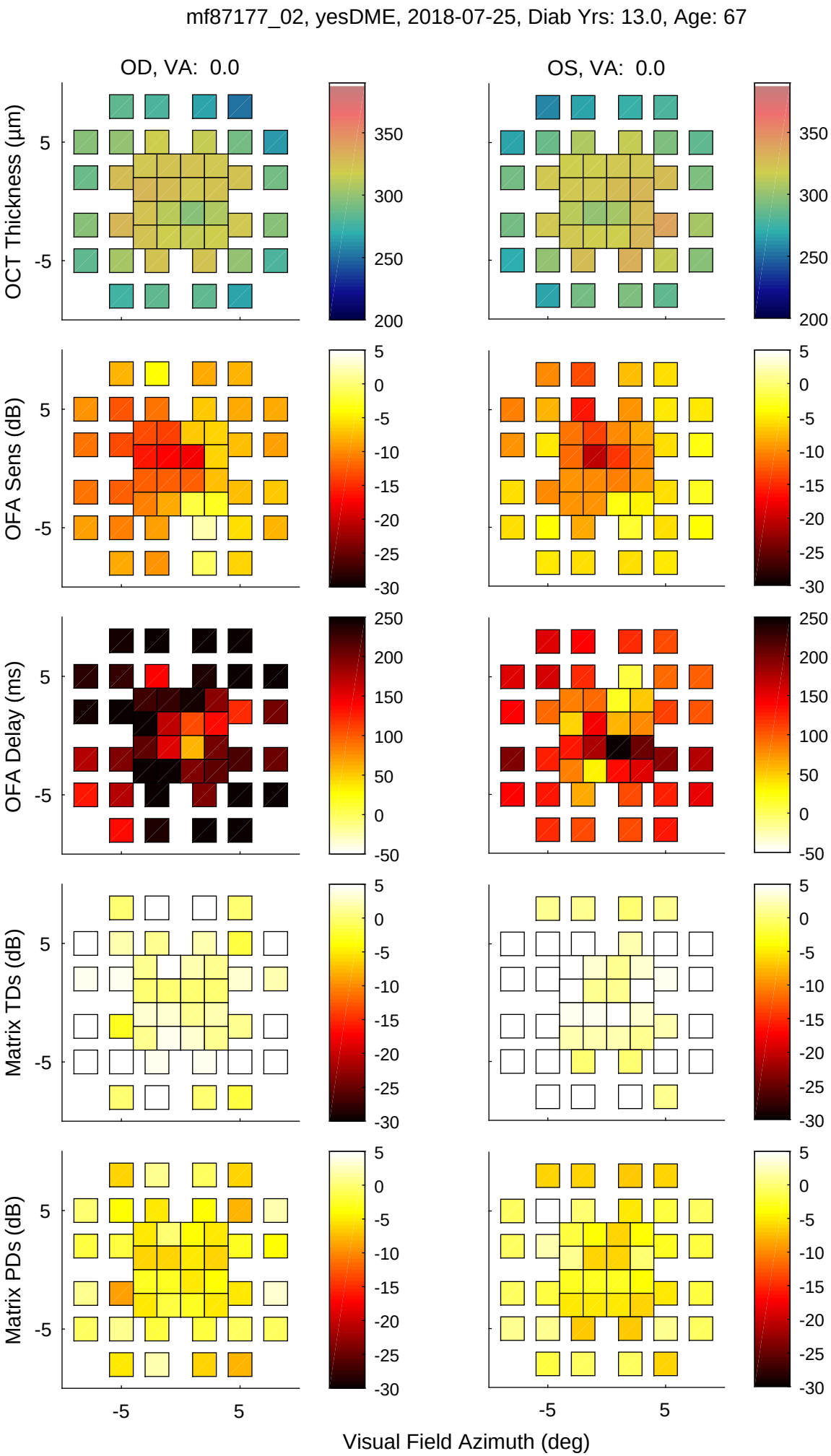
mf87177_02, yesDME, 2018-07-25, Diab Yrs: 13.0, Age: 67
OD, VA: 0.0
OS, VA: 0.0
OCT Thickness (µm)
OFA Sens (dB)
OFA Delay (ms)
Matrix TDs (dB)
Matrix PDs (dB)
Visual Field Azimuth (deg)

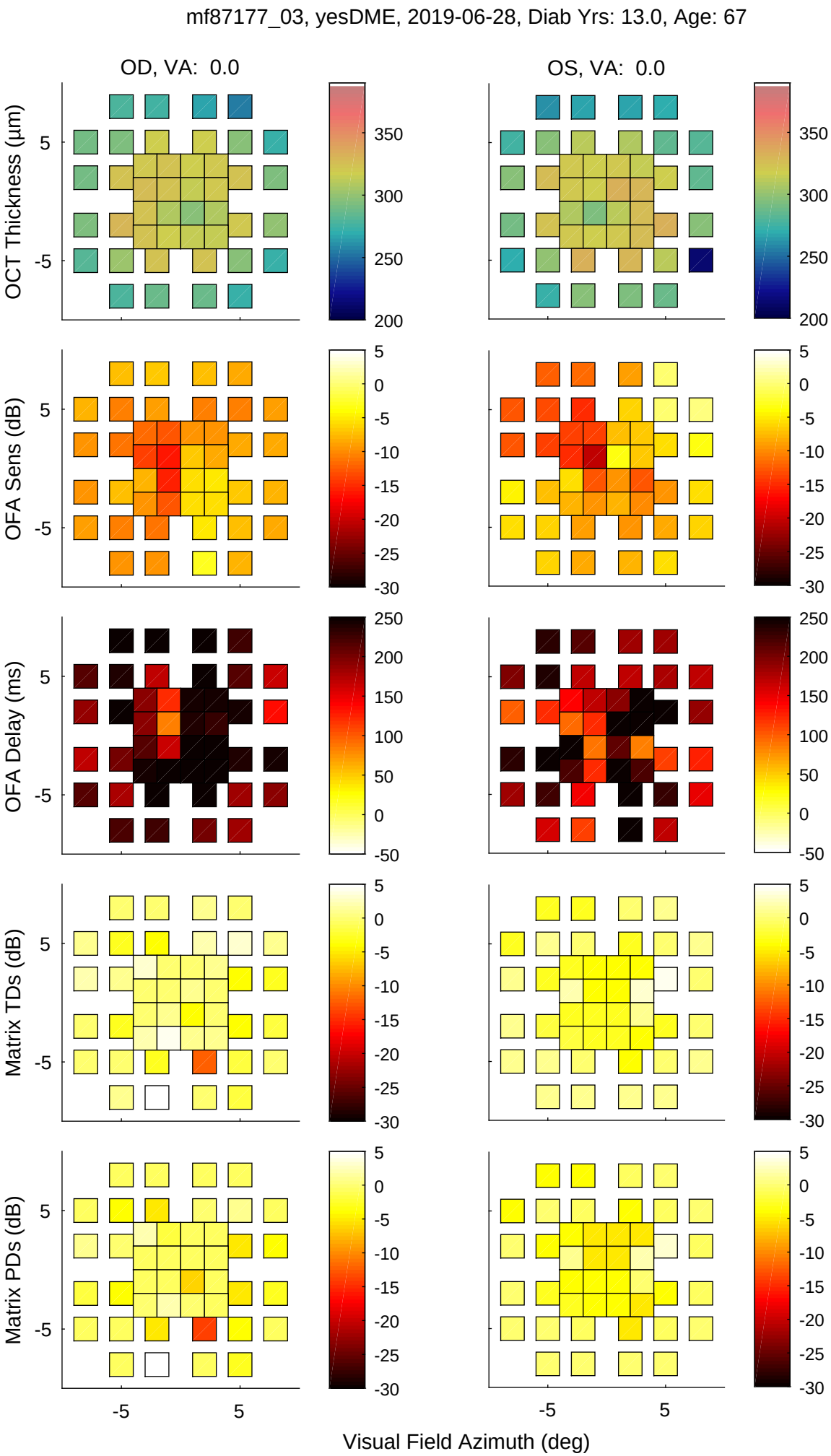
mf87177_03, yesDME, 2019-06-28, Diab Yrs: 13.0, Age: 67
OD, VA: 0.0
OS, VA: 0.0
OCT Thickness (µm)
OFA Sens (dB)
OFA Delay (ms)
Matrix TDs (dB)
Matrix PDs (dB)
Visual Field Azimuth (deg)

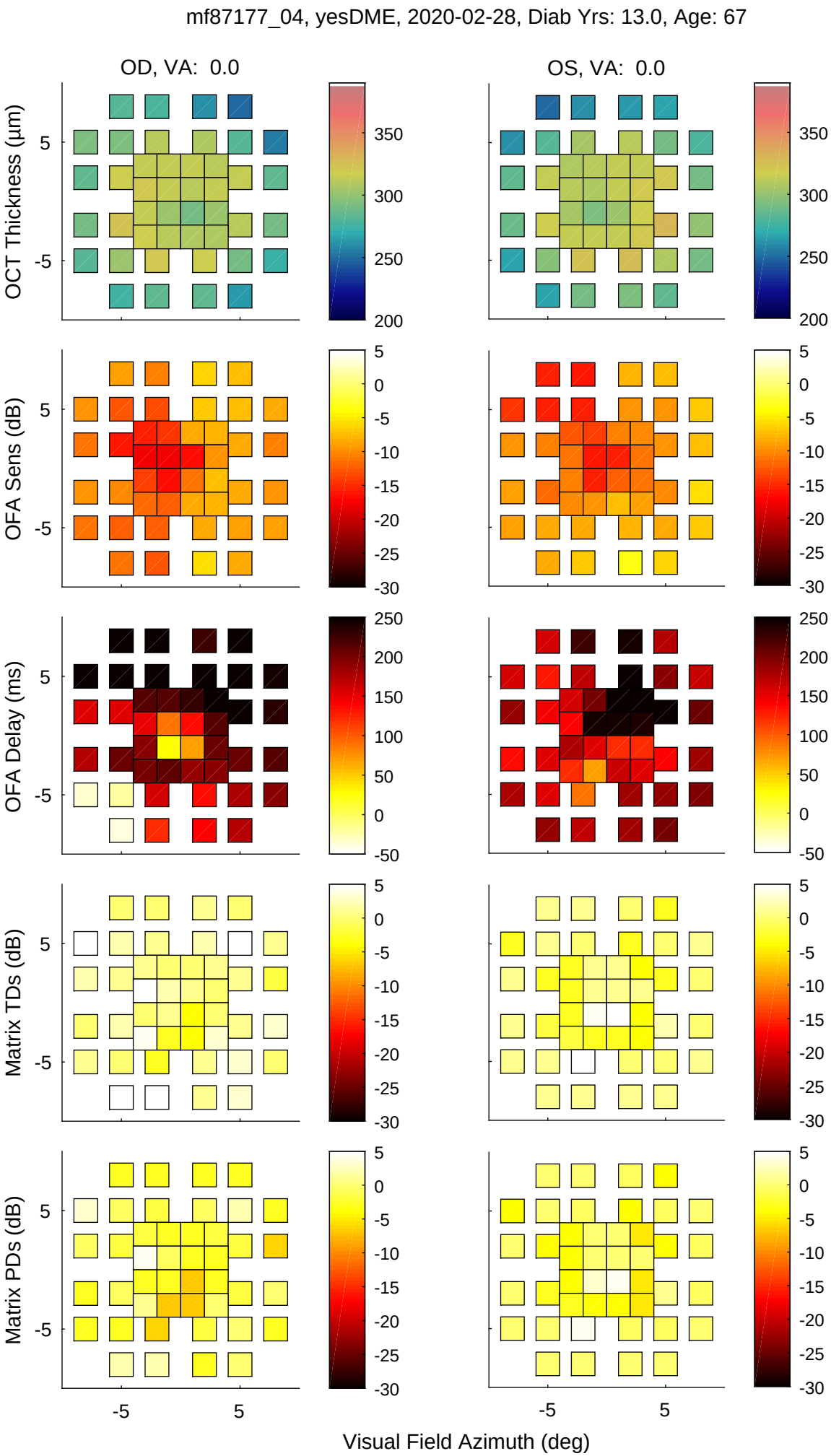
mf87177_04, yesDME, 2020-02-28, Diab Yrs: 13.0, Age: 67
OD, VA: 0.0
OS, VA: 0.0
OCT Thickness (µm)
OFA Sens (dB)
OFA Delay (ms)
Matrix TDs (dB)
Matrix PDs (dB)
Visual Field Azimuth (deg)

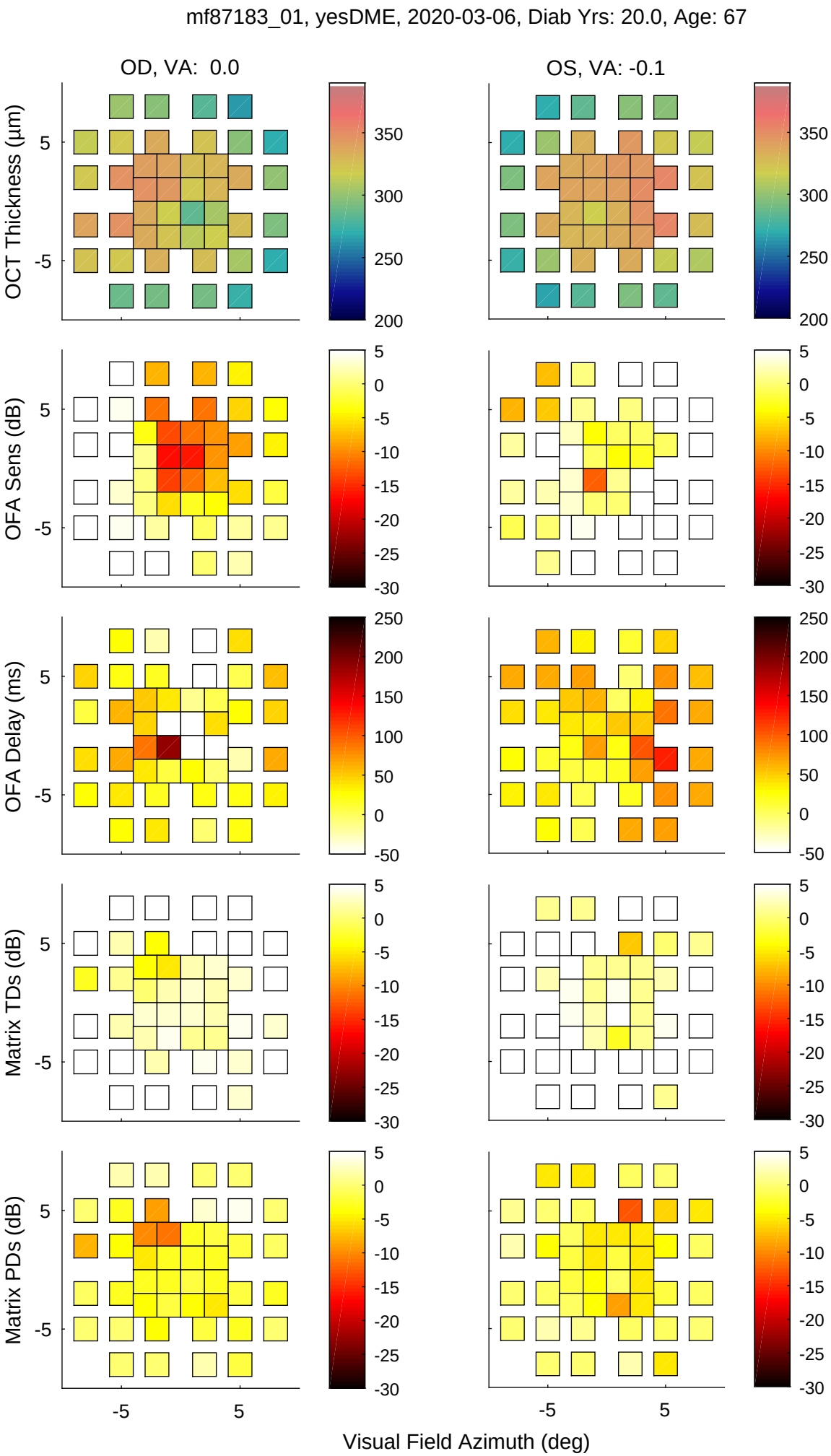
mf87183_01, yesDME, 2020-03-06, Diab Yrs: 20.0, Age: 67
OD, VA: 0.0
OS, VA: -0.1
OCT Thickness (µm)
OFA Sens (dB)
OFA Delay (ms)
Matrix TDs (dB)
Matrix PDs (dB)
Visual Field Azimuth (deg)

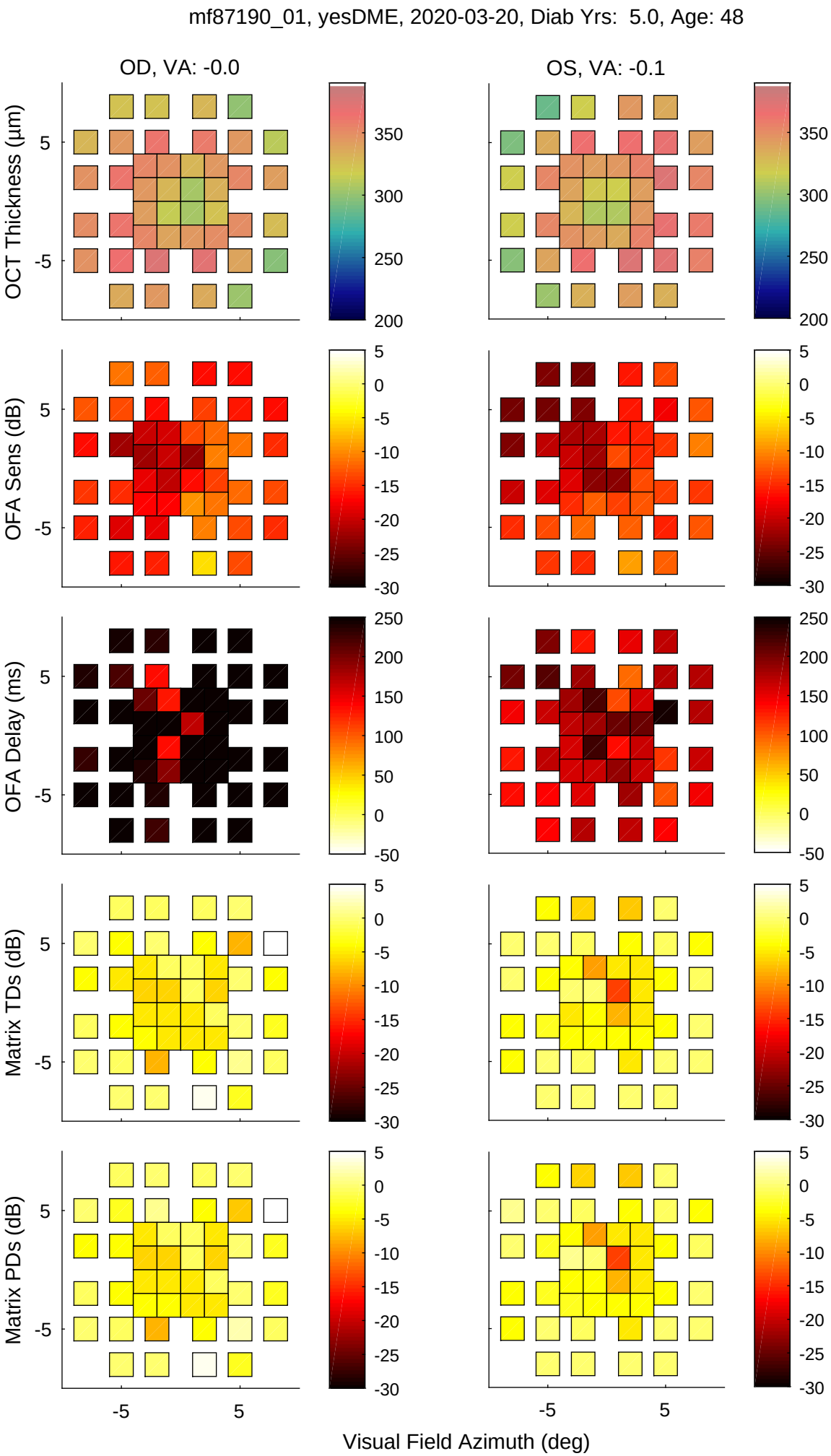
mf87190_01, yesDME, 2020-03-20, Diab Yrs: 5.0, Age: 48
OD, VA: -0.0
OS, VA: -0.1
OCT Thickness (µm)
OFA Sens (dB)
OFA Delay (ms)
Matrix TDs (dB)
Matrix PDs (dB)
Visual Field Azimuth (deg)